US Army Corps of Engineers
Waterways Experiment Station

Miscellaneous Paper EL-95-7
September 1995

Temperature and Dissolved Oxygen Simulations for the Upper Missouri River Reservoirs

by Thomas M. Cole, Michael L. Schneider, John G. Skogerboe, Ronald E. Heath, Herman O. Turner

Approved For Public Release; Distribution Is Unlimited

Prepared for Headquarters, U.S. Army Corps of Engineers

and U.S. Army Engineer Division, Missouri River

Miscellaneous Paper EL-95-7
September 1995

Temperature and Dissolved Oxygen Simulations for the Upper Missouri River Reservoirs

by Thomas M. Cole, Michael L. Schneider, John G. Skogerboe,
Ronald E. Heath, Herman O. Turner

U.S. Army Corps of Engineers
Waterways Experiment Station
3909 Halls Ferry Road
Vicksburg, MS 39180-6199

Final report

Prepared for U.S. Army Corps of Engineers
Washington, DC 20314-1000

and U.S. Army Engineer Division, Missouri River
Omaha, NE 68101-0103

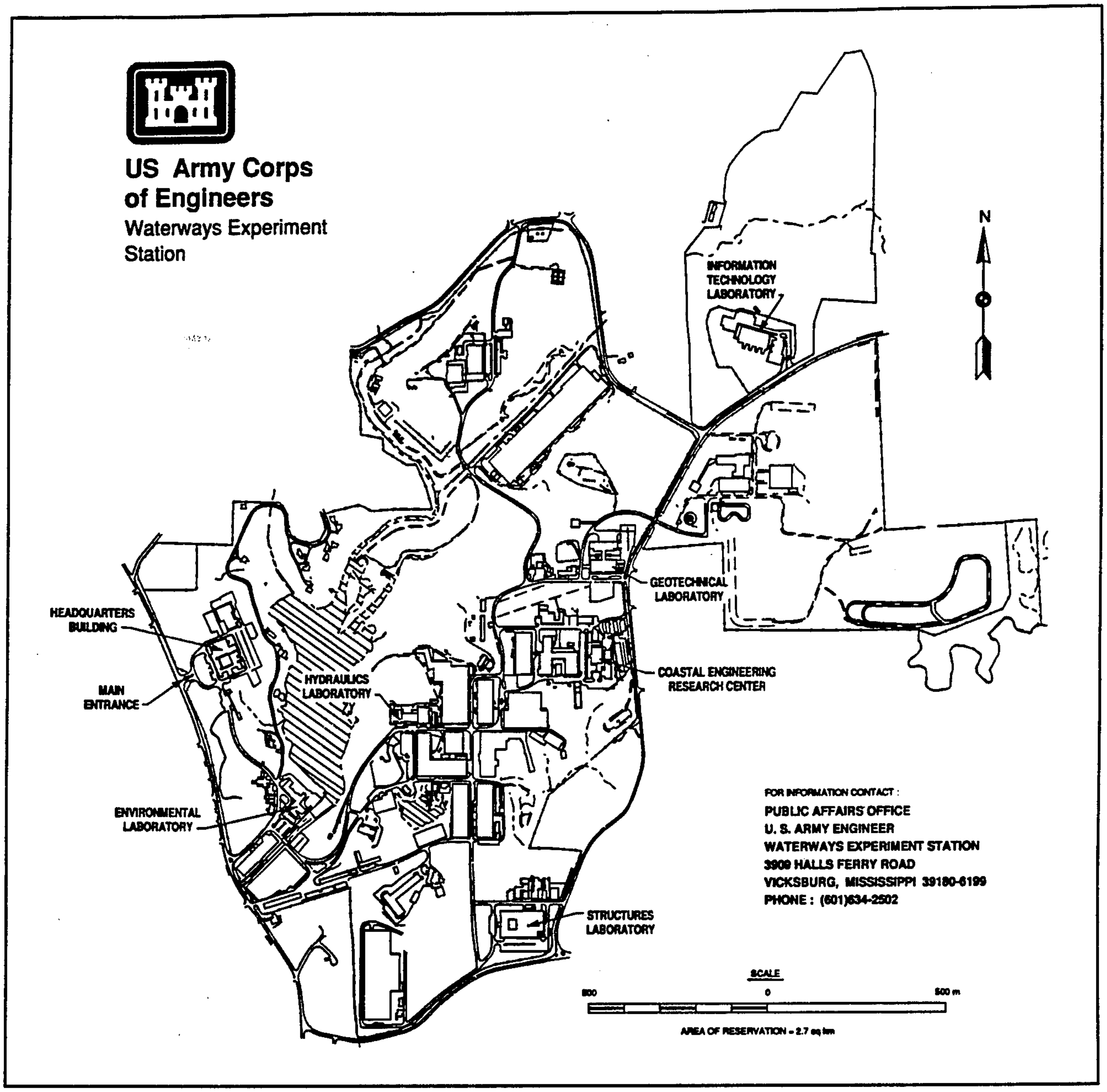

Waterways Experiment Station Cataloging-in-Publication Data

Temperature and dissolved oxygen simulations for the upper Missouri River reservoirs / by Thomas M. Cole ... [et al.] ; prepared for U.S. Army Corps of Engineers and U.S. Army Engineer Division, Missouri River.

284 p. : ill. ; 28 cm. -- (Miscellaneous paper ; EL-95-7)

Includes bibliographic references.

1. Reservoirs -- Missouri River. 2. Water temperature -- Missouri River. 3. Missouri River. 4. Water quality -- Missouri River. I. Cole, Thomas M. II. United States. Army. Corps of Engineers. Missouri River Division. III. U.S. Army Engineer Waterways Experiment Station. IV. Environmental Laboratory (U.S. Army Engineer Waterways Experiment Station) V. Series: Miscellaneous paper (U.S. Army Engineer Waterways Experiment Station) ; EL-95-7.

TA7 W34m no.EL-95-7

Contents

List of Figures

List of Tables

Preface

The report herein was prepared by the Environmental Laboratory (EL), U.S. Army Engineer Waterways Experiment Station (WES), Vicksburg, MS, for use by engineers, scientists, and resource managers in the U.S. Army Engineer Division, Missouri River. It provides information on determining the effects of operational changes in the Upper Missouri River Reservoir System on suitable coldwater fish habitat. The study was sponsored by the Missouri River Division as part of the Missouri River Water Control Manual Review.

The authors of this report were Messrs. Thomas M. Cole and John G. Skogerboe, EL, and Messrs. Michael L. Schneider, Ronald E. Heath, and Herman O. Turner, Hydraulics Laboratory (HL), WES. This report was prepared under the direct supervision of Mr. Cole and under the general supervision of Dr. Mark S. Dortch, Chief, Water Quality and Contaminant Modeling Branch, EL; Mr. Donald L. Robey, Chief, Environmental Processes and Effects Division, EL; and Dr. John W. Keeley, Director, EL. Mr. Frank Hermann was Director, HL.

At the time of publication of this report, Director of WES was Dr. Robert W. Whalin. Commander was COL Bruce K. Howard, EN.

This report should be cited as follows:

Cole, T. M., Schneider, M. L., Skogerboe, J. G., Heath, R. E., and Turner, H. O. (1995). "Temperature and dissolved oxygen simulations for the Upper Missouri River reservoirs," Miscellaneous Report EL-95-7, U.S. Army Engineer Waterways Experiment Station, Vicksburg, MS.

Conversion Factors, Non-SI to SI Units of Measurement

Non-Si units of measurement used in this report can be converted to SI units as follows:

Multiply	By	To Obtain
acres	4,046.873	square meters
acre-feet	1,233,489	cubic meters
cubic feet	0.02831685	cubic meters
feet	0.3048	meters
Fahrenheit degrees	5/9	Celsius degrees[1]
miles (U.S. statute)	1.609347	kilometers

[1] To obtain Celsius (C) temperature readings from Fahrenheit (F) readings, use the following formula: $C = (5/9)(F - 32)$.

1 Introduction

Background

The U.S. Army Engineer Division, Missouri River (MRD) controls water resources on the main stem Missouri River to fulfill project purposes authorized in the 1930's and 1940's. Since authorization, considerable demographic, social, economic, and political changes have occurred in the region. In 1990, MRD began reevaluating the Missouri River Master Water Control Manual to meet the changing priorities of the system. The goal was to develop methods of impact assessment that would help MRD identify and promote equitable use of resources for authorized purposes.

Purpose

The purpose of this study was to provide MRD with the ability to predict the effects of reservoir operational changes on suitable coldwater fish habitat in Fort Peck Lake, Lake Sakakawea, Lake Oahe, and Lake Francis Case. Coldwater fish habitat is defined as water less than or equal to 15°C and greater than or equal to 5 $mg\,l^{-1}$ DO. The only system operational variables which can be changed are end-of-month stages and monthly average releases. Results of this study must therefore predict suitable coldwater fish habitat as a function of these two variables. The results will be incorporated into MRD's *L*ong *R*ange *S*ystem model (LRS) and will be used to predict suitable coldwater fish habitat under various operational alternatives.

Approach

Fort Peck Lake, Lake Sakakawea, and Lake Oahe are long, narrow, deep-storage reservoirs. Reservoirs of this type typically exhibit both longitudinal and vertical water quality gradients (Cole and Hannan, 1990). The likelihood of two-dimensional (2D) water quality gradients dictated the use of a 2D water quality model. The 2D water quality model, CE-QUAL-W2, was chosen to model temperature and dissolved oxygen (DO) and ultimately suitable coldwater fish habitat. Although Lake Francis Case more closely resembles a run-of-the-river reservoir in which longitudinal gradients may be negligable, it was also modeled using CE-QUAL-W2.

Since operational changes in an upstream reservoir could affect the downstream reservoir, the four reservoirs were modeled in series in which releases from the upstream reservoir were routed to the downstream reservoir. This required developing temperature and DO routing equations for the riverine reaches between reservoirs.

Evaluation of operational alternatives using the LRS model involves modeling a 92 year period using historical flows. Meteorologic data necessary to drive the water quality model during this historical period were not available prior to 1950. Therefore, a different approach was needed to produce results for coldwater fish habitat analysis for the 92 year period. The approach used was to model 30 years and produce regression relationships relating stage and discharge to suitable coldwater fish habitat.

The 30 years had to encompass the expected range of operating conditions used in the 92 year LRS simulations - specifically, the drought of the 1930's had to be incorporated into the 30 year simulations. The drought of the 1930's was represented by surrogate years in which years with available meteorologic data were chosen to represent the drought based on yearly runoff from above Sioux City, SD. Table 1 shows the correspondence between surrogate years and drought years. Nine 30 year operational scenarios developed by MRD were then run to produce monthly regressions relating stage and discharge to suitable coldwater fish habitat. The monthly regressions will be used to predict habitat for all of the operational alternatives proposed by the MRD.

Typically, DO is modeled along with a full suite of water quality variables including algal/nutrient interactions. Lack of available algal/nutrient data necessitated a different approach. DO was assumed to be a function of sediment and water column oxygen demands which were adjusted during calibration to reproduce the average DO depletion during summer stratification. The drawback to this approach is that operational changes which might affect algal/nutrient interactions cannot be predicted. This approach also precluded modeling algal blooms and die-offs during model calibration. Results from this study show only how physical factors relating to changes in reservoir stage and discharge affect DO.

Model Description

CE-QUAL-W2 is a 2-D (longitudinal-vertical), hydrodynamic and water quality model developed for rivers, lakes, reservoirs, and estuaries (Environmental and Hydraulics Laboratories, 1986; Martin, 1987; Martin, 1988). It is based upon the LARM model originally developed by Edinger and Buchak (1978). The model is capable of making long-term predictions of hydrodynamics and in-pool and release temperature and water quality con-

Table 1. Correspondence between 1930's drought years and surrogate years

Drought Year	Runoff (acre-ft)	Surrogate Year	Runoff (acre-ft)
1930	18,452,000	1980	18,687,000
1931	10,701,000	1988	12,352,000
1932	19,463,000	1956	19,418,000
1933	18,166,000	1989	17,700,000
1934	11,164,000	1988	12,352,000
1935	14,323,000	1977	16,080,000
1936	14,339,000	1977	16,080,000
1937	14,315,000	1977	16,080,000
1938	20,652,000	1980	18,687,000
1939	17,271,000	1989	17,700,000
1940	12,101,000	1988	12,352,000
1941	16,714,000	1955	16,410,000

stituents. It is best suited for waterbodies that are relatively long and narrow exhibiting water quality gradients in both the longitudinal and vertical directions. The model has been used extensively by Government and private firms in the United States and throughout the world to investigate water quality problems. An extensive bibliography is given as a separate section in the References.

The model represents a reservoir as a grid of longitudinal segments and vertical layers having a length and height defined by the user. The width for each cell is defined as the surface area at the mid-height of the cell divided by the segment length. Predictions from the model represent values of temperature or a water quality constituent averaged over the length, height, and width of a cell. CE-QUAL-W2 has the following capabilities that were important in this study:

1. Multiple branches
2. Autostepping (automatic adjustment of timestep to maintain hydrodynamic stability)
3. Layer/segment addition and subtraction
4. Ice cover

The following improvements to the model were implemented during calibration to the Upper Missouri River reservoirs:

1. A higher-order explicit transport algorithm (QUICKEST, Leonard, 1979) in the longitudinal and vertical, and a time-weighted, implicit transport algorithm in the vertical

were added to the model. These improvements were necessary to more accurately reproduce the temperature gradient in the thermocline.

2. A fully implicit, vertical diffusion algorithm was implemented to eliminate density inversions during periods of rapid cooling.
3. An improved ice-cover algorithm was implemented to more accurately reproduce ice-in and ice-out dates.
4. A selective withdrawal algorithm was implemented to more accurately reproduce observed release temperatures.

Site Description

The modeled system consists of five reservoirs and two stretches of the Missouri River - Fort Peck Lake, Lake Sakakawea, Lake Oahe, Lake Sharp, Lake Francis Case, and the Missouri River below Fort Peck Dam and Garrison Dam (Lake Sakakawea) (Figure 1). Lake Sharpe was treated similarly to the Missouri River stretches. Release temperatures from Oahe Dam were routed as inflows to Lake Francis Case taking into account the travel time in Lake Sharpe (see page 29 for further details on the routing procedure).

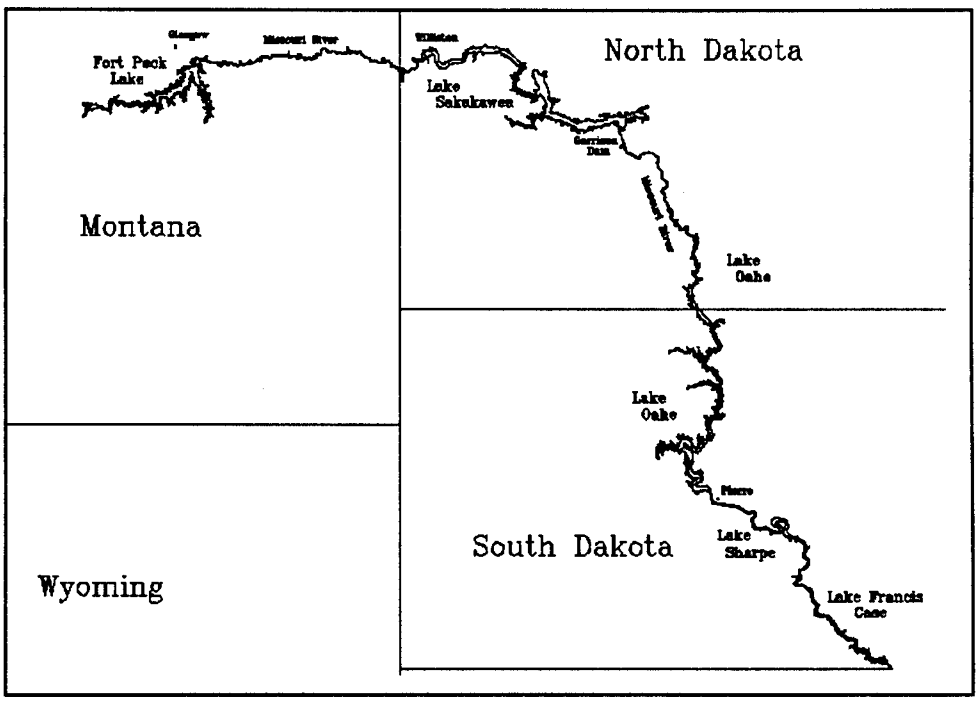

Figure 1. Map of the Upper Missouri River system modeled for this study

Fort Peck Lake

Fort Peck Dam is located in eastern Montana on the Missouri River about 18 miles southeast of Glasglow (Figure 2). The major tributaries to the main body of Fort Peck Lake are the Missouri River and the Musselshell River. Because of the proximity of the upstream boundary and the confluence with the Musselshell River, inflows from both rivers were combined and treated as a single inflow at the upstream boundary. The primary inflow to the southern branch of Fort Peck Lake is Little Dry Creek. The two sampling stations used in calibration are located near the dam and midway up the reservoir near Hell Creek.

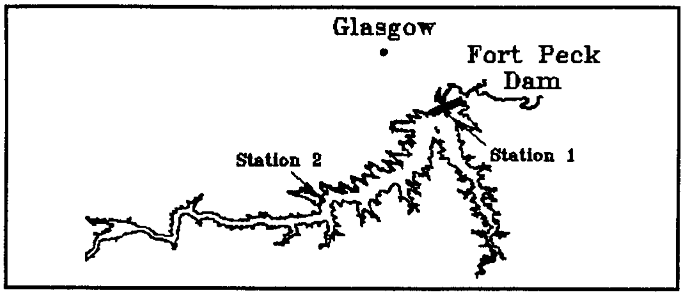

Figure 2. Fort Peck Lake study area showing sampling stations

Lake Sakakawea

Garrison Dam is located in central North Dakota at Missouri River mile 1390 about 75 miles northwest of Bismark (Figure 3). The major tributaries to Lake Sakakawea are the Missouri River and the Little Missouri River. The Missouri River enters Lake Sakakawea upstream of Williston, MT. Flows at this point consist primarily of inflows from the Yellowstone and Milk Rivers and releases from Fort Peck Dam. The two sampling stations used in calibrating the model are located near the dam and a little over midway upstream from the dam near New Town.

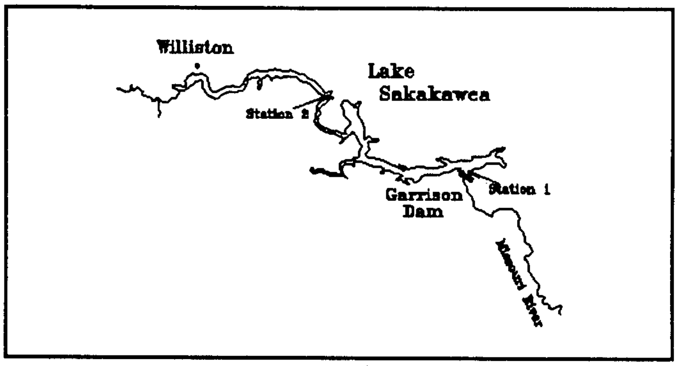

Figure 3. Lake Sakakawea study area showing sampling stations

Lake Oahe

Oahe Dam is located in central South Dakota on the Missouri River just north of Pierre, South Dakota (Figure 4). The Missouri River enters Lake Oahe just downstream from Bismarck, ND. Flow at this point is primarily from Garrison dam releases. The Cheyenne River is the other significant inflow. The two sampling stations used in calibrating the model are located near the dam and about two-thirds of the way upstream from the dam near Pollack.

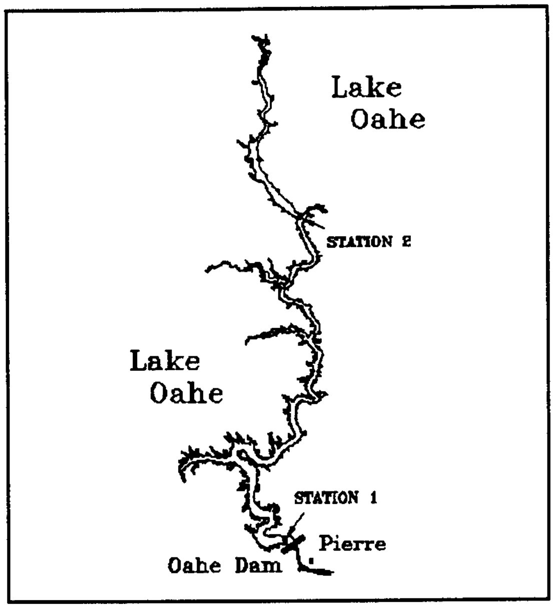

Figure 4. Lake Oahe study area showing sampling station locations

Lake Francis Case

Fort Randall Dam is located on the Missouri River in southeastern South Dakota near the Nebraska state line (Figure 5). Lake Francis Case, formed by Fort Randall Dam, is 107 miles in length. The upstream boundary of Lake Francis Case is Big Bend Dam (river mile 988). Inflows to Lake Francis Case are from the White River and Crow Creek and releases from Big Bend Dam. The two sampling stations used in calibrating the model are located near Fort Randall Dam and a little over midway upstream from the dam near Elm Creek.

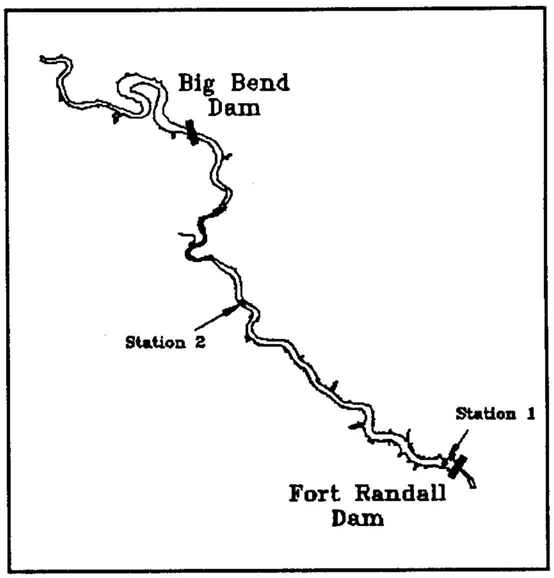

Figure 5. Lake Francis Case study area showing sampling station locations

2 Input Data

Bathymetry

CE-QUAL-W2 requires the reservoir be discretized into longitudinal segments and vertical layers that may vary in length and height. An average width must then be defined for each active cell where an active cell is defined as potentially containing water. Additionally, every branch has inactive cells at the upstream and downstream segments and top layer. Inactive cells are also located below the bottom active cell in each segment. Segment lengths and layer heights for all four reservoirs were constant for a given branch.

Once the segment lengths and layer weights were finalized, average widths were then determined for each cell from sediment range data obtained from the Omaha district. A computer program was written to average widths for each cell using linear interpolation.

Fort Peck Lake

The computational grid is shown in Figure 6. The reservoir was discretized into two branches with a total of 49 segments and 32 layers. Segments are numbered horizontally and layers are numbered vertically. Inactive cells are seen as blank spaces on the grid (i.e, segments 35 and 36). Branch one (segments 1-35) is the mainstem portion of Lake Fort Peck and branch two (segments 36-49) is the Big Dry Creek arm of the reservoir. Cells were 5km long and 2m high. A comparison of computed volume-area-elevation curves and U.S. Army Corps of Engineers (USACE) data is given in Figure 7.

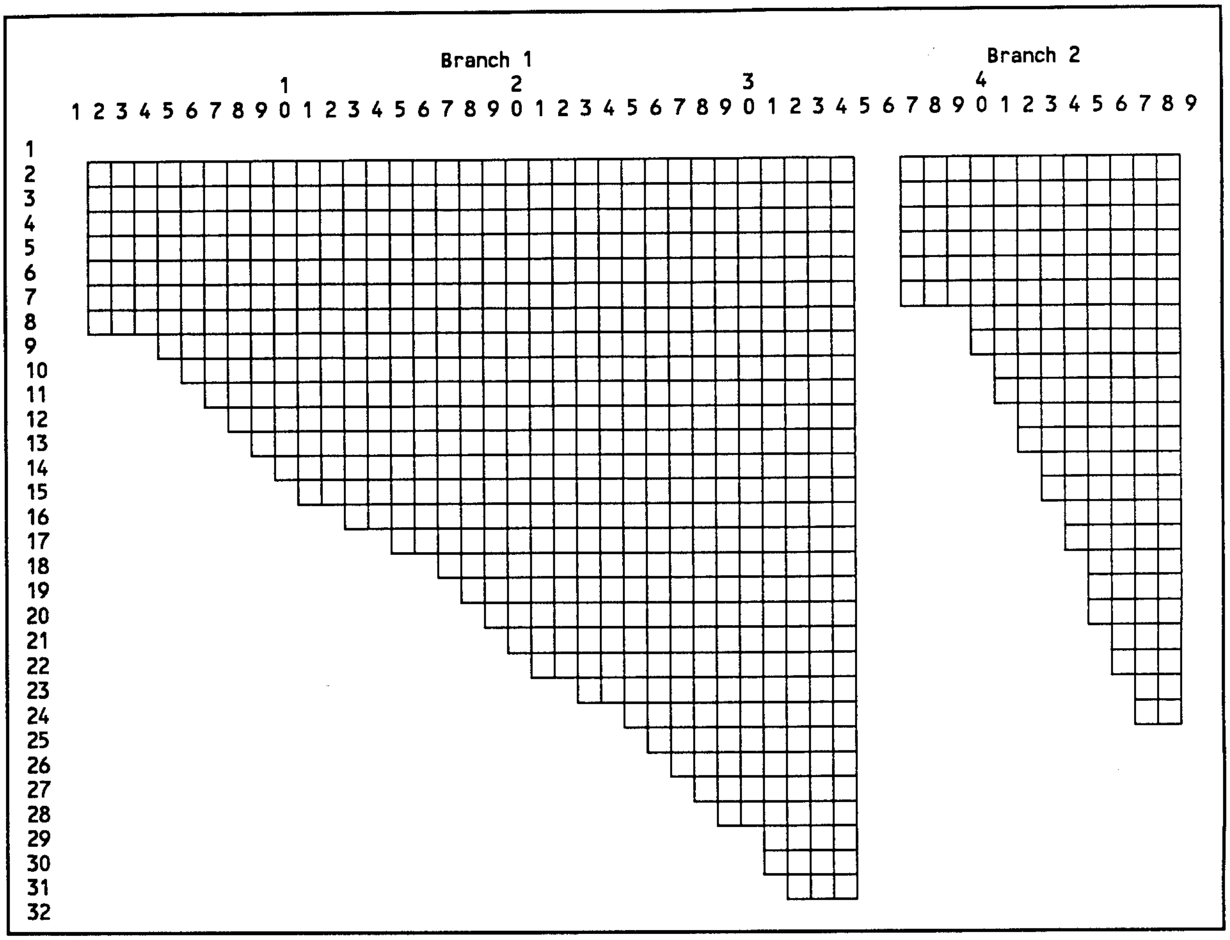

Figure 6. Fort Peck Lake computational grid

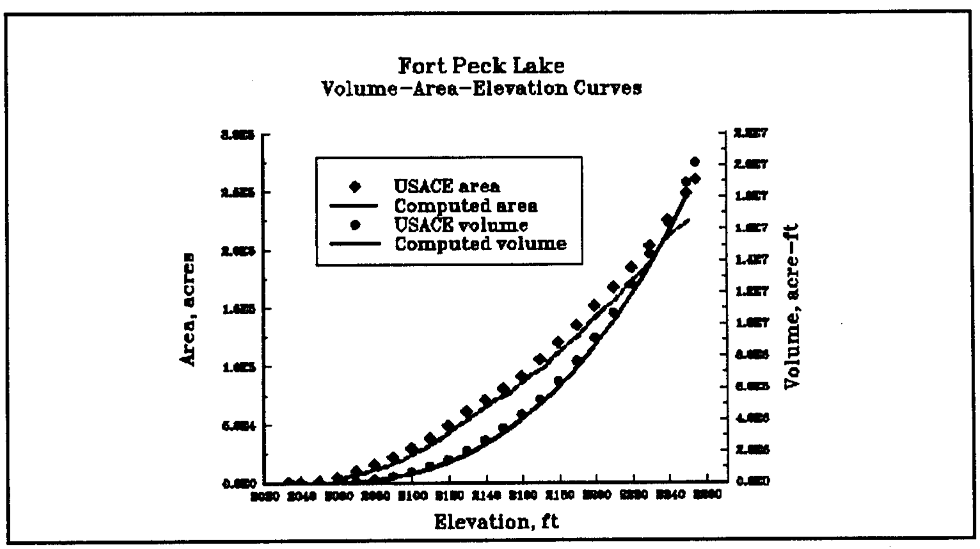

Figure 7. Fort Peck Lake computed versus USACE volume-area-elevation curves.

Lake Sakakawea

The computational grid is shown in Figure 8. The reservoir was discretized into two branches with a total of 66 segments and 31 layers. Branch one (segments 1-55) is the mainstem portion of Lake Sakakawea and branch two (segments 56-66) is the Little Missouri River arm of the reservoir. Cells were 5 km long and 2 m high. A comparison of computed volume-area-elevation curves and USACE data is given in Figure 9.

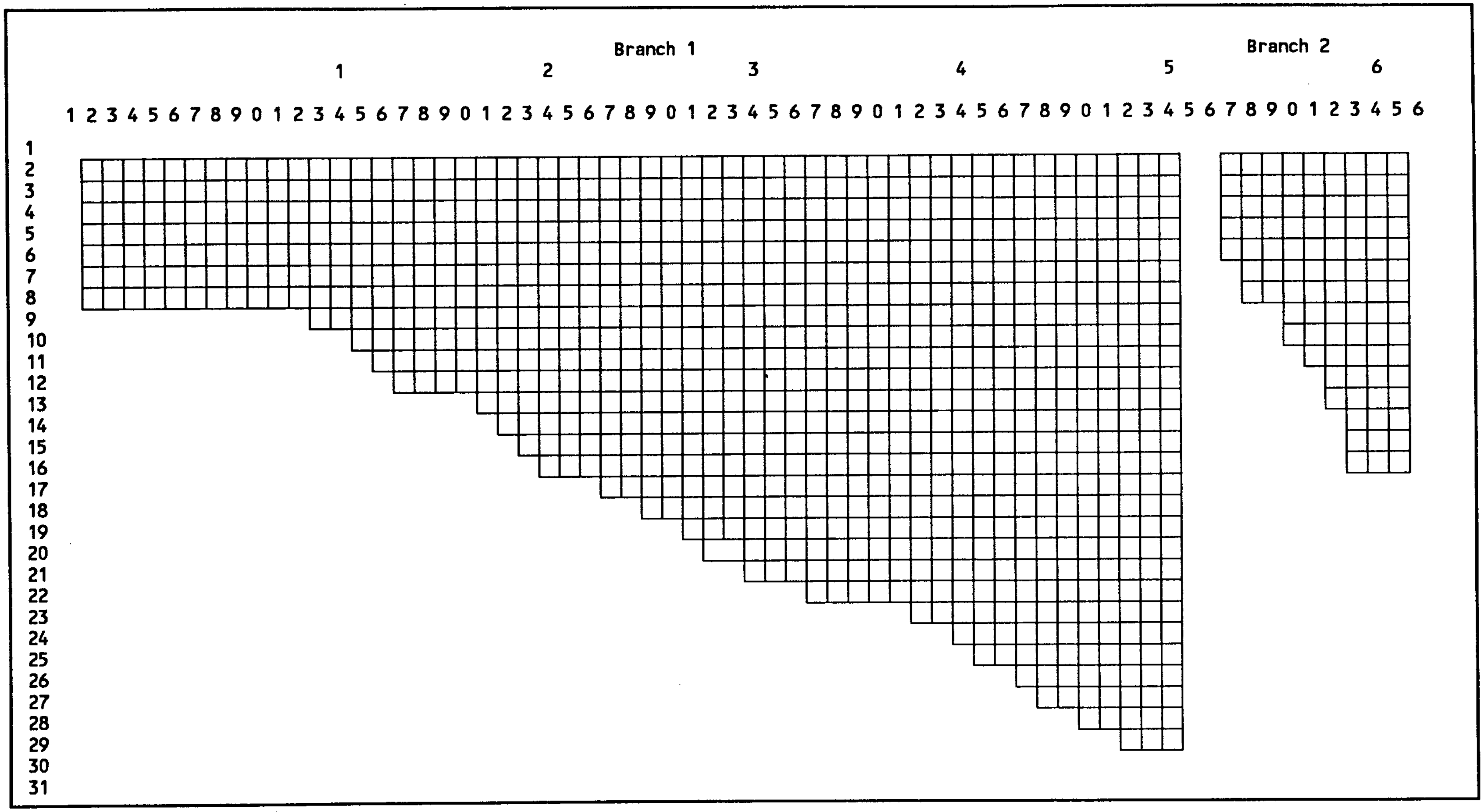

Figure 8. Lake Sakakawea computational grid

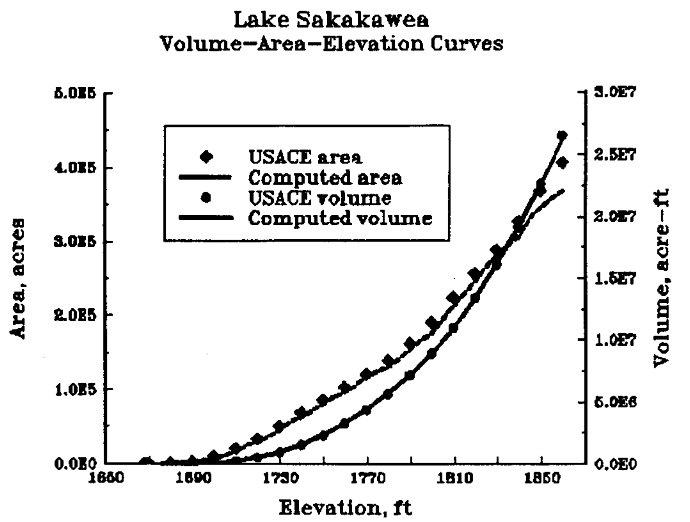

Figure 9. Lake Sakakawea computed versus USACE volume-area-elevation curves.

Lake Oahe

The computational grid is shown in Figure 10. The reservoir was discretized into two branches with a total of 47 segments and 34 layers. Branch one (segments 1-37) is the mainstem portion of Lake Oahe and branch two (segments 38-47) is the Cheyenne River arm of the reservoir. Cells in branch one were 10 km long and 2 m high. Cells in branch two were 5 km long and 2 m high. A comparison of computed volume-area-elevation curves and USACE data is given in Figure 11.

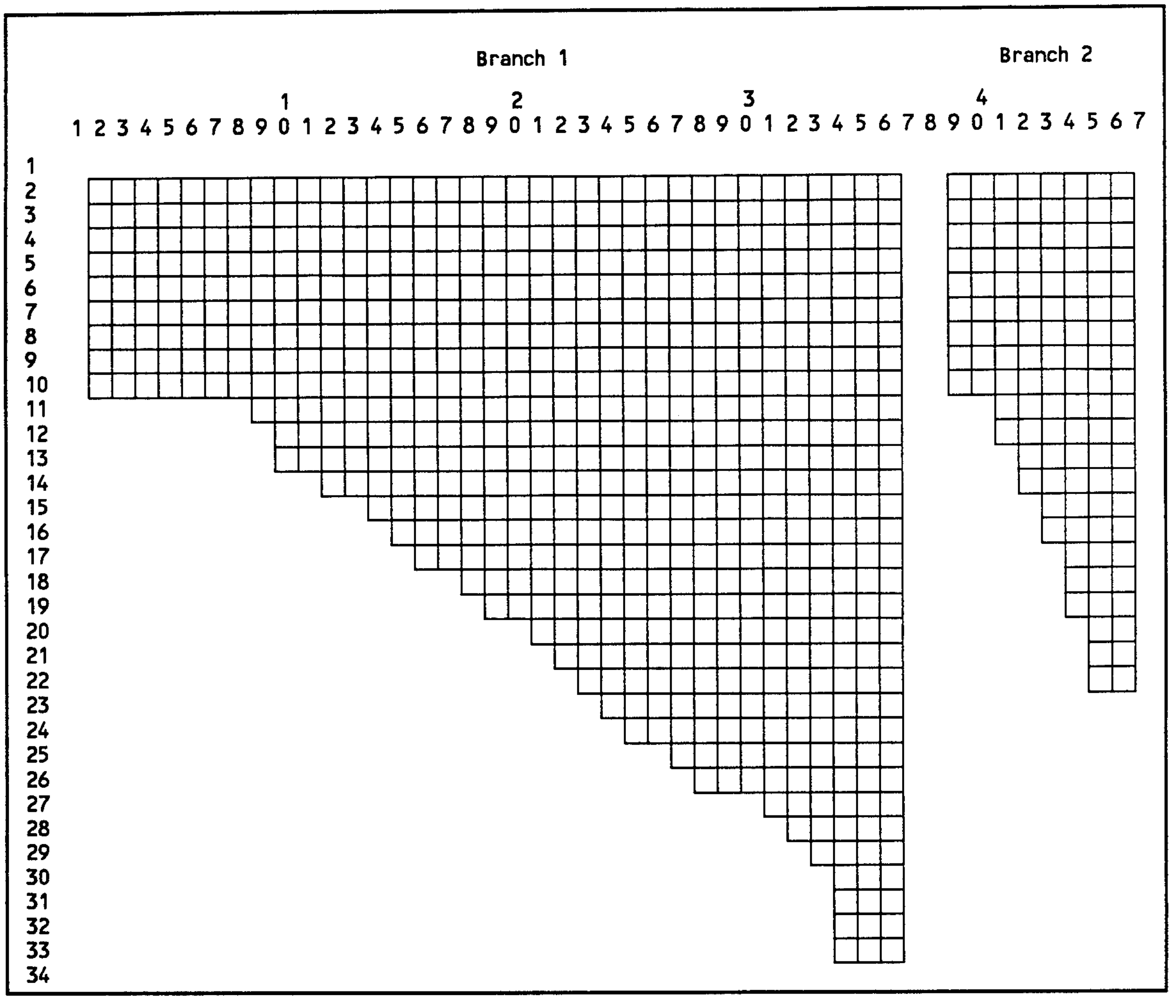

Figure 10. Lake Oahe computational grid

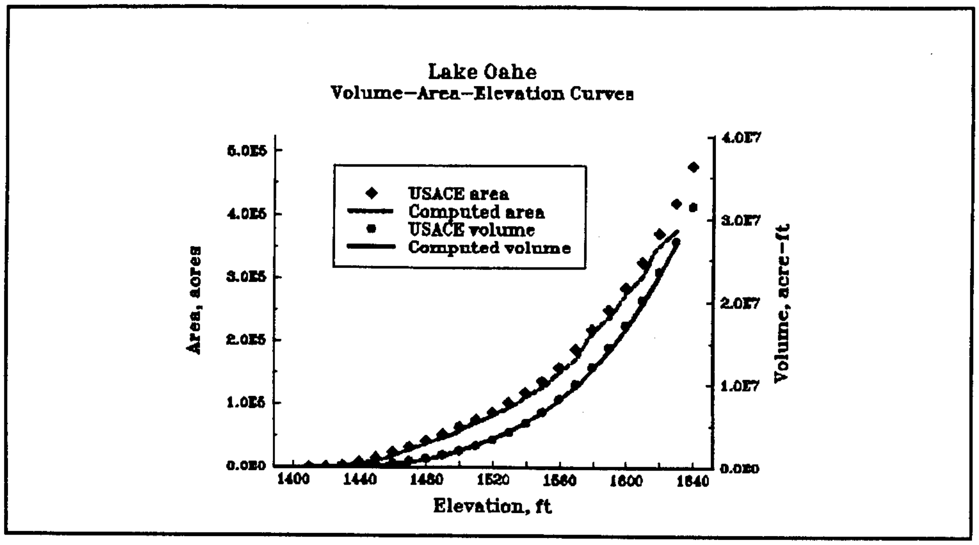

Figure 11. Lake Oahe computed versus USACE volume-area-curves.

Lake Francis Case

The computational grid is shown in Figure 12. The reservoir was discretized into one branch with a total of 45 segments and 25 layers. Cells were 4km long and 2m high. A comparison of computed volume-area-elevation curves and USACE data is given in Figure 13.

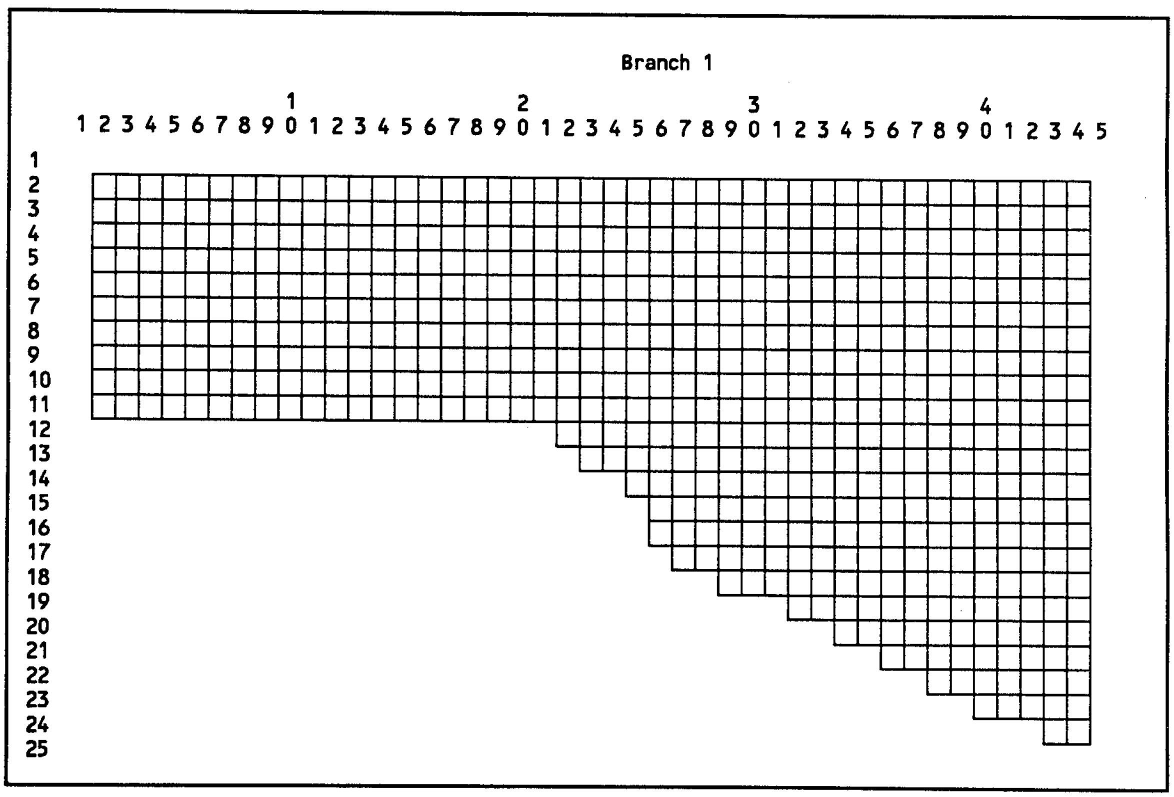

Figure 12. Lake Francis Case computational grid

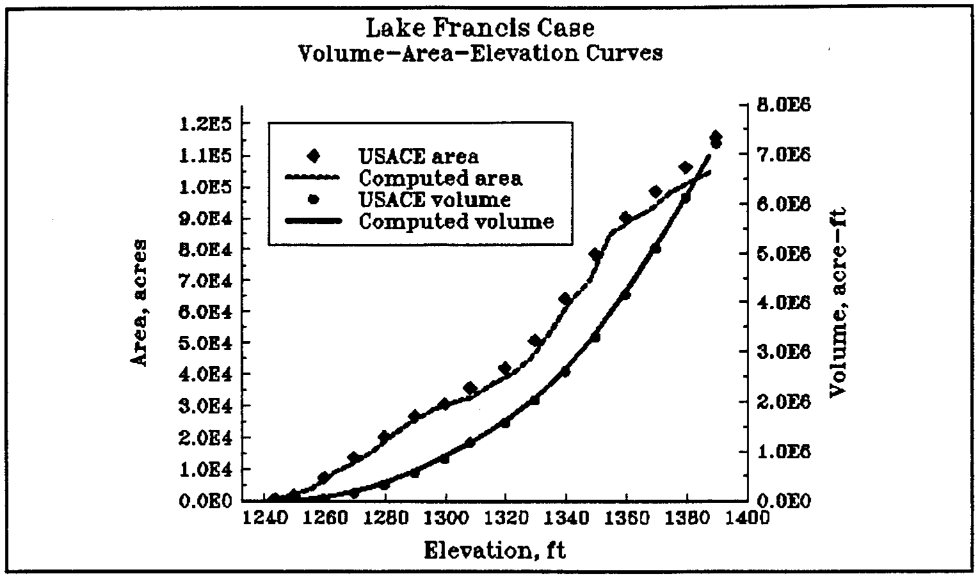

Figure 13. Lake Francis Case computed versus USACE volume-area-elevation curves.

Inflow and Outflow

When determining which years to include for calibration, one of the first considerations is to choose years or conditions that reflect as wide a range of pool elevations, inflow/outflow, and meteorologic conditions as possible. The years 1978 and 1980 had the widest range of inflow/outflow of the years that had sufficient water quality data for calibration. Table 2 summarizes the flows and residence times for each reservoir for 1978 and 1980. Inflows and outflows are shown in Figure 14-Figure 21.

Table 2. Summary of reservoir hydrology for 1978 and 1979

Reservoir	Year	Statistic	Inflow cfs	Outflow cfs	Elevation, ft	Residence Time, years
Fort Peck Lake	1978	Min	2,291	0	2,227.5	2.0
		Max	90,425	15,285	2,250.0	
		Mean	14,971	11,671	2,241.5	
	1980	Min	32	5,789	2,234.6	2.1
		Max	30,283	14,579	2,242.1	
		Mean	8,952	10,463	2,237.8	
Lake Sakakawea	1978	Min	5,189	6,321	1,826.2	0.9
		Max	120,831	39,687	1,849.5	
		Mean	30,474	28,111	1,839.4	
	1980	Min	2,316	16,803	1,833.6	1.1
		Max	44,587	29,703	1,842.1	
		Mean	19,153	22,994	1,838.0	
Lake Oahe	1978	Min	9,473	0	1,594.8	0.9
		Max	58,500	54,306	1,616.2	
		Mean	29,064	29,768	1,608.7	
	1980	Min	5,449	0	1,596.3	0.7
		Max	38,676	54,607	1,608.4	
		Mean	22,282	35,598	1,602.7	
Lake Francis Case	1978	Min	8	801	1,337.8	0.2
		Max	100,033	53,208	1,362.6	
		Mean	31,235	32,453	1,363.7	
	1980	Min	10	6,297	1,338.1	0.2
		Max	69,011	41,689	1,358.7	
		Mean	25,331	25,621	1,360.3	

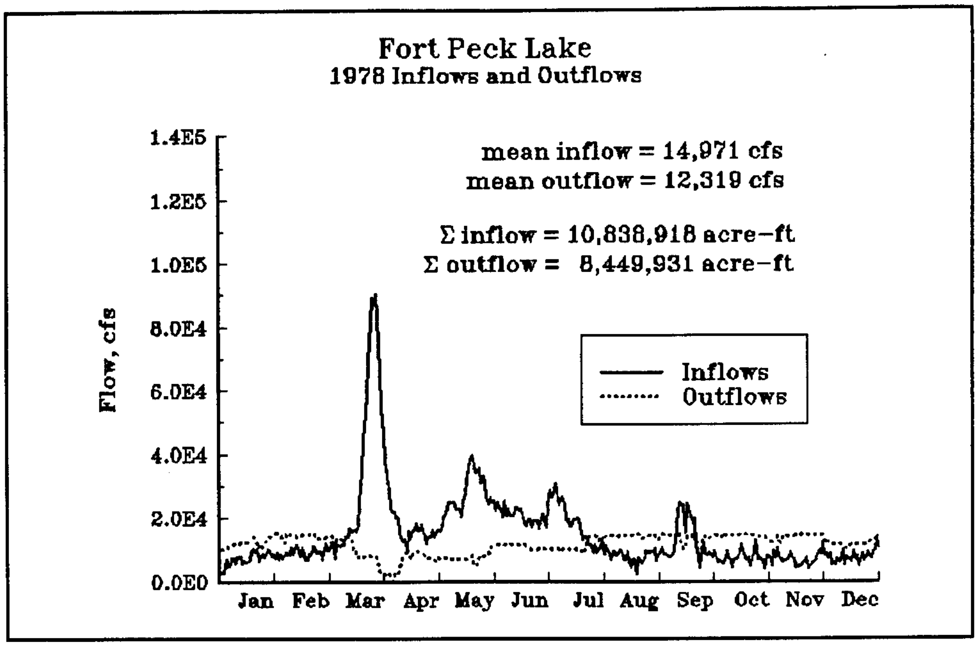

Figure 14. Fort Peck Lake 1978 inflows and outflows

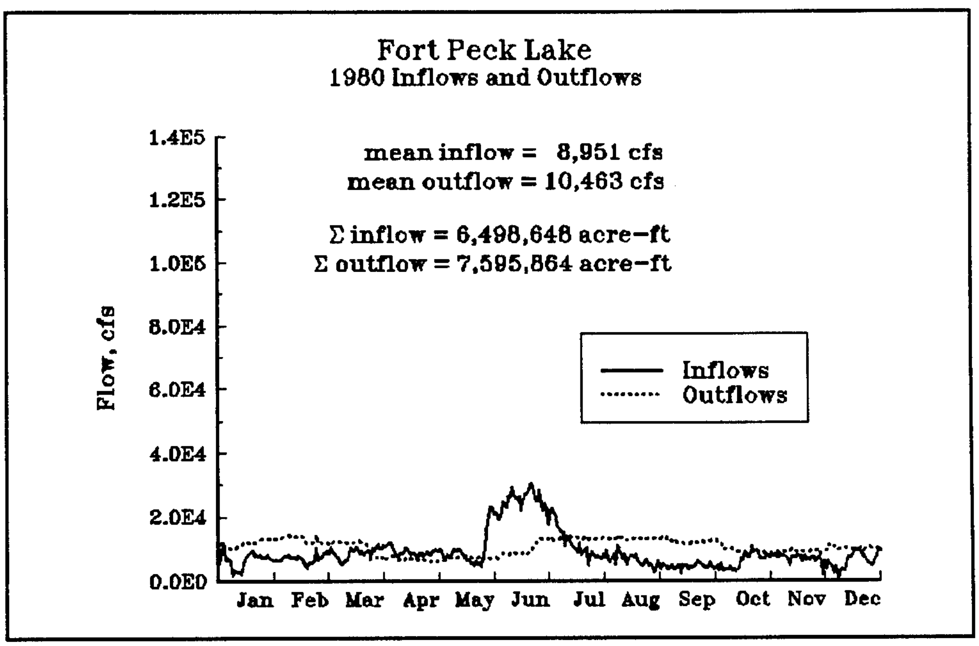

Figure 15. Fort Peck Lake 1980 inflows and outflows

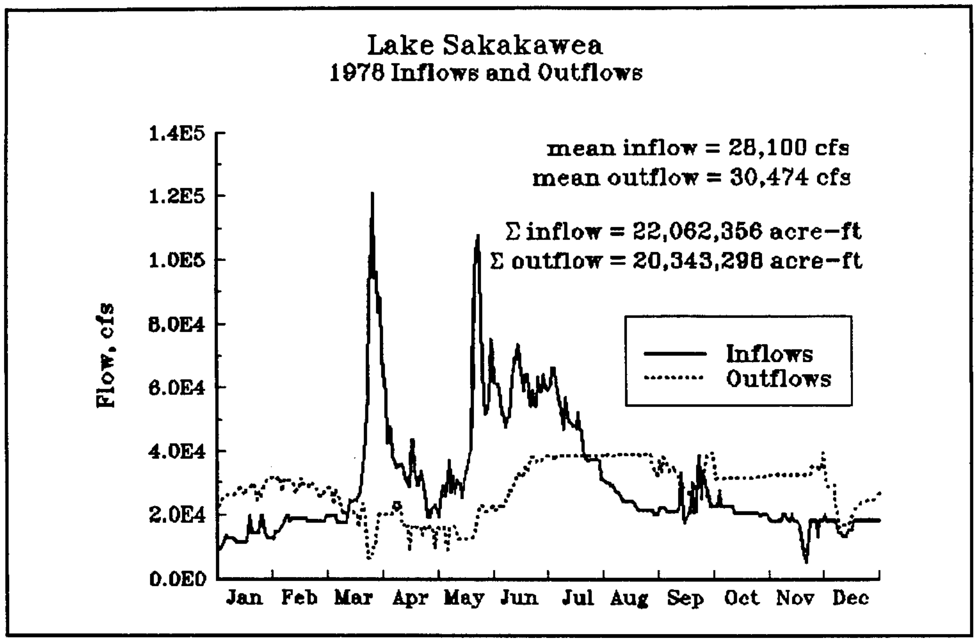

Figure 16. Lake Sakakawea 1978 inflows and outflows

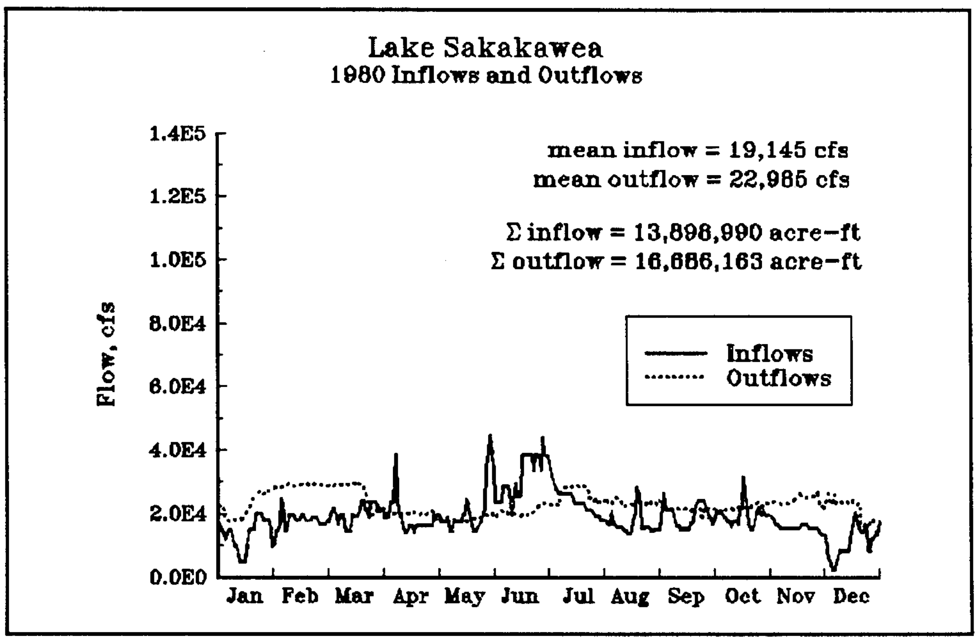

Figure 17. Lake Sakakawea 1980 inflows and outflows

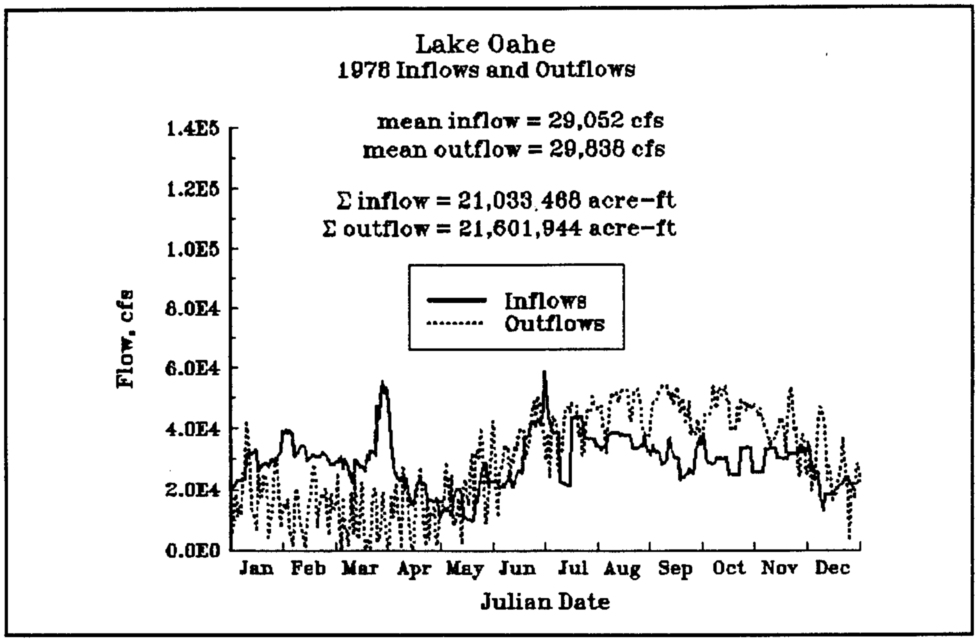

Figure 18. Lake Oahe 1978 inflows and outflows

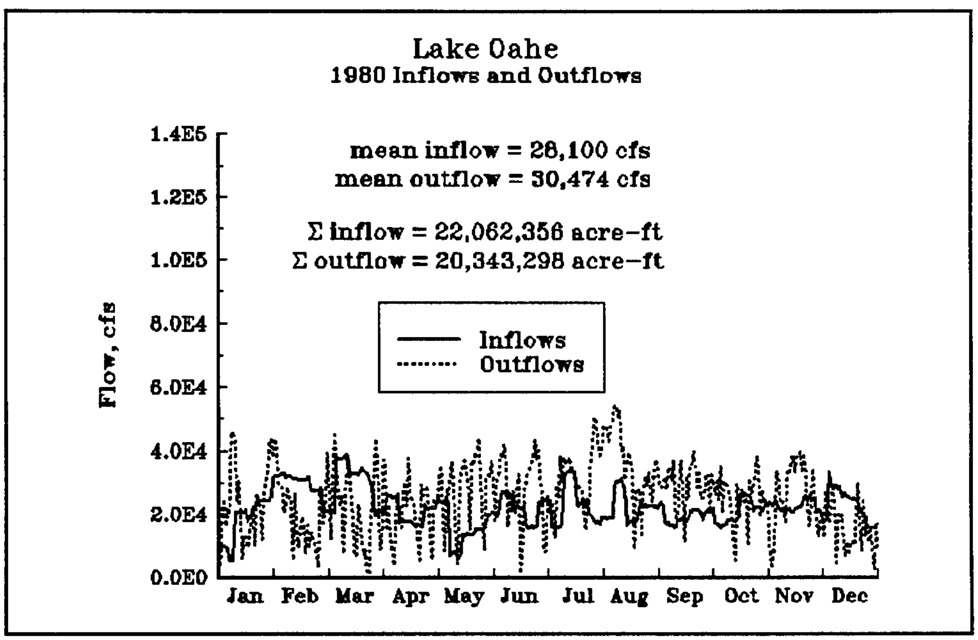

Figure 19. Lake Oahe 1980 inflows and outflows

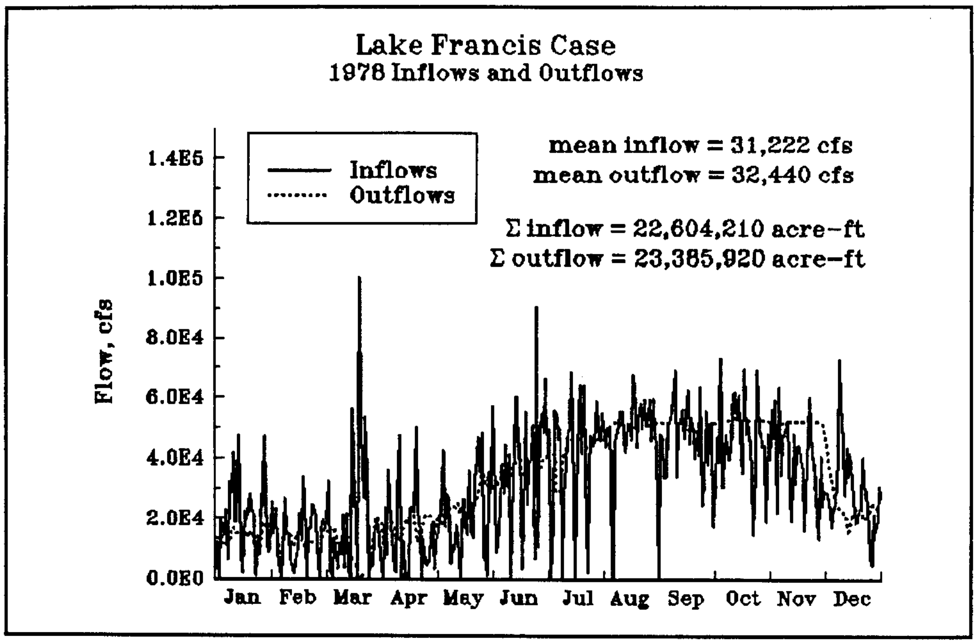

Figure 20. Lake Francis Case 1978 inflows and outflows

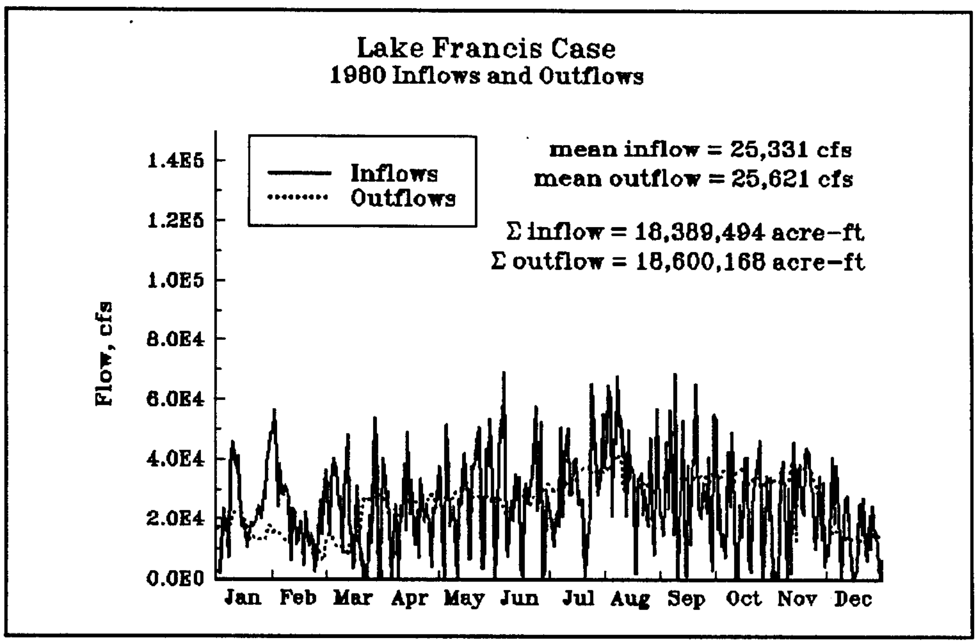

Figure 21. Lake Francis Case 1980 inflows and outflows

Meteorology

CE-QUAL-W2 requires air and dew-point temperature, wind speed and direction, and cloud cover for surface heat exchange and ice-cover computations. Previously, equilibrium temperatures were used in computing heat exchange and ice-cover. The new ice-cover algorithm employs a term-by-term solution in which the individual components of surface heat exchange are computed from the same meteorologic variables used previously in the equilibrium temperature computations. Hourly values for all meteorologic variables were obtained from first-order weather stations located in Glasgow, MT, Williston, ND, and Pierre, SD. Meteorologic inputs are shown in Figure 22-Figure 39.

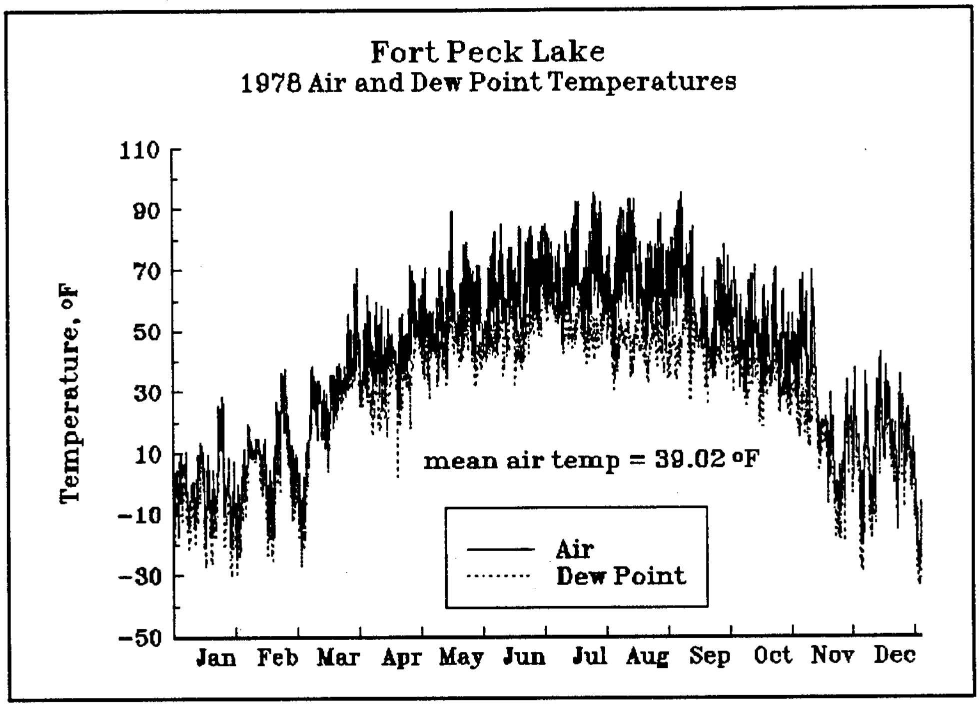

Figure 22. Fort Peck Lake 1978 air/dew-point temperatures from Glasgow, MT

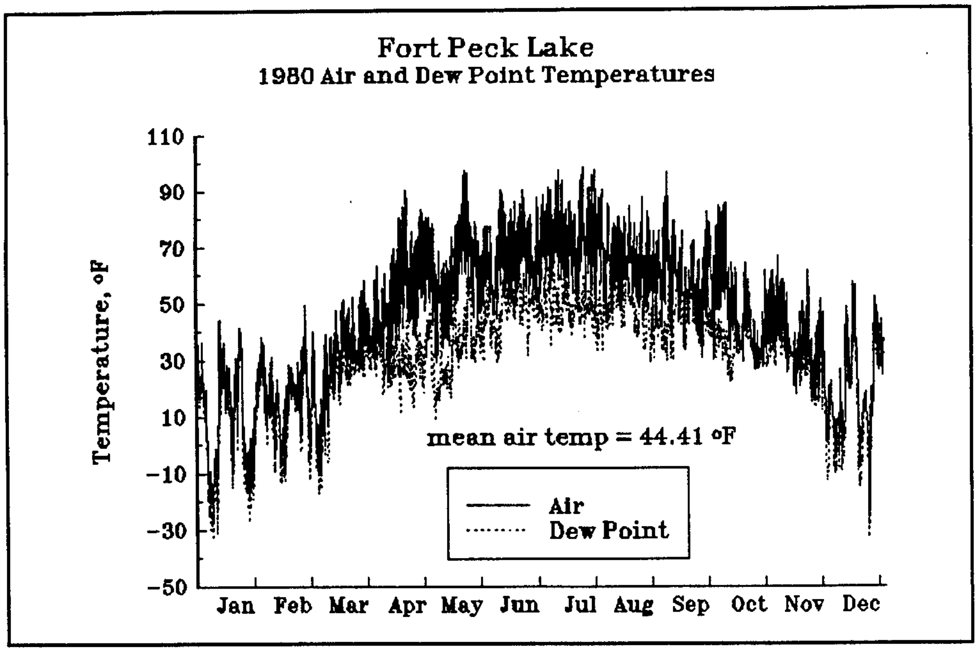

Figure 23. Fort Peck Lake 1980 air/dew-point temperatures for Glasgow, MT

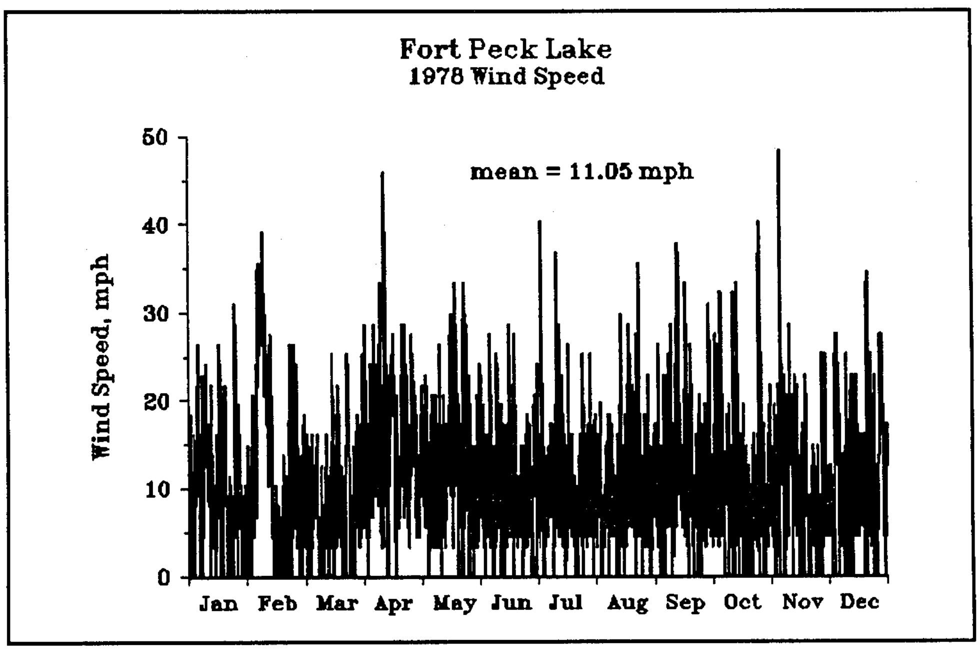

Figure 24. Fort Peck Lake 1978 wind speeds from Glasgow, MT

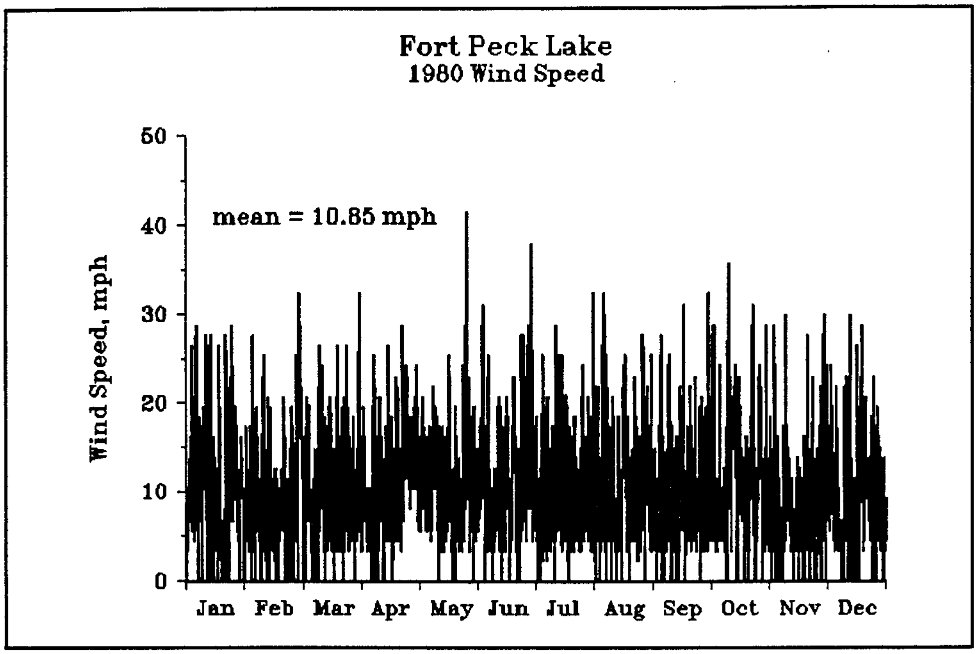

Figure 25. Fort Peck Lake 1980 wind speeds from Glasgow, MT

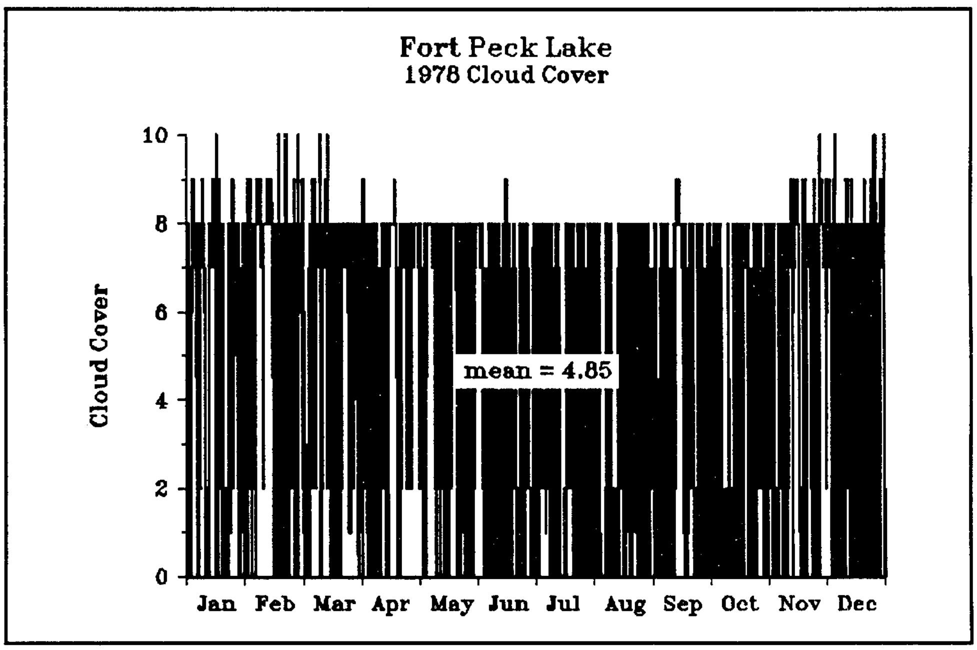

Figure 26. Fort Peck Lake 1978 cloud cover from Glasgow, MT

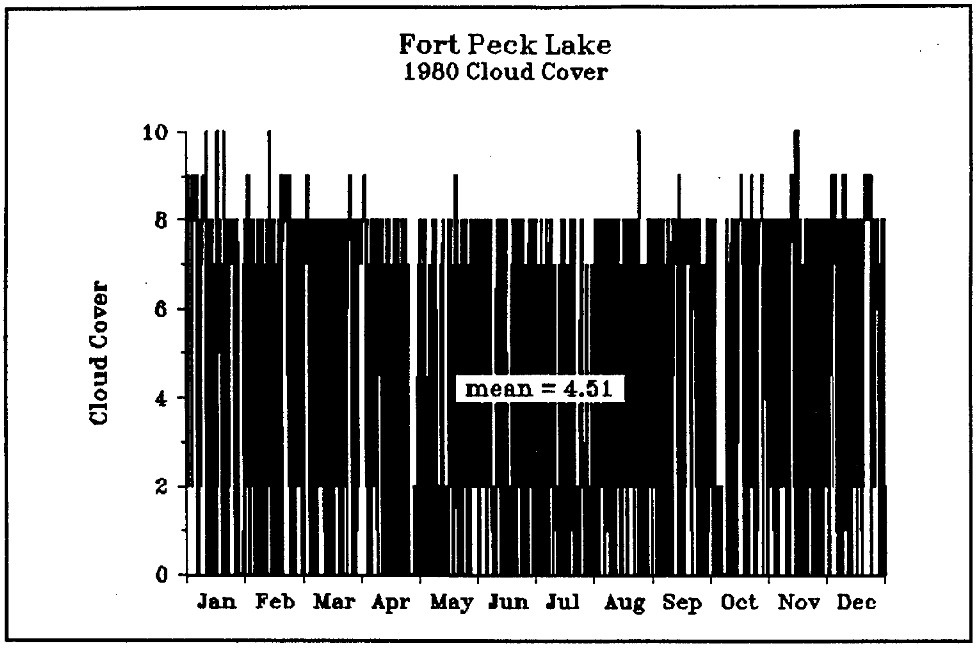

Figure 27. Fort Peck Lake 1980 cloud cover from Glasgow, MT

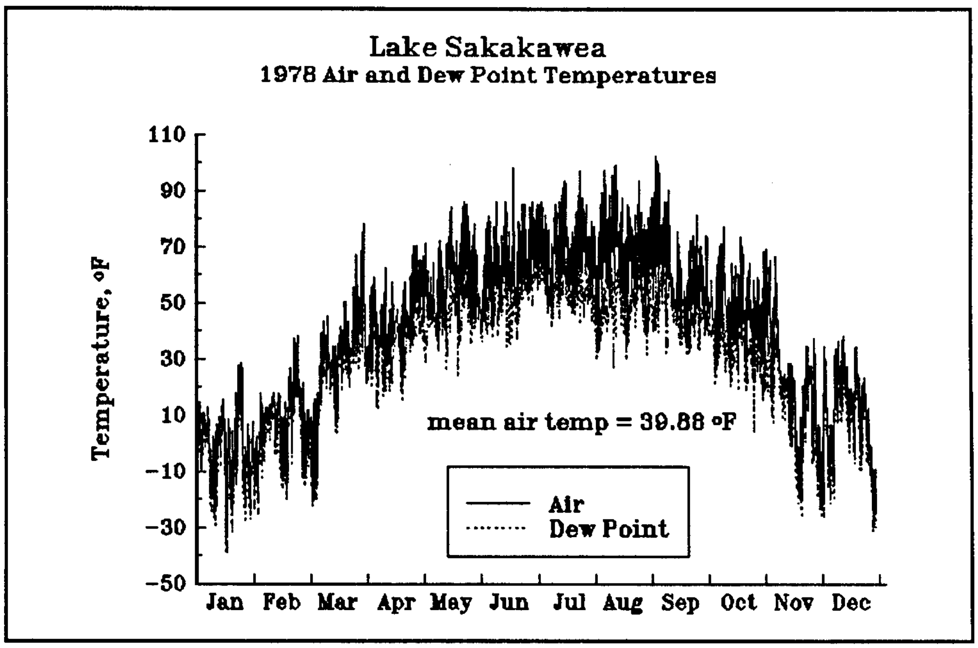

Figure 28. Lake Sakakawea 1978 air/dew-point temperatures from Williston, ND

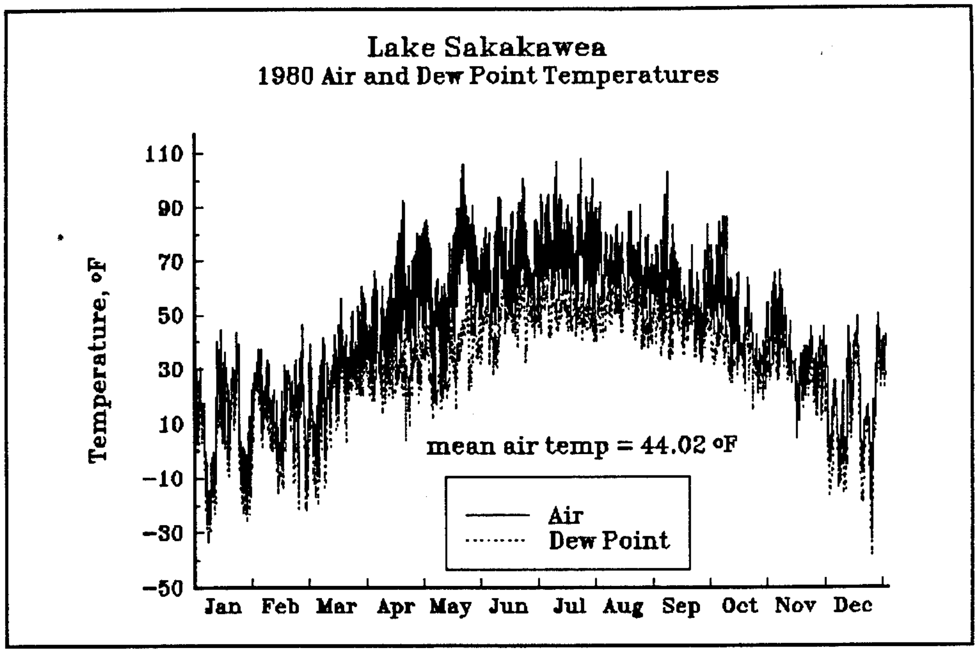

Figure 29. Lake Sakakawea 1980 air/dew-point temperatures for Williston, ND

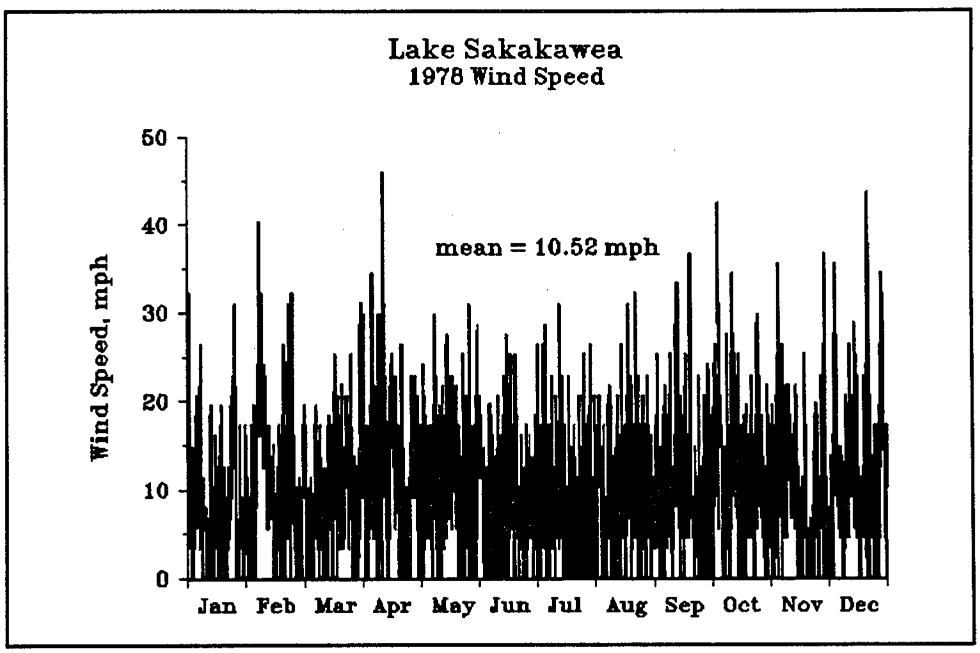

Figure 30. Lake Sakakawea 1978 wind speeds from Williston, ND

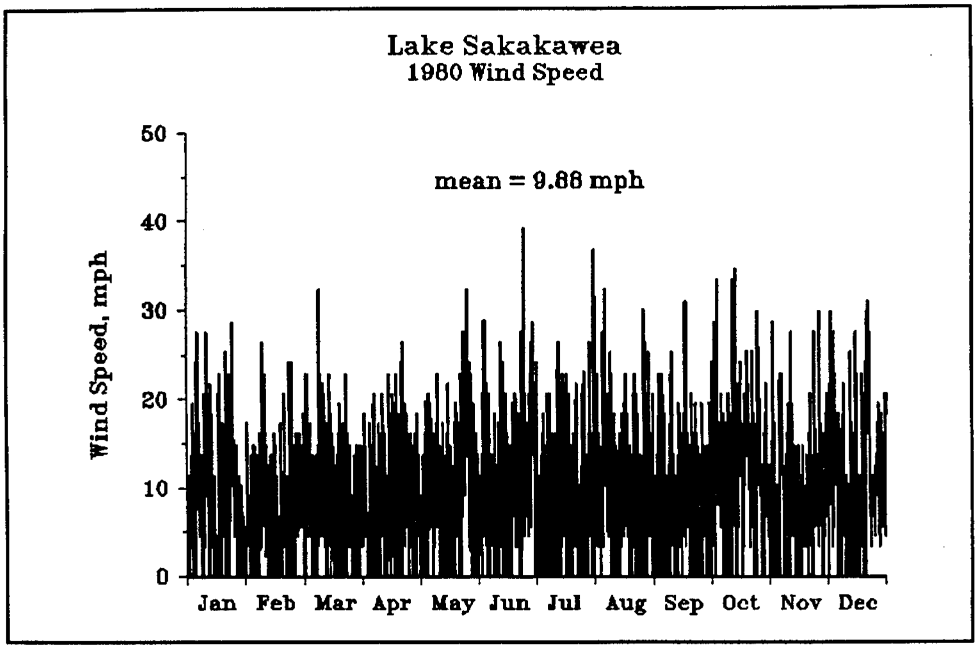

Figure 31. Lake Sakakawea 1980 wind speeds from Williston, ND

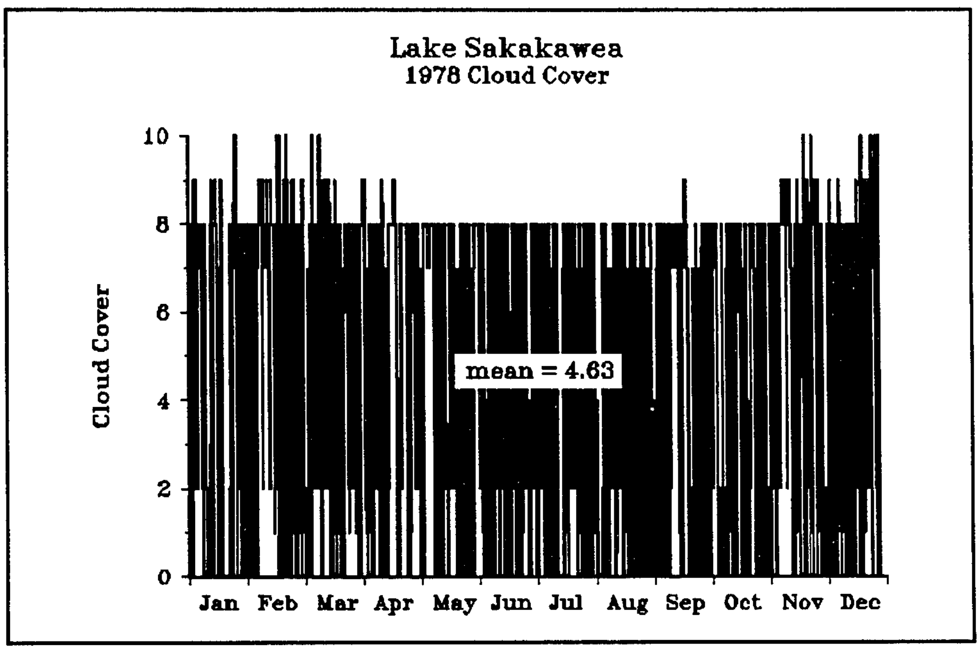

Figure 32. Lake Sakakawea 1978 cloud cover from Williston, ND

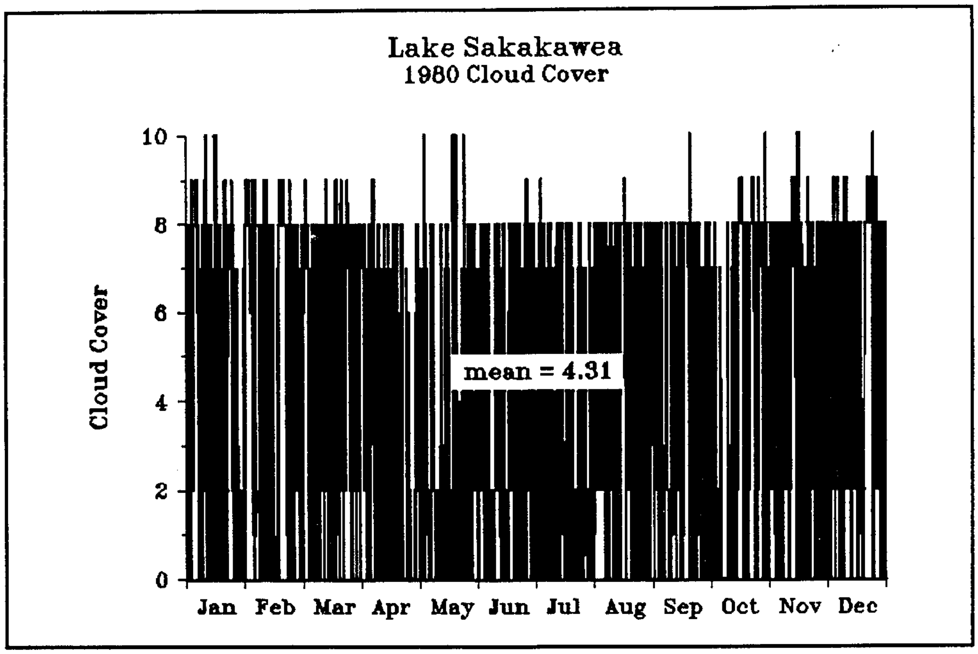

Figure 33. Lake Sakakawea 1980 cloud cover from Williston, ND

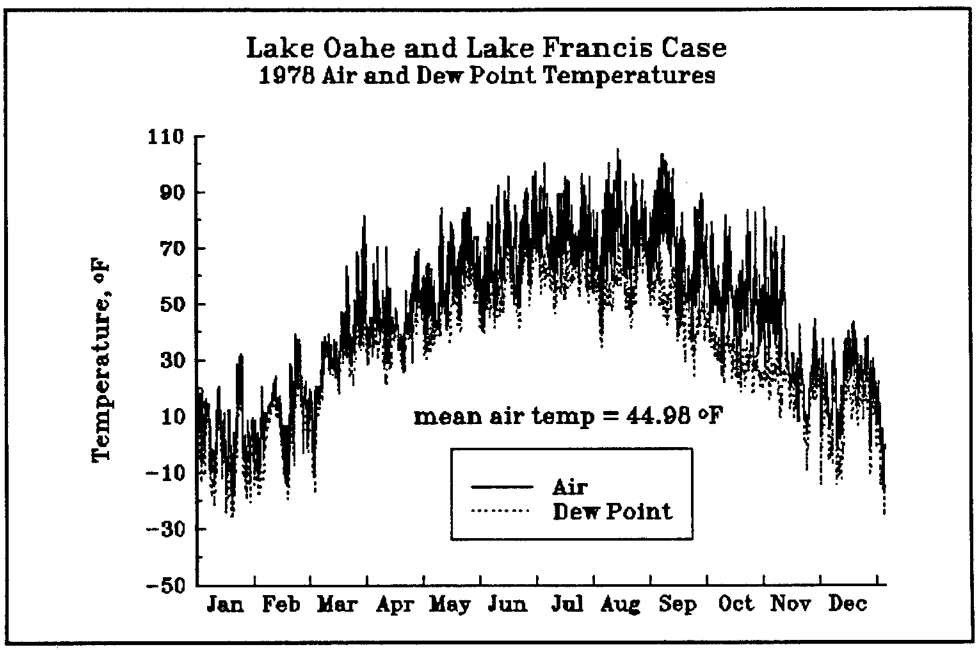

Figure 34. Lake Oahe and Lake Francis Case 1978 air/dew-point temperatures from Pierre, SD

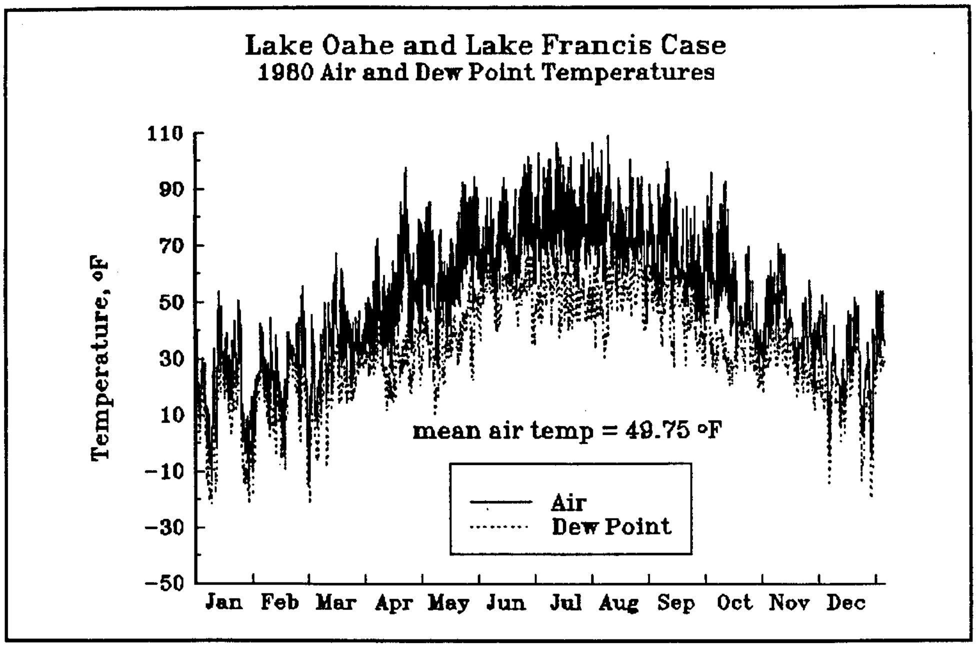

Figure 35. Lake Oahe and Lake Francis Case 1980 air/dew-point temperatures from Pierre, SD

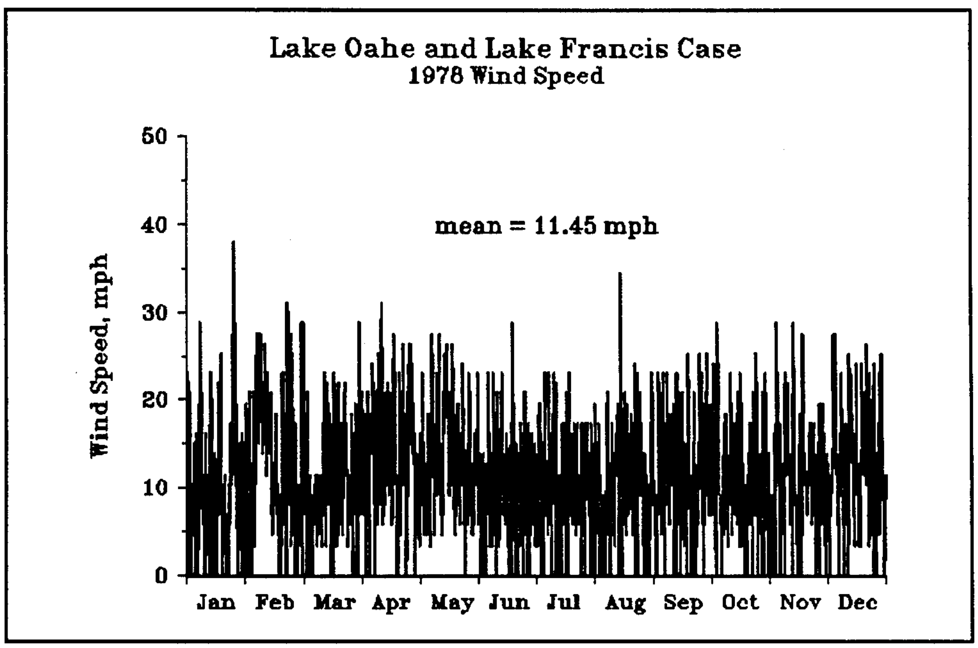

Figure 36. Lake Oahe and Lake Francis Case 1978 wind speeds from Pierre, SD

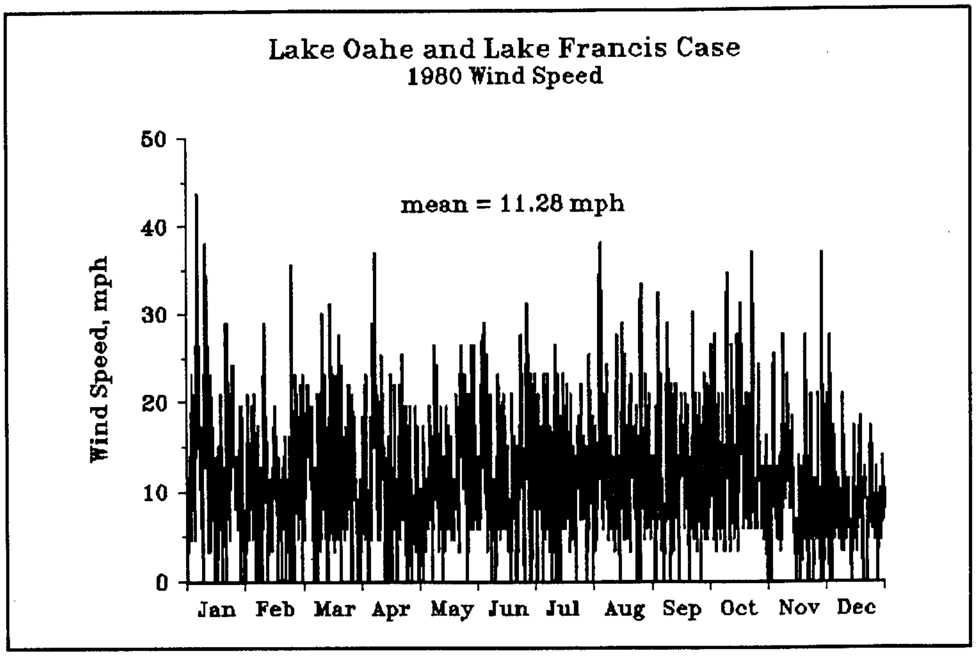

Figure 37. Lake Oahe and Lake Francis Case 1980 wind speeds from Pierre, SD

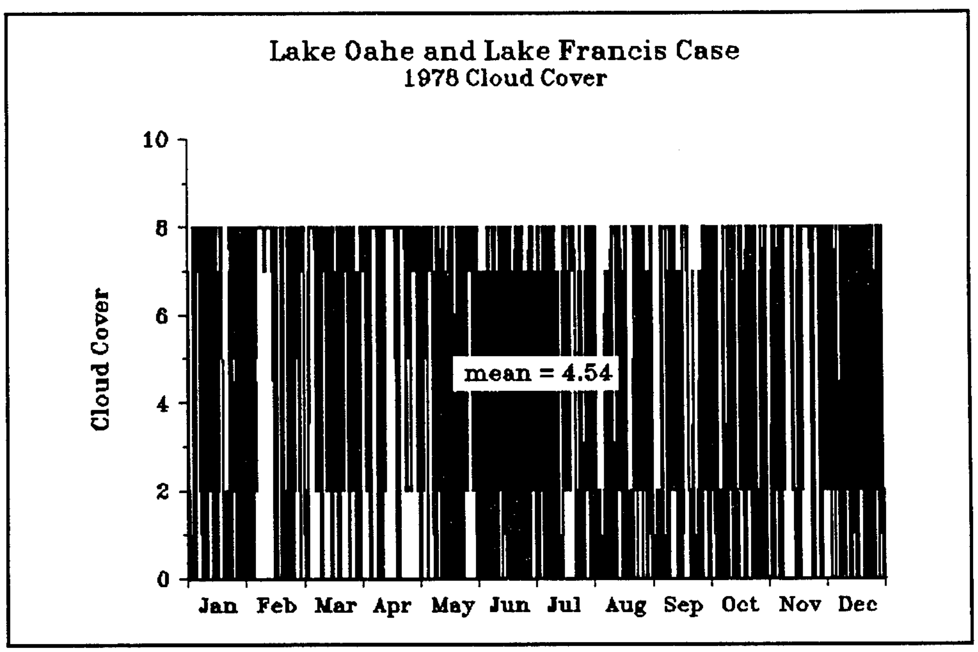

Figure 38. Lake Oahe and Lake Francis Case 1978 cloud cover from Pierre, SD

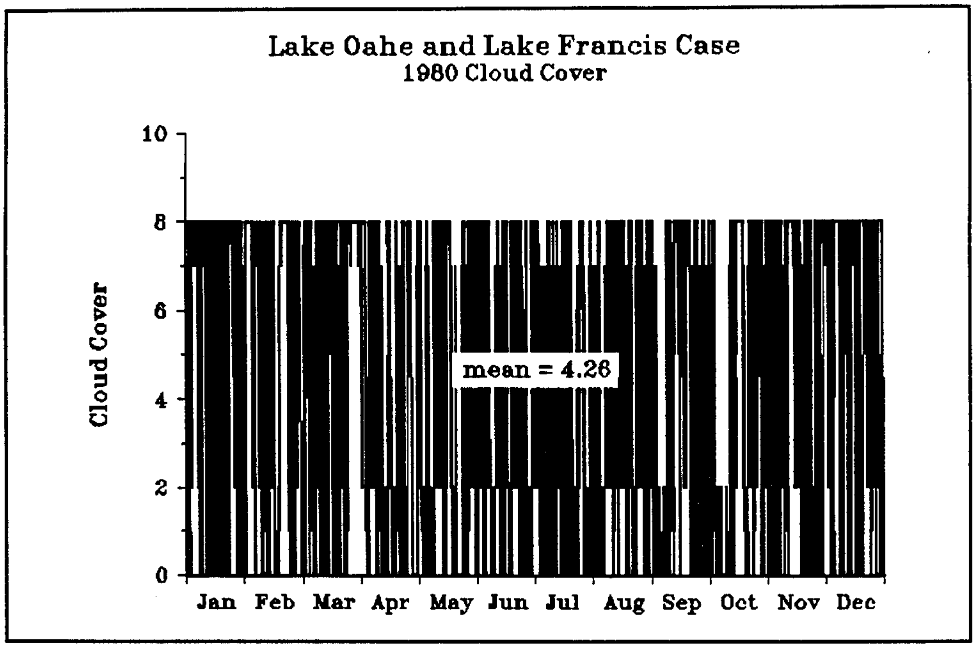

Figure 39. Lake Oahe and Lake Francis Case 1980 cloud cover from Pierre, SD

Inflow Temperatures

Daily inflow temperatures were determined from regressions relating observed inflow temperatures to equilibrium temperatures. These values were used during the initial calibration of the reservoirs. However, since the scenarios would require linking the reservoirs in series with release temperatures routed downstream and used as inflow boundary conditions to the lower reservoir, this same method was used to obtain inflow temperatures for the lower three reservoirs during final calibration. The original regressed inflow temperatures were used for Fort Peck Lake.

Daily average values were used for routing inflow temperatures. Equation (1) was used to route the temperatures.

$$T_r = T_e + (T_o - T_e)e^{\left(\frac{-K_h}{h}\right)t} \tag{1}$$

where

T_r = routed inflow temperature
T_e = average daily equilibrium temperature
T_o = upstream release temperature
K_h = coefficient of surface heat exchange
h = average river depth over the reach
t = travel time from upstream dam

Inflow temperatures are shown in Figure 40-Figure 47.

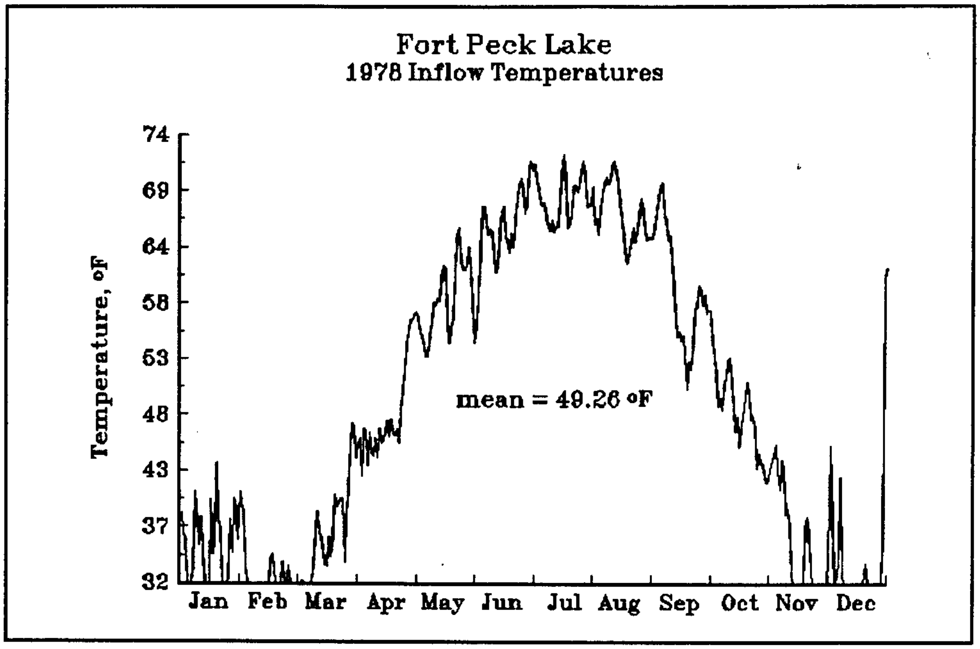

Figure 40. Fort Peck Lake 1978 regressed inflow temperatures

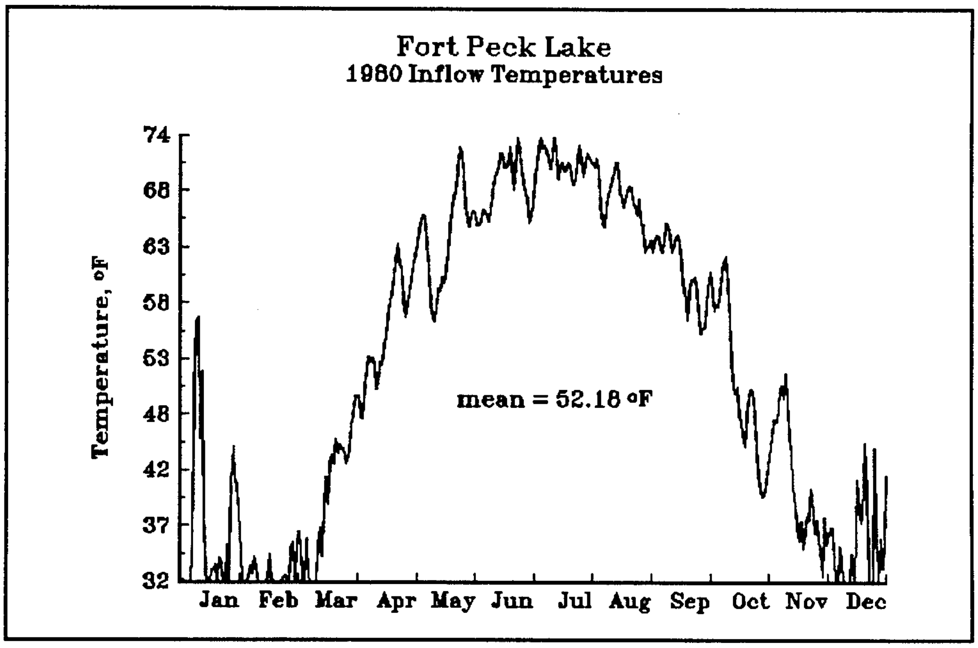

Figure 41. Fort Peck Lake 1980 regressed inflow temperatures

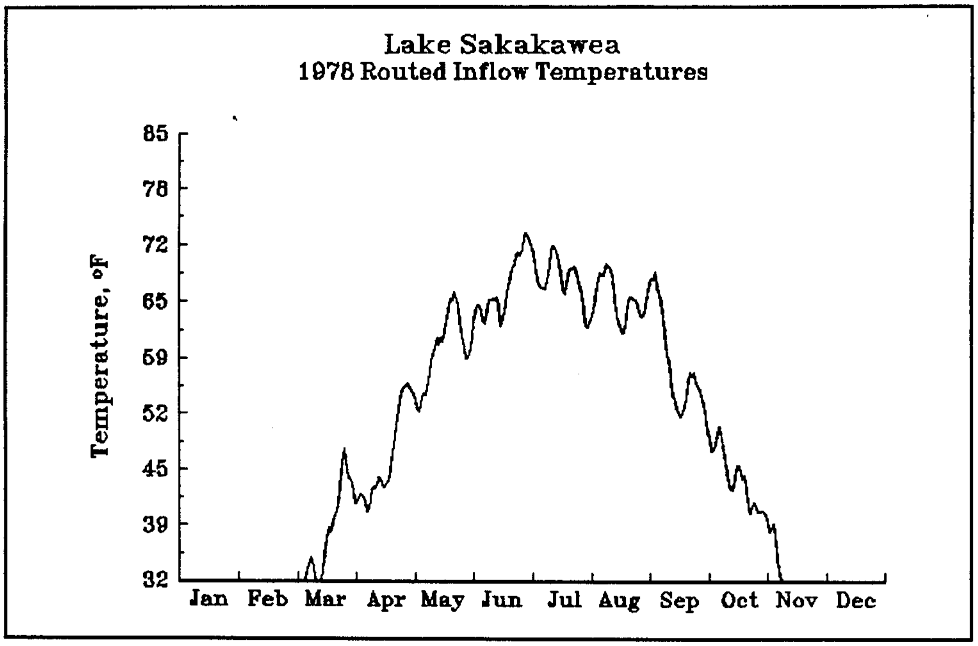

Figure 42. Lake Sakakawea 1978 routed inflow temperatures

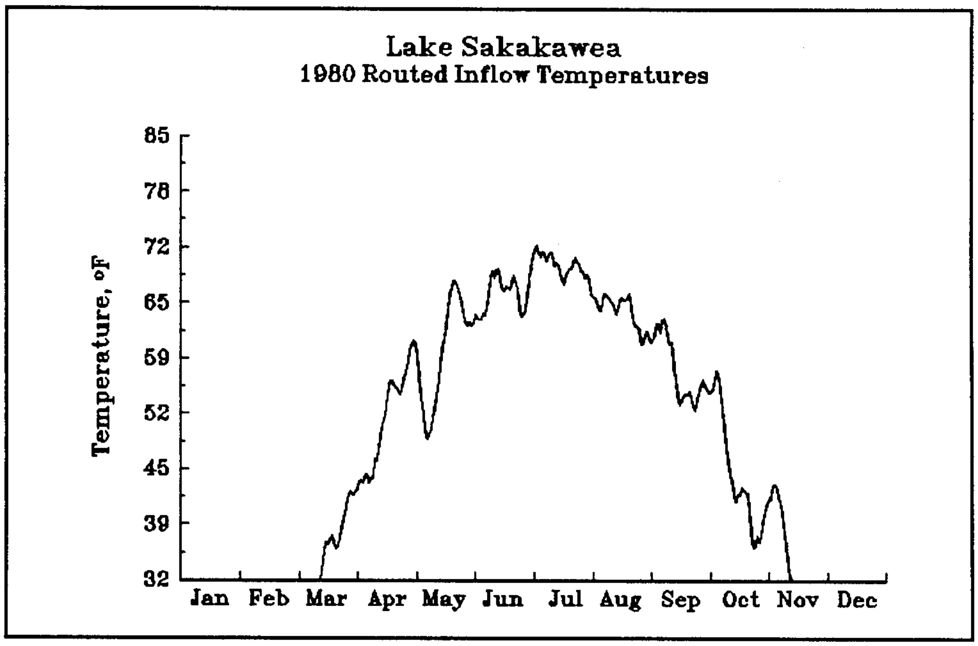

Figure 43. Lake Sakakawea 1980 routed inflow temperatures

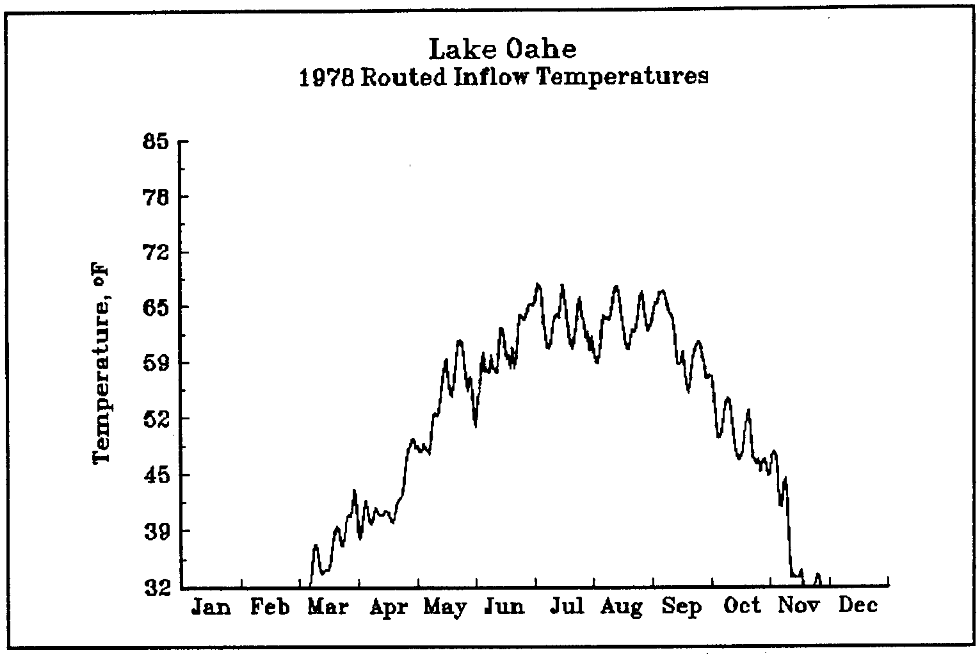

Figure 44. Lake Oahe 1978 routed inflow temperatures

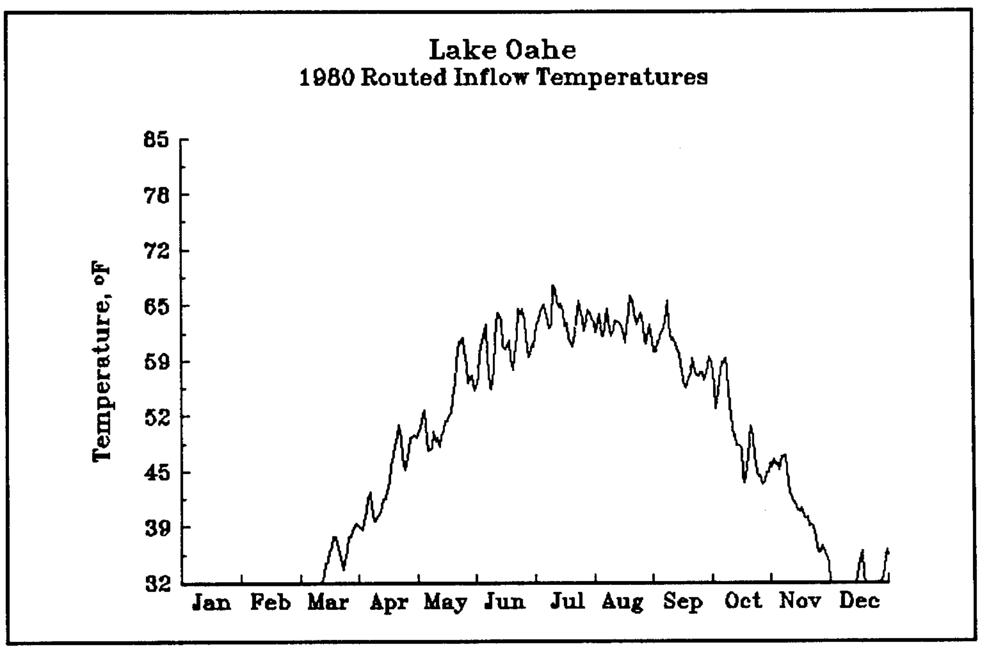

Figure 45. Lake Oahe 1980 routed inflow temperatures

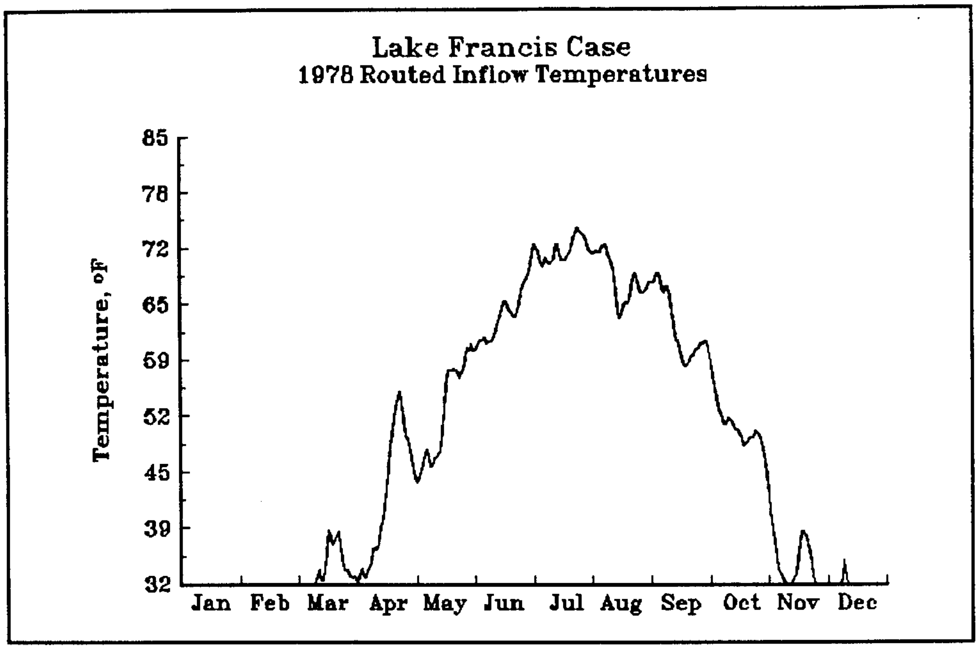

Figure 46. Lake Francis Case 1978 routed inflow temperatures

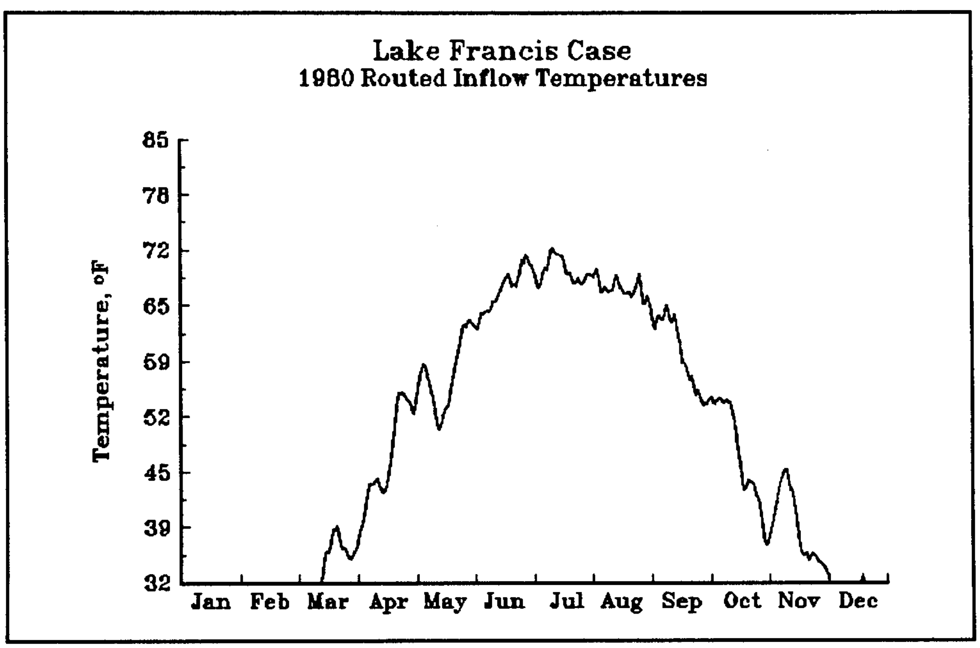

Figure 47. Lake Francis Case 1980 routed inflow temperatures

Inflow DO

Data were not available for inflow DO for the calibration years. The assumption was made that all inflow DO concentrations were saturated. Saturated DO concentrations were calculated from equation (2) in the same routing program used in determining inflow temperatures:

$$DO = e^{7.7117-1.314*[\ln(T_r+45.93)]}\left[1-\frac{E_i}{44.3}\right]^{5.25} \tag{2}$$

where

DO = dissolved oxygen concentration, mg l^{-1}
T_r = routed temperature, °C
E_i = elevation at the inflow, m

Inflow DO is shown in Figure 48-Figure 55.

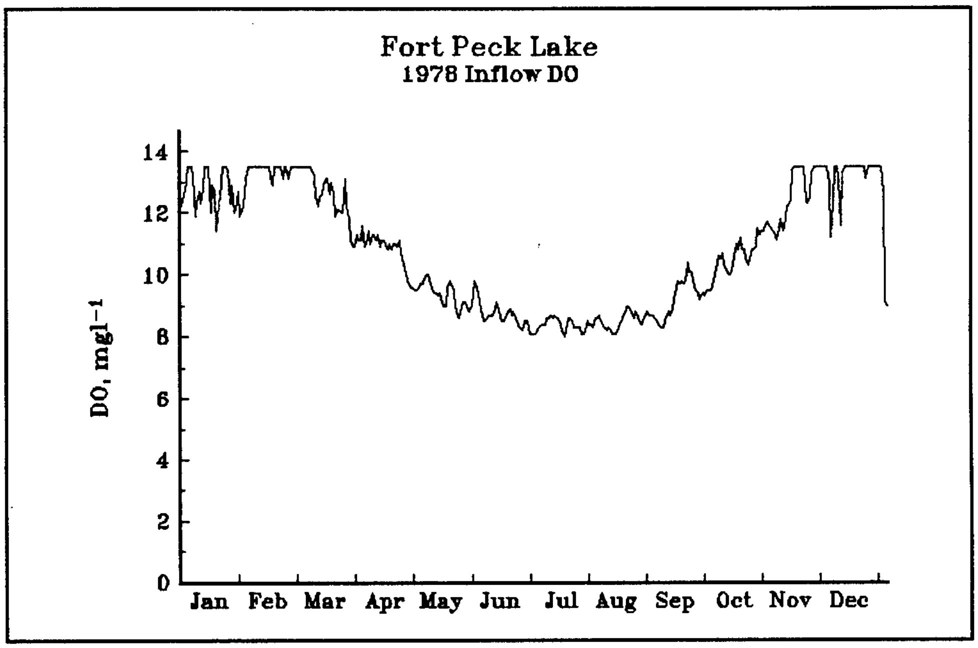

Figure 48. Fort Peck Lake 1978 inflow DO

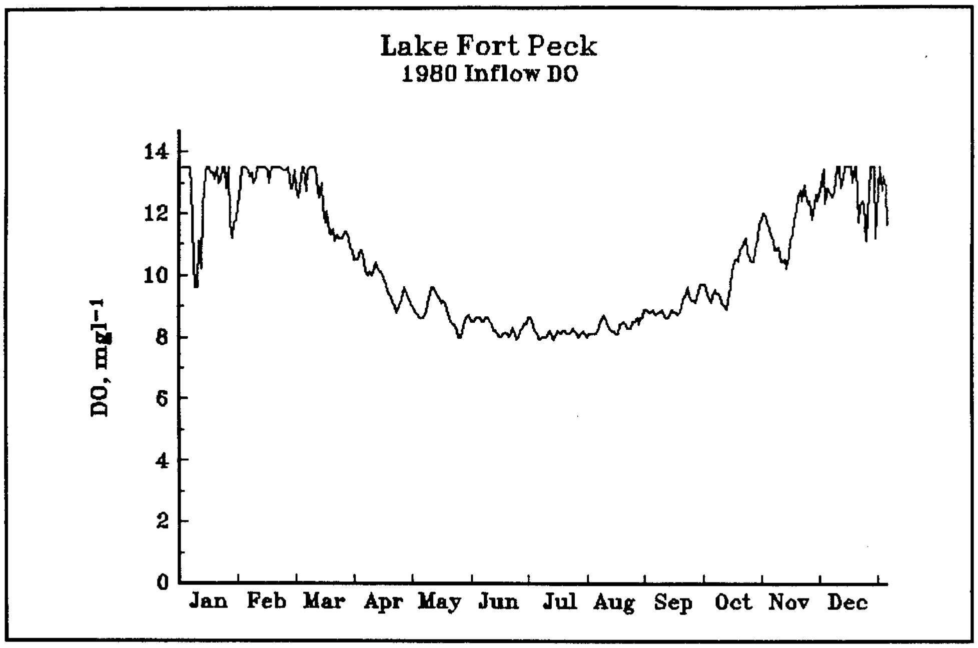

Figure 49. Fort Peck Oahe 1980 inflow DO

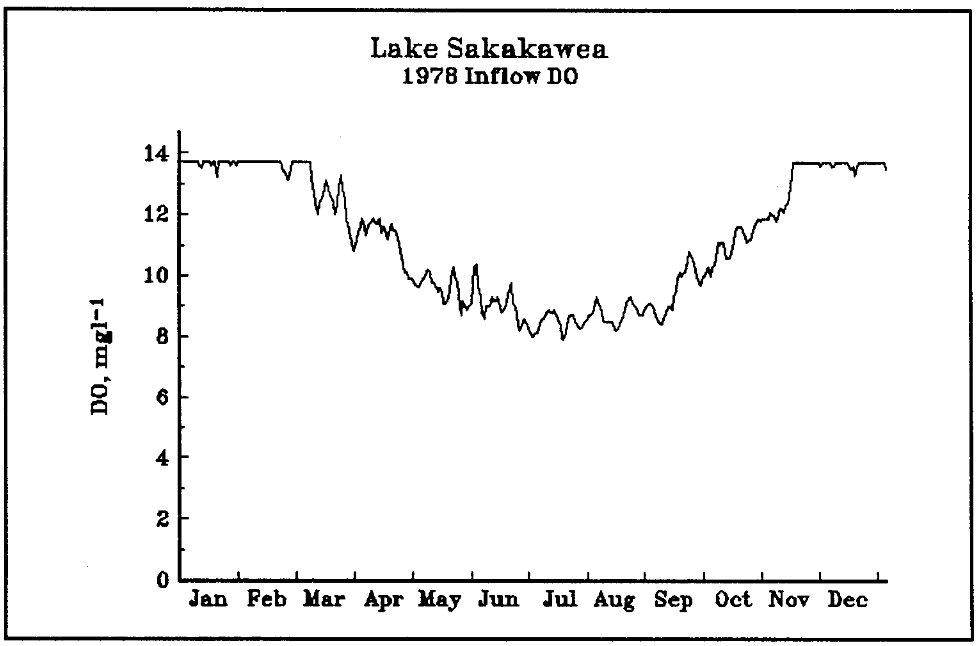

Figure 50. Lake Sakakawea 1978 inflow DO

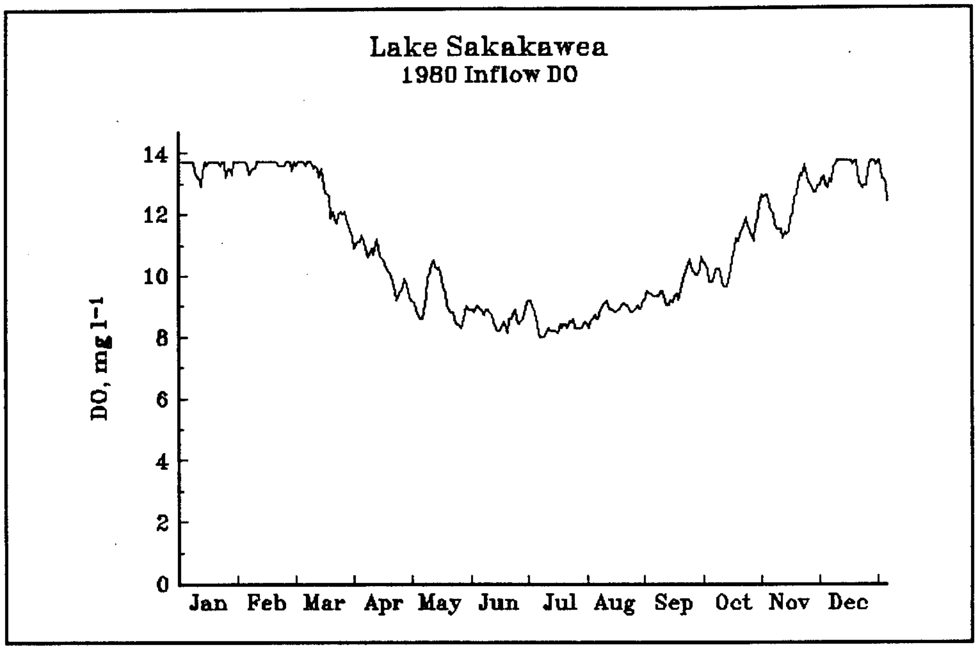

Figure 51. Lake Sakakawea 1980 inflow DO

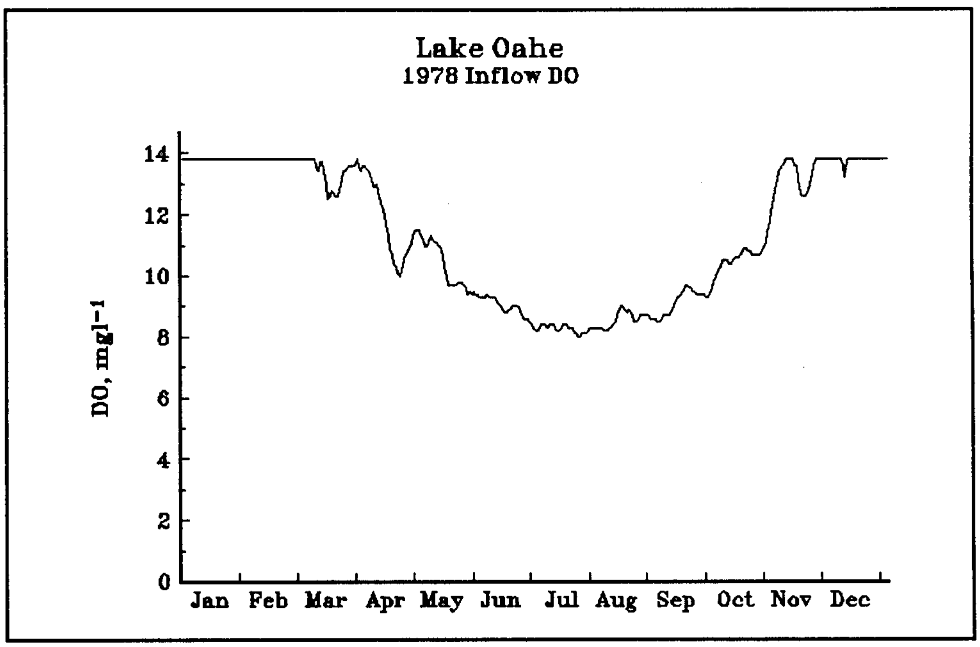

Figure 52. Lake Oahe 1978 inflow DO

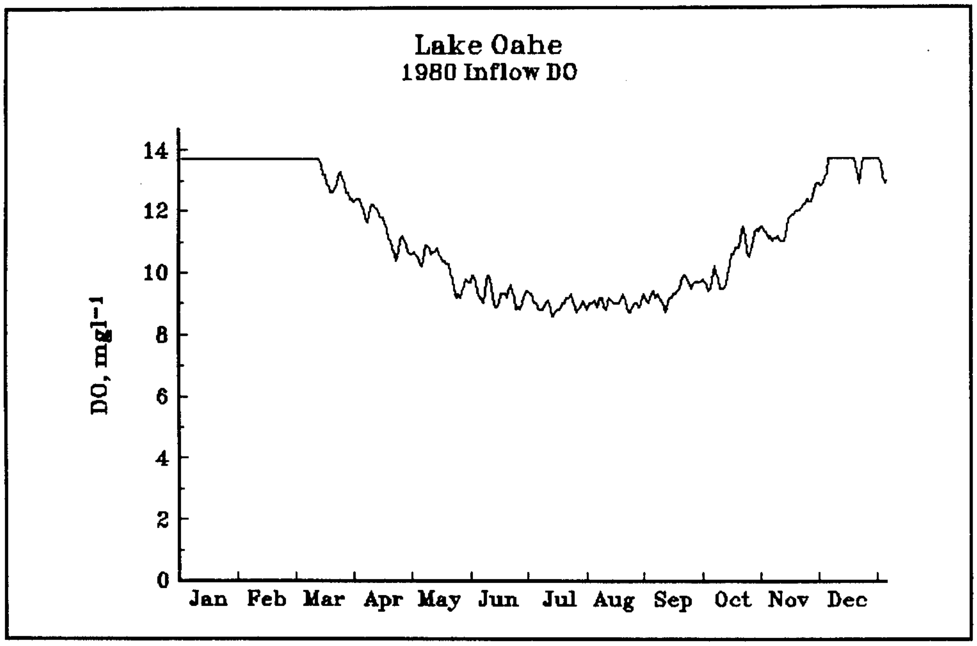

Figure 53. Lake Oahe 1980 inflow DO

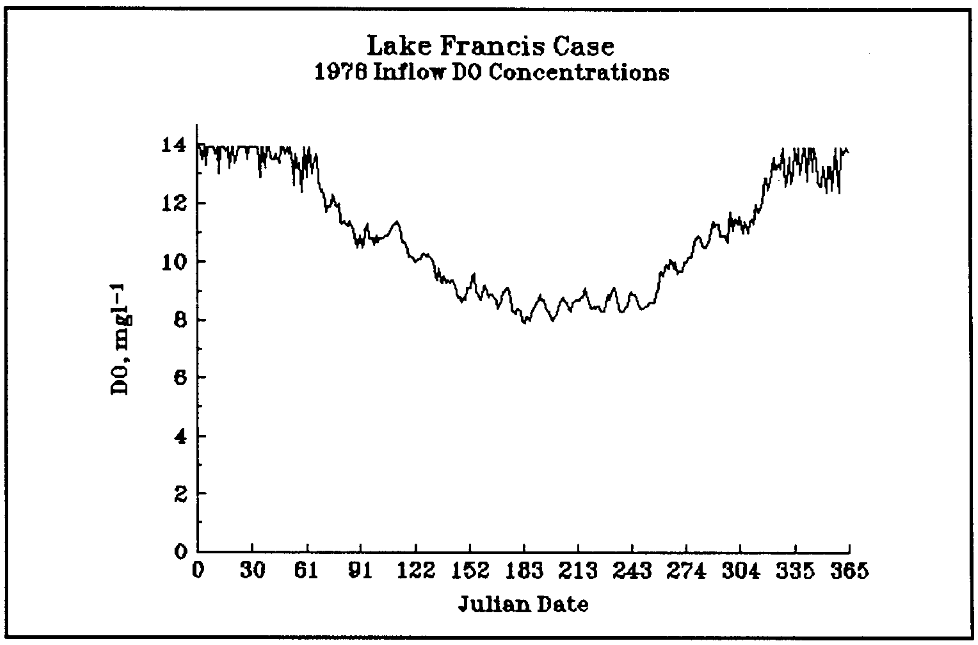

Figure 54. Lake Francis Case 1978 inflow DO

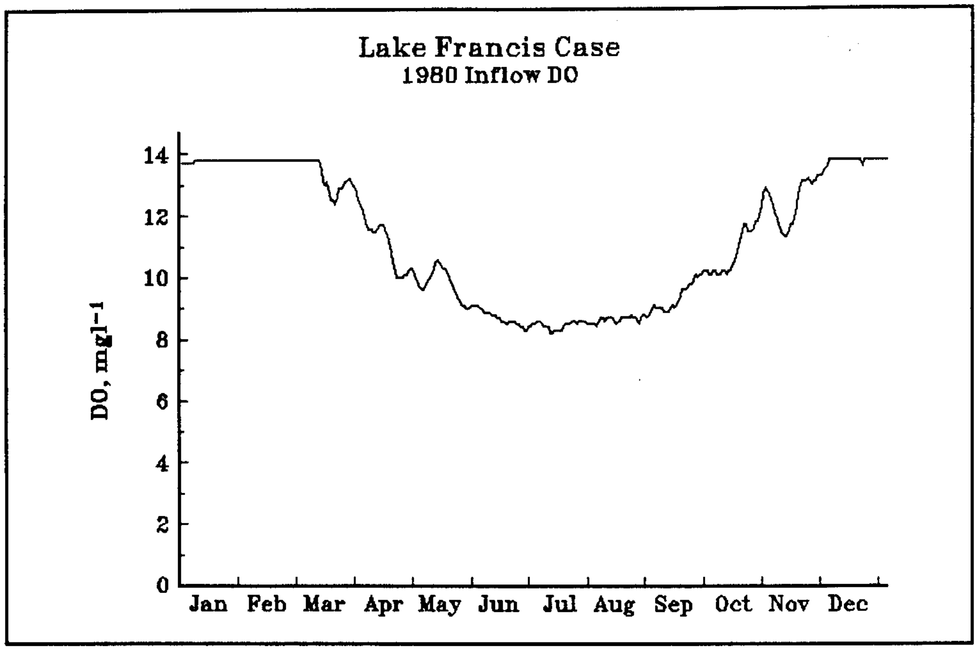

Figure 55. Lake Francis Case 1980 inflow DO

3 Calibration

Fort Peck Lake 1978 Simulation

Water Surface Elevations

Computed and observed 1978 water surface elevations are shown in Figure 56. The net increase in storage was 12.7 ft with elevations ranging from 2,227.7 ft to 2,249.6 ft. Differences in computed and observed stages were less than 0.5 ft throughout the year.

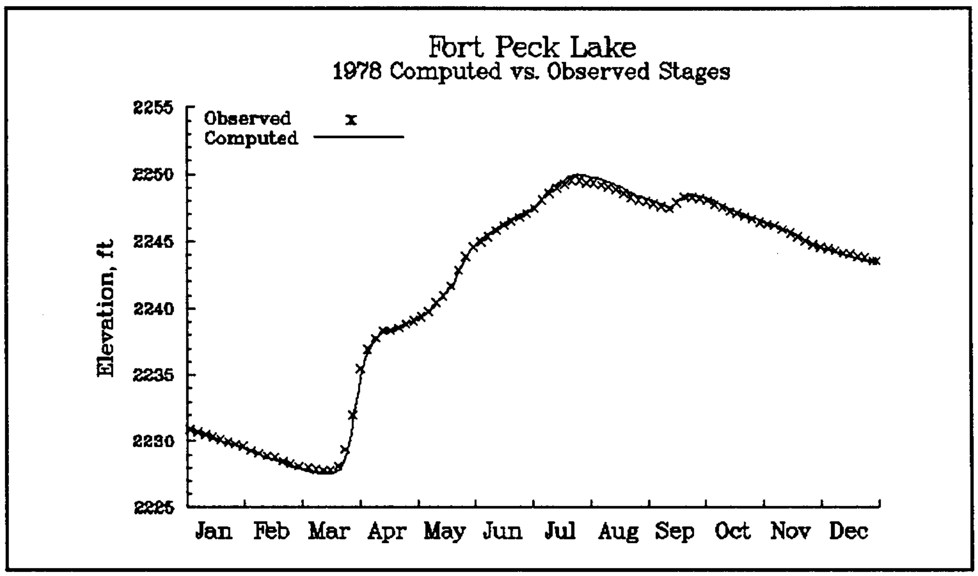

Figure 56. Fort Peck Lake 1978 computed versus observed water surface elevations at dam.

Ice Cover

Computed ice cover is shown in Figure 57. Ice-out was predicted on April 17. Reported ice-out occurred on April 18. Reported ice-in occurred on January 14, 1979. No ice-in date was available from the 1978 simulation since the run did not continue into 1979.

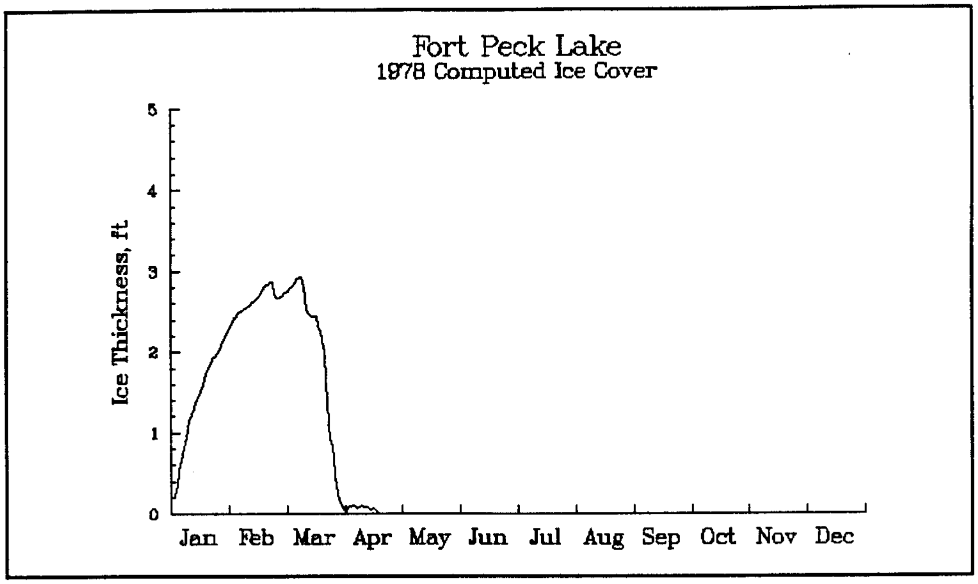

Figure 57. Fort Peck Lake 1978 computed ice cover

Temperature

There are several important points to keep in mind when interpreting temperature predictions from CE-QUAL-W2. First, temperature predictions are averaged over the length, height, and width of a cell. Observed data represent temperature at a specific point in space. Also, predictions for all stations were output at 12 noon that may or may not be the same time of day at which measurements were taken since there was no record of when observed measurements were taken during the day. Also, meteorologic data from one station is applied to the entire reservoir. These caveats are most evident in discrepancies between predicted and observed epilimnetic temperatures when observed data may be taken early in the morning or late in the afternoon or when a weather front has moved through the reservoir at a different time than at the meteorologic station.

Table 3 shows the values of all coefficients that affect temperature and ice computations. Although nearly all values were varied during the calibration, all values were set back to their default values for the final calibration. Also, all values were the same for the four reservoirs. Temperature predictions were most sensitive to changes in the wind sheltering coefficient.

Station Near Dam. Observed and computed temperature profiles are shown in Figure 58 and Figure 59. Computed and observed profiles were generally in close agreement until July 21 when the model predicted lower hypolimnetic temperatures than observed. The August 3 profile showed similar discrepancies. However, by August 21, the computed hypolimnetic temperatures were considerably warmer than the observed. Observed hypolimnetic temperatures show considerable cooling took place between August 3 and August 21 that the model did not capture. Analysis of observed air temperatures (Figure 22, page

Table 3. Final values for coefficients adjusted during Fort Peck Lake temperature calibration

Coefficient	Value
Horizontal eddy viscosity	1.0 $m^2 s^{-1}$
Minimum vertical eddy viscosity	1.4 x 10^{-7} m^2 s^{-1}
Horizontal eddy diffusivity	1.0 m^2 s^{-1}
Minimum vertical eddy diffusivity	1.4 x 10^{-6} m^2 s^{-1}
Bottom frictional resistance	70.0 $m^{1/2} s^{-1}$
Fraction of solar radiation absorbed at the water surface	0.45
Light extinction - water	0.40 m^{-1}
Fraction of solar radiation absorbed in the ice surface.	0.60
Light extinction - ice	0.07 m^{-1}
Wind sheltering coefficient	1.0
Ice albedo	0.25
Water-to-ice heat exchange	10.0 W m^{-2} $°C^{-1}$

20) shows that the first significant cooling event occurred in the middle of September and not between August 3 and August 21. Since the meteorological data drive the temperature predictions, the model could not capture the observed changes in temperature during this time period. On September 14, the model significantly underpredicted the epilimnetic temperature. This is the time of the previously mentioned cold spell in the observed data and the model is responding to the colder air temperatures. By October 5, the reservoir had overturned. The model predicts nearly complete overturn.

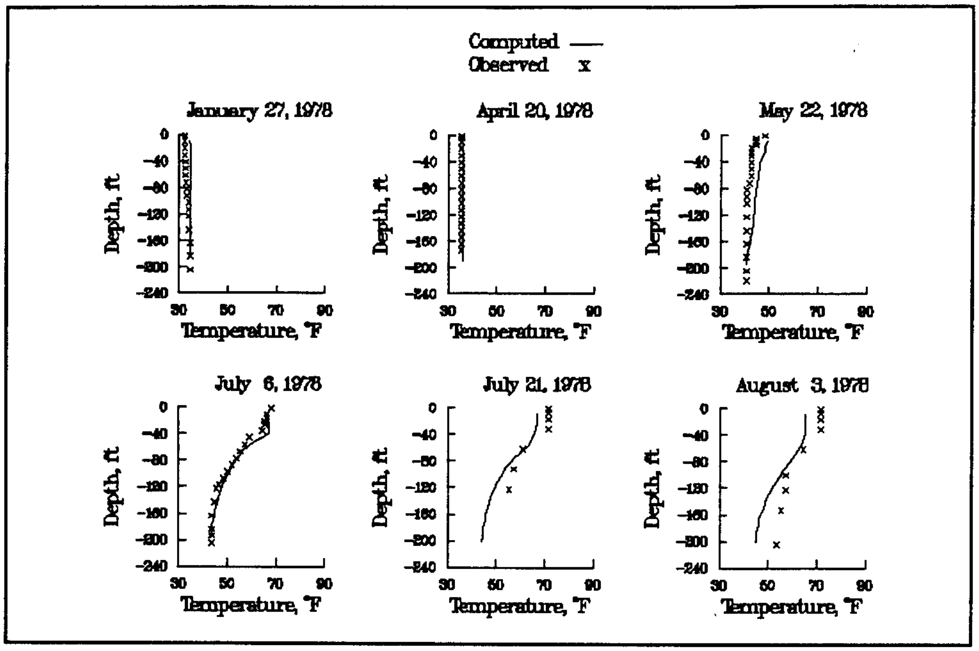

Figure 58. Fort Peck Lake 1978 computed versus observed temperatures at station near dam, January 27 - August 3

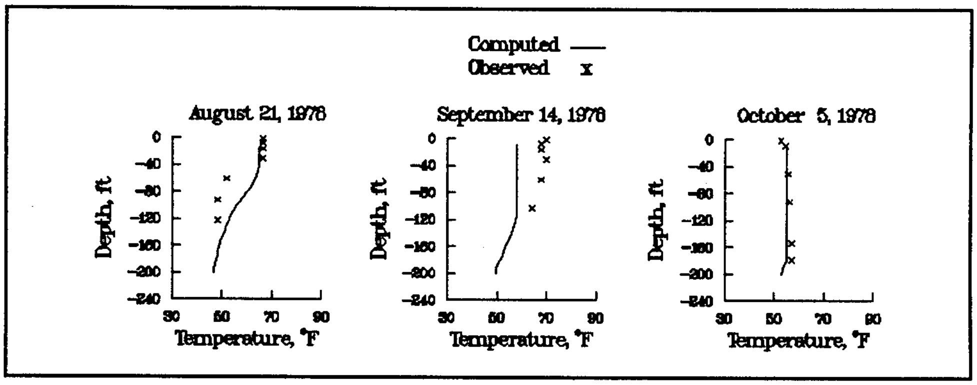

Figure 59. Fort Peck Lake 1978 computed versus observed temperatures at station near dam, August 21 - October 5

Station Near Hell Creek. Observed and computed temperature profiles are given in Figure 60 and Figure 61. Computed versus observed temperatures follow the same trend as temperatures at the station near the dam with the exception that the October 3 computed profile had undergone fall overturn whereas the observed profile was still stratified. Apparently, the reservoir was in the process of overturn in the first week of October since the October 5 observed profile at the dam was isothermal.

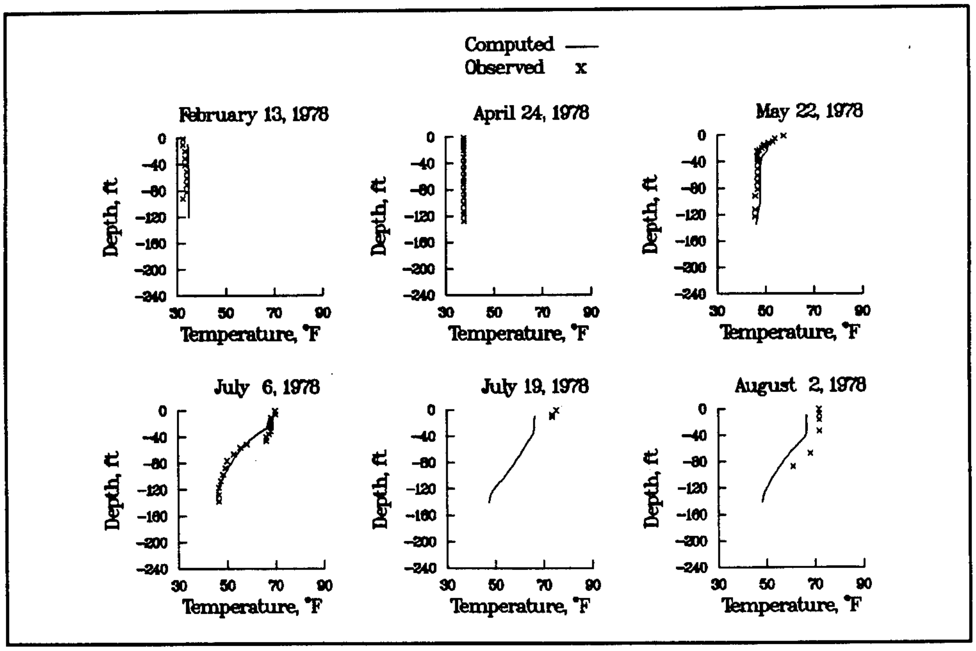

Figure 60. Fort Peck Lake 1978 computed versus observed temperature profiles at station near Hell Creek, February 13 - August 2

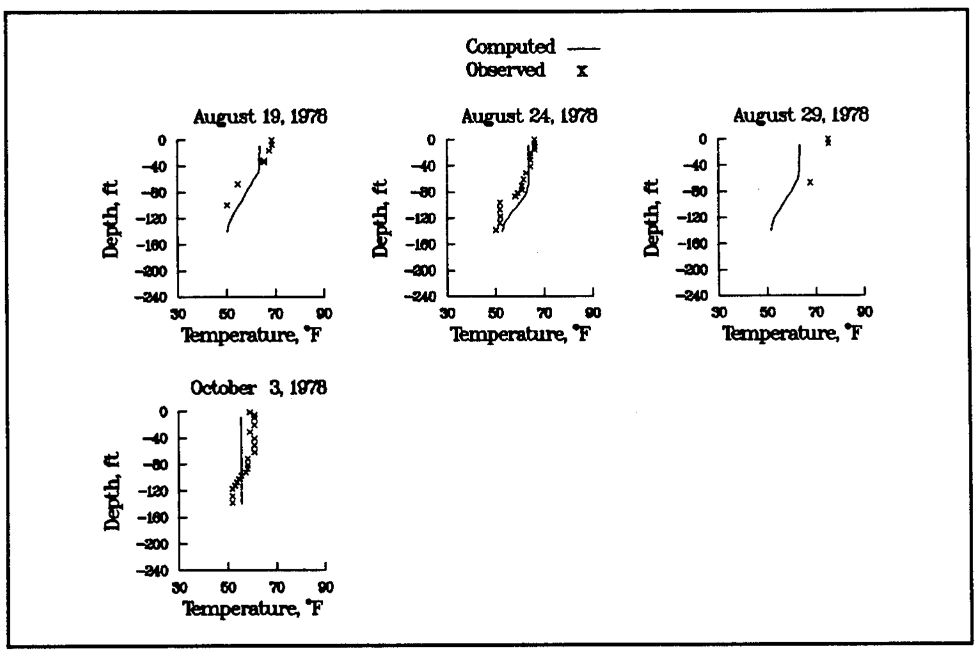

Figure 61. Fort Peck Lake 1978 computed versus observed temperature profiles at station near Hell Creek, August 19 - October 3

Release Temperature. Computed and observed release temperatures are shown in Figure 62. They are in close agreement until October when the model predicts colder release temperatures than observed. Again, air temperatures (Figure 22, page 20) show a marked decrease at the beginning of October consistent with model predictions and not with observed release temperatures. The computed rate of increase and decrease and the maximum release temperature are nearly identical to observed.

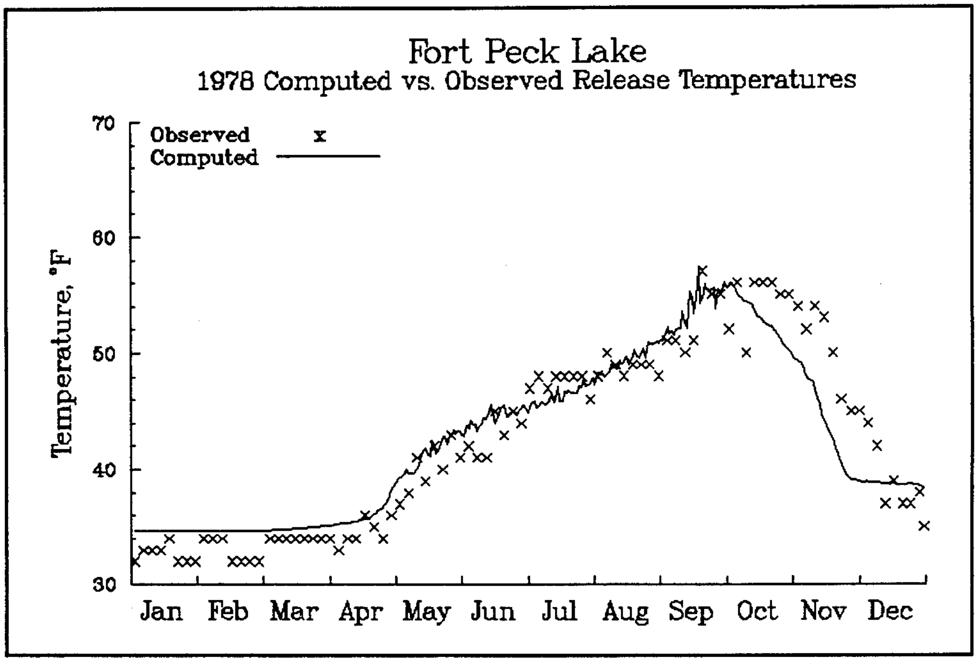

Figure 62. Fort Peck Lake 1978 computed versus observed release temperatures.

Dissolved Oxygen

As previously stated, insufficient water quality data existed to model algal/nutrient/DO dynamics. Instead, a "black box" approach was used that required specifying a zero-order sediment and water column oxygen demand. Values were adjusted until a reasonable fit with observed data was obtained which best represented the average oxygen demand during summer stratification. Final values for sediment and water column oxygen demand are given in Table 4.

Table 4. Lake Fort Peck calibrated sediment and water column oxygen demand

Segment	Sediment, g m^2 day^{-1}	Water Column, g m^3 day^{-1}
1-17	0.3	0.06
19-27	0.3	0.04-0.2
27-33	0.3	0.01

Station Near Dam. Initial DO concentrations were set at saturated values for the beginning of the simulation. As a result, predicted DO on January 27 was much greater than observed throughout the water column. After overturn in April, the model was in close agreement with observed data (Figure 63). By July 6, observed hypolimnetic DO had decreased by ≈ 3 mg l^{-1}. Computed DO was slightly higher. The observed data for August 21 indicate that hypolimnetic DO had increased which is questionable. Computed and observed DO are in close agreement on October 5 just after overturn.

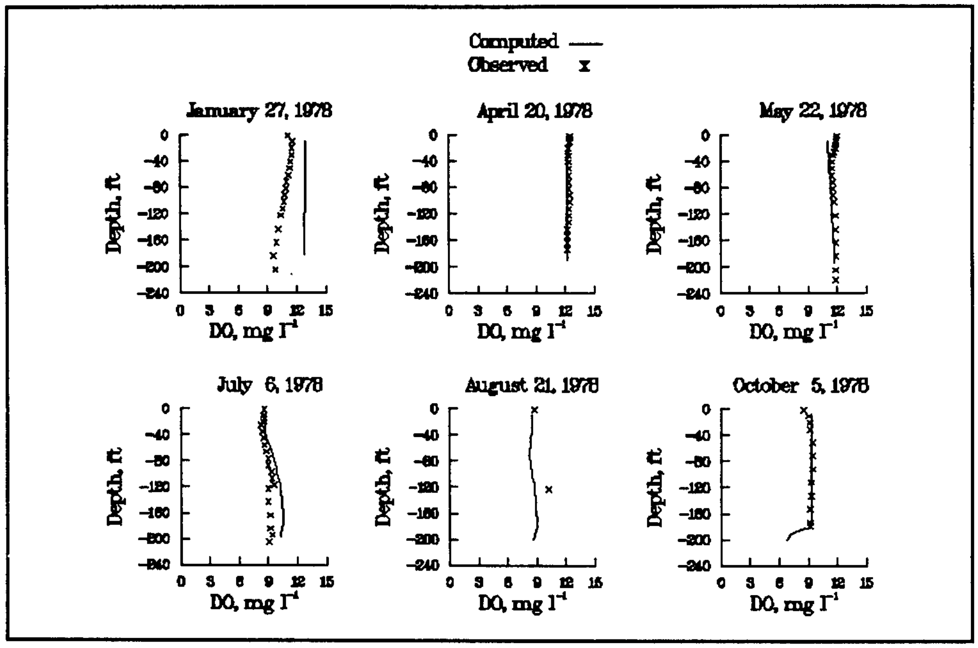

Figure 63. Fort Peck Lake 1978 computed versus observed DO at station near dam

Station Near Hell Creek. Computed DO is in close agreement with observed until May 22 when there was a significant oxygen deficit the model did not capture (Figure 64 and Figure 65). This event is most likely due to a spring phytoplankton bloom and die-off that the formulation for DO used in this study would not be able to capture. By August 19, computed and observed DO were back in agreement. The discrepancy between computed and observed DO on October 3 is due to the model having predicted overturn at this station that is not in agreement with observed temperature data.

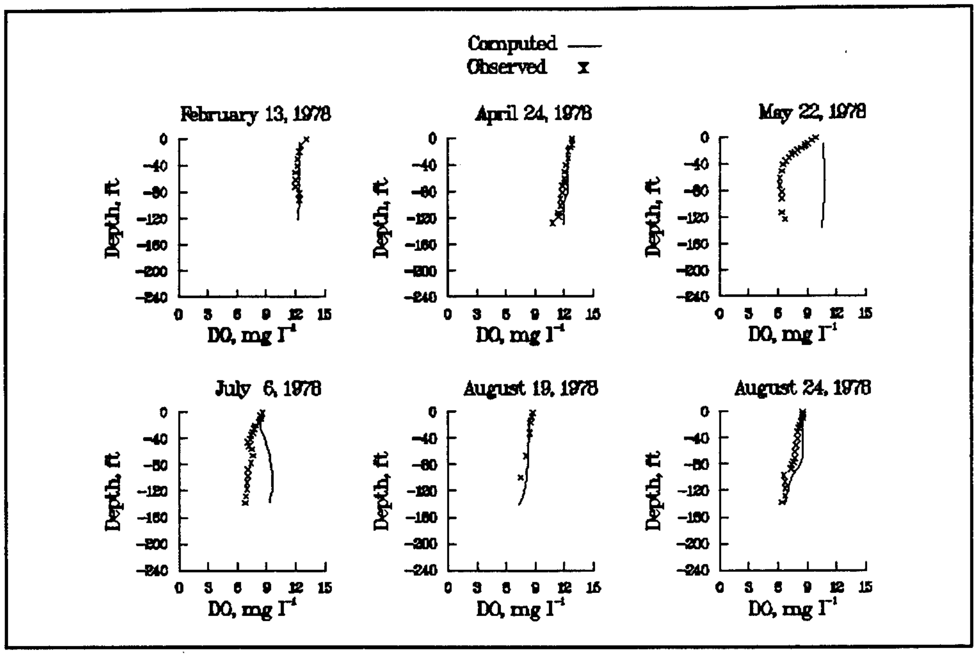

Figure 64. Fort Peck Lake 1978 computed versus observed DO at station near Hell Creek, February 13 - August 24

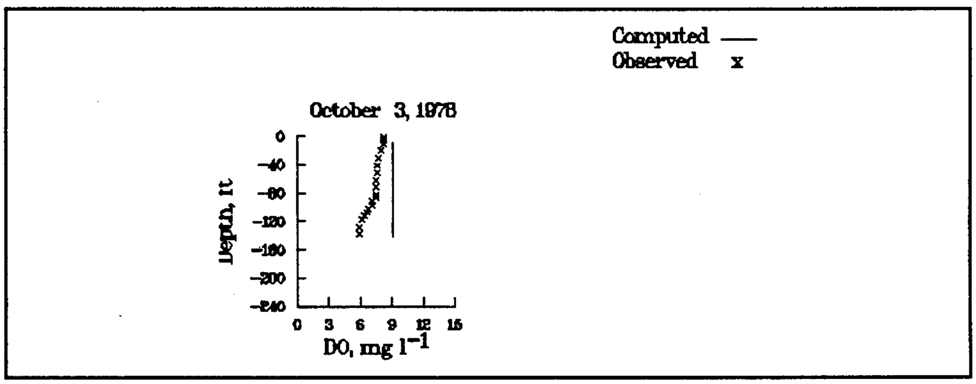

Figure 65. Fort Peck Lake 1978 computed versus observed DO at station near Hell Creek, October 3

Release DO. Computed release DO concentrations are shown in Figure 66.

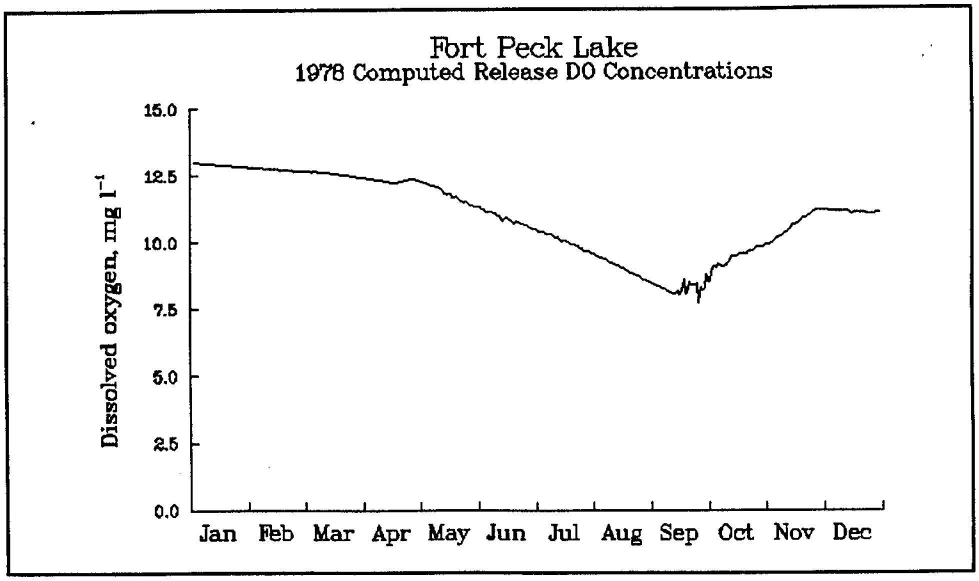

Figure 66. Fort Peck Lake 1978 computed release DO

Fort Peck Lake 1980 Simulation

Water Surface Levels

Computed and observed 1980 water surface elevations are shown in Figure 67. The net decrease in storage was 6.1 ft with elevations ranging from 2,235.9 ft to 2,242.0 ft. Differences in computed and observed stages were less than 0.5 ft throughout the year.

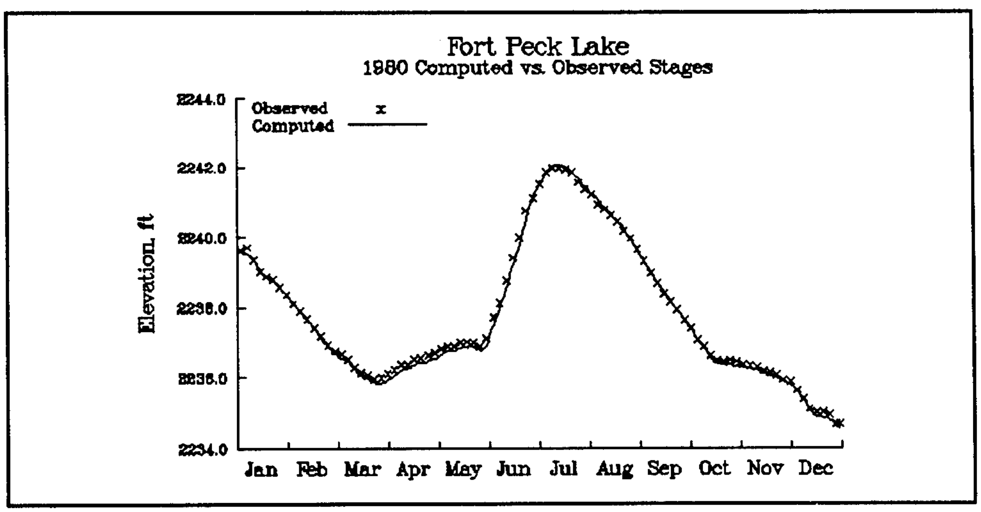

Figure 67. Fort Peck Lake 1980 computed versus observed water surface elevations at dam

Ice Cover

Computed ice cover is shown in Figure 68. Reported ice-out was on April 18 and computed ice-out was on April 19. Reported ice-in occurred on February 12, 1981. No computed ice-in date was available from the 1980 simulation since the run did not continue into 1981.

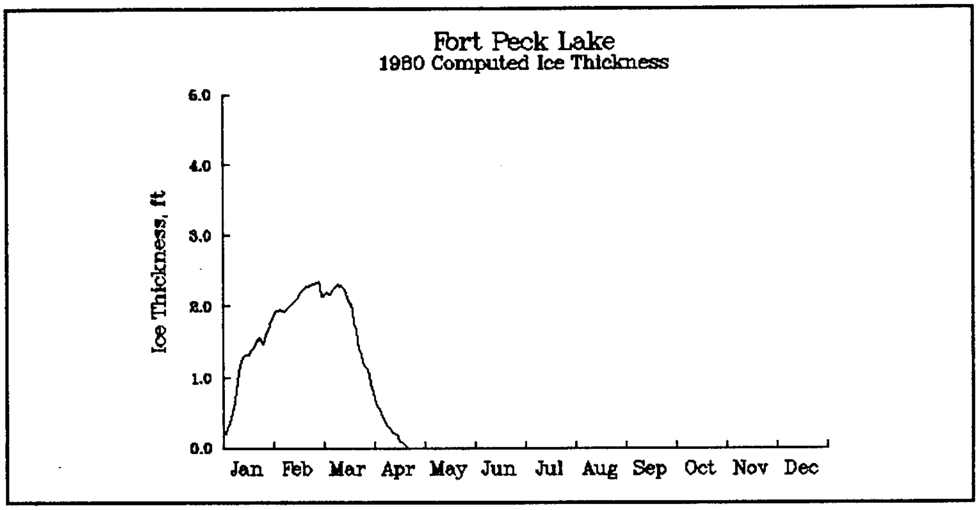

Figure 68. Fort Peck Lake 1980 computed ice cover

Temperature

Station Near Dam. Observed and computed temperature profiles are shown in Figure 69 and Figure 70. Computed and observed profiles are in close agreement until July 21 when the model predicted much lower hypolimnetic temperatures than observed. Temperatures were in closer agreement by August 11 when the observed hypolimnetic temperatures had cooled by several degrees. By August 22, computed and observed temperatures were in nearly exact agreement. Between July 21 and August 22, observed hypolimnetic temperatures had decreased by ≈ 8 °F. If the observed data were correct, then the most likely explanation for the decrease in hypolimnetic temperatures during the hottest part of summer is displacement of hypolimnetic water near the dam because of internal seiching. More evidence of this phenomena can be seen in both Lake Sakakawea and Lake Oahe. By October 8, the model predicts nearly complete overturn while the observed data show the presence of a thermocline near 120ft.

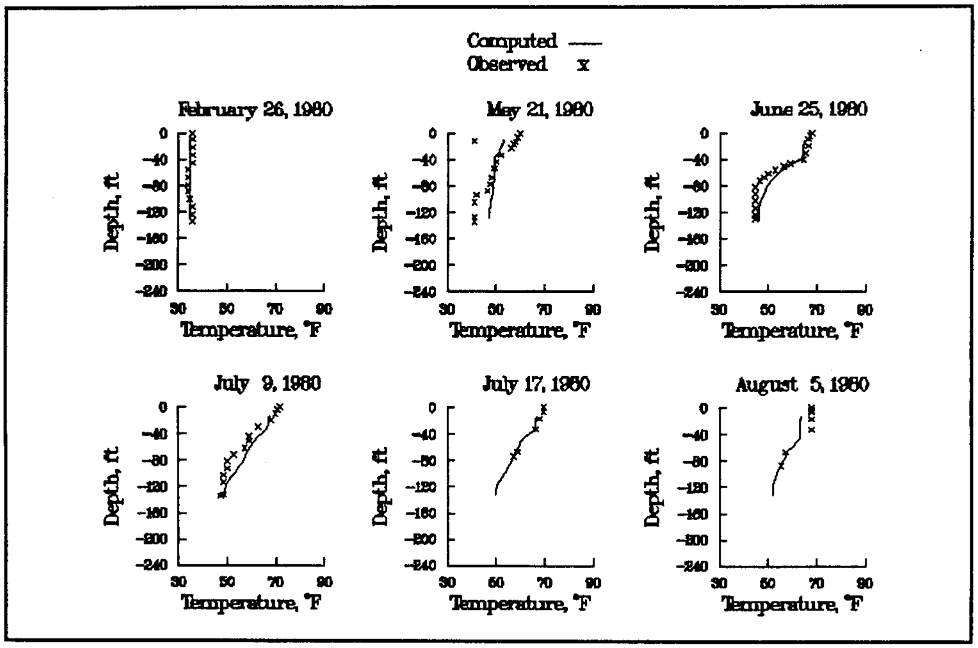

Figure 69. Fort Peck Lake 1980 computed versus observed temperatures at station near Hell Creek, February 26 - August 5

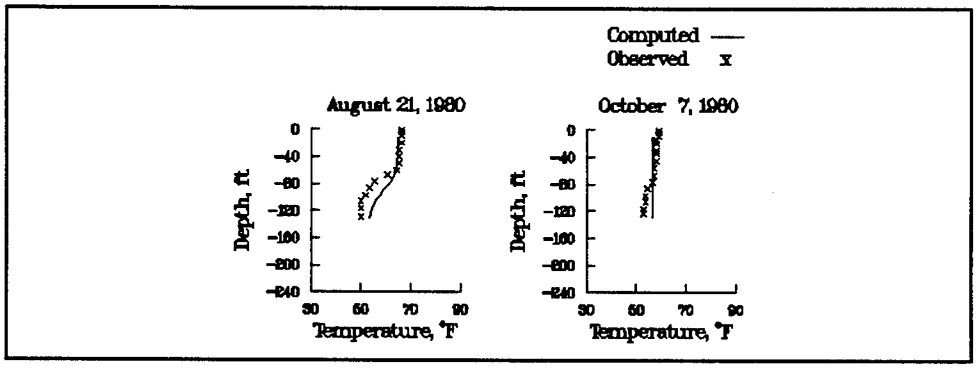

Figure 70. Fort Peck Lake 1980 computed versus observed temperatures at station near Hell Creek, August 21 - October 7

Station Near Hell Creek. Computed versus observed temperatures are shown in Figure 71 and Figure 72. With the exception of May 21, computed and observed temperatures are in reasonable agreement. The erosion of the thermocline between June 25 and July 9 was captured by the model. The model predicted complete overturn by October 7 while observed data still showed some stratification.

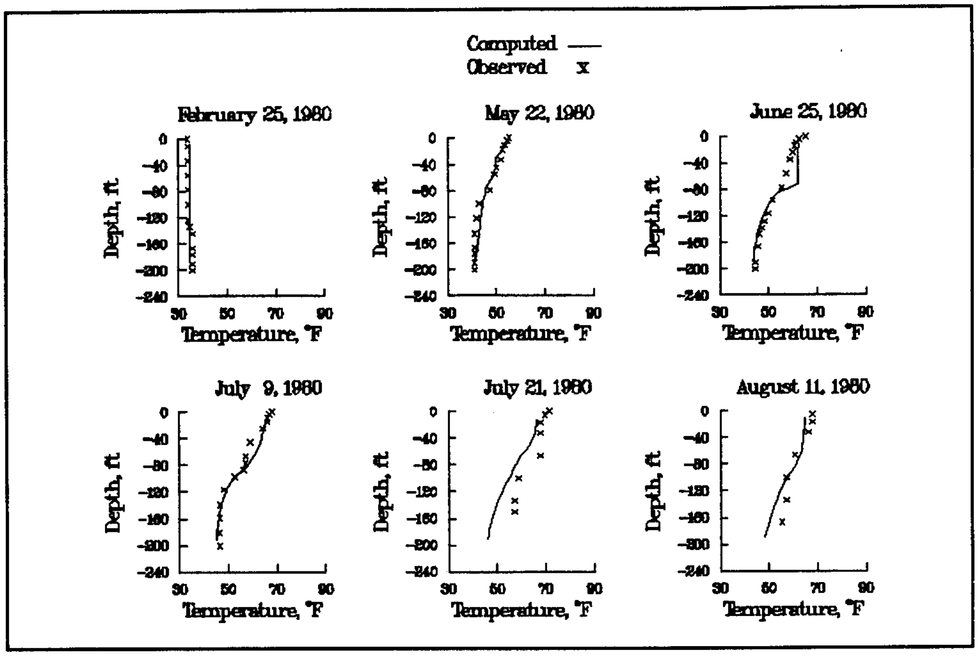

Figure 71. Fort Peck Lake 1980 computed versus observed temperatures at station near dam, February 25 - August 11

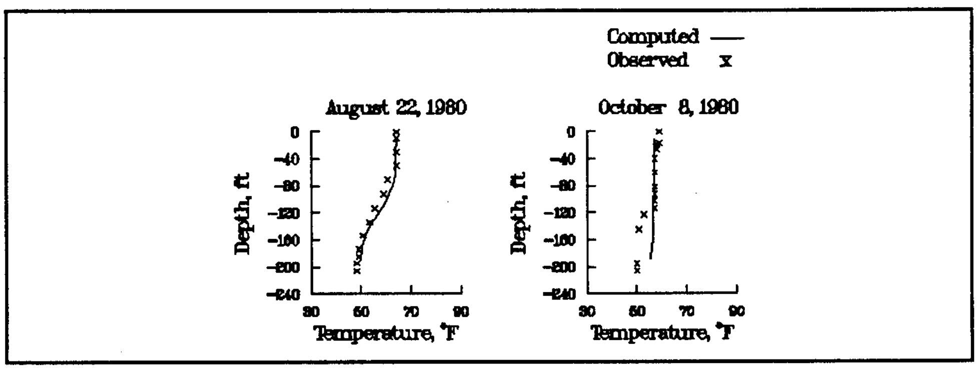

Figure 72. Fort Peck Lake 1980 computed versus observed temperatures at station near dam, August 22 - October 8

Release Temperature. Computed and observed release temperatures are shown in Figure 73. Computed temperatures are in close agreement with observations with the exception that release temperatures decreased earlier in the fall than observed, although not as early as in 1978. As in 1978, the rate of increase and decrease and maximum release temperature were nearly identical.

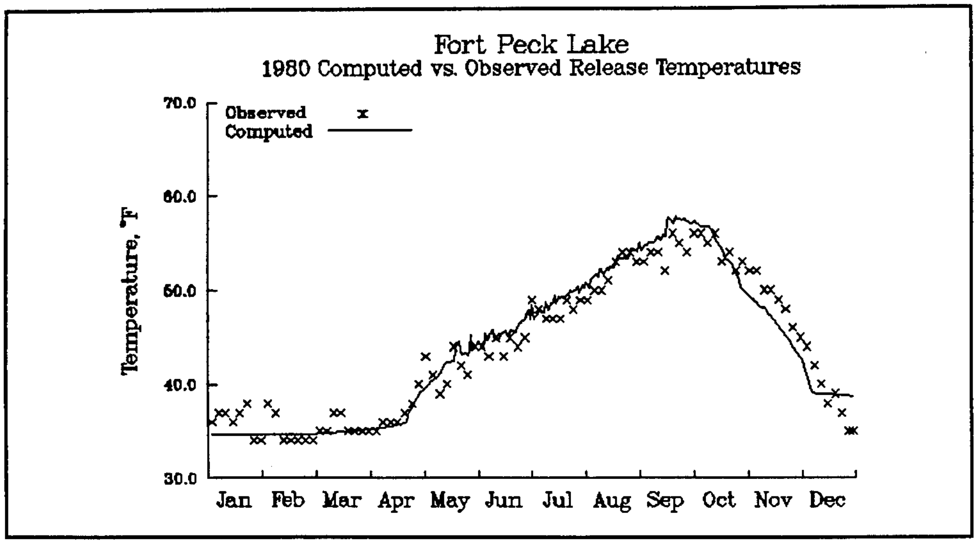

Figure 73. Fort Peck Lake 1980 computed versus observed release temperatures

Dissolved Oxygen

Station Near Dam. Computed versus observed DO profiles are given in Figure 73, Figure 74. With the exception of October 8, computed and observed profiles are in general agreement. In June and July, Fort Peck Lake exhibited a classic clinograde DO profile typical of dimictic, oligotrophic lakes. The model also reflected this pattern. The rapid decline in DO between the end of August and October is again most likely due to a phytoplankton bloom and die-off that has exerted a tremendous water column oxygen demand. The depth of the thermocline at this date is ≈ 120ft and DO should be nearly saturated in the epilimnion as the reservoir is undergoing fall overturn. The presence of a significant oxygen deficit in the epilimnion suggests rapid decay or tremendous phytoplankton respiration.

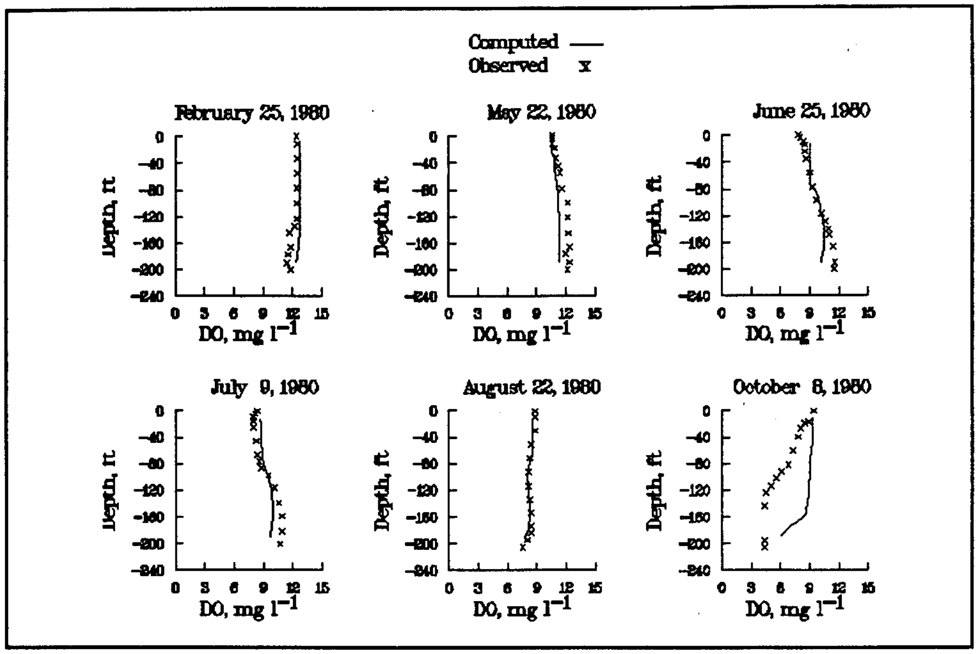

Figure 74. Fort Peck Lake 1980 computed versus observed DO at station near dam

Station Near Hell Creek. Computed and observed DO profiles are shown in Figure 75. As in 1978, greater discrepancies between computed and observed DO profiles are found at this station than at the dam suggesting that phytoplankton blooms play a more important role in determining variations in DO. With the exceptions of July 9 and October 7, the model captures the trends in DO at this station. The model does not capture the DO deficits in spring and fall. However, the model does predict the overall oxygen demand during summer stratification by predicting fairly closely the observed DO on August 21. As in the station near the dam, there is evidence of a large phytoplankton bloom and die-off on October 7 that the model cannot capture.

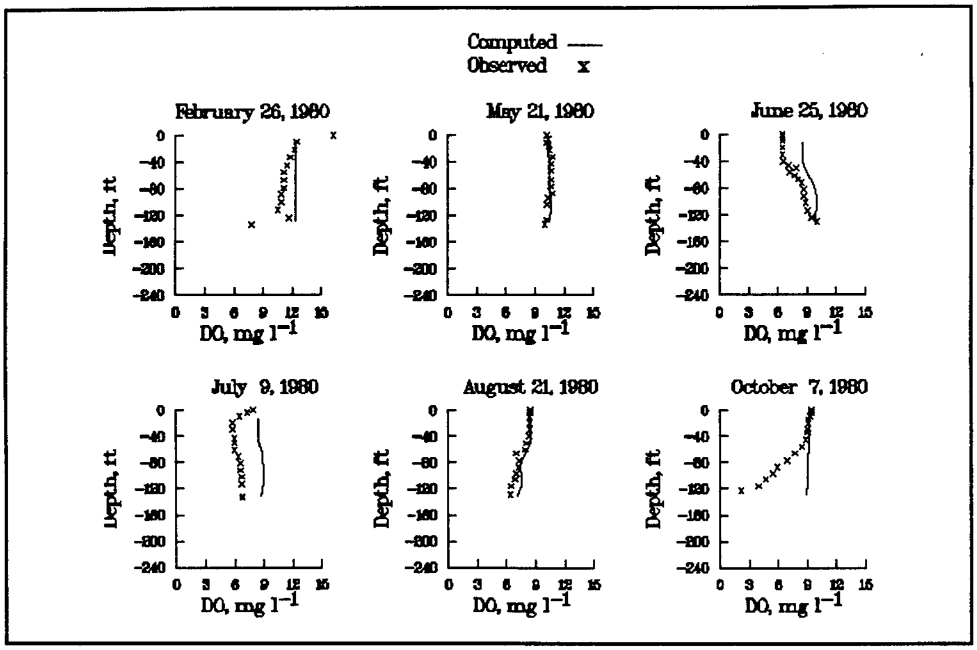

Figure 75. Fort Peck Lake 1980 computed versus observed DO at station near Hell Creek

Release DO. Computed release DO concentrations are shown in Figure 76.

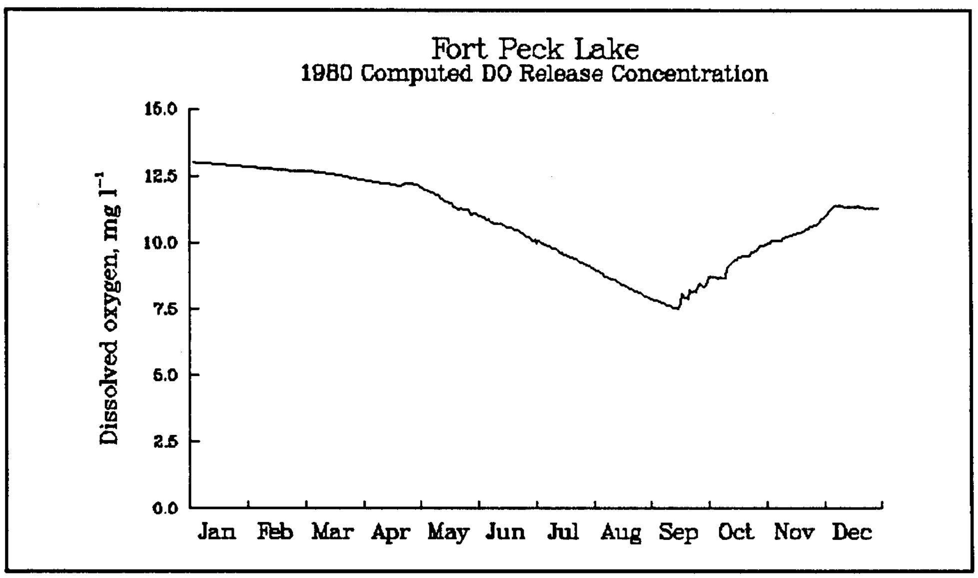

Figure 76. Fort Peck Lake 1980 computed release DO

Lake Sakakawea 1978 Simulation

Water Surface Elevations

Computed and observed 1978 water surface elevations are shown in Figure 77. The net increase in storage was 24.5 ft with elevations ranging from 1,825.0 ft to 1,849.5 ft. Differences in computed and observed stages were less than 0.5 ft throughout the year.

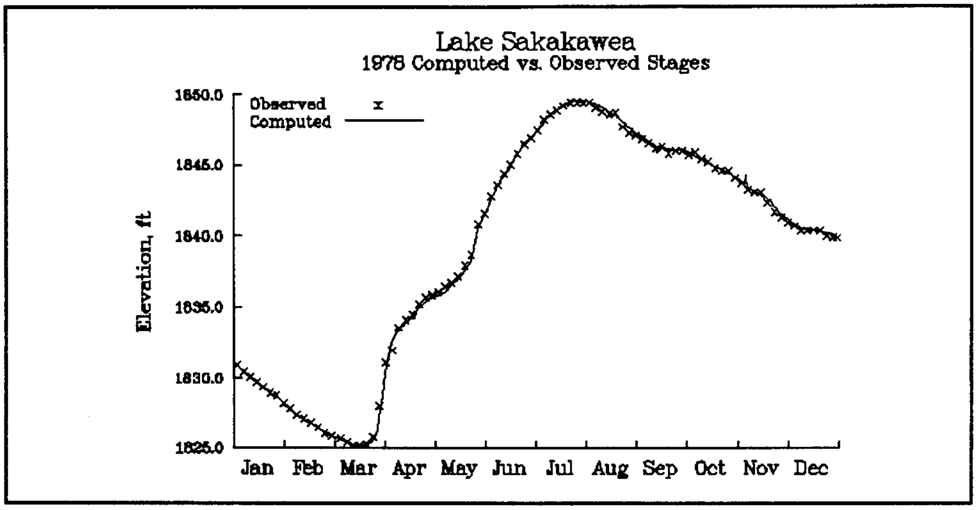

Figure 77. Lake Sakakawea 1978 computed versus observed water surface elevations at dam

Ice Cover

Computed ice cover is shown in Figure 78. Reported ice-out was on April 22 and computed ice-out was on April 16. Reported ice-in occurred on January 17, 1979. No ice-in date was available from the 1978 simulation since it did not continue into 1979.

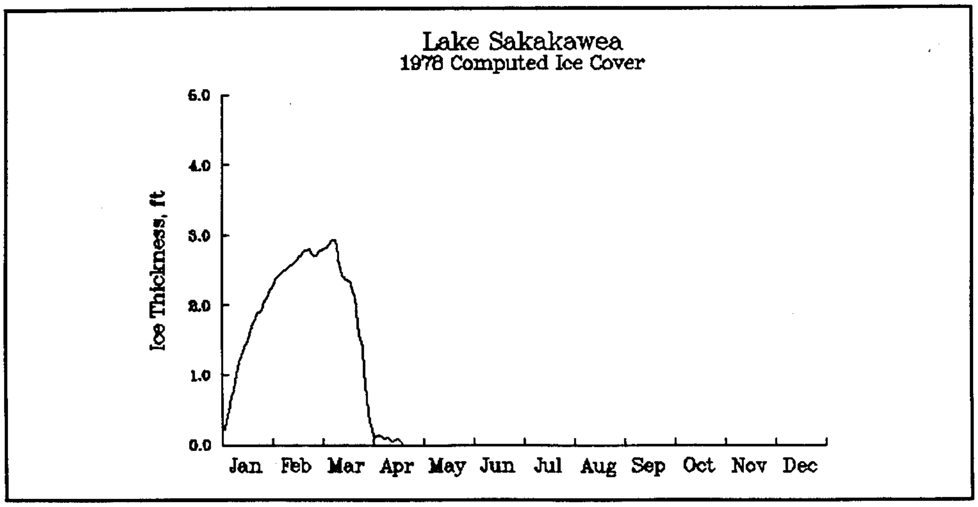

Figure 78. Lake Sakakawea 1978 computed ice cover

Temperature

Table 5 gives the values of all coefficients affecting temperature and ice computations. As in the Fort Peck calibration, all values except for the minimum vertical eddy diffusivity were reset to default values for the final calibration run.

Table 5. Final values for coefficients adjusted during Lake Sakakawea temperature calibration

Coefficient	Value
Horizontal eddy viscosity	1.0 $m^2 s^{-1}$
Minimum vertical eddy viscosity	$1.4 \times 10^{-7} m^2 s^{-1}$
Horizontal eddy diffusivity	1.0 $m^2 s^{-1}$
Minimum vertical eddy diffusivity	$1.4 \times 10^{-6} m^2 s^{-1}$
Bottom frictional resistance	70.0 $m^{1/2} s^{-1}$
Fraction of solar radiation absorbed at the water surface	0.45
Light extinction - water	0.40 m^{-1}
Fraction of solar radiation absorbed in the ice surface	0.60
Light extinction - ice	0.07 m^{-1}
Wind sheltering coefficient	1.0
Ice albedo	0.25
Water-to-ice heat exchange	10.0 $W m^{-2} °C^{-1}$

Station Near Dam. Observed and computed temperature profiles are shown in Figure 79 and Figure 80. Computed and observed profiles were generally in close agreement until August when profiles were taken one day apart. These two profiles illustrate some of the problems when calibrating water quality models to observed data. Although they were taken only one day apart, there is a discernable difference in temperature at 100 ft. The model overpredicts hypolimnetic temperatures for both dates, but the difference appears to be more pronounced on August 16. On September 20, observed data indicate that the reser-

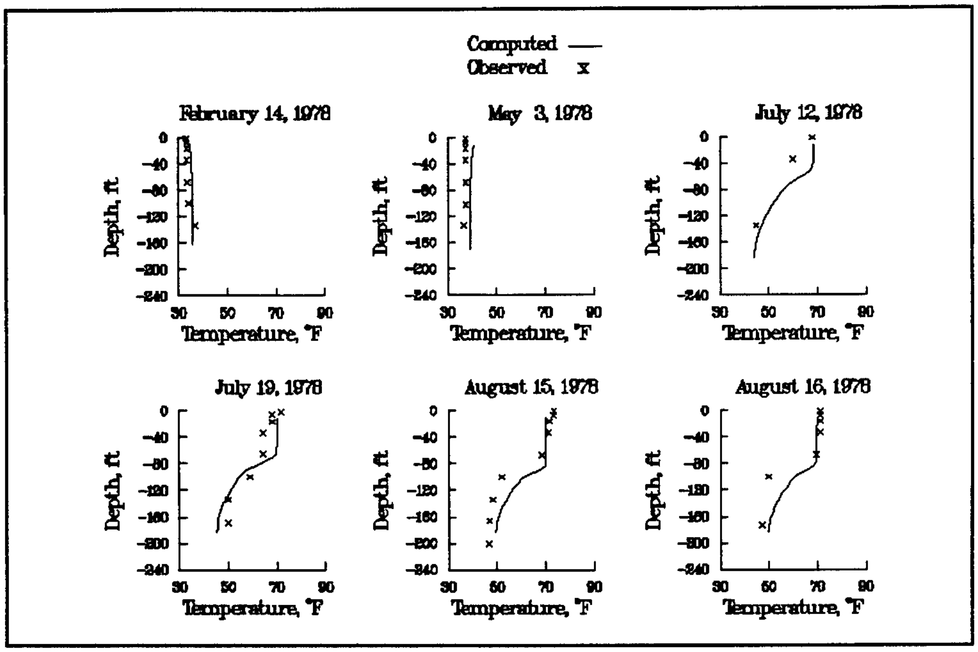

Figure 79. Lake Sakakawea 1978 computed versus observed temperatures at station near dam, February 14 - August 15

voir had overturned and then restratified while the model predicts nearly complete overturn but temperatures are ≈ 8°F higher than observed. By October 11, the reservoir has overturned and computed and observed temperatures are in close agreement. Between September 20 and October 11, the observed data show the reservoir has heated up by ≈5°F. The model predicts a temperature decrease during this time that appears more reasonable based on air temperature during this period.

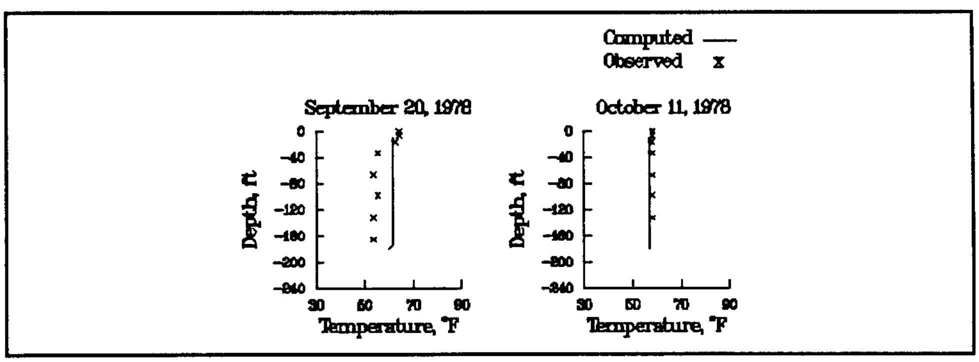

Figure 80. Lake Sakakawea 1978 computed versus observed temperatures at station near dam, September 20 - October 11

Station near New Town. Computed versus observed temperatures are shown in Figure 81 and Figure 82. Except for the profile on May 4, computed temperatures are in fairly close agreement with observed temperatures. Profiles on August 17 and 18 illustrate the day-to-day variability that can occur in temperature. Computed hypolimnetic temperatures are warmer than observed while one day later they are colder. Observed data in September show that the reservoir at this station had overturned as do the computed temperatures.

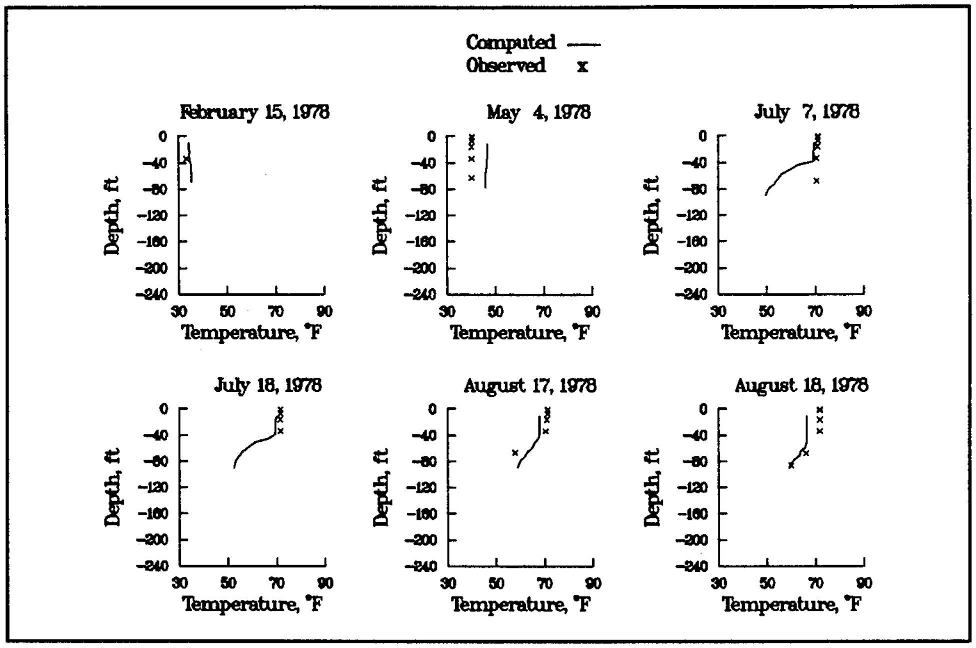

Figure 81. Lake Sakakawea 1978 computed versus observed temperatures at station near New Town, February - August 18

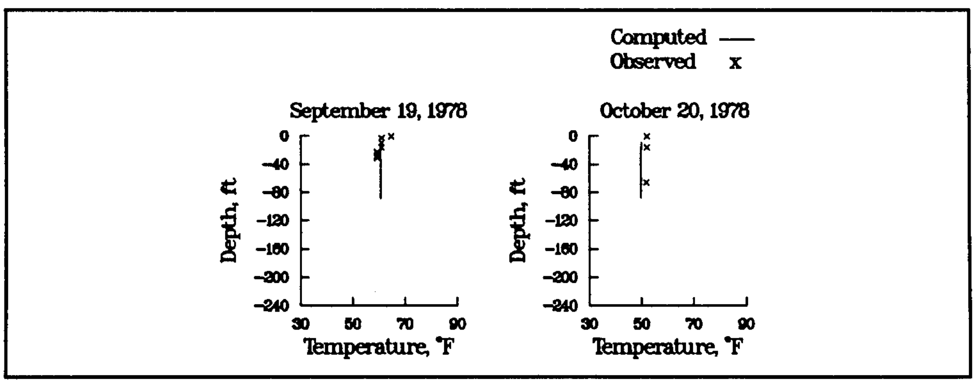

Figure 82. Lake Sakakawea 1978 computed versus observed temperatures at station near New Town, September 19 - October 20

Release Temperature. Computed versus observed release temperatures are shown in Figure 83. Computed release temperatures are generally in close agreement with observed release temperatures. The greatest discrepancies occur in June and July where computed temperatures are less than observed. As in Fort Peck Lake, the model predicts colder temperatures during the fall although the differences are not as pronounced. The model does not capture the lowest temperatures during December.

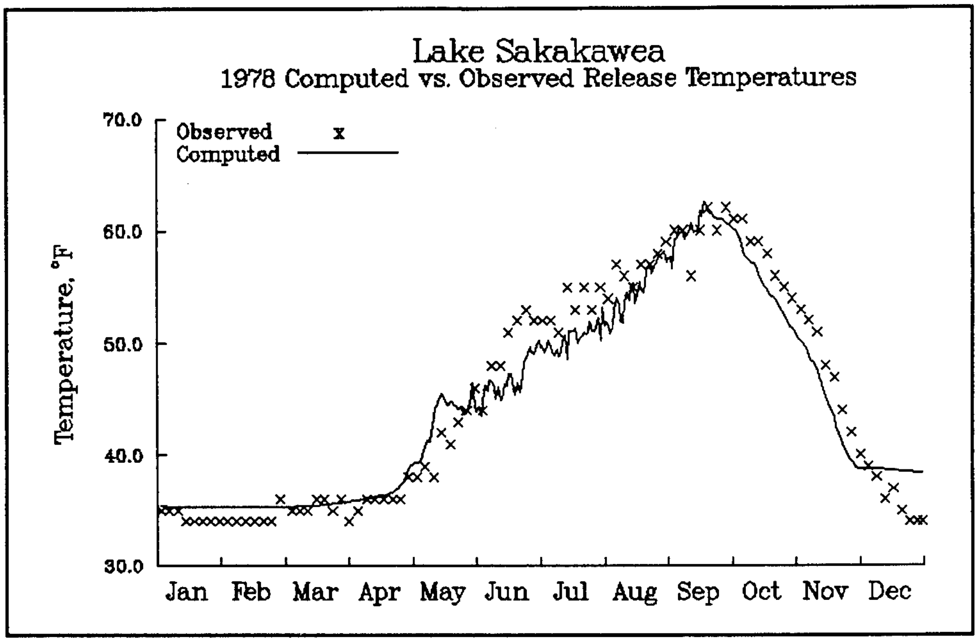

Figure 83. Lake Sakakawea 1978 computed versus observed release temperatures

Dissolved Oxygen

Table 6. Lake Sakakawea calibrated sediment and water column oxygen demand

Segment	Sediment, g m^2 day^{-1}	Water Column, g m^3 day^{-1}
1-10	0.3	0.1
11-20	0.3-0.2	0.1-0.01
21-54	0.2	0.01

Values for sediment and water column oxygen demand were adjusted until a reasonable fit with observed data was obtained that best represented the average oxygen demand during summer stratification. Although oxygen deficits occurred during the winter months, only a small emphasis was placed on calibrating DO during the winter months. The assumption was made that the winter DO and temperature profiles would not have an impact on suitable fish habitat.

Station Near Dam. Computed versus observed DO concentrations are shown in Figure 84 and Figure 85. The February 14 observed profile shows that a considerable oxygen demand existed during the winter months when the reservoir was under ice cover. The model did not capture the observed decrease in hypolimnetic DO. Apparently, there is a greater hypolimnetic oxygen demand during the winter months than during the summer since the minimum observed DO is less in February than in August. The present formulation for DO would not be able to account for the low DO in February. The formulation for DO demand in the model reduces oxygen uptake with decreasing temperatures. Either respiration rates are not dependent upon temperature in Lake Sakakawea (highly unlikely) or there is a greater concentration of organic matter during the winter. The remainder of the profiles are in close agreement. The clinograde profiles are typical of deep, oligotrophic lakes.

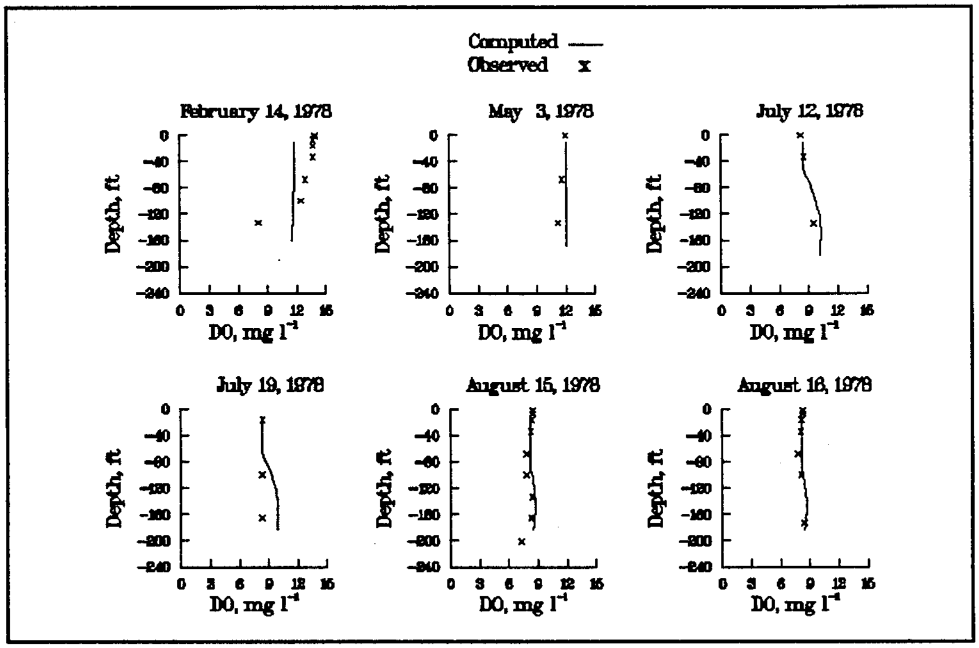

Figure 84. Lake Sakakawea 1978 computed versus observed DO at station near dam, February 14 - August 16

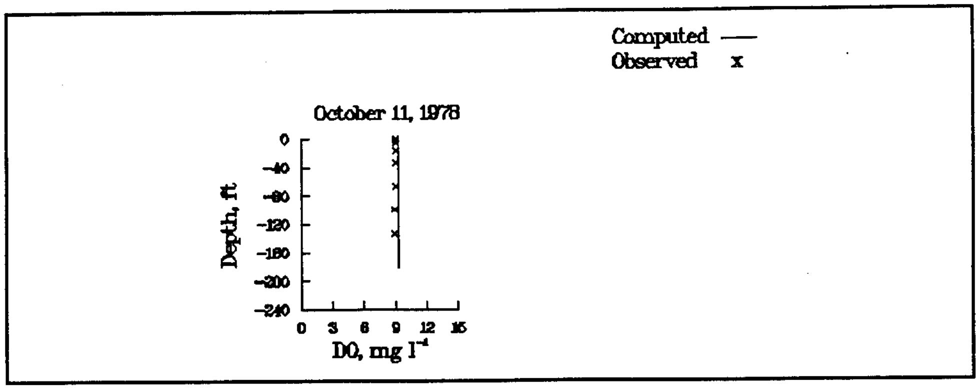

Figure 85. Lake Sakakawea 1978 computed versus observed DO at station near dam

Station Near New Town. Computed versus observed DO concentrations are shown in Figure 86 and Figure 87. Unlike the predictions near the dam on February 15, the model is predicting a relatively large decrease in DO with depth. Computed DO concentrations are in close agreement throughout the remainder of the year. A greater oxygen depletion is apparent at this station than at the dam that is consistent with the model predictions.

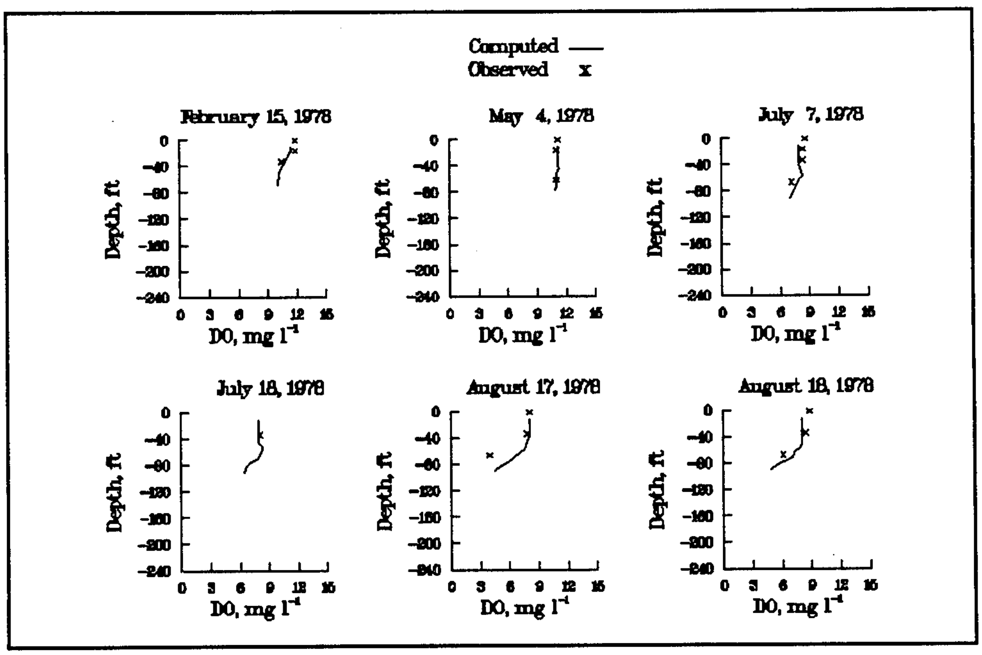

Figure 86. Lake Sakakawea 1978 computed versus observed DO at station near New Town, February 15 - August 18

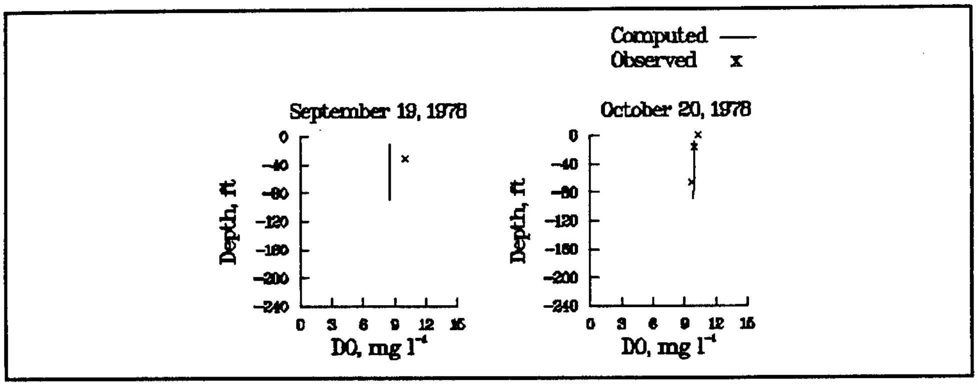

Figure 87. Lake Sakakawea 1978 computed versus observed DO at station near New Town, September 19 - October 20

Release DO. Computed release DO concentrations are shown in Figure 88. As stated previously, the model did not capture the observed DO depletion during the winter months at the station near the dam. However, the release DO did show a constant decrease throughout the winter until ice-out.

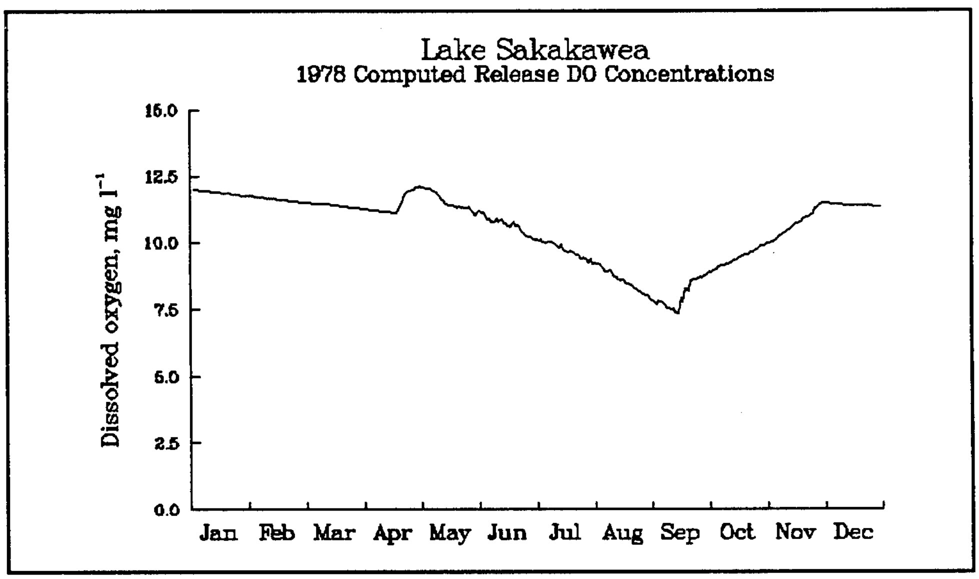

Figure 88. Lake Sakakawea 1980 release DO

Lake Sakakawea 1980 Simulation

Water Surface Elevations

Computed versus observed water surface elevations are shown in Figure 89. The net decrease in storage was 8.4 ft with elevations ranging from 1,842.0 ft to 1,833.6 ft. Differences in computed and observed stages were less than 0.5 ft throughout the year.

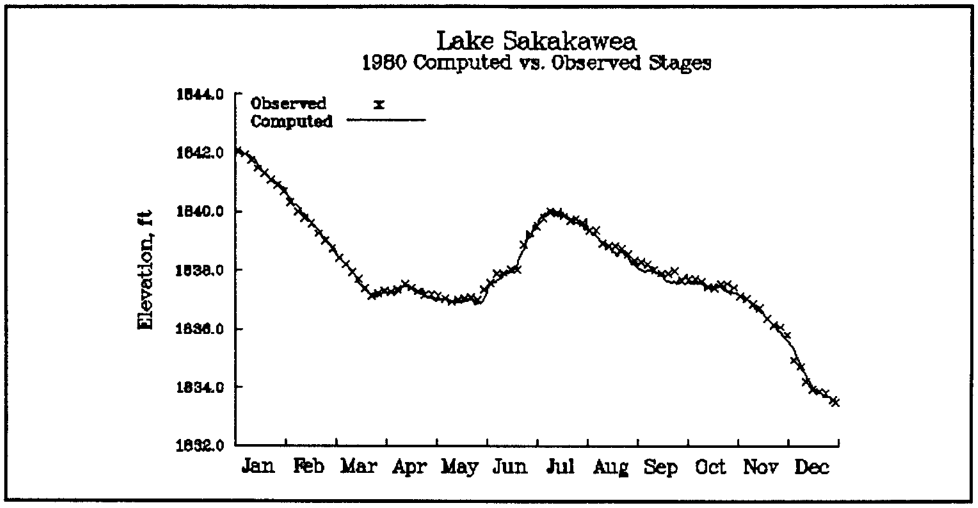

Figure 89. Lake Sakakawea 1980 computed versus observed water surface elevations at dam

Ice Cover

Computed ice cover is shown in Figure 90. Reported ice-out was on April 24 and computed ice-out was on April 17. Reported ice-in was on January 3, 1979. No ice-in date was available from the 1980 simulation since it did not continue into 1981.

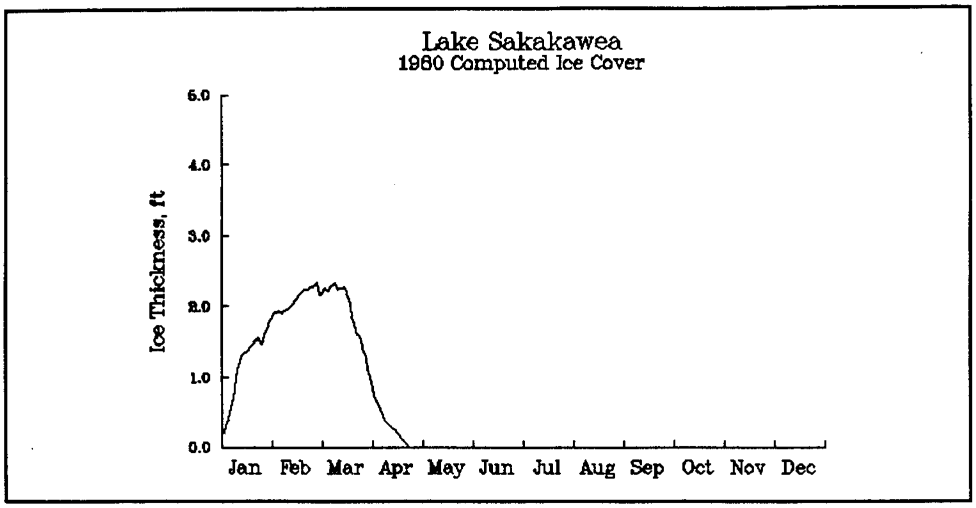

Figure 90. Lake Sakakawea 1980 computed ice cover

Temperature

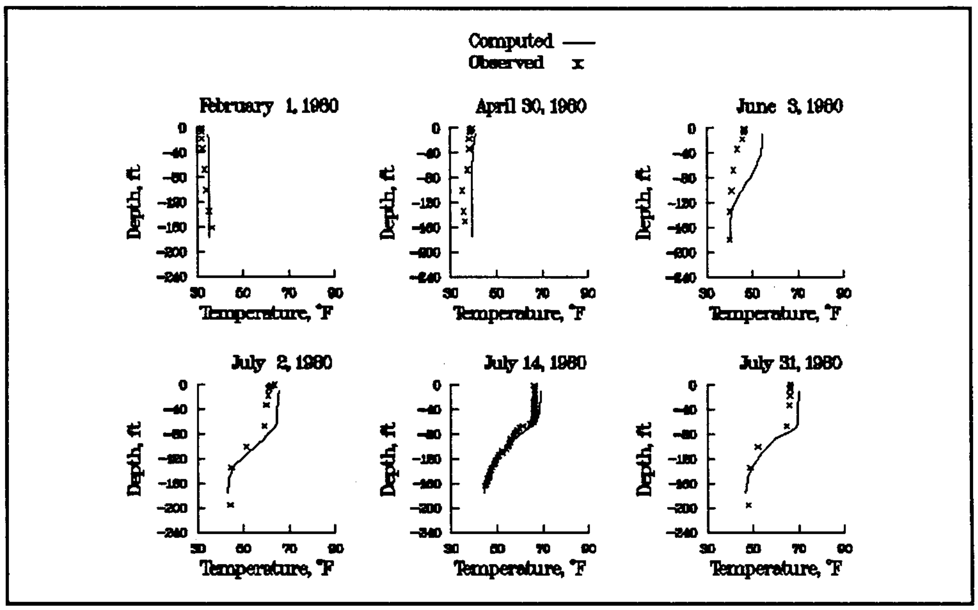

Figure 91. Lake Sakakawea 1980 computed versus observed temperatures at station near dam, February 1 - July 31

Station Near Dam. Computed versus observed temperatures are shown in Figure 91 and Figure 92. Temperatures are generally in close agreement with the exception of June 3 when the model overpredicts epilimnetic temperatures by ≈ 8°F.

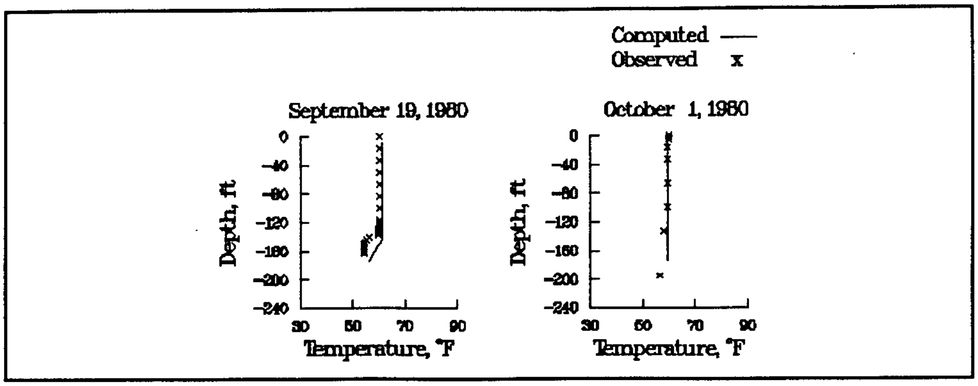

Figure 92. Lake Sakakawea 1980 computed versus observed temperatures at station near dam, September 19 - October 1

Station near New Town. Computed versus observed temperatures are shown in Figure 93 and Figure 94. Computed temperatures during the summer stratification period are in fairly close agreement with observed data. Computed temperatures during the spring and fall are consistently higher than observed temperatures.

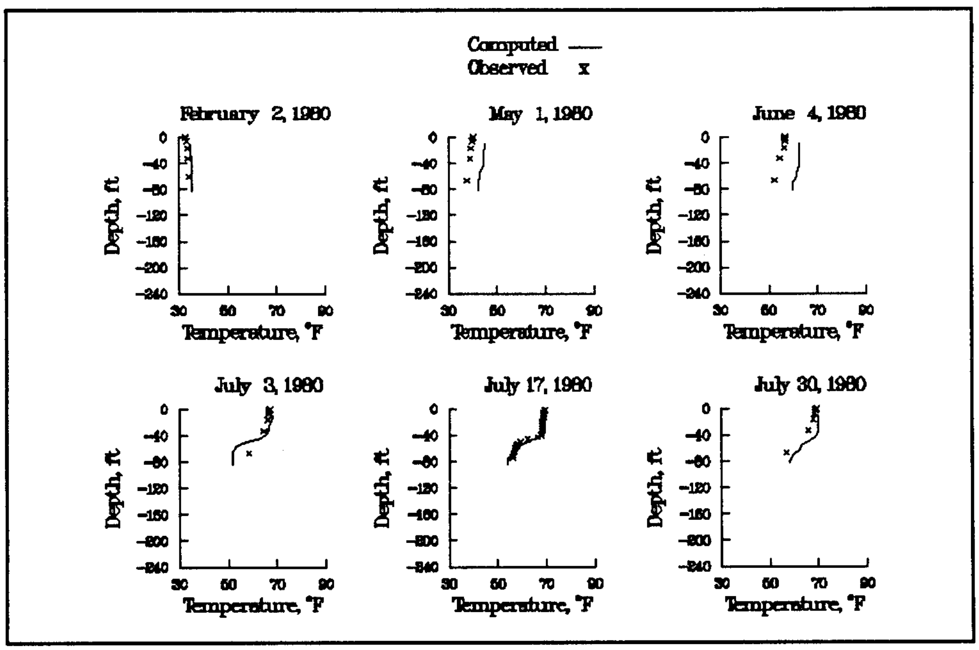

Figure 93. Lake Sakakawea 1980 computed versus observed temperatures at station near New Town, February 2 - July 17

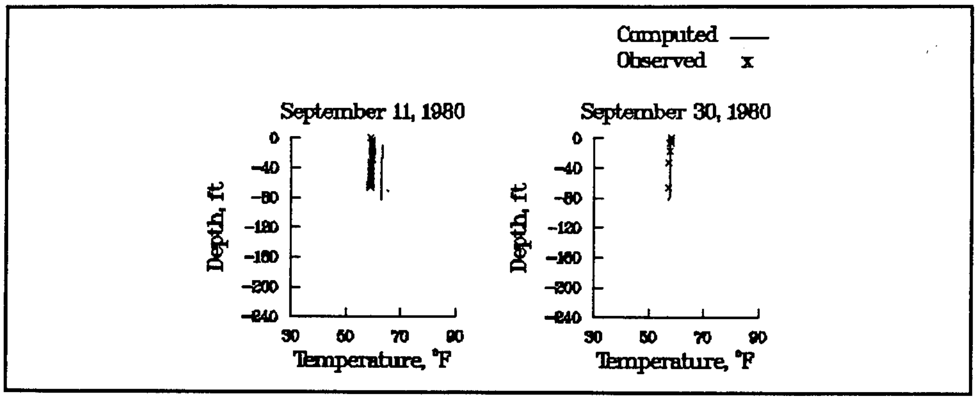

Figure 94. Lake Sakakawea 1980 computed versus observed temperatures at station near New Town, September 11 - september 30

Release Temperatures. Computed versus observed release temperatures are shown in Figure 95. Computed temperatures are in close agreement with observed until the beginning of October when they begin to decrease. Observed release temperatures do not begin to decrease until the end of October. Air temperatures drop rapidly at the beginning of October and the model is responding to the drop in air temperature.

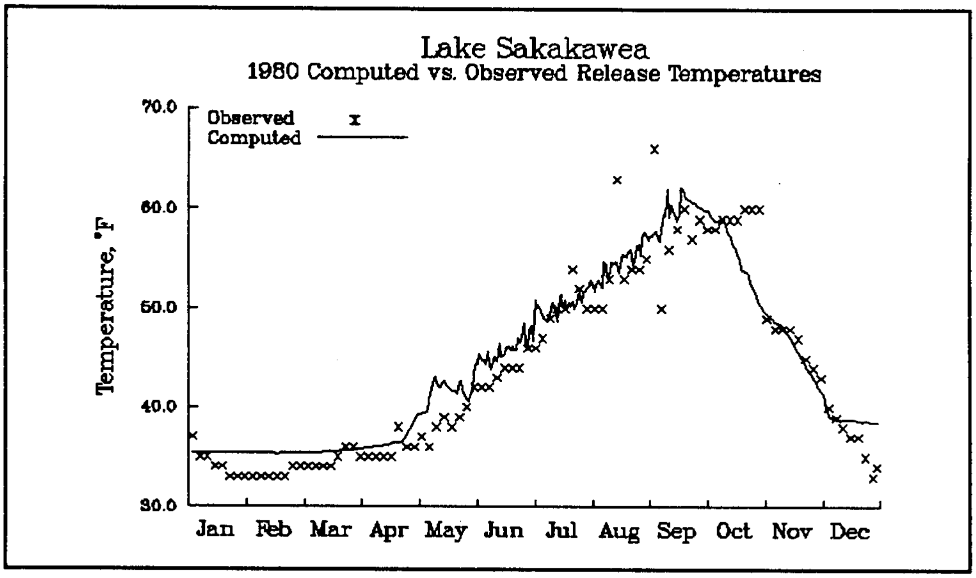

Figure 95. Lake Sakakawea 1980 release temperatures

Dissolved Oxygen

Station Near Dam. Computed versus observed DO concentrations are shown in Figure 96 and Figure 97. A significant oxygen demand during the winter months is again evident in 1980. The April 30 observed data show a decrease of $\approx 6\,mg\,l^{-1}$ from the surface to the bottom. By June 3 following spring overturn, computed DO is in close agreement with observed. The profile on July

14 shows almost complete agreement between computed and observed data while the model overpredicts hypolimnetic DO on July 2 and July 31. More faith was placed in the July 14 data set for two reasons. First, the observed data were more extensive. Second, if the July 2 observed data is correct, then hypolimnetic DO has increased $\approx$ 2-3 mg l^{-1} between July 2 and July 14 (assuming that the July 14 data set is correct). There is no mechanism in the model that would allow the hypolimnetic DO to increase during summer stratification.

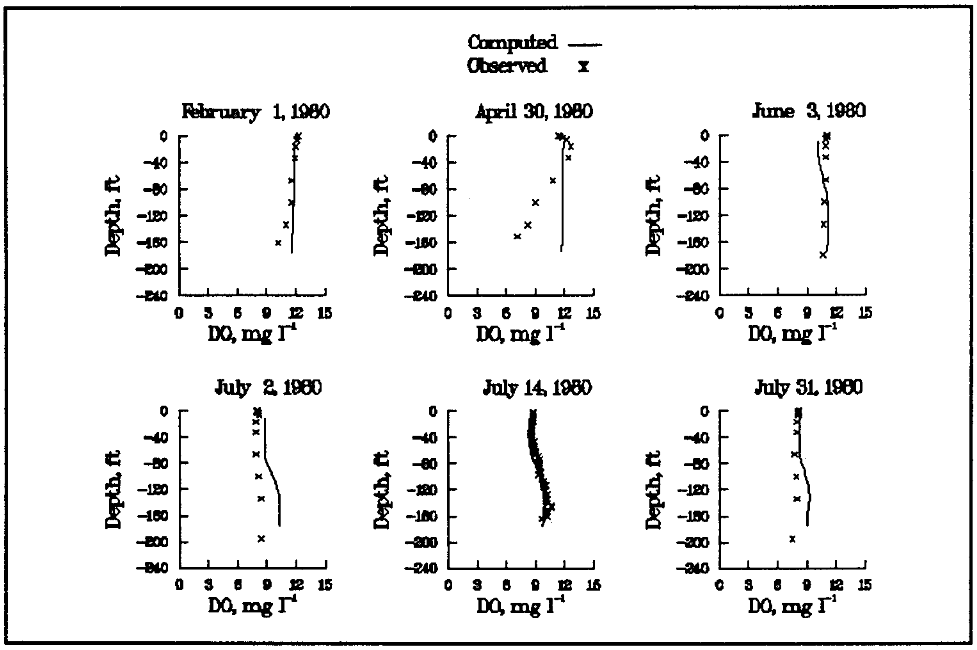

Figure 96. Lake Sakakawea 1980 computed versus observed DO at station near dam, February 1 - July 31

On September 19, the reservoir is in the process of fall overturn. Again, if the more extensive data set on this date is assumed to be correct, then hypolimnetic DO must have increased from the end of July to the middle of September. The October 1 observed profile shows a significant oxygen deficit in the hypolimnion even though the temperature profile on this date shows that the reservoir has overturned. There is no mechanism in the DO formulation that could account for this.

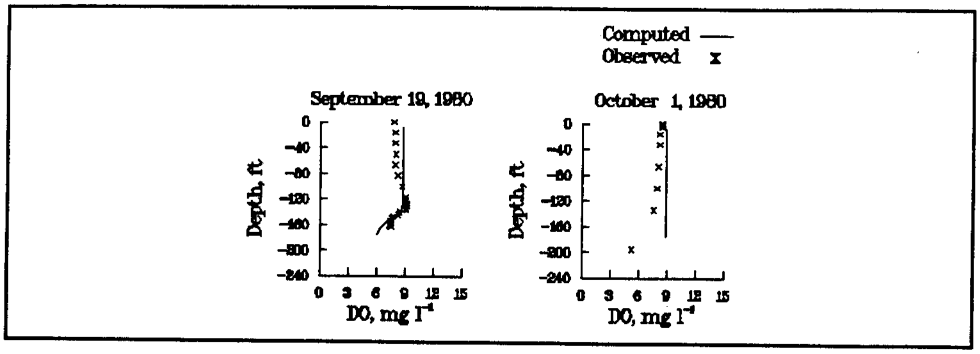

Figure 97. Lake Sakakawea 1980 computed versus observed DO at station near dam, September 19 - October 1

Station Near New Town. Computed versus observed profiles are shown in Figure 98 and Figure 99. During the winter and spring, the supersaturated DO indicate a large algal bloom was present at the upstream station that the model cannot capture. DO is also consistently overpredicted during the summer. Water column and sediment oxygen demand could have been increased to more closely match the observed data, but this would affect the 1978 predictions that were in close agreement. The judgement was that the DO at this station was responding to the winter/spring algal bloom that resulted in a much higher oxygen demand at this station during 1980. It was assumed that this bloom was atypical after reviewing water quality data from other years. Therefore, values for water column and sediment oxygen demand were used from the 1978 simulation and were not adjusted for the 1980 data.

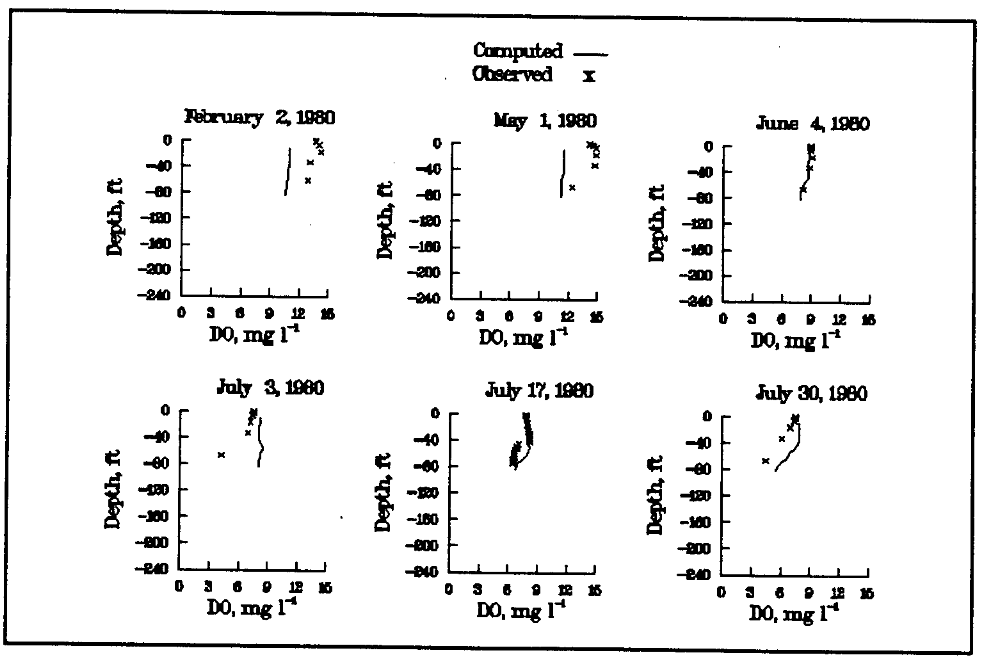

Figure 98. Lake Sakakawea 1980 computed versus observed DO at station near New Town, February 2 - July 30

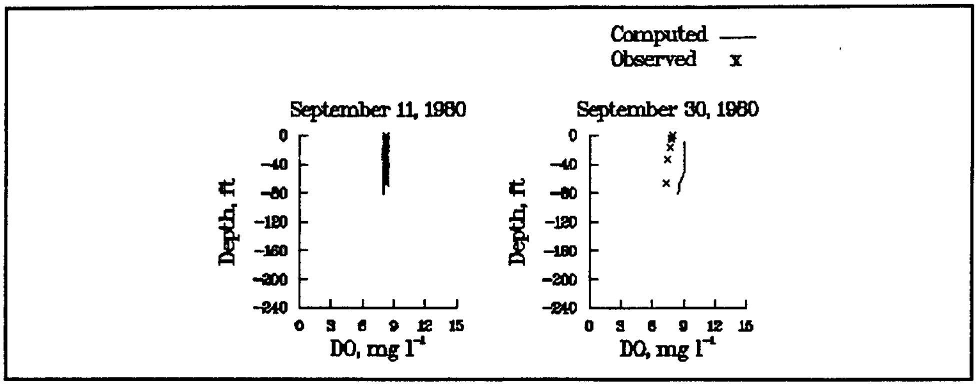

Figure 99. Lake Sakakawea 1980 computed versus observed DO at station near New Town, September 11 - September 30

Release DO. Computed release DO concentrations are given in Figure 100.

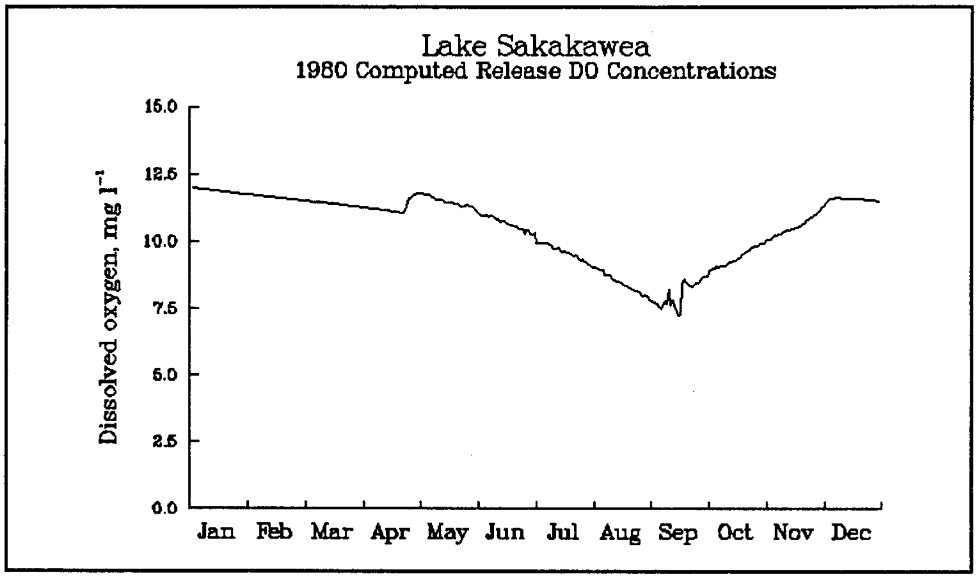

Figure 100. Lake Sakakawea 1980 release DO

Lake Oahe 1978 Simulation

Water Surface Elevations

Computed versus observed 1978 water surface elevations are shown in Figure 101. The net increase in storage was 21 ft with elevations ranging from 1595 ft to 1616 ft. Computed and observed stages were in close agreement throughout the year.

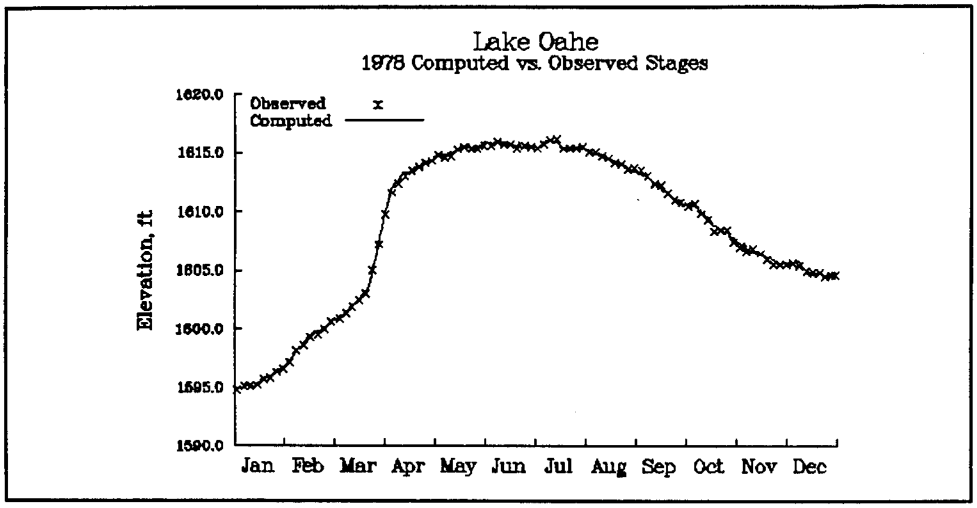

Figure 101. Lake Oahe 1978 computed versus observed water surface elevations at dam

Ice Cover

Computed ice cover is shown in Figure 102. Predicted ice-out occurred on April 7 while reported ice-out occurred on April 8. Reported ice-in occurred on January 3, 1979. No ice-in date was available from the 1978 simulation since the run did not continue into 1979.

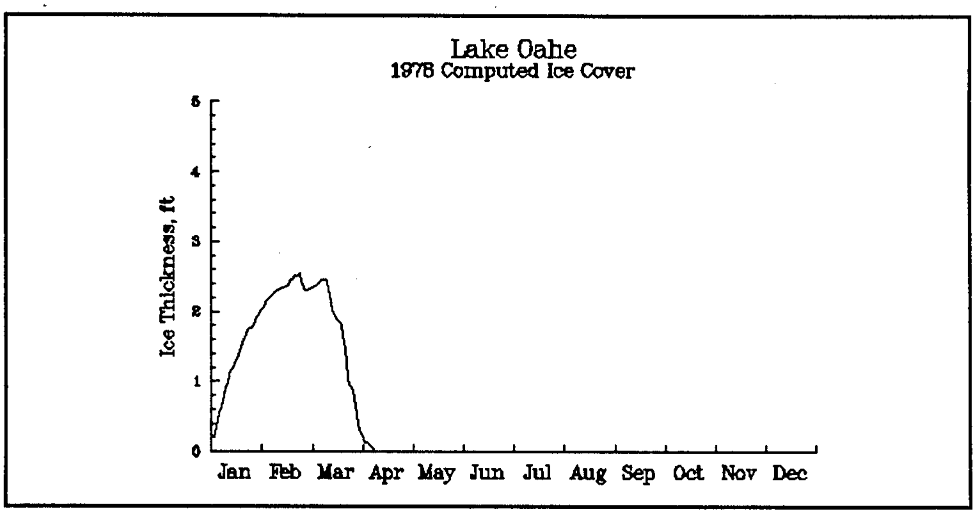

Figure 102. Lake Oahe 1978 computed ice cover

Temperature

Table 7 gives the values of all coefficients affecting temperature and ice computations. As in the Fort Peck and Sakakawea calibrations, all values except for the minimum vertical eddy diffusivity were reset to default values for the final calibration runs.

Table 7. Final values for coefficients adjusted during Lake Oahe temperature calibration

Coefficient	Value
Horizontal eddy viscosity	1.0 $m^2\ s^{-1}$
Minimum vertical eddy viscosity	1.4 x $10^{-7}\ m^2\ s^{-1}$
Horizontal eddy diffusivity	1.0 $m^2\ s^{-1}$
Minimum vertical eddy diffusivity	1.4 x $10^{-6}\ m^2\ s^{-1}$
Bottom frictional resistance	70.0 $m^{1/2}\ s^{-1}$
Fraction of solar radiation absorbed at the water surface	0.45
Light extinction - water	0.40 m^{-1}
Fraction of solar radiation absorbed in the ice surface	0.60
Light extinction - ice	0.07 m^{-1}
Wind sheltering coefficient	1.0
Ice albedo	0.25
Water-to-ice heat exchange	10.0 $W\ m^{-2}\ {}^{o}C^{-1}$

Station near Dam. Computed versus observed temperatures are given in Figure 103 and Figure 104. Observed hypolimnetic temperatures exhibited an interesting behavior of periodically increasing and then decreasing temperatures throughout the summer stratification period. Although not as prevalent, this behavior was also observed in the 1980 data. Assuming that the data are correct, the most likely explanation for this behavior is internal seiching due to winds that causes the thermocline to tilt back and forth. As the thermocline tilts downwards at the dam, hypolimnetic temperatures would increase. As the thermocline tilted upwards at the dam, hypolimnetic temperatures would decrease. This is speculation, but lacking any further data, is a plausible explanation of the observed temperatures. Computed temperatures are in close agreement on July 24 and August 17 but are several degrees colder on July 14 and August 9. Overall, they are in good agreement with the observed data throughout the entire year.

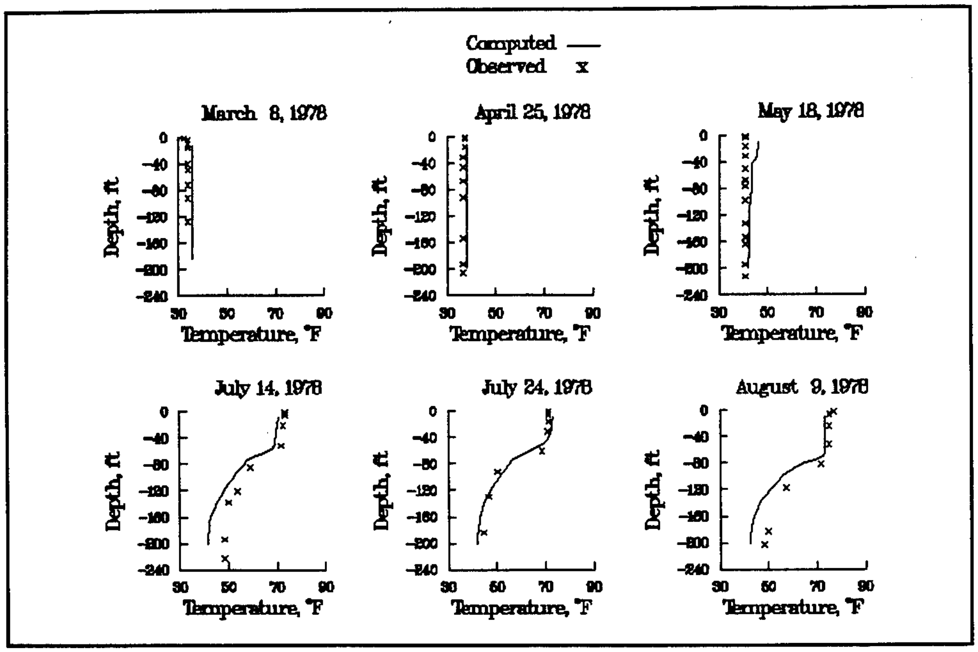

Figure 103. Lake Oahe 1978 computed versus observed temperatures at station near dam, March 8 - August 9

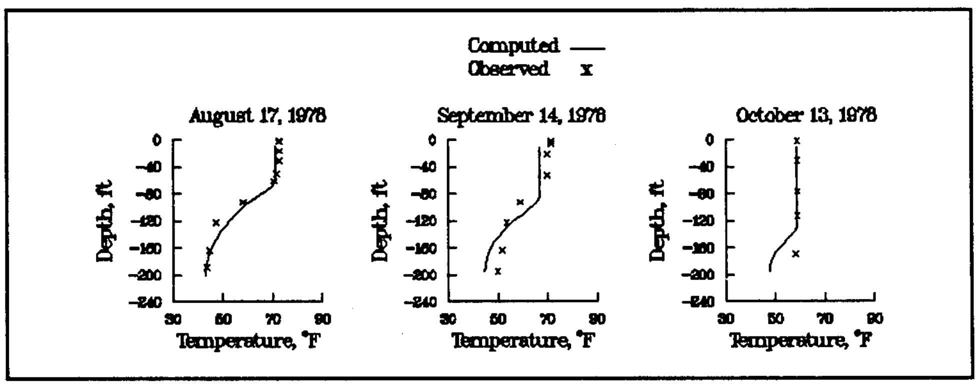

Figure 104. Lake Oahe 1978 computed versus observed temperatures at station near dam, August 17 - October 13

Station near Pollack. Computed versus observed temperatures are shown in Figure 105. Computed temperatures capture the trends throughout the year. The March, April, and October computed profiles are isothermal as are the observed profiles. The May, July, and August profiles are slightly stratified as are the observed profiles.

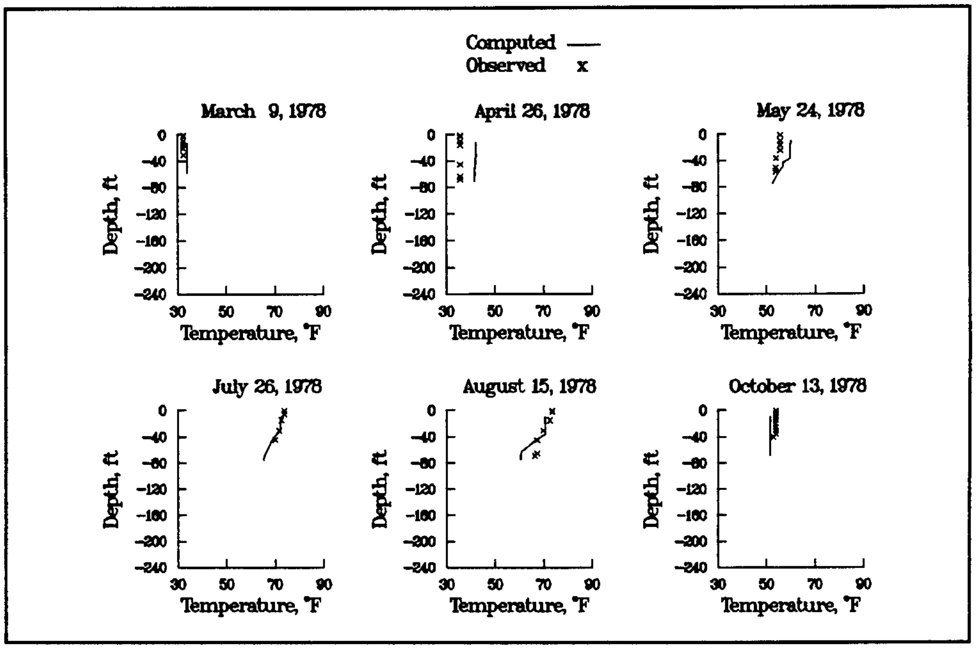

Figure 105. Lake Oahe 1978 computed versus observed temperatures at station near Pollack

Release Temperatures. Computed versus observed release temperatures are shown in Figure 106. Computed temperatures are in general agreement with observed. Unlike Fort Peck Lake and, to a lesser extent Lake Sakakawea, the computed time at which release temperatures begin to decline is in close agreement with the observed time. A much greater variability in computed release temperatures occurs in Lake Oahe compared to Fort Peck Lake and Lake Sakakawea most likely due to the greater variability in releases.

Dissolved Oxygen

Table 8. Lake Oahe calibrated sediment and water column oxygen demand

Segment	Sediment, g m^{-2} day^{-1}	Water Column, g m^{-3} day^{-1}
1-13	0.2	0.05
14-22	0.19-0.11	0.04-0.02
23-43	0.1	0.02

Values for sediment and water column oxygen demand were adjusted until a reasonable fit with observed data was obtained that best represented the average oxygen demand during summer stratification. Table 8 shows the values used for sediment and

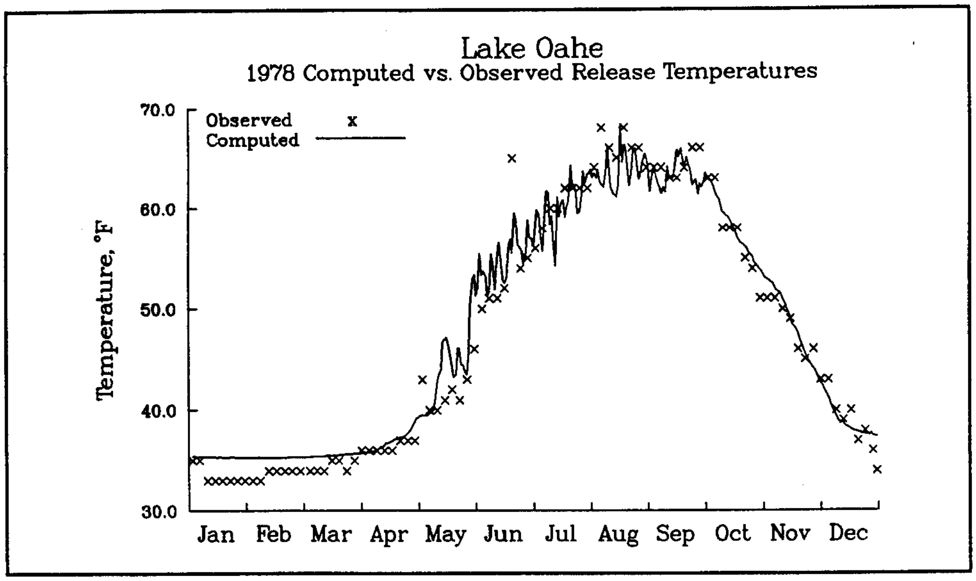

Figure 106. Lake Oahe 1978 computed versus observed release temperatures

water oxygen demand for both years of calibration.

Station Near Dam. Computed versus observed DO concentrations are shown in Figure 107. Observed DO in March and April under ice cover are supersaturated from algal production of DO. The May profile shows close agreement between computed and observed DO just after spring overturn. The July and August computed profiles during summer stratification are typical clinograde DO profiles and are also in close agreement with observed DO. The October profile does not capture the supersaturated conditions at the dam. The supersaturation is likely due to an algal bloom that the present formulation for DO cannot reproduce.

Station Near Pollack. Computed versus observed DO concentrations are shown in Figure 108. With the exception of the August profile, computed DO is in agreement with observed DO. The increase in DO from top to bottom in the computed August profile must be due to an underflow bringing oxygenated waters to the hypolimnion since the reservoir is stratified at this station on this date.

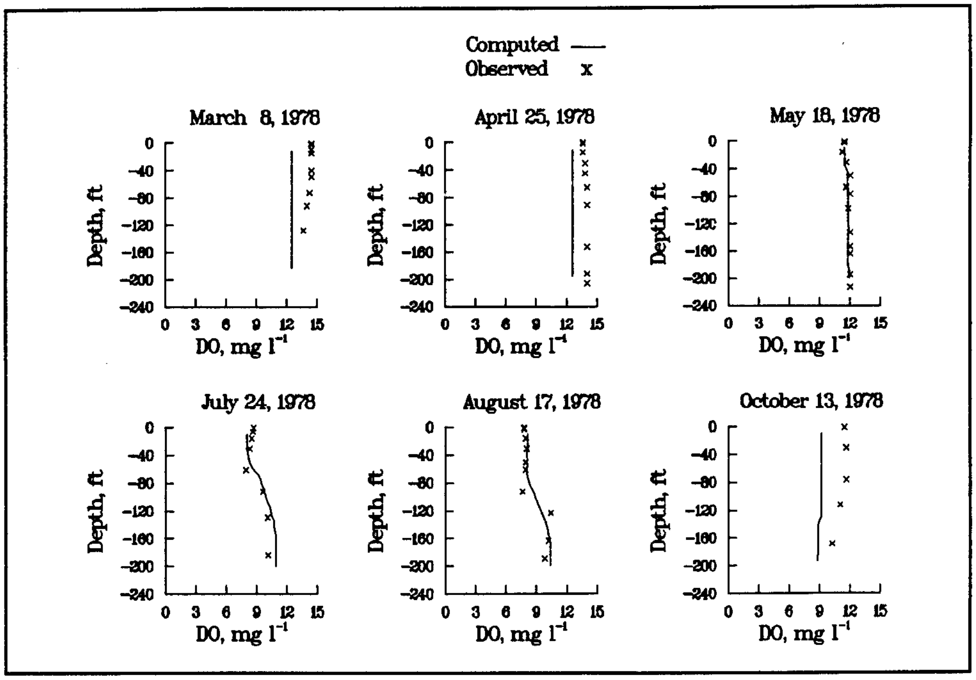

Figure 107. Lake Oahe 1978 computed versus observed DO at station near dam

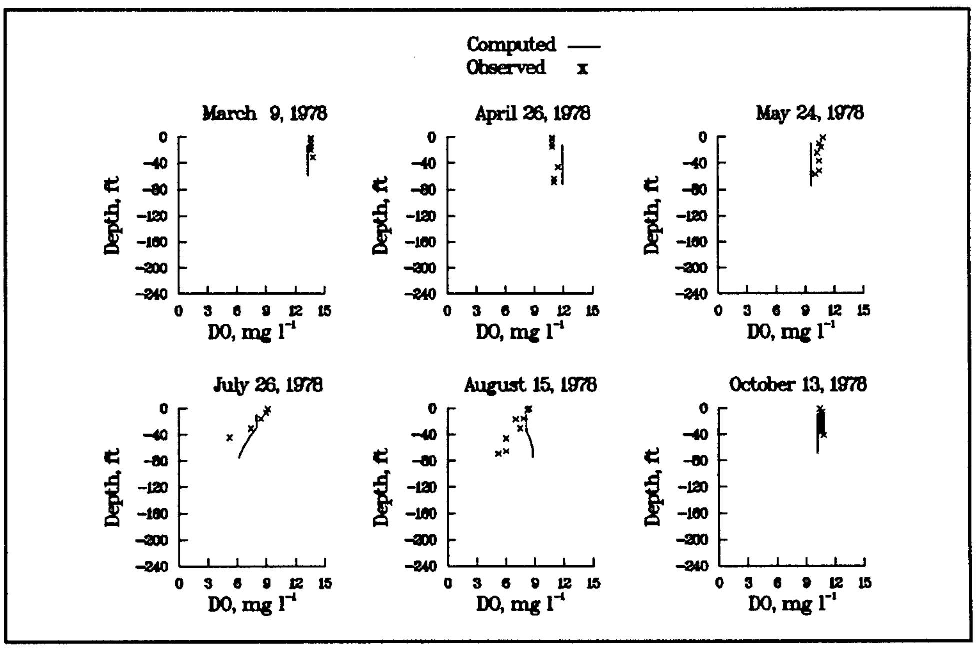

Figure 108. Lake Oahe 1978 computed versus observed DO at station near Pollack

Release DO. Computed release DO is shown in Figure 109.

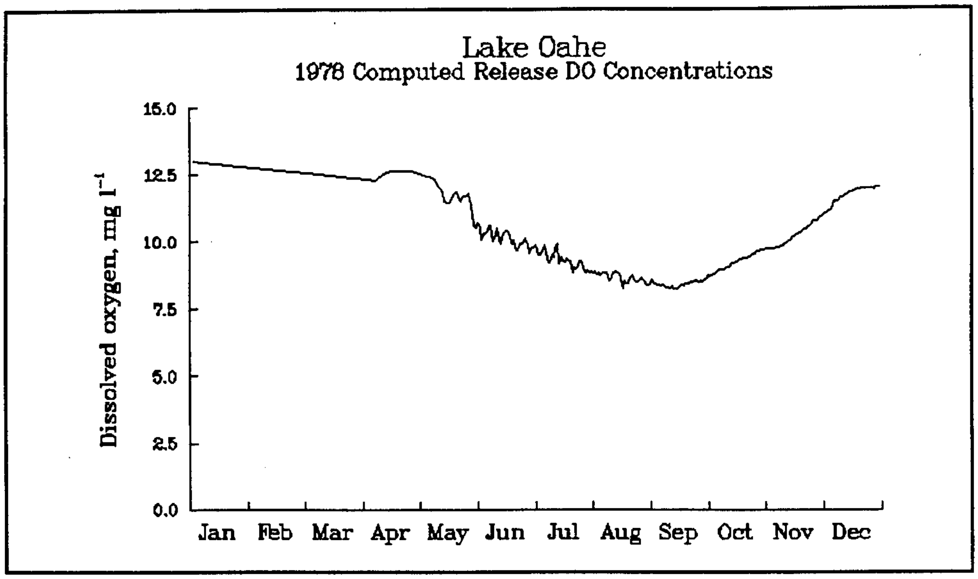

Figure 109. Lake Oahe 1978 release DO

Lake Oahe 1980 Simulation

Water Surface Elevations

Computed versus observed water surface elevations are shown in Figure 110. The net decrease in storage was 11.8 ft with elevations ranging from 1,596.4 ft to 1,608.2 ft. Differences in computed and observed stages were less than 0.5 ft throughout the year.

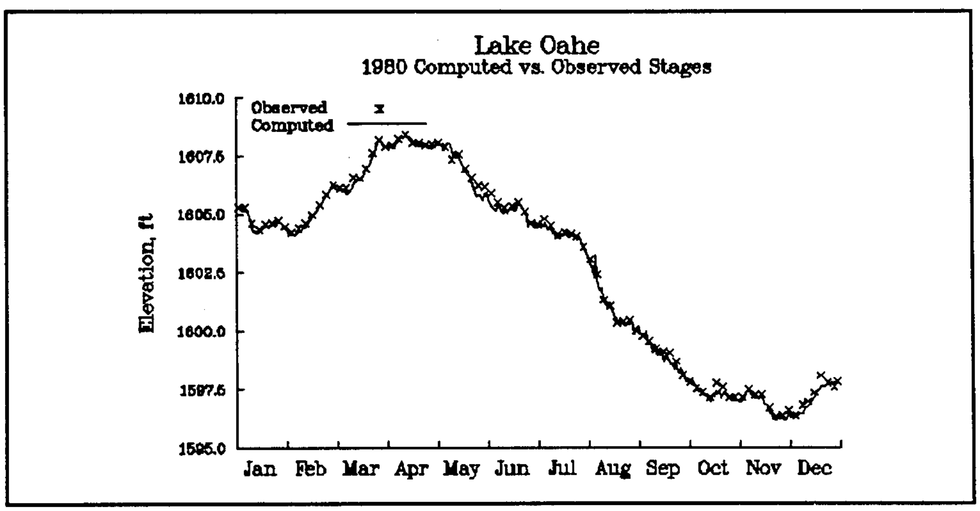

Figure 110. Lake Oahe 1980 computed versus observed water surface elevations

Ice Cover

Computed ice cover is shown in Figure 111. Ice-out was predicted on April 19 and reported ice-out occurred on April 8. Reported ice-in occurred on January 3, 1981. No ice-in date was available from the 1980 simulation since the run did not continue into 1981.

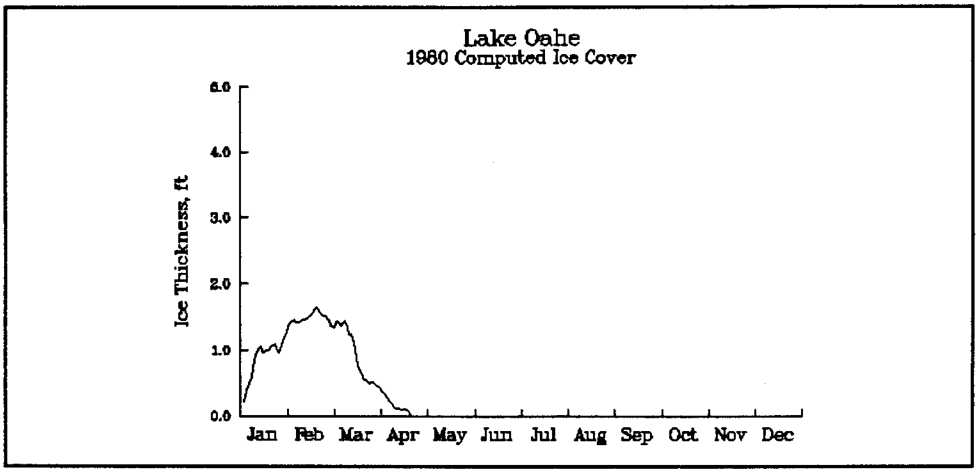

Figure 111. Lake Oahe 1980 computed ice cover

Temperature

Station Near Dam. Computed versus observed temperatures are shown in Figure 112 and Figure 113. The April and May computed profiles are in close agreement with observed data. The observed hypolimnetic temperature in June is > 5°F warmer than in July possibly due to seiching. Computed temperatures are lower than observed in June, but the July and August profiles are in close agreement. At the start of overturn in September, the computed depth of the thermocline is below the observed depth. Six days later, the observed depth of the thermocline is deeper than the computed depth. This is an excellent demonstration of the variability of temperature profiles during fall overturn. Computed temperatures may have been in much closer agreement either one day earlier or later. By October 22, the model predicted complete overturn. Observed data showed the reservoir was slightly stratified.

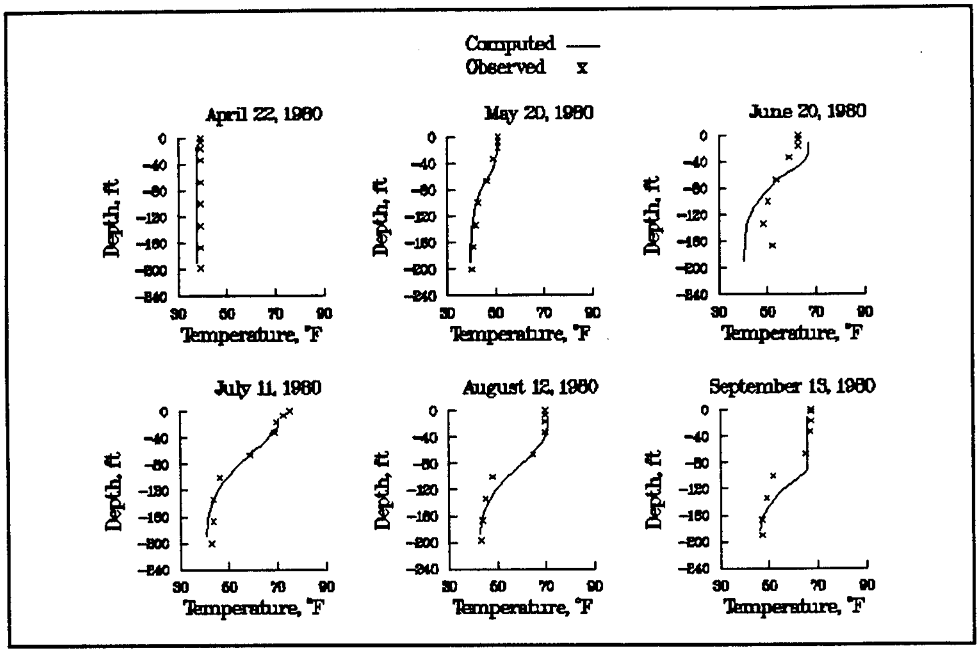

Figure 112. Lake Oahe 1980 computed versus observed temperatures at station near Dam, April 22 - September 13

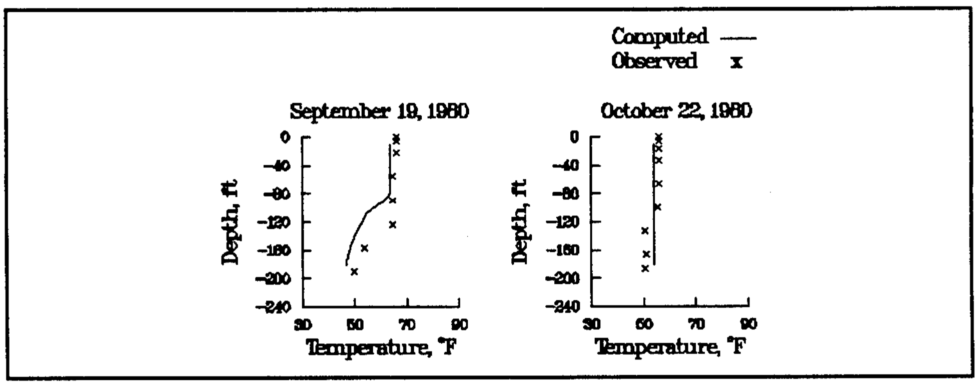

Figure 113. Lake Oahe 1980 computed versus observed temperatures at station near Dam, September 19 - October 22

Station Near Pollock. Computed versus observed temperatures are shown in Figure 114 and Figure 115. Computed temperatures are in close agreement with observed throughout the year. The model correctly predicts stratified conditions in April and May with virtually no stratification throughout the summer.

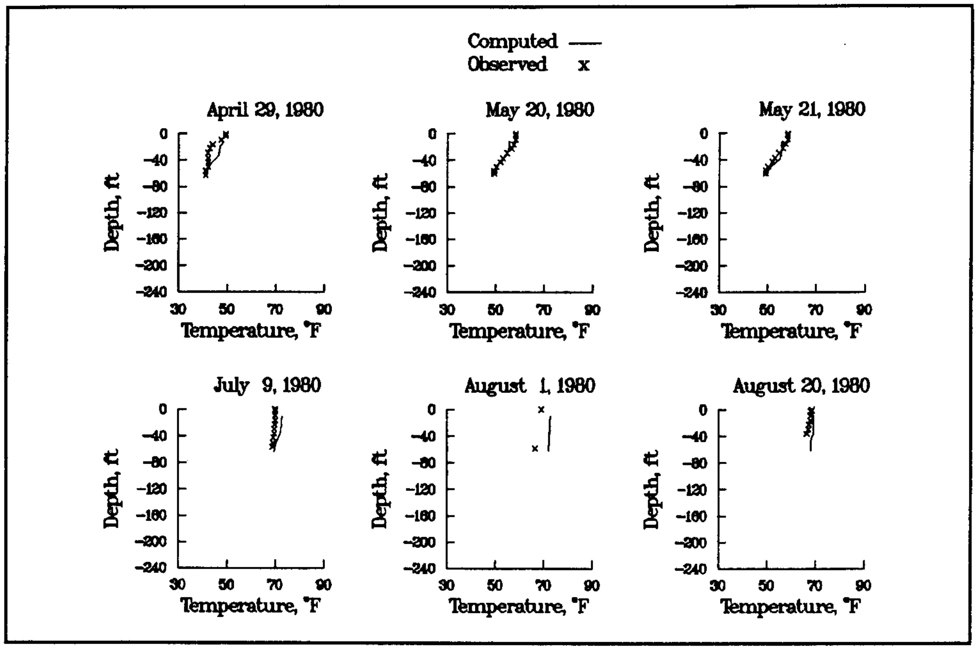

Figure 114. Lake Oahe 1980 computed versus observed temperatures at station near Pollack, April 29 - August 20

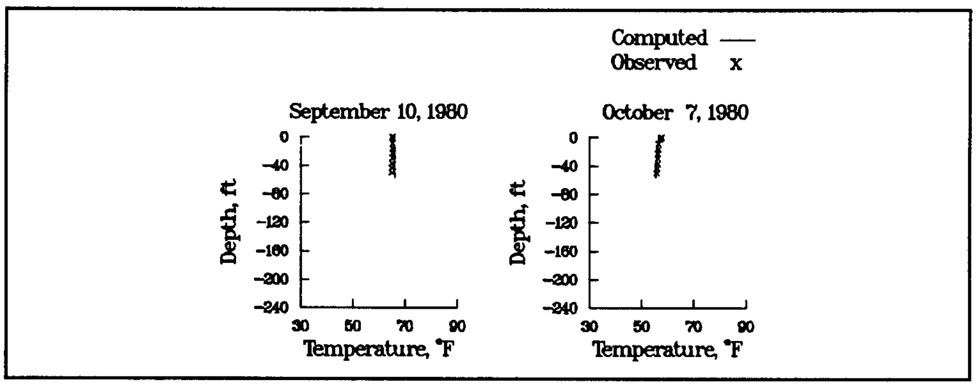

Figure 115. Lake Oahe 1980 computed versus observed temperatures at station near Pollack, September 10 - October 7

Release Temperature. Computed versus observed release temperatures are shown in Figure 116. Computed temperatures are in general agreement with observed throughout the year. Computed release temperatures showed a much greater variability than any of the other reservoirs which is some evidence that the model may be capturing some of the internal seiching suspected to occur.

Dissolved Oxygen

Station near Dam. Computed versus observed DO concentrations are shown in Figure 117. Again, the model did not reproduce the supersaturated conditions in spring that were most likely due to an algal bloom. The remainder of the computed profiles were in general agreement with observed data. The

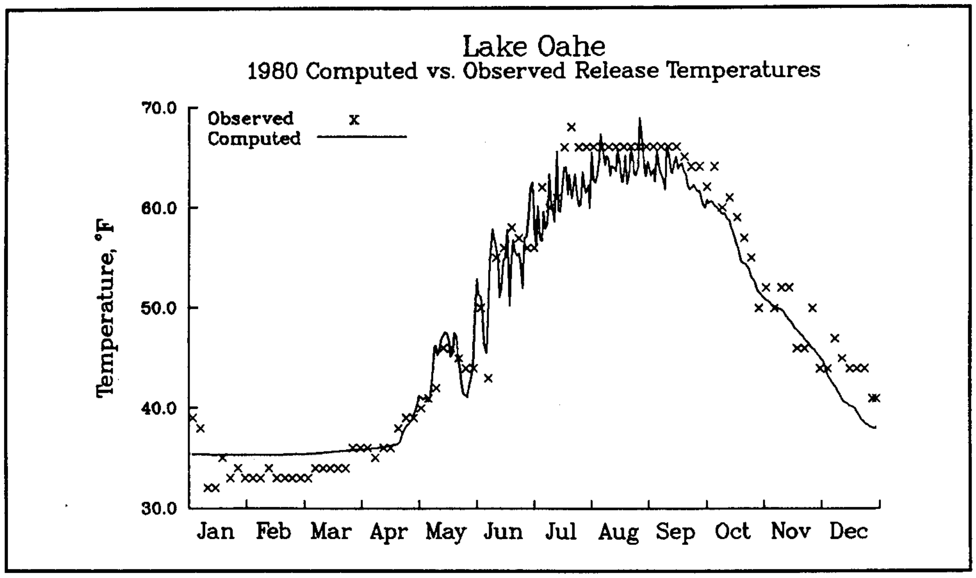

Figure 116. Lake Oahe 1980 computed versus observed release temperatures

computed profiles did not capture all of the hypolimnetic DO depletion in September and October.

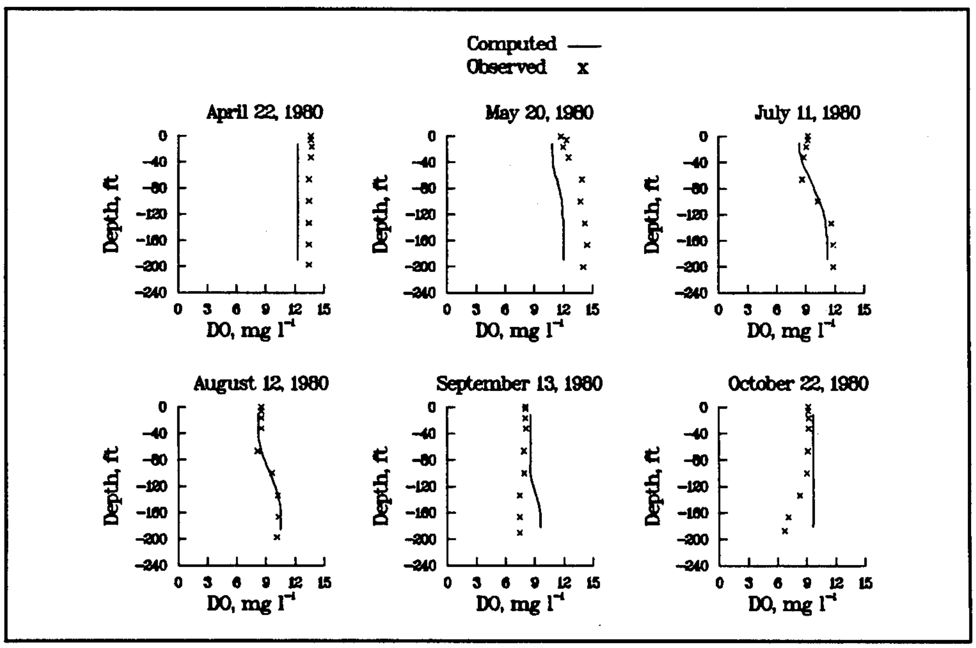

Figure 117. Lake Oahe 1980 computed versus observed DO at station near dam

Station Near Pollack. Computed versus observed DO concentrations are shown in Figure 118 and Figure 119. For reasons mentioned previously, the model does not capture the supersaturated conditions in April and May. The remainder of the computed profiles are in general agreement with observed data.

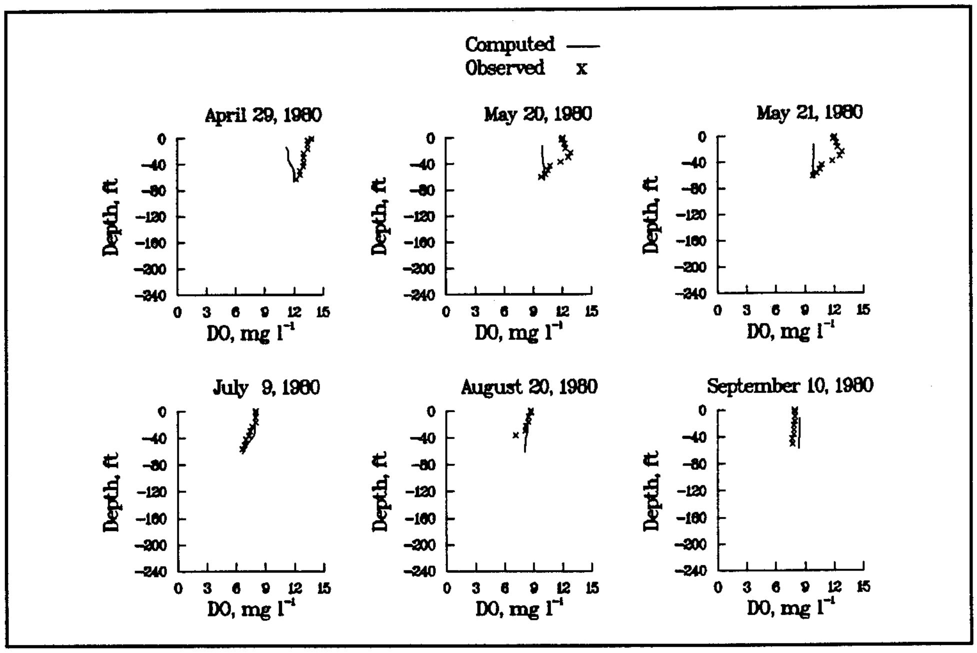

Figure 118. Lake Oahe 1980 computed versus observed DO at station near Pollack, April 29 - September 10

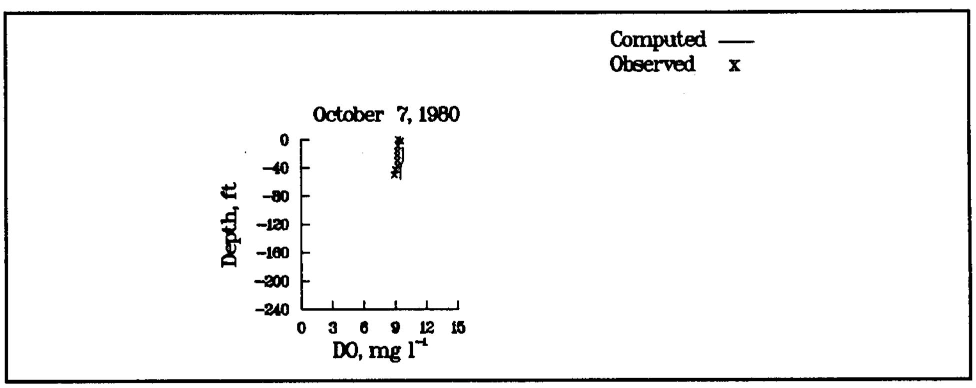

Figure 119. Lake Oahe 1980 computed versus observed DO at station near Pollack, October 7

Release DO. Computed release DO concentrations are shown in Figure 120.

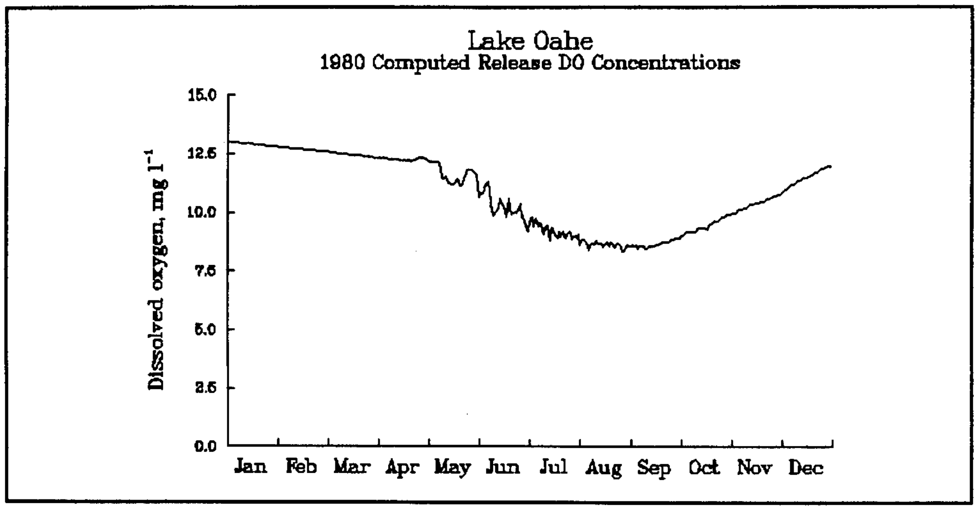

Figure 120. Lake Oahe 1980 computed release DO

Lake Francis Case 1978 Simulation

Water Surface Elevations

Computed versus observed water surface elevations are shown in Figure 121. The net decrease in storage was 3 ft with elevations ranging from 1337.8 ft to 1362.6 ft. Differences in computed and observed stages were less than 0.5 ft throughout the year.

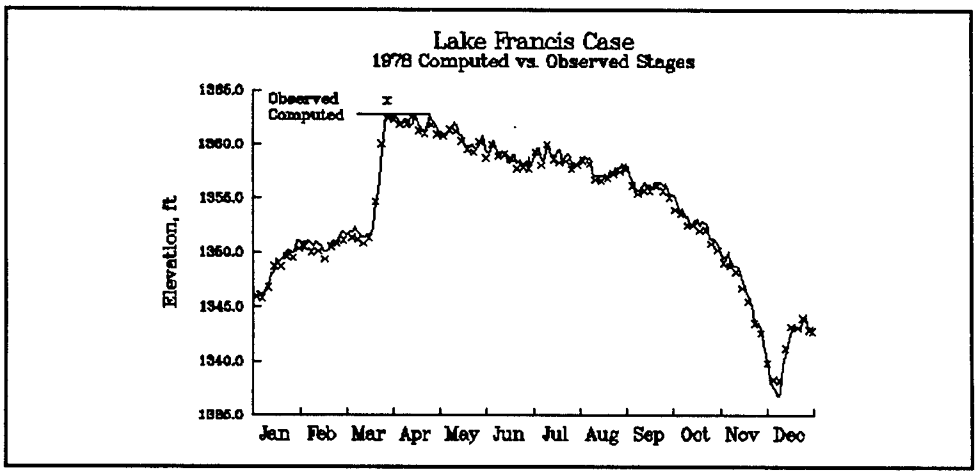

Figure 121. Lake Francis Case 1978 computed versus observed stages at dam

Ice Cover

Computed ice cover is shown in Figure 122. Reported ice-out was on April 3 and computed ice-out was on April 7. Reported ice-in was on December 24, 1978 and computed ice-in was on December 17. This is the only year out of 1978 and 1980 for all four reservoirs that reported ice-in and ice-out occurred during the same year. This is also the only year for all four reservoirs in which computed ice-in and ice-out occurred during the same year.

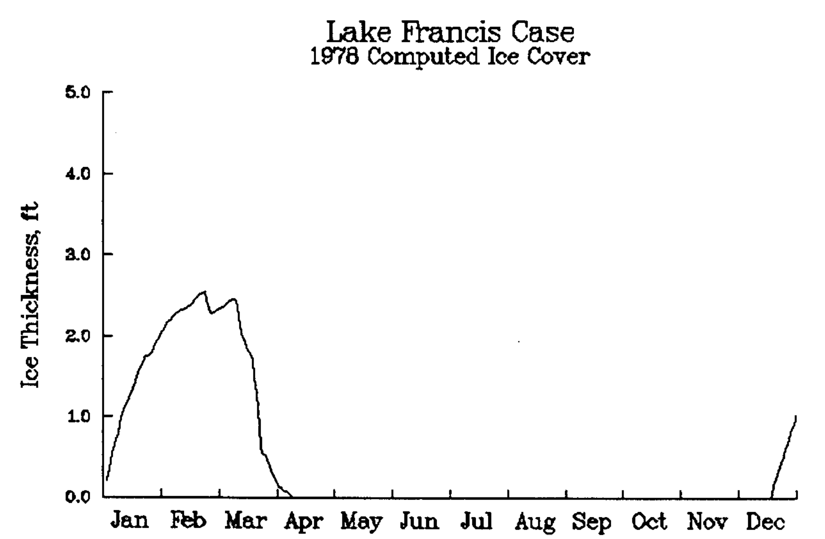

Figure 122. Lake Francis Case 1978 computed ice cover

Temperature

Unlike the upper three reservoirs, inflows to Lake Francis Case play a more dominant role in the heat budget. Residence time in 1978 for Lake Francis Case was ≈ 2 months compared to ≈ 2 years for Fort Peck Lake, ≈ 1 year for Lake Sakakawea, and ≈ 1 year for Lake Oahe. As a result, Lake Francis Case undergoes intermittent stratification during the summer. Table 9 gives the values of all coefficients affecting temperature and ice computations. As in the other three reservoirs, all values except for the minimum eddy diffusivity were reset to default values for the final calibration runs.

Station Near Dam. As mentioned previously, Lake Francis Case stratifies only briefly during the summer with much warmer hypolimnetic temperatures than the three upper reservoirs. The July 7 and 21 profiles are the only observed profiles that are stratified. These are the only times that computed profiles are stratified to any degree. The remainder of the observed profiles are essentially isothermal. Computed temperatures are in general agreement with observed for these dates (Figure 123 and Figure 124).

Table 9. Final values for coefficients adjusted during Lake Francis Case temperature calibration

Coefficient	Value
Horizontal eddy viscosity	1.0 m^2 s^{-1}
Minimum vertical eddy viscosity	1.4 x 10^{-7} m^2 s^{-1}
Horizontal eddy diffusivity	1.0 m^2 s^{-1}
Minimum vertical eddy diffusivity	1.4 x 10^{-6} m^2 s^{-1}
Bottom frictional resistance	70.0 $m^{1/2}$ s^{-1}
Fraction of solar radiation absorbed at the water surface	0.45
Light extinction - water	0.4 m^{-1}
Fraction of solar radiation absorbed in the ice surface	0.60
Light extinction - ice	0.07 m^{-1}
Wind sheltering coefficient	1.0
Ice albedo	0.25
Water-to-ice heat exchange	10.0 W m^{-2} $°C^{-1}$

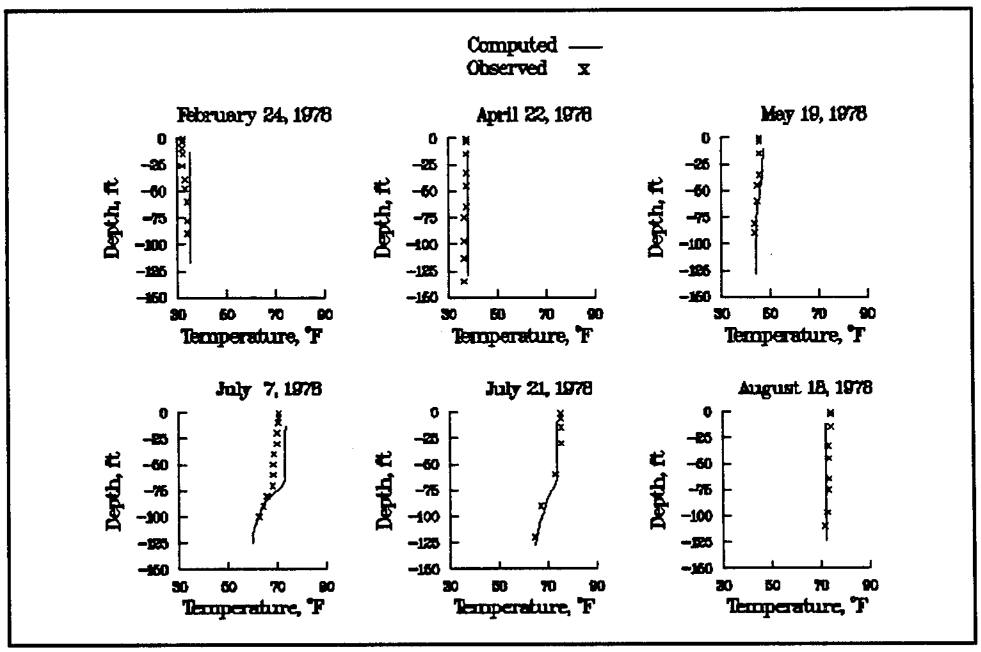

Figure 123. Lake Francis Case 1978 computed versus observed temperatures at station near dam, February 24 - August 18

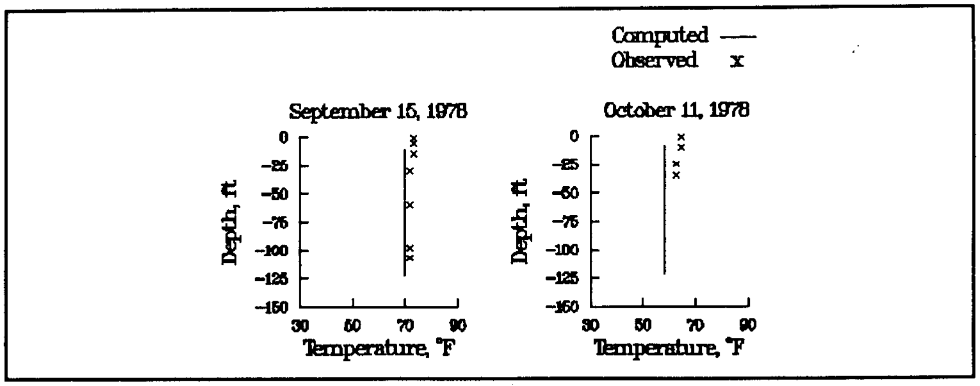

Figure 124. Lake Francis Case 1978 computed versus observed temperatures at station near dam, September 15 - October 11

Station near Elm Creek. Computed versus observed temperatures are shown in Figure 125. With the exception of May 19, computed temperatures are in fairly close agreement with observed. This station shows no stratification during summer.

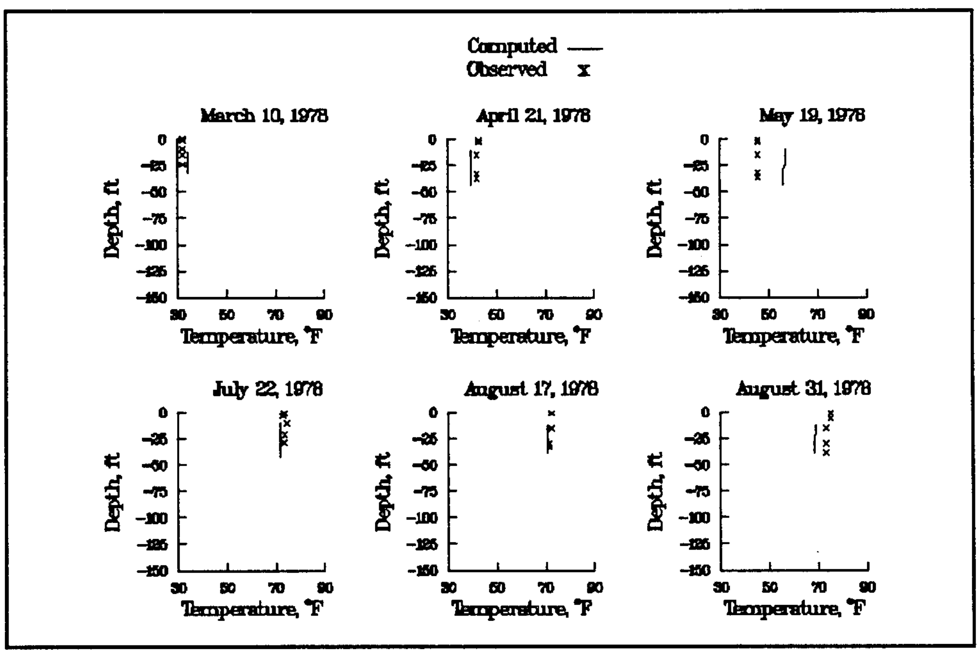

Figure 125. Lake Francis Case 1978 computed versus observed temperatures at station near Elm Creek

Release Temperatures. Computed versus observed release temperatures are shown in Figure 126. Computed release temperatures are in close agreement until August when computed temperatures are ≈ 5°F colder than observed. During this time, observed in-pool temperatures at the dam are 74°F at the surface to 7 °F at the bottom, computed in-pool temperatures are 72.4°F from top to bottom, and observed release temperatures are 75°F. Since observed release temperatures are greater than observed in-pool temperatures, there is obviously some error associated with either the observed release temperatures or observed in-pool temperatures. In any case, the maximum difference between computed and observed release temperatures is 3°F. As in Fort Peck Lake and Lake Sakakawea, computed release temperatures begin to decrease earlier in the fall than observed.

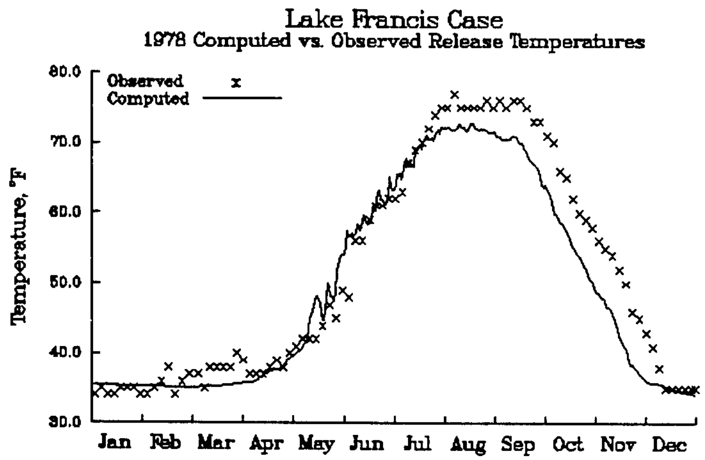

Figure 126. Lake Francis Case 1978 computed versus observed release temperatures

Dissolved Oxygen

Table 10. Lake Francis Case calibrated sediment and water column oxygen demand

Segment	Sediment, g m^{-3} day^{-1}	Water Column, g m^{-2} day^{-1}
1-40	0.5	0.08

Values for sediment and water column oxygen demand were adjusted until a reasonable fit with observed data was obtained that best represented the average oxygen demand during summer stratification. Table 10 gives the values for sediment and water column oxygen demand used in the 1978 and 1980 calibrations. Because of the short residence time, oxygen demand did not vary longitudinally as in the upstream reservoirs.

Station Near Dam. Computed versus observed DO concentrations are shown in Figure 127 and Figure 128. Except for April 22 and October 11 when the observed DO was supersaturated, computed and observed DO profiles are in general agreement. During July when Lake Francis Case was stratified, computed hypolimnetic DO is in close agreement with observed.

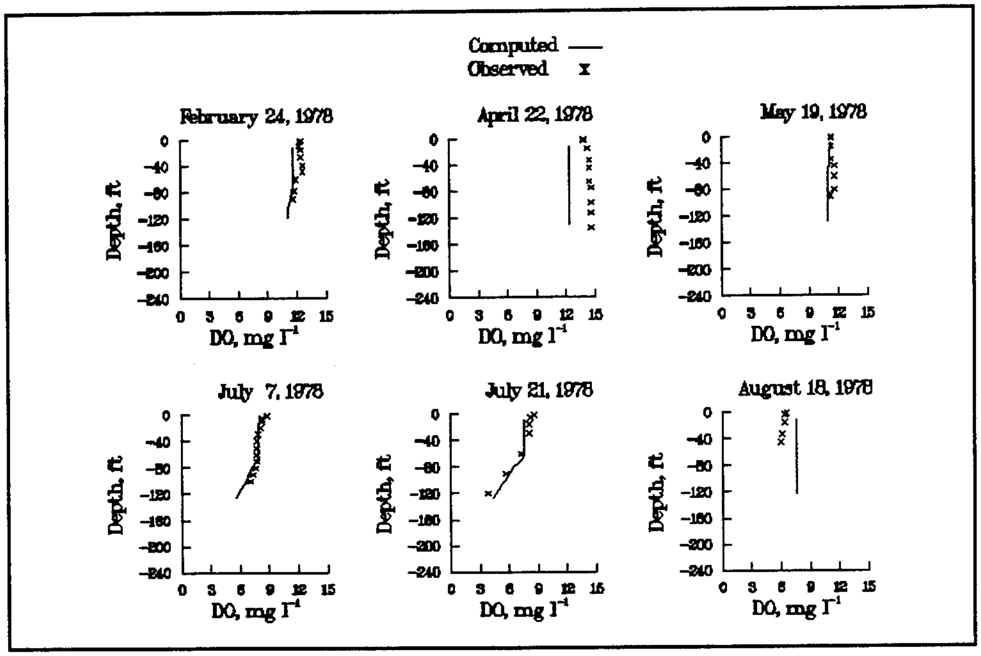

Figure 127. Lake Francis Case 1978 computed versus observed DO at station near dam, February 24 - August 18

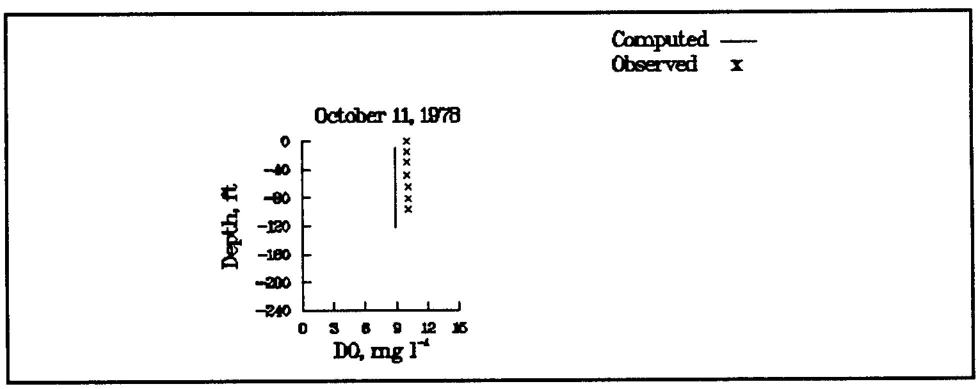

Figure 128. Lake Francis Case 1978 computed versus observed DO at station near dam, October 11

Station Near Elm Creek. Computed versus observed DO concentrations are shown in Figure 129. Since this station does not stratify, computed DO is saturated throughout the year. Deviations from observed data are due to DO uptake under ice-cover and algal produced supersaturation.

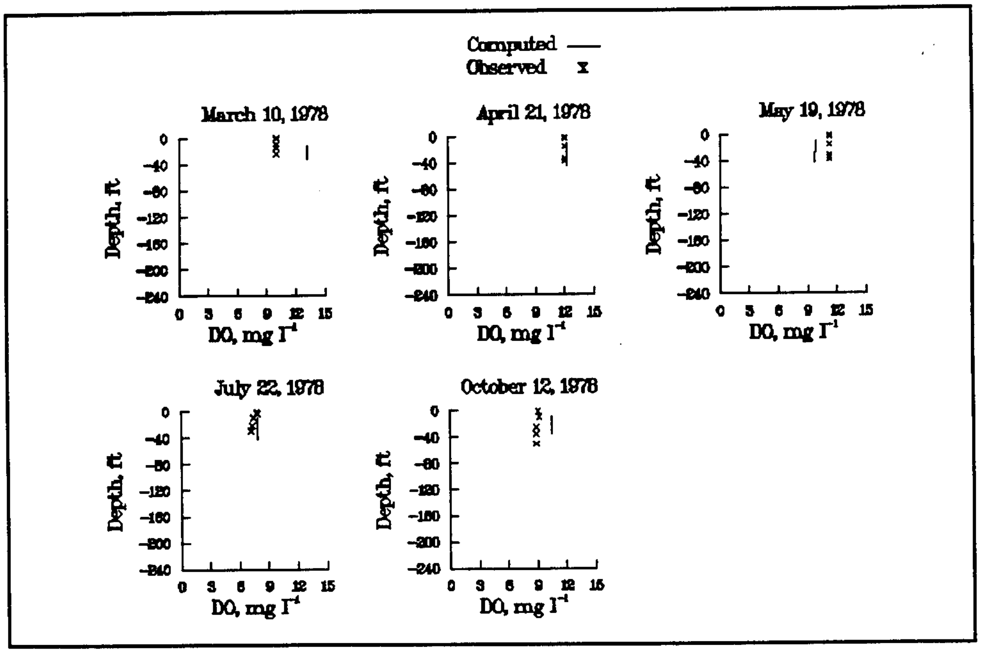

Figure 129. Lake Francis Case 1978 computed versus observed DO at station near Elm Creek

Release DO. Computed release DO concentrations are shown in Figure 130. Release DO concentration approaches 5 $mg\,l^{-1}$ in August which is the lowest of the modeled reservoirs.

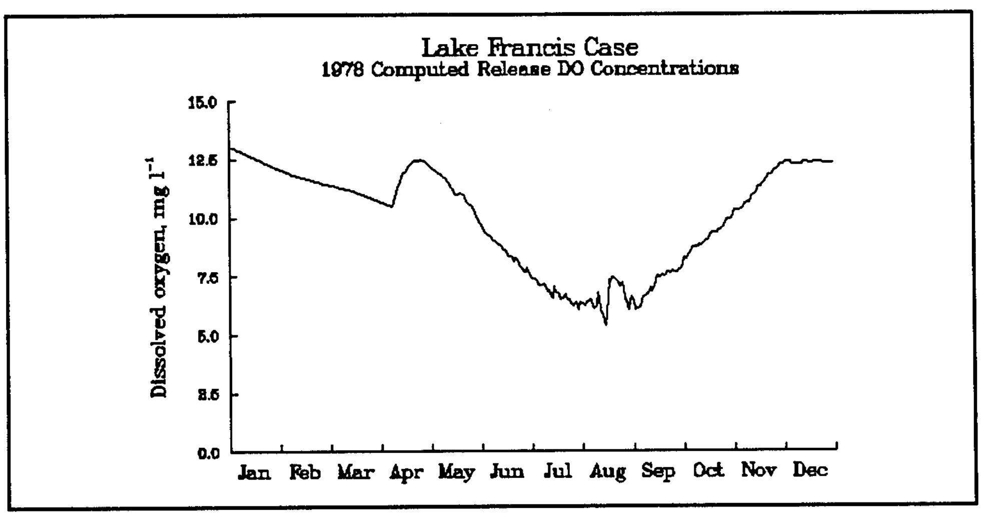

Figure 130. Lake Francis Case 1978 release DO

Lake Francis Case 1980 Simulation

Water Surface Elevations

Computed versus observed water surface elevations are shown in Figure 131. Water surface level decreased by 0.4 ft during 1980. Elevations ranged from 1,338.1 ft to 1,358.7 ft. Differences in computed and observed stages were less than 1 ft throughout the year.

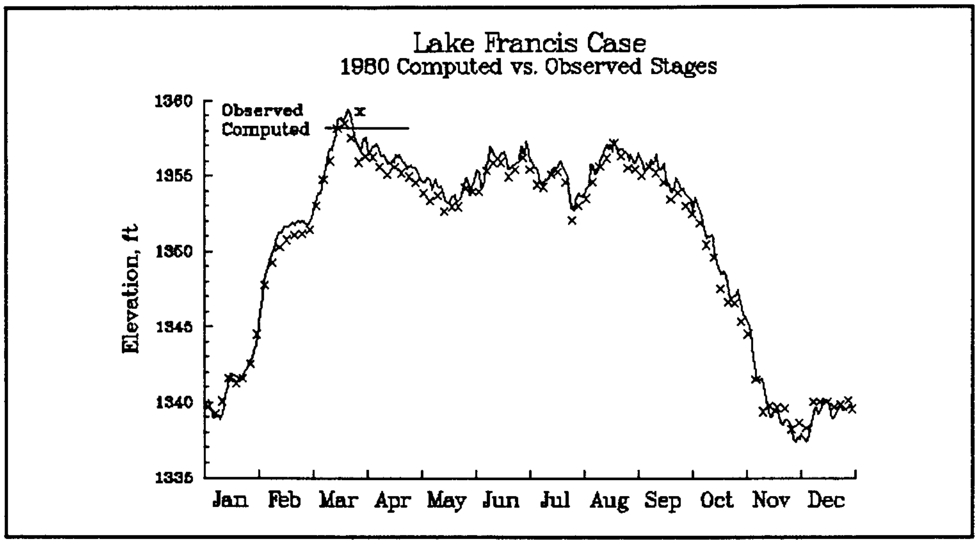

Figure 131. Lake Francis Case 1980 computed versus observed stages at dam

Ice Cover

Computed ice cover is shown in Figure 132. Reported ice-out was on April 3 and computed ice-out was on April 19. Reported ice-in was on January 8, 1981. No ice-in date was available from the 1980 simulation since it did not continue into 1981.

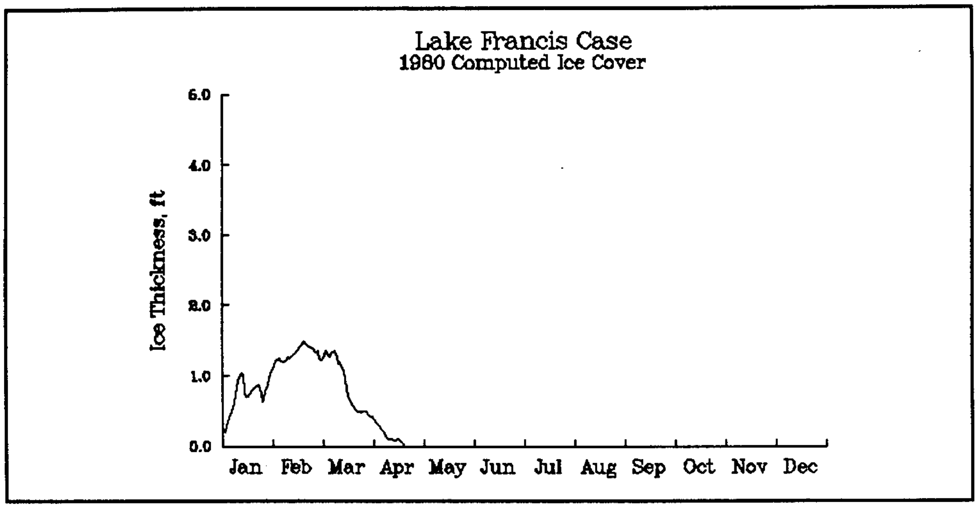

Figure 132. Lake Francis Case 1980 computed ice cover

Temperature

Station Near Dam. Computed versus observed temperatures are shown in Figure 133 and Figure 134. Computed temperatures are consistently lower than observed temperatures throughout the simulation by ≈ 3-4°F with the exception of the profile in June. There are two possible sources of error for the under-prediction. Meteorologic data used in the heat exchange computations were obtained from Pierre, SD which is located upstream of Lake Sharpe approximately 120 miles northwest of the dam. Another possible source of error is the inflow temperatures obtained from Lake Sharpe releases since the residence time is so short in Lake Francis Case. The problem in determining the source of error is that the 1978 temperature predictions are in much closer agreement with observed data than the 1980 simulations. In any event, the model did show that the reservoir was slightly stratified from March to June which is in agreement with observed data. By August, both computed and observed profiles showed that the reservoir was very nearly isothermal.

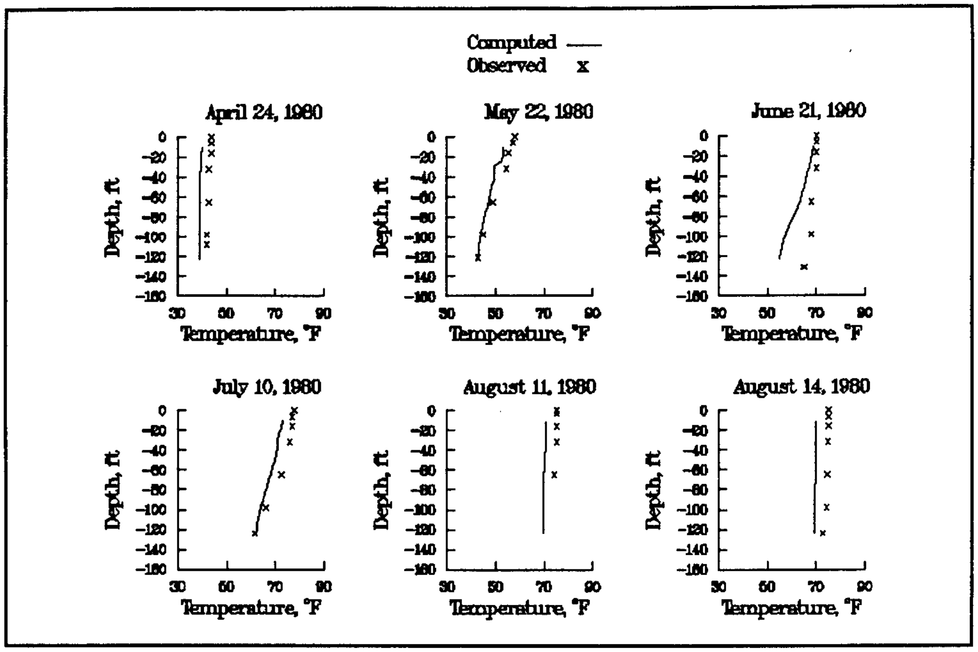

Figure 133. Lake Francis Case 1980 computed versus observed temperatures at station near dam, April 24 - August 14

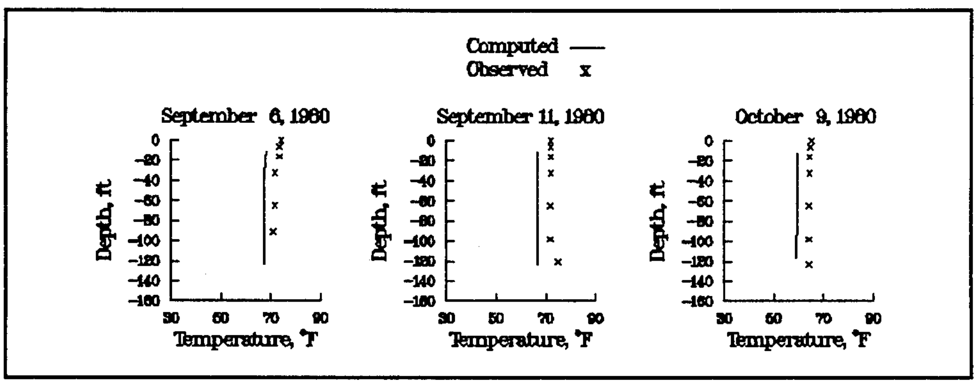

Figure 134. Lake Francis Case 1980 computed versus observed temperatures at station near dam, September 6 - October 9

Station Near Elm Creek. Computed versus observed temperatures are shown in Figure 135. Again, the model consistently underpredicts observed temperatures. The discrepancy is even greater at this station suggesting that the most likely source of error in temperature predictions is the inflow temperatures.

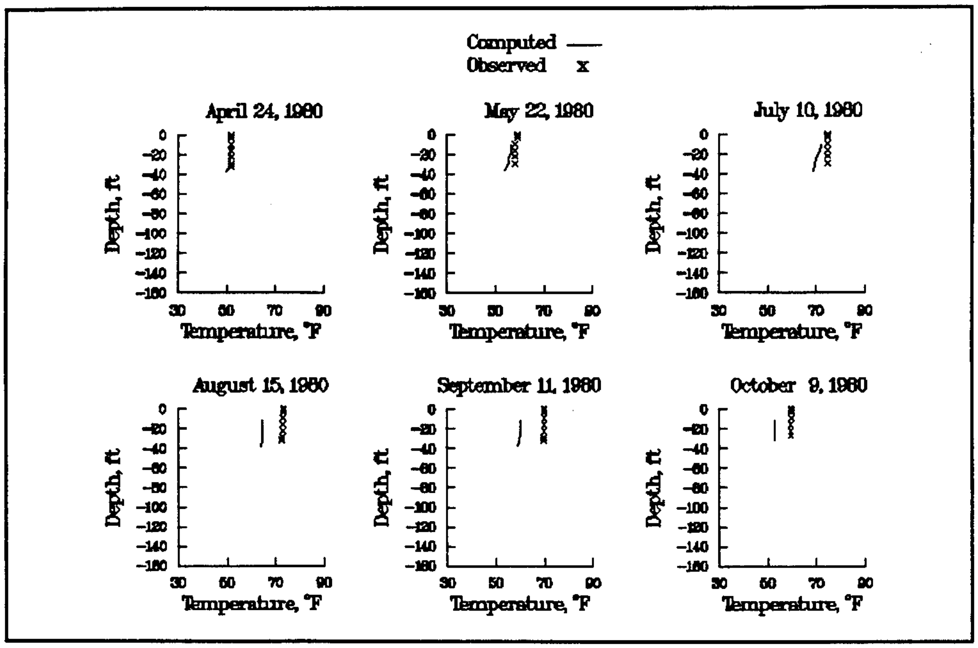

Figure 135. Lake Francis Case 1980 computed versus observed temperatures at station near Elm Creek

Release Temperature. Computed versus observed release temperatures are shown in Figure 136. As in 1978, computed release temperatures are consistently less than observed release temperatures starting in late July and continuing until late December. One source of error is the previously mentioned underprediction of temperatures at the dam. However, there is a discrepancy in the observed data in that the release temperatures in August are ≈ 2°F greater than the observed temperatures at the dam. For example, on August 11 the maximum in-pool temperature at the dam was 75°F while the observed release temperature was 78.8°.

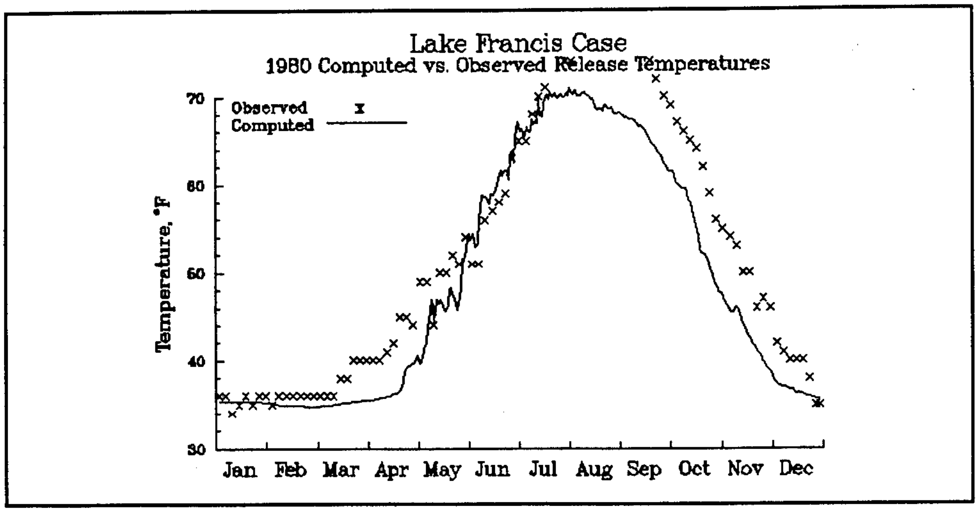

Figure 136. Lake Francis Case 1980 computed versus observed release temperatures

Dissolved Oxygen

Station Near Dam. Computed versus observed DO concentrations are shown in Figure 137. With the exception of April and May when the water column was supersaturated, computed and observed DO profiles are in close agreement.

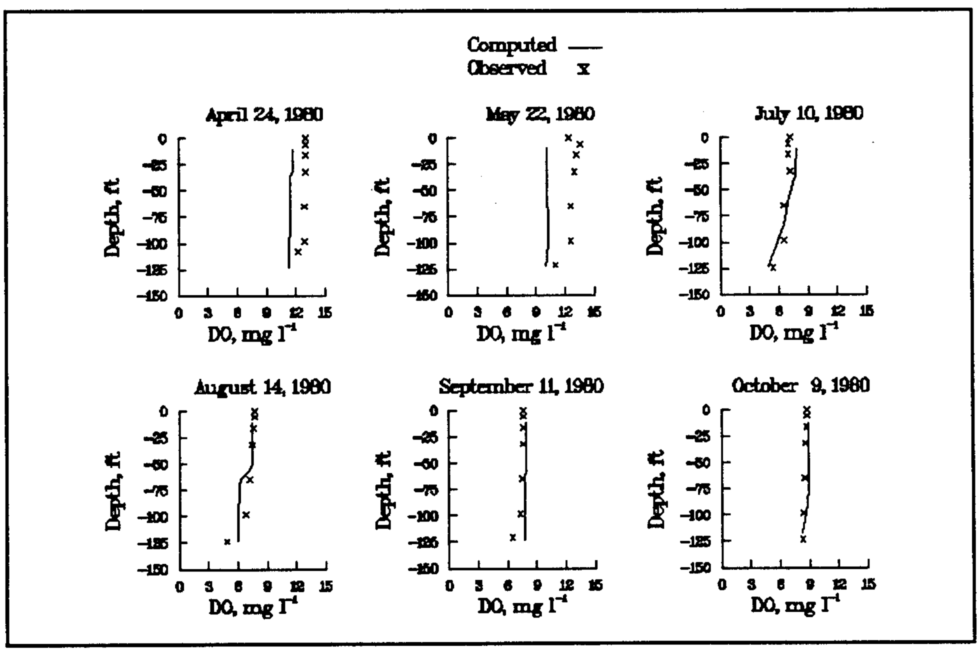

Figure 137. Lake Francis Case 1980 computed versus observed DO at station near dam.

Station Near Elm Creek. Computed versus observed DO concentrations are shown in Figure 138. Observed DO profiles in April and May were supersaturated. An oxygen deficit existed in September and October which the model did not capture. Computed temperatures in July and August are in general agreement with observed.

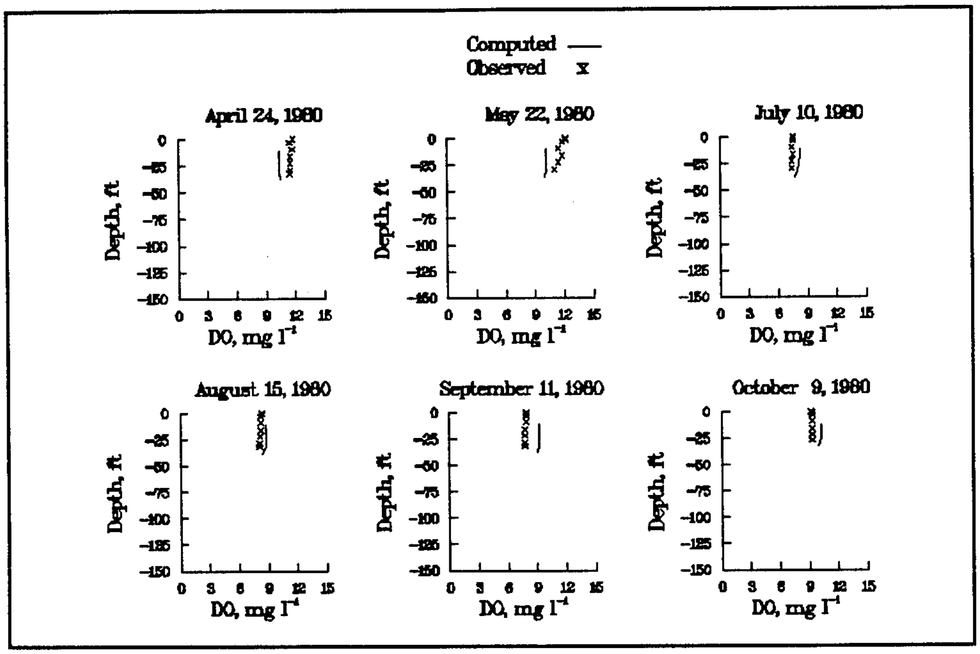

Figure 138. Lake Francis Case 1980 computed versus observed DO at station near Elm Creek

Release DO. Computed release DO concentrations are shown in Figure 139.

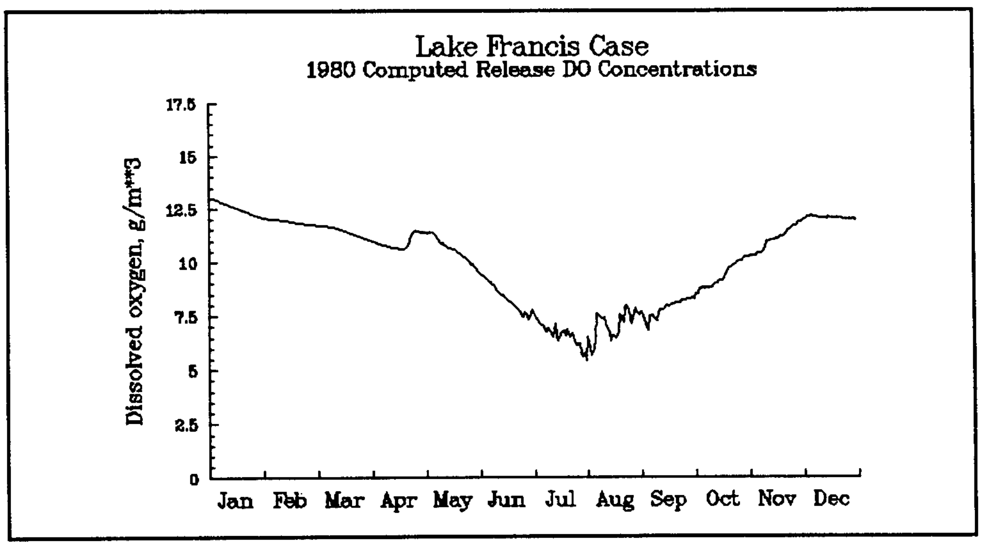

Figure 139. Lake Francis Case 1980 computed release DO

4 Operational Scenarios

As stated in the introduction, nine operational scenarios were conducted that encompassed a 30 year period from 1960-1990. The first 11 years consisted of surrogate years that were intended to represent the drought of the 1930's while the remainder used actual data from 1972-1990. Table 11 summarizes the nine operational scenarios.

Table 11. Summary of scenarios

Scenario	Study ID	Minimum Pool (acre-ft x 10^6)	Non-Navigation Releases (cfs x 10^3)	
			Winter	Summer
1	AFWQ1209	18.3	12	9
2	AIWQ1225	18.3	12	25
3	CFWQ1209	31.0	12	9
4	CHWQ1218	31.0	12	18
5	EFWQ1209	44.0	12	9
6	EHWQ1218	44.0	12	18
7	PFWQ1209	power series	12	9
8	PIWQ1225	power series	12	25
9	EVQ1			

Input Data

Inflows

Inflows for the surrogate years were obtained by combining the inflow and evaporation data with the actual depletion data for 1930-1941. The remaining years consisted of the actual inflow, evaporation, and depletion data.

Fort Peck Lake. Inflows for each scenario are given in Figure 140-Figure 148. Although differences in inflows existed for all nine scenarios, the differences were not as pronounced when compared to the other three reservoirs.

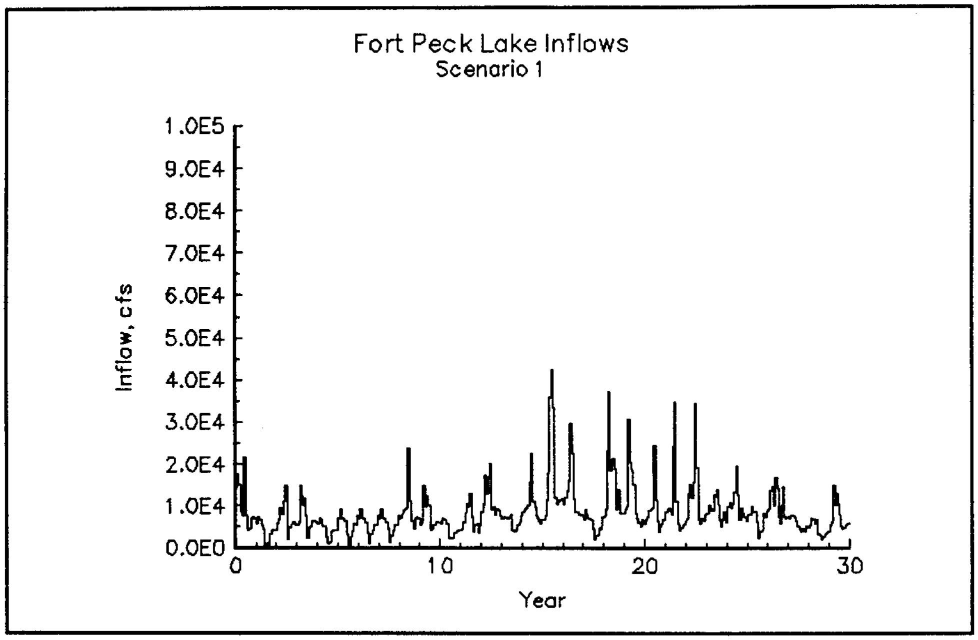

Figure 140. Fort Peck Lake scenario 1 inflows

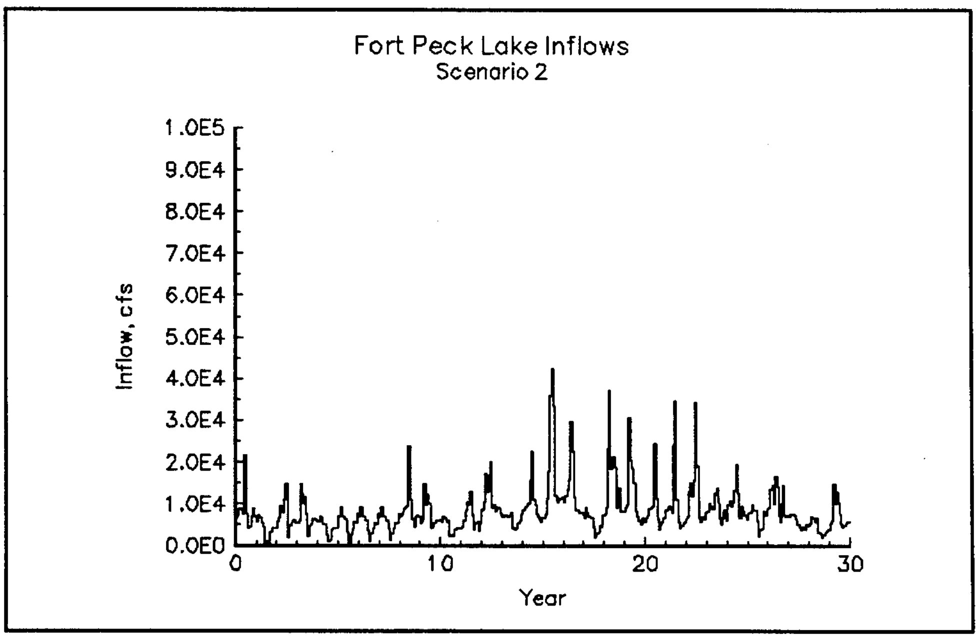

Figure 141. Fort Peck Lake scenario 2 inflows

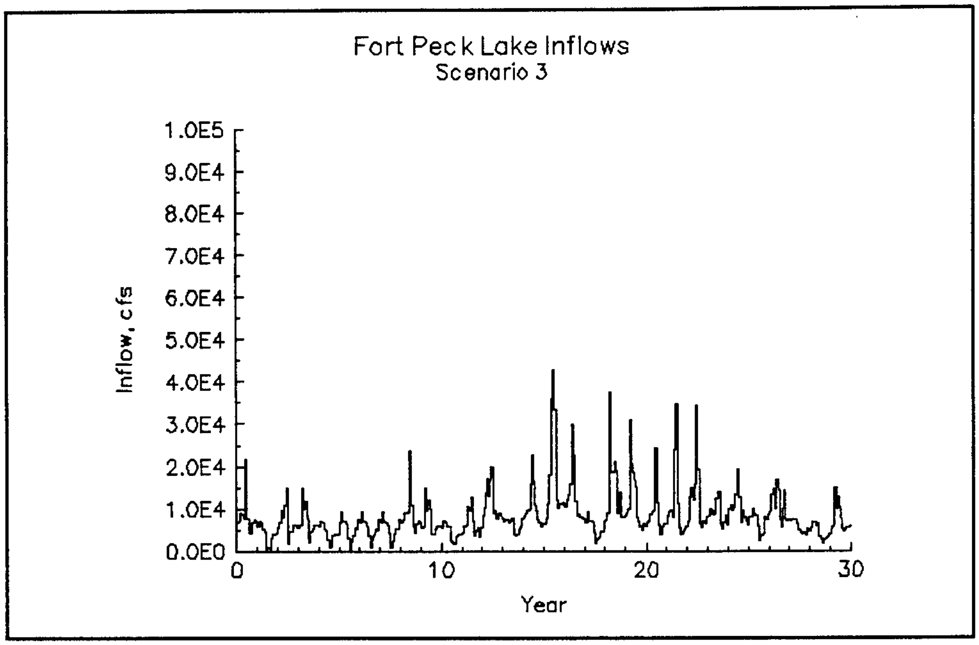

Figure 142. Fort Peck Lake scenario 3 inflows

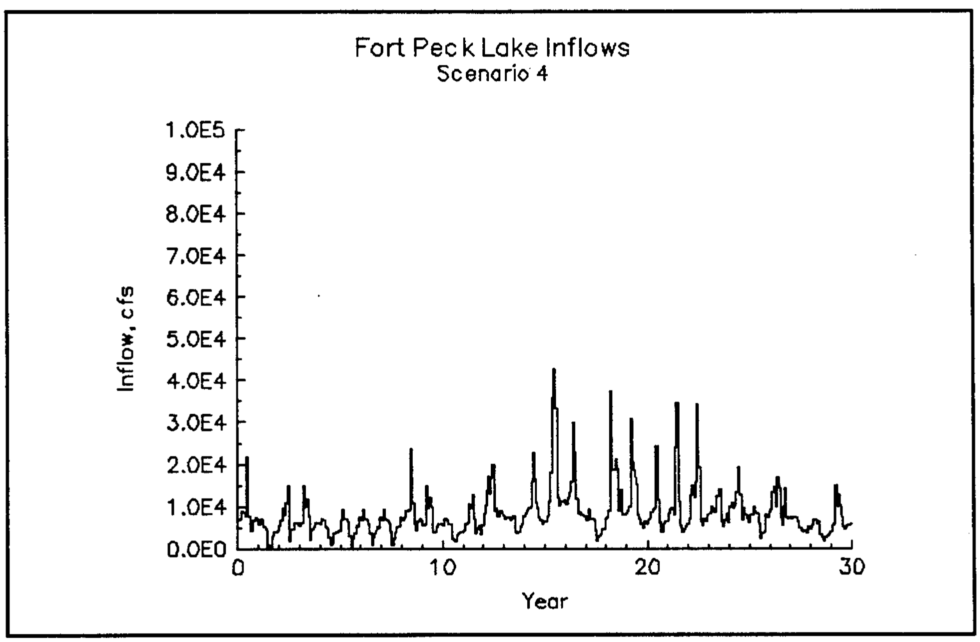

Figure 143. Fort Peck Lake scenario 4 inflows

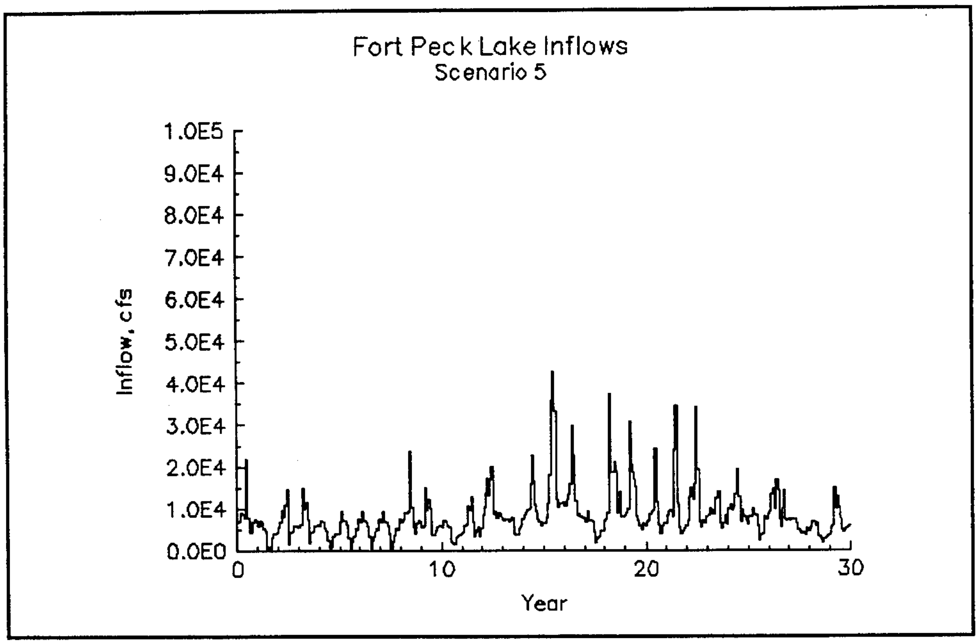

Figure 144. Fort Peck Lake scenario 5 inflows

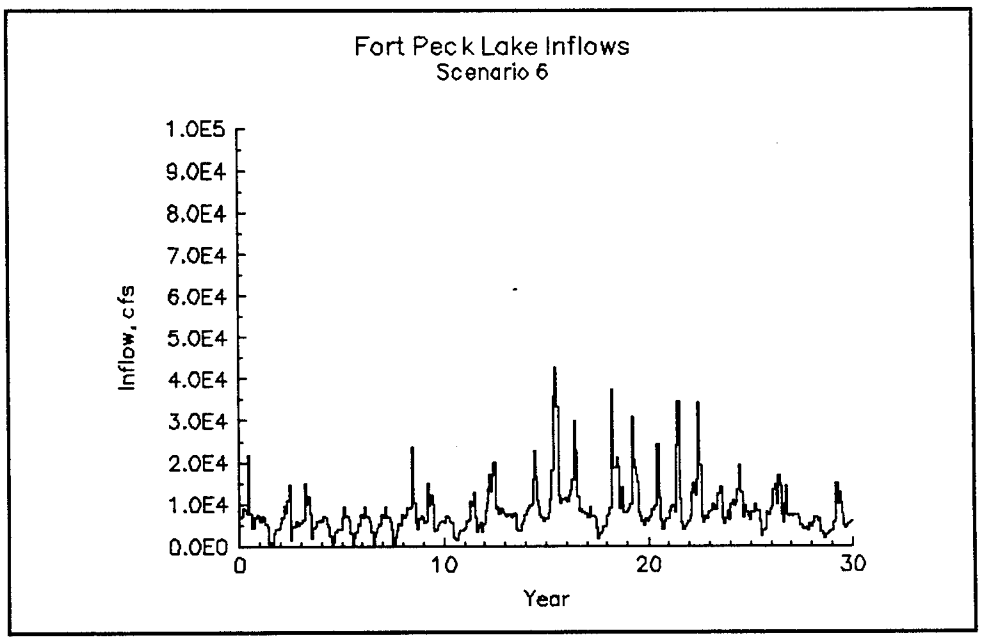

Figure 145. Fort Peck Lake scenario 6 inflows

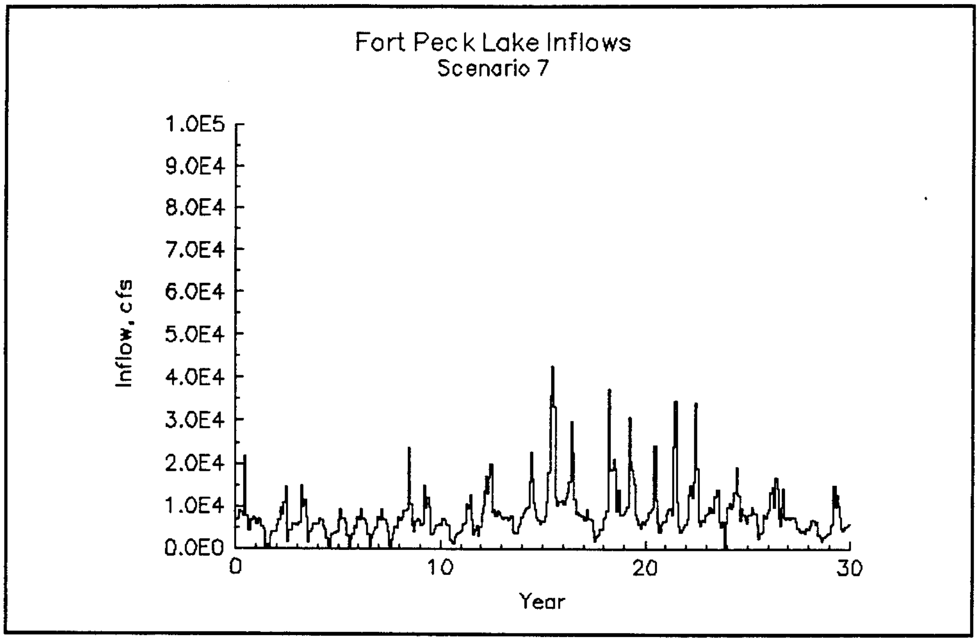

Figure 146. Fort Peck Lake scenario 7 inflows

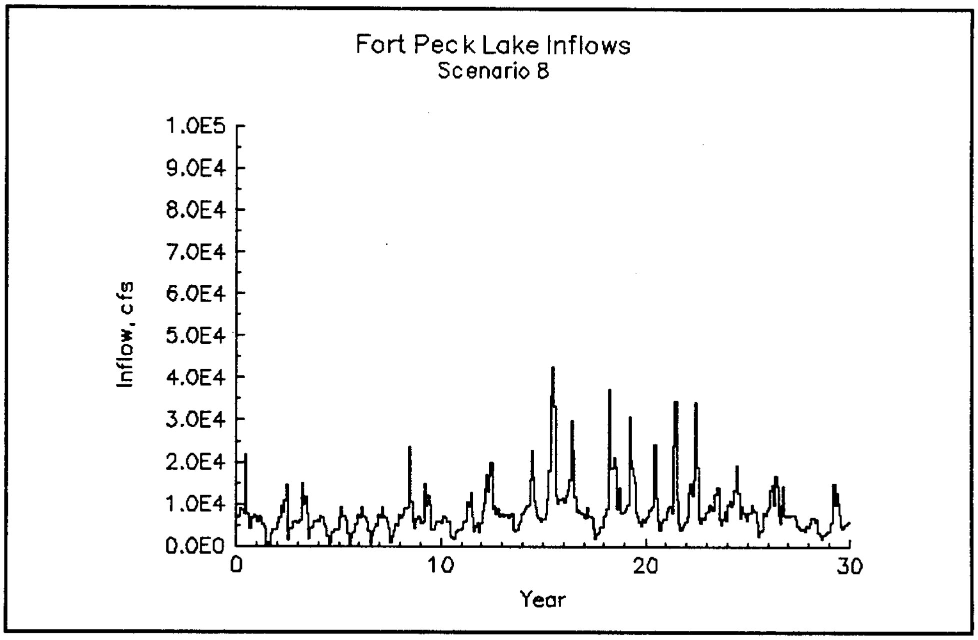

Figure 147. Fort Peck Lake scenario 8 inflows

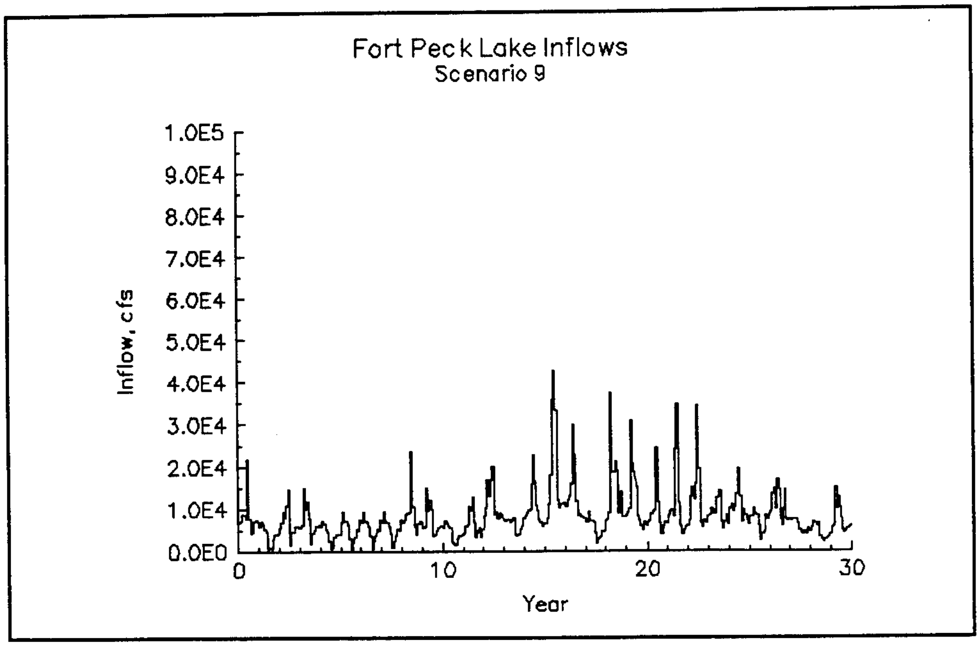

Figure 148. Fort Peck Lake scenario 9 inflows

Lake Sakakawea. Inflows for the nine scenarios are given in Figure 149-Figure 157. Differences between scenarios are most obvious when comparing maximum and minimum flows for a given year. For example, the minimum inflows for years 5, 6, and 10 are much less for scenario two than for scenario one.

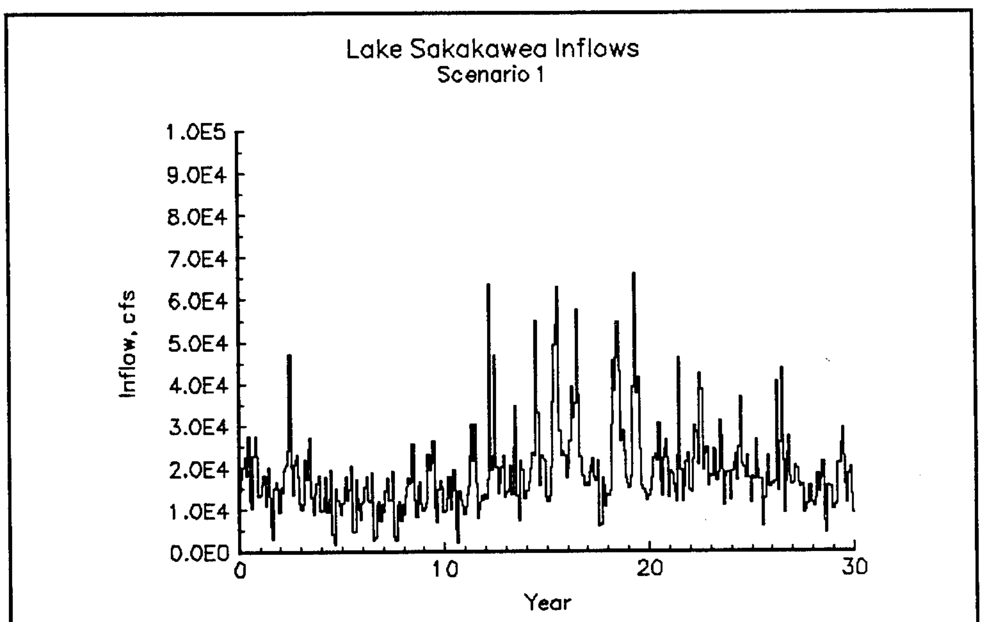

Figure 149. Lake Sakakawea scenario 1 inflows

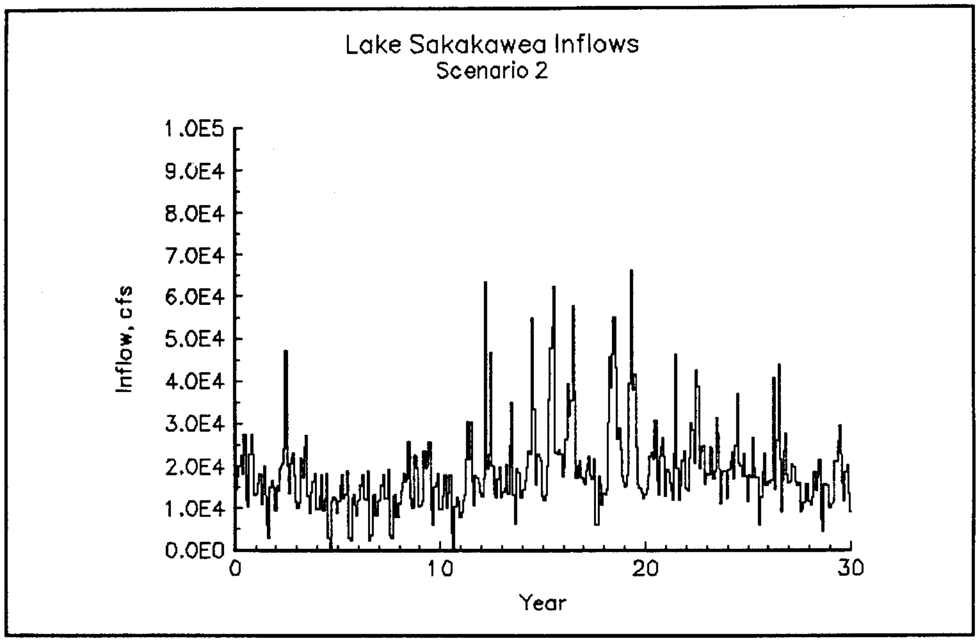

Figure 150. Lake Sakakawea scenario 2 inflows

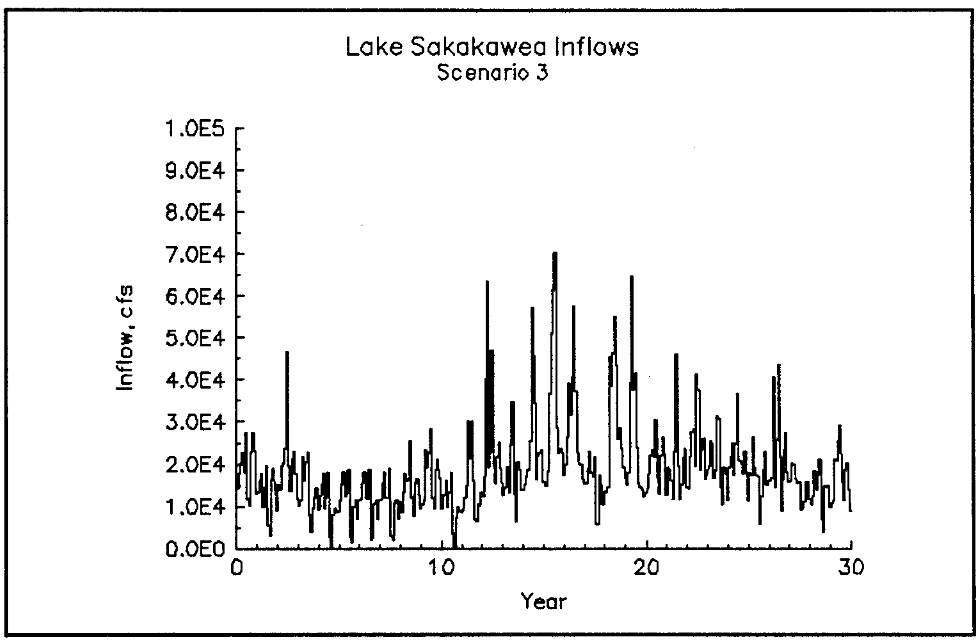

Figure 151. Lake Sakakawea scenario 3 inflows

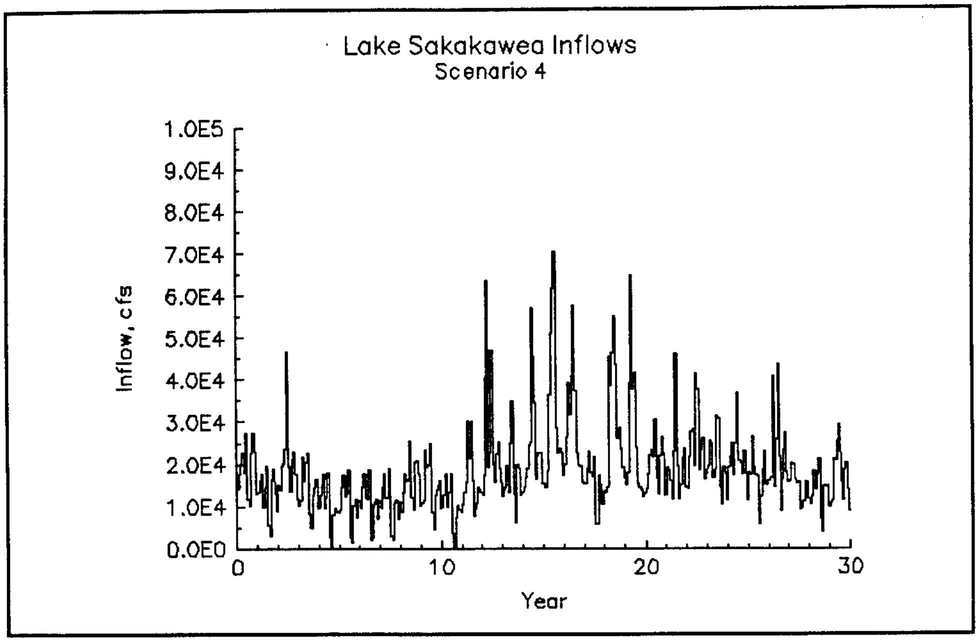

Figure 152. Lake Sakakawea scenario 4 inflows

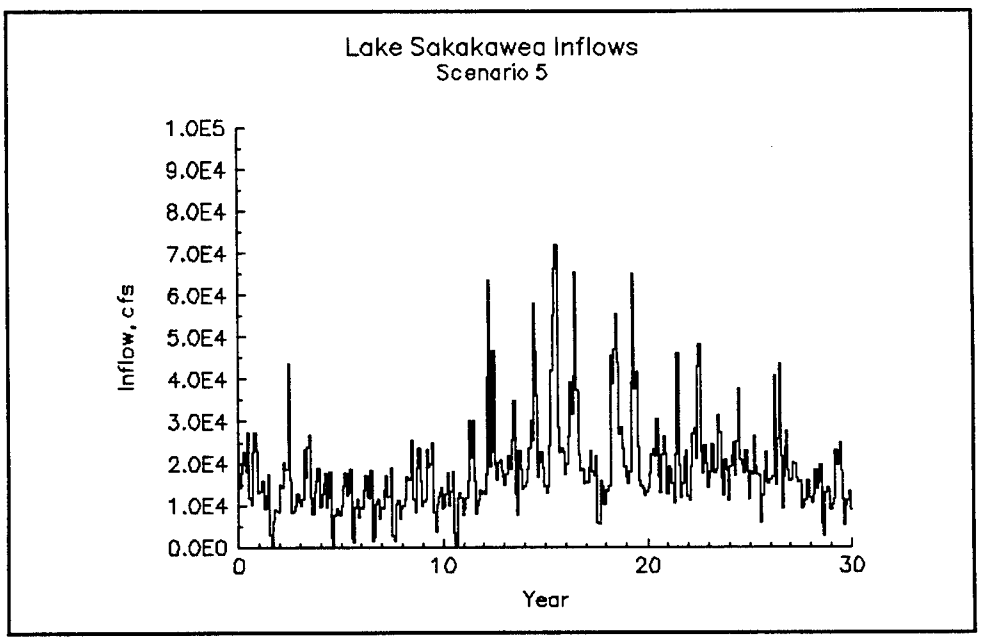

Figure 153. Lake Sakakawea scenario 5 inflows

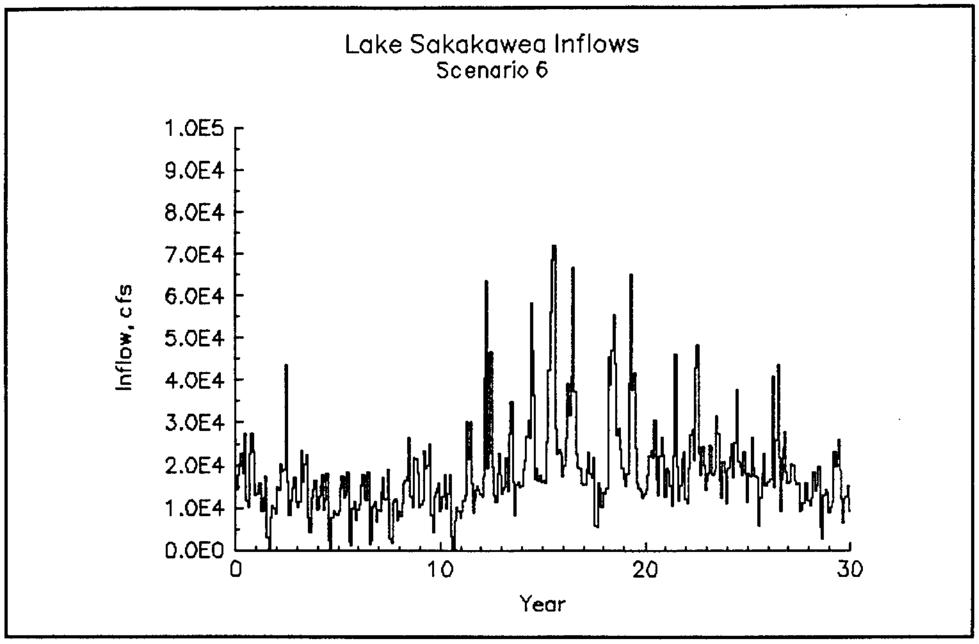

Figure 154. Lake Sakakawea scenario 6 inflows

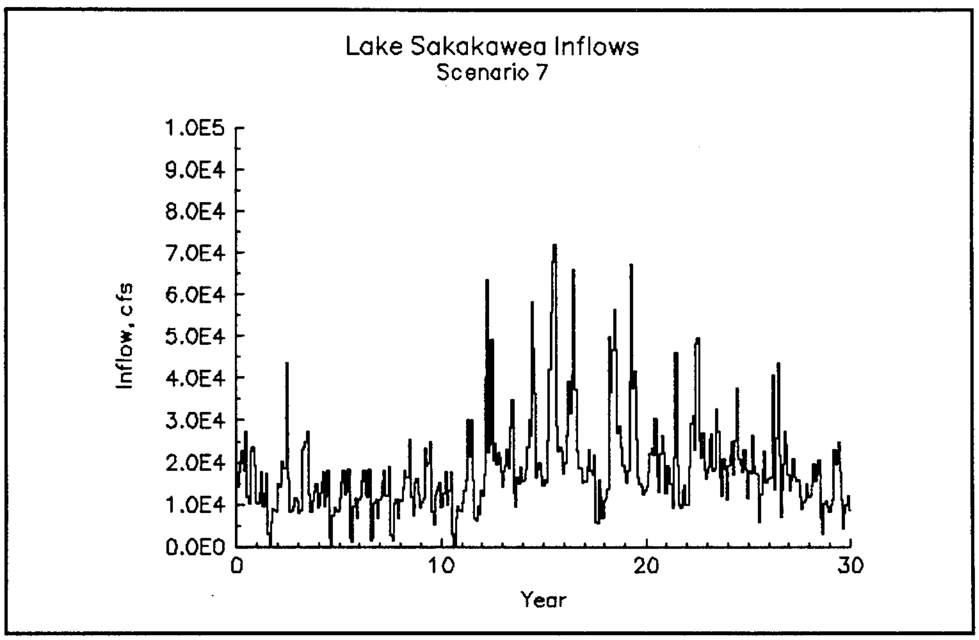

Figure 155. Lake Sakakawea scenario 7 inflows

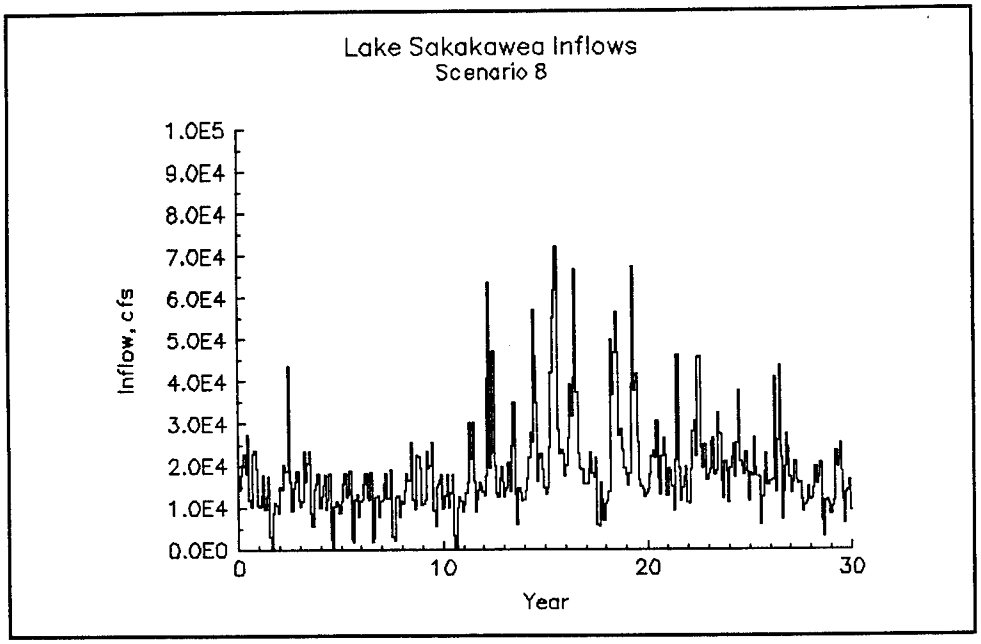

Figure 156. Lake Sakakawea scenario 8 inflows

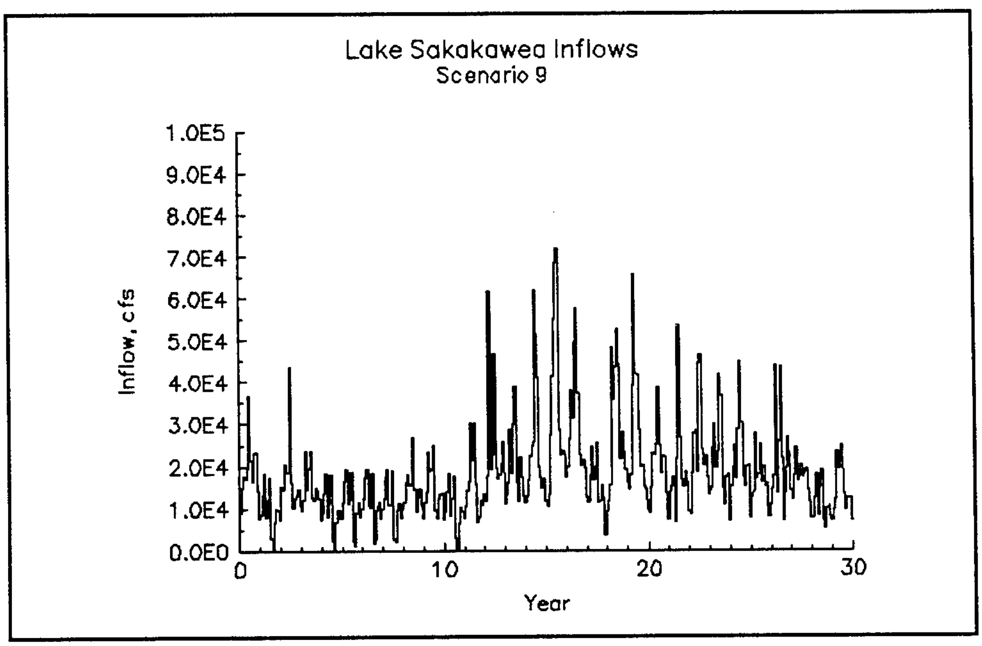

Figure 157. Lake Sakakawea scenario 9 inflows

Lake Oahe. Inflows for the nine scenarios are given in Figure 158-Figure 166.

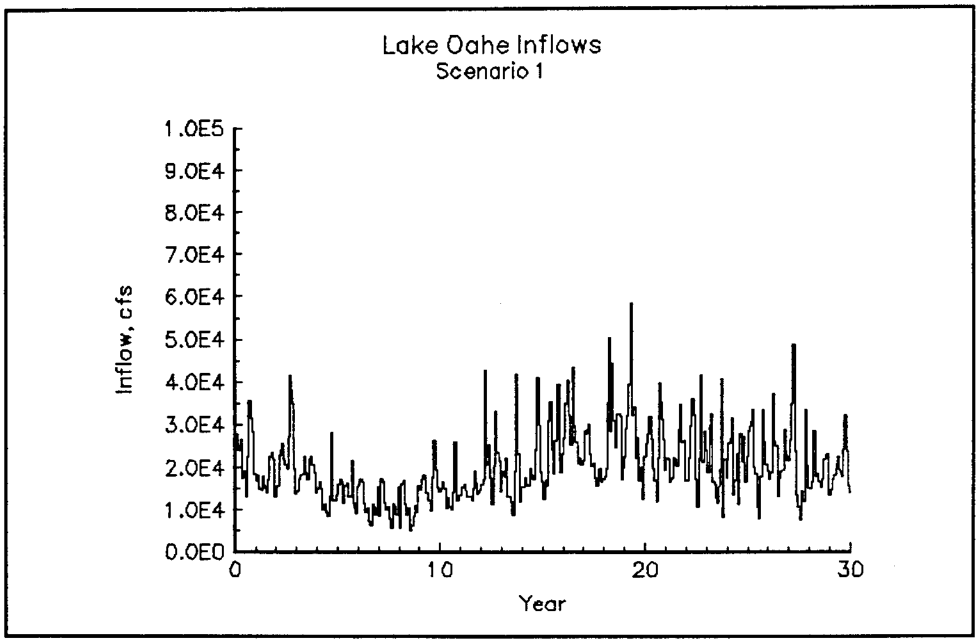

Figure 158. Lake Oahe scenario 1 inflows

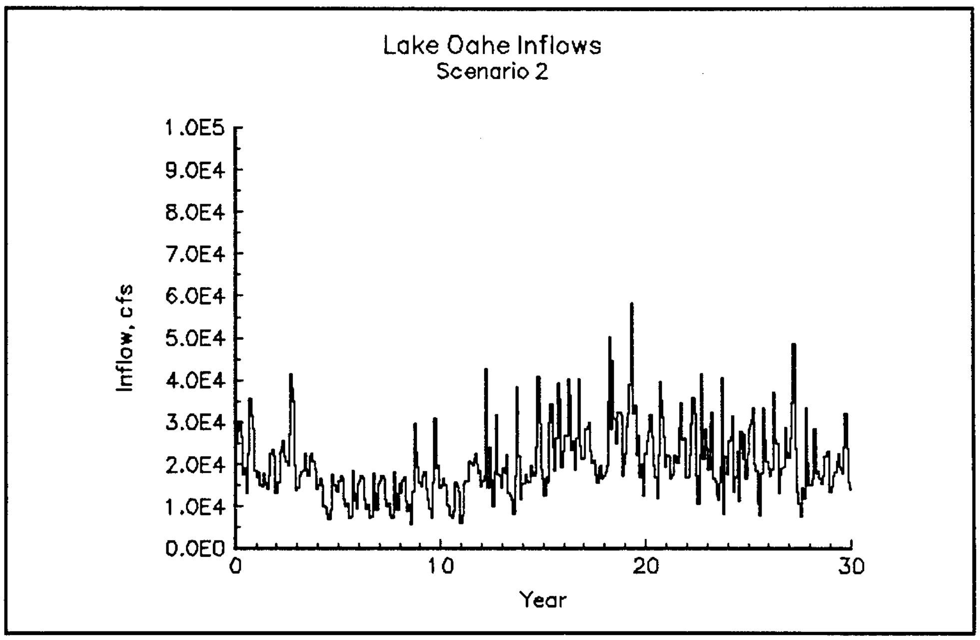

Figure 159. Lake Oahe scenario 2 inflows

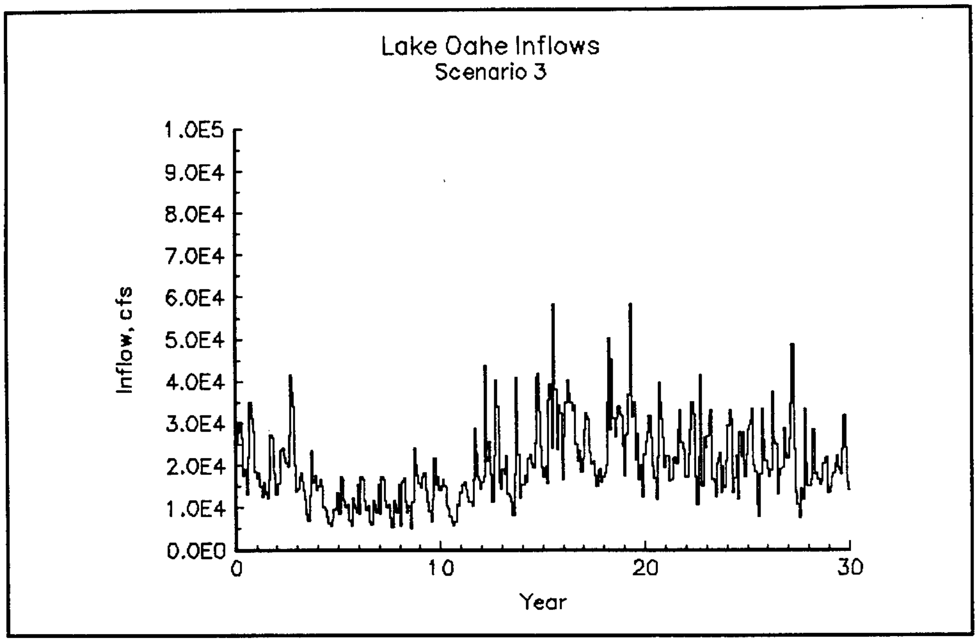

Figure 160. Lake Oahe scenario 3 inflows

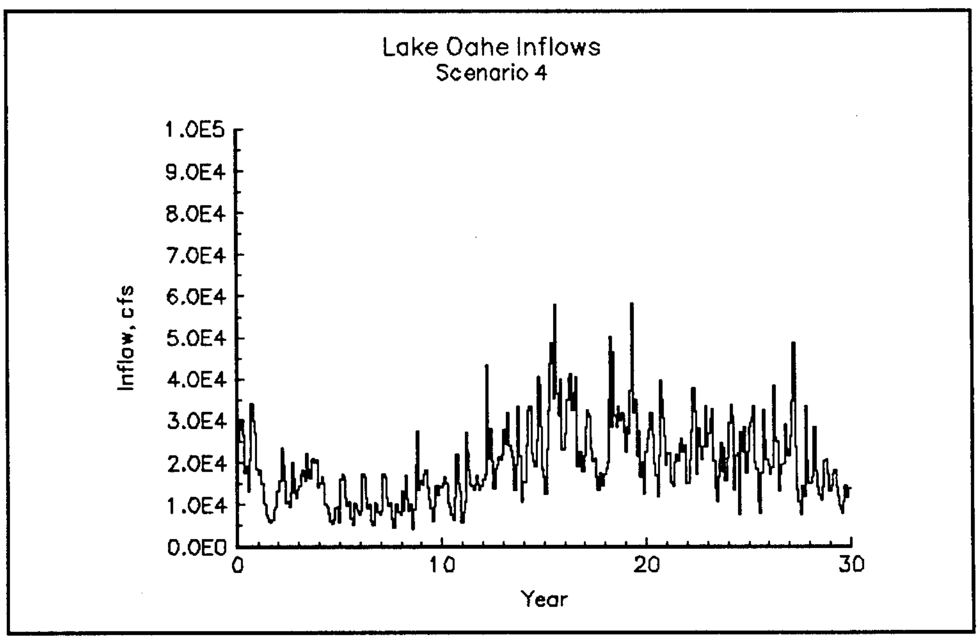

Figure 161. Lake Oahe scenario 4 inflows

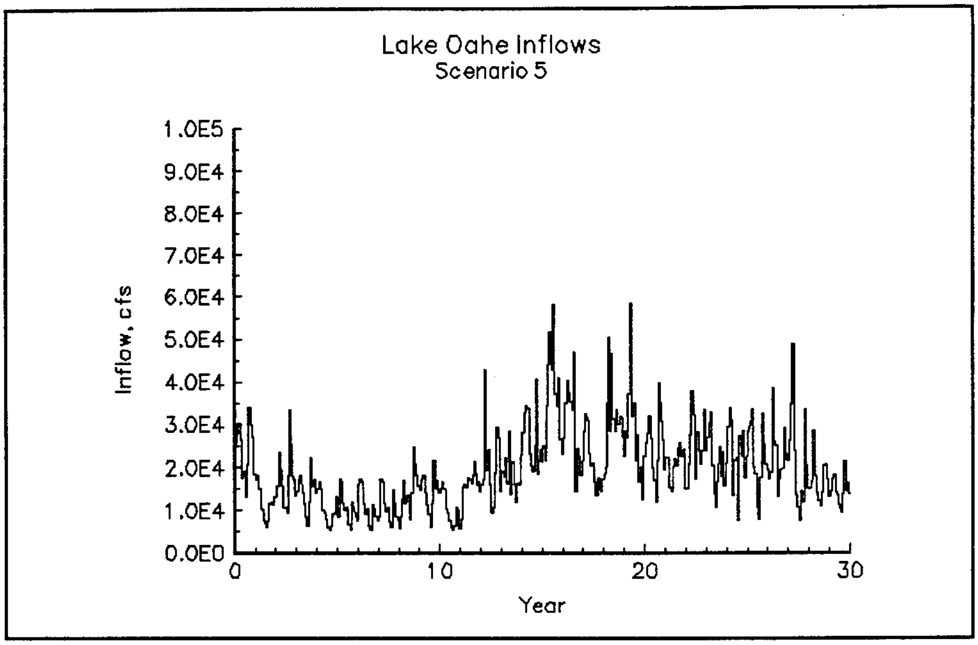

Figure 162. Lake Oahe scenario 5 inflows

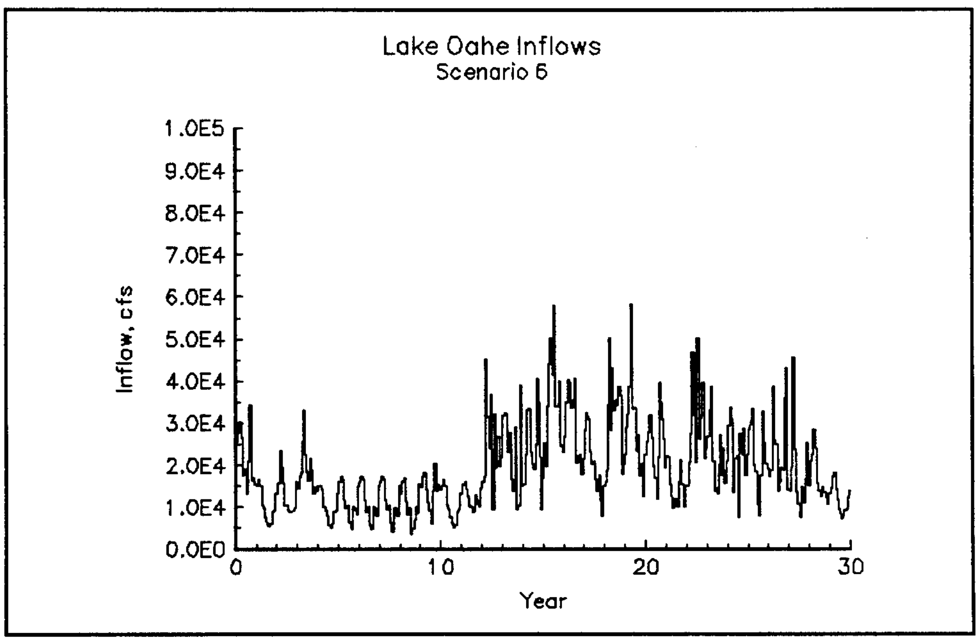

Figure 163. Lake Oahe scenario 6 inflows

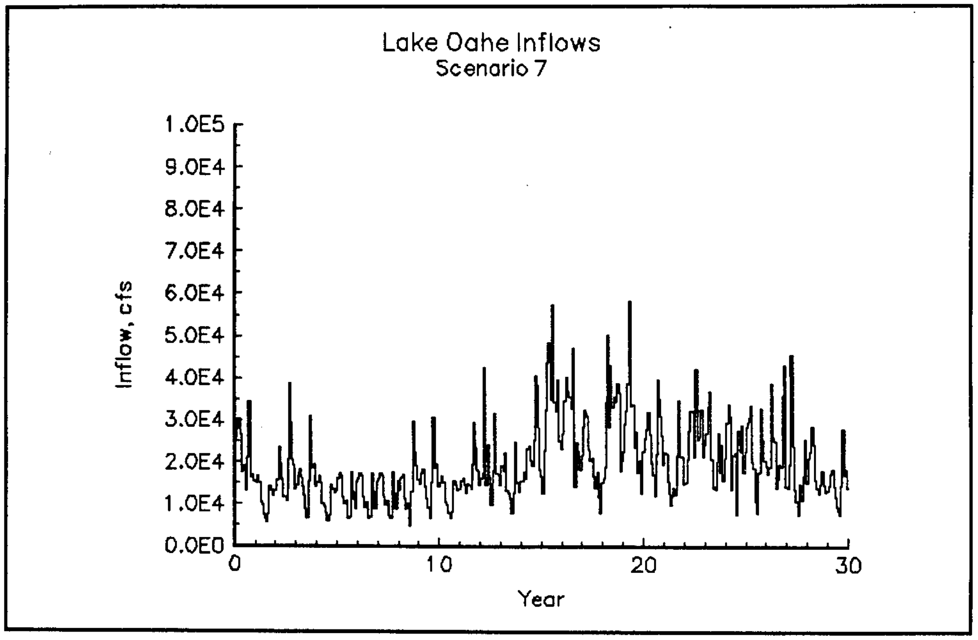

Figure 164. Lake Oahe scenario 7 inflows

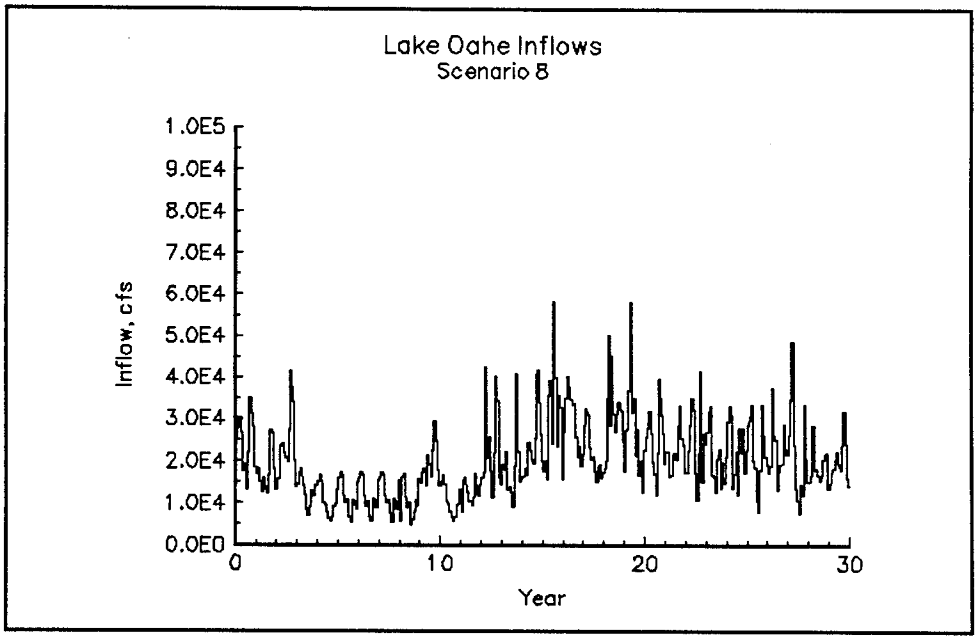

Figure 165. Lake Oahe scenario 8 inflows

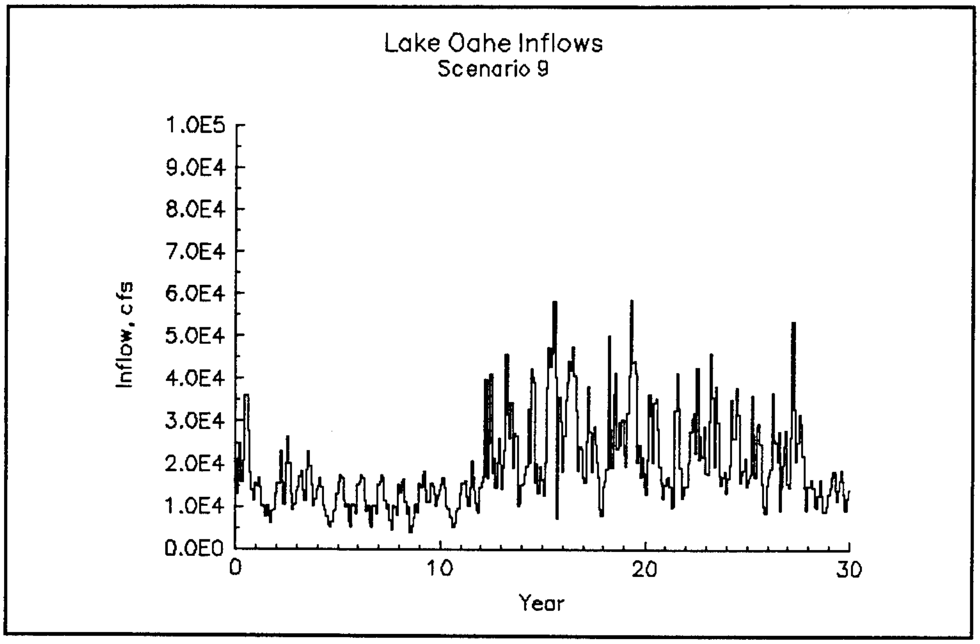

Figure 166. Lake Oahe scenario 9 inflows

Lake Francis Case. Inflows for the nine scenarios are given in Figure 167-Figure 175.

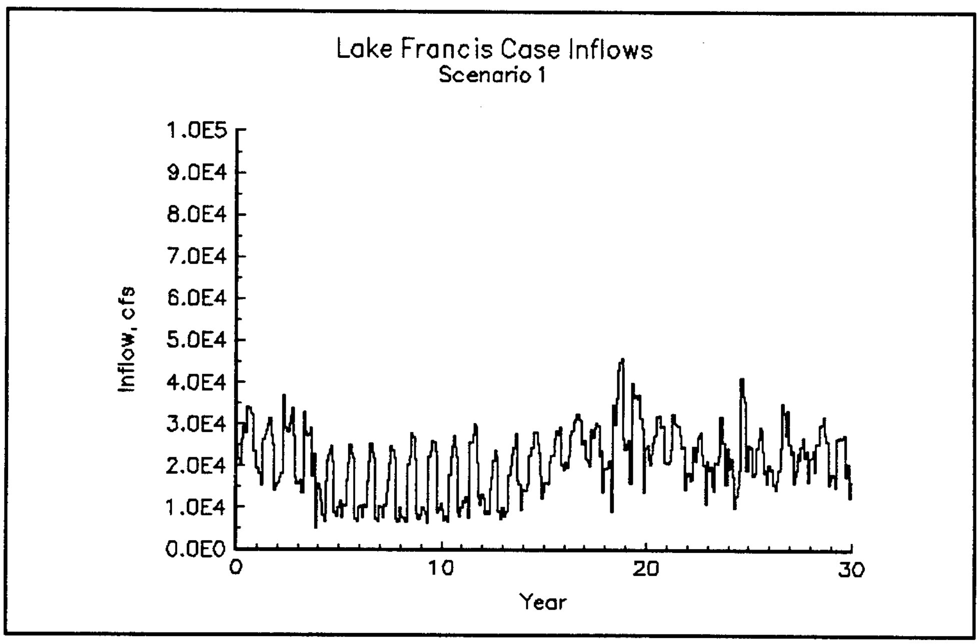

Figure 167. Lake Francis Case scenario 1 inflows

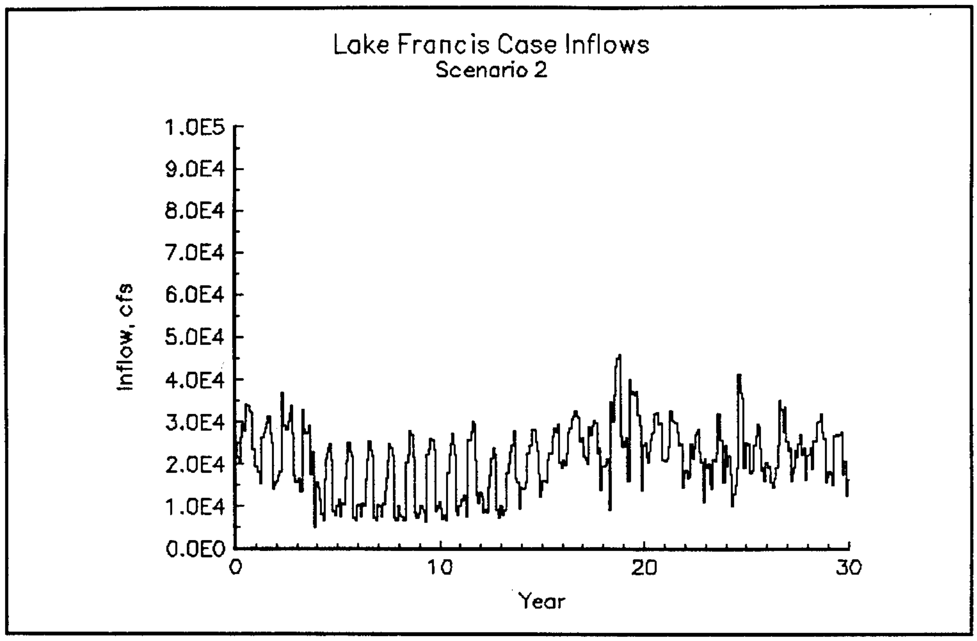

Figure 168. Lake Francis Case scenario 2 inflows

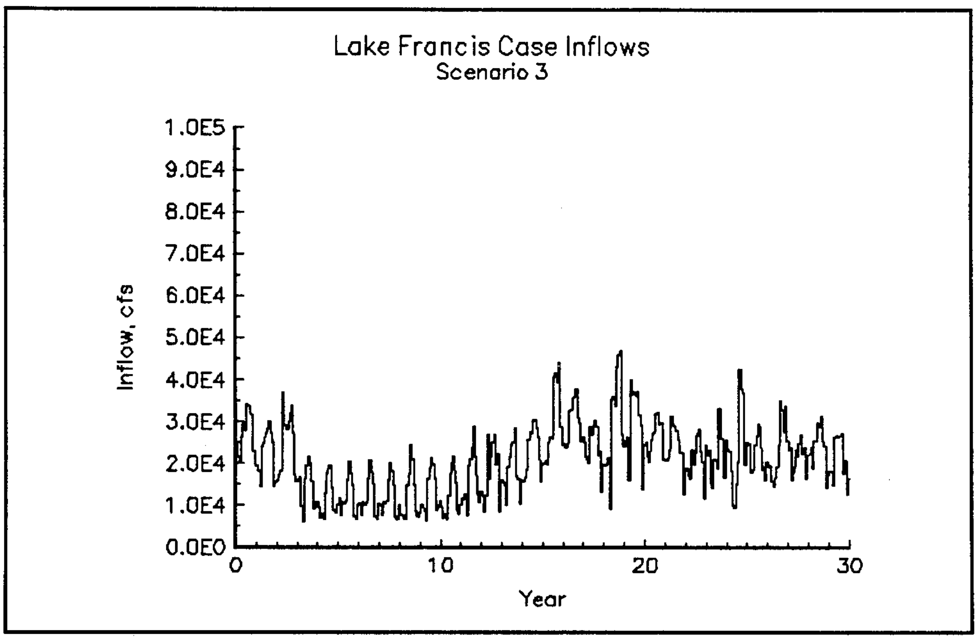

Figure 169. Lake Francis Case scenario 3 inflows

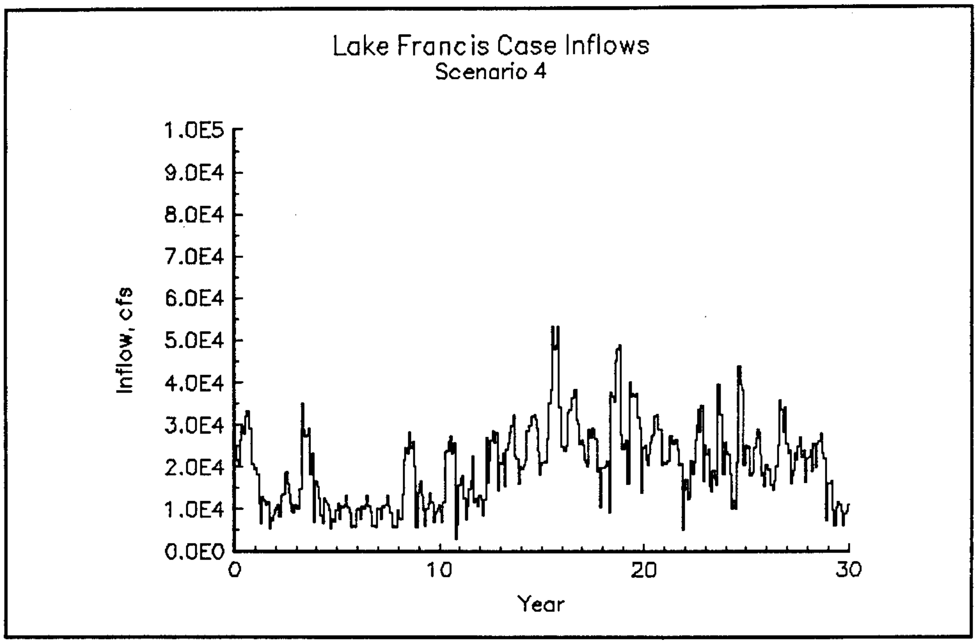

Figure 170. Lake Francis Case scenario 4 inflows

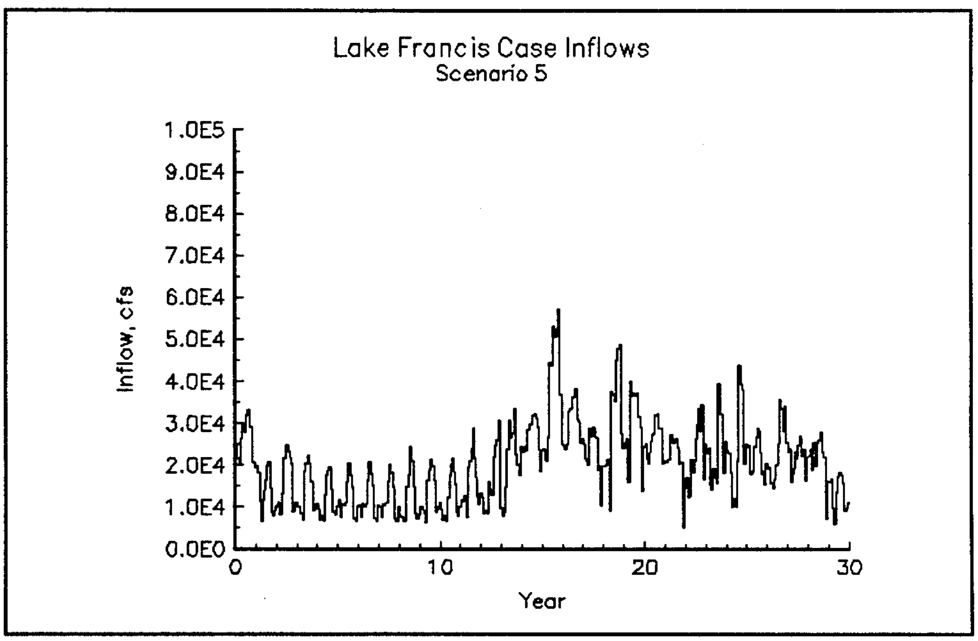

Figure 171. Lake Francis Case scenario 5 inflows

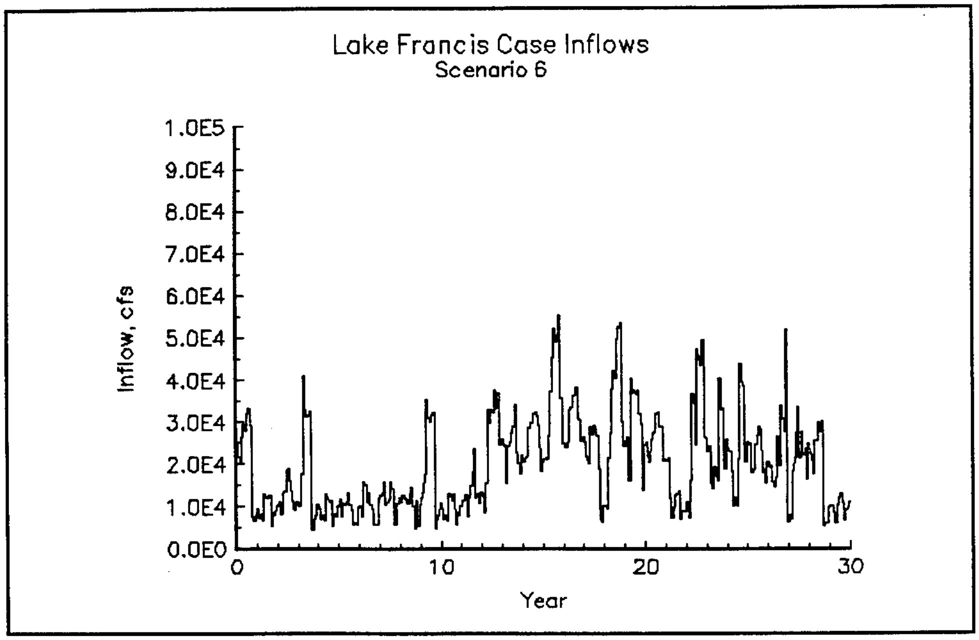

Figure 172. Lake Francis Case scenario 6 inflows

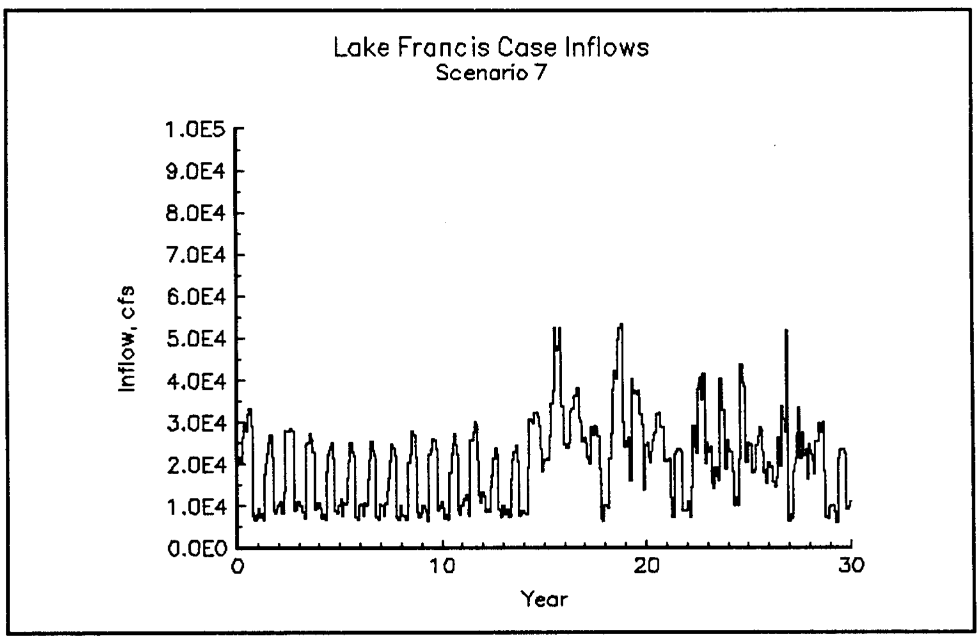

Figure 173. Lake Francis Case scenario 7 inflows

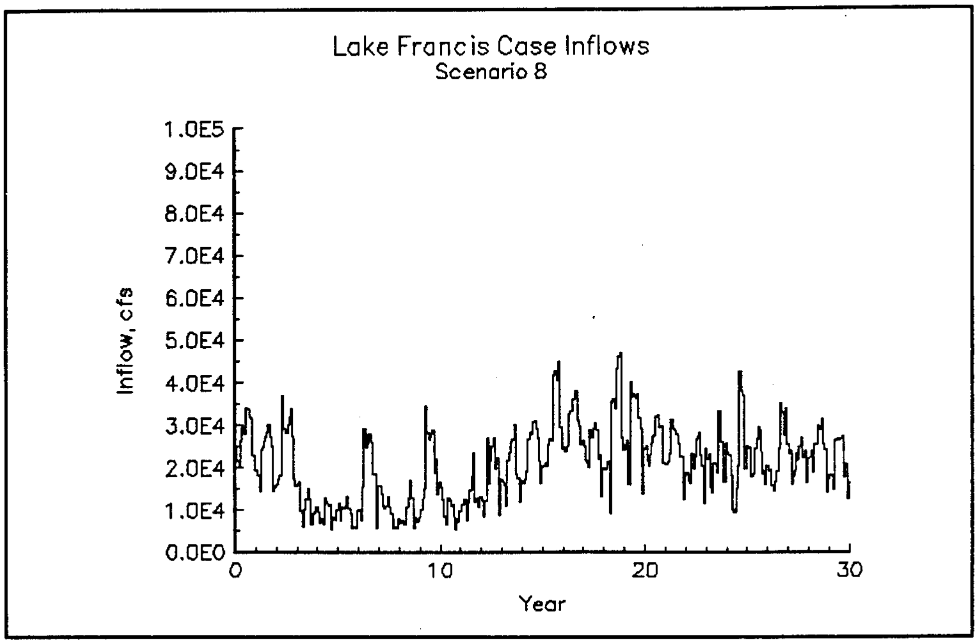

Figure 174. Lake Francis Case scenario 8 inflows

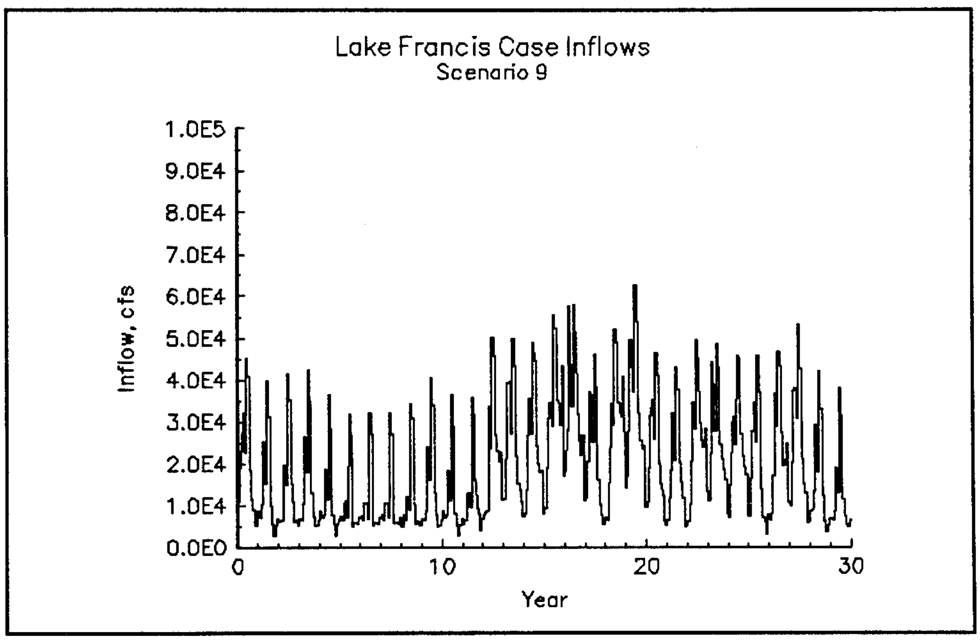

Figure 175. Lake Francis Case scenario 9 inflows

Releases

Fort Peck Lake. Releases for the nine scenarios are given in Figure 176-Figure 184.

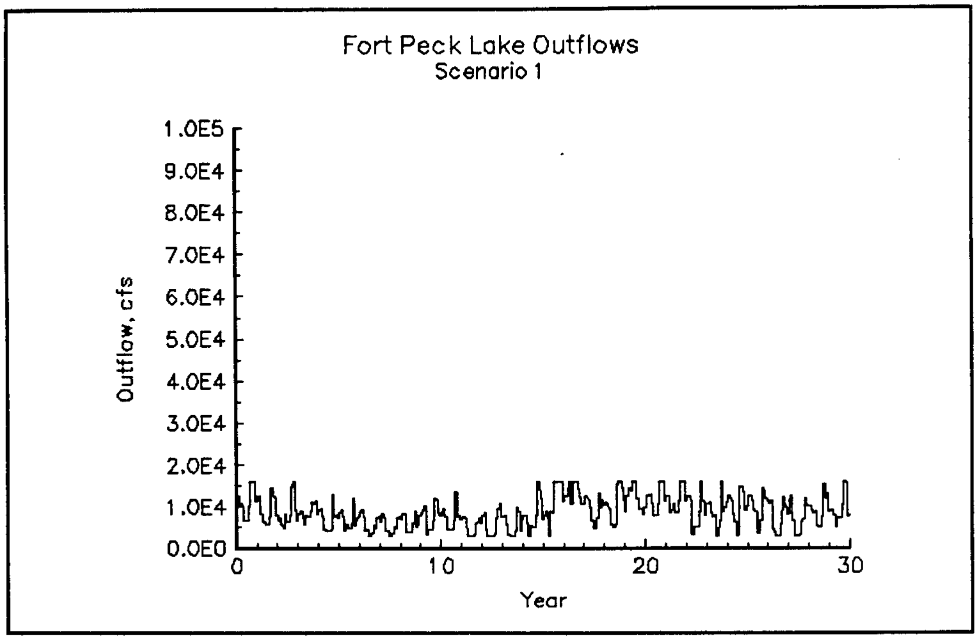

Figure 176. Fort Peck Lake scenario 1 outflows

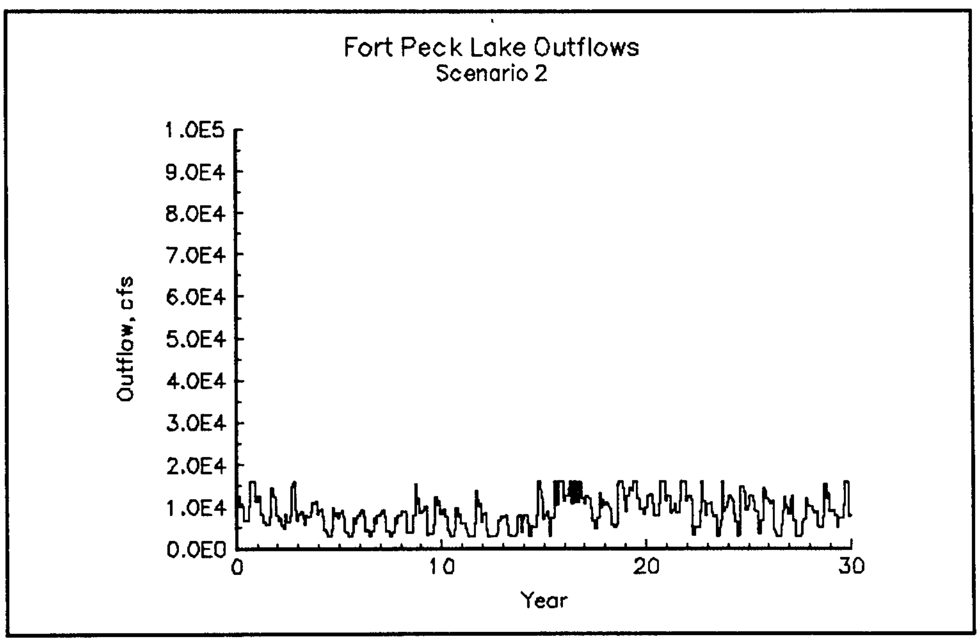

Figure 177. Fort Peck Lake scenario 2 outflows

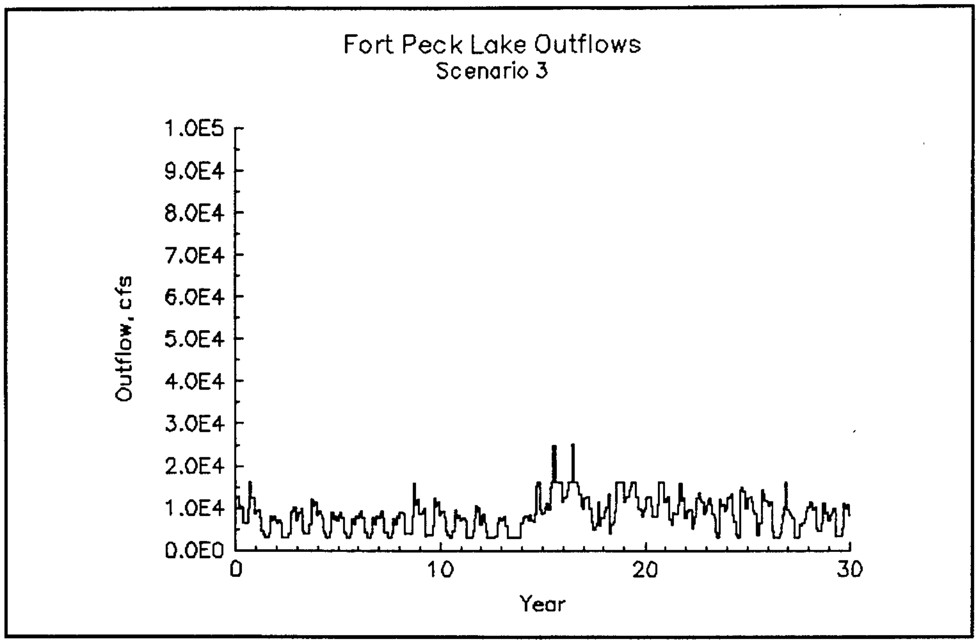

Figure 178. Fort Peck Lake scenario 3 outflows

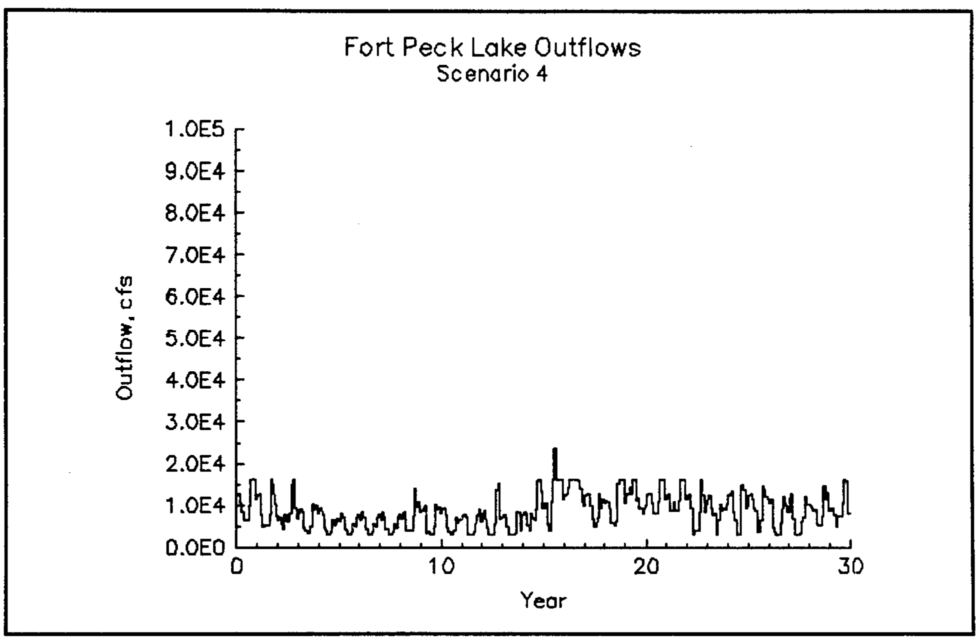

Figure 179. Fort Peck Lake scenario 4 outflows

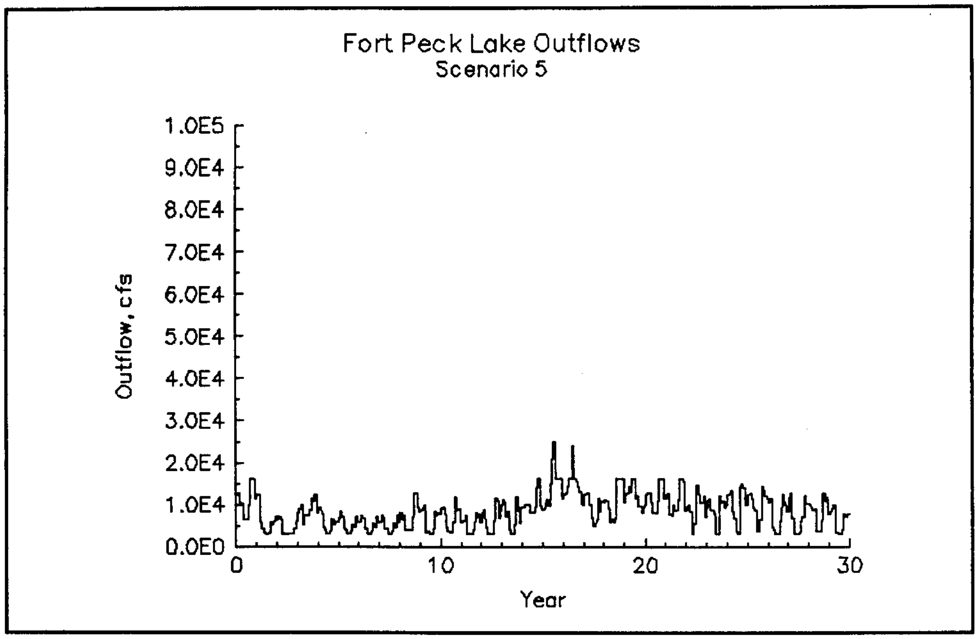

Figure 180. Fort Peck Lake scenario 5 outflows

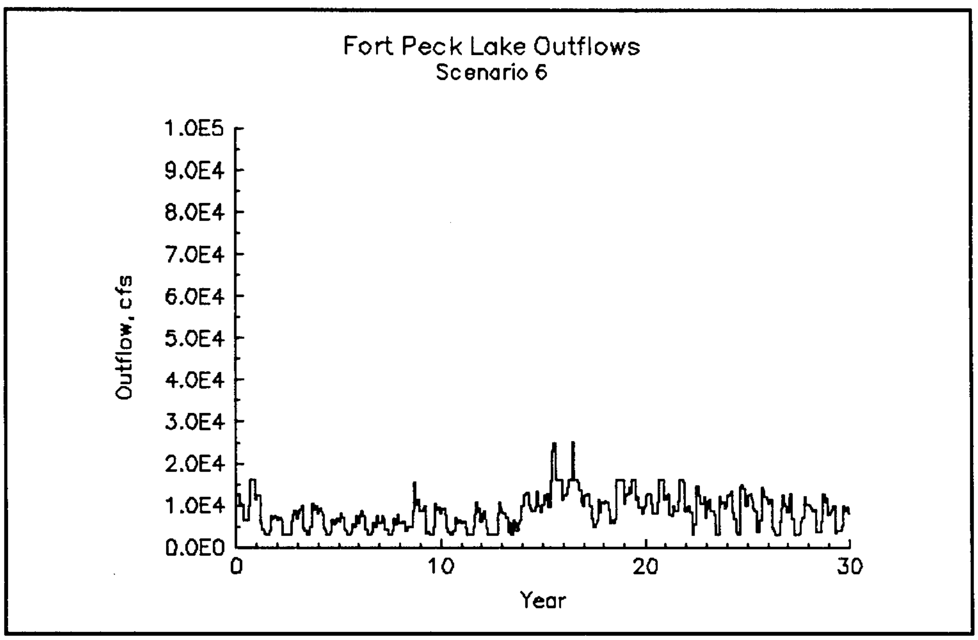

Figure 181. Fort Peck Lake scenario 6 outflows

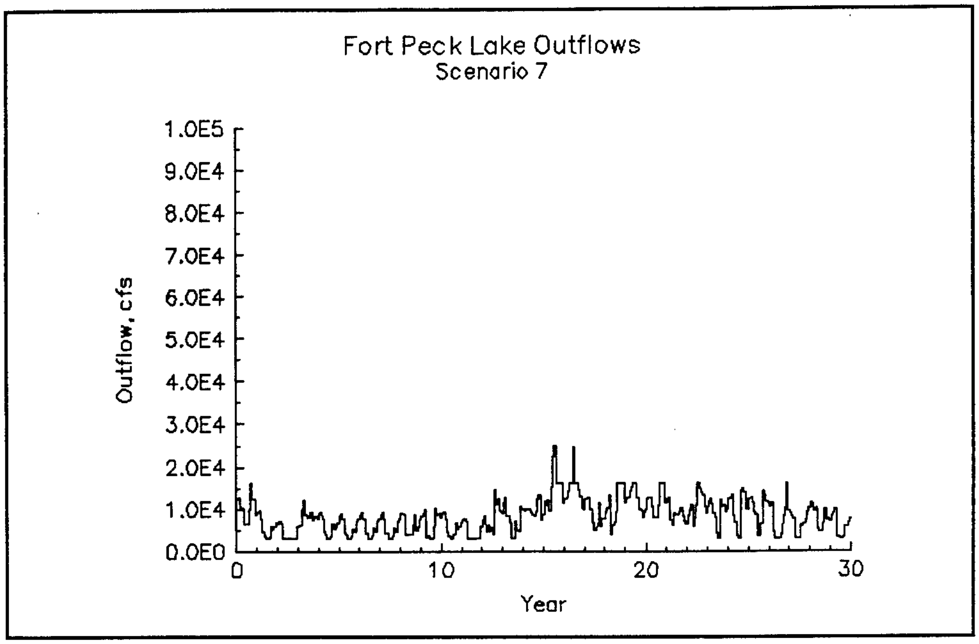

Figure 182. Fort Peck Lake scenario 7 outflows

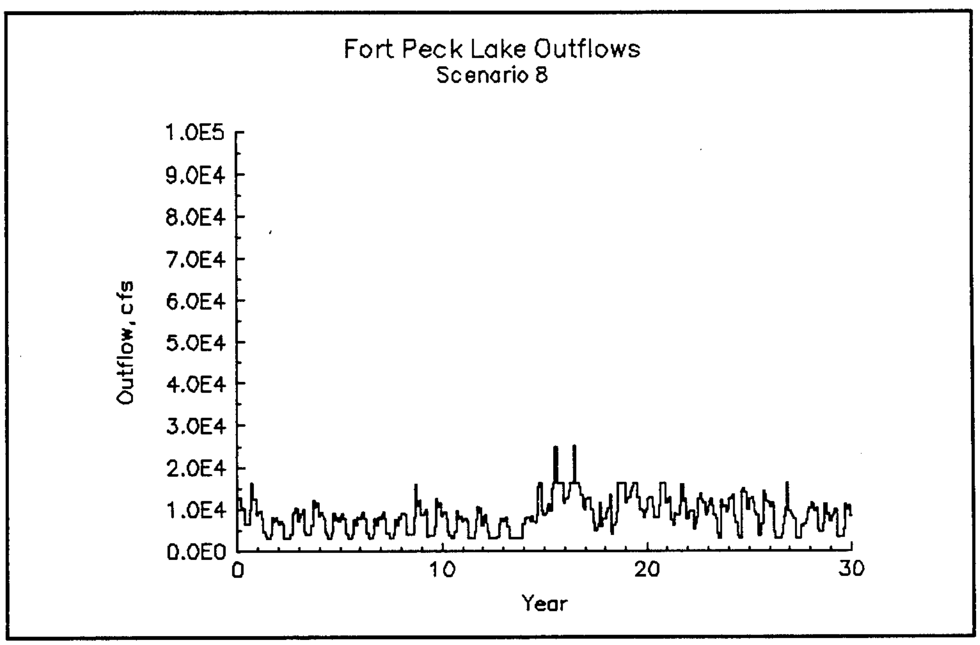

Figure 183. Fort Peck Lake scenario 8 outflows

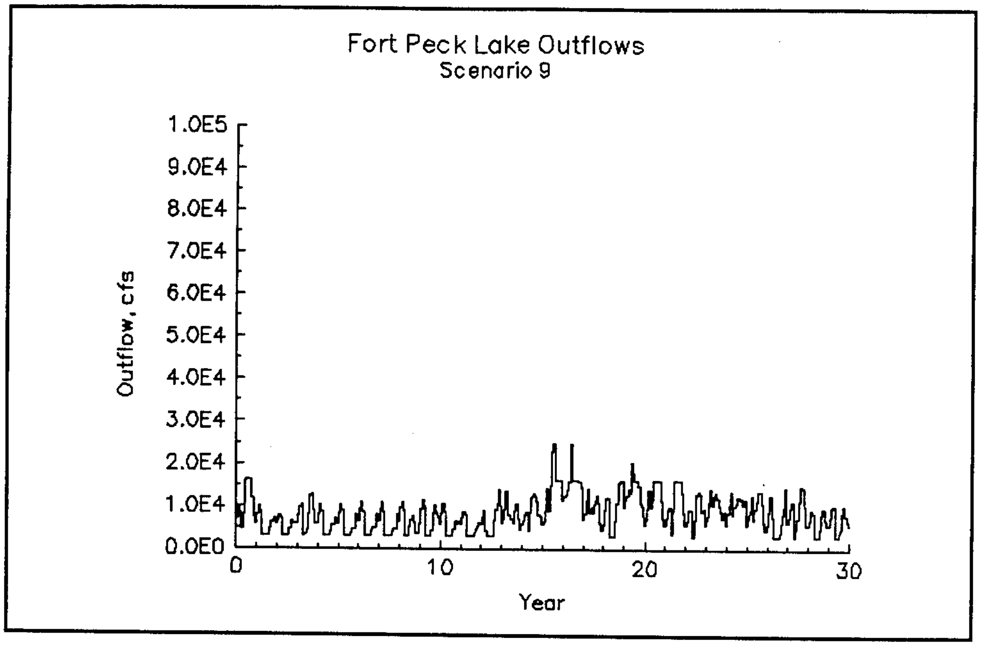

Figure 184. Fort Peck Lake scenario 9 outflows

Lake Sakakawea. Releases for the nine scenarios are given in Figure 185-Figure 193.

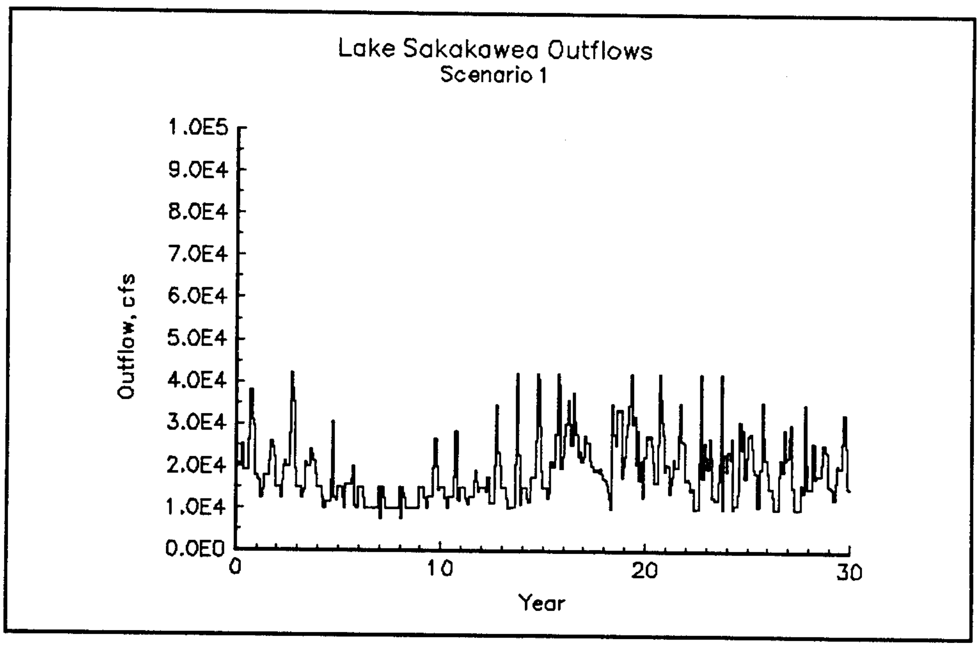

Figure 185. Lake Sakakawea scenario 1 outflows

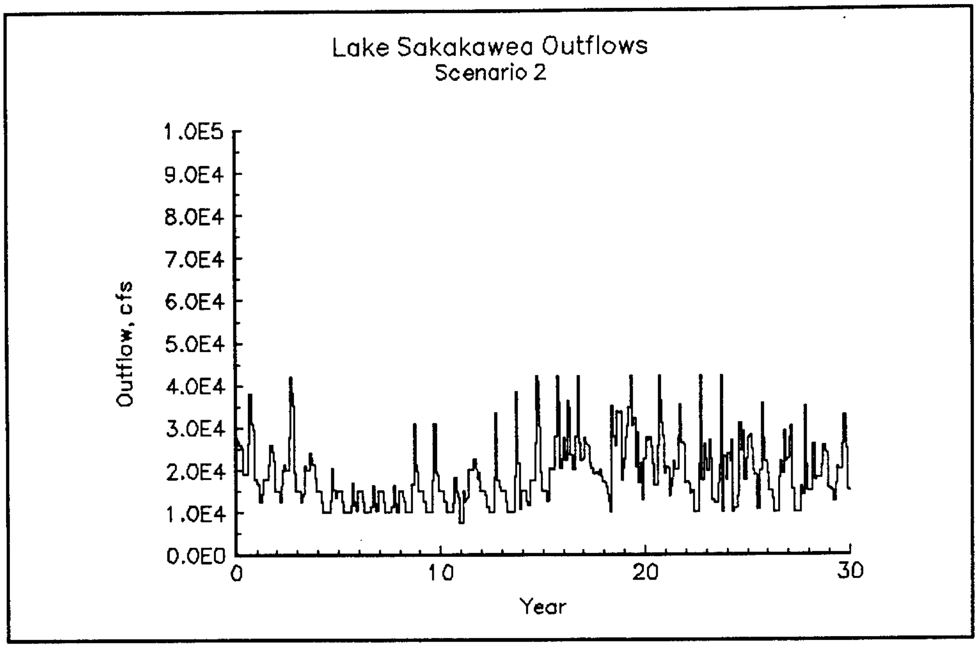

Figure 186. Lake Sakakawea scenario 2 outflows

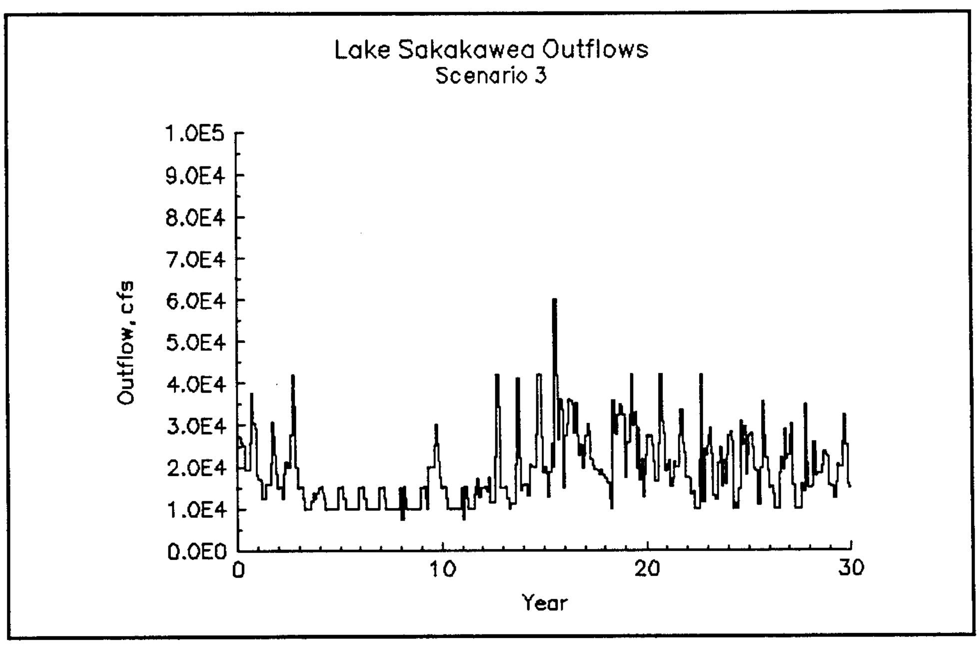

Figure 187. Lake Sakakawea scenario 3 outflows

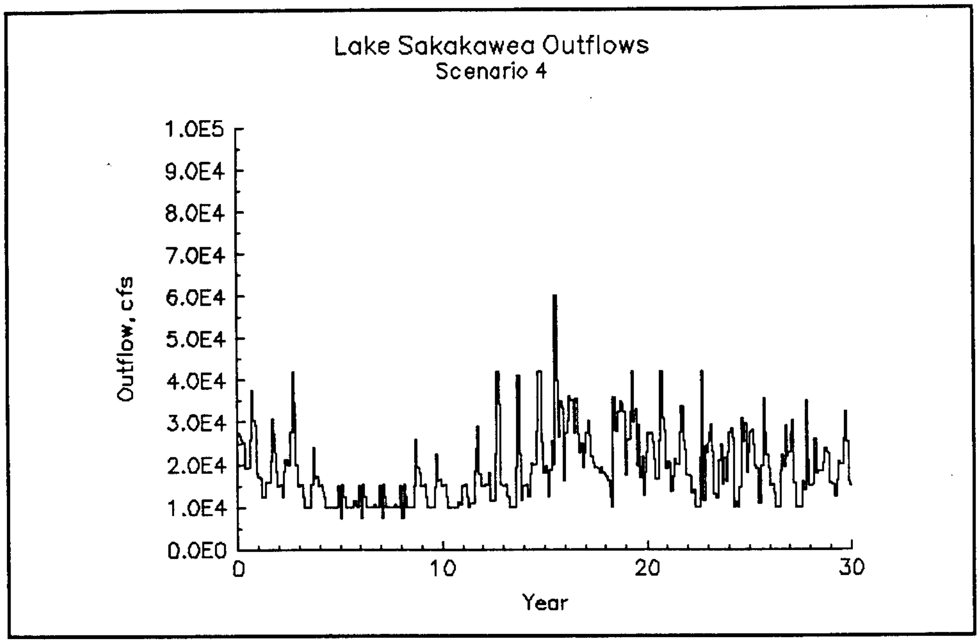

Figure 188. Lake Sakakawea scenario 4 outflows

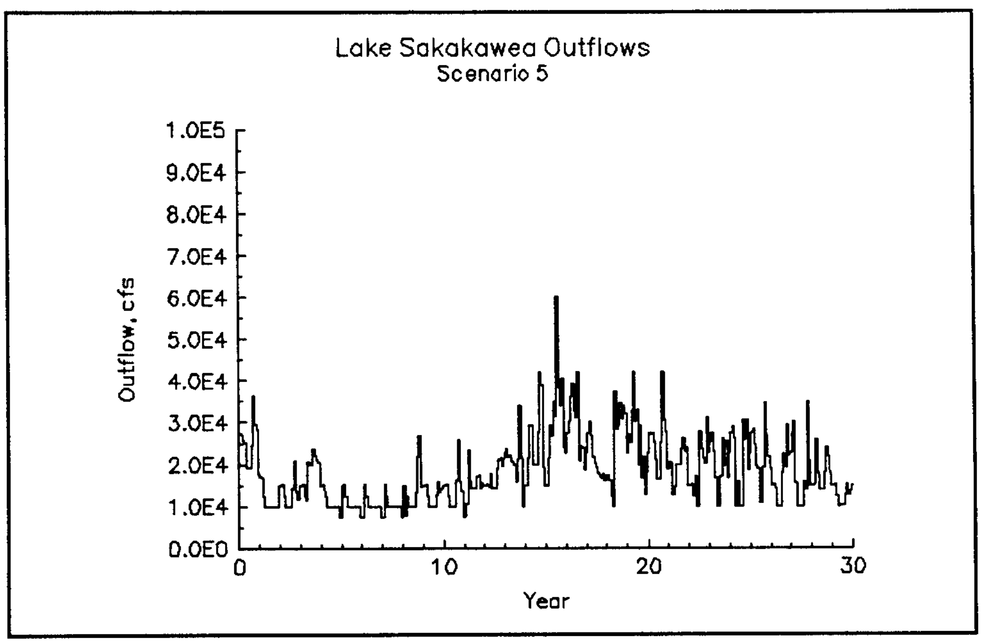

Figure 189. Lake Sakakawea scenario 5 outflows

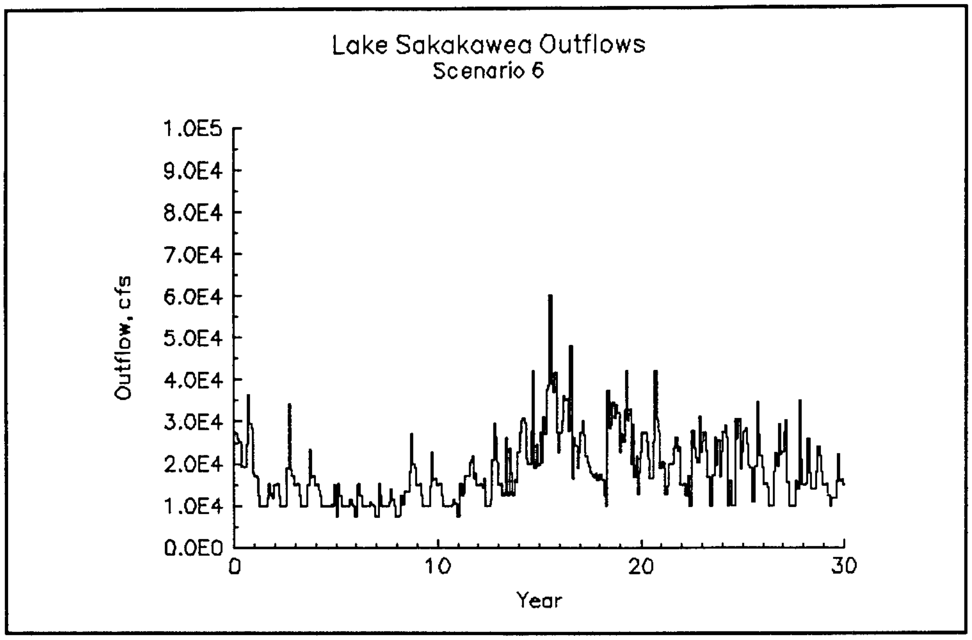

Figure 190. Lake Sakakawea scenario 6 outflows

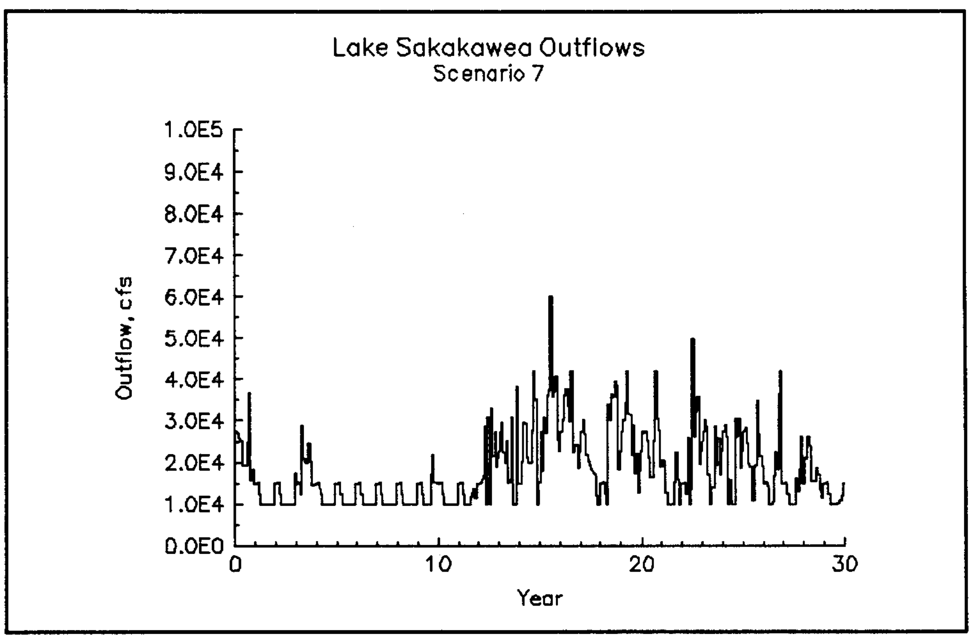

Figure 191. Lake Sakakawea scenario 7 outflows

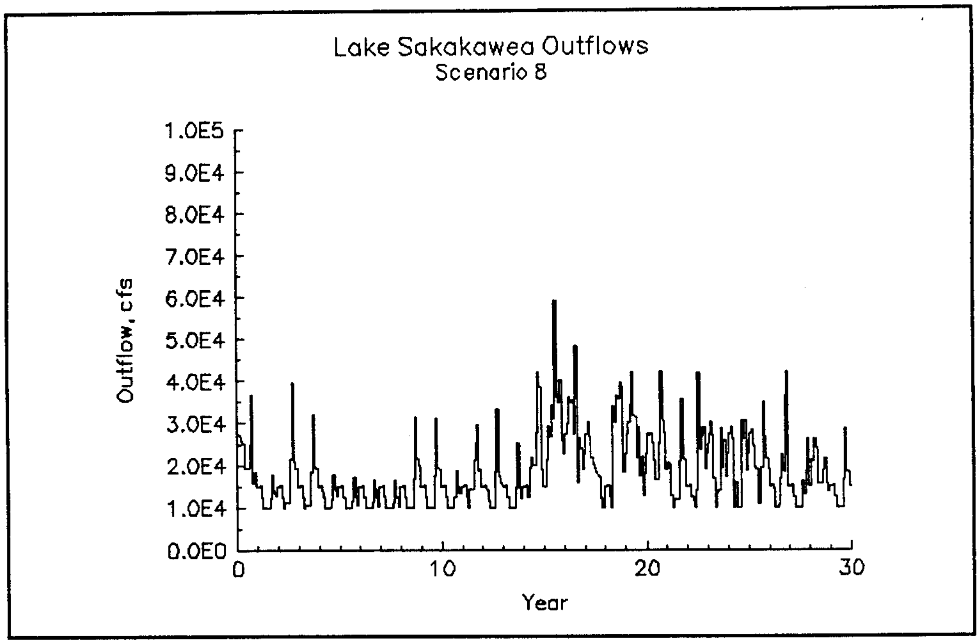

Figure 192. Lake Sakakawea scenario 8 outflows

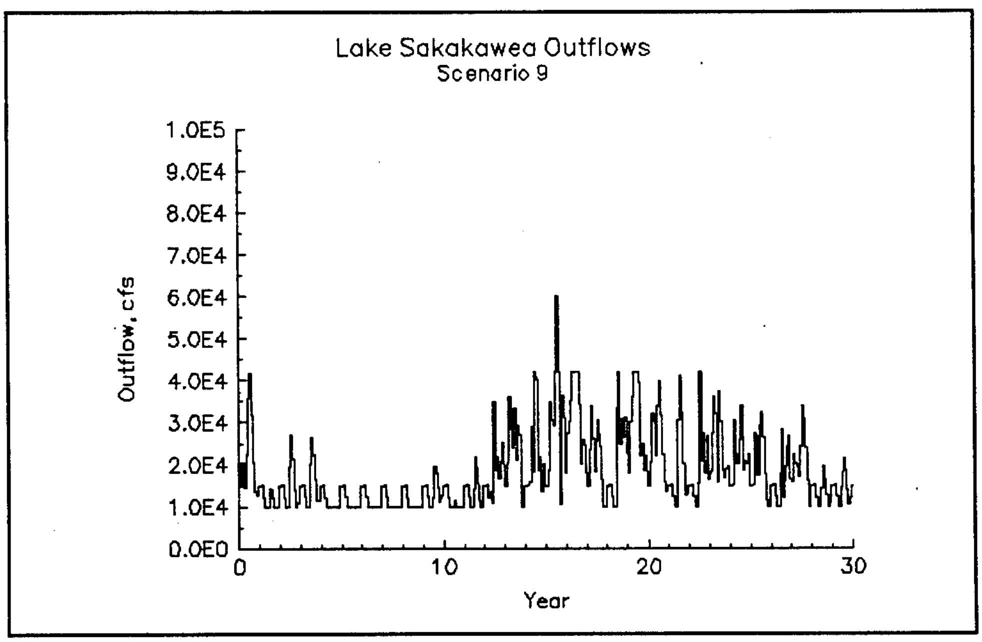

Figure 193. Lake Sakakawea scenario 9 outflows

Lake Oahe. Releases for the nine scenarios are given in Figure 194-Figure 202.

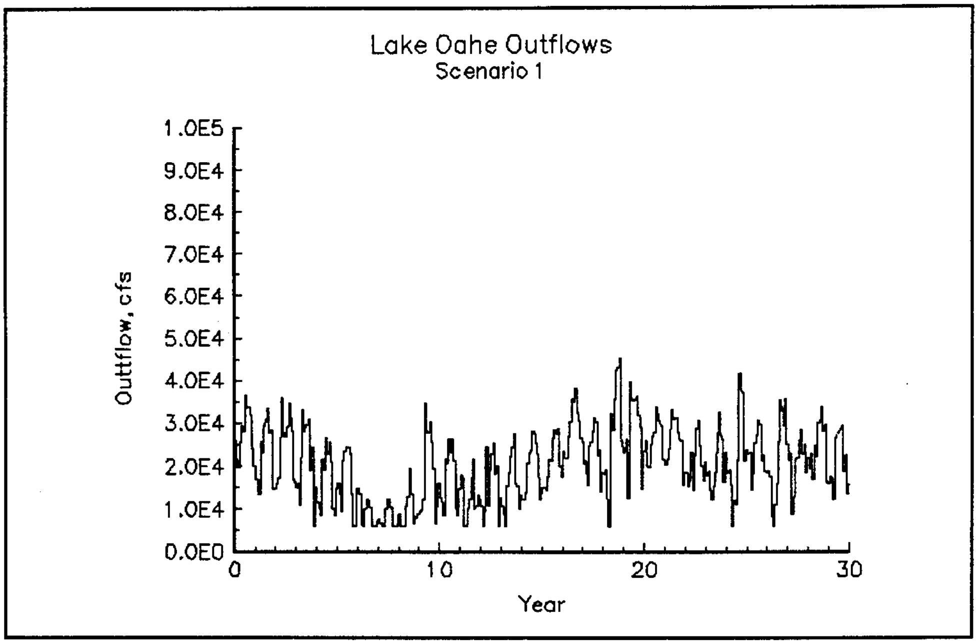

Figure 194. Lake Oahe scenario 1 outflows

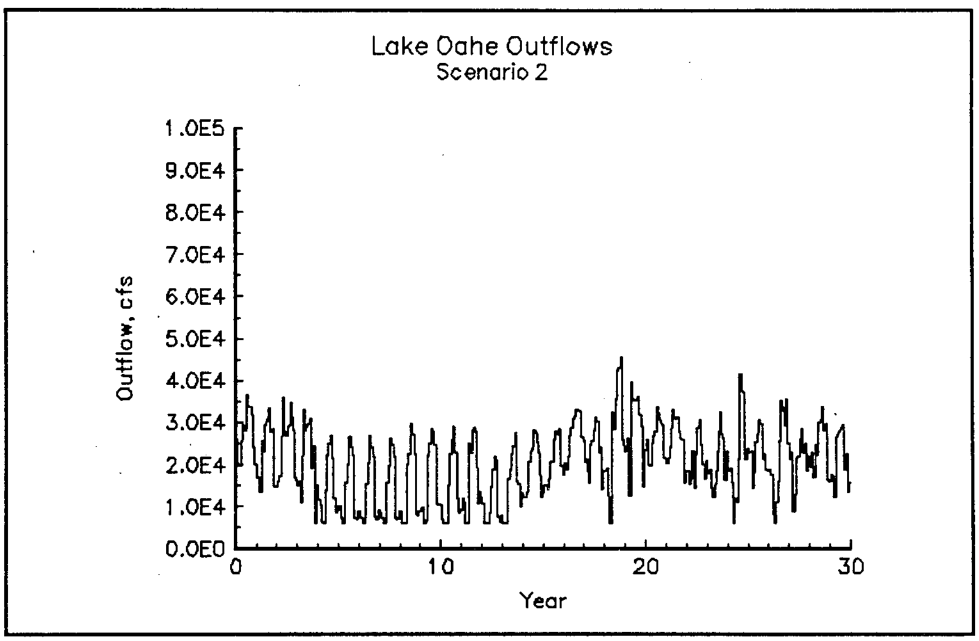

Figure 195. Lake Oahe scenario 2 outflows

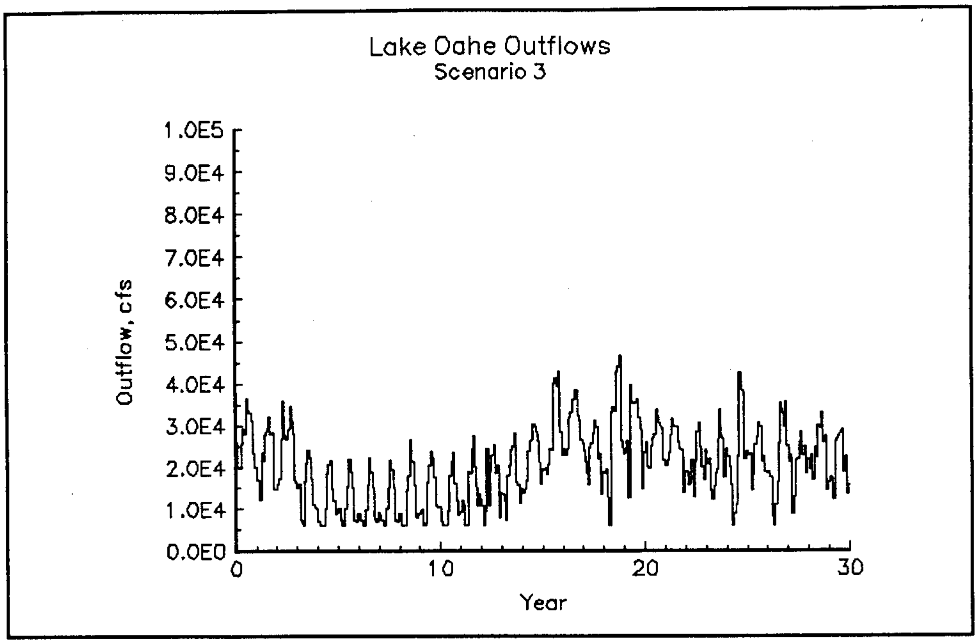

Figure 196. Lake Oahe scenario 3 outflows

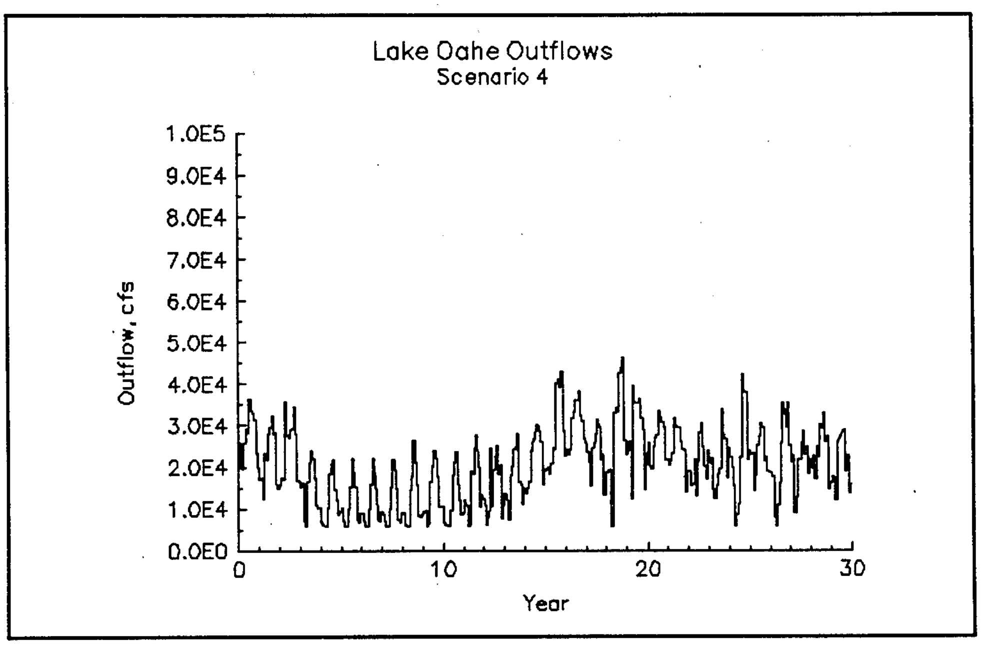

Figure 197. Lake Oahe scenario 4 outflows

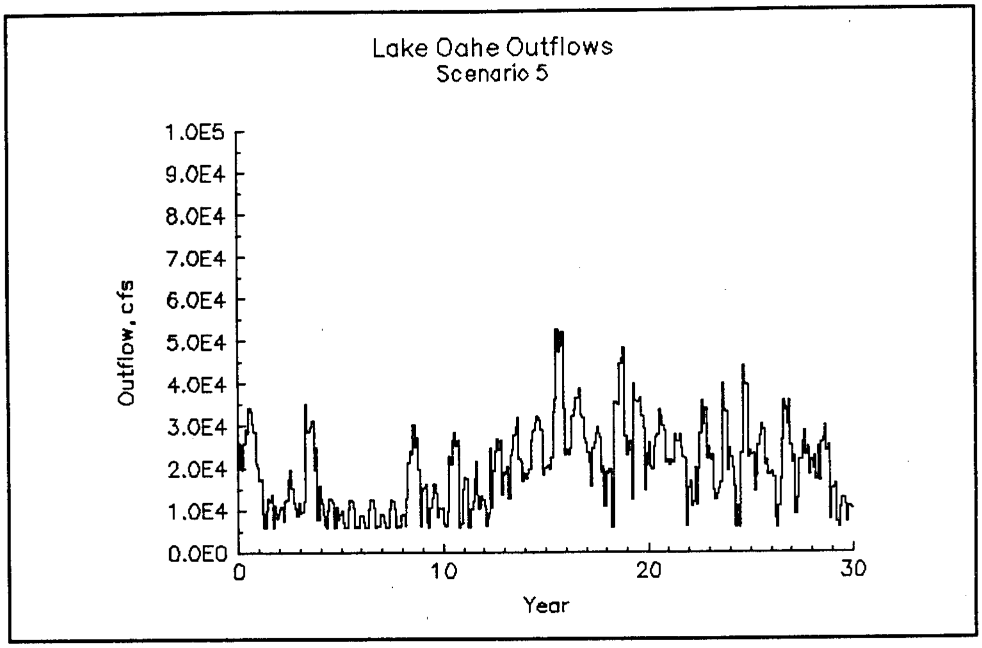

Figure 198. Lake Oahe scenario 5 outflows

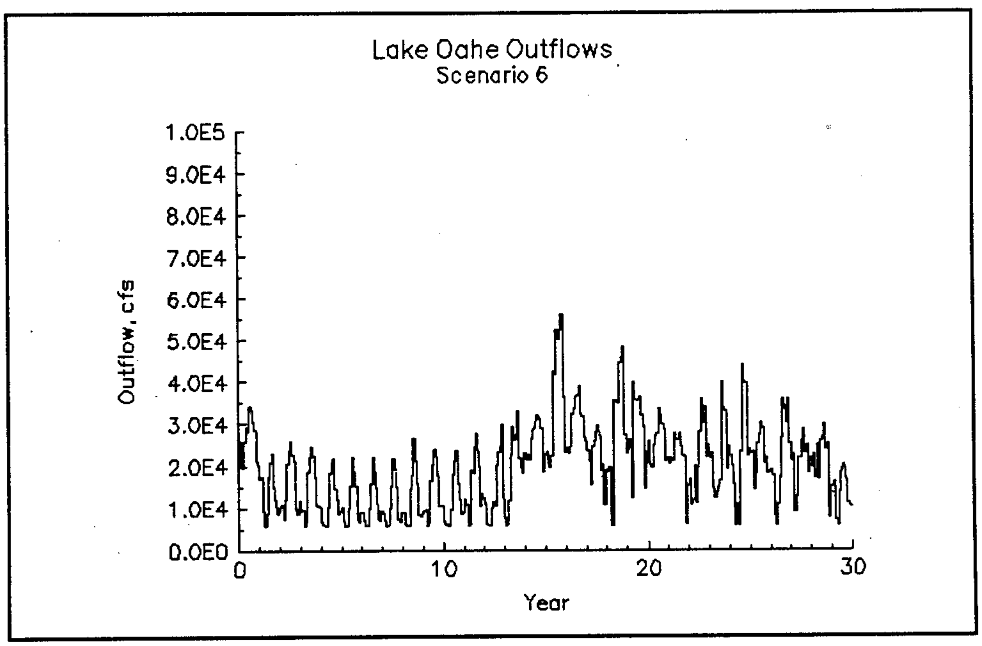

Figure 199. Lake Oahe scenario 6 outflows

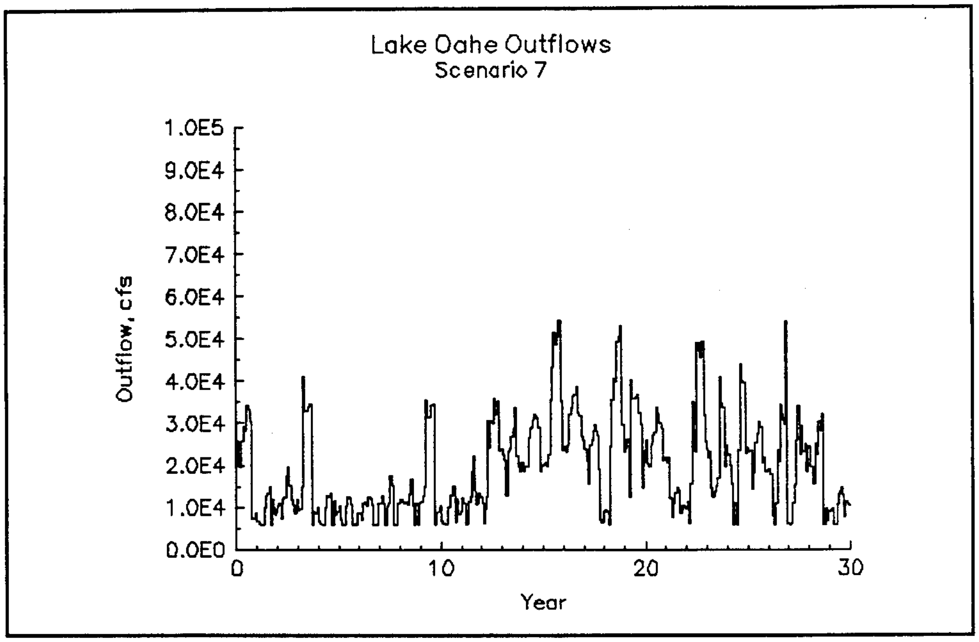

Figure 200. Lake Oahe scenario 7 outflows

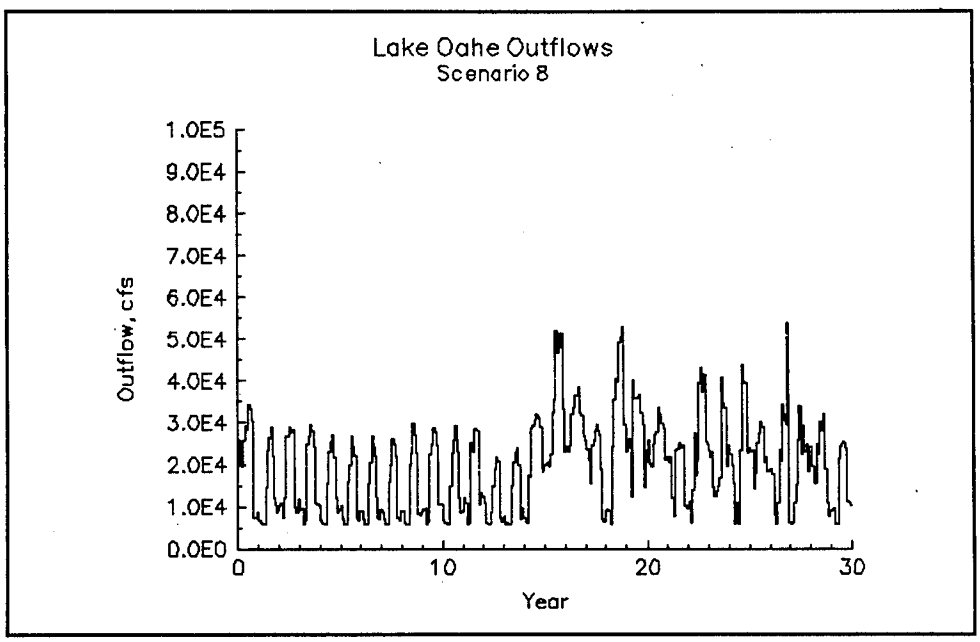

Figure 201. Lake Oahe scenario 8 outflows

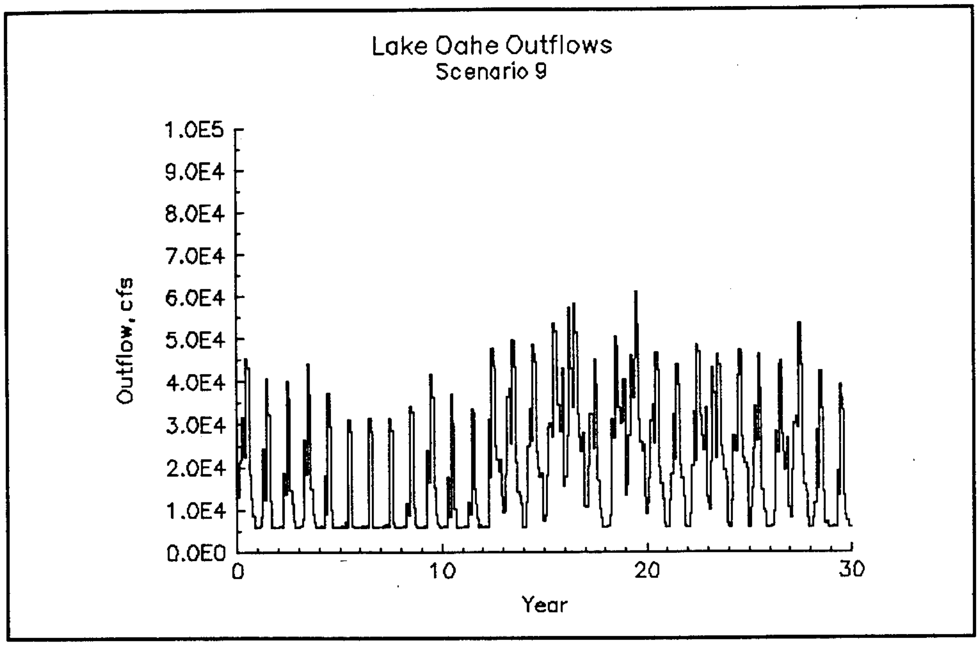

Figure 202. Lake Oahe scenario 9 outflows

Lake Francis Case. Releases for the nine scenarios are given in Figure 203-Figure 211.

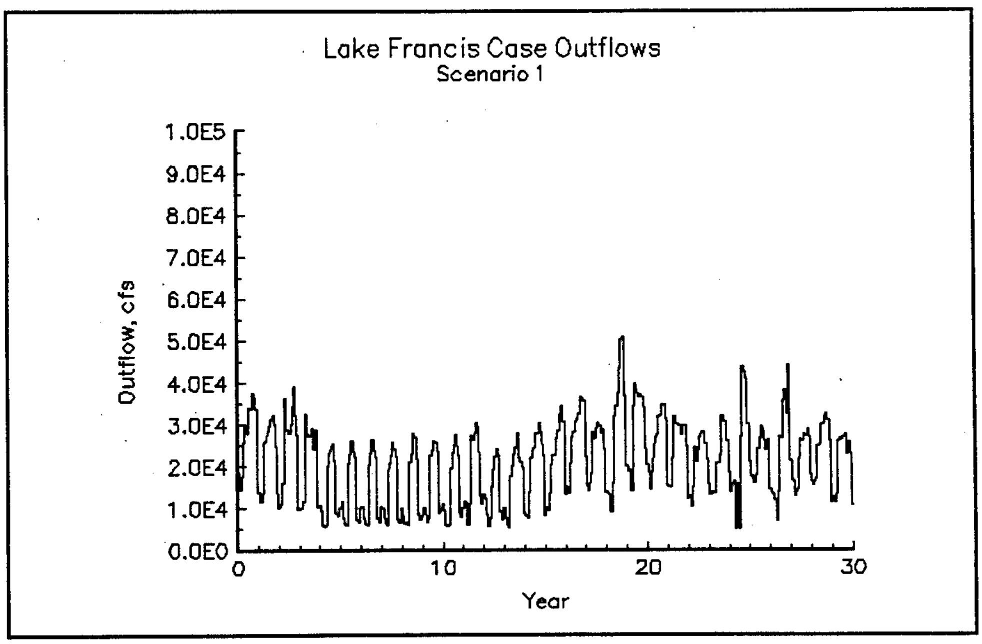

Figure 203. Lake Francis Case scenario 1 outflows

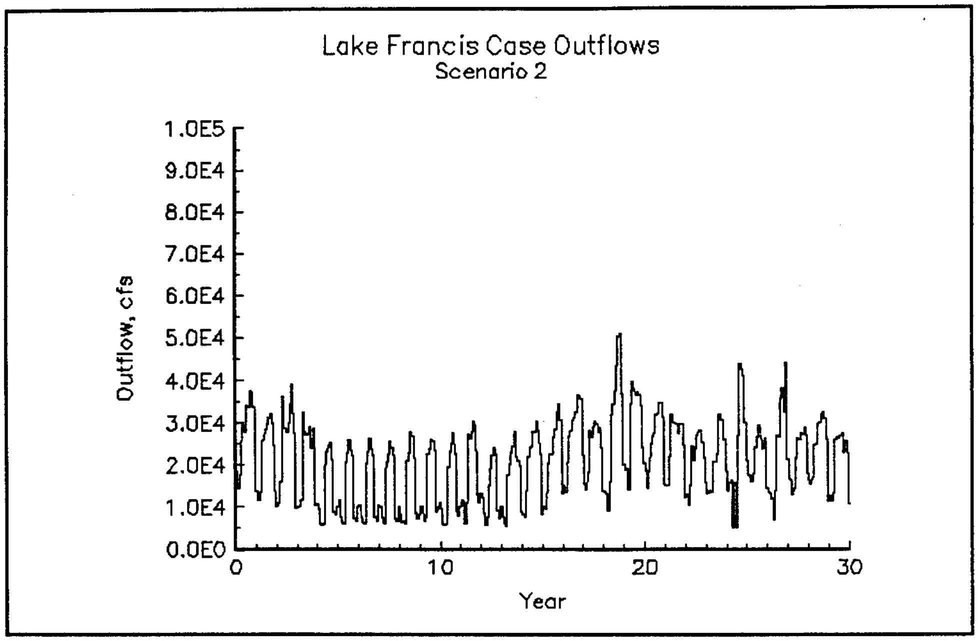

Figure 204. Lake Francis Case scenario 2 outflows

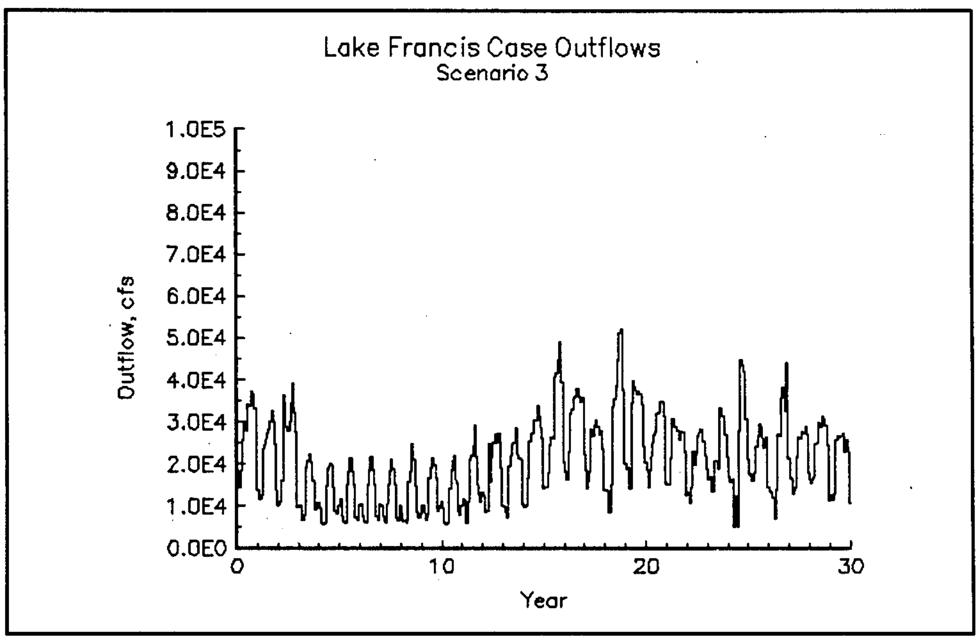

Figure 205. Lake Francis Case scenario 3 outflows

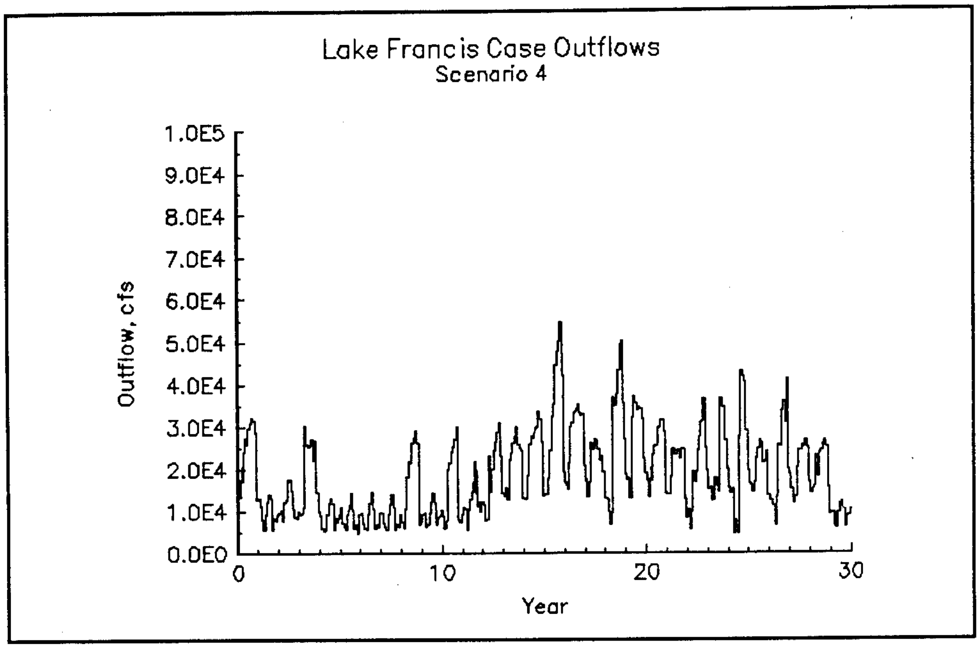

Figure 206. Lake Francis Case scenario 4 outflows

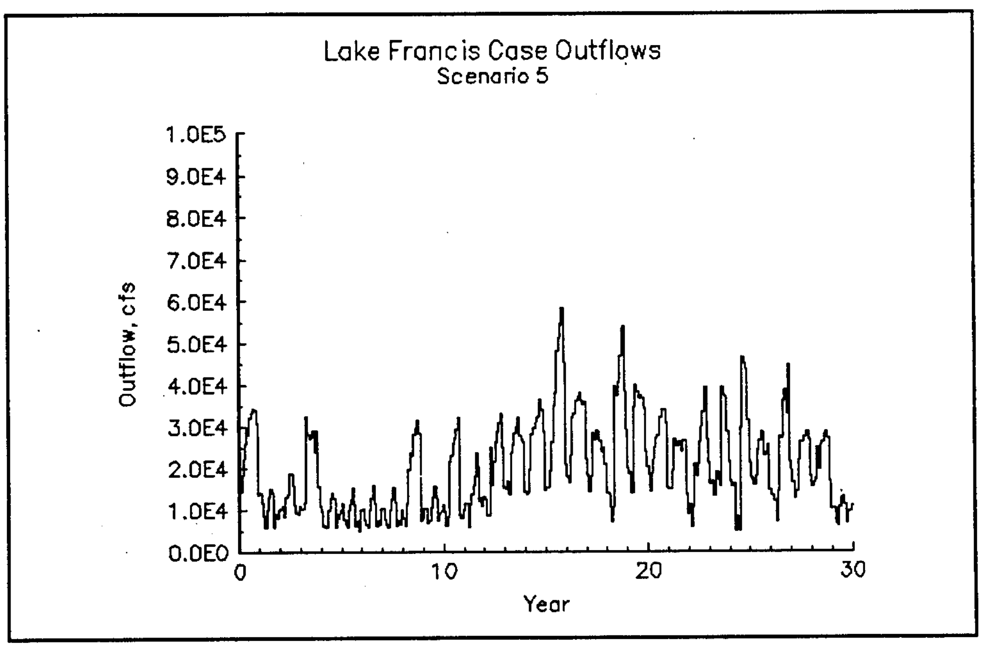

Figure 207. Lake Francis Case scenario 5 outflows

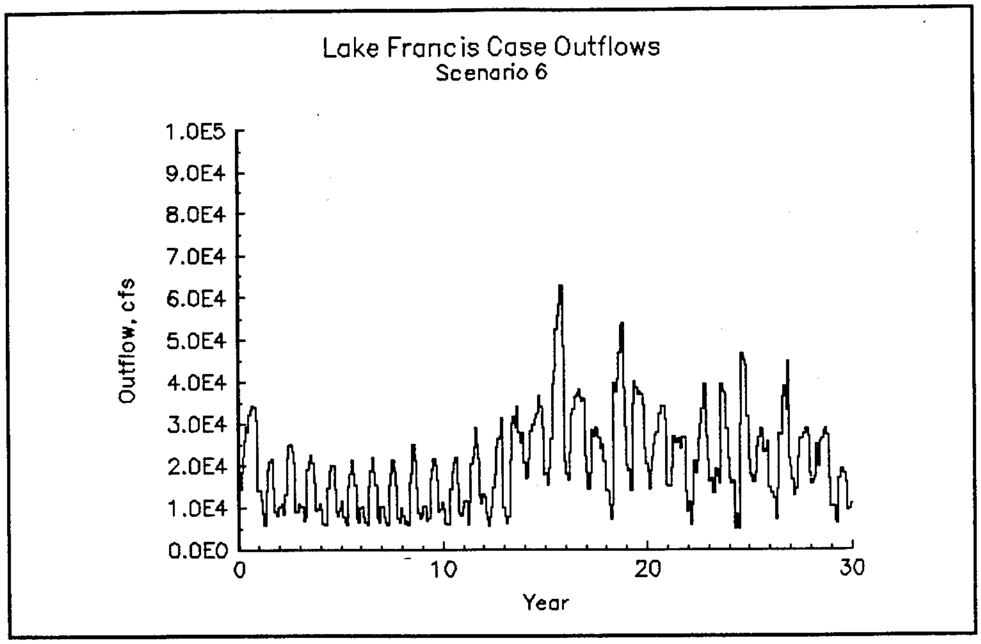

Figure 208. Lake Francis Case scenario 6 outflows

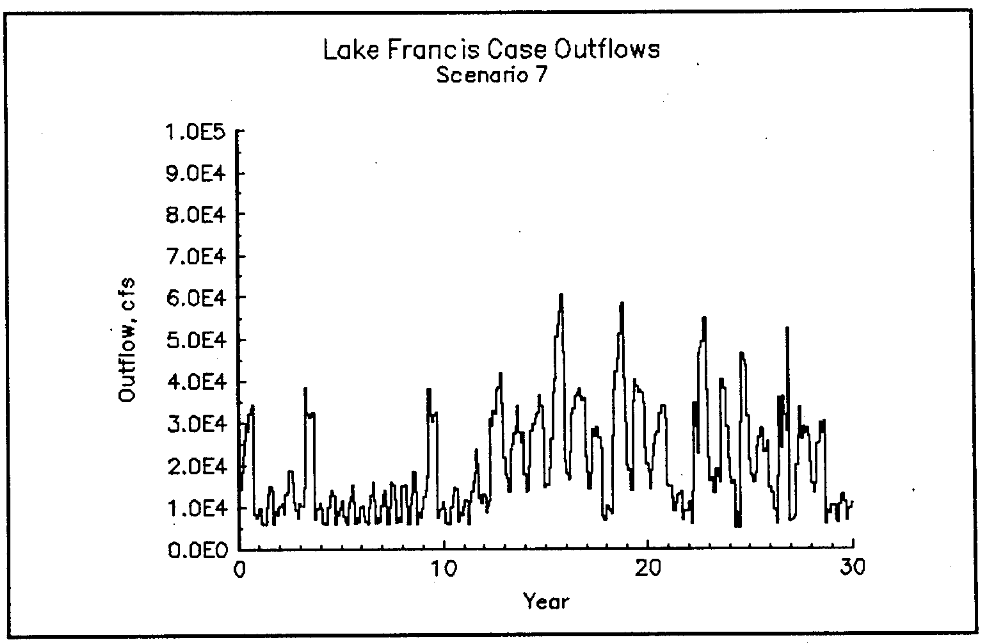

Figure 209. Lake Francis Case scenario 7 outflows

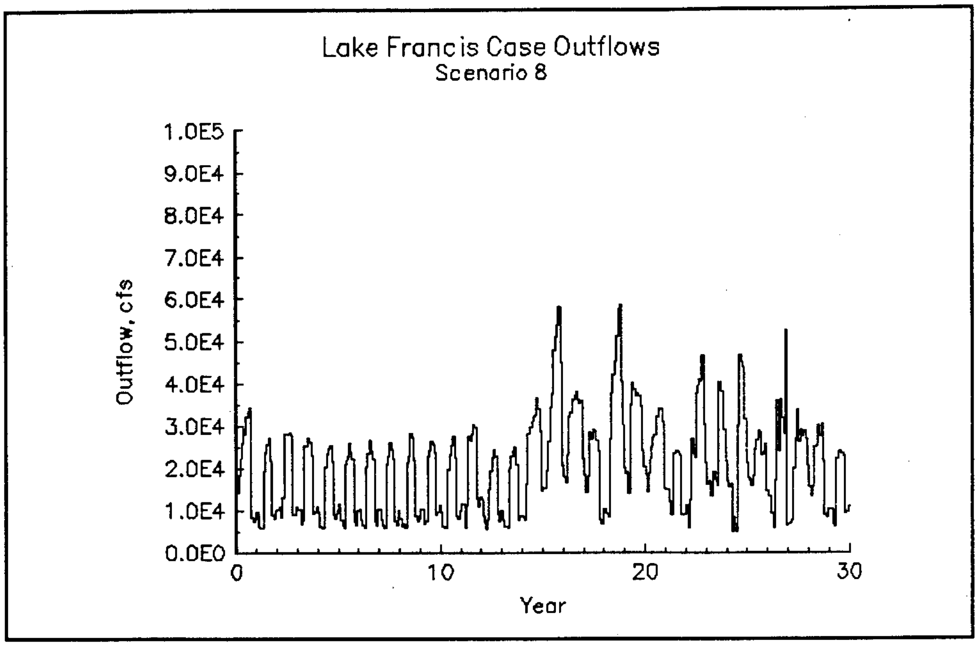

Figure 210. Lake Francis Case scenario 8 outflows

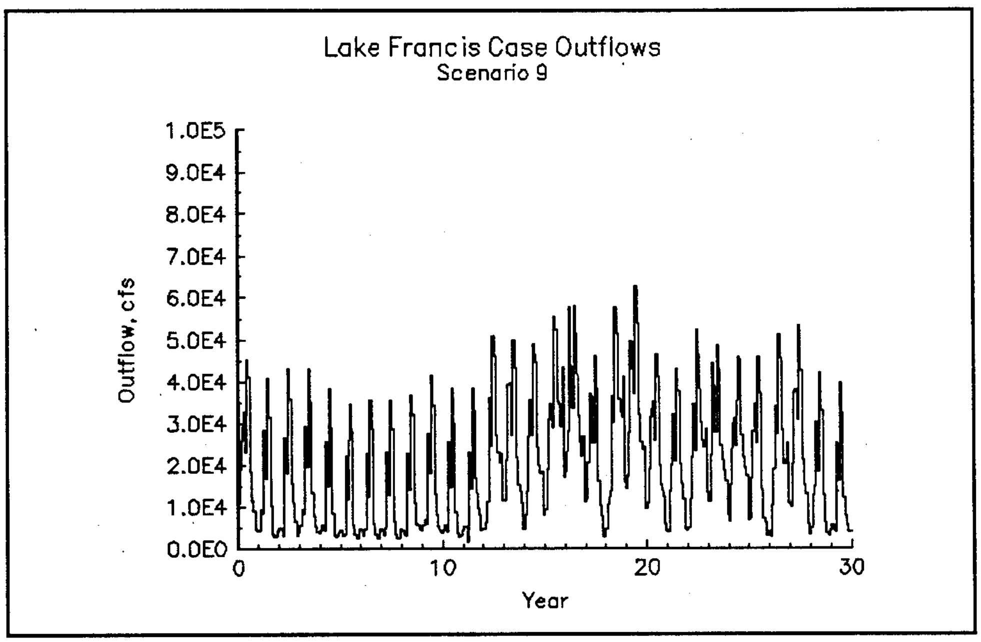

Figure 211. Lake Francis Case scenario 9 outflows

Inflow Temperatures

Fort Peck Lake. Inflow temperatures for the nine scenarios are the same and are given in Figure 212.

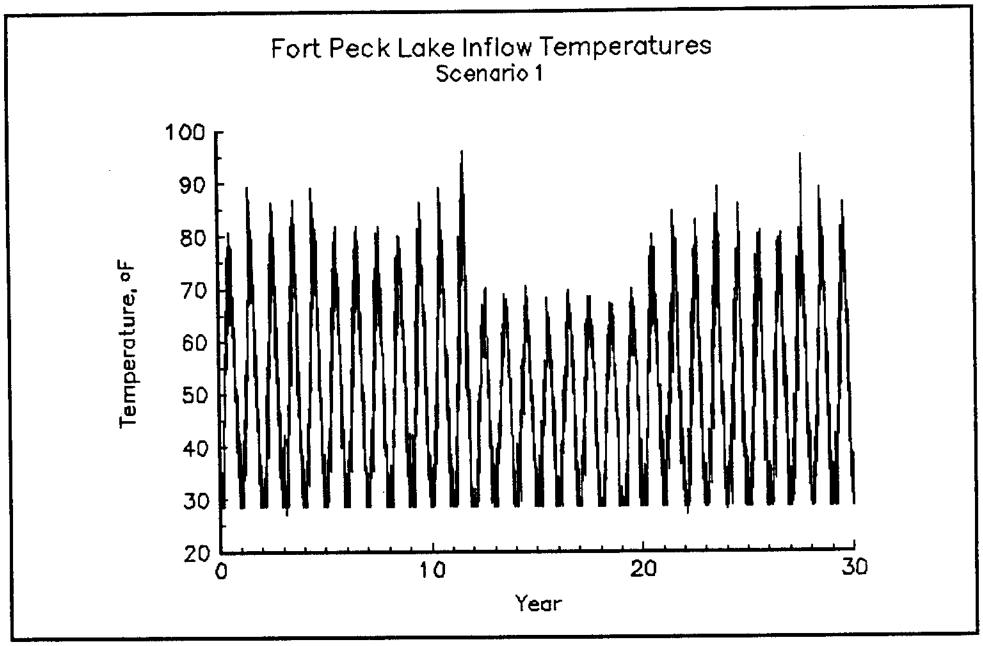

Figure 212. Fort Peck Lake scenario 1 inflow temperatures

Lake Sakakawea. Inflow temperatures for the nine scenarios are given in Figure 213-Figure 221.

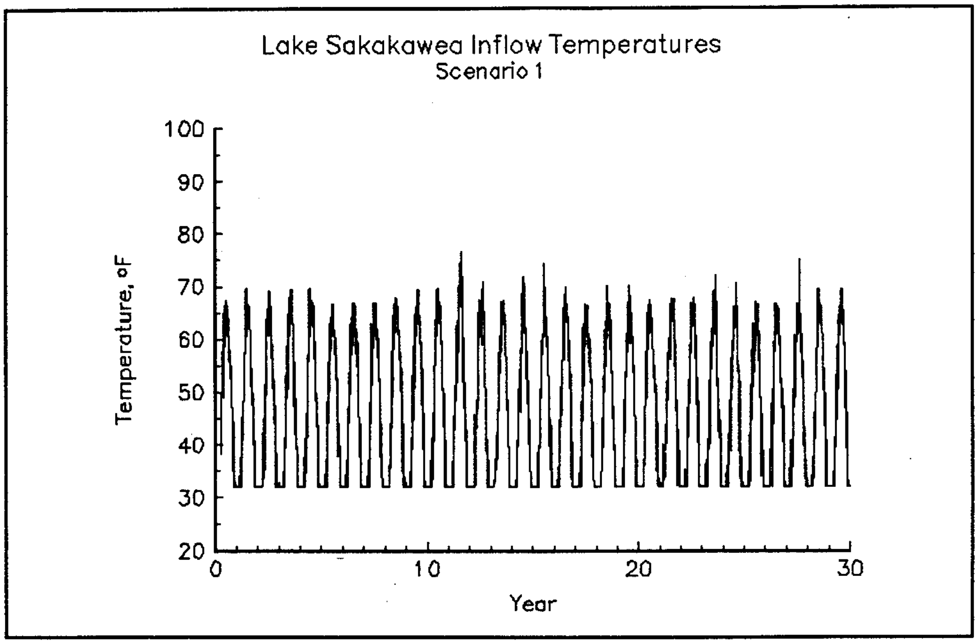

Figure 213. Lake Sakakawea scenario 1 inflow temperatures

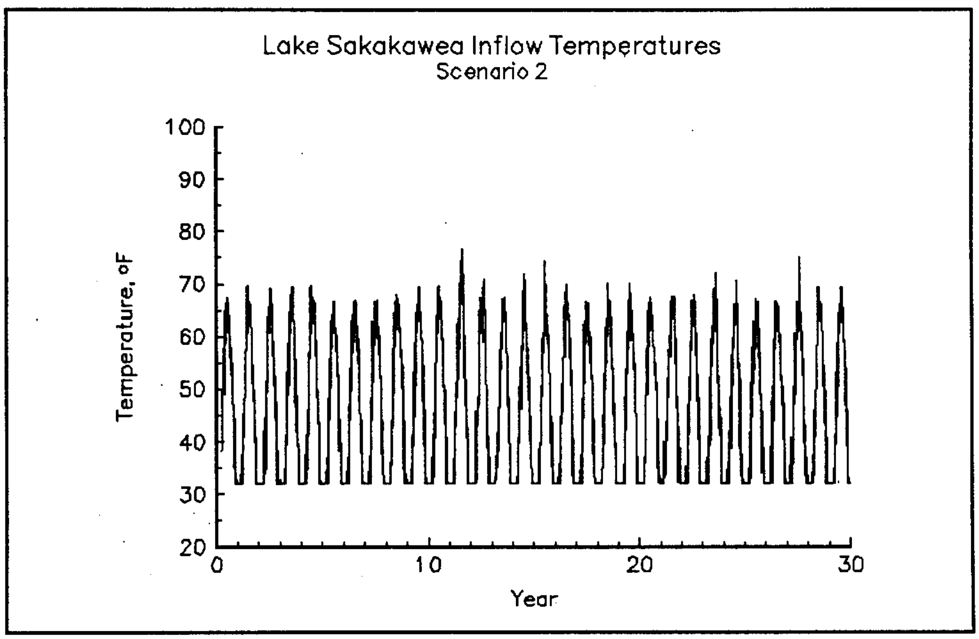

Figure 214. Lake Sakakawea scenario 2 inflow temperatures

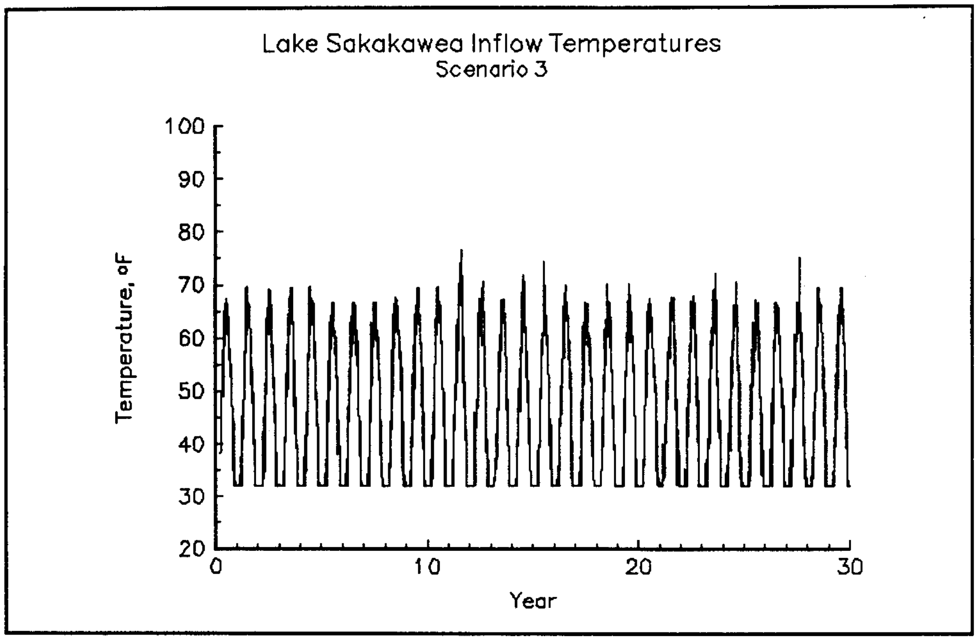

Figure 215. Lake Sakakawea scenario 3 inflow temperatures

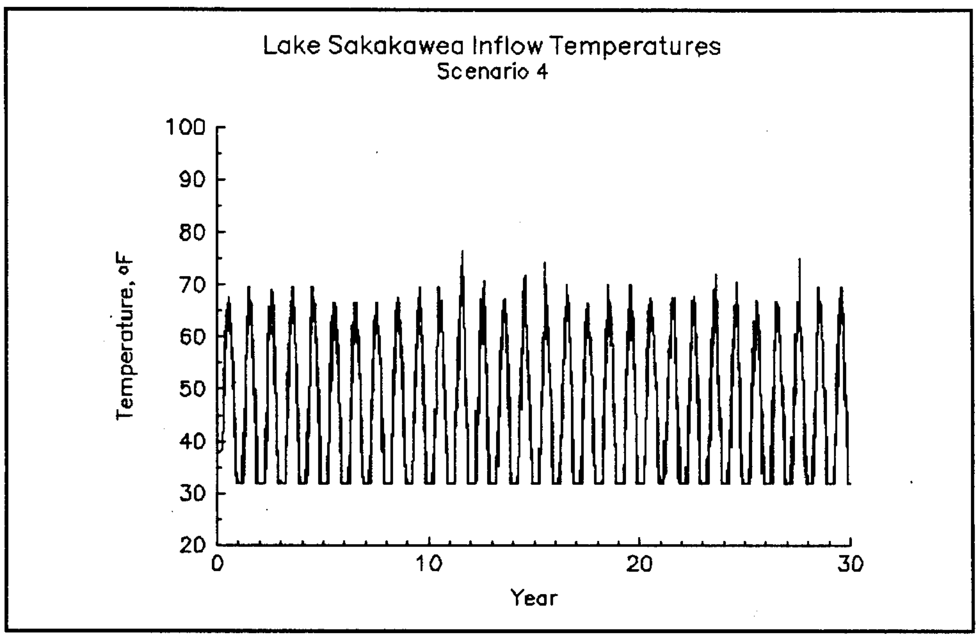

Figure 216. Lake Sakakawea scenario 4 inflow temperatures

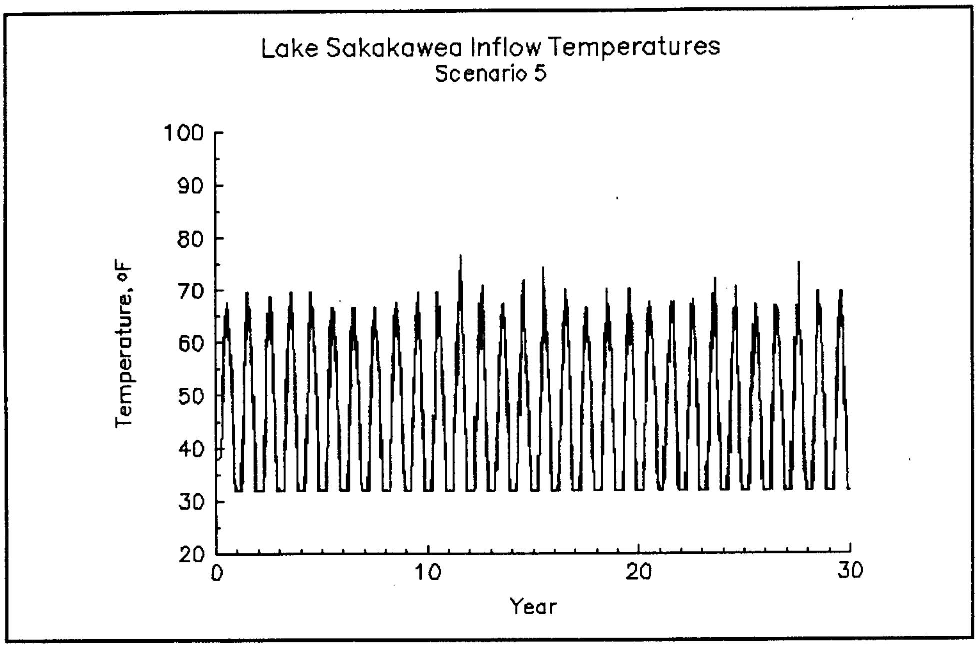

Figure 217. Lake Sakakawea scenario 5 inflow temperatures

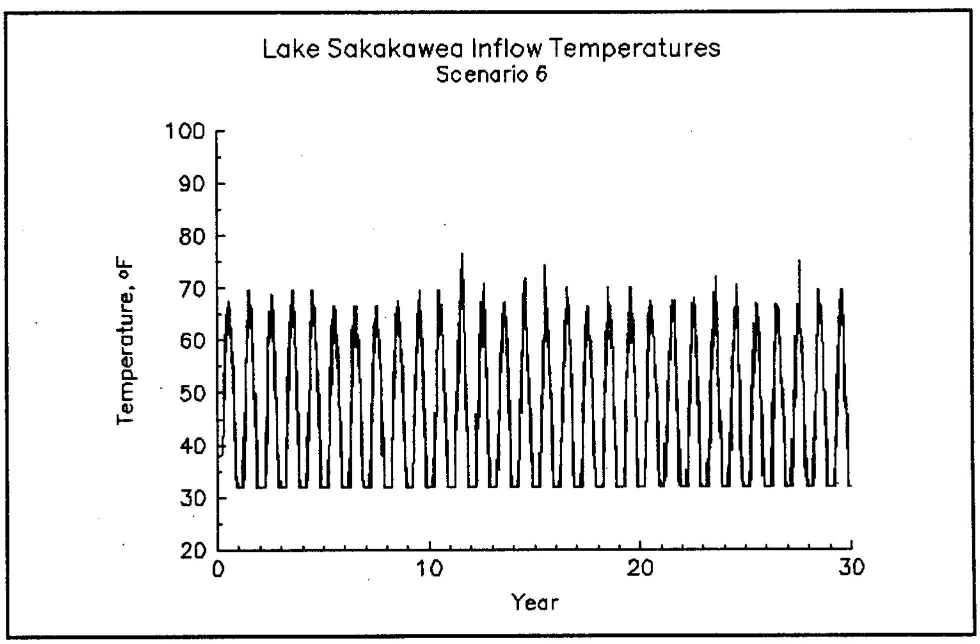

Figure 218. Lake Sakakawea scenario 6 inflow temperatures

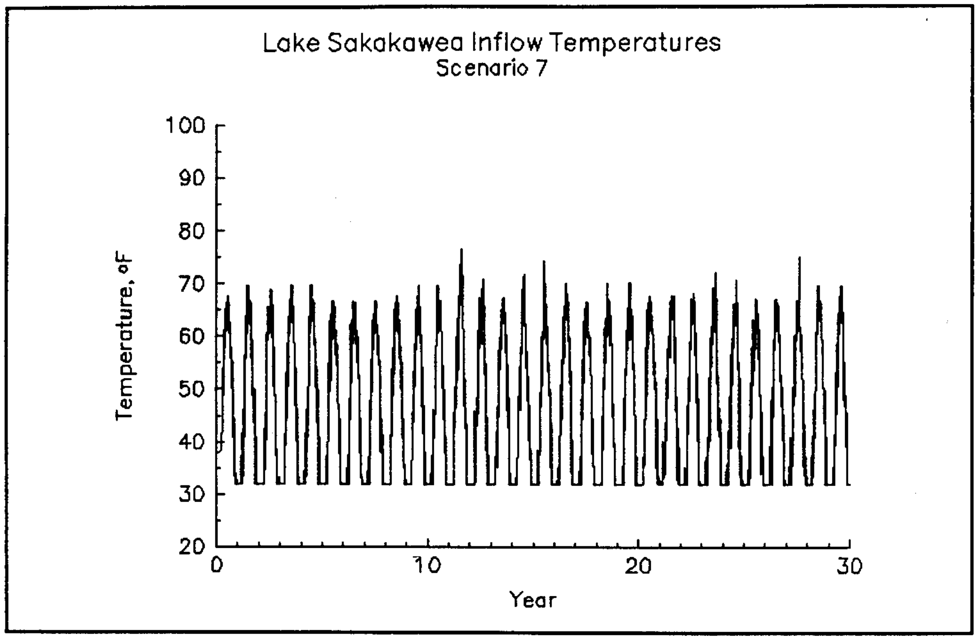

Figure 219. Lake Sakakawea scenario 7 inflow temperatures

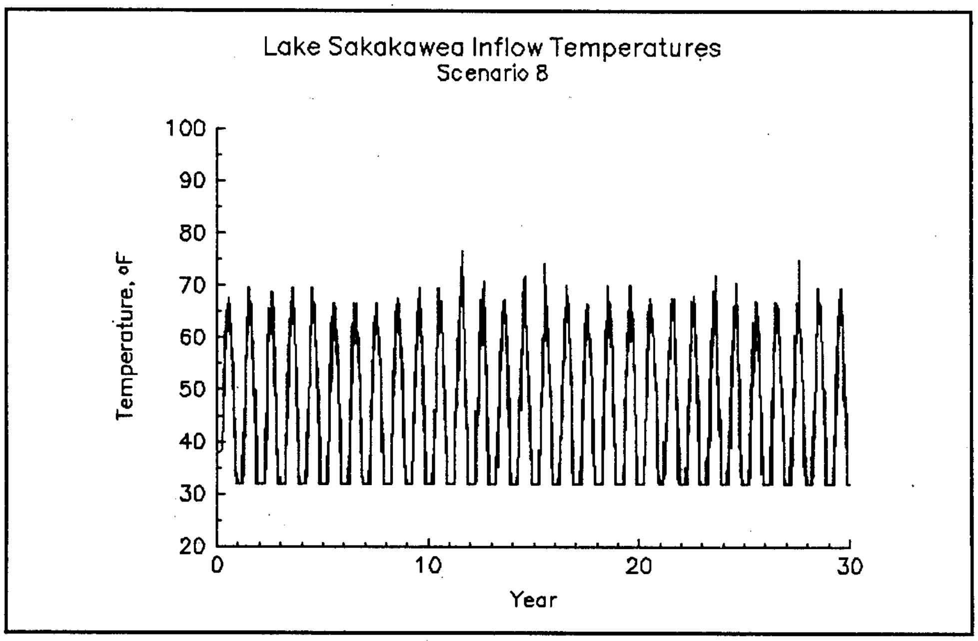

Figure 220. Lake Sakakawea scenario 8 inflow temperatures

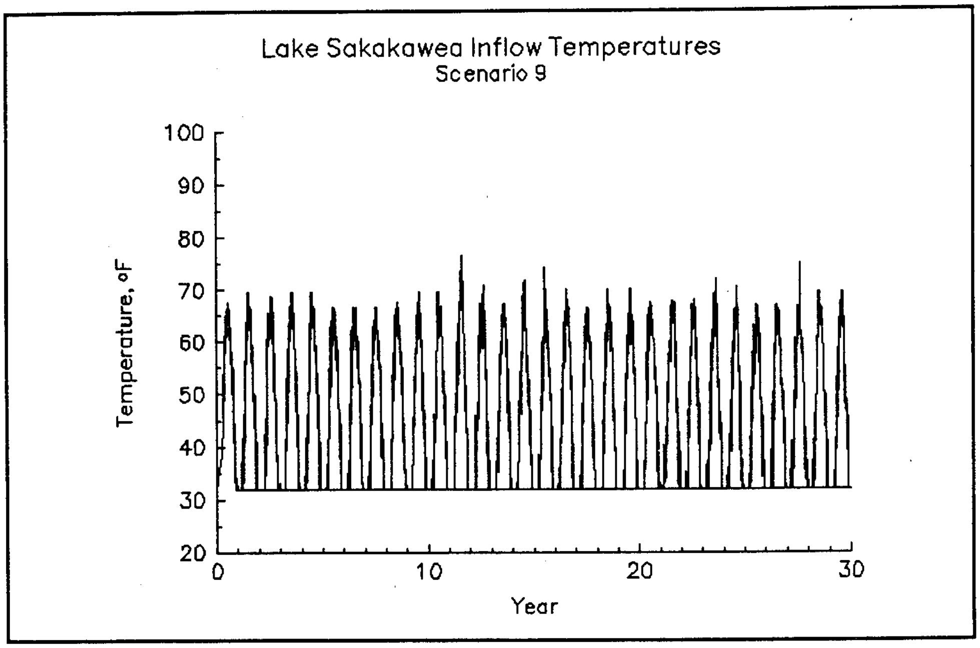

Figure 221. Lake Sakakawea scenario 9 inflow temperatures

Lake Oahe. Inflow temperatures for the nine scenarios are given in Figure 222-Figure 230.

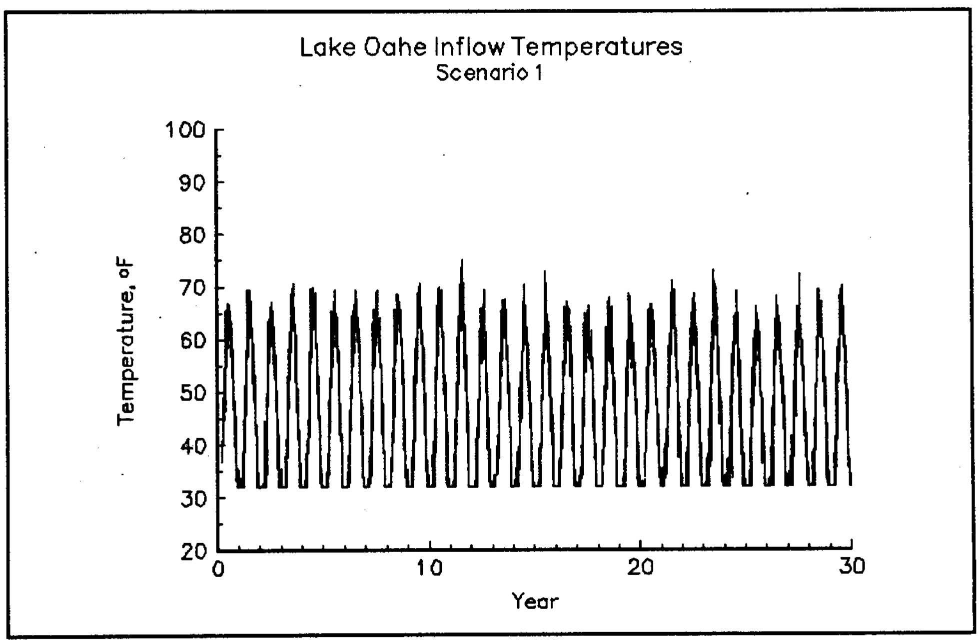

Figure 222. Lake Oahe scenario 1 inflow temperatures

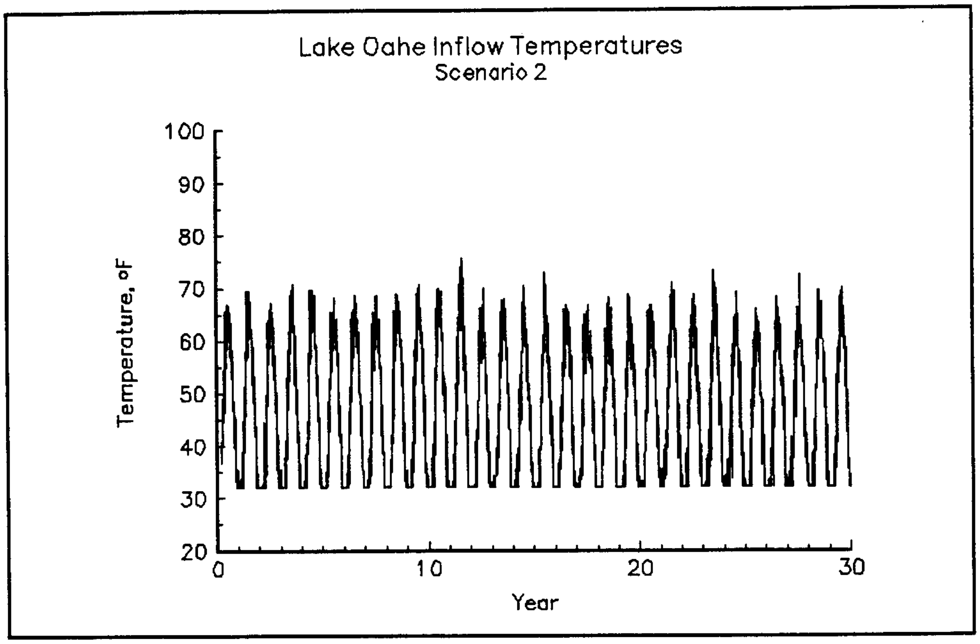

Figure 223. Lake Oahe scenario 2 inflow temperatures

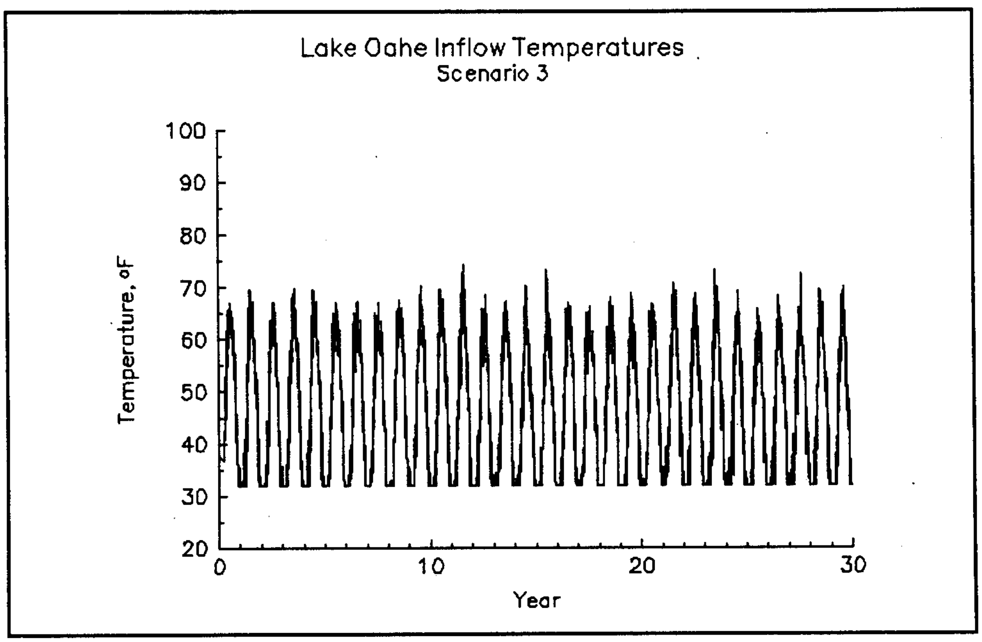

Figure 224. Lake Oahe scenario 3 inflow temperatures

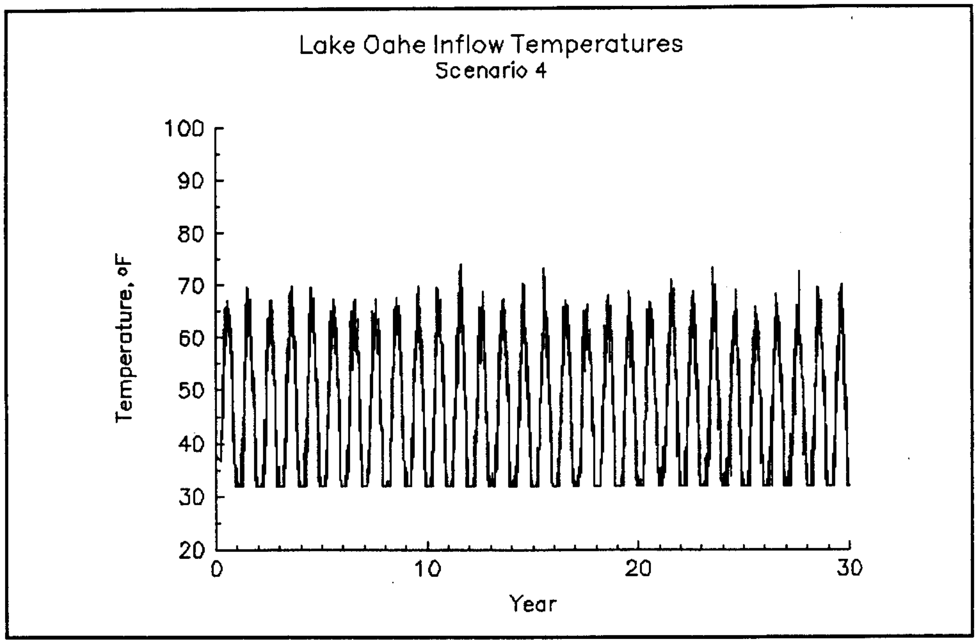

Figure 225. Lake Oahe scenario 4 inflow temperatures

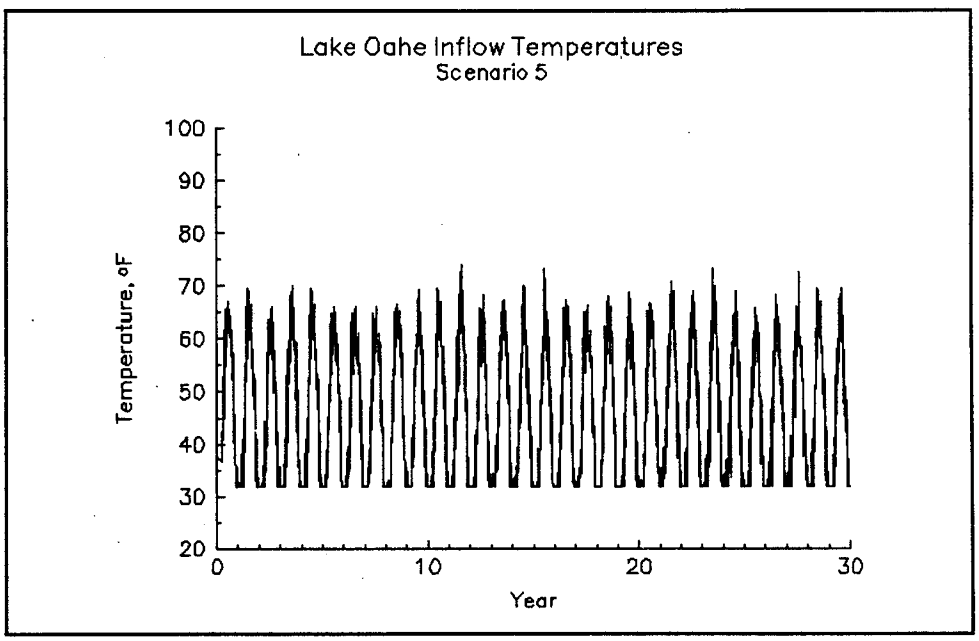

Figure 226. Lake Oahe scenario 5 inflow temperatures

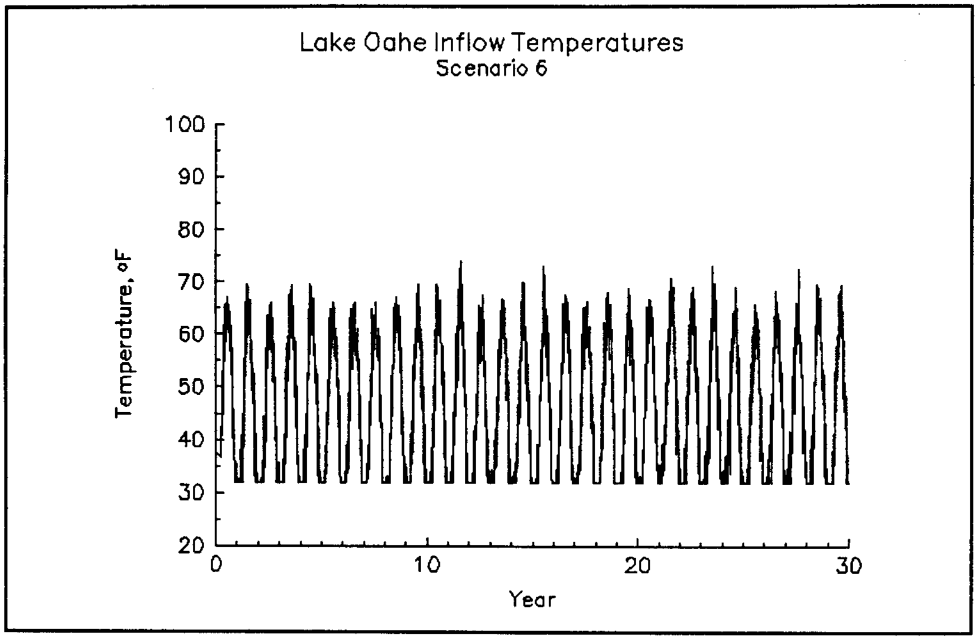

Figure 227. Lake Oahe scenario 6 inflow temperatures

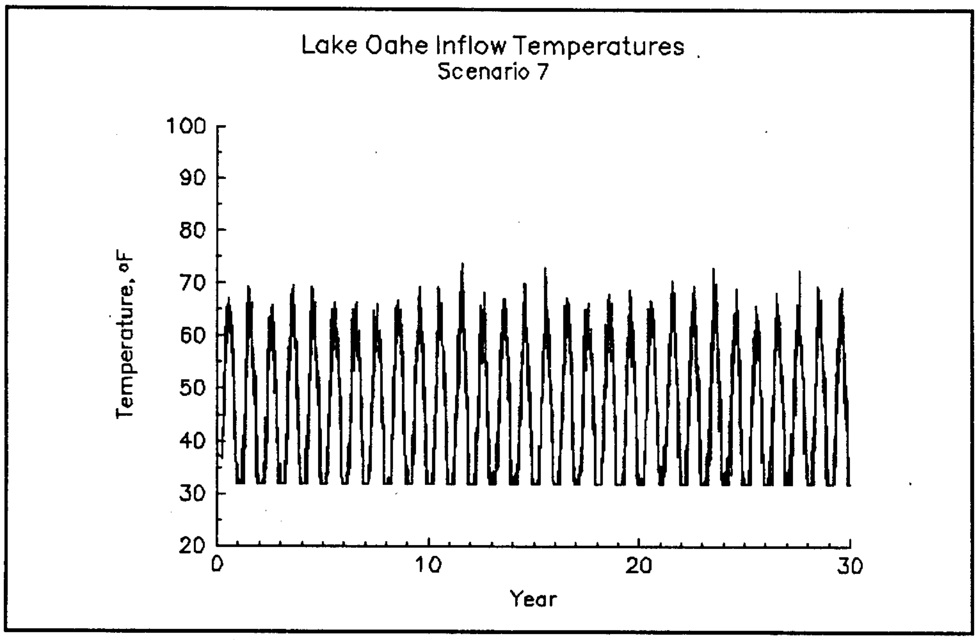

Figure 228. Lake Oahe scenario 7 inflow temperatures

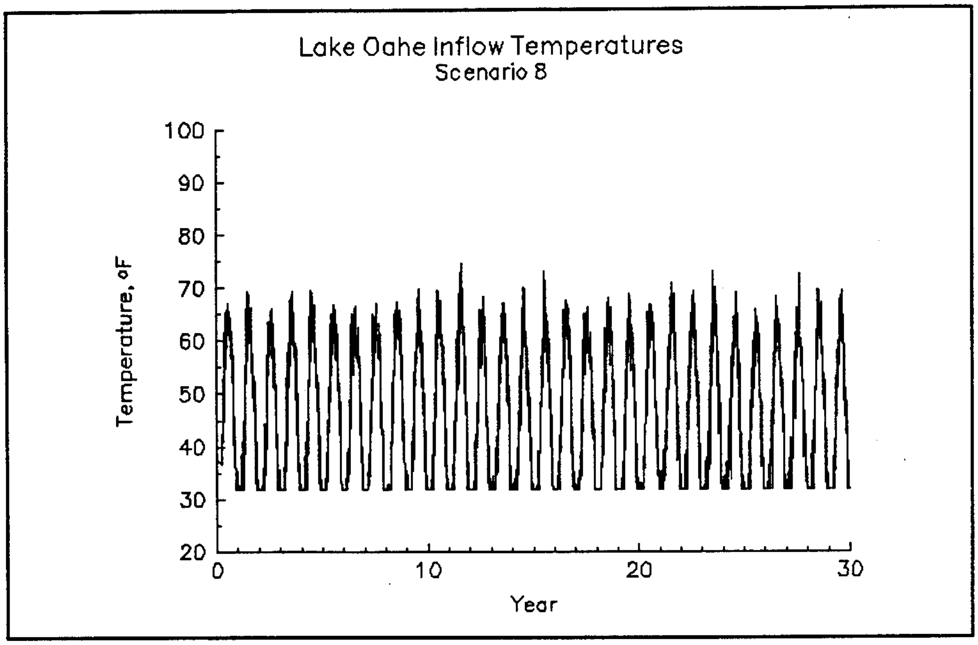

Figure 229. Lake Oahe scenario 8 inflow temperatures

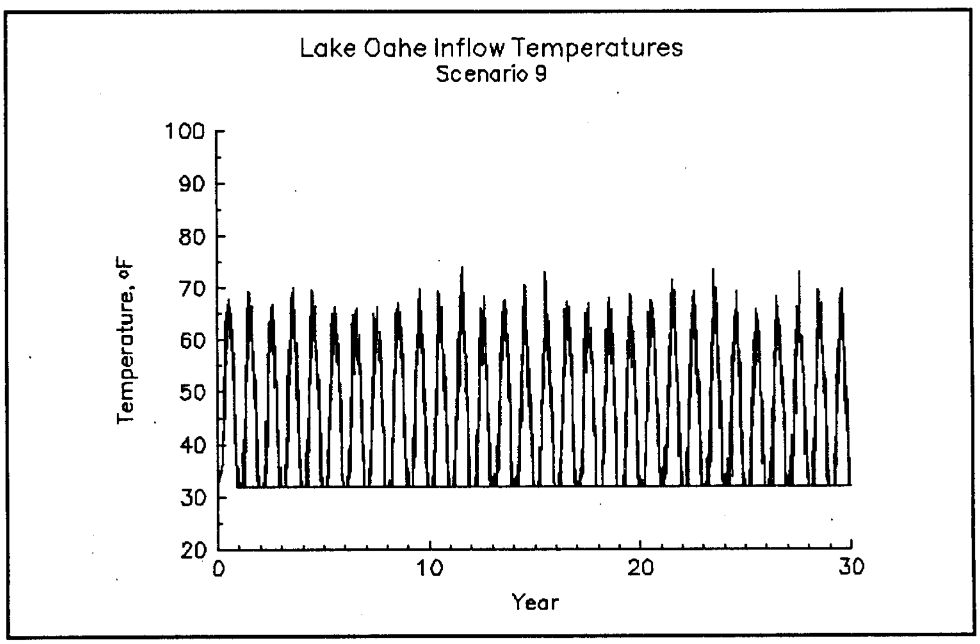

Figure 230. Lake Oahe scenario 9 inflow temperatures

Lake Francis Case. Inflow temperatures for the nine scenarios are given in Figure 231-Figure 239.

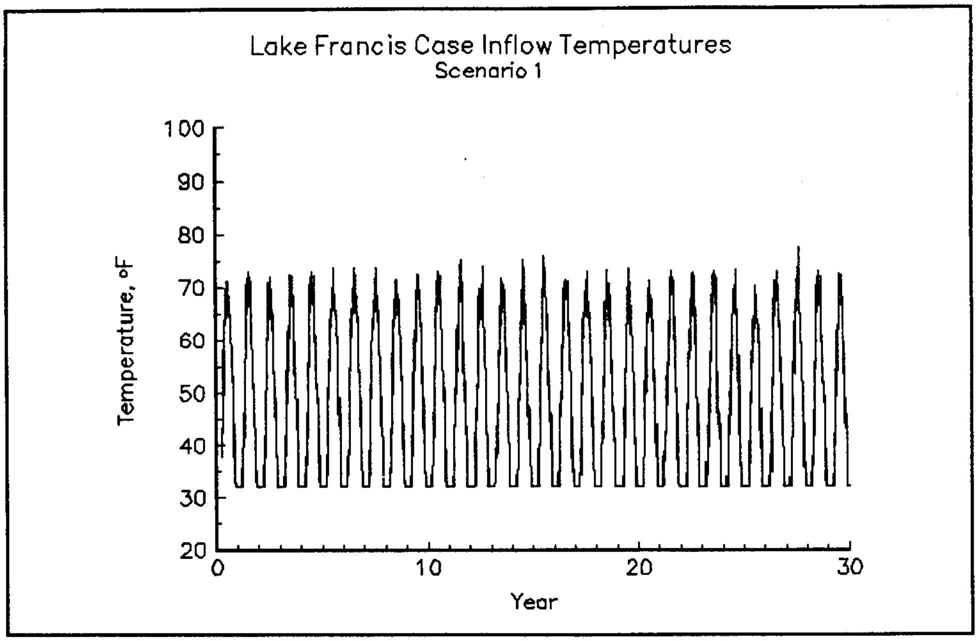

Figure 231. Lake Francis Case scenario 1 inflow temperatures

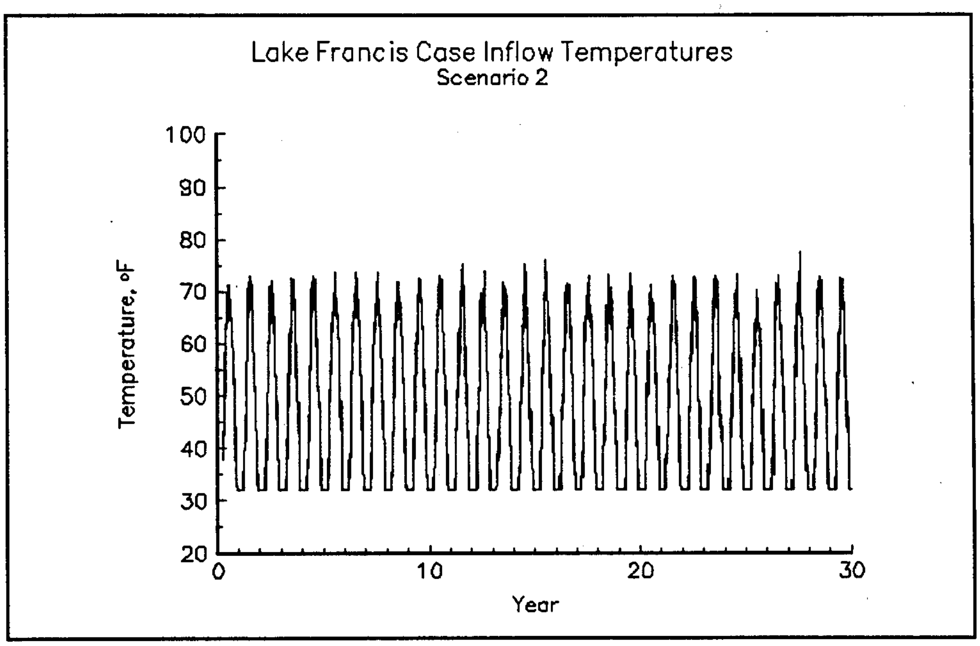

Figure 232. Lake Francis Case scenario 2 inflow temperatures

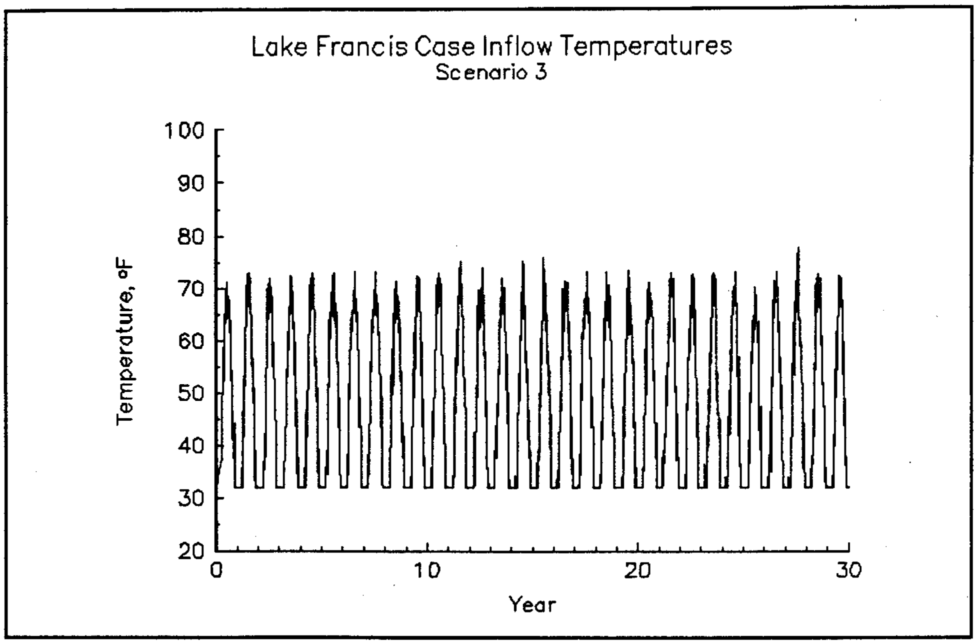

Figure 233. Lake Francis Case scenario 3 inflow temperatures

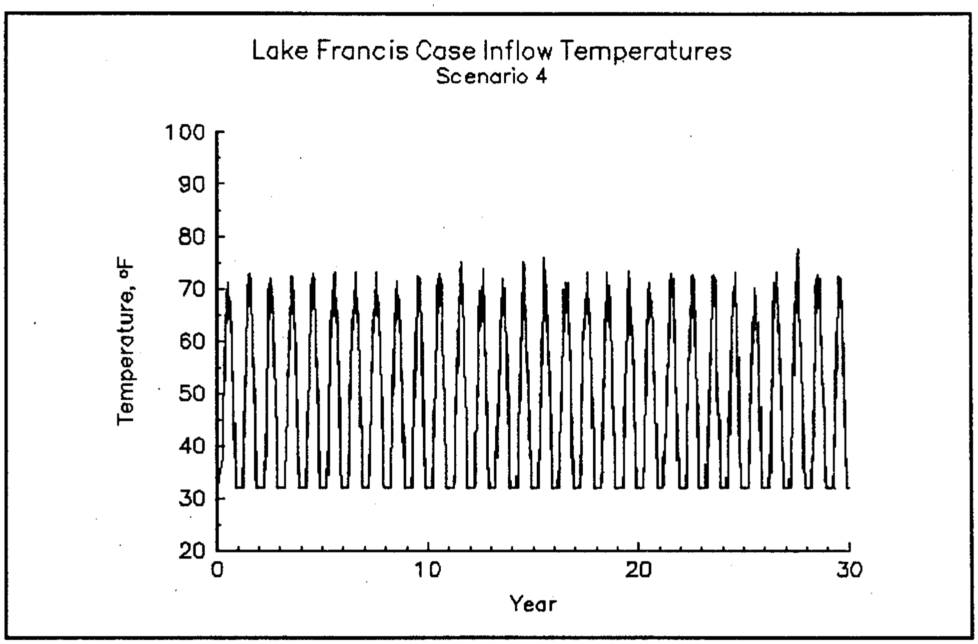

Figure 234. Lake Francis Case scenario 4 inflow temperatures

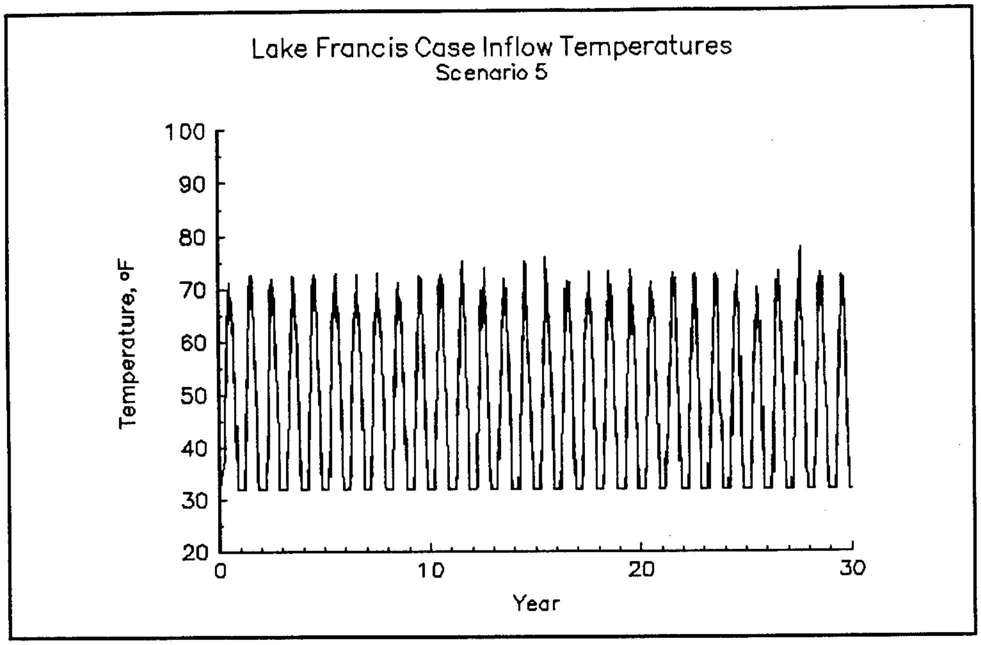

Figure 235. Lake Francis Case scenario 5 inflow temperatures

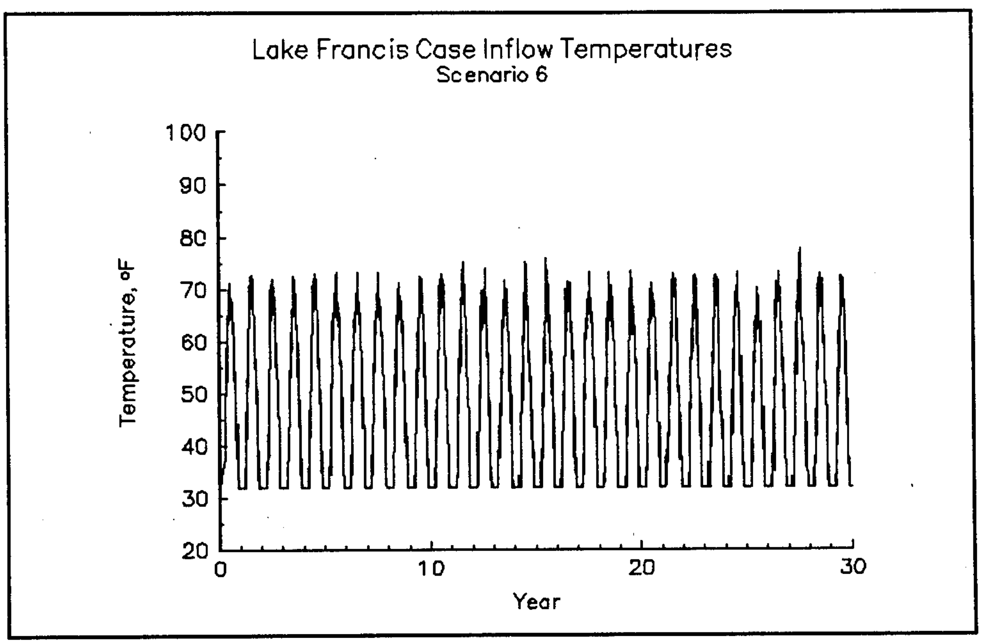

Figure 236. Lake Francis Case scenario 6 inflow temperatures

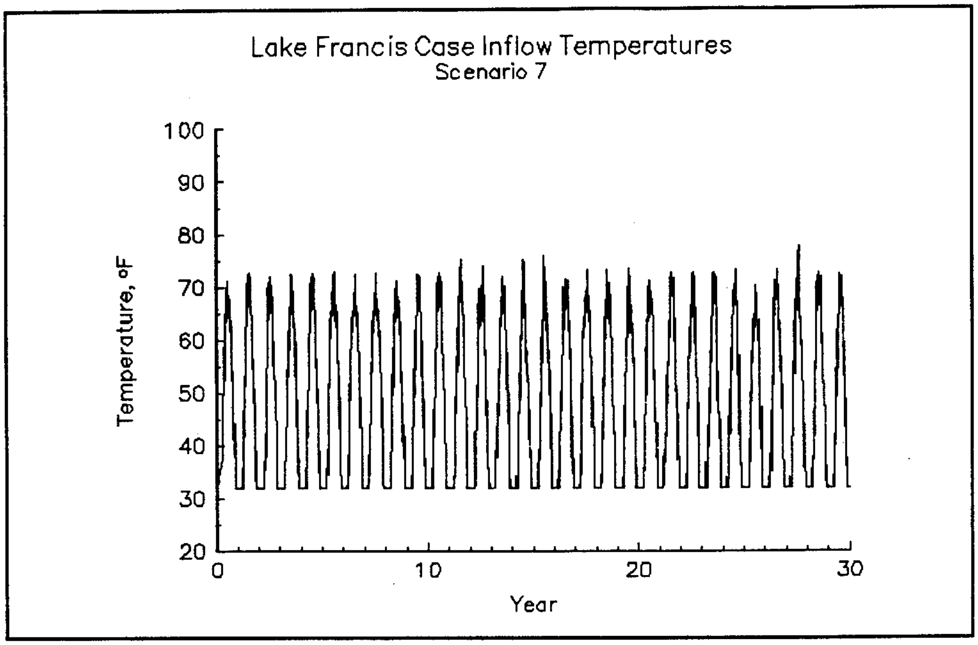

Figure 237. Lake Francis Case scenario 7 inflow temperatures

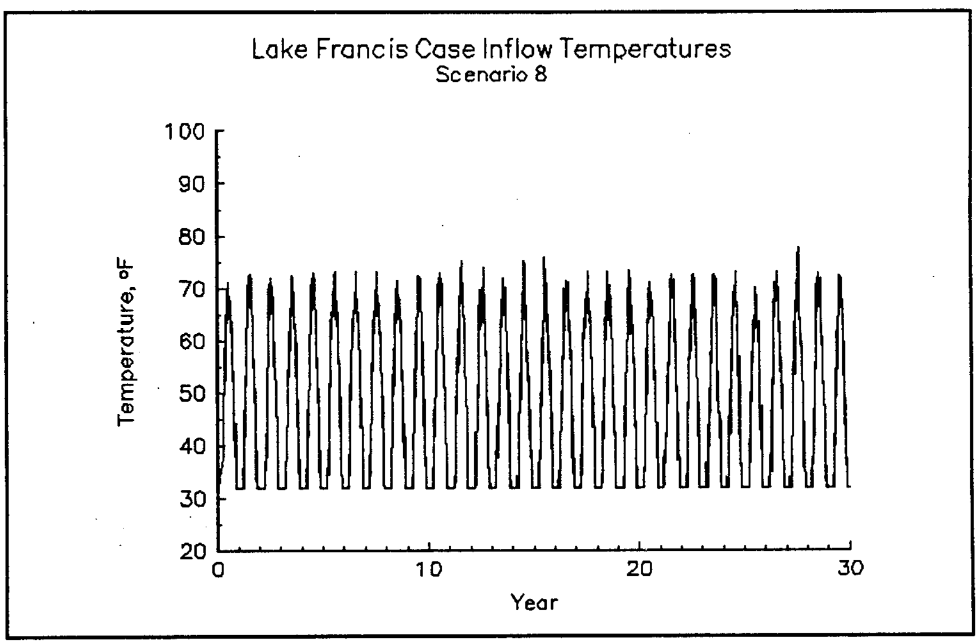

Figure 238. Lake Francis Case scenario 8 inflow temperatures

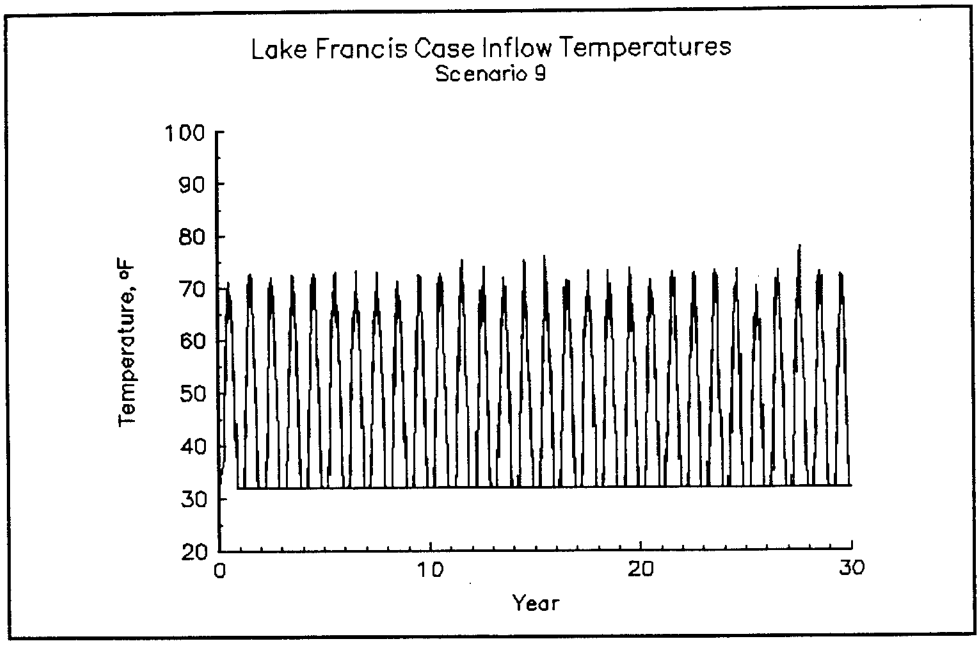

Figure 239. Lake Francis Case scenario 9 inflow temperatures

Inflow DO

Fort Peck Lake. Inflow DO for the nine scenarios are the same and are given in Figure 240.

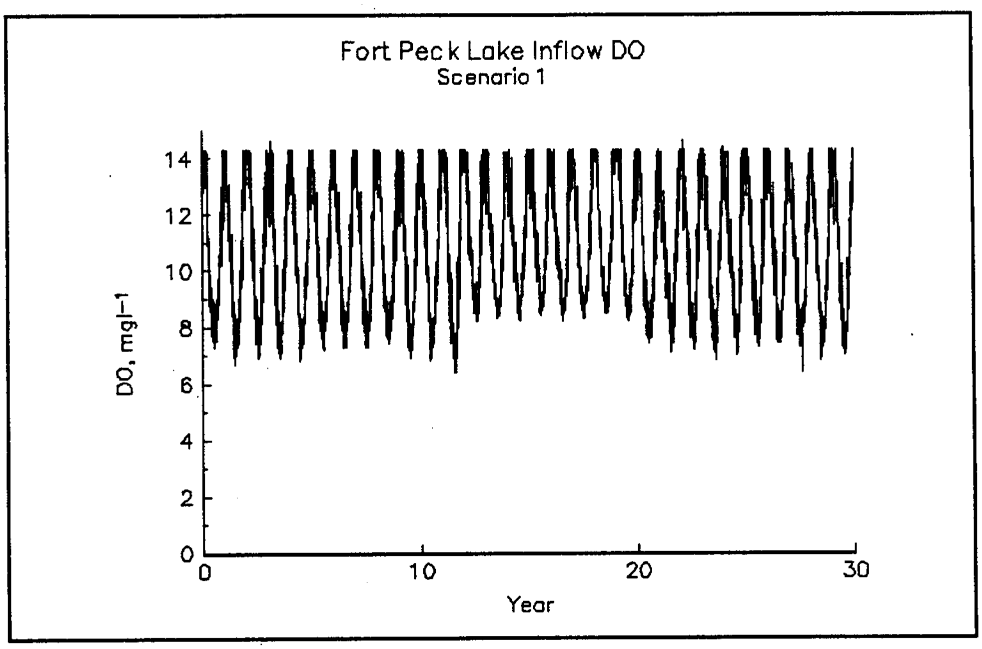

Figure 240. Fort Peck Lake scenario 1 inflow DO

Lake Sakakawea. Inflow DO for the nine scenarios are given in Figure 241-Figure 249.

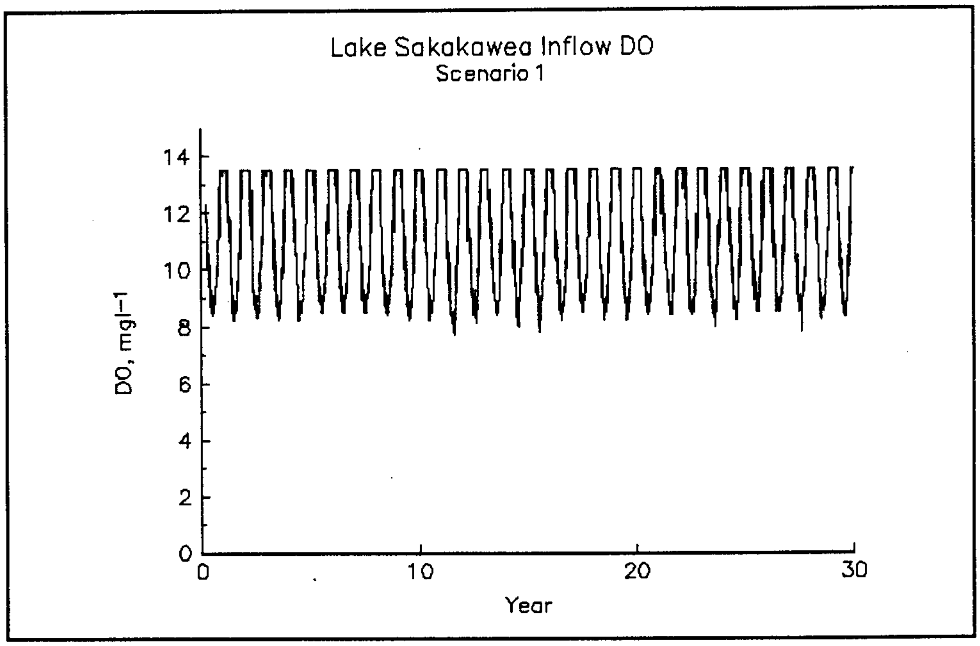

Figure 241. Lake Sakakawea scenario 1 inflow DO

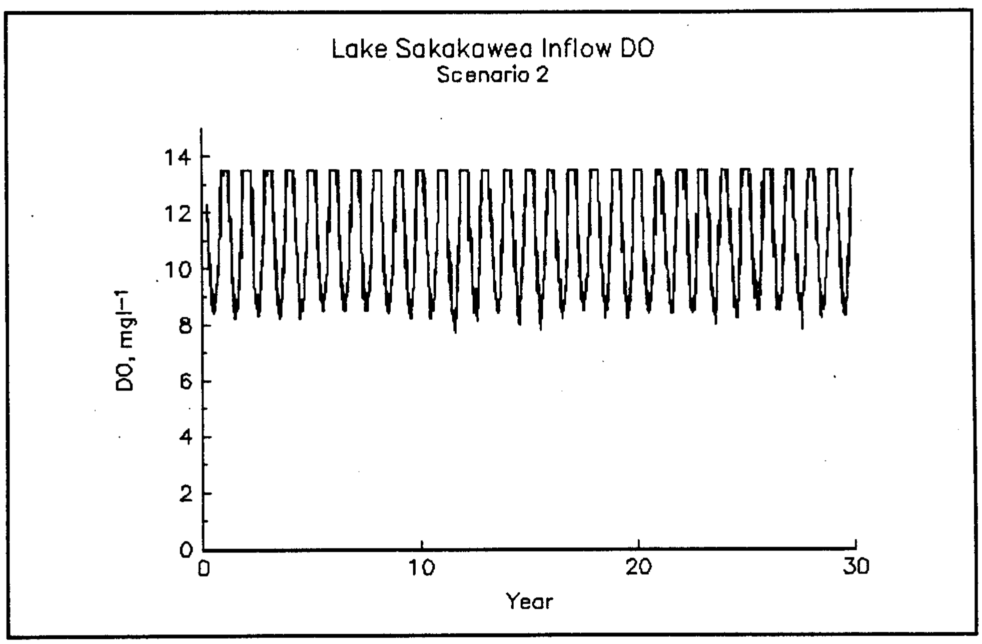

Figure 242. Lake Sakakawea scenario 2 inflow DO

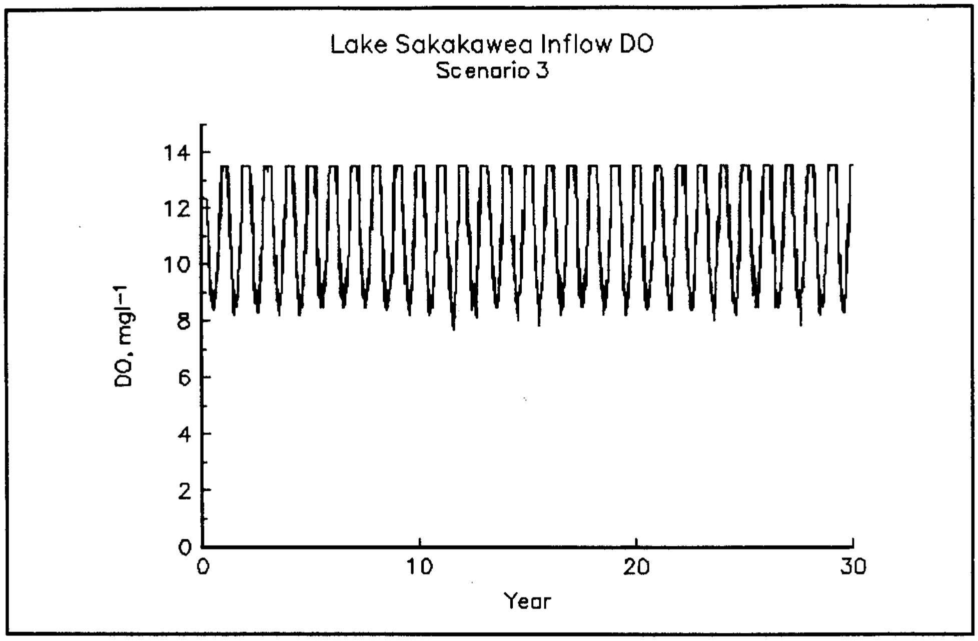

Figure 243. Lake Sakakawea scenario 3 inflow DO

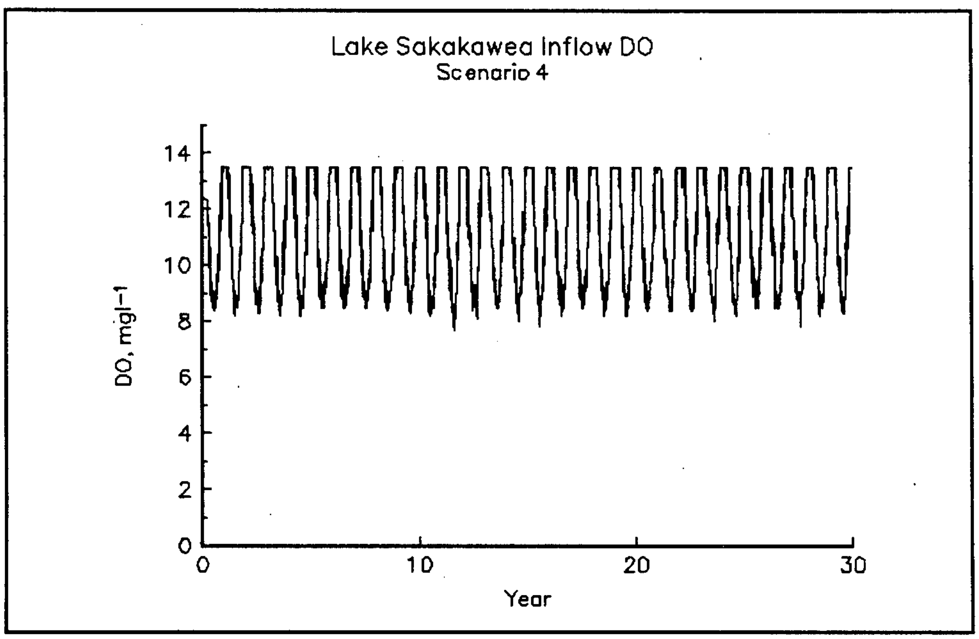

Figure 244. Lake Sakakawea scenario 4 inflow DO

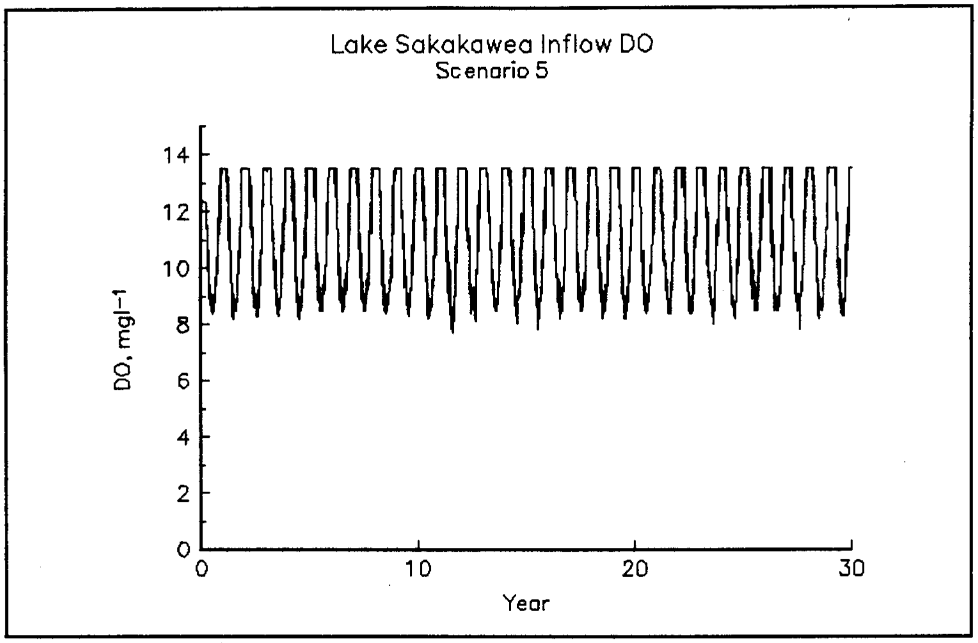

Figure 245. Lake Sakakawea scenario 5 inflow DO

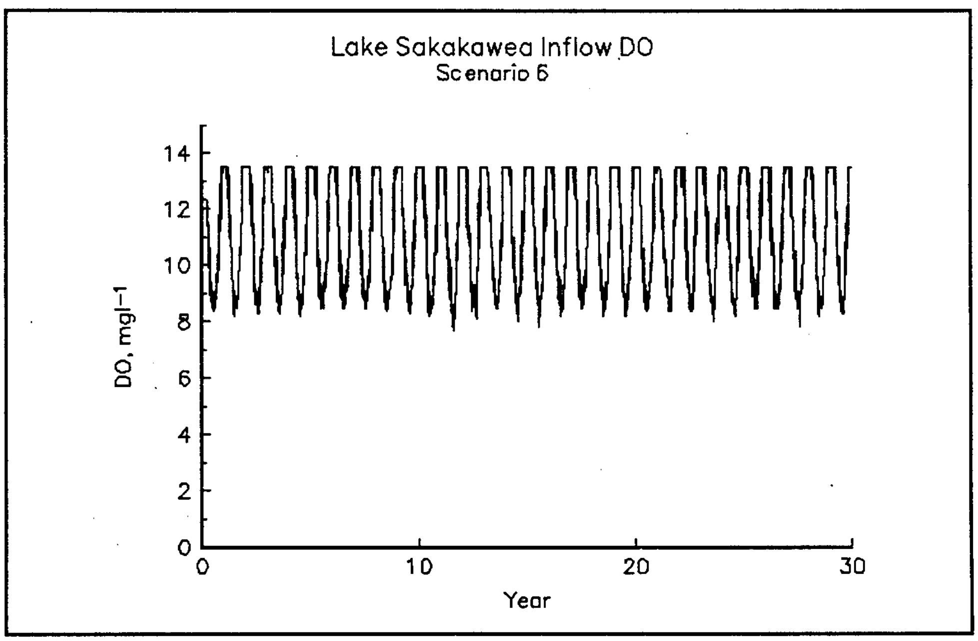

Figure 246. Lake Sakakawea scenario 6 inflow DO

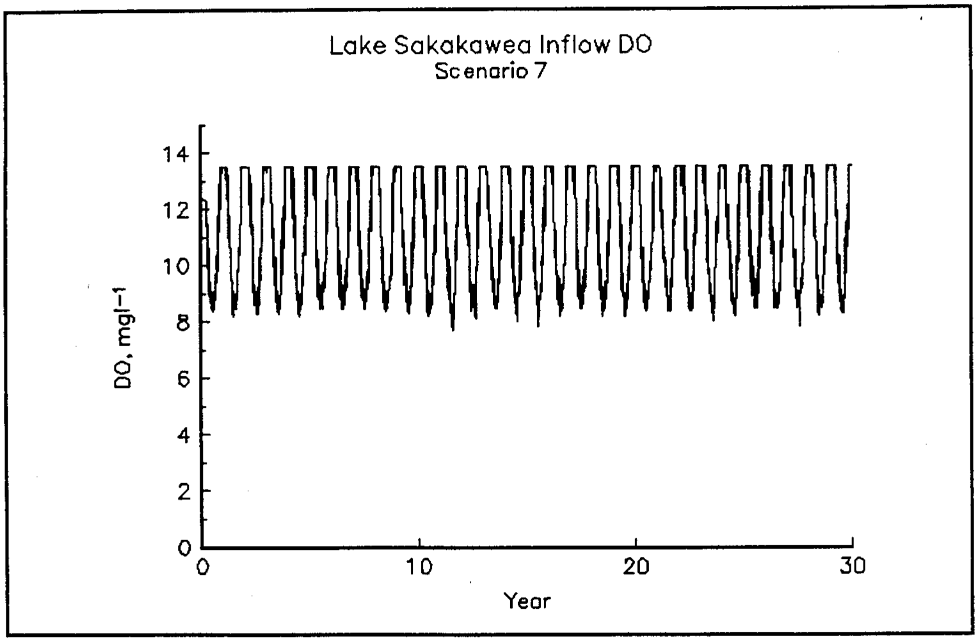

Figure 247. Lake Sakakawea scenario 7 inflow DO

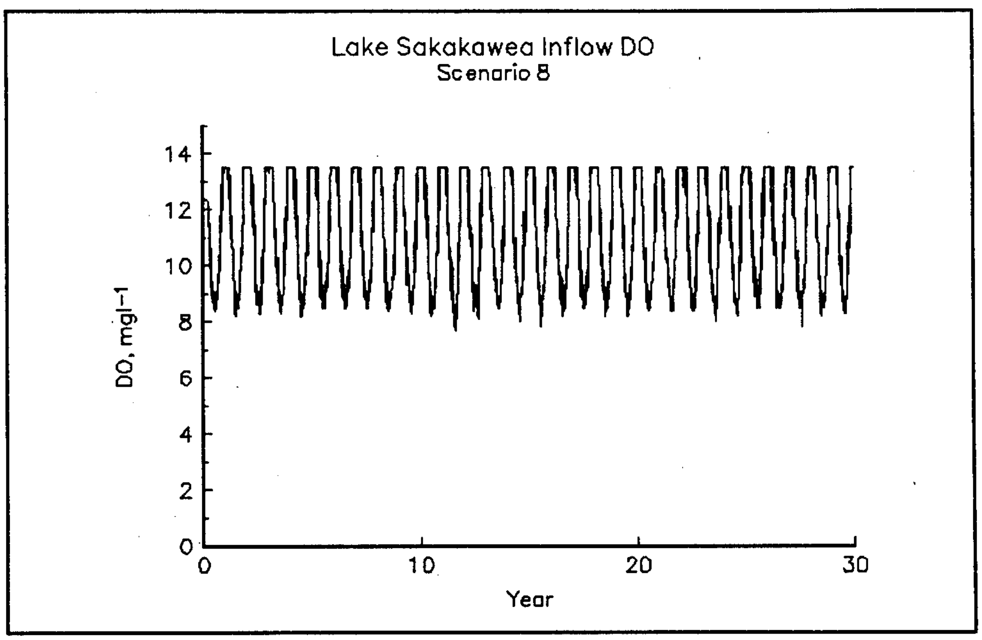

Figure 248. Lake Sakakawea scenario 8 inflow DO

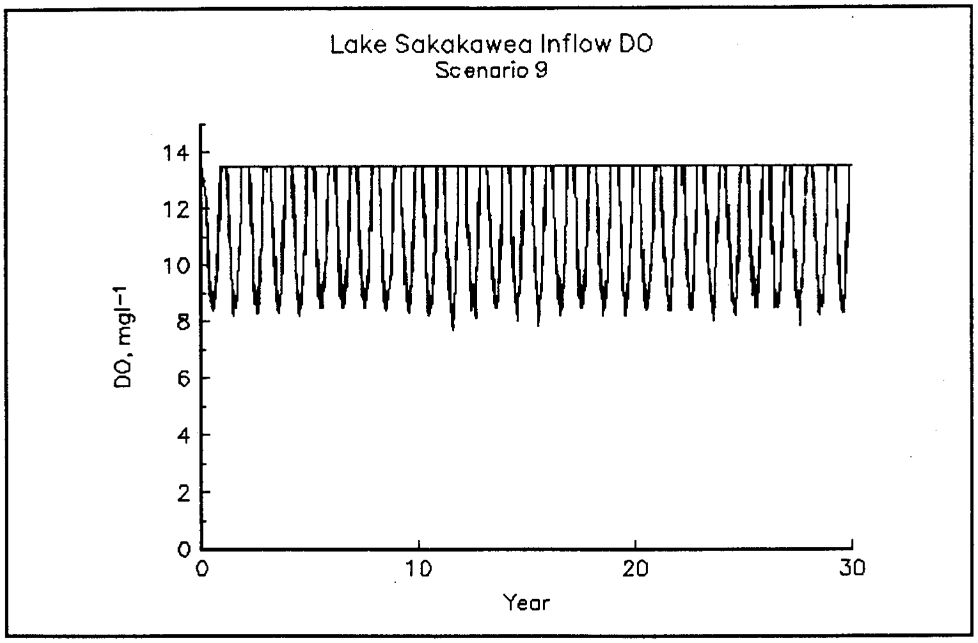

Figure 249. Lake Sakakawea scenario 9 inflow DO

Lake Oahe. Inflow DO for the nine scenarios are given in Figure 250-Figure 258

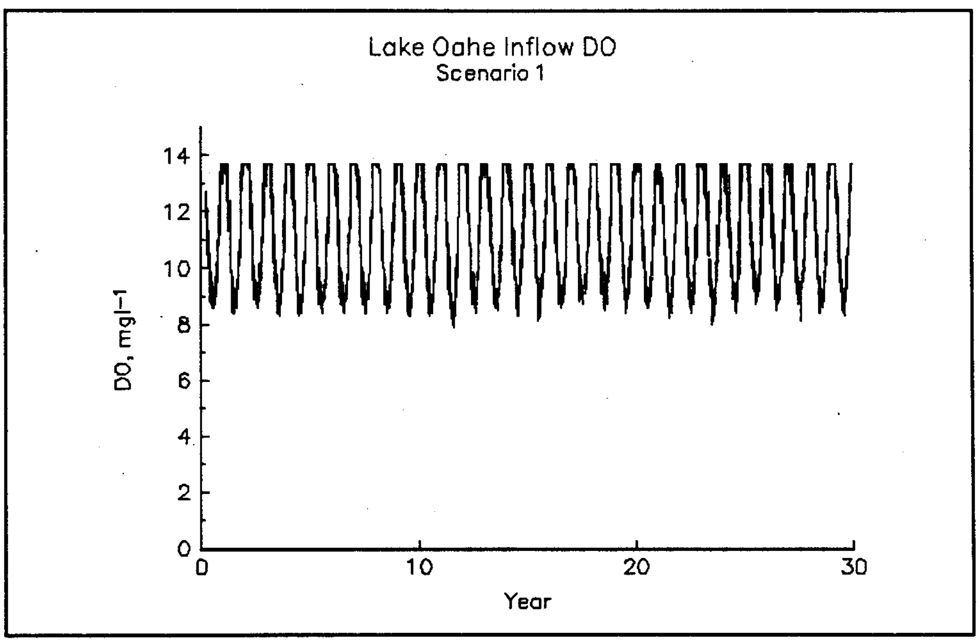

Figure 250. Lake Oahe scenario 1 inflow DO

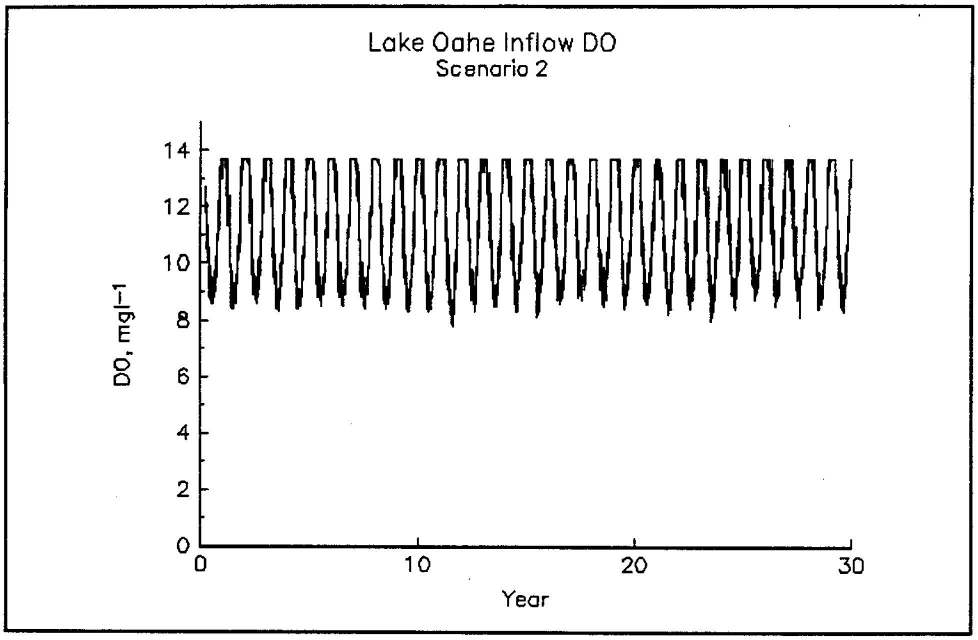

Figure 251. Lake Oahe scenario 2 inflow DO

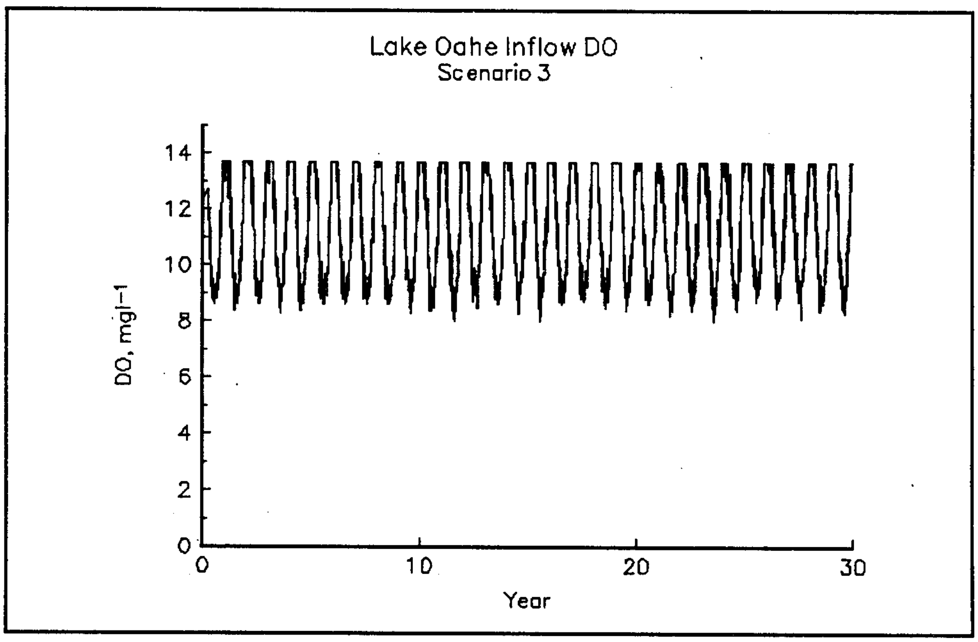

Figure 252. Lake Oahe scenario 3 inflow DO

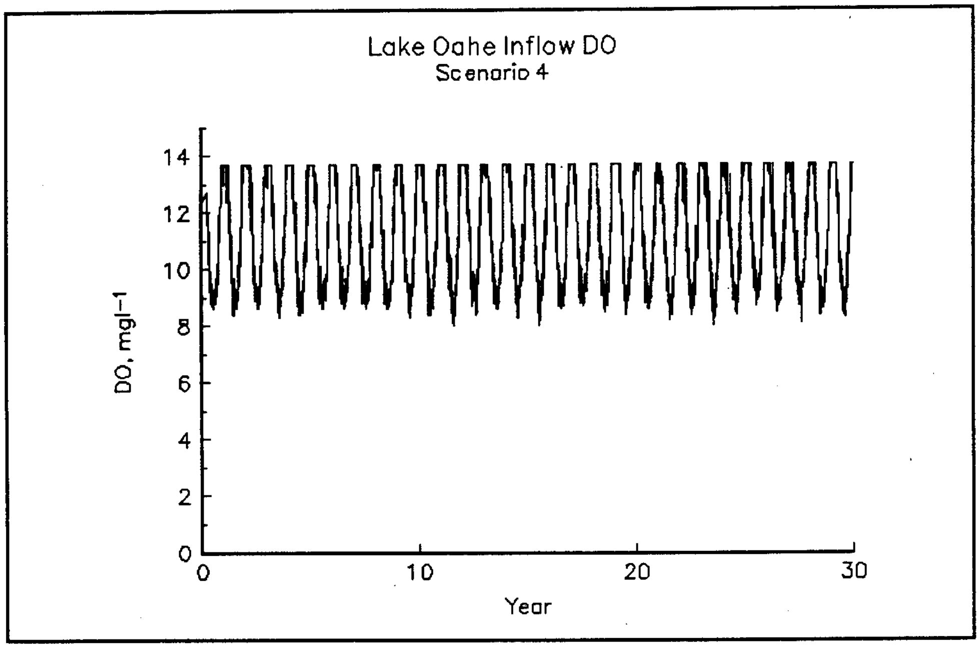

Figure 253. Lake Oahe scenario 4 inflow DO

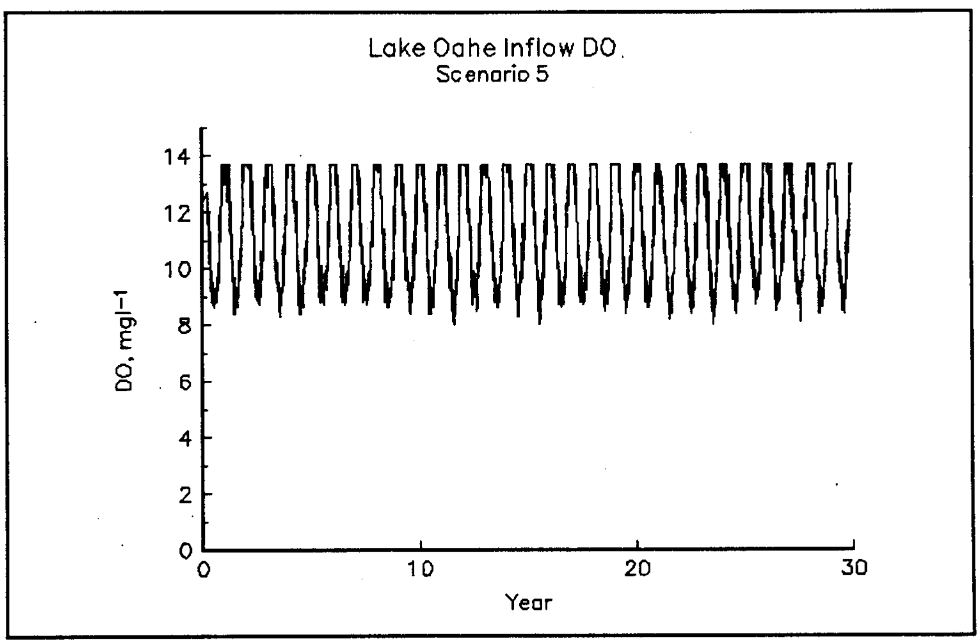

Figure 254. Lake Oahe scenario 5 inflow DO

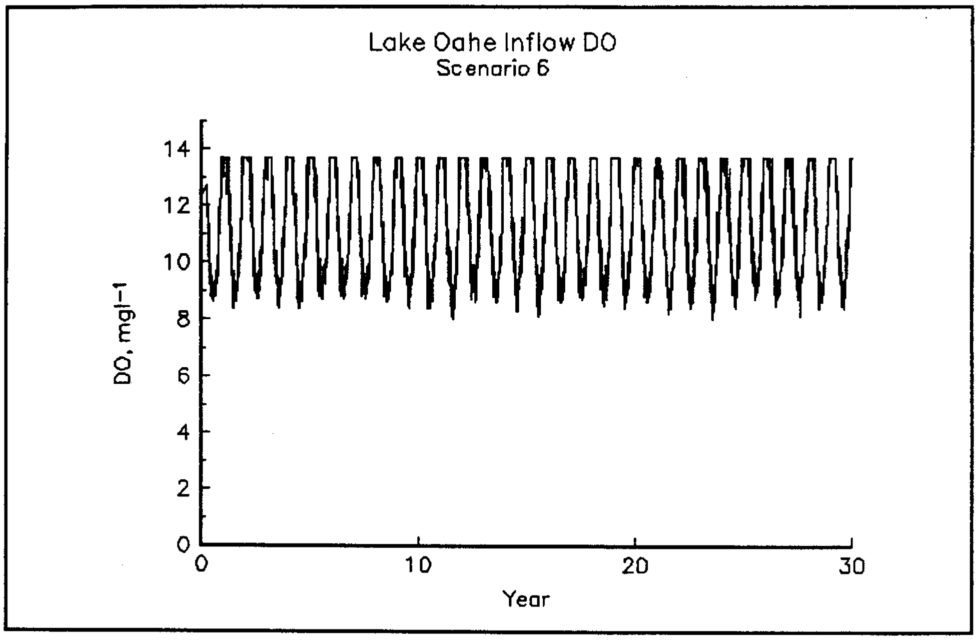

Figure 255. Lake Oahe scenario 6 inflow DO

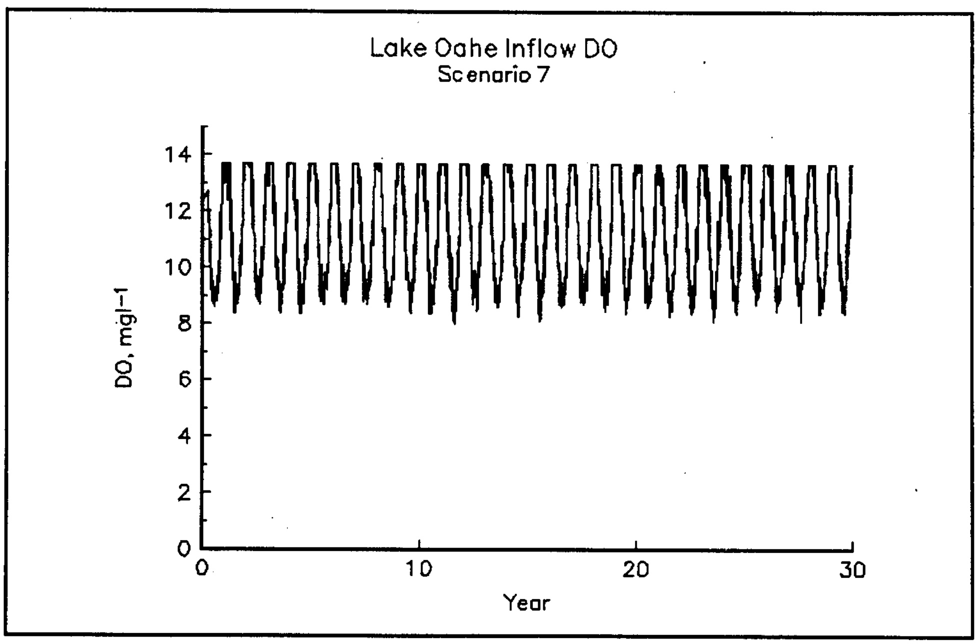

Figure 256. Lake Oahe scenario 7 inflow DO

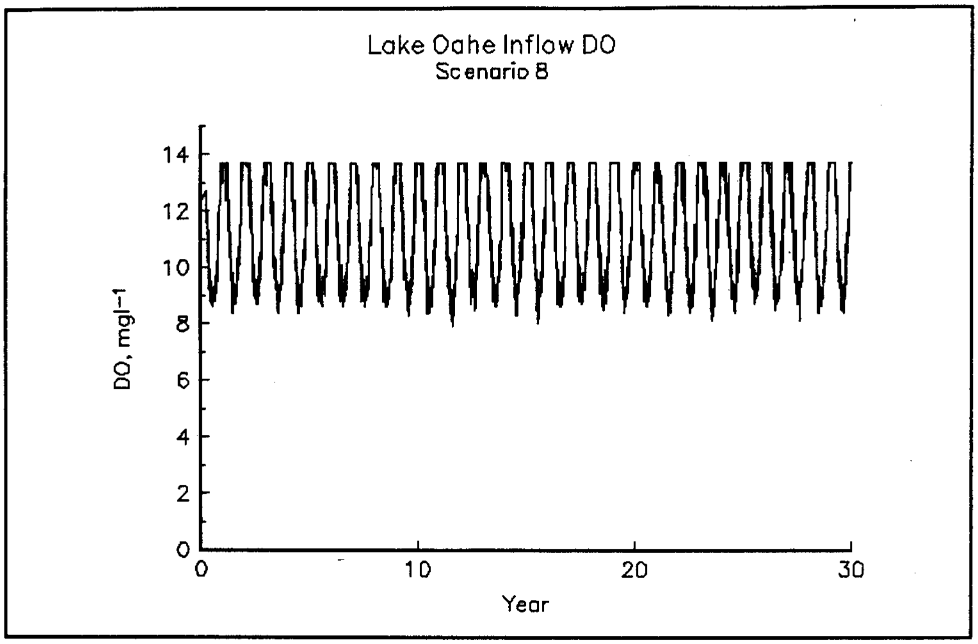

Figure 257. Lake Oahe scenario 8 inflow DO

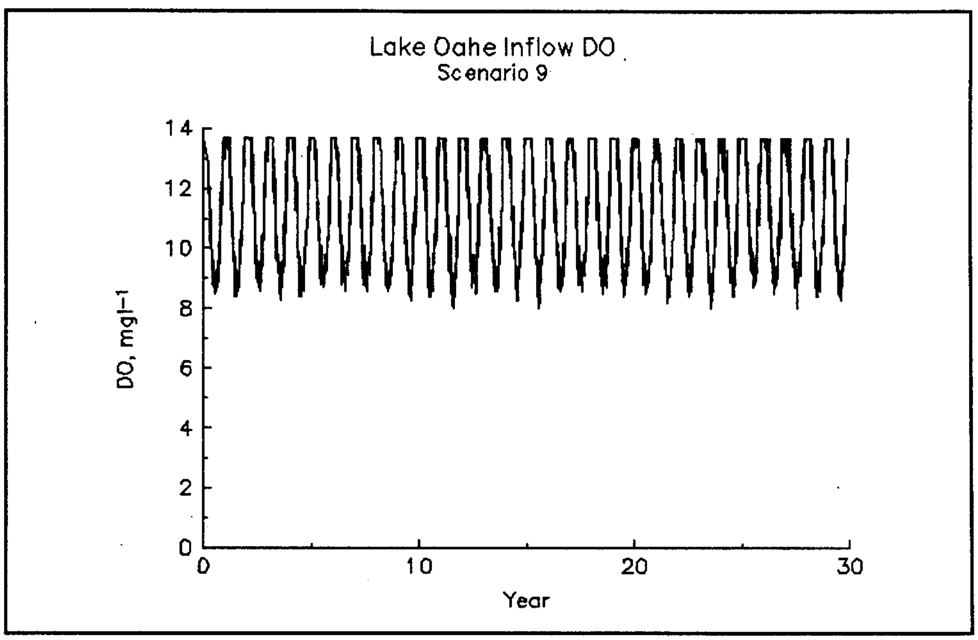

Figure 258. Lake Oahe scenario 9 inflow DO

Lake Francis Case. Inflow DO for the nine scenarios are given in Figure 259-Figure 267.

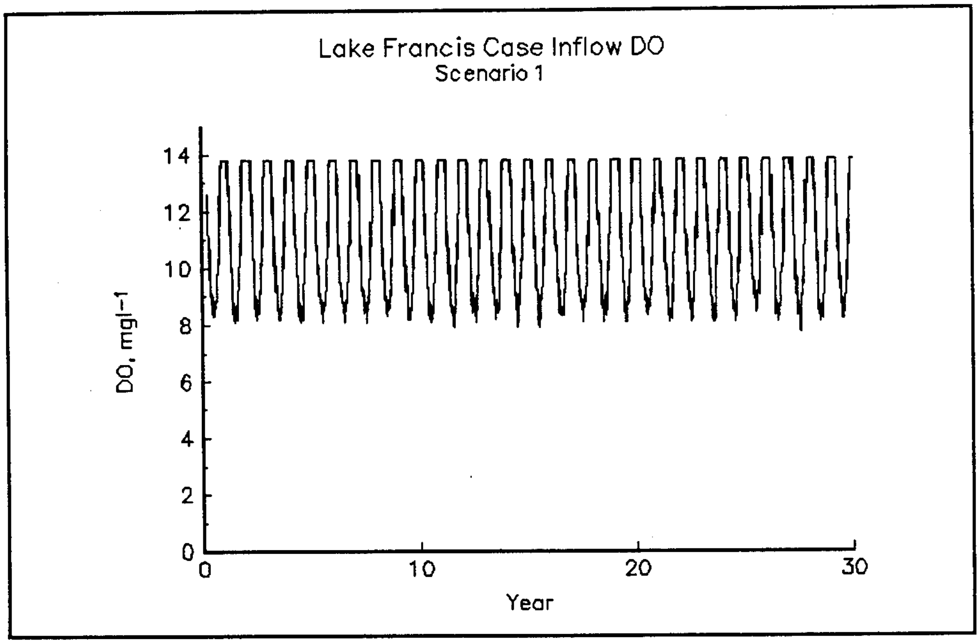

Figure 259. Lake Francis Case scenario 1 inflow DO

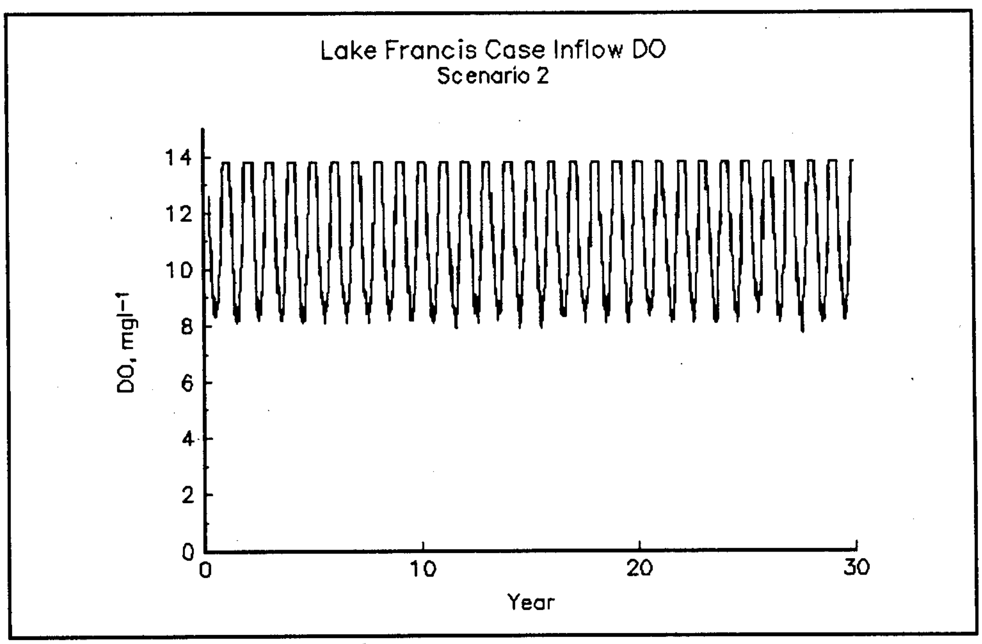

Figure 260. Lake Francis Case scenario 2 inflow DO

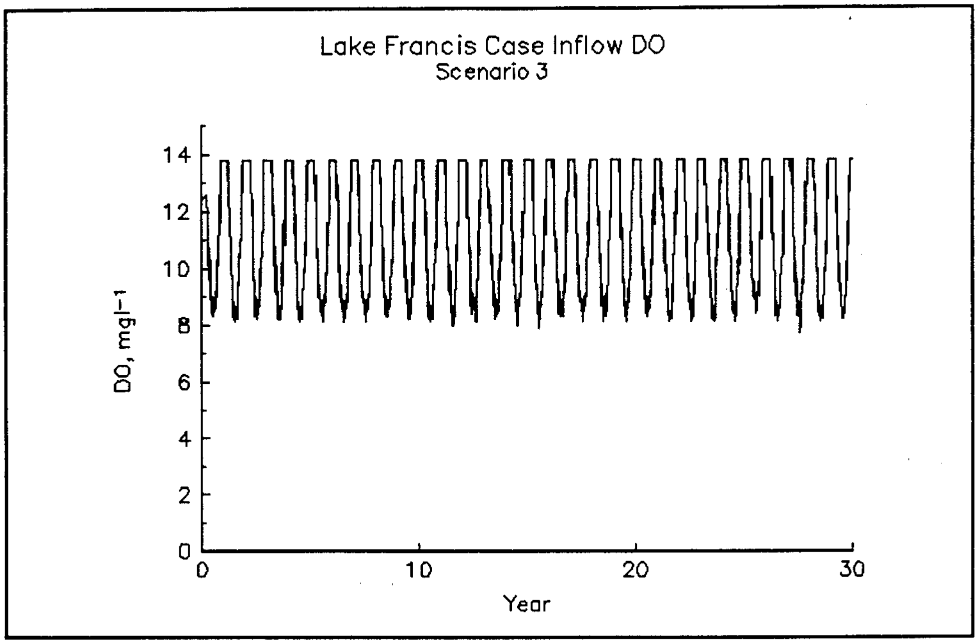

Figure 261. Lake Francis Case scenario 3 inflow DO

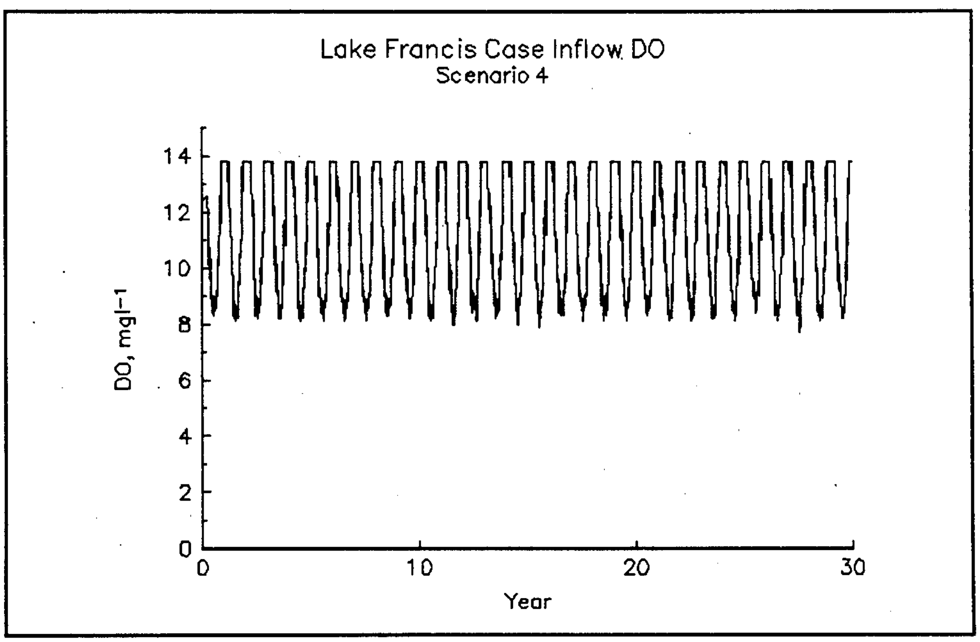

Figure 262. Lake Francis Case scenario 4 inflow DO

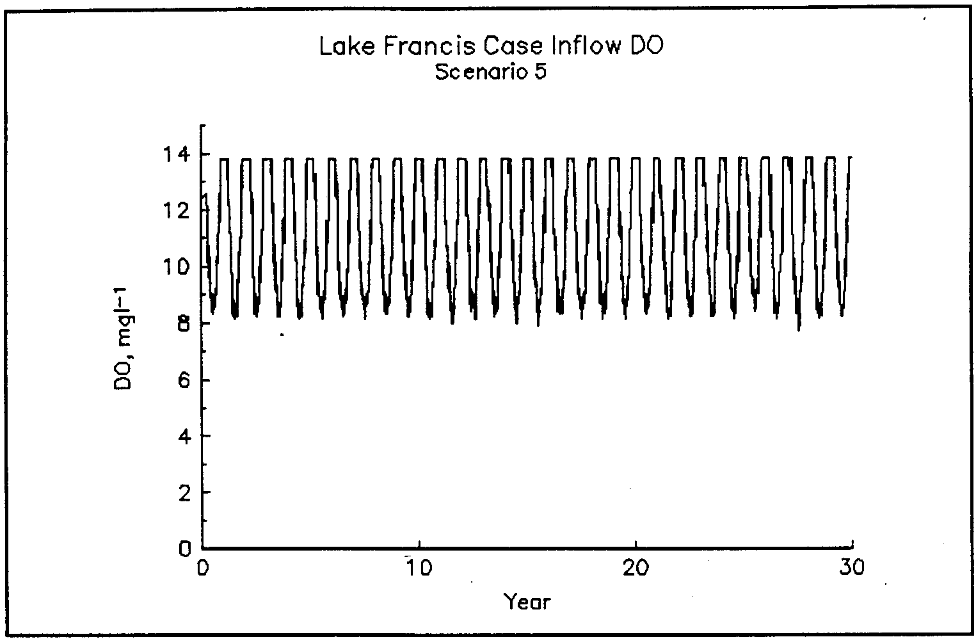

Figure 263. Lake Francis Case scenario 5 inflow DO

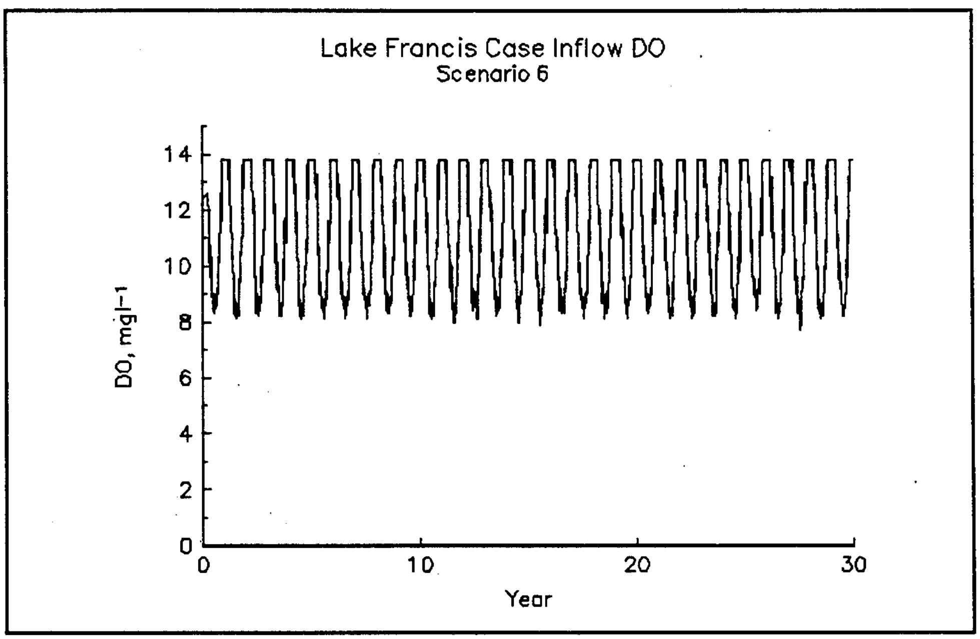

Figure 264. Lake Francis Case scenario 6 inflow DO

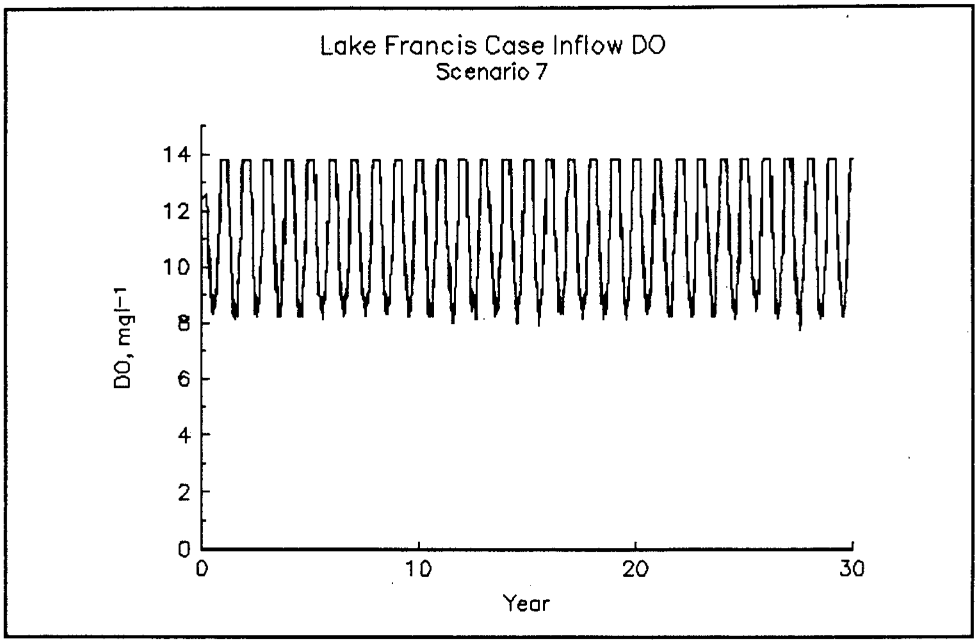

Figure 265. Lake Francis Case scenario 7 inflow DO

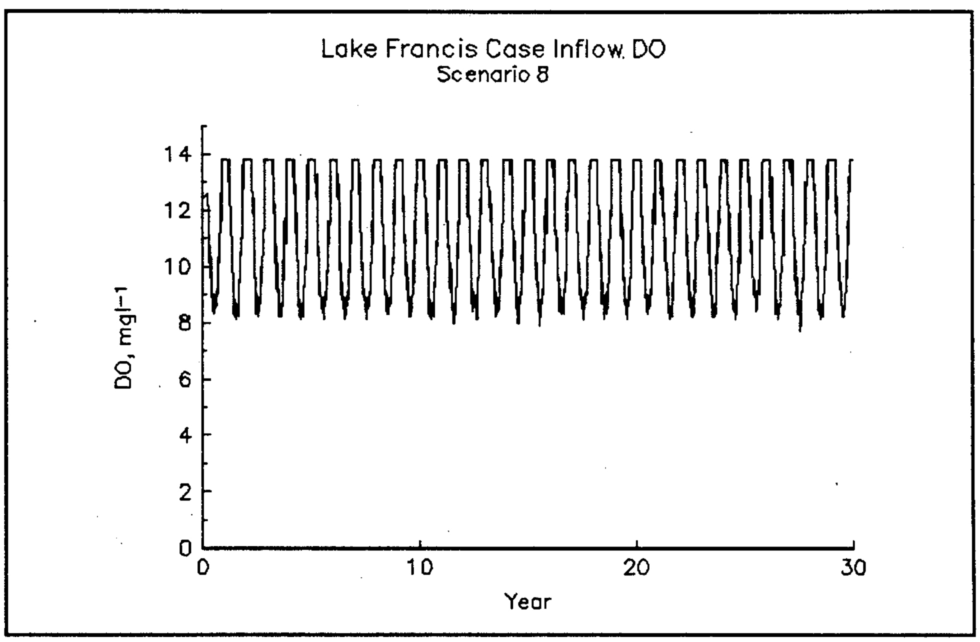

Figure 266. Lake Francis Case scenario 8 inflow DO

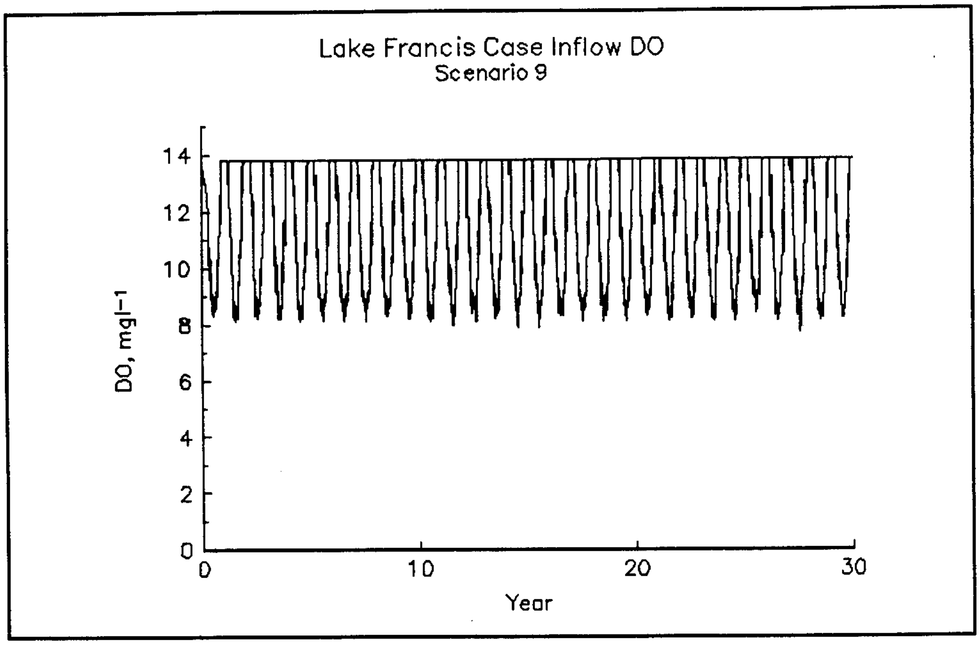

Figure 267. Lake Francis Case scenario 9 inflow DO

Scenarios

Fort Peck Lake

Water Surface Elevations. Water surface elevations for the nine scenarios are given in Figure 268-Figure 276. CE-QUAL-W2 predictions are in close agreement with LRS results.

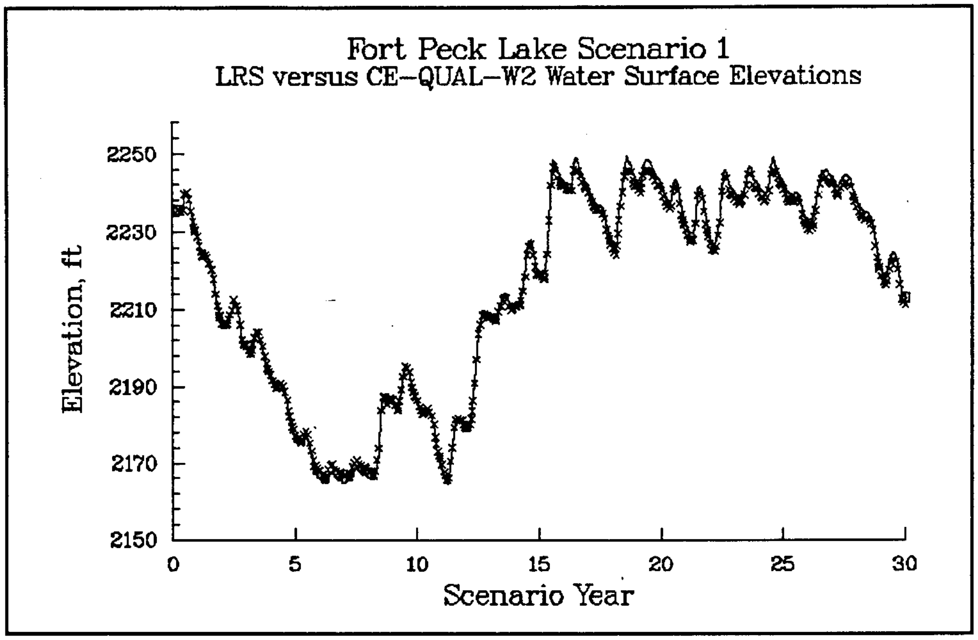

Figure 268. Fort Peck Lake LRS versus CE-QUAL-W2 water surface elevations for scenario 1

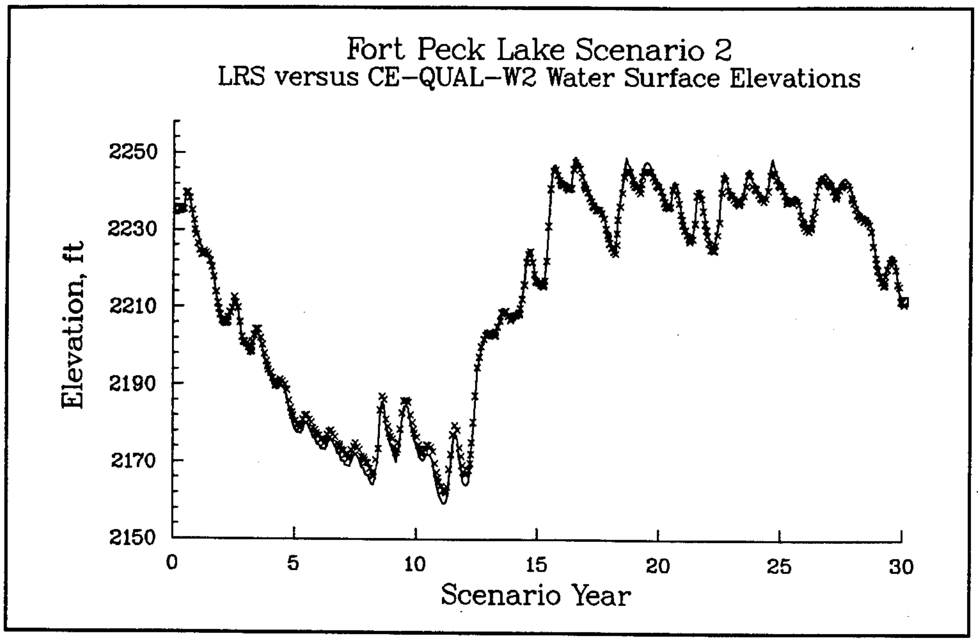

Figure 269. Fort Peck Lake LRS versus CE-QUAL-W2 water surface elevations for scenario 2

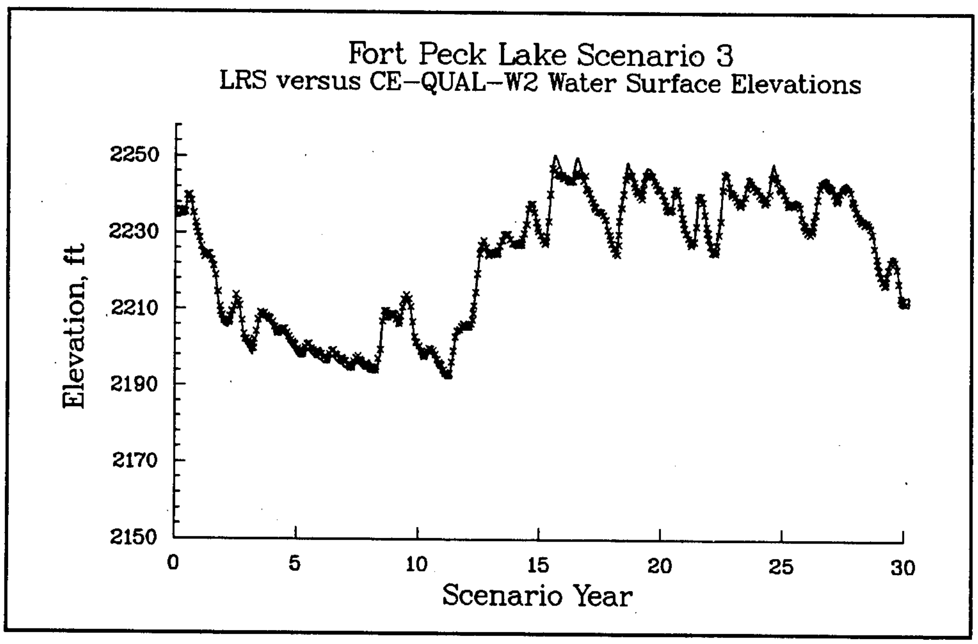

Figure 270. Fort Peck Lake LRS versus CE-QUAL-W2 water surface elevations for scenario 3

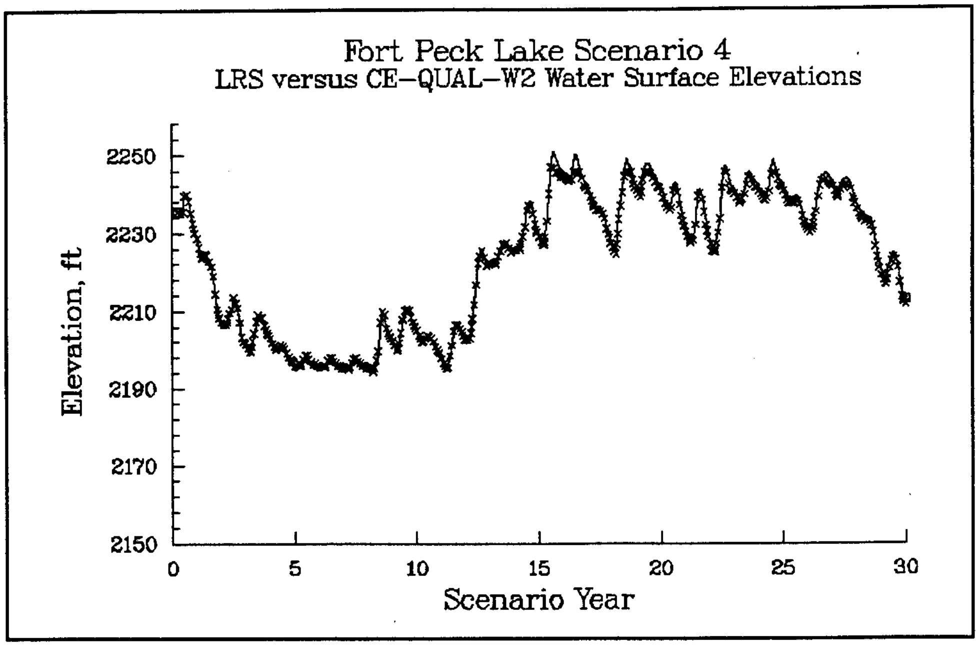

Figure 271. Fort Peck Lake LRS versus CE-QUAL-W2 water surface elevations for scenario 4

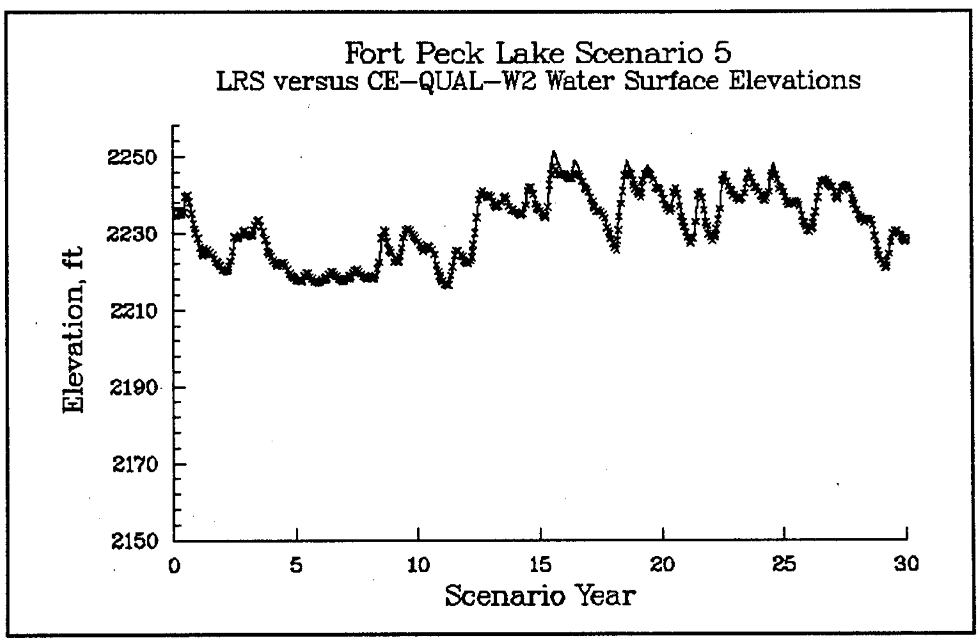

Figure 272. Fort Peck Lake LRS versus CE-QUAL-W2 water surface elevations for scenario 5

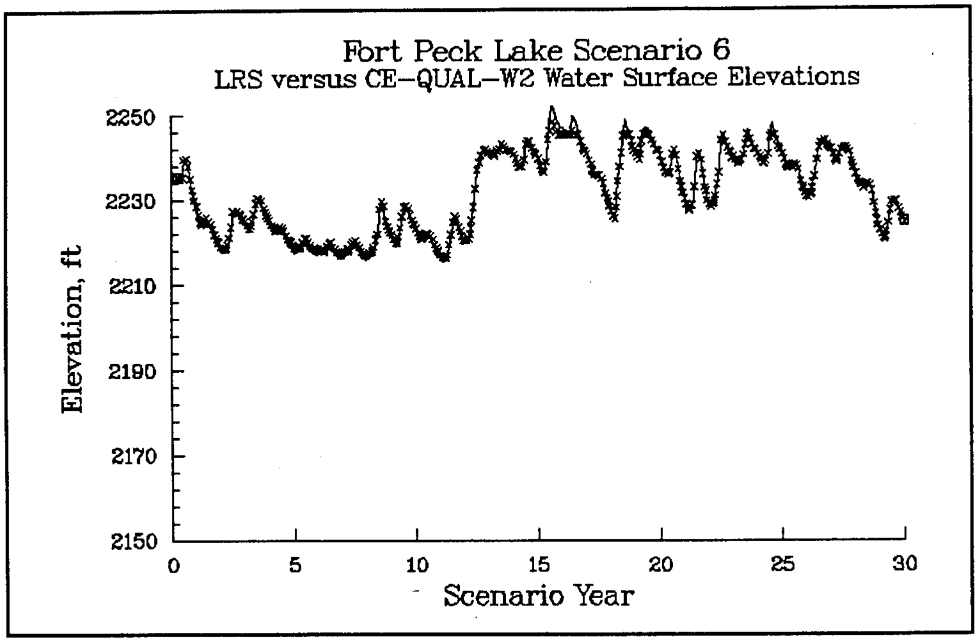

Figure 273. Fort Peck Lake LRS versus CE-QUAL-W2 water surface elevations for scenario 6

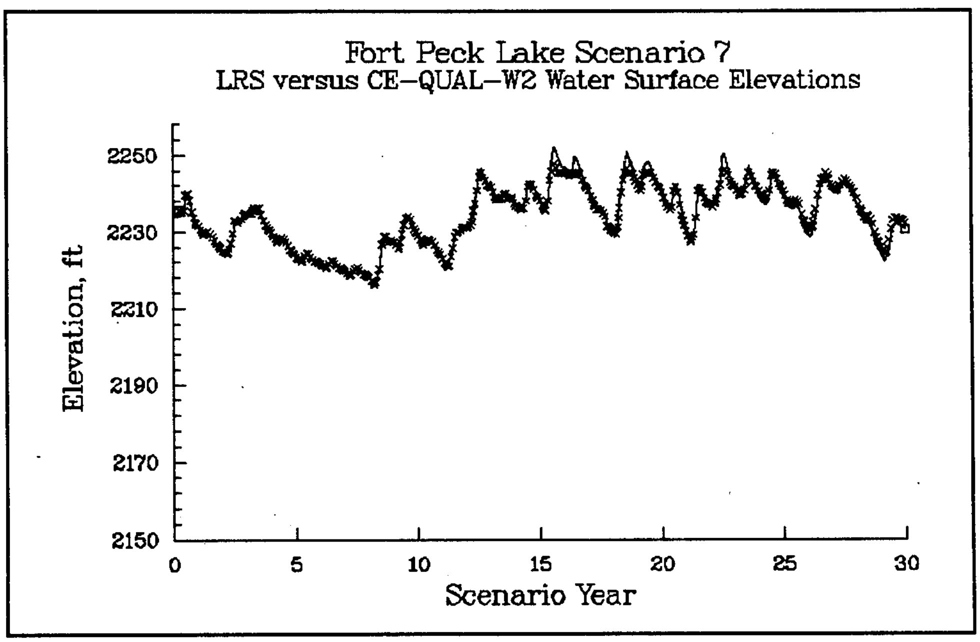

Figure 274. Fort Peck Lake LRS versus CE-QUAL-W2 water surface elevations for scenario 7

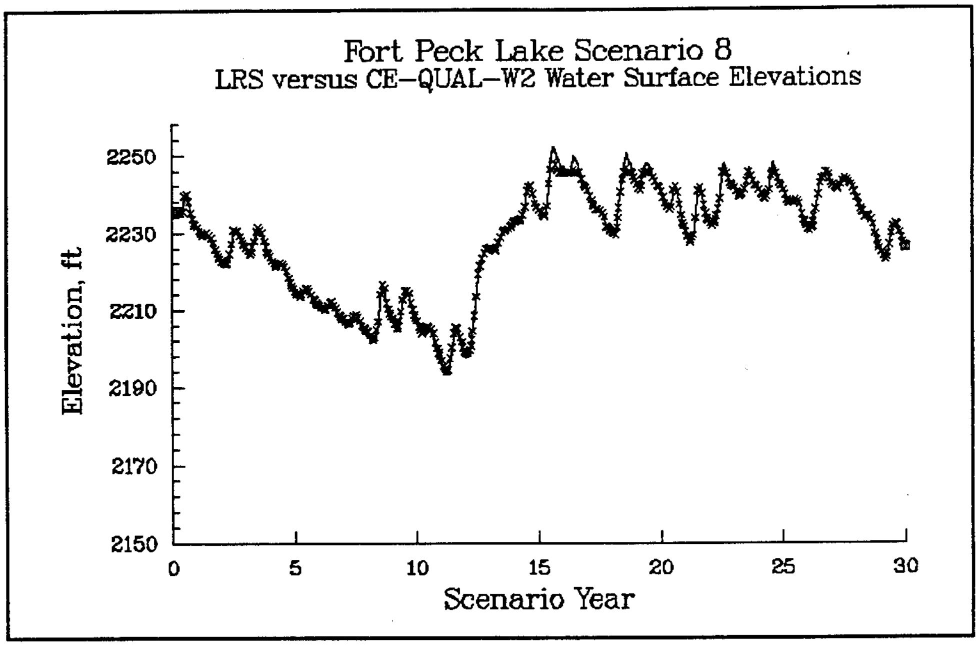

Figure 275. Fort Peck Lake LRS versus CE-QUAL-W2 water surface elevations for scenario 8

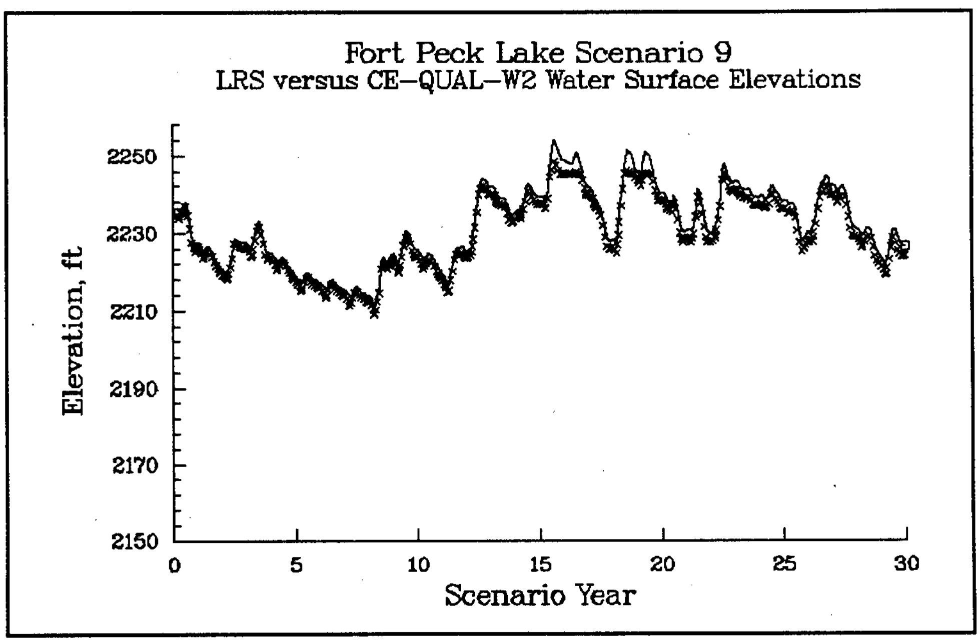

Figure 276. Fort Peck Lake LRS versus CE-QUAL-W2 water surface elevations for scenario 9

Release Temperatures. Release temperatures for the nine scenarios are given in Figure 277-Figure 285. Release temperatures are indicative of the temperature regime in the reservoir and can be used to identify which scenarios provide the most coldwater habitat. Scenarios one and two result in the highest release temperatures which is consistent with the water surface elevations that are the lowest of the nine scenarios.

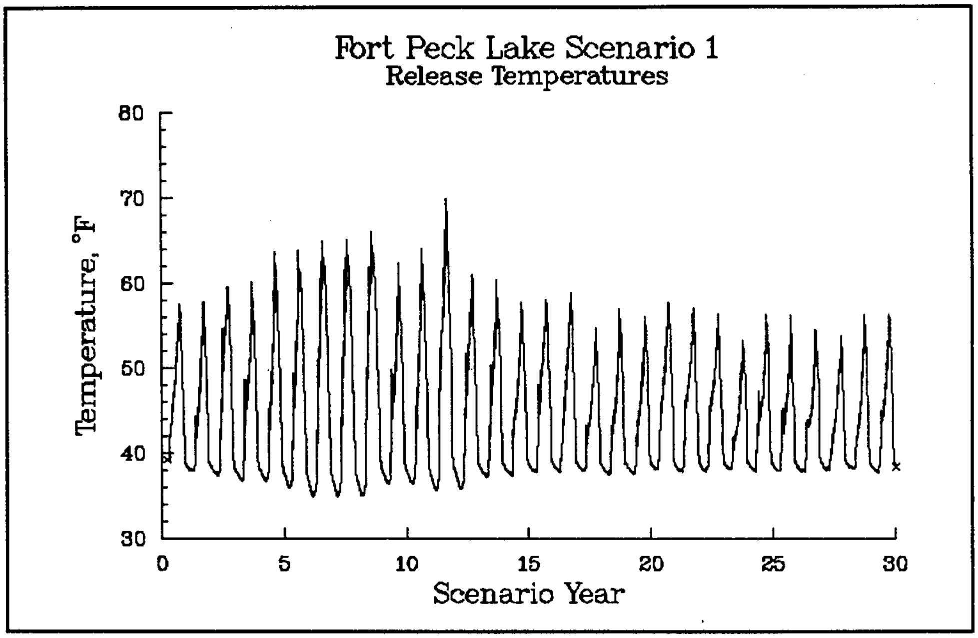

Figure 277. Fort Peck Lake computed release temperatures for scenario 1

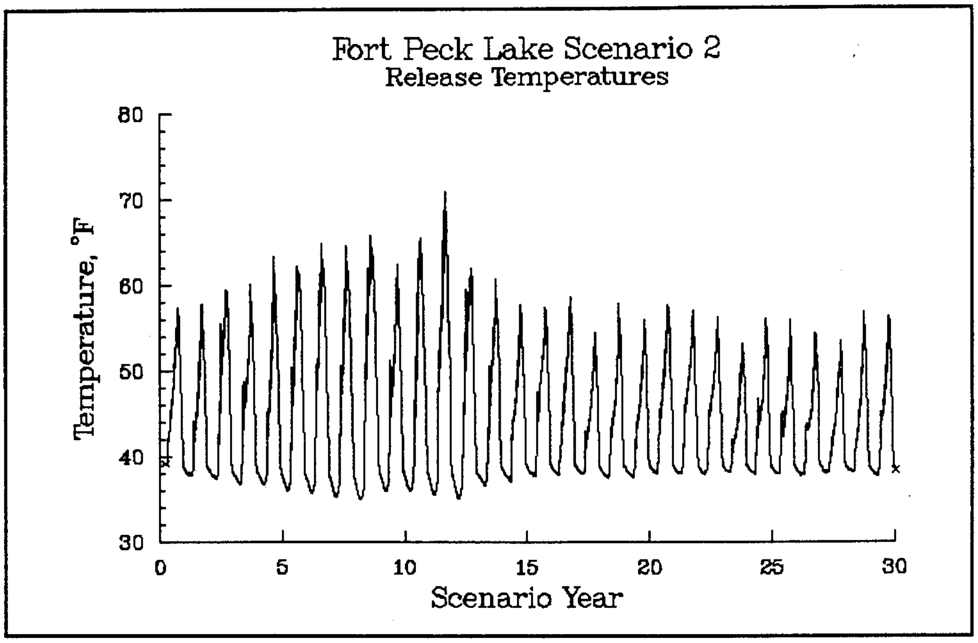

Figure 278. Fort Peck Lake computed release temperatures for scenario 2

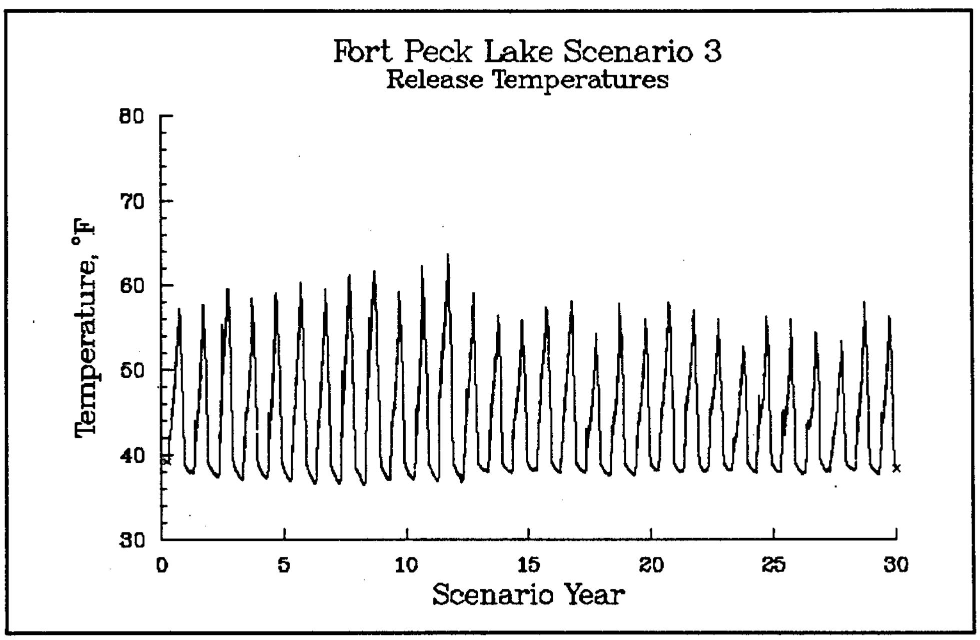

Figure 279. Fort Peck Lake computed release temperatures for scenario 3

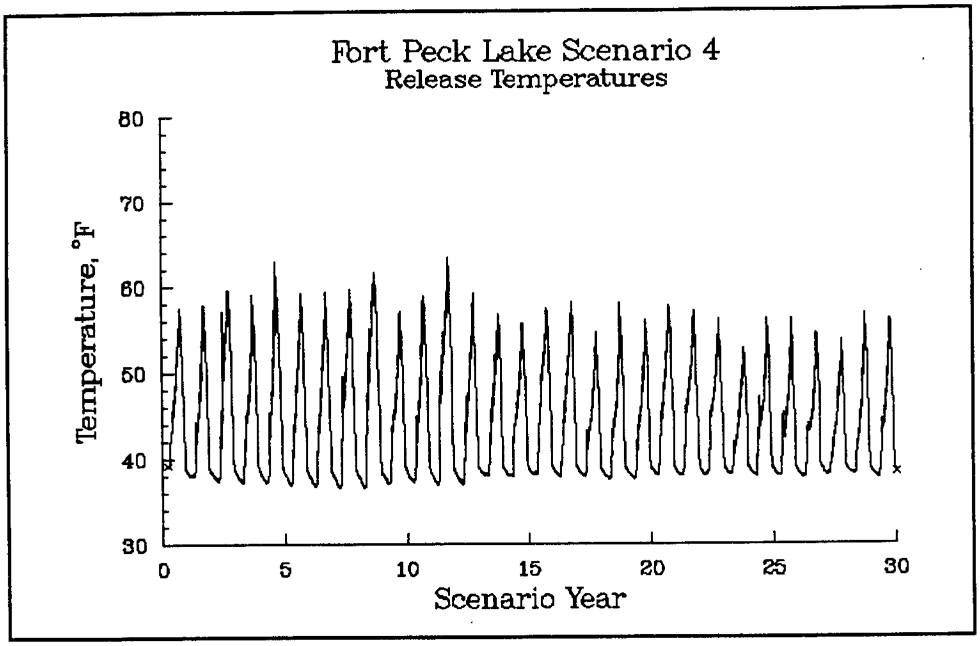

Figure 280. Fort Peck Lake computed release temperatures for scenario 4

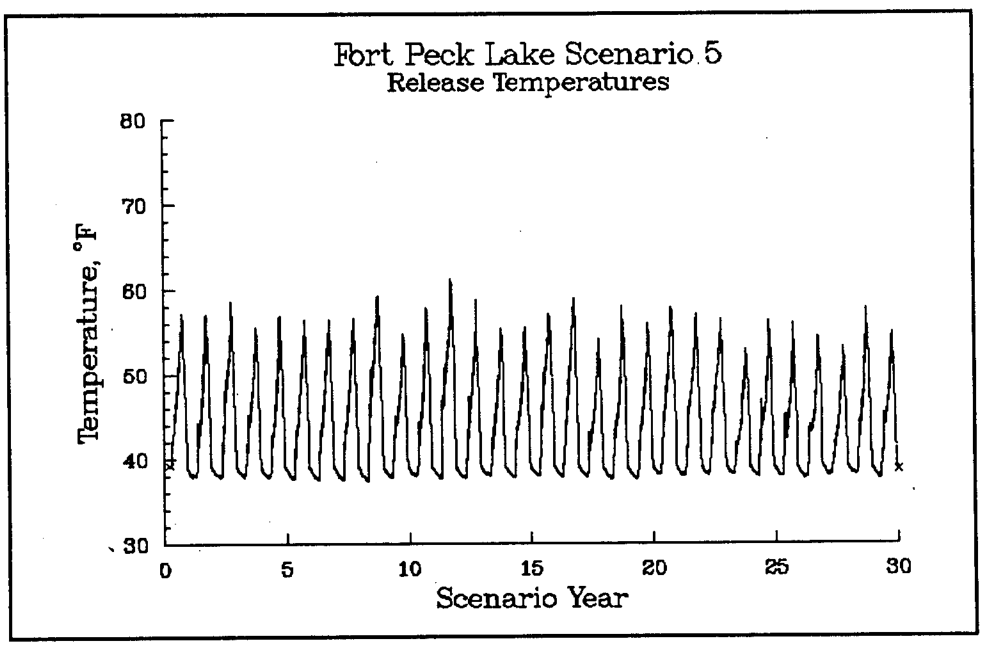

Figure 281. Fort Peck Lake computed release temperatures for scenario 5

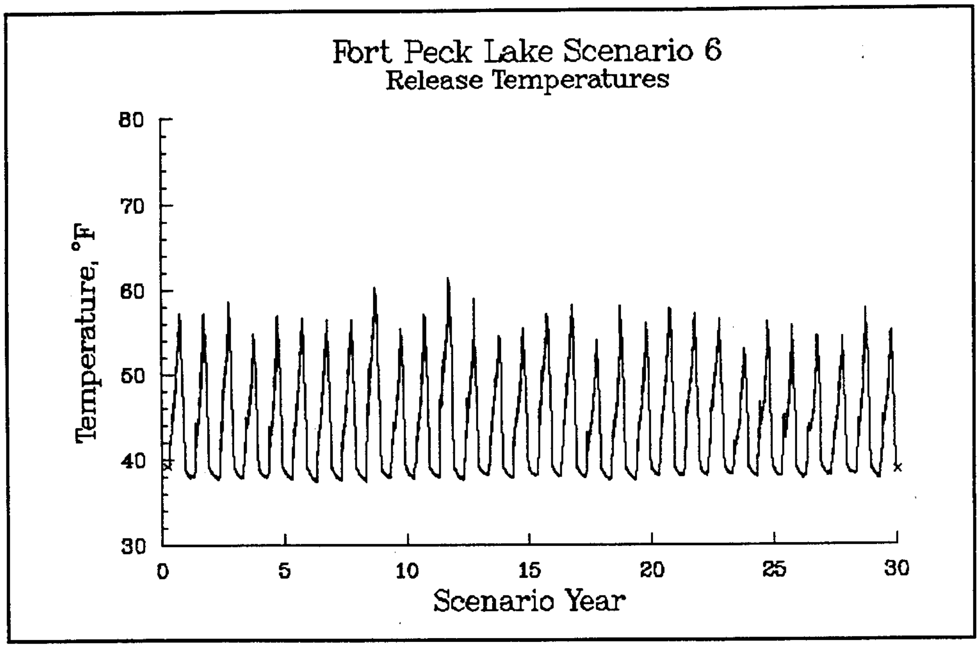

Figure 282. Fort Peck Lake computed release temperatures for scenario 6

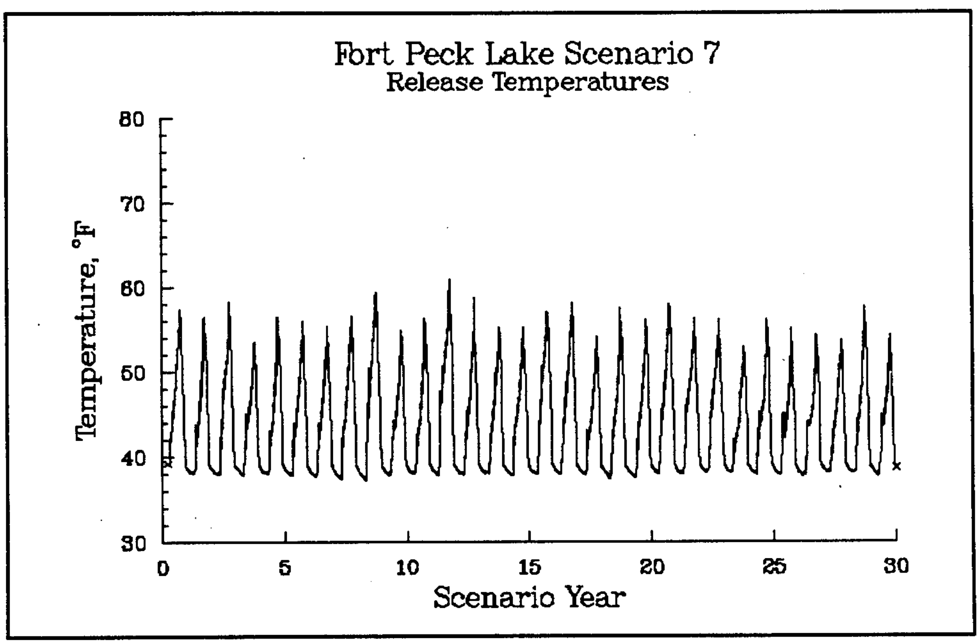

Figure 283. Fort Peck Lake computed release temperatures for scenario 7

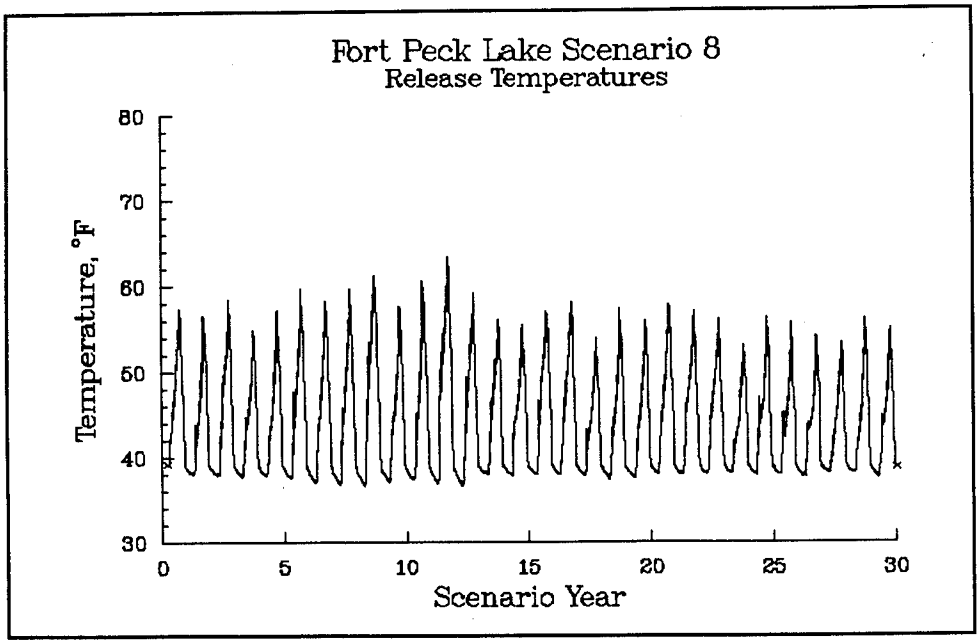

Figure 284. Fort Peck Lake computed release temperatures for scenario 8

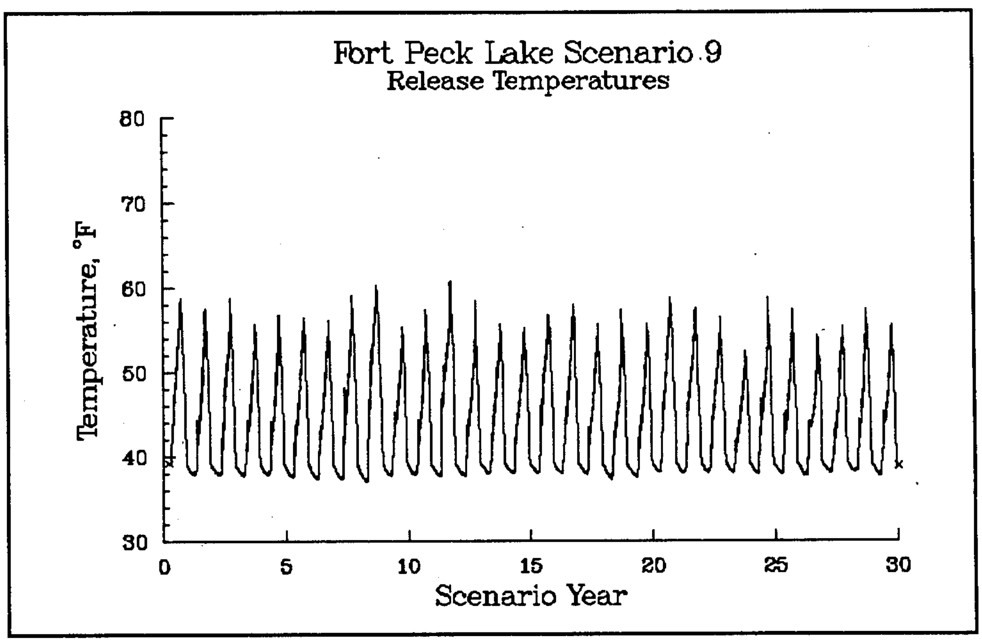

Figure 285. Fort Peck Lake computed release temperatures for scenario 9

Release DO. Release DO concentrations for the nine scenarios are given in Figure 286-Figure 294.

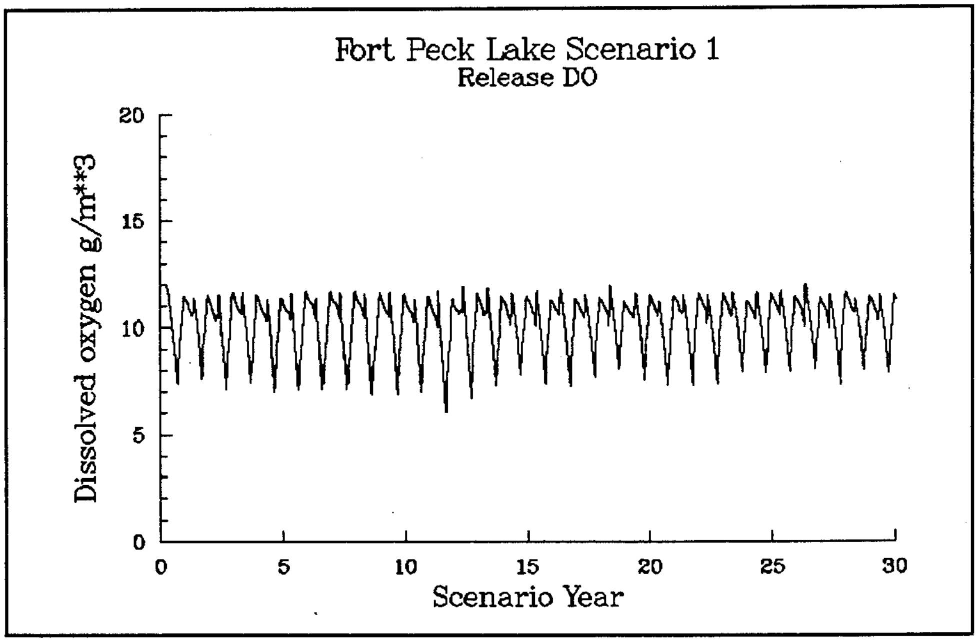

Figure 286. Fort Peck Lake release DO concentrations for scenario 1

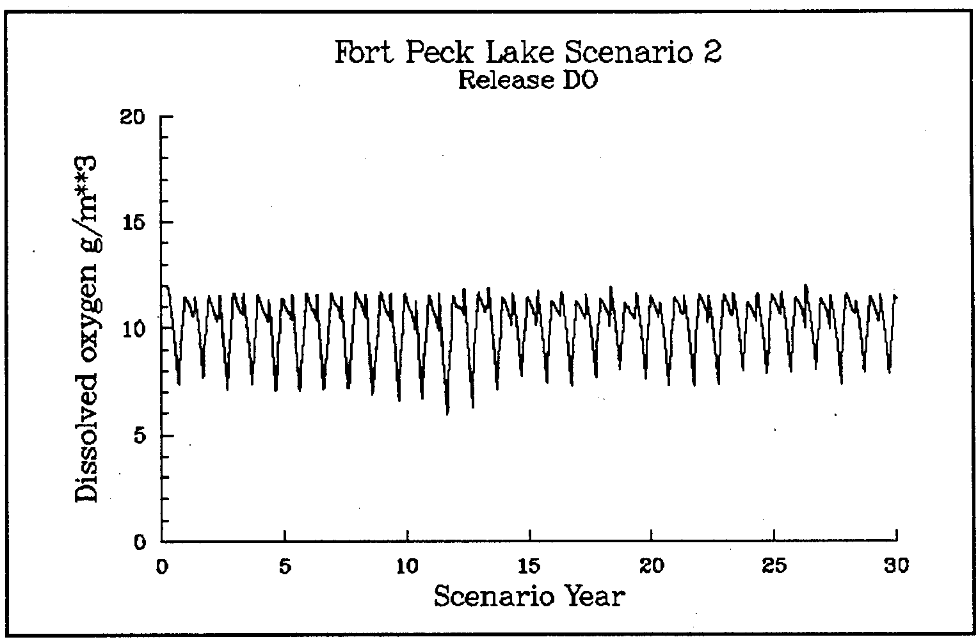

Figure 287. Fort Peck Lake release DO concentrations for scenario 2

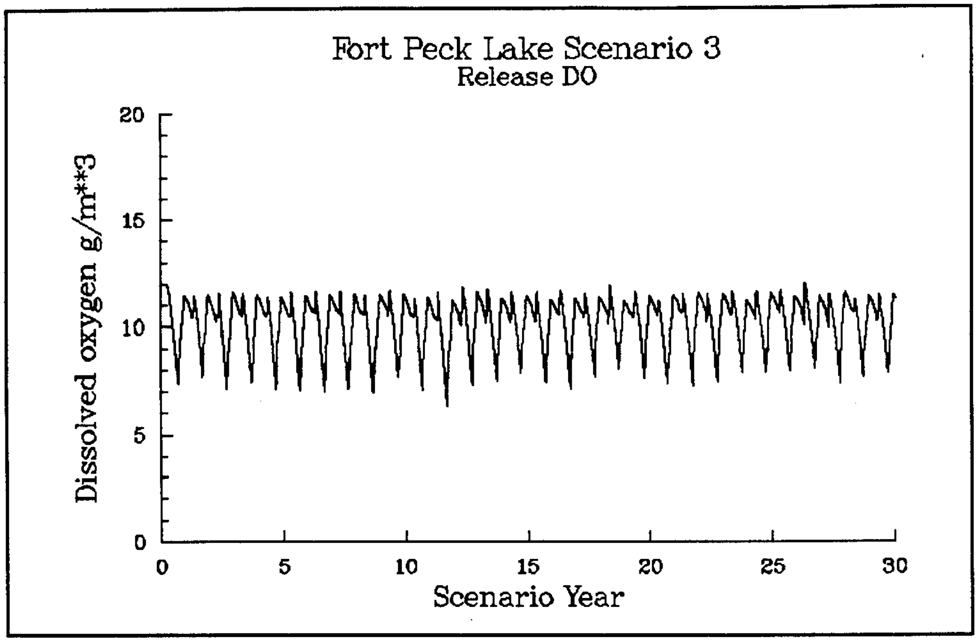

Figure 288. Fort Peck Lake release DO concentrations for scenario 3

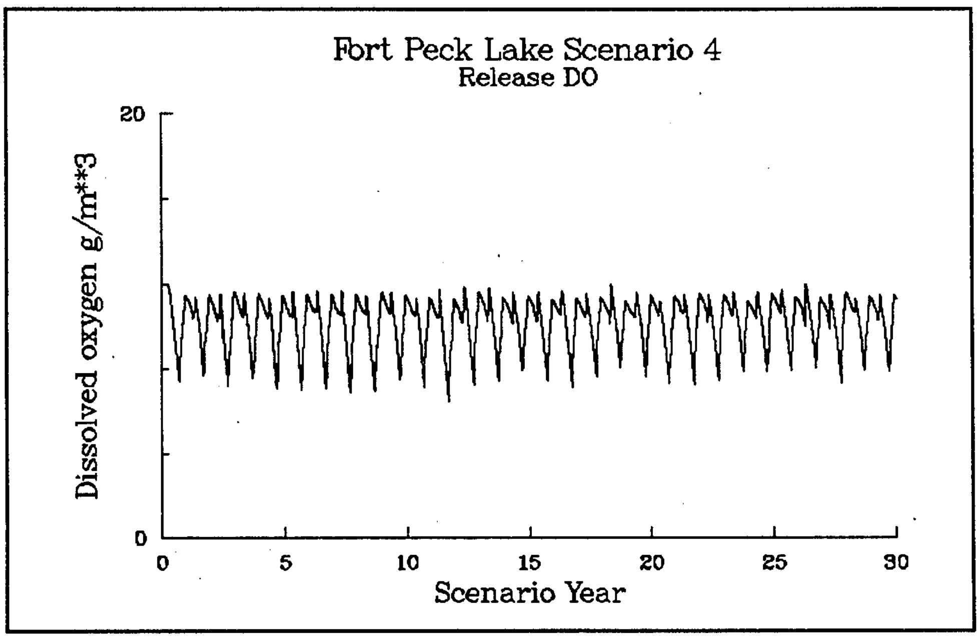

Figure 289. Fort Peck Lake release DO concentrations for scenario 4

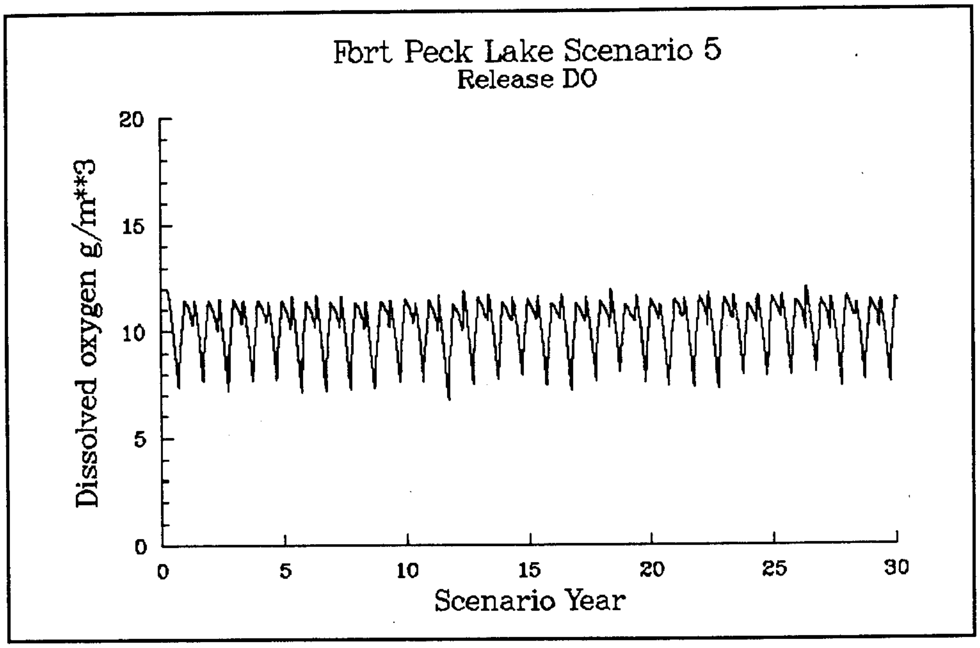

Figure 290. Fort Peck Lake release DO concentrations for scenario 5

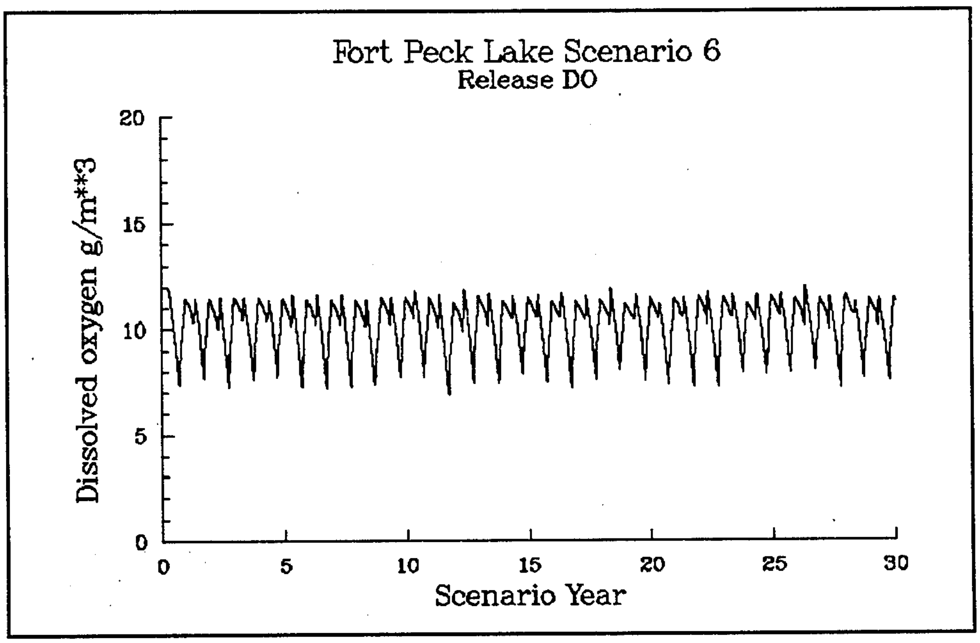

Figure 291. Fort Peck Lake release DO concentrations for scenario 6

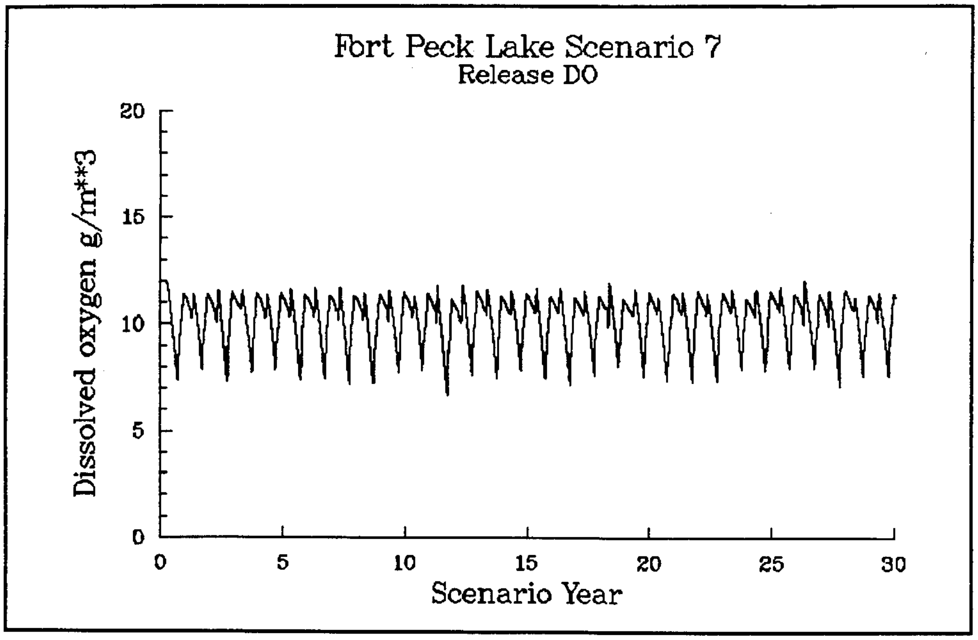

Figure 292. Fort Peck Lake release DO concentrations for scenario 7

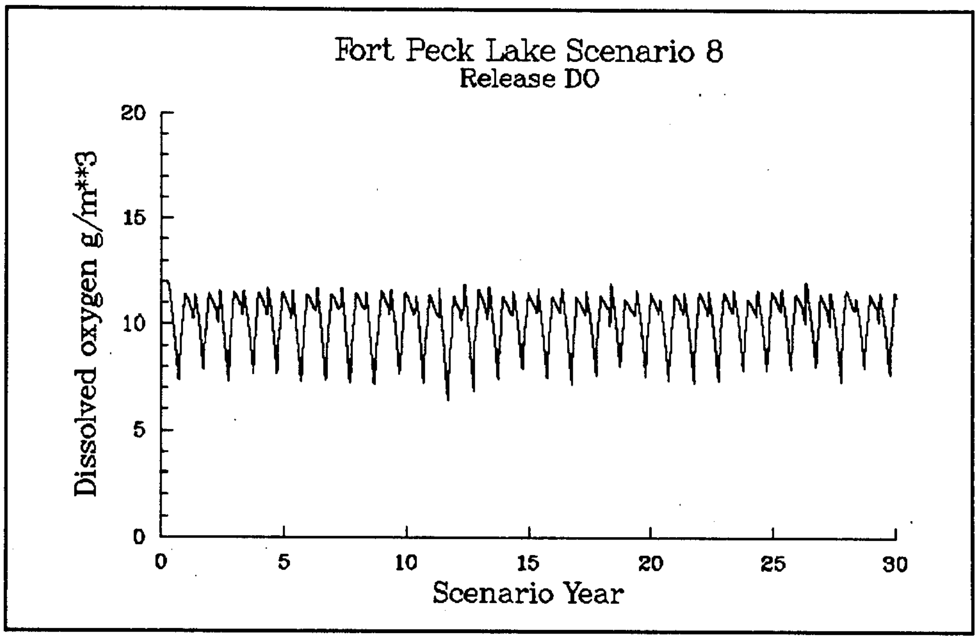

Figure 293. Fort Peck Lake release DO concentrations for scenario 8

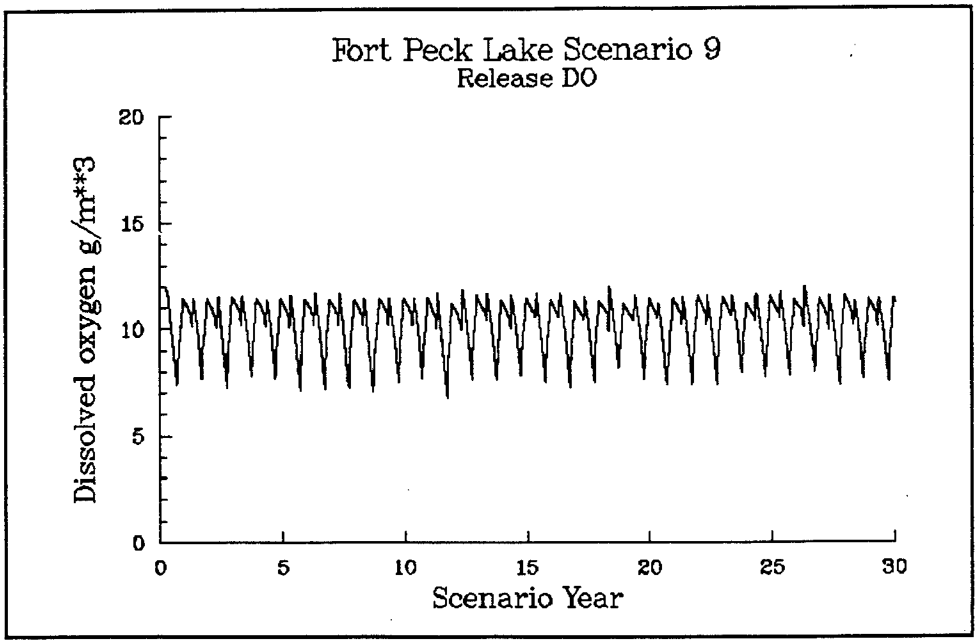

Figure 294. Fort Peck Lake release DO concentrations for scenario 9

Lake Sakakawea

Water Surface Elevations. Water surface elevations for the nine scenarios are given in Figure 295-Figure 303.

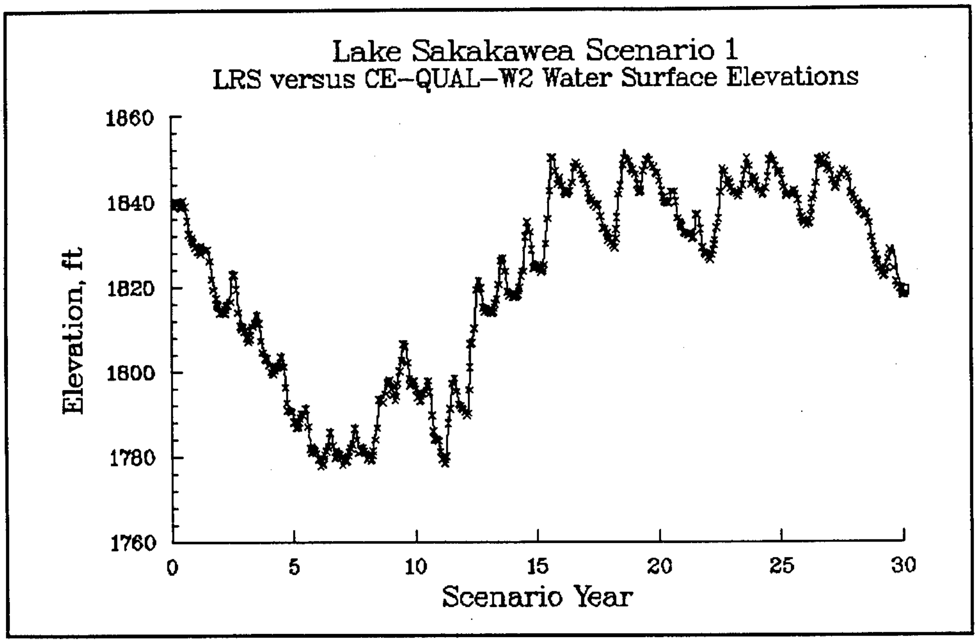

Figure 295. Lake Sakakawea LRS versus CE-QUAL-W2 water surface elevations for scenario 1

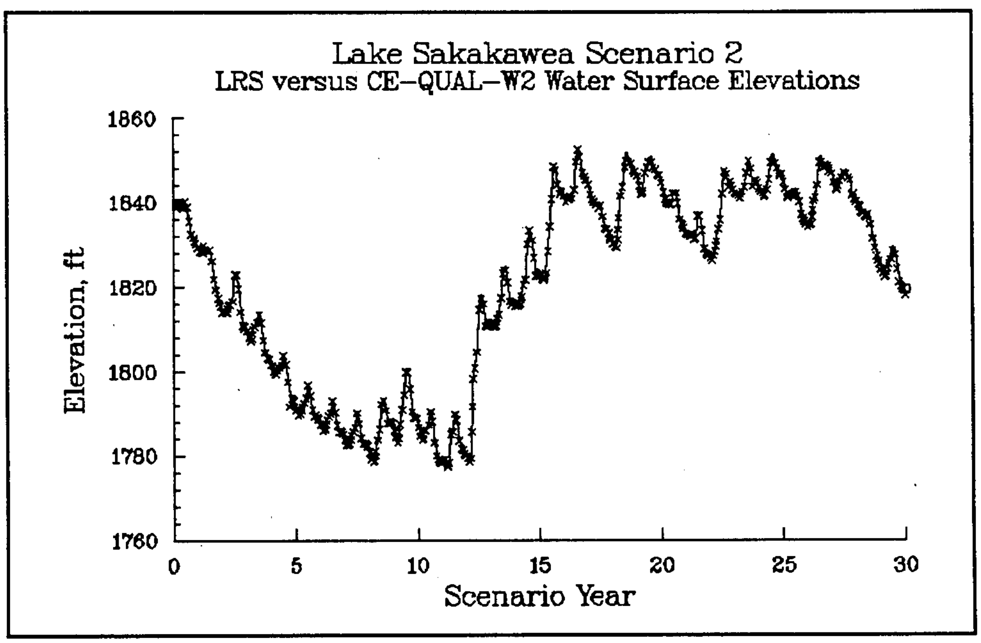

Figure 296. Lake Sakakawea LRS versus CE-QUAL-W2 water surface elevations for scenario 2

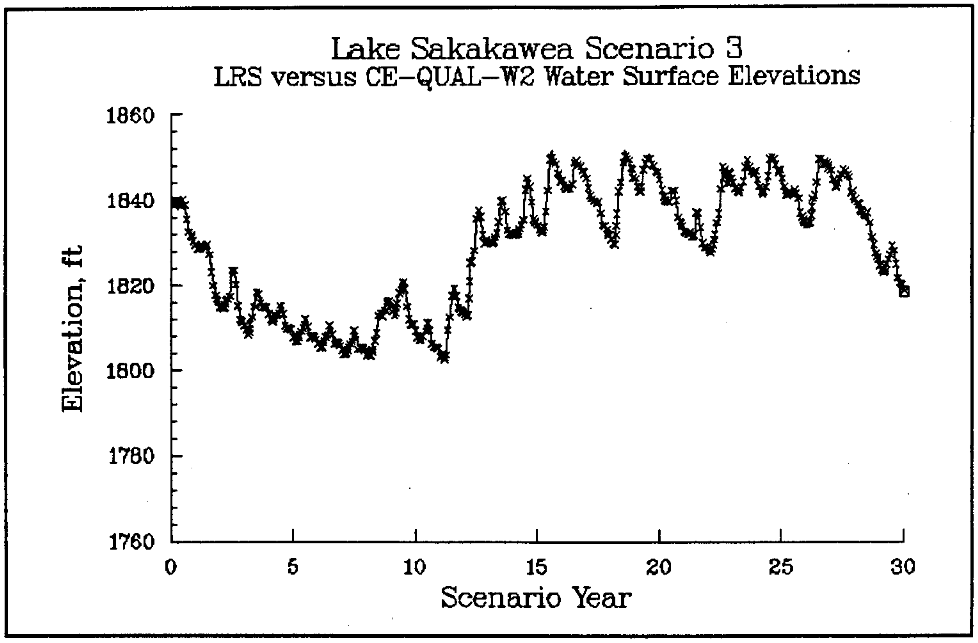

Figure 297. Lake Sakakawea LRS versus CE-QUAL-W2 water surface elevations for scenario 3

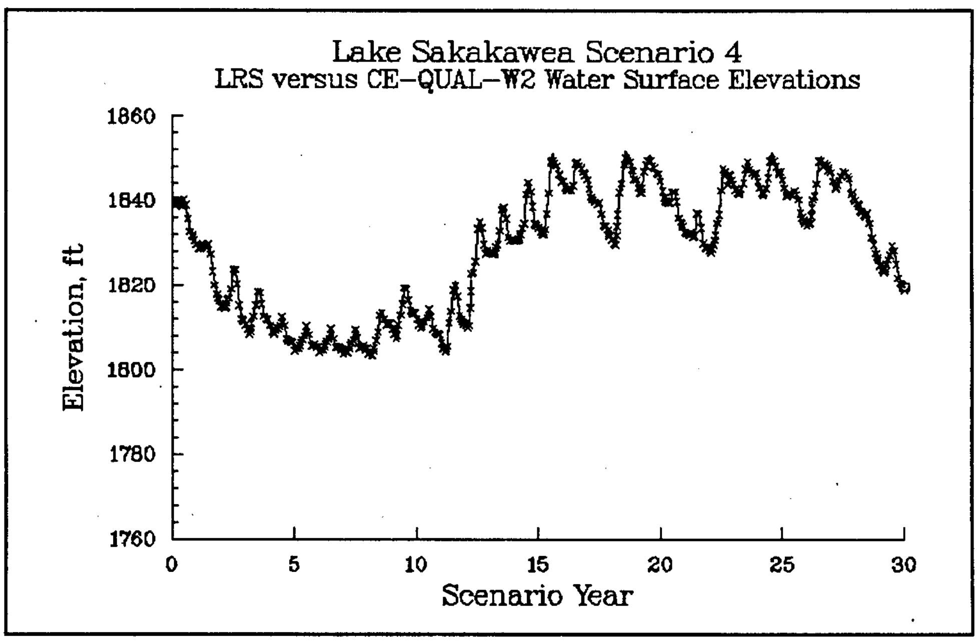

Figure 298. Lake Sakakawea LRS versus CE-QUAL-W2 water surface elevations for scenario 4

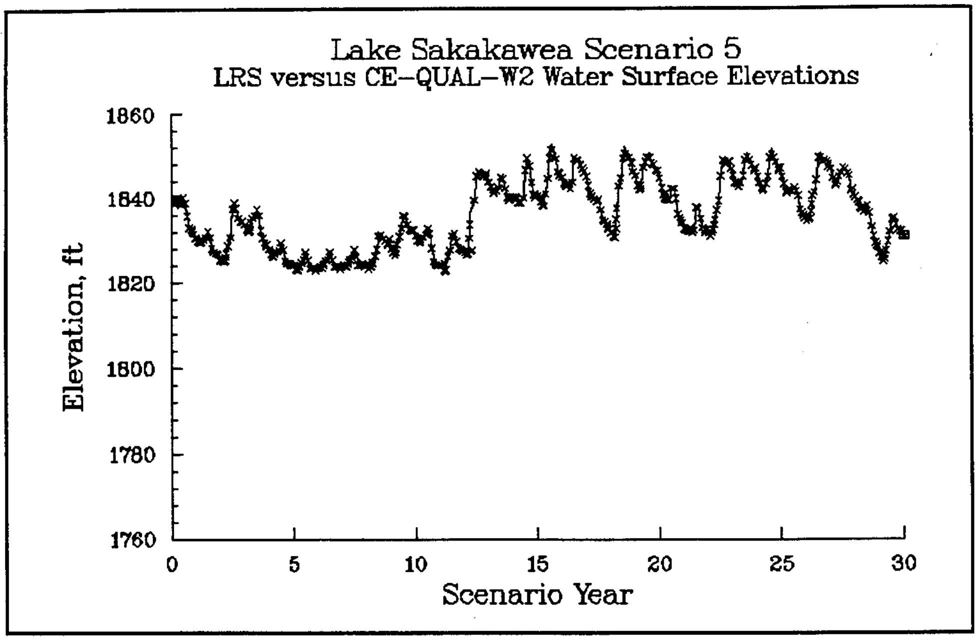

Figure 299. Lake Sakakawea LRS versus CE-QUAL-W2 water surface elevations for scenario 5

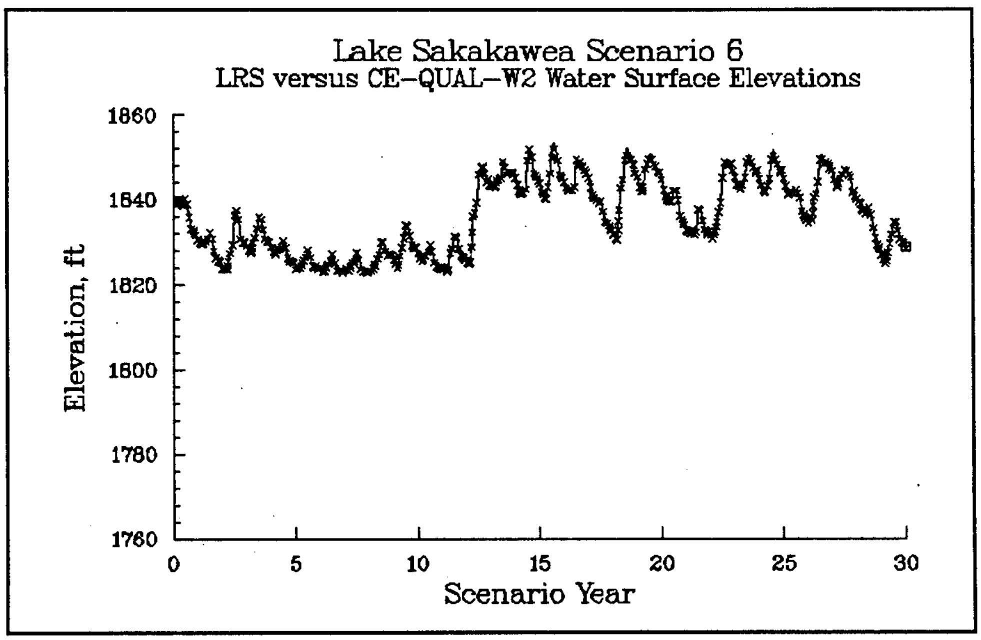

Figure 300. Lake Sakakawea LRS versus CE-QUAL-W2 water surface elevations for scenario 6

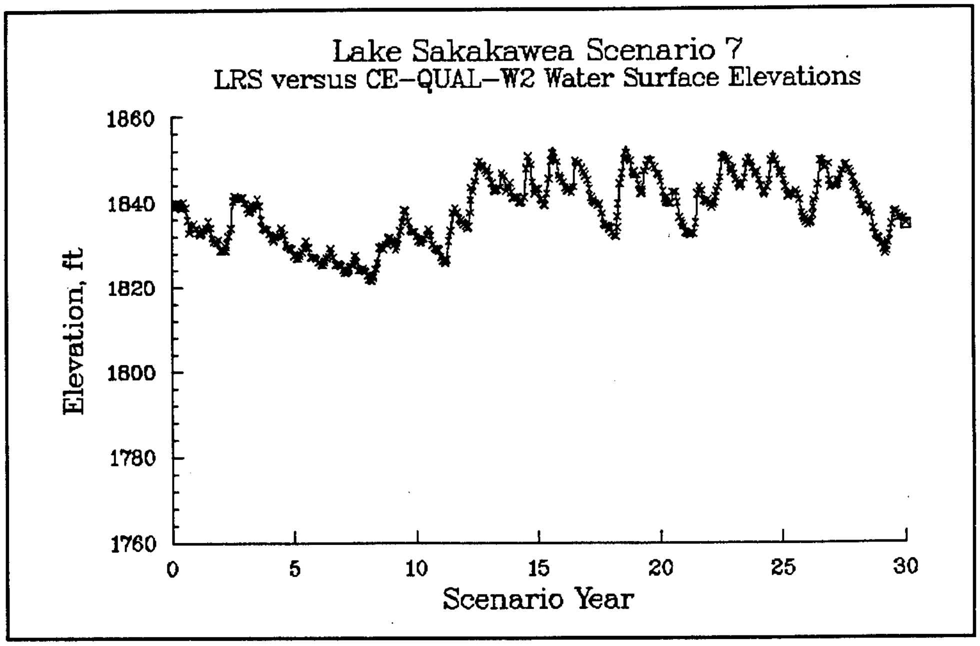

Figure 301. Lake Sakakawea LRS versus CE-QUAL-W2 water surface elevations for scenario 7

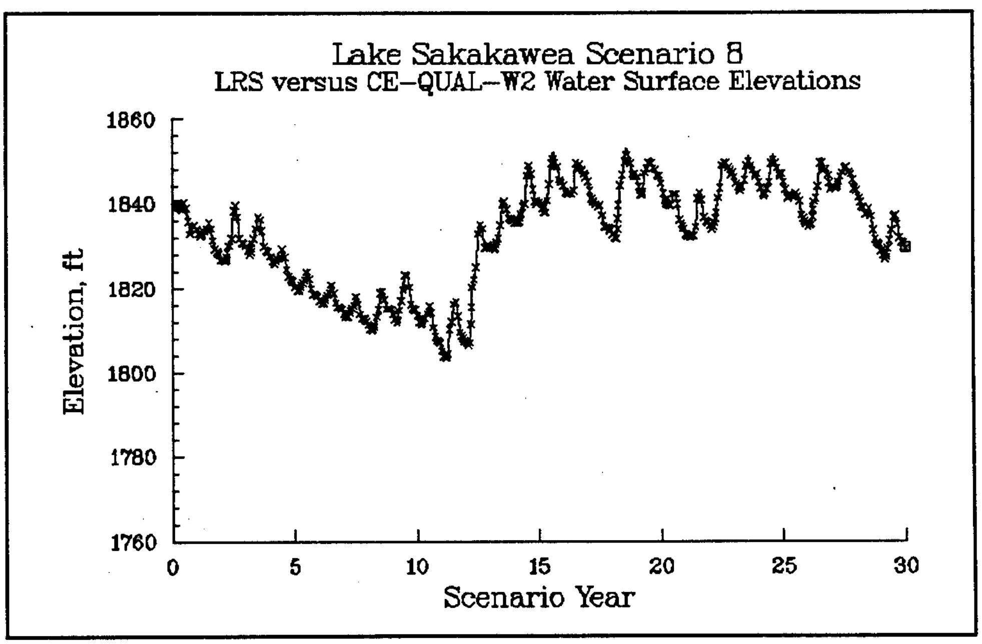

Figure 302. Lake Sakakawea LRS versus CE-QUAL-W2 water surface elevations for scenario 8

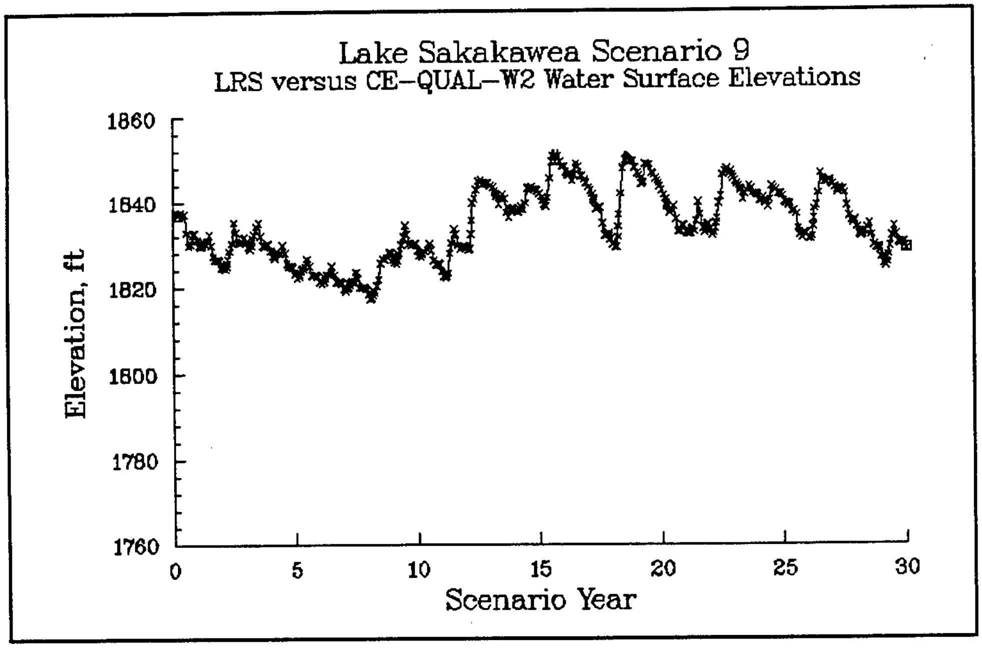

Figure 303. Lake Sakakawea LRS versus CE-QUAL-W2 water surface elevations for scenario 9

Release Temperature. Release temperatures for the nine scenarios are given in Figure 304-Figure 312.

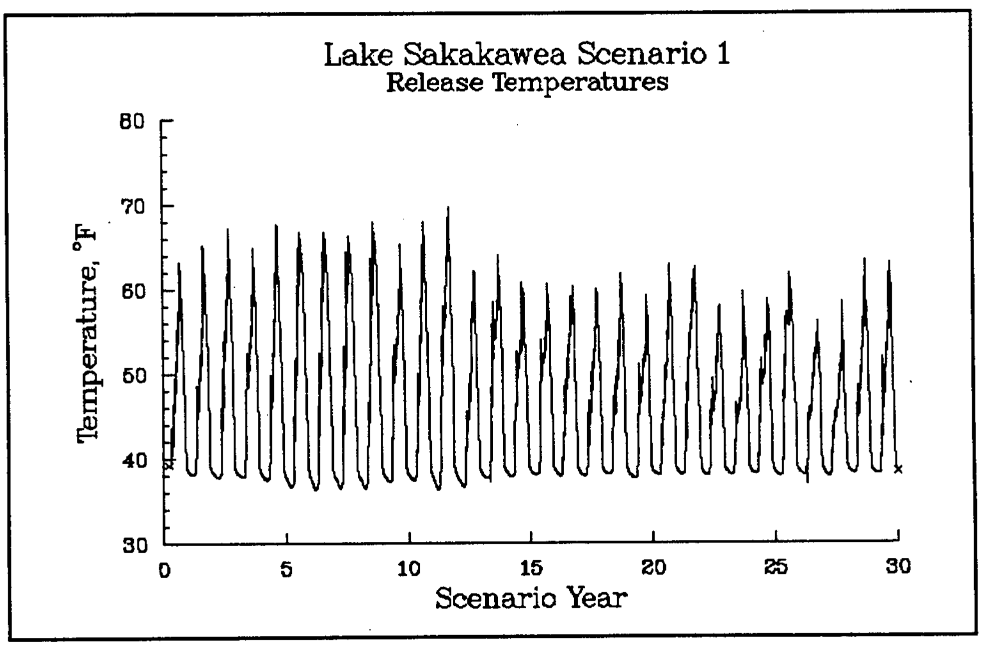

Figure 304. Lake Sakakawea release temperatures for scenario 1

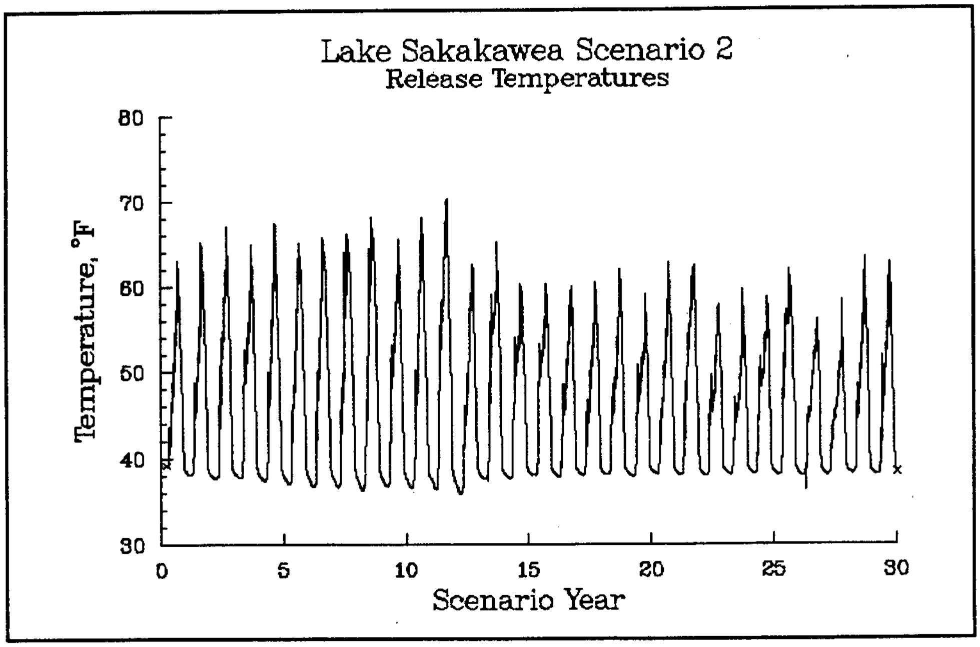

Figure 305. Lake Sakakawea release temperatures for scenario 2

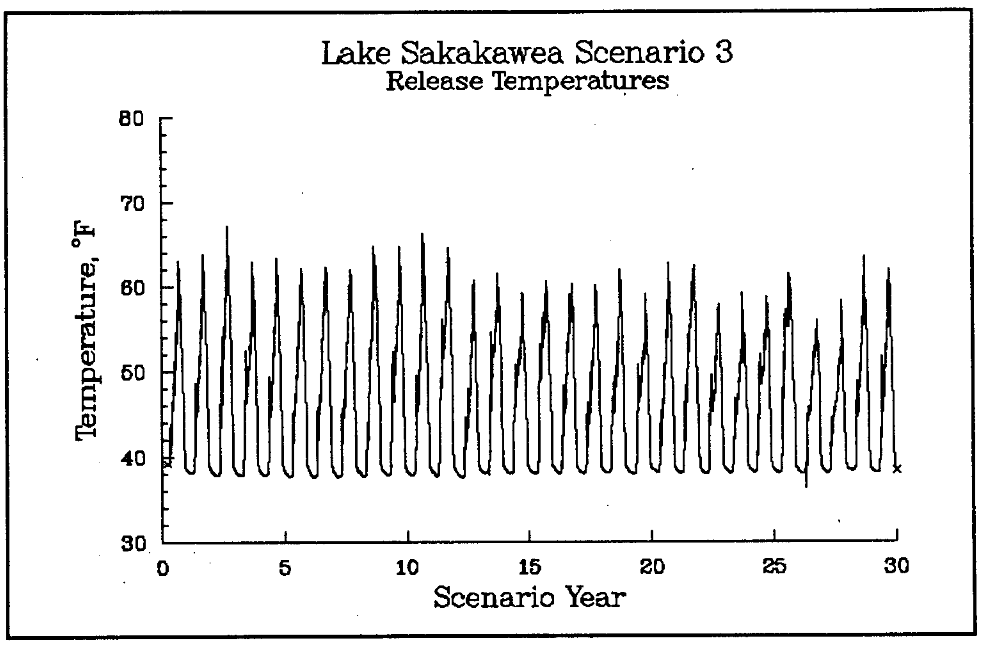

Figure 306. Lake Sakakawea release temperatures for scenario 3

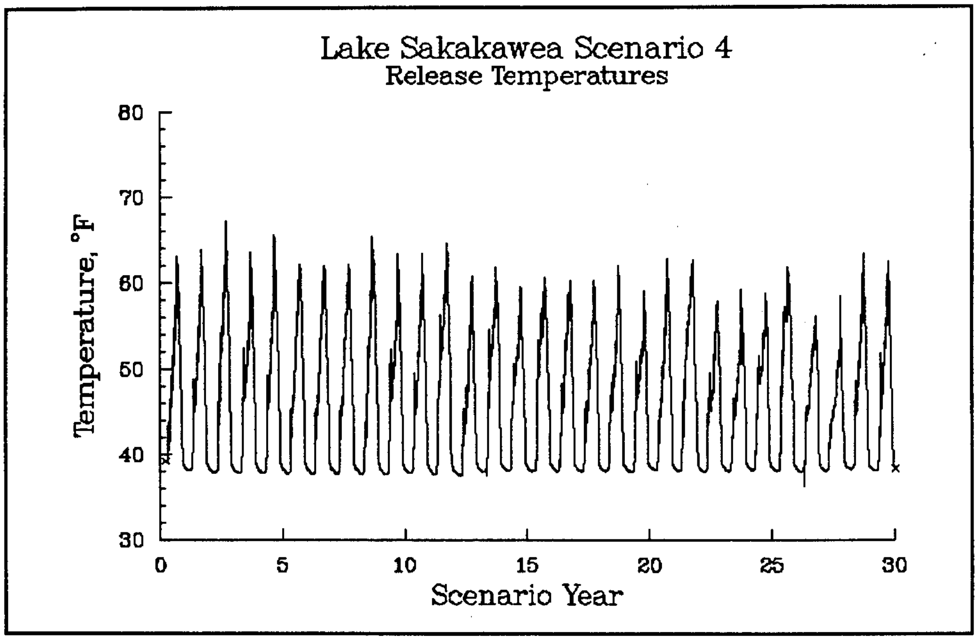

Figure 307. Lake Sakakawea release temperatures for scenario 4

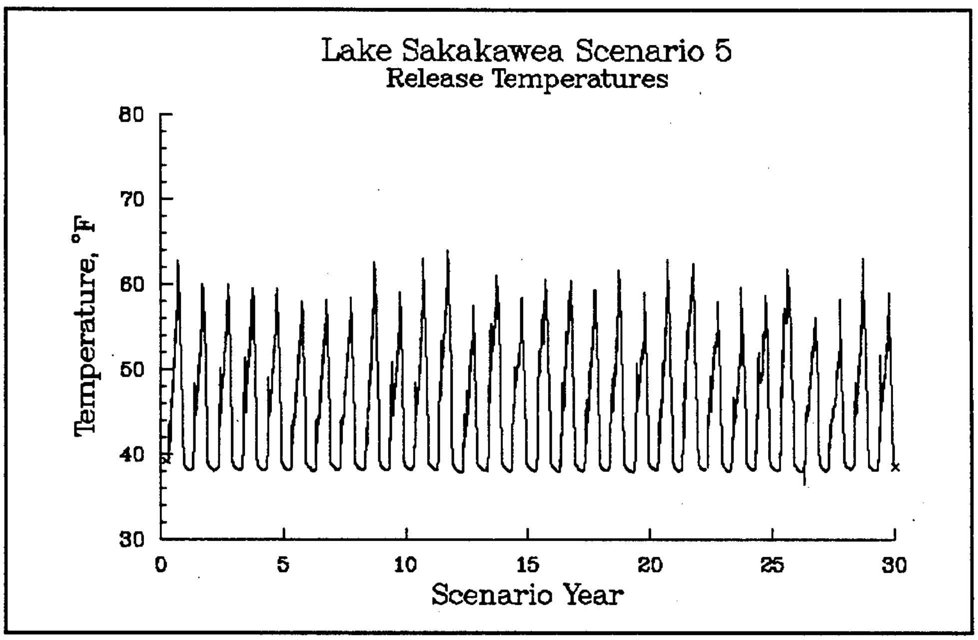

Figure 308. Lake Sakakawea release temperatures for scenario 5

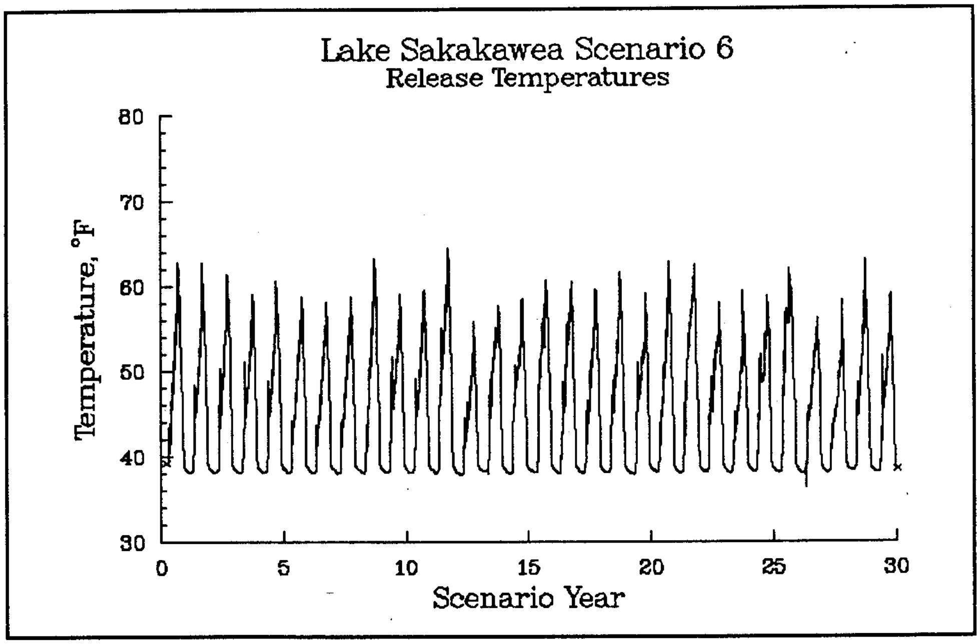

Figure 309. Lake Sakakawea release temperatures for scenario 6

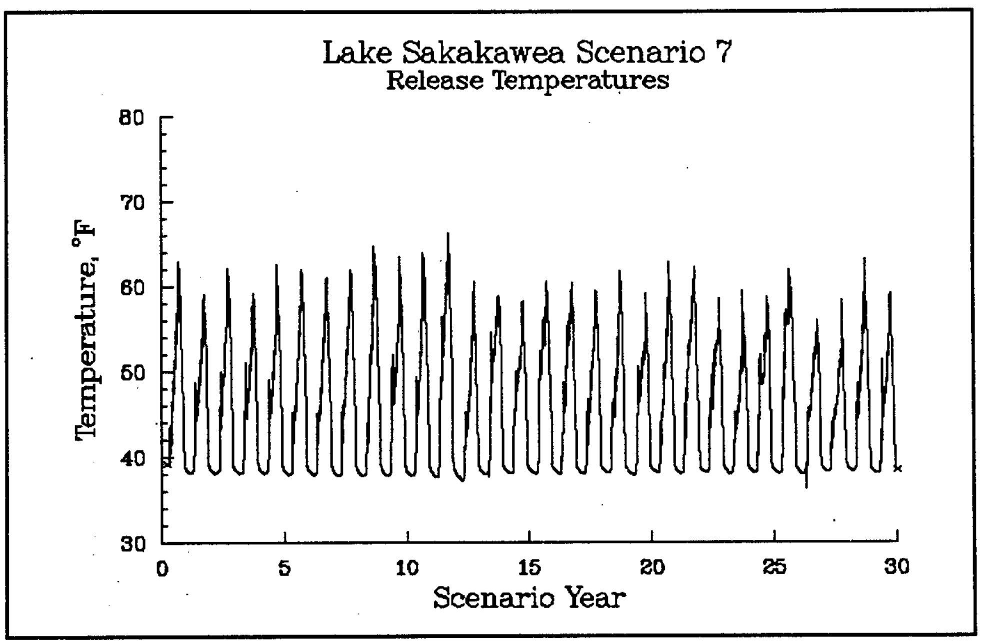

Figure 310. Lake Sakakawea release temperatures for scenario 7

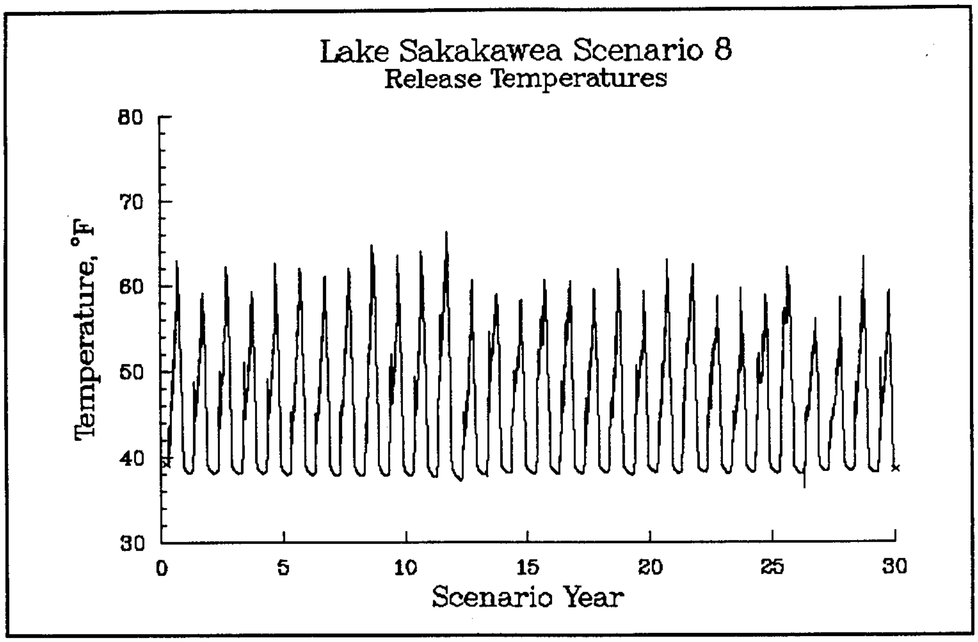

Figure 311. Lake Sakakawea release temperatures for scenario 8

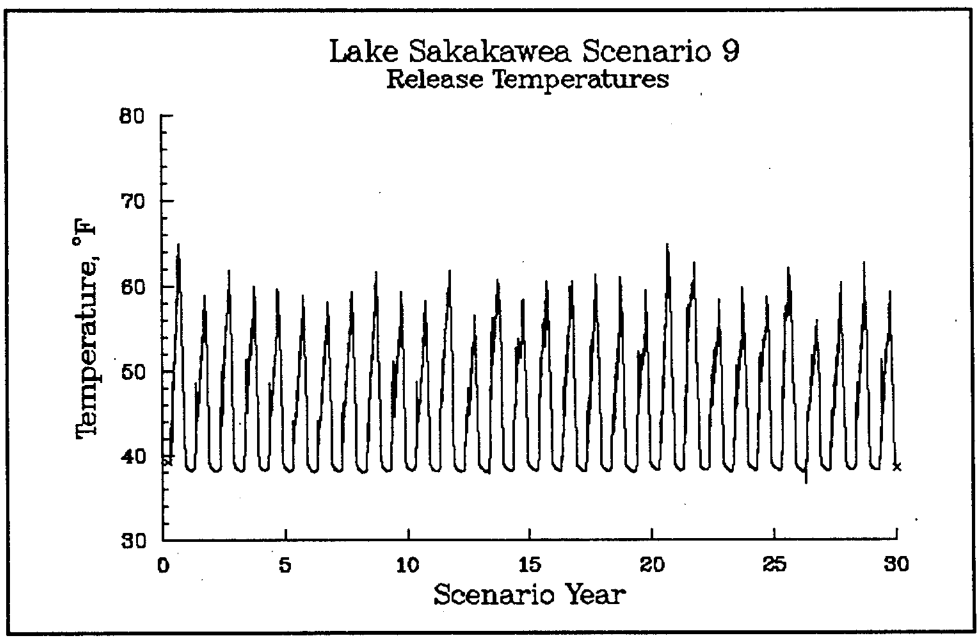

Figure 312. Lake Sakakawea release temperatures for scenario 9

Release DO. Release DO concentrations for the nine scenarios are given in Figure 313-Figure 321.

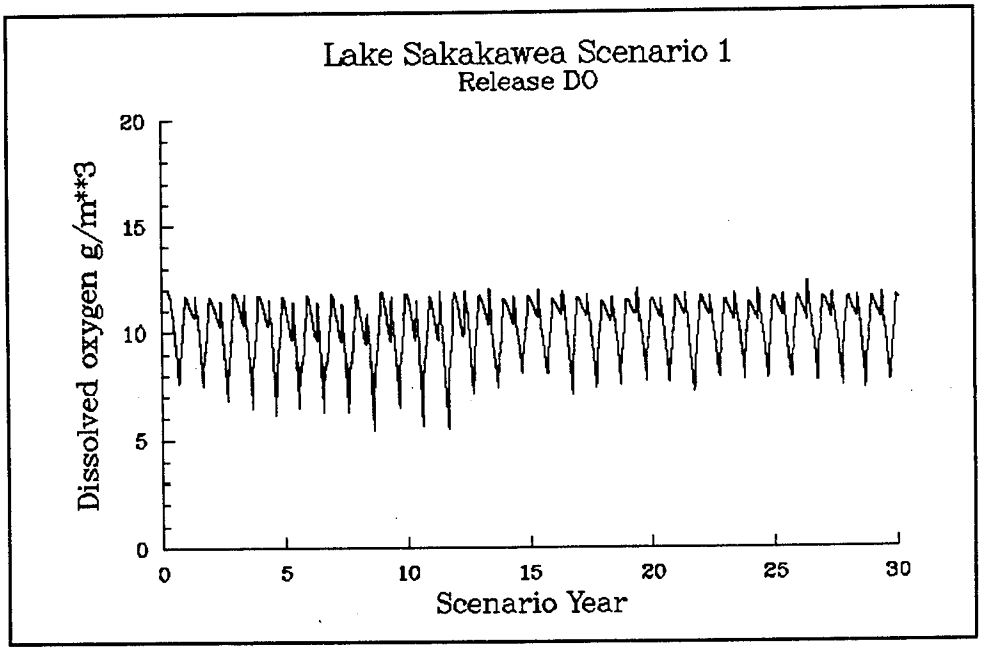

Figure 313. Lake Sakakawea release DO concentrations for scenario 1

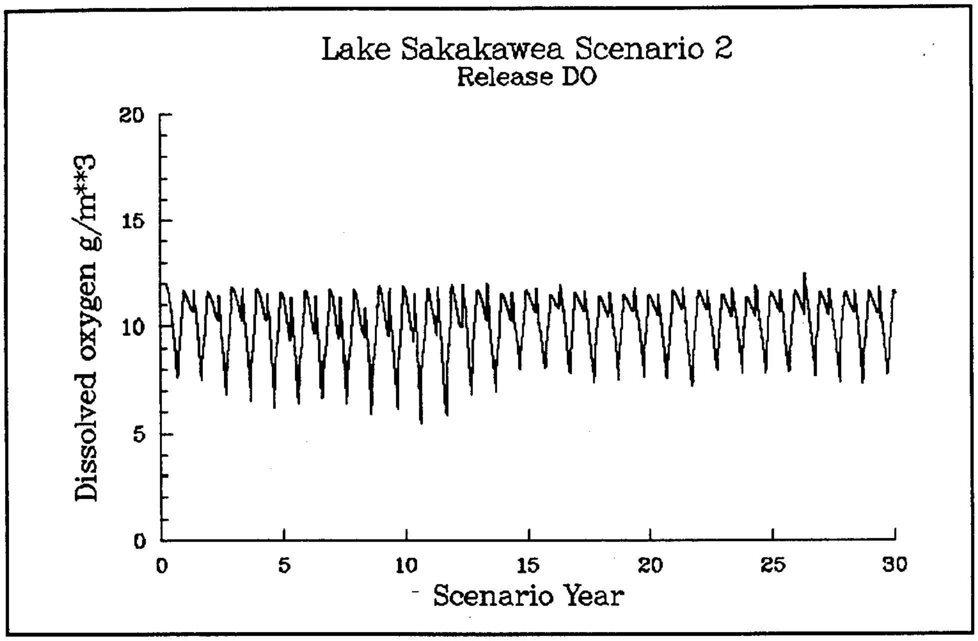

Figure 314. Lake Sakakawea release DO concentrations for scenario 2

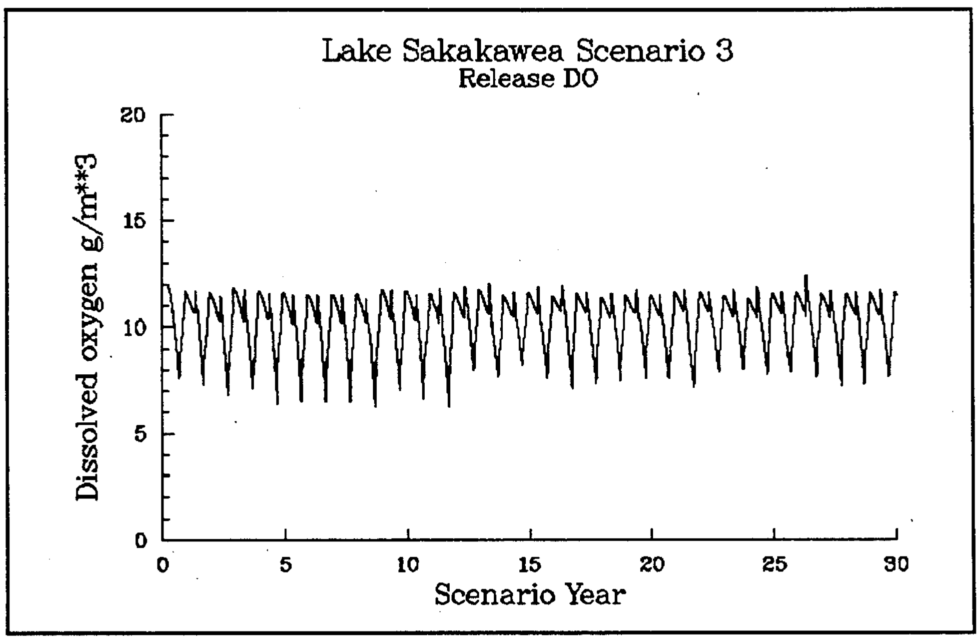

Figure 315. Lake Sakakawea release DO concentrations for scenario 3

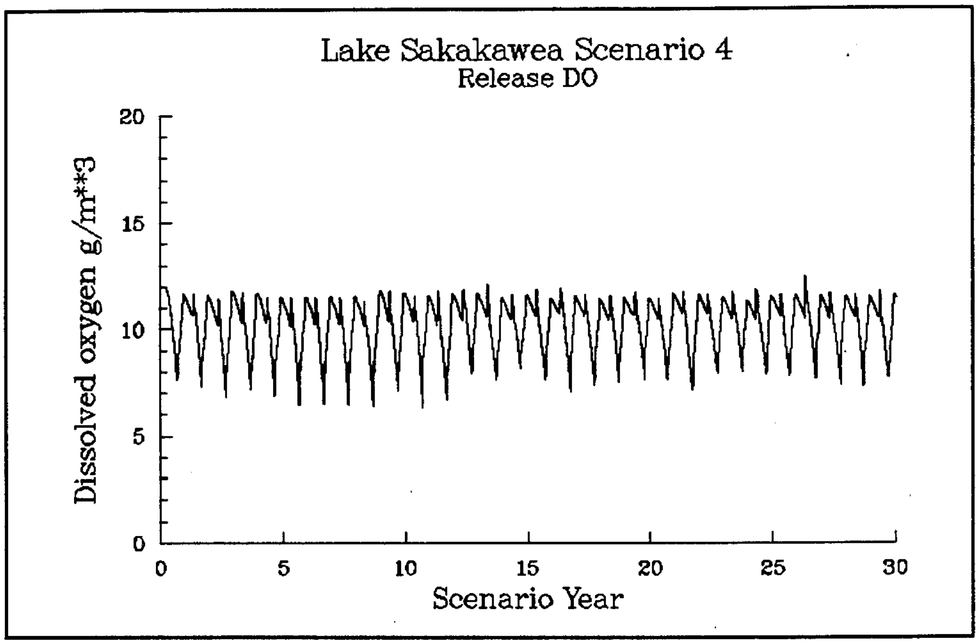

Figure 316. Lake Sakakawea release DO concentrations for scenario 4

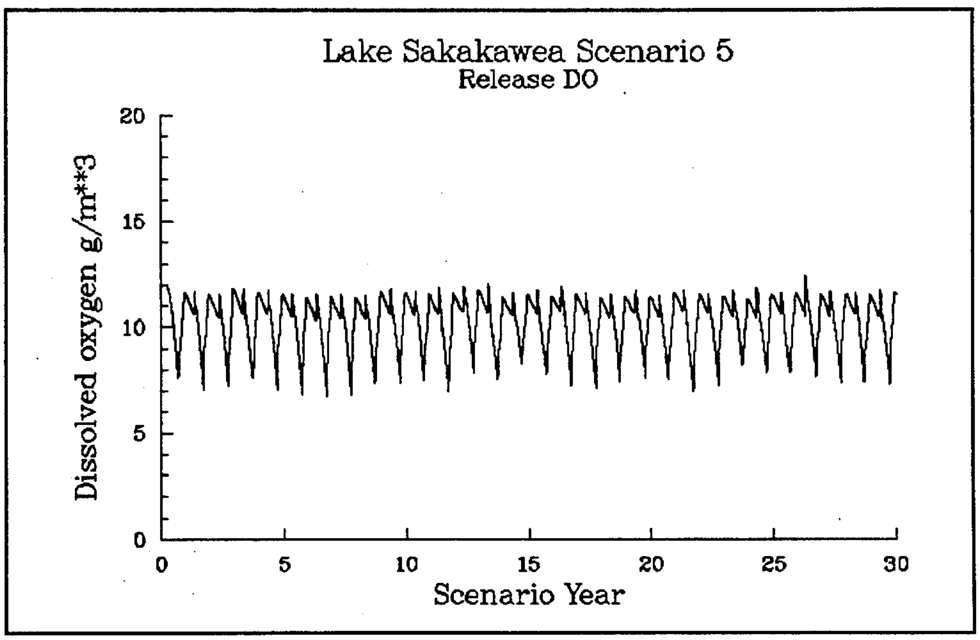

Figure 317. Lake Sakakawea release DO concentrations for scenario 5

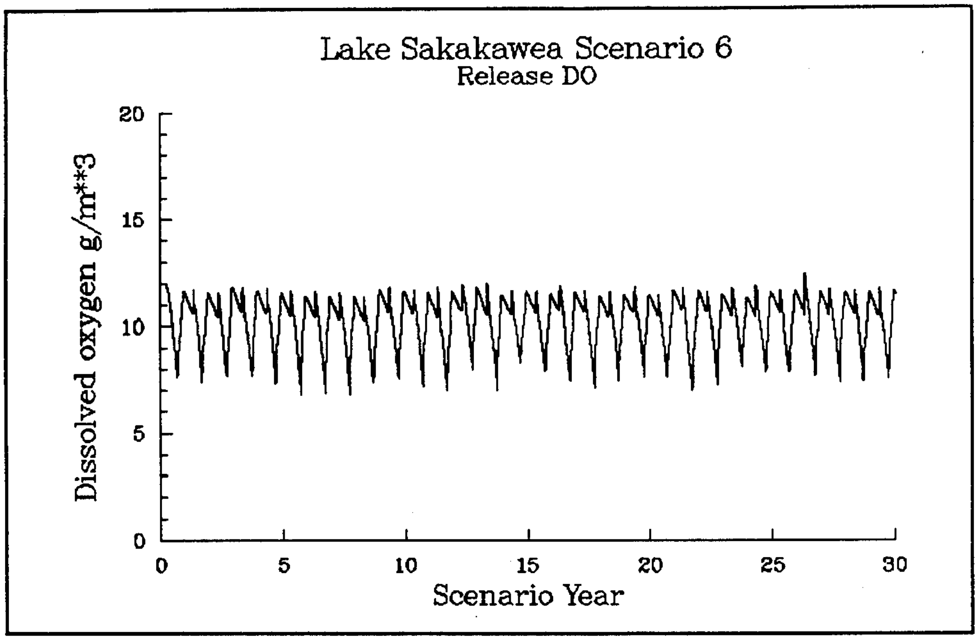

Figure 318. Lake Sakakawea release DO concentrations for scenario 6

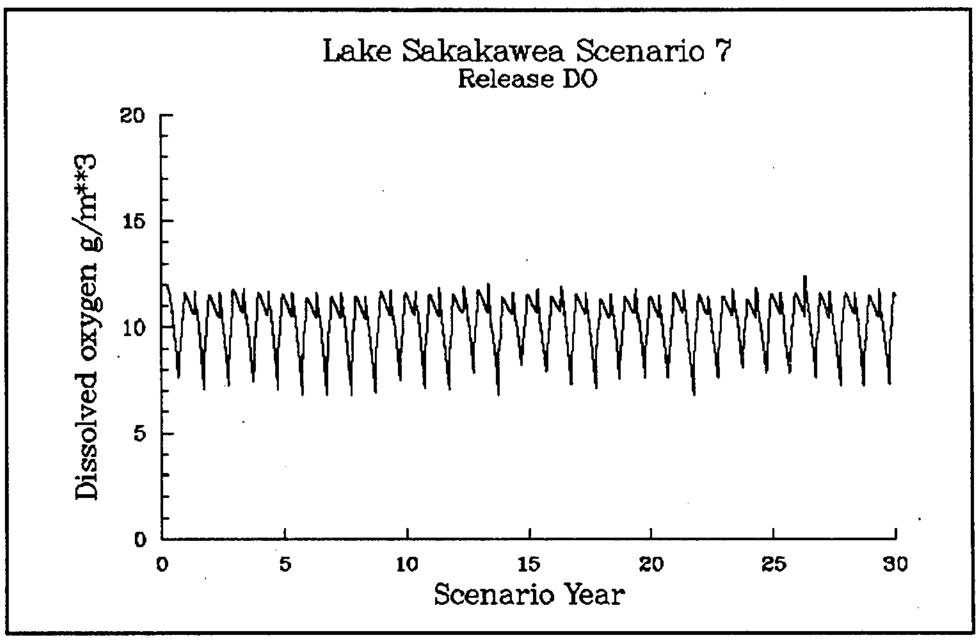

Figure 319. Lake Sakakawea release DO concentrations for scenario 7

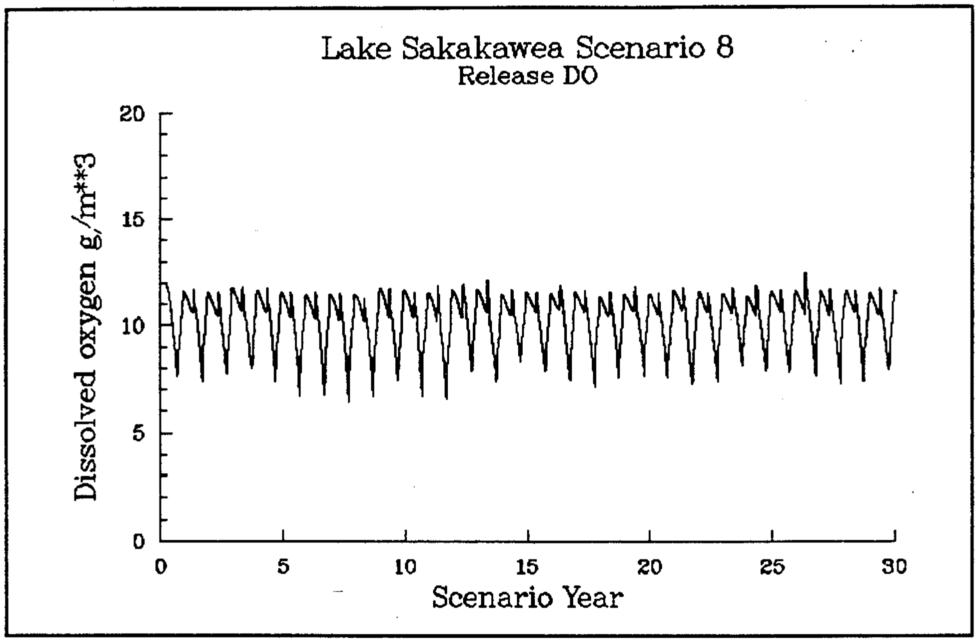

Figure 320. Lake Sakakawea release DO concentrations for scenario 8

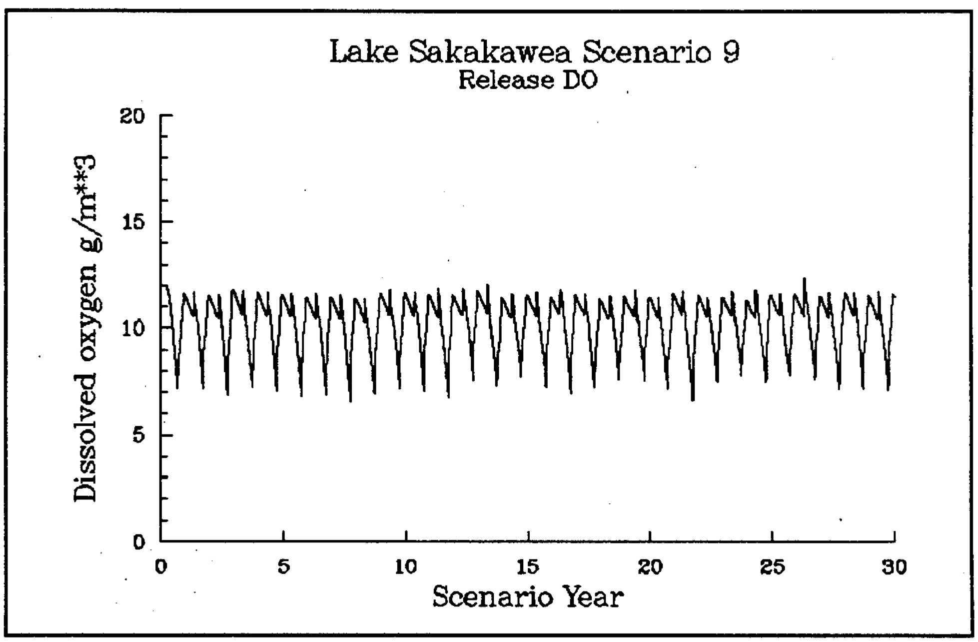

Figure 321. Lake Sakakawea release DO concentrations for scenario 9

Lake Oahe

Water Surface Elevations. Water surface elevations for the nine scenarios are given in Figure 322-Figure 330.

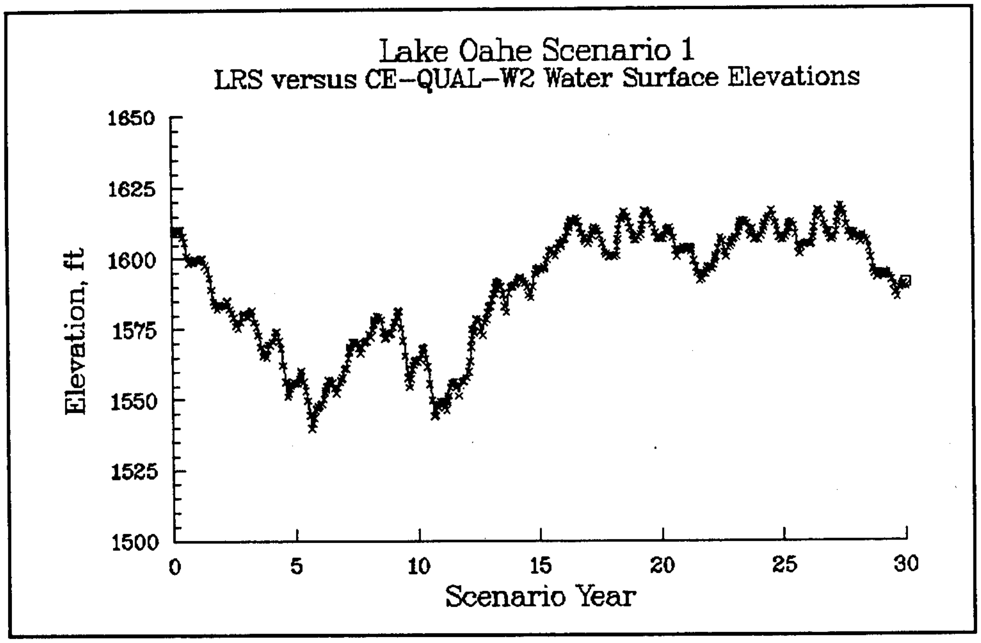

Figure 322. Lake Oahe LRS versus CE-QUAL-W2 water surface elevations for scenario 1

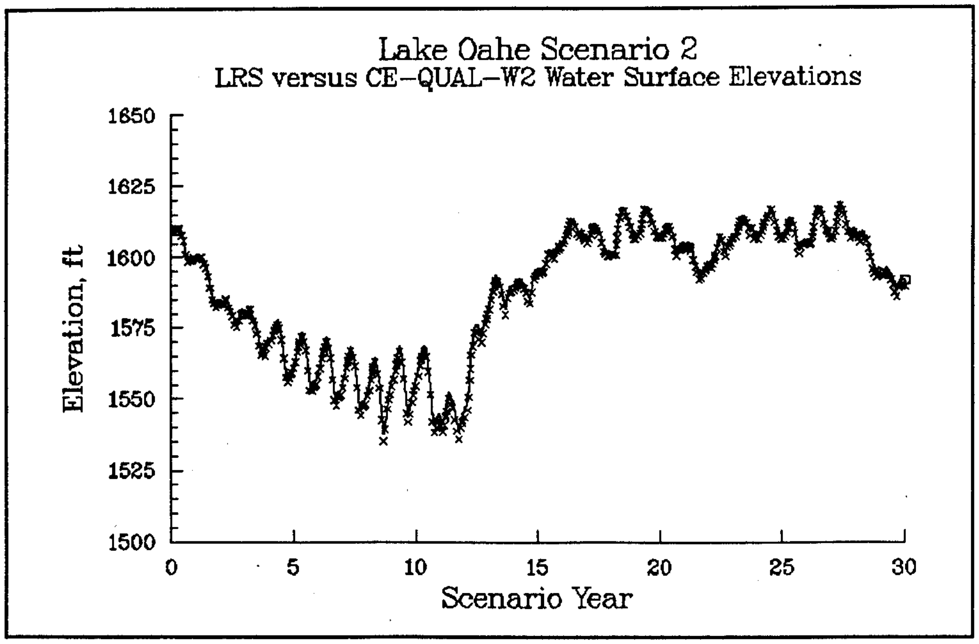

Figure 323. Lake Oahe LRS versus CE-QUAL-W2 water surface elevations for scenario 2

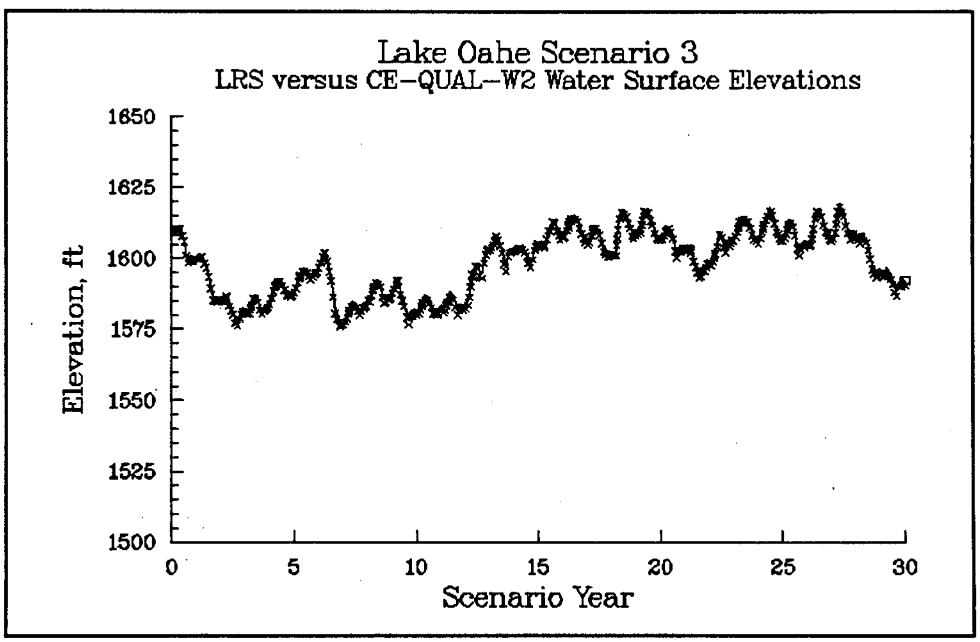

Figure 324. Lake Oahe LRS versus CE-QUAL-W2 water surface elevations for scenario 3

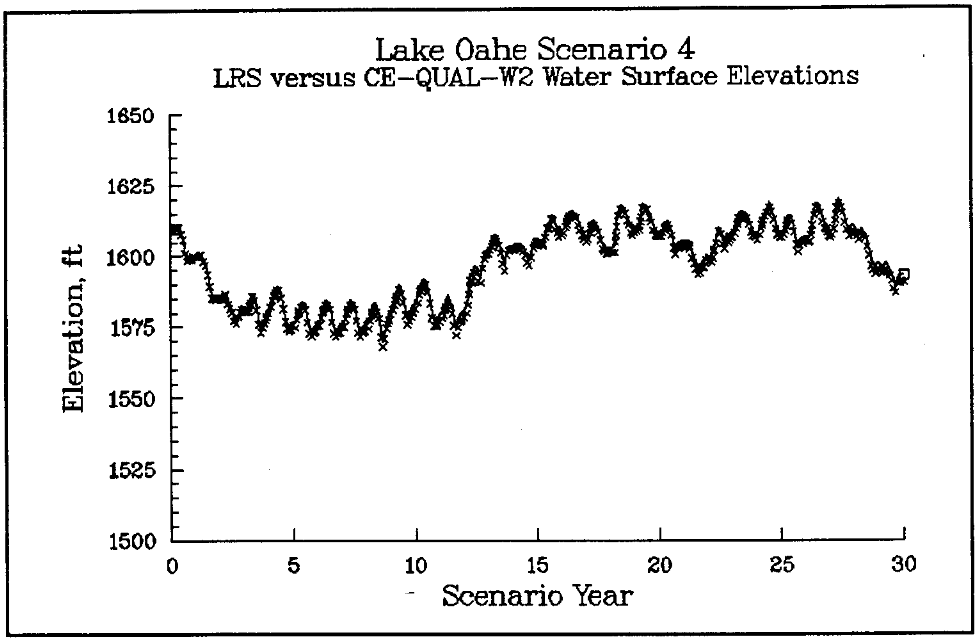

Figure 325. Lake Oahe LRS versus CE-QUAL-W2 water surface elevations for scenario 4

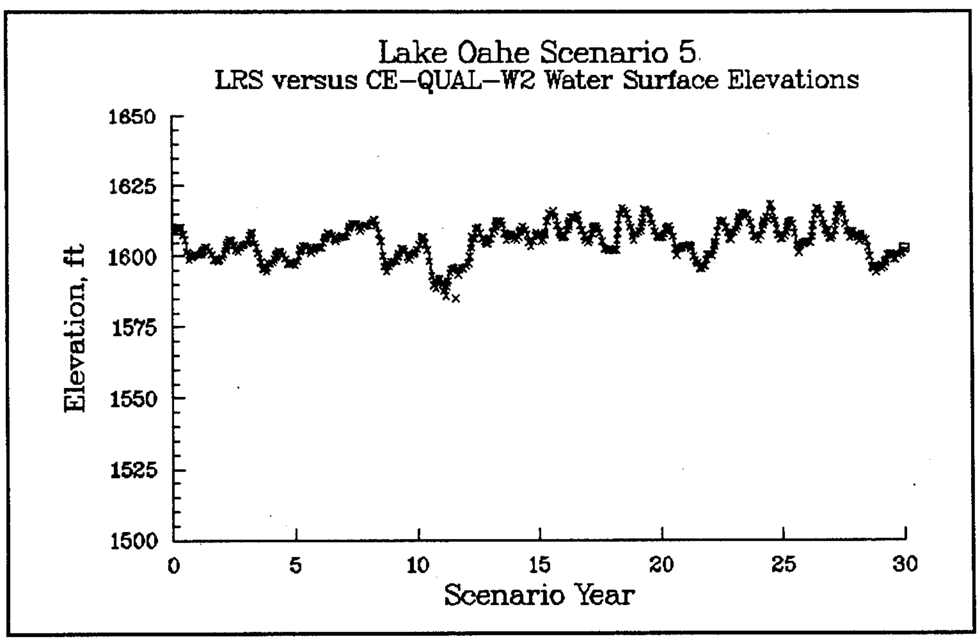

Figure 326. Lake Oahe LRS versus CE-QUAL-W2 water surface elevations for scenario 5

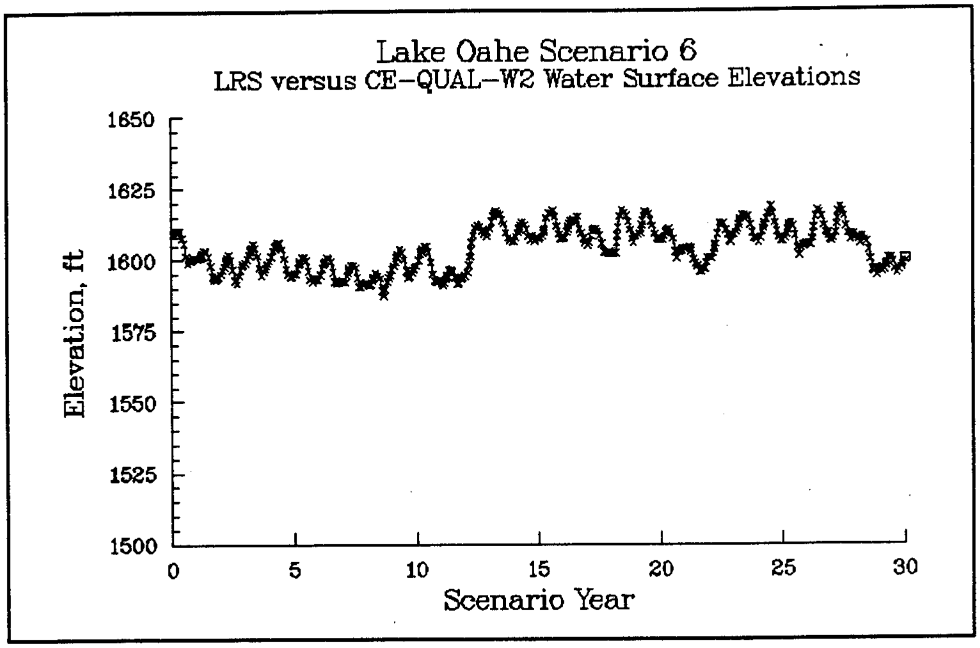

Figure 327. Lake Oahe LRS versus CE-QUAL-W2 water surface elevations for scenario 6

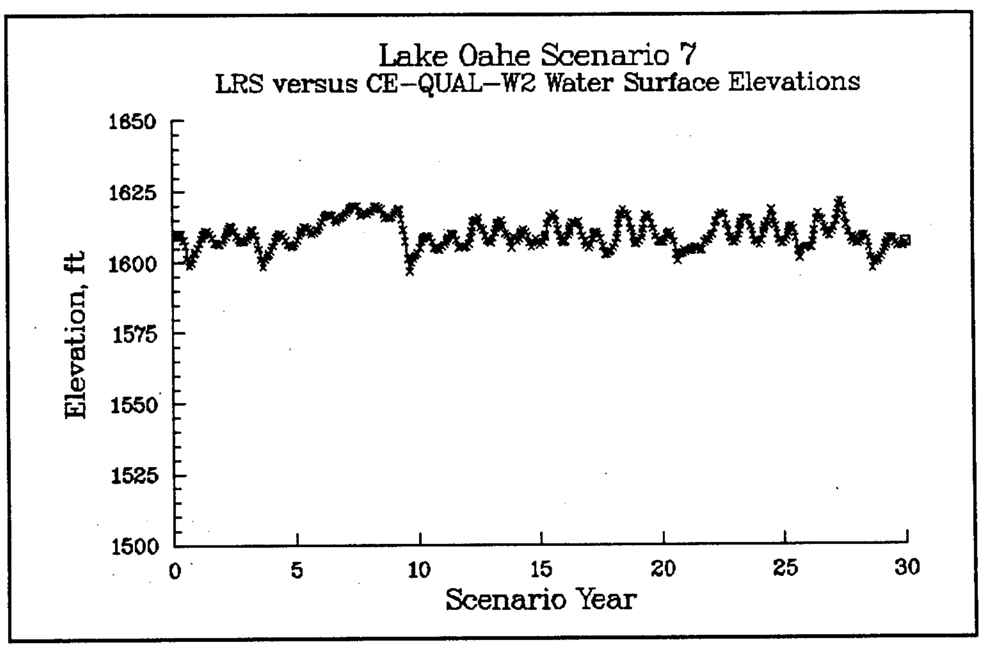

Figure 328. Lake Oahe LRS versus CE-QUAL-W2 water surface elevations for scenario 7

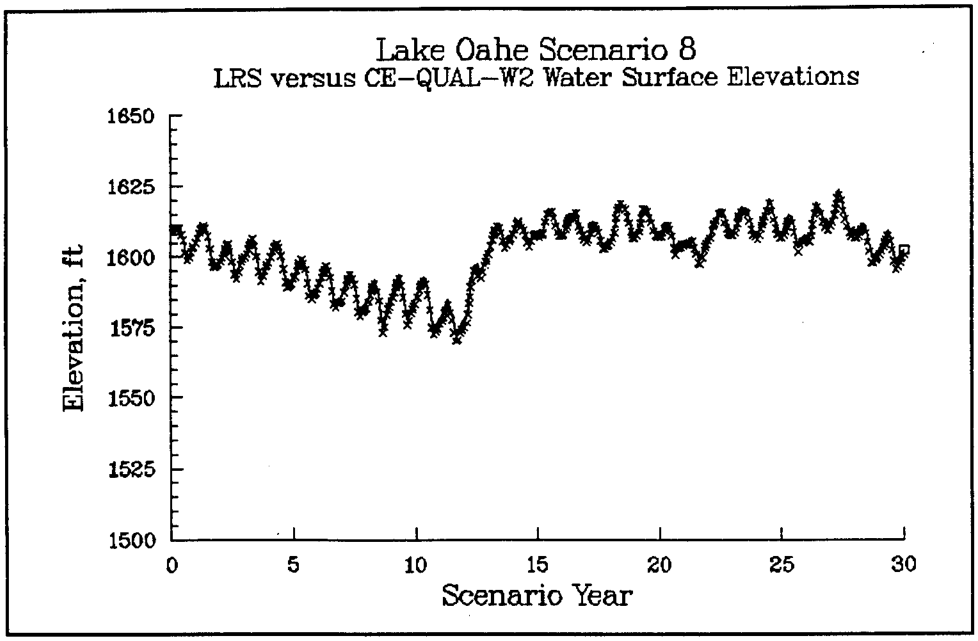

Figure 329. Lake Oahe LRS versus CE-QUAL-W2 water surface elevations for scenario 8

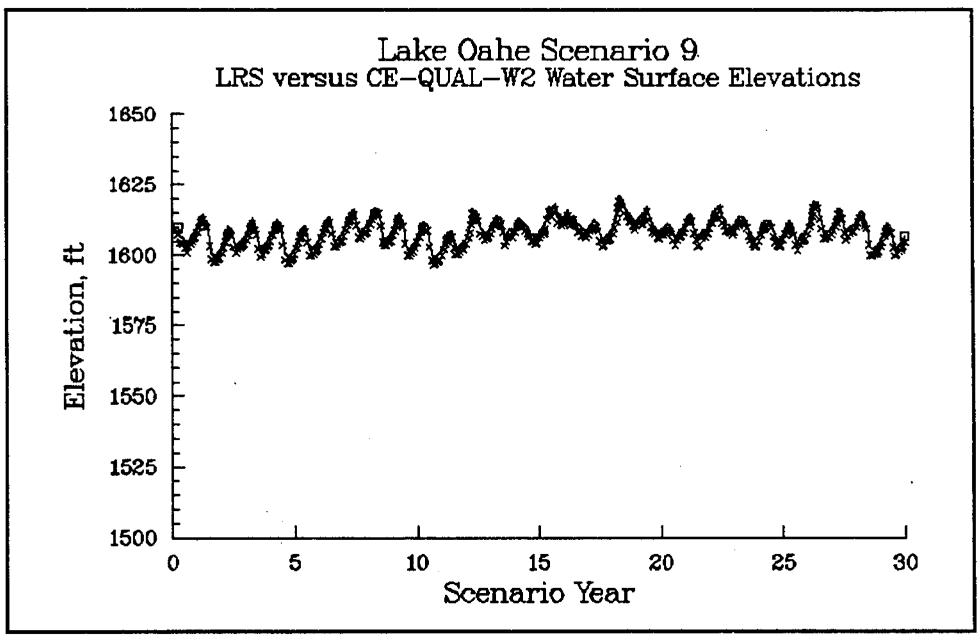

Figure 330. Lake Oahe LRS versus CE-QUAL-W2 water surface elevations for scenario 9

Release Temperature. Release temperatures for the nine scenarios are given in Figure 331-Figure 339.

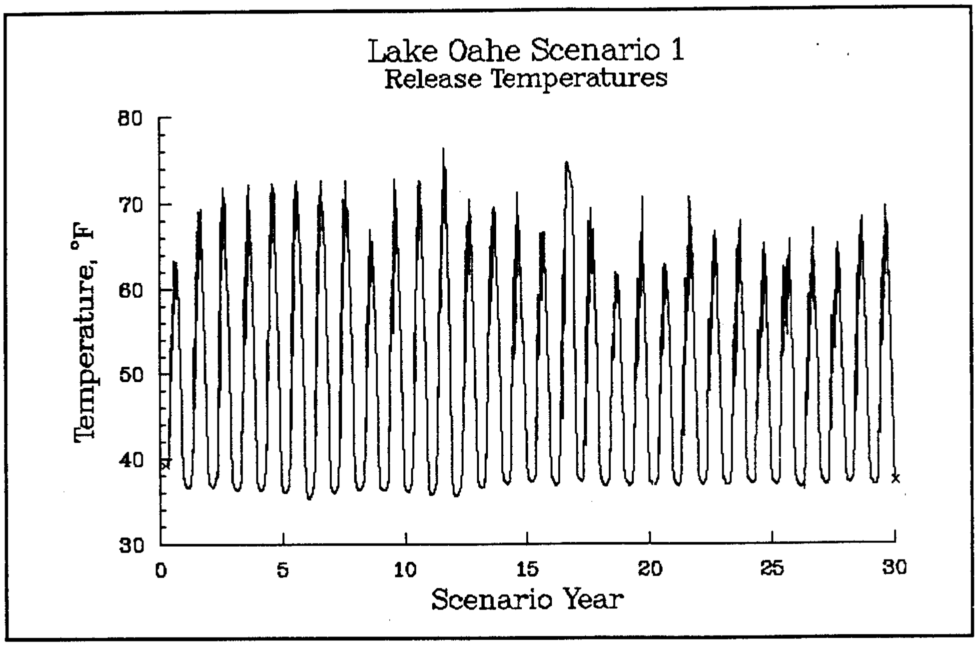

Figure 331. Lake Oahe release temperatures for scenario 1

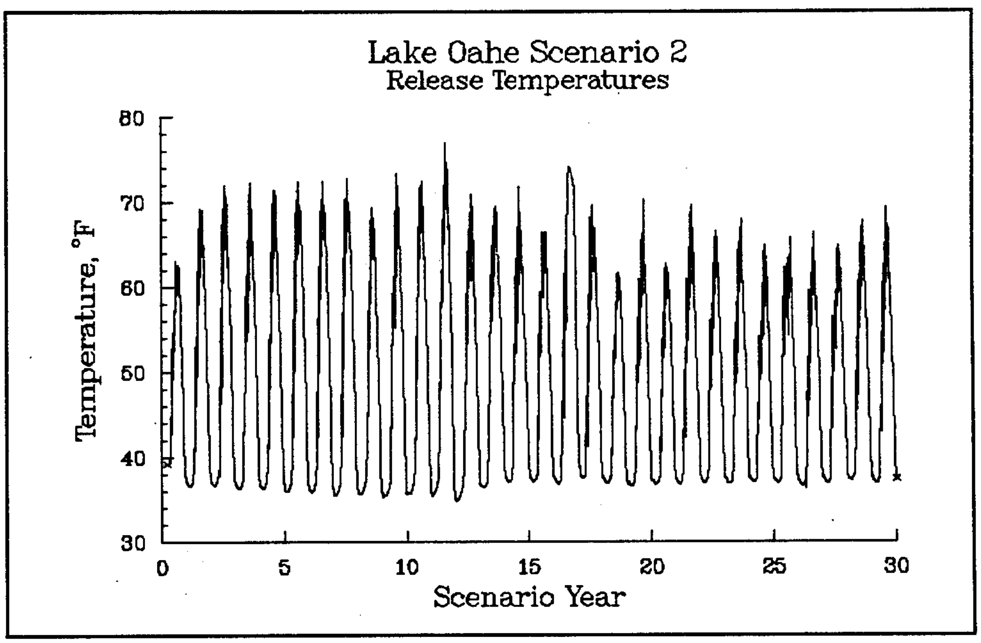

Figure 332. Lake Oahe release temperatures for scenario 2

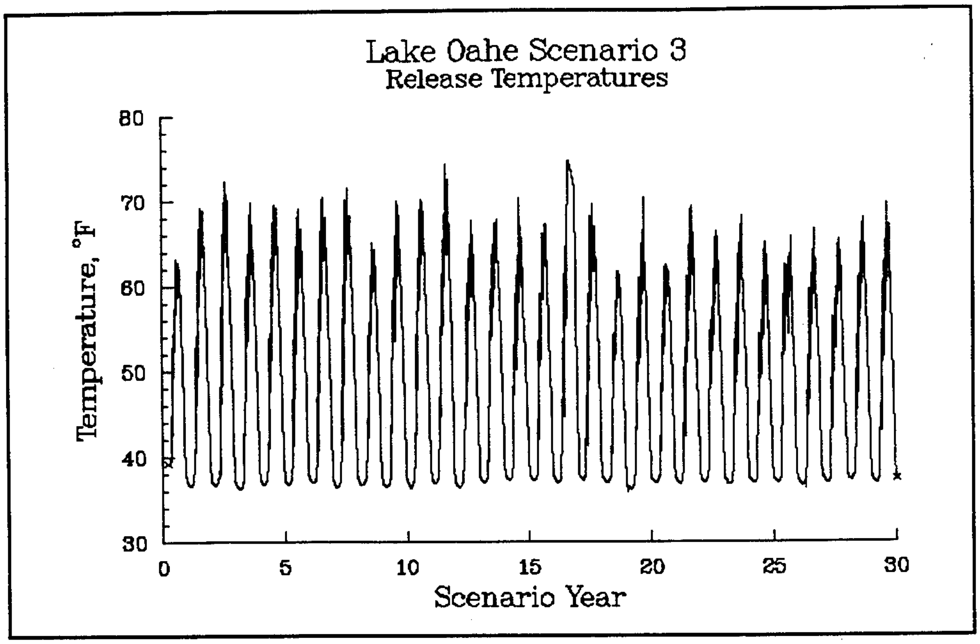

Figure 333. Lake Oahe release temperatures for scenario 3

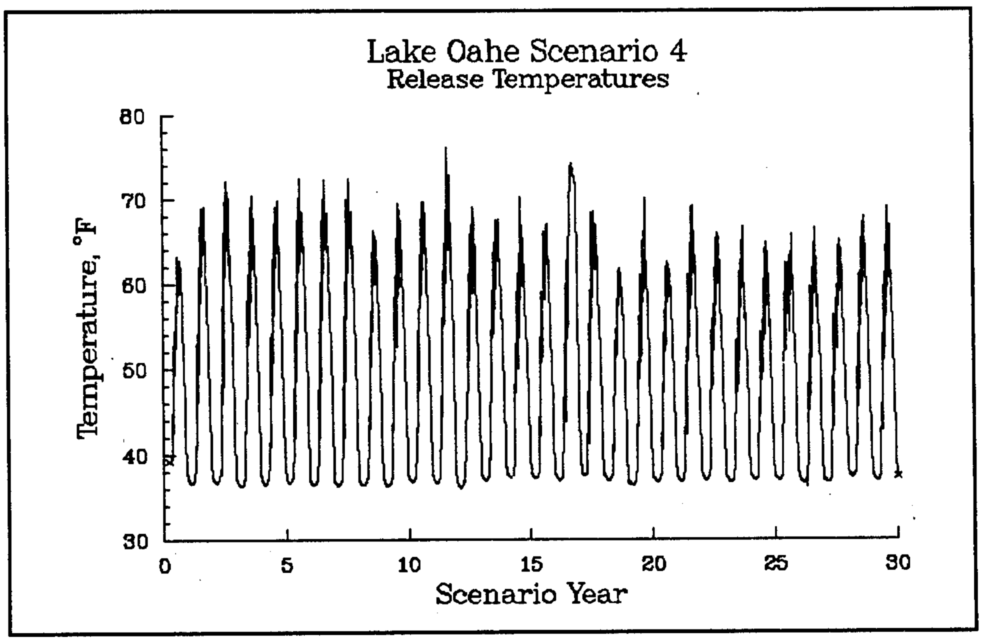

Figure 334. Lake Oahe release temperatures for scenario 4

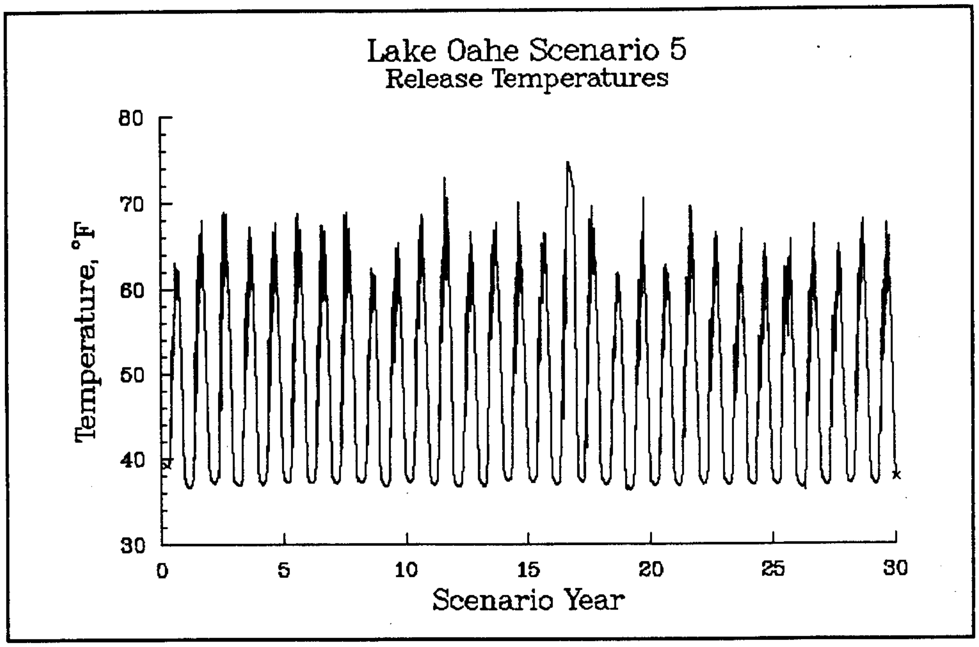

Figure 335. Lake Oahe release temperatures for scenario 5

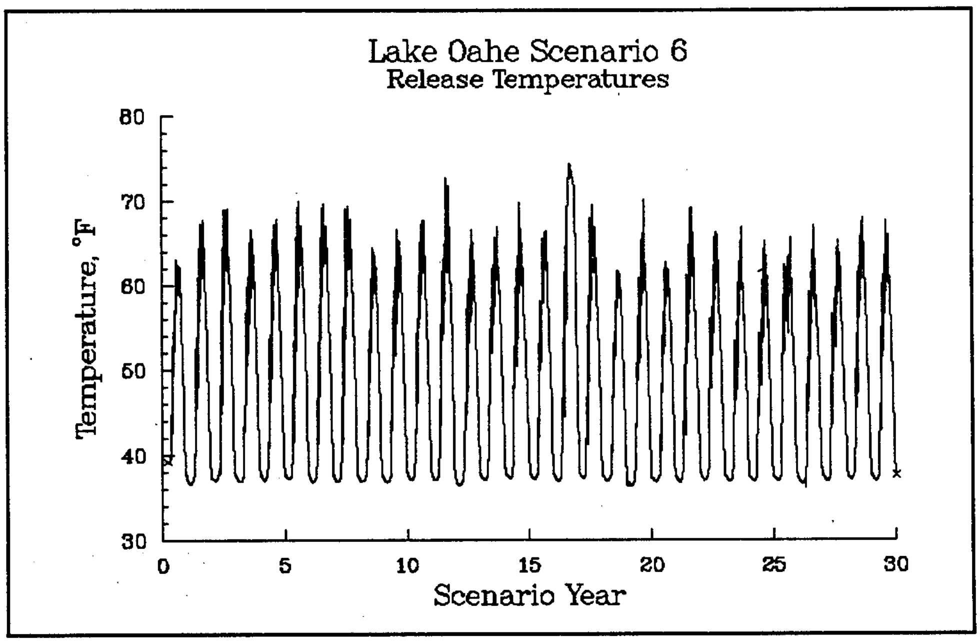

Figure 336. Lake Oahe release temperatures for scenario 6

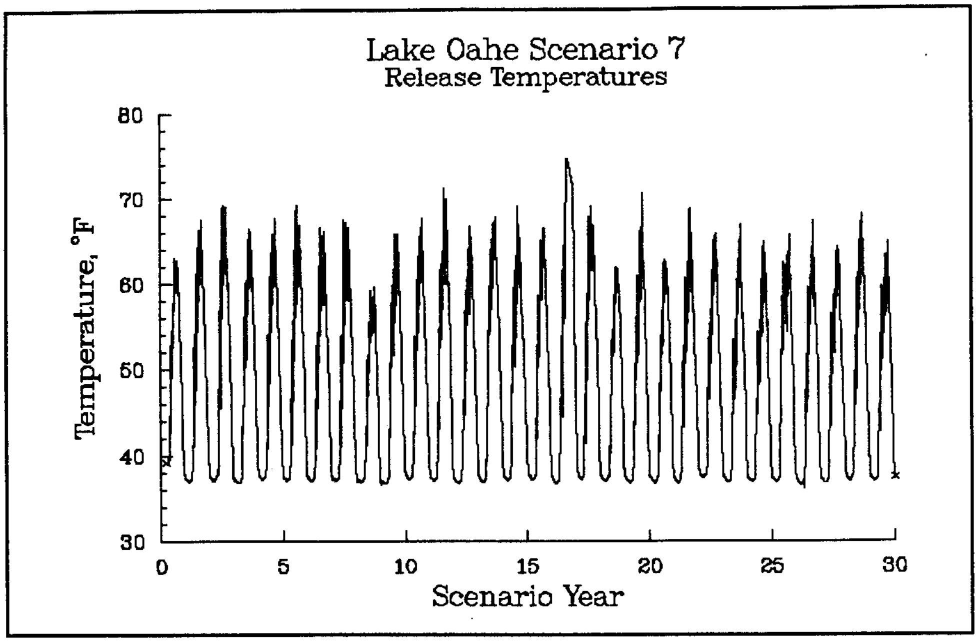

Figure 337. Lake Oahe release temperatures for scenario 7

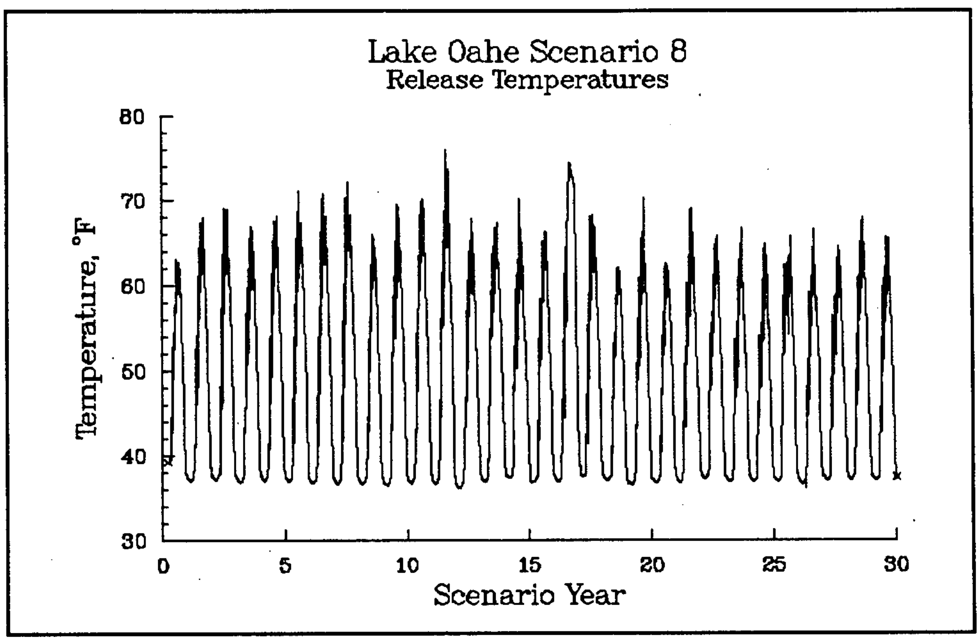

Figure 338. Lake Oahe release temperatures for scenario 8

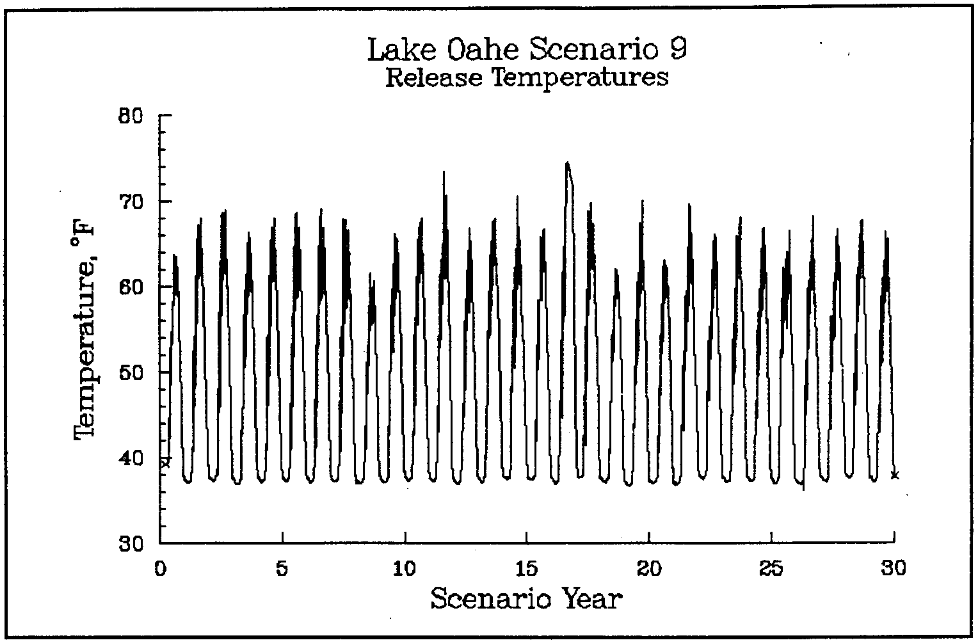

Figure 339. Lake Oahe release temperatures for scenario 9

Release DO. Release DO concentrations for the nine scenarios are given in Figure 340-Figure 348.

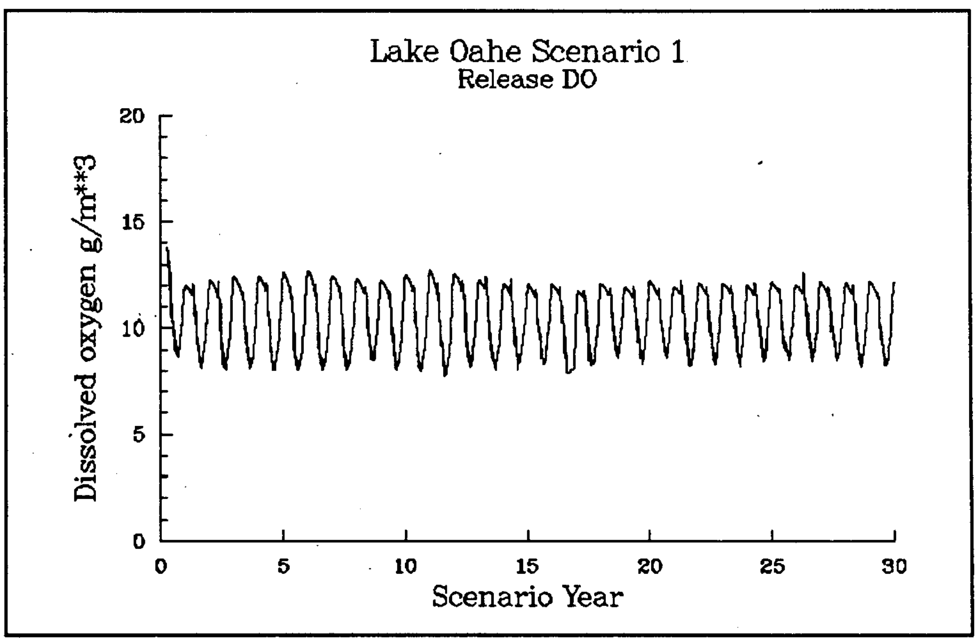

Figure 340. Lake Oahe release DO concentrations for scenario 1

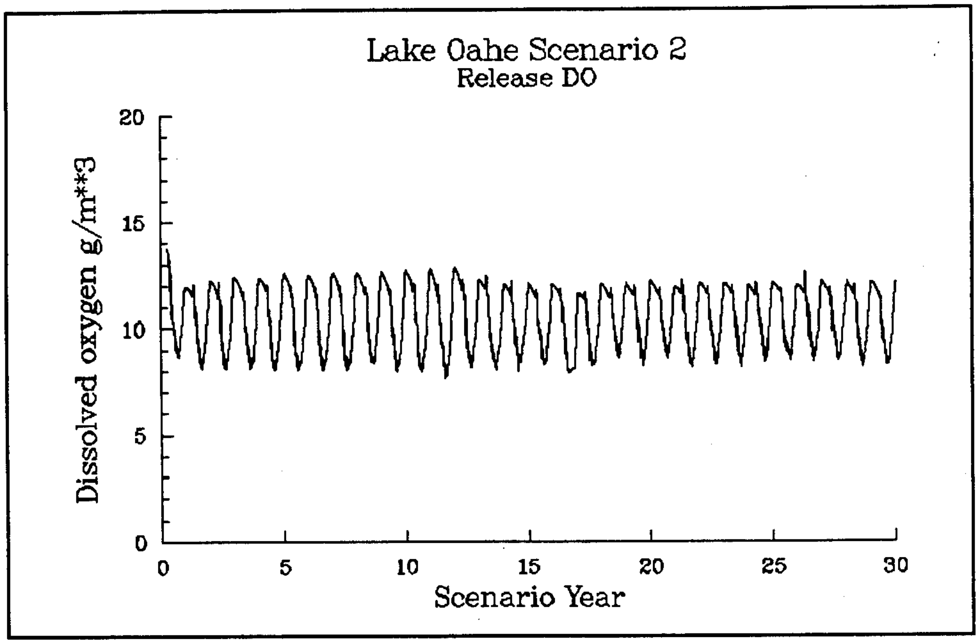

Figure 341. Lake Oahe release DO concentrations for scenario 2

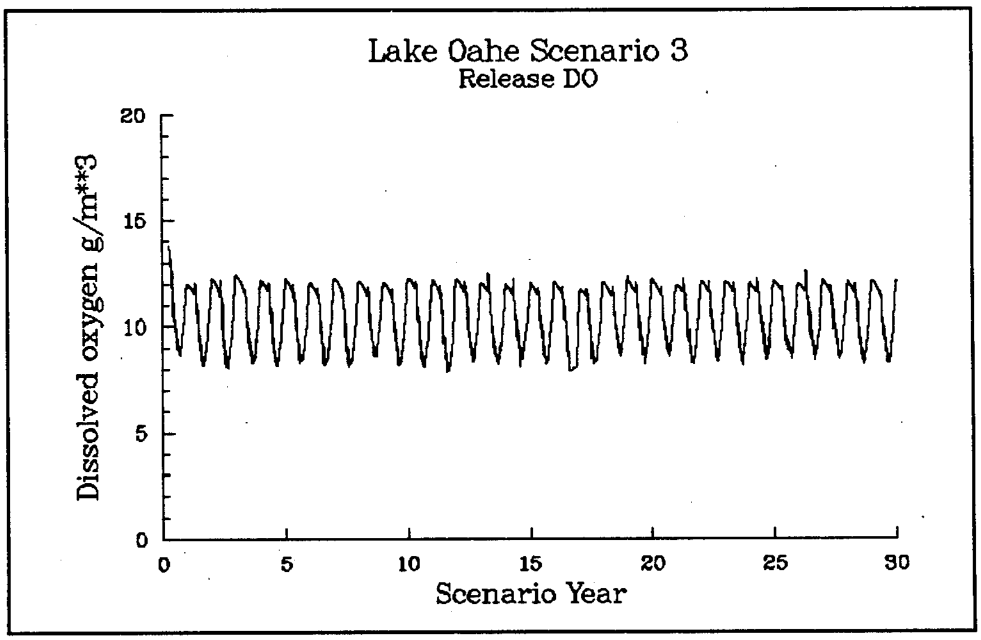

Figure 342. Lake Oahe release DO concentrations for scenario 3

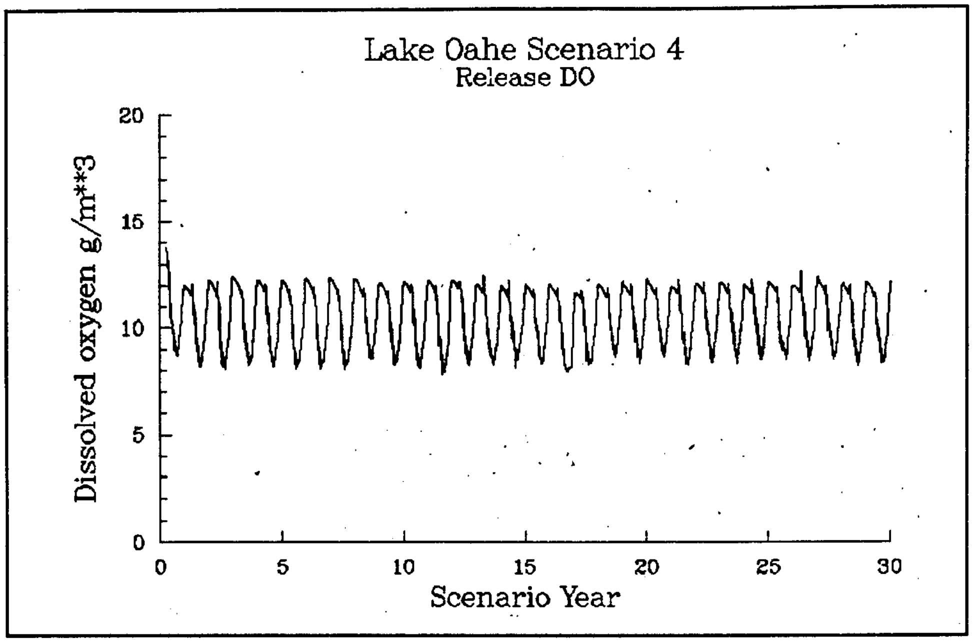

Figure 343. Lake Oahe release DO concentrations for scenario 4

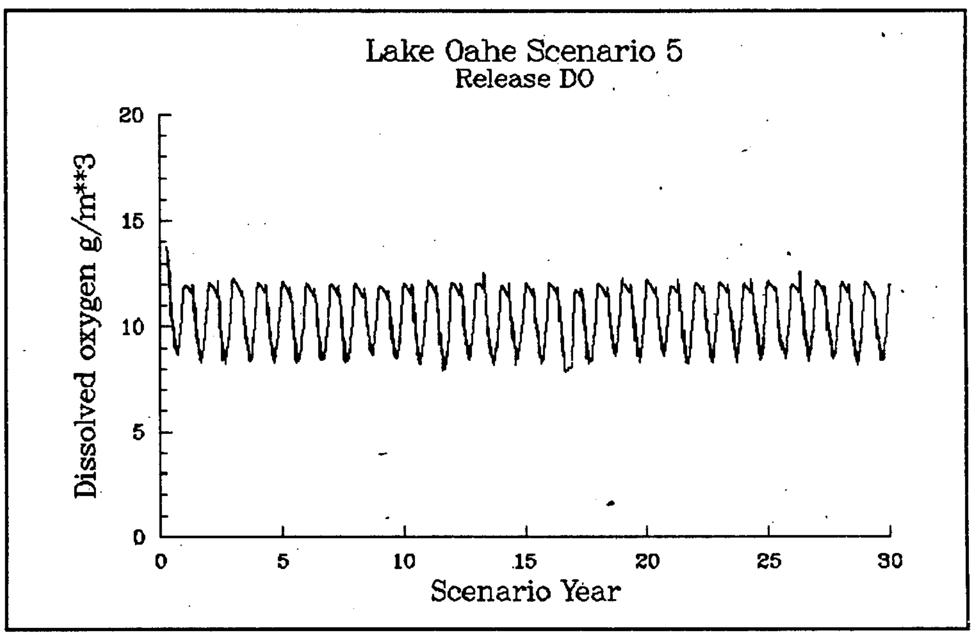

Figure 344. Lake Oahe release DO concentrations for scenario 5

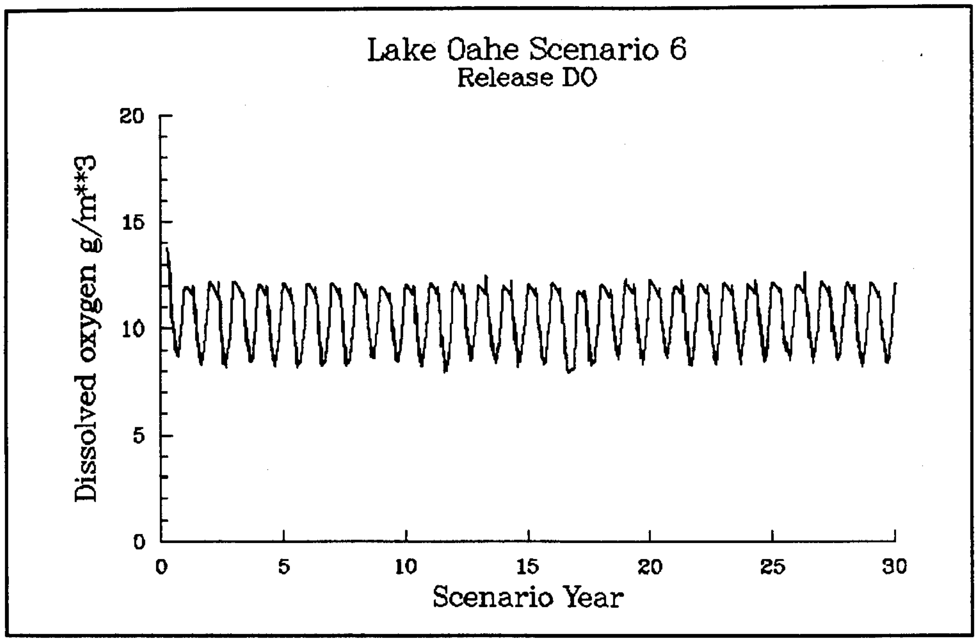

Figure 345. Lake Oahe release DO concentrations for scenario 6

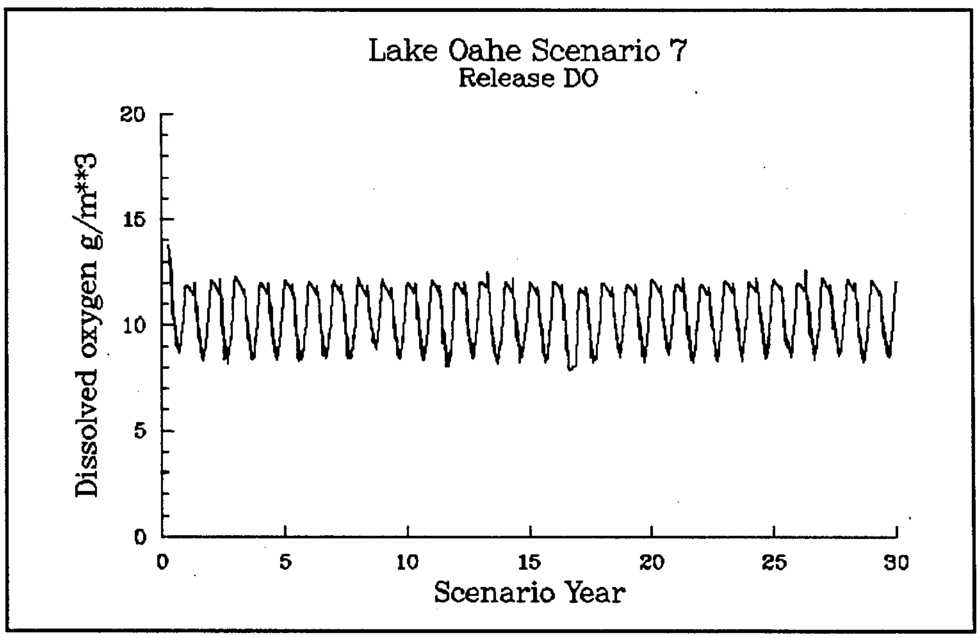

Figure 346. Lake Oahe release DO concentrations for scenario 7

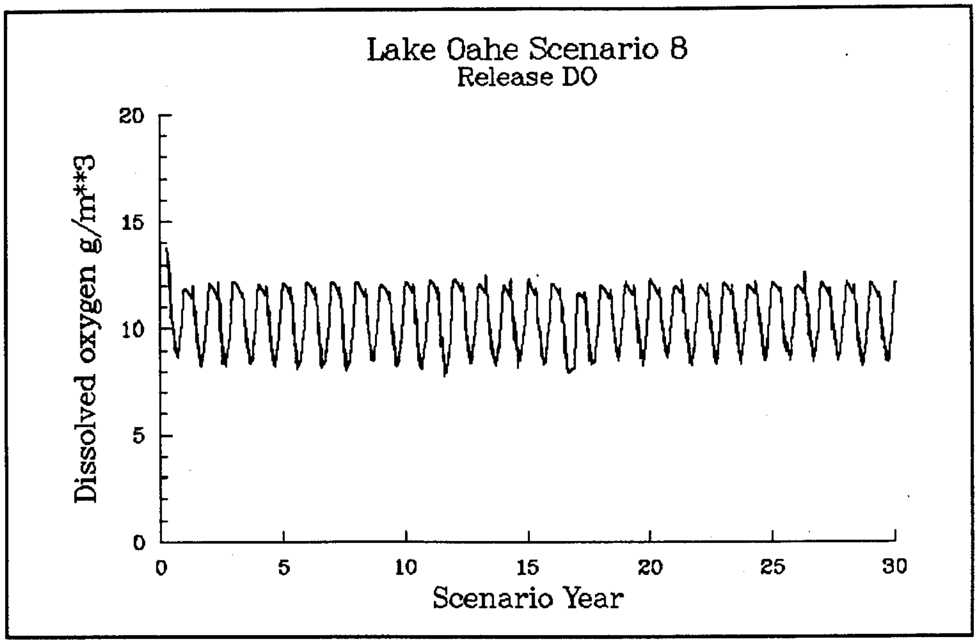

Figure 347. Lake Oahe release DO concentrations for scenario 8

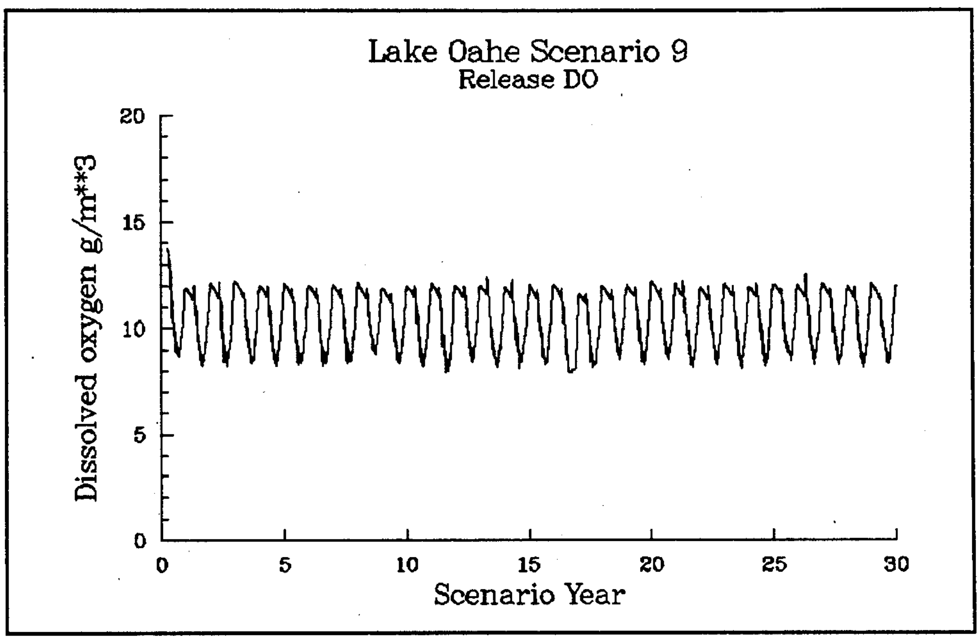

Figure 348. Lake Oahe release DO concentrations for scenario 9

Lake Francis Case

Water Surface Elevations. Water surface elevations for the nine scenarios are given in Figure 349-Figure 357.

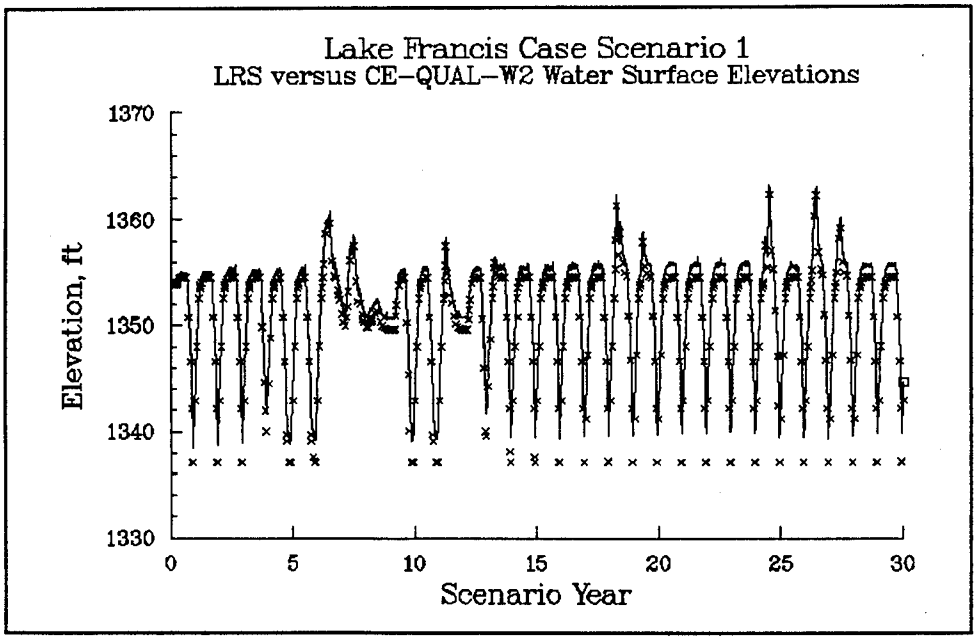

Figure 349. Lake Francis Case LRS versus CE-QUAL-W2 water surface elevations for scenario 1

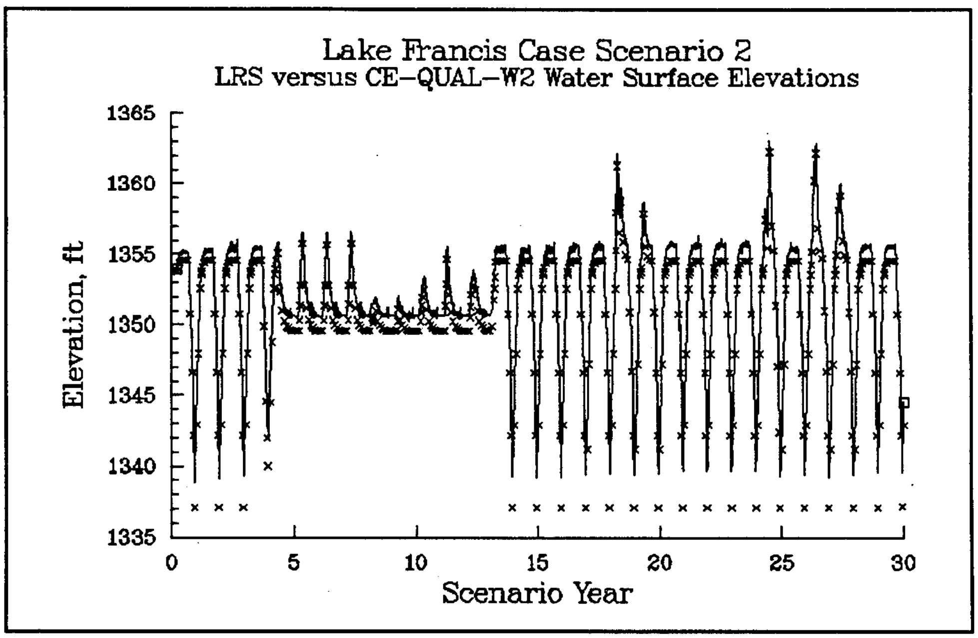

Figure 350. Lake Francis Case LRS versus CE-QUAL-W2 water surface elevations for scenario 2

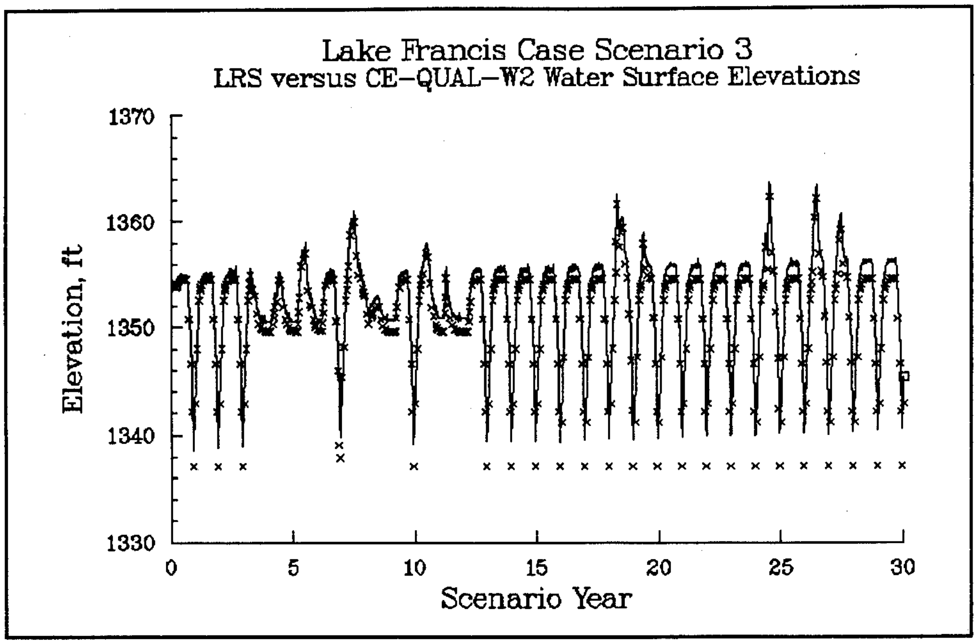

Figure 351. Lake Francis Case LRS versus CE-QUAL-W2 water surface elevations for scenario 3

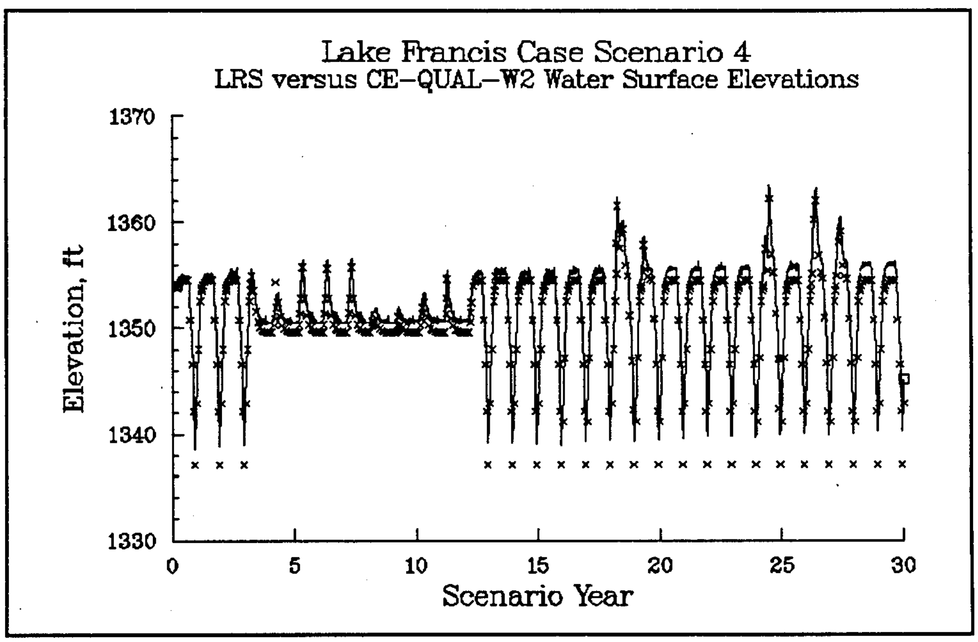

Figure 352. Lake Francis Case LRS versus CE-QUAL-W2 water surface elevations for scenario 4

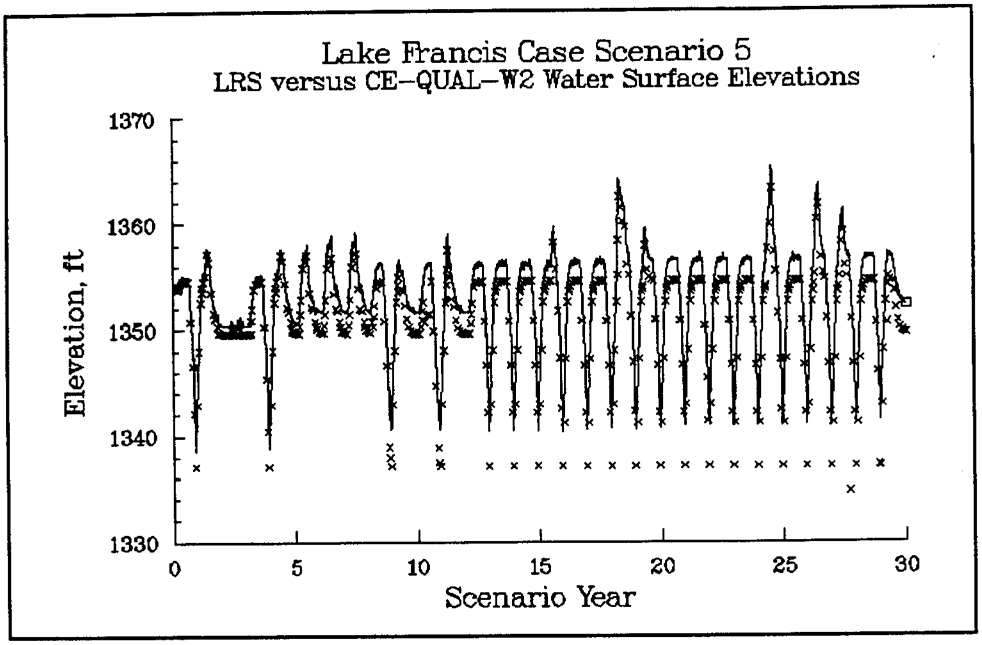

Figure 353. Lake Francis Case LRS versus CE-QUAL-W2 water surface elevations for scenario 5

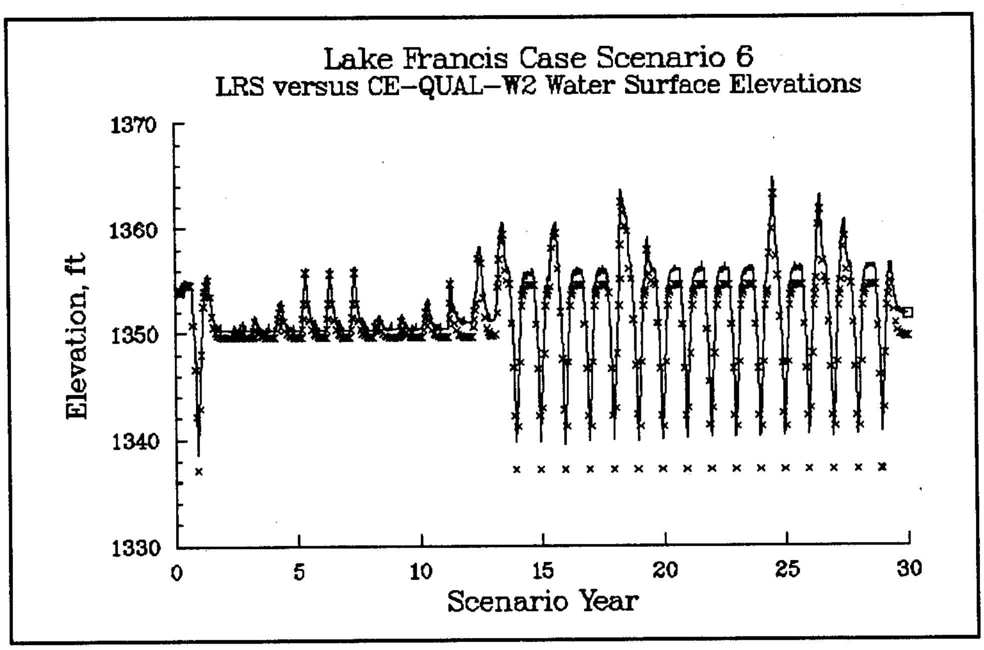

Figure 354. Lake Francis Case LRS versus CE-QUAL-W2 water surface elevations for scenario 6

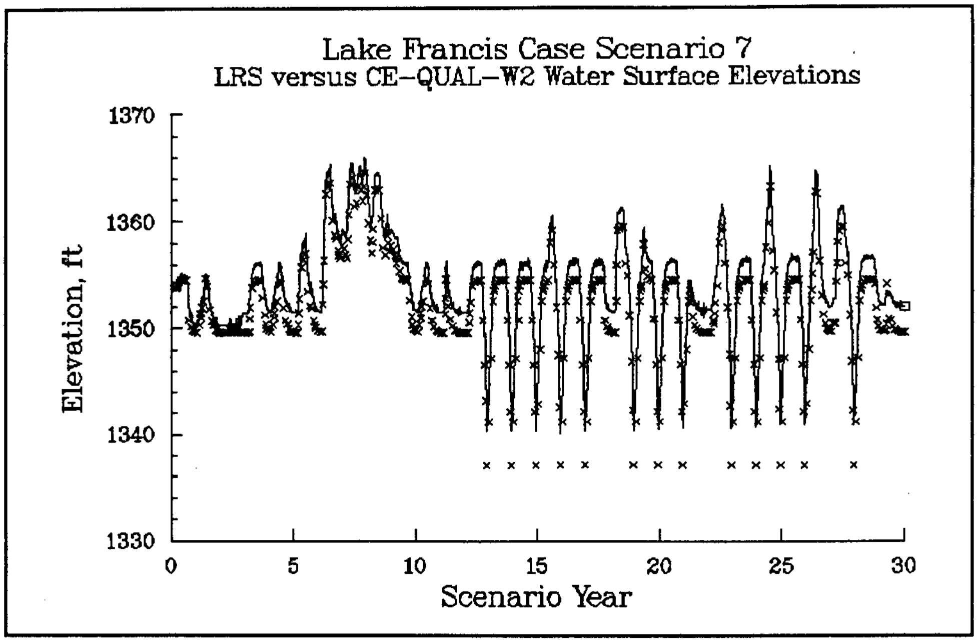

Figure 355. Lake Francis Case LRS versus CE-QUAL-W2 water surface elevations for scenario 7

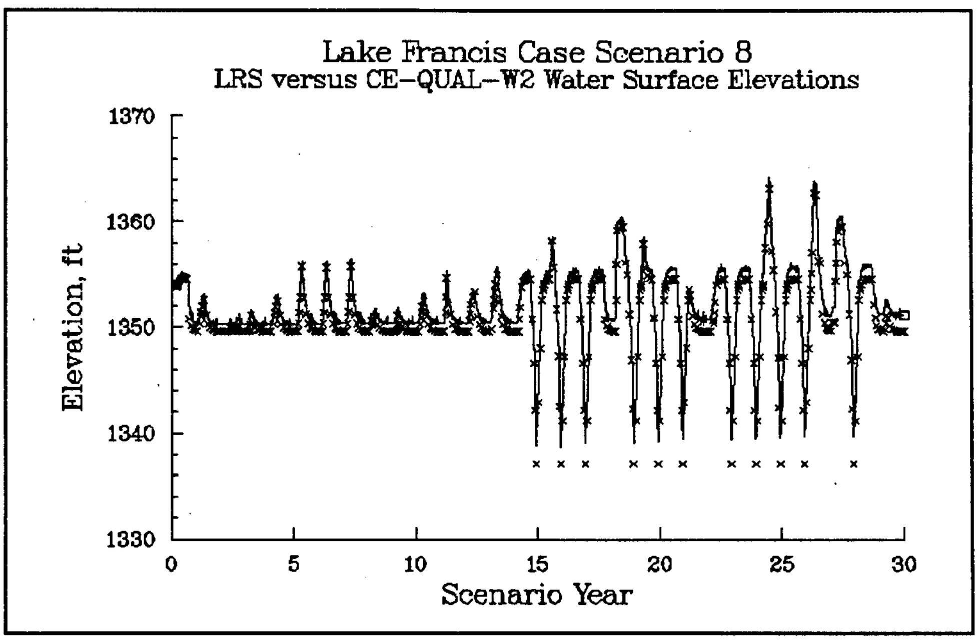

Figure 356. Lake Francis Case LRS versus CE-QUAL-W2 water surface elevations for scenario 8

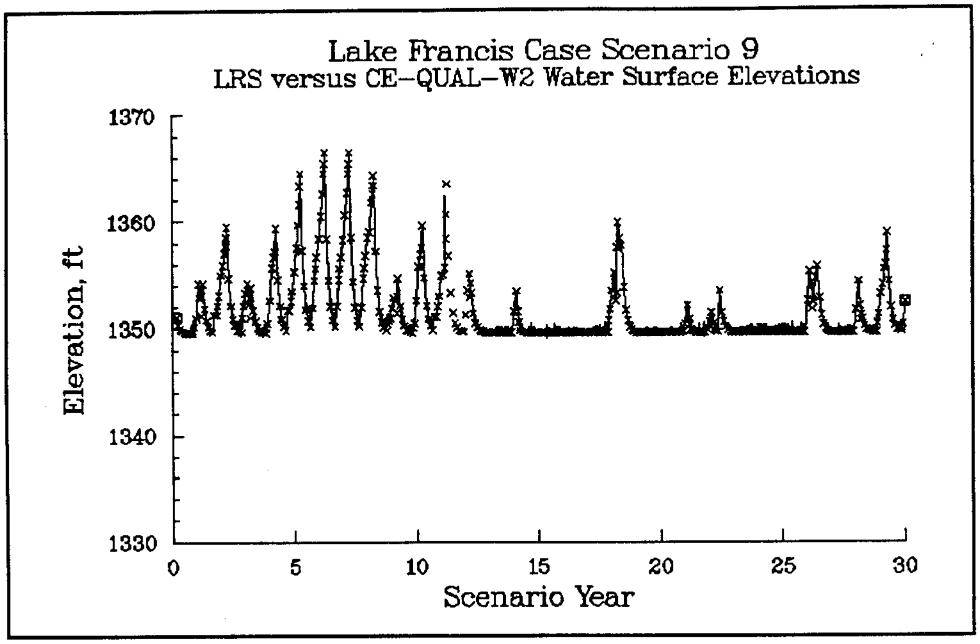

Figure 357. Lake Francis Case LRS versus CE-QUAL-W2 water surface elevations for scenario 9

Release Temperature. Release temperatures for the nine scenarios are given in Figure 358-Figure 366.

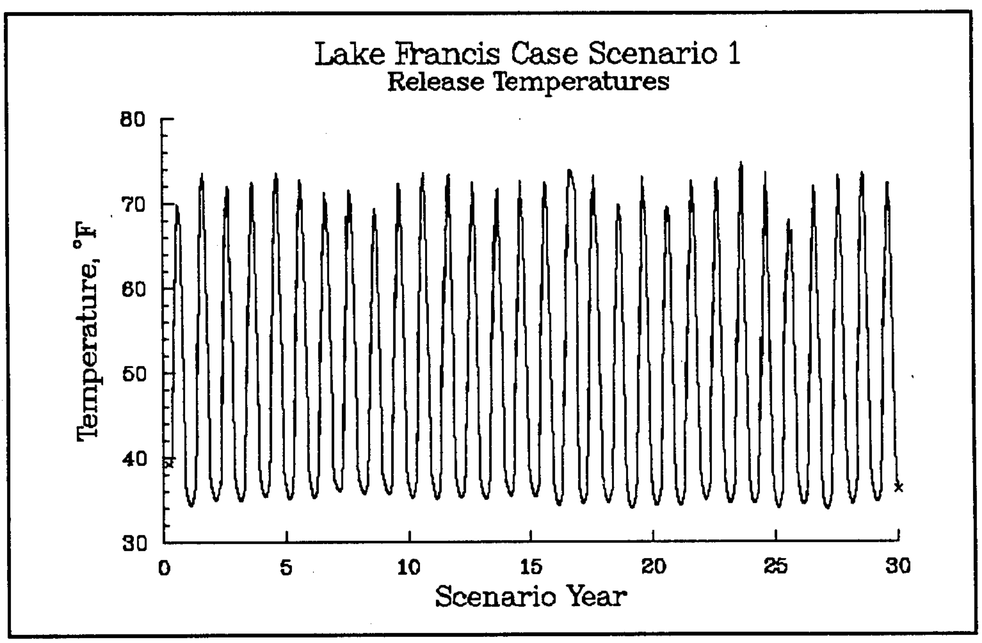

Figure 358. Lake Francis Case release temperatures for scenario 1

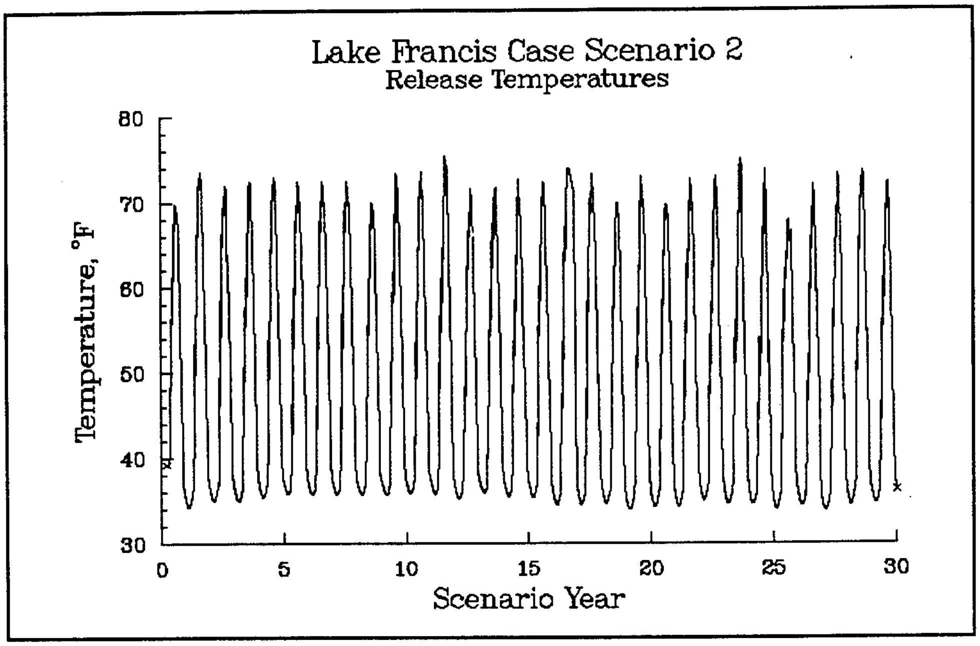

Figure 359. Lake Francis Case release temperatures for scenario 2

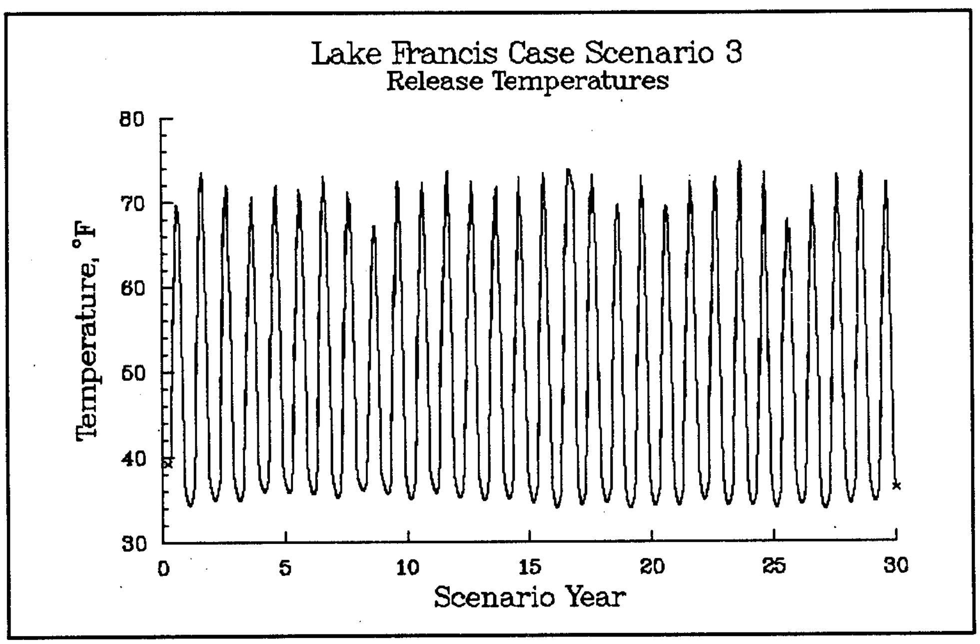

Figure 360. Lake Francis Case release temperatures for scenario 3

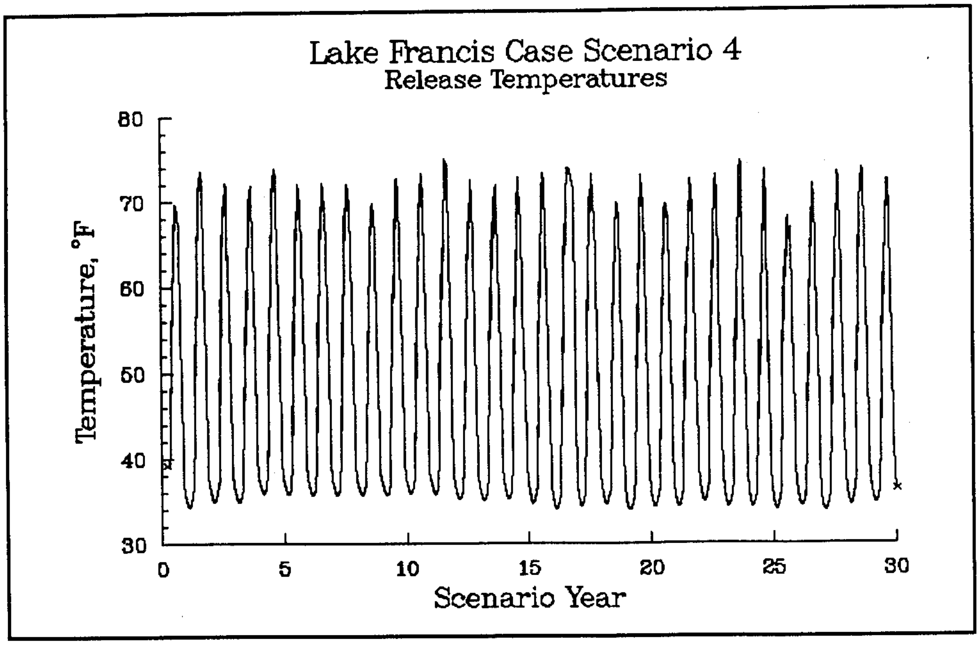

Figure 361. Lake Francis Case release temperatures for scenario 4

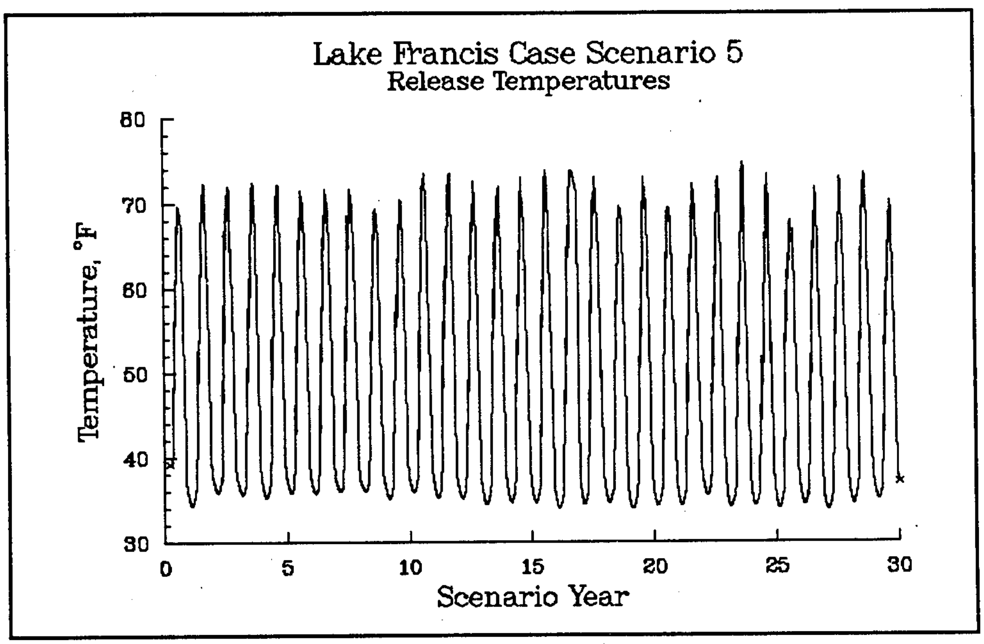

Figure 362. Lake Francis Case release temperatures for scenario 5

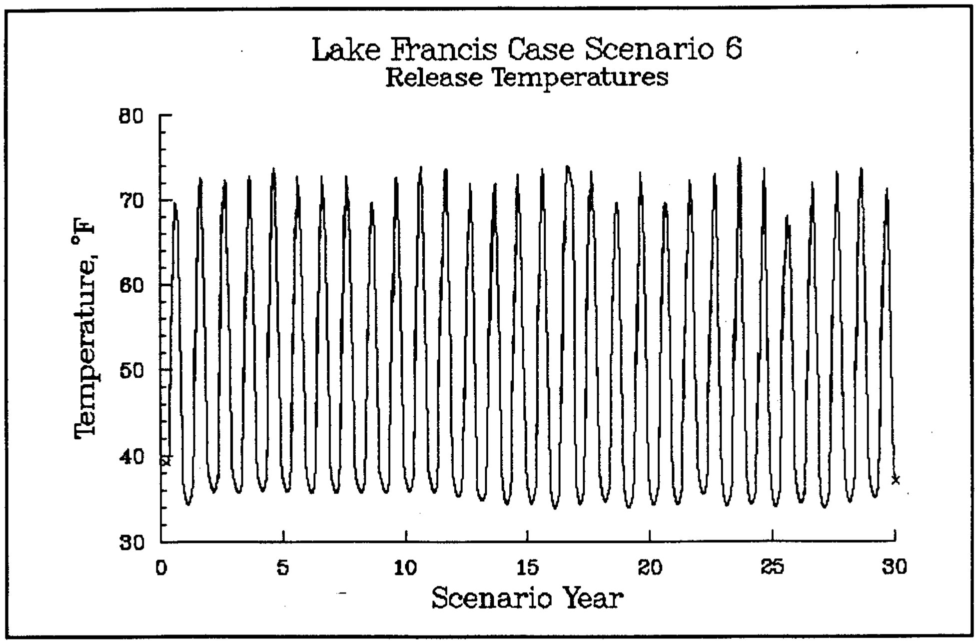

Figure 363. Lake Francis Case release temperatures for scenario 6

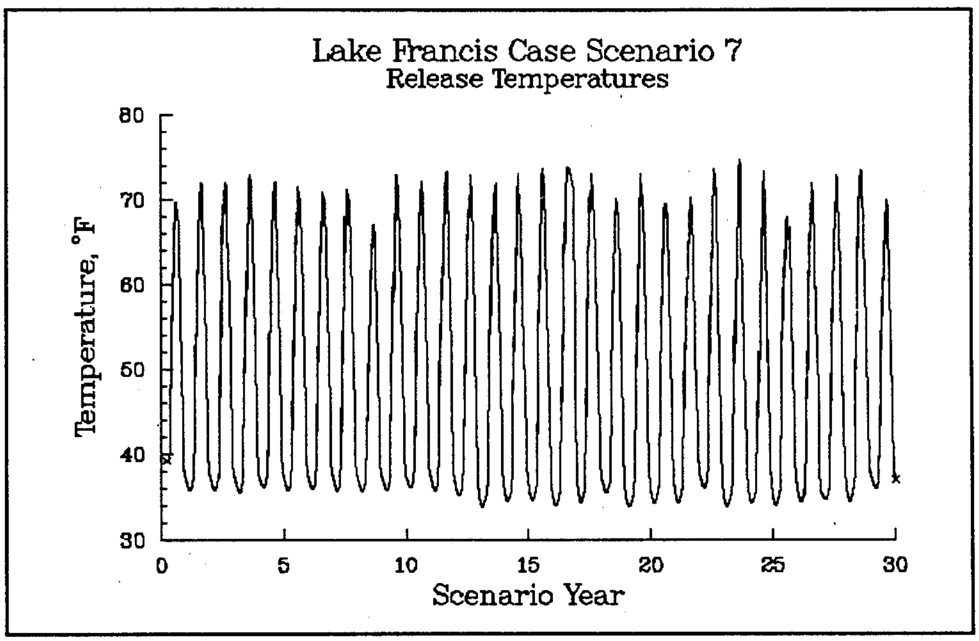

Figure 364. Lake Francis Case release temperatures for scenario 7

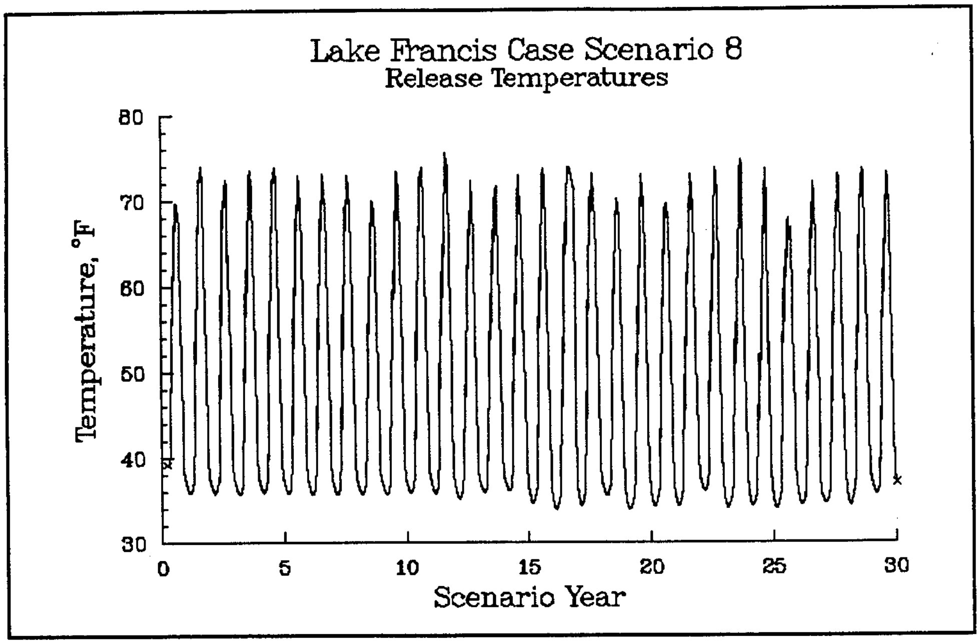

Figure 365. Lake Francis Case release temperatures for scenario 8

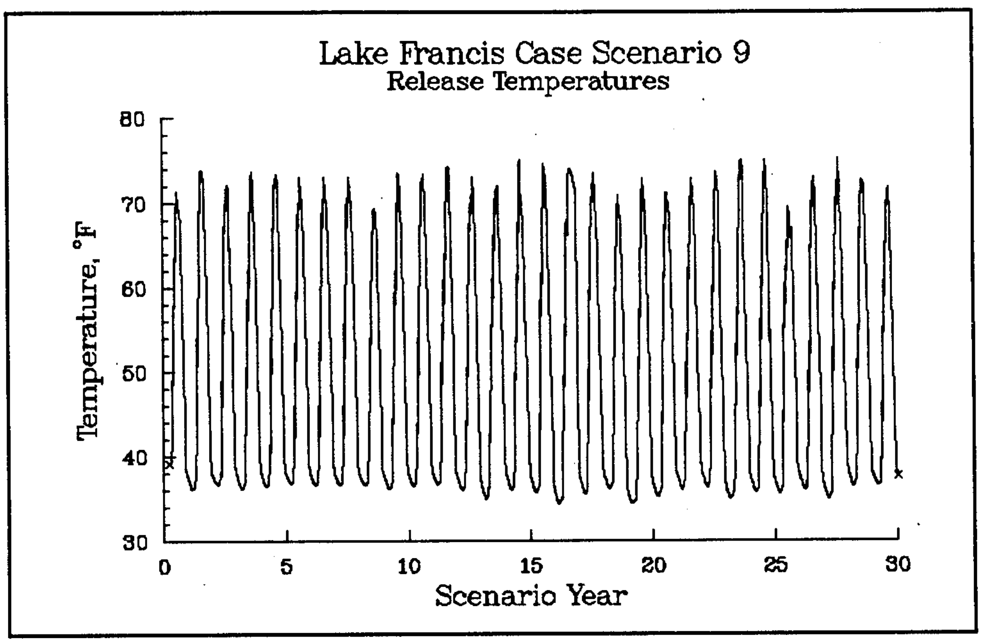

Figure 366. Lake Francis Case release temperatures for scenario 9

Release DO. Release DO concentrations for the nine scenarios are given in Figure 367-Figure 375.

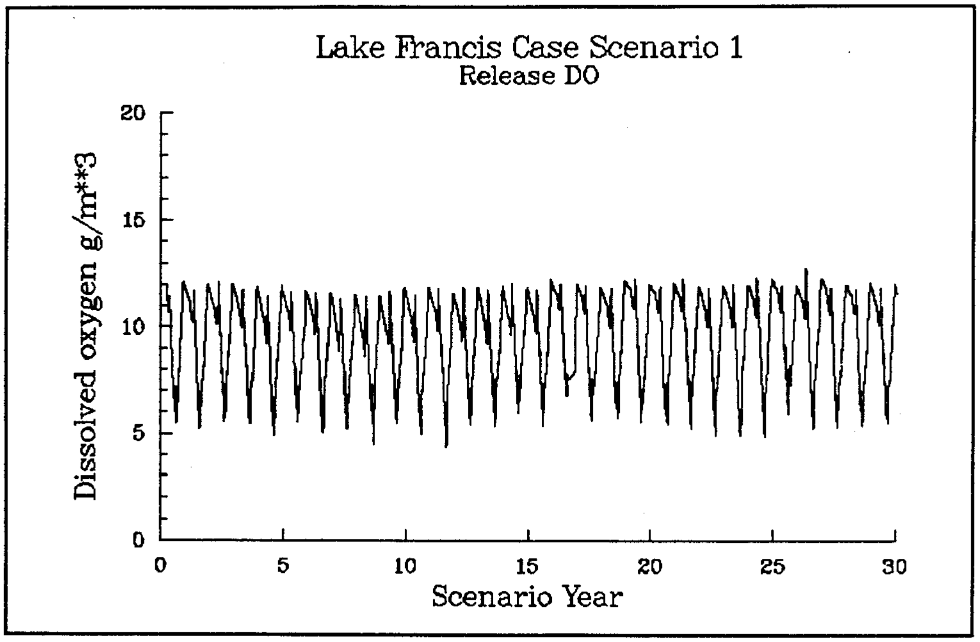

Figure 367. Lake Francis Case release DO for scenario 1

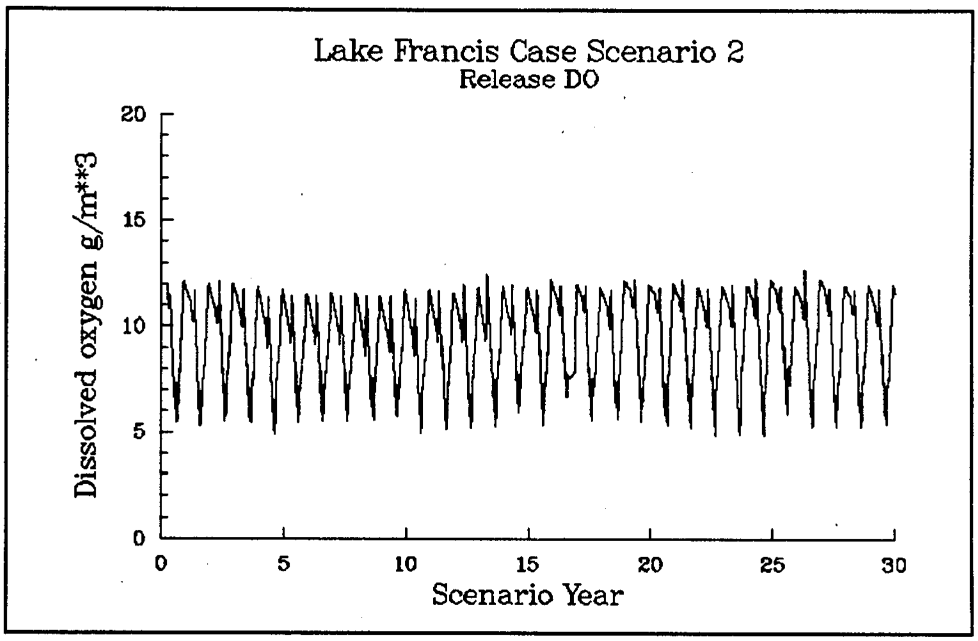

Figure 368. Lake Francis Case release DO for scenario 2

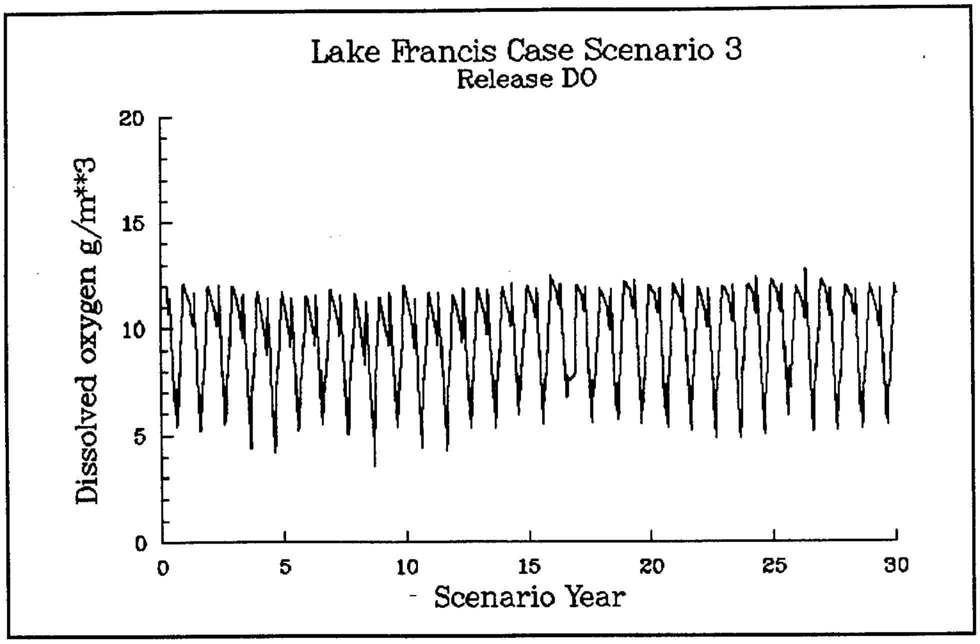

Figure 369. Lake Francis Case release DO for scenario 3

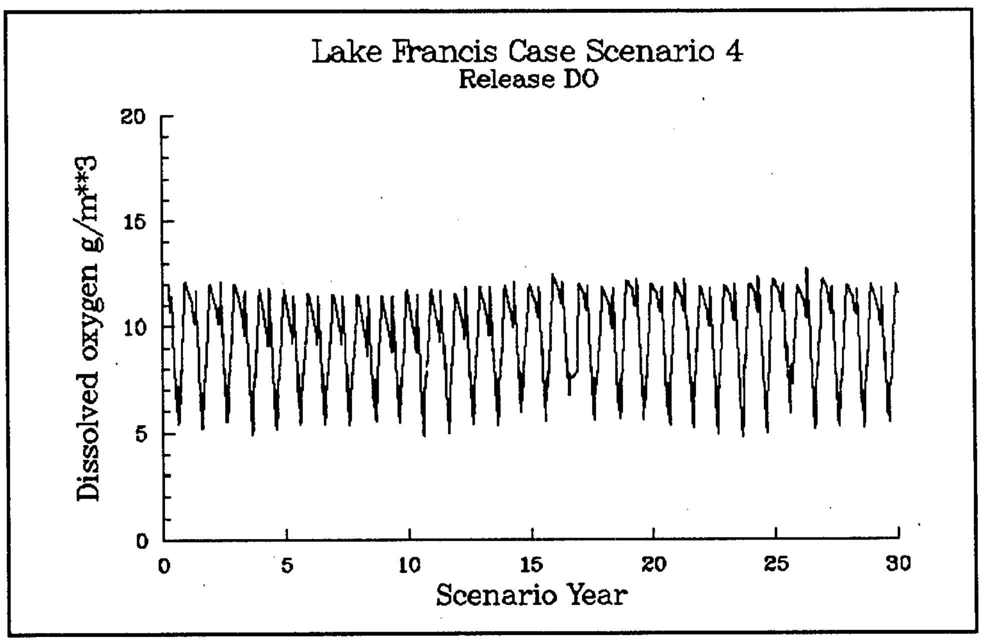

Figure 370. Lake Francis Case release DO for scenario 4

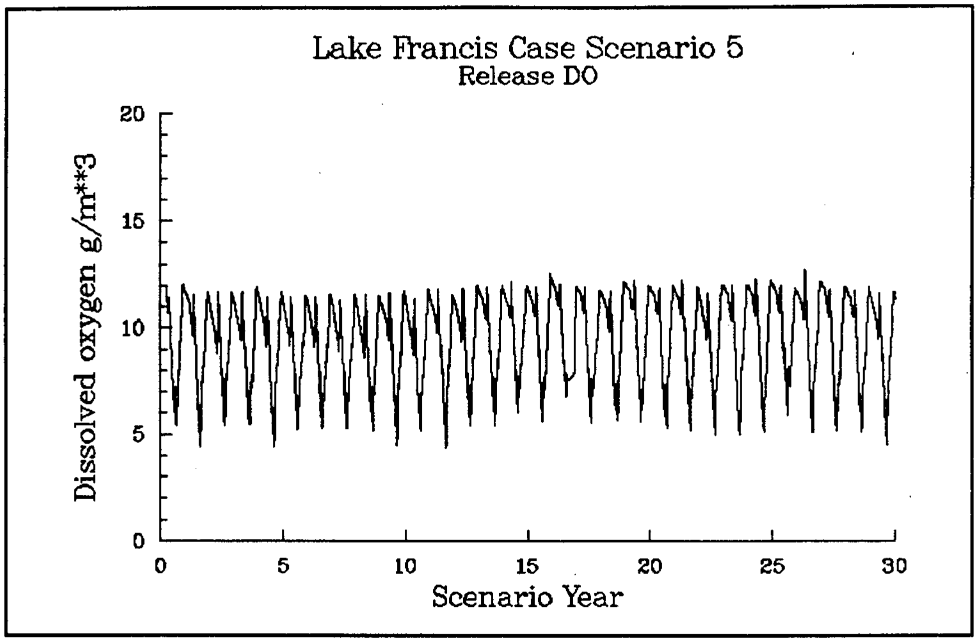

Figure 371. Lake Francis Case release DO for scenario 5

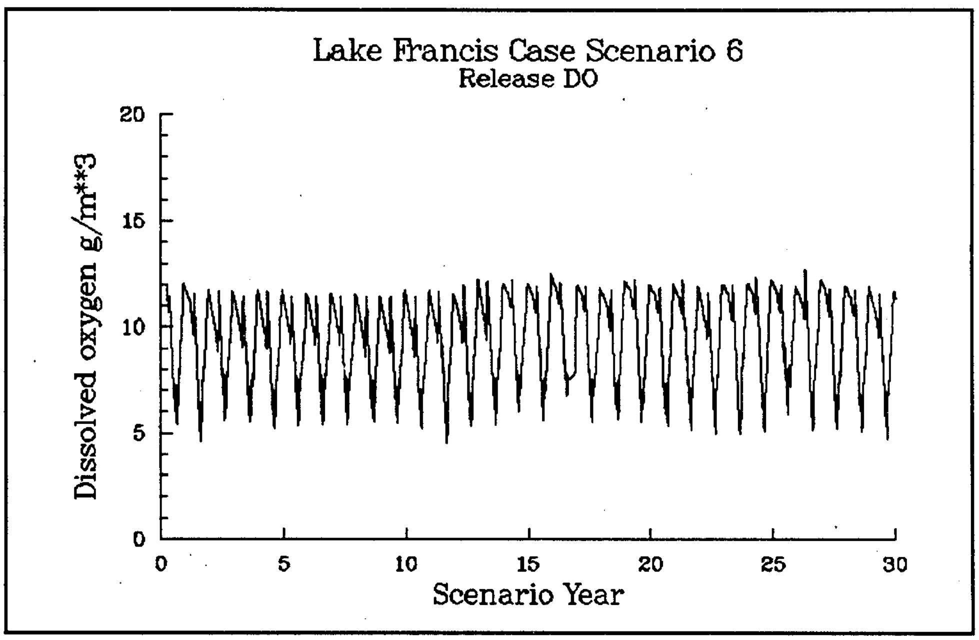

Figure 372. Lake Francis Case release DO for scenario 6

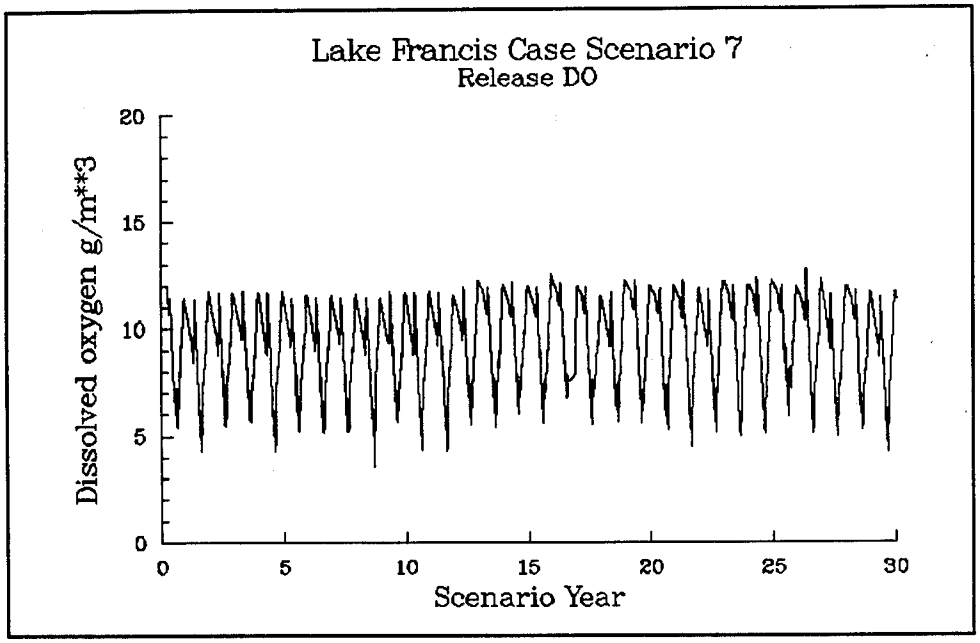

Figure 373. Lake Francis Case release DO for scenario 7

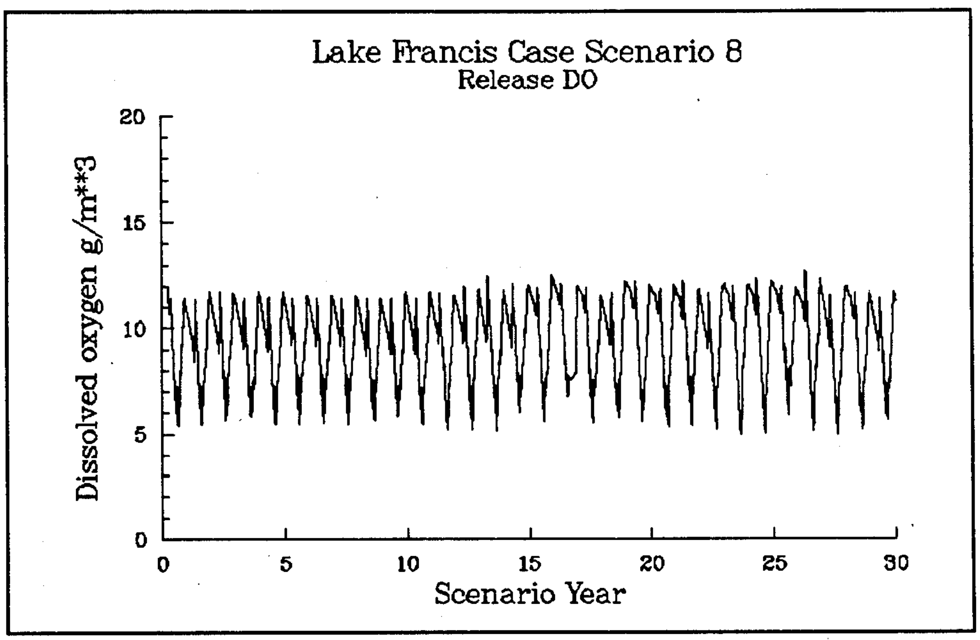

Figure 374. Lake Francis Case release DO for scenario 8

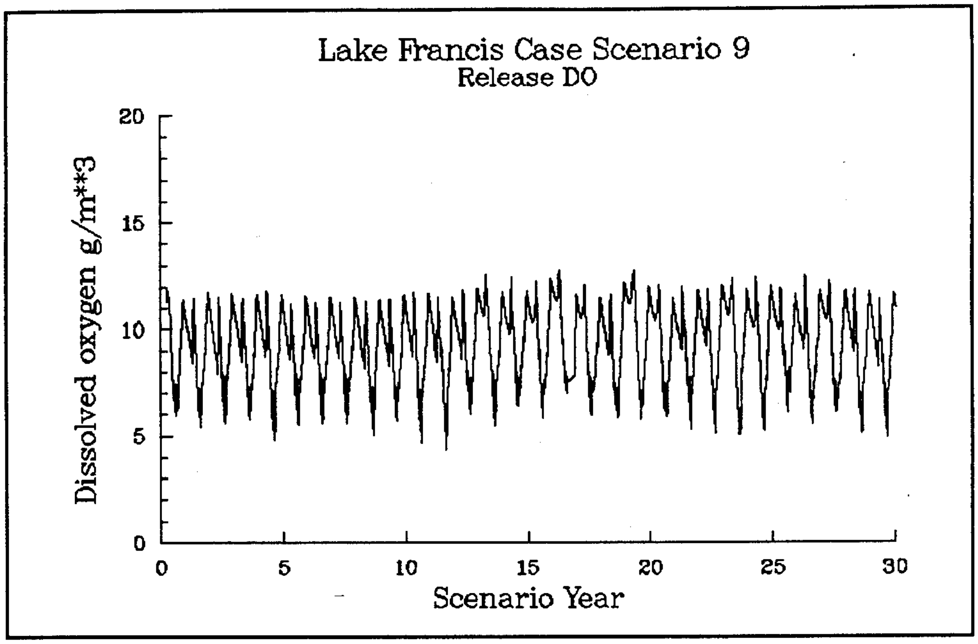

Figure 375. Lake Francis Case release DO for scenario 9

5 Suitable Habitat Regressions

The volume of suitable cold water fish habitat in each reservoir was calculated from reservoir water temperature and dissolved oxygen concentrations generated during the 30 year scenario model runs. Regression equations were then developed for each reservoir and month to correlate the suitable cold water fish habitat to reservoir stage and discharge. Using the SAS statistical analysis software, multiple linear regressions were conducted by month in which suitable habitat was the dependent variable and stage, stage squared, and discharge were the independent variables. Other independent variables were tried including stage cubed and discharge squared but they did not add significantly to the R^2 value. Results were best during the winter months and declined during summer as the water temperatures increased. The poorest correlations usually occurred in October during overturn.

Fort Peck Lake

Regression results are summarized in Table 12. Plots of stage and discharge versus suitable coldwater fish habitat are shown in Figure 376-Figure 387. These plots do not include the stage squared variable that was included in the regressions. However, they do give some insight into how well the regressions are predicting suitable fish habitat. In the figures, the gridded plane is the predicted regression plane and the points represent model predictions of suitable habitat. The vertical lines connected to the points are used to indicate the location above or below and the distance to the regression plane.

Table 12. Fort Peck Lake suitable habitat regression coefficients and statistics

Month	Intercept	Discharge	Stage	$Stage^2$	R^2	Pr > F
January	1.33×10^{14}	3.30×10^{7}	-4.15×10^{11}	3.24×10^{8}	0.998	0.0
February	1.29×10^{14}	4.17×10^{7}	-4.03×10^{11}	3.15×10^{8}	0.997	0.0001
March	1.48×10^{14}	0.84×10^{7}	-4.60×10^{11}	3.56×10^{8}	0.995	0.0001
April	1.47×10^{14}	-8.25×10^{7}	-4.56×10^{11}	3.53×10^{8}	0.716	0.0001
May	1.16×10^{14}	3.21×10^{7}	-3.64×10^{11}	2.86×10^{8}	0.992	0.0001
June	1.43×10^{14}	-1.67×10^{7}	-4.45×10^{11}	3.47×10^{8}	0.995	0.0001
July	2.57×10^{14}	4.33×10^{7}	-7.83×10^{11}	5.96×10^{8}	0.797	0.0001
August	1.11×10^{14}	-6.21×10^{7}	-3.40×10^{11}	2.62×10^{8}	0.894	0.0001
September	1.16×10^{14}	-12.3×10^{7}	-3.54×10^{11}	2.70×10^{8}	0.833	0.0001
October	-1.67×10^{14}	4.06×10^{7}	4.85×10^{11}	-3.52×10^{8}	0.260	0.0001
November	0.91×10^{14}	5.79×10^{7}	-2.91×10^{11}	2.32×10^{8}	0.983	0.0001
December	1.18×10^{14}	4.61×10^{7}	-3.71×10^{11}	2.91×10^{8}	0.999	0.0

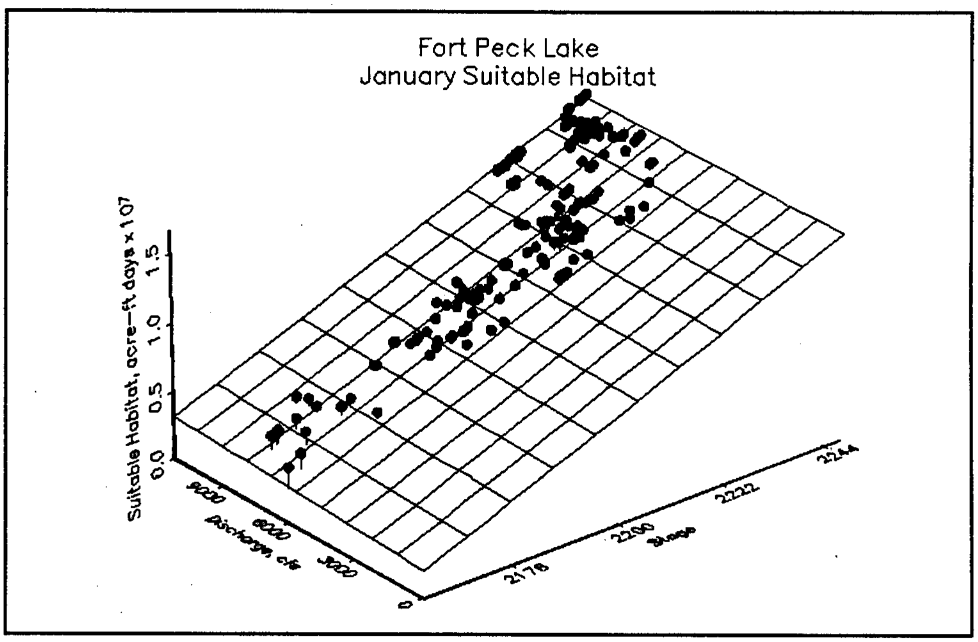

Figure 376. Fort Peck Lake plot of stage-discharge versus suitable habitat for January

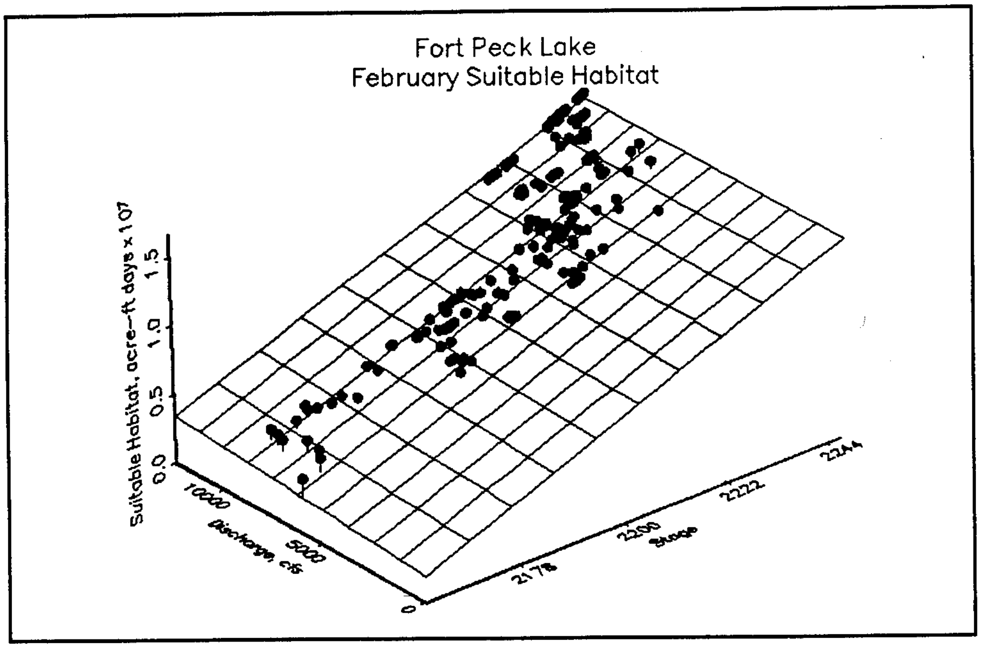

Figure 377. Fort Peck Lake plot of stage-discharge versus suitable habitat for February

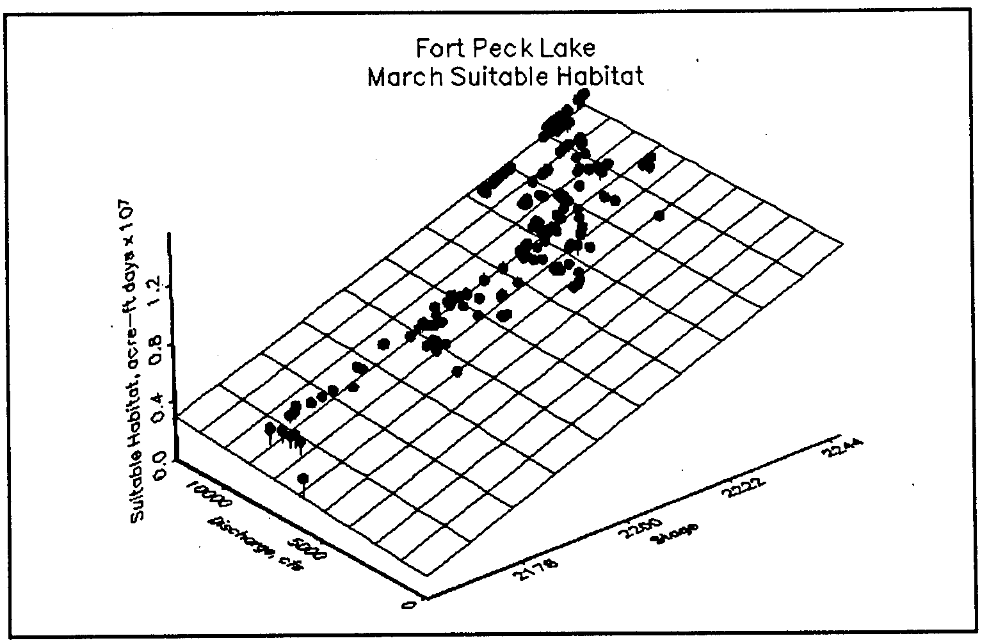

Figure 378. Fort Peck Lake plot of stage-discharge versus suitable habitat for March

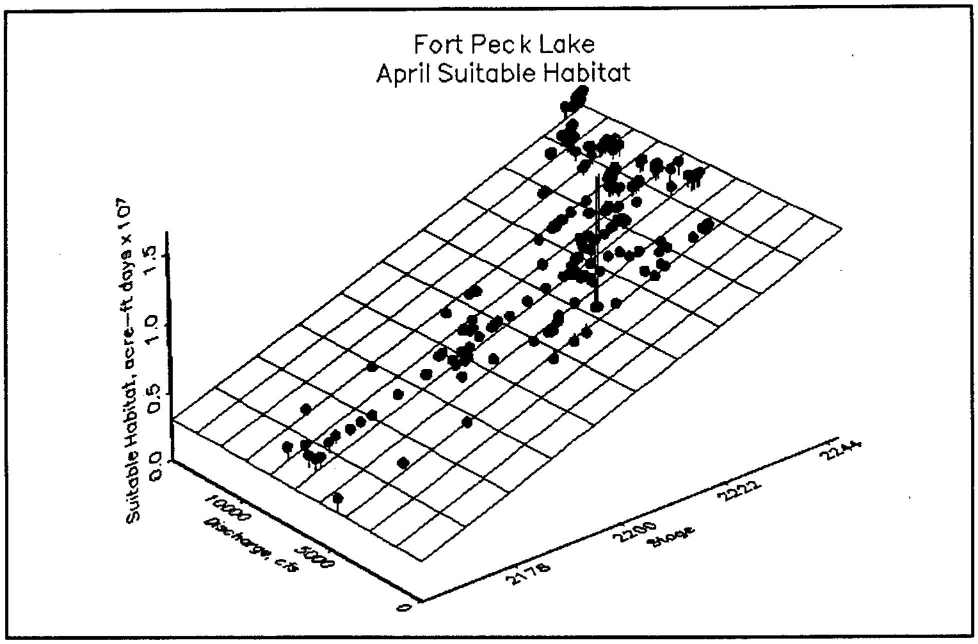

Figure 379. Fort Peck Lake plot of stage-discharge versus suitable habitat for April

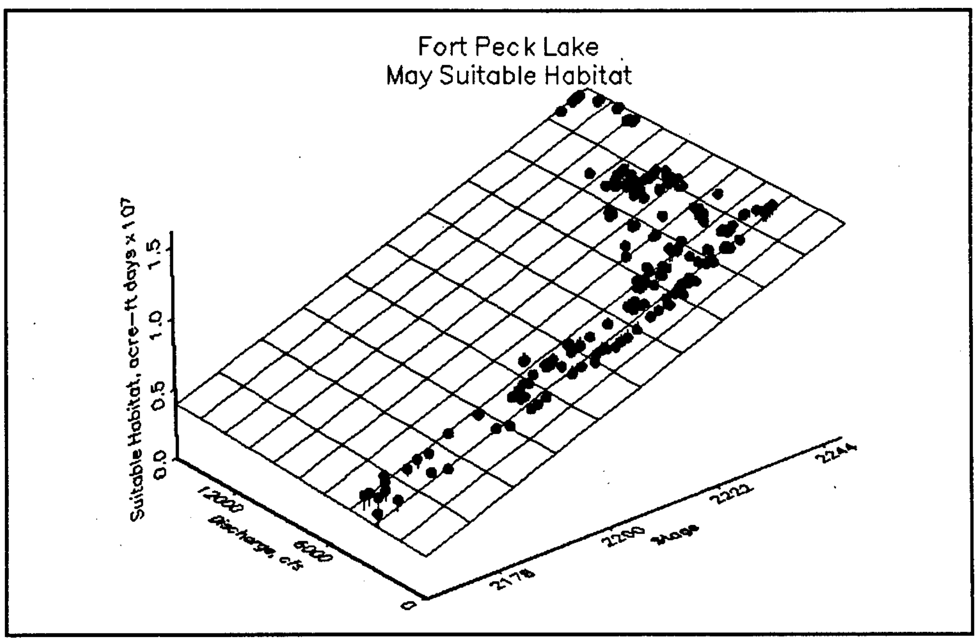

Figure 380. Fort Peck Lake plot of stage-discharge versus suitable habitat for May

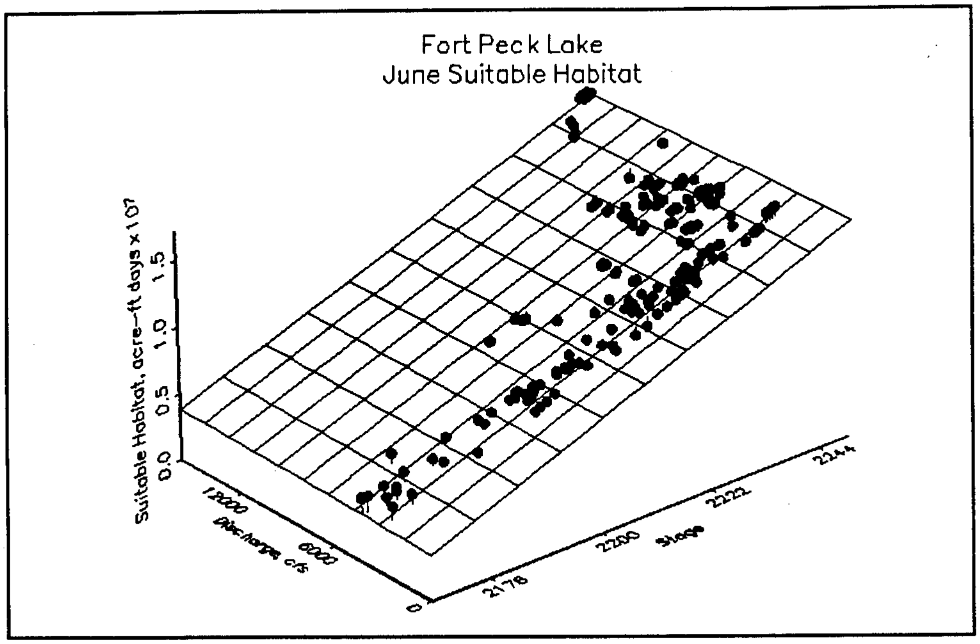

Figure 381. Fort Peck Lake plot of stage-discharge versus suitable habitat for June

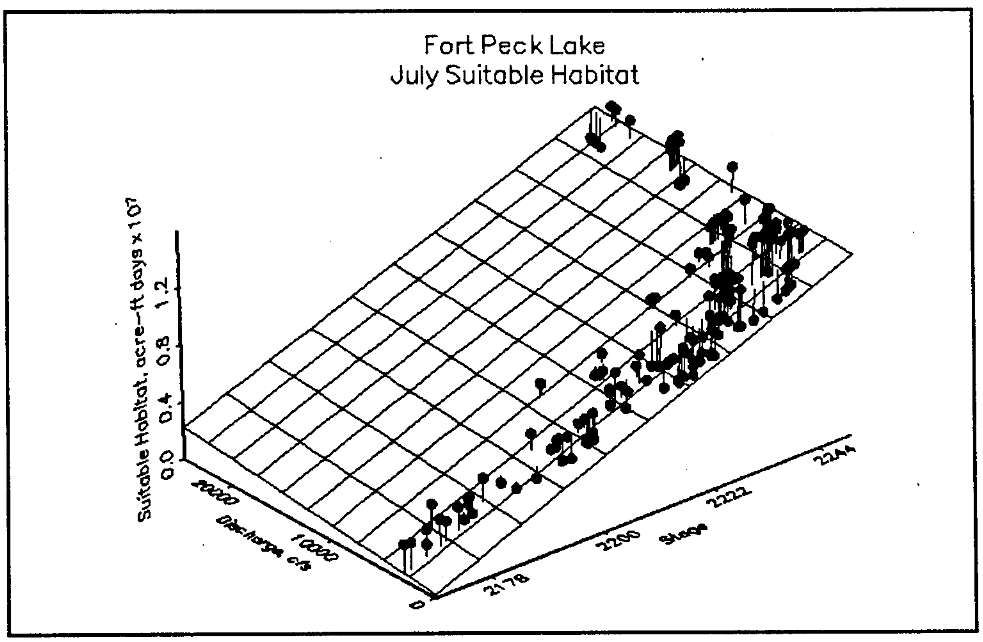

Figure 382. Fort Peck Lake plot of stage-discharge versus suitable habitat for July

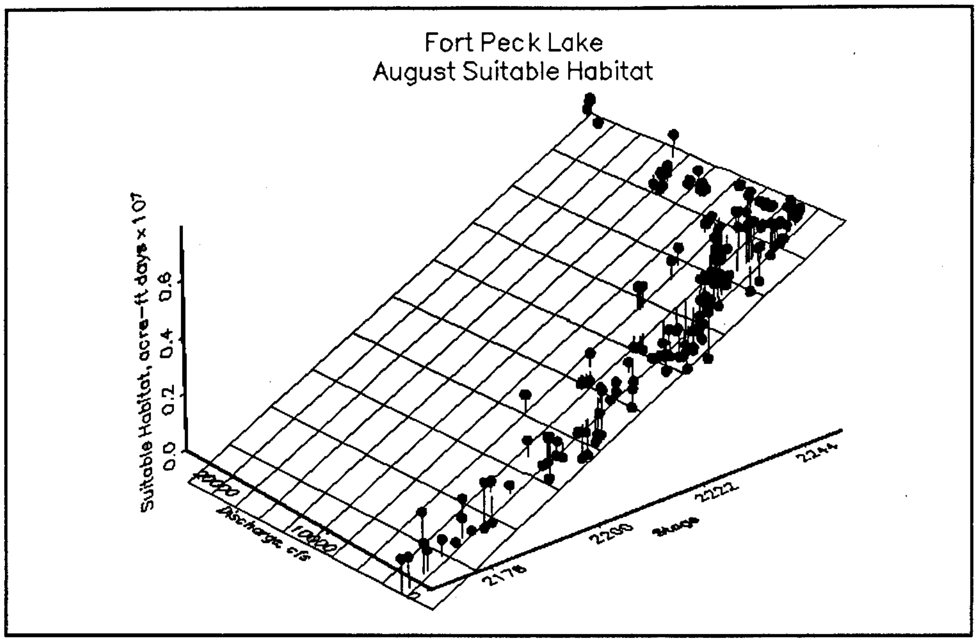

Figure 383. Fort Peck Lake plot of stage-discharge versus suitable habitat for August

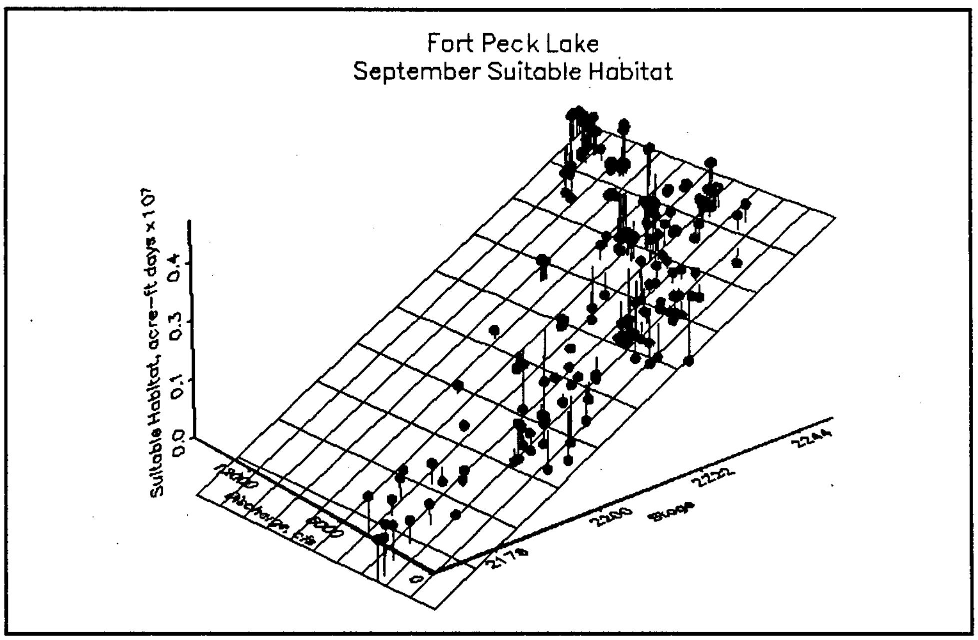

Figure 384. Fort Peck Lake plot of stage-discharge versus suitable habitat for September

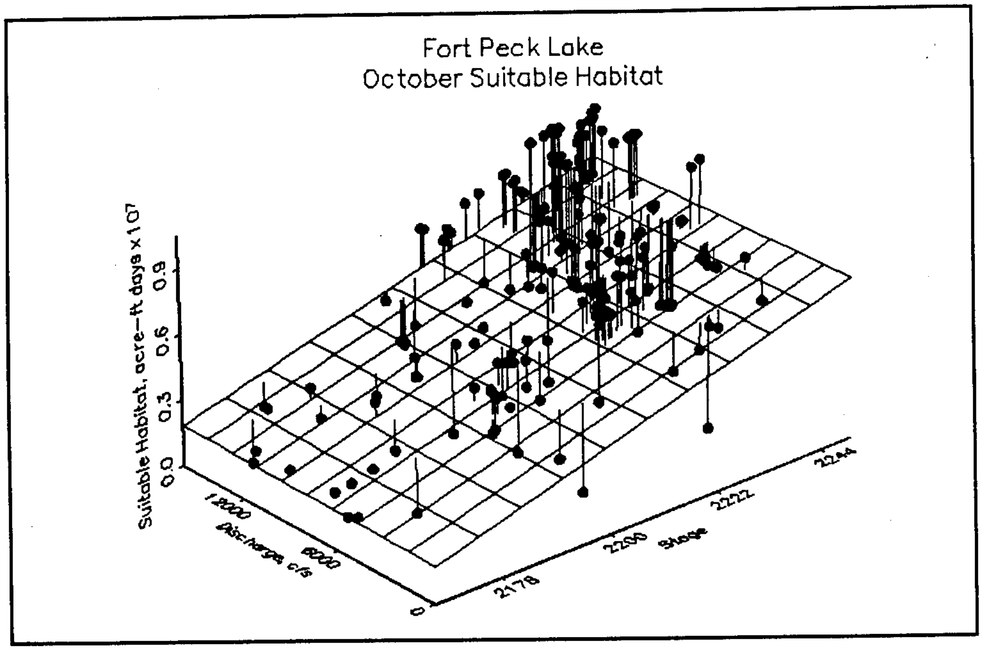

Figure 385. Fort Peck Lake plot of stage-discharge versus suitable habitat for October

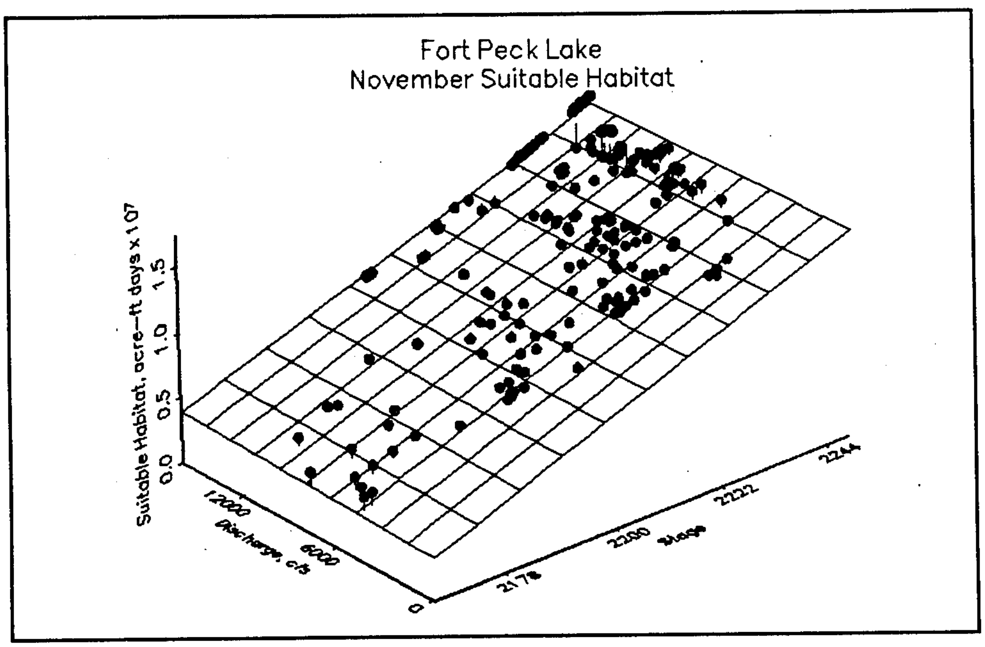

Figure 386. Fort Peck Lake plot of stage-discharge versus suitable habitat for November

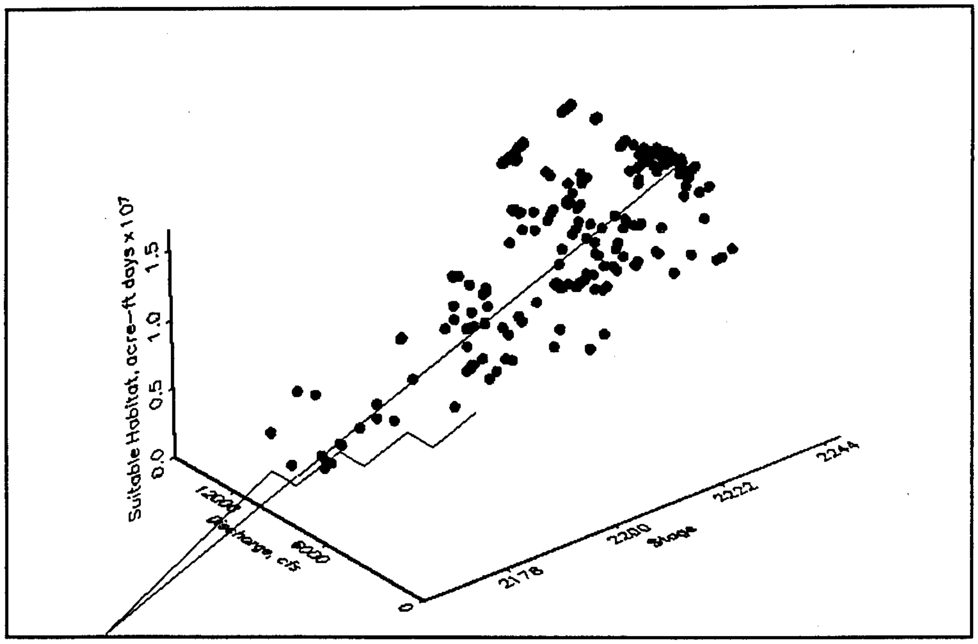

Figure 387. Fort Peck Lake plot of stage-discharge versus suitable habitat for December

Lake Sakakawea

Regression results are summarized in Table 12. Plots of stage and discharge are shown in Figure 388-Figure 399.

Table 13. Lake Sakakawea suitable habitat regression coefficients and statistics

Month	Intercept	Discharge	Stage	Stage^2	R^2	Pr > F
January	1.91×10^{14}	3.72×10^{7}	-7.21×10^{11}	6.81×10^{8}	0.999	0.0
February	1.96×10^{14}	3.50×10^{7}	-7.39×10^{11}	6.97×10^{8}	0.999	0.0
March	2.03×10^{14}	3.16×10^{7}	-7.61×10^{11}	7.14×10^{8}	0.994	0.0001
April	2.18×10^{14}	-3.98×10^{7}	-8.14×10^{11}	7.63×10^{8}	0.667	0.0001
May	1.73×10^{14}	0.32×10^{7}	-6.55×10^{11}	6.20×10^{8}	0.993	0.0001
June	2.20×10^{14}	-0.54×10^{7}	-8.27×10^{11}	7.78×10^{8}	0.990	0.0001
July	5.13×10^{14}	0.02×10^{7}	-10.9×10^{11}	17.2×10^{8}	0.601	0.0001
August	1.95×10^{14}	-3.85×10^{7}	-7.16×10^{11}	6.58×10^{8}	0.839	0.0001
September	1.50×10^{14}	-6.16×10^{7}	-3.54×10^{11}	2.70×10^{8}	0.833	0.0001
October	1.06×10^{14}	0.61×10^{7}	-3.91×10^{11}	3.60×10^{8}	0.243	0.0001
November	1.45×10^{14}	2.12×10^{7}	-5.53×10^{11}	5.27×10^{8}	0.927	0.0001
December	1.91×10^{14}	2.49×10^{7}	-7.20×10^{11}	6.79×10^{8}	0.998	0.0

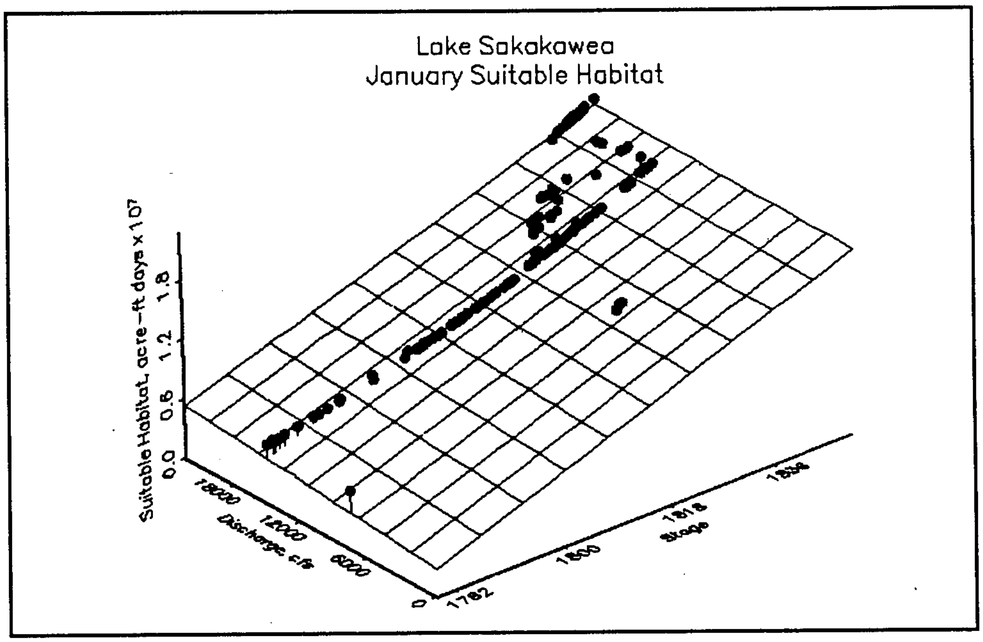

Figure 388. Lake Sakakawea plot of stage-discharge versus suitable habitat for January

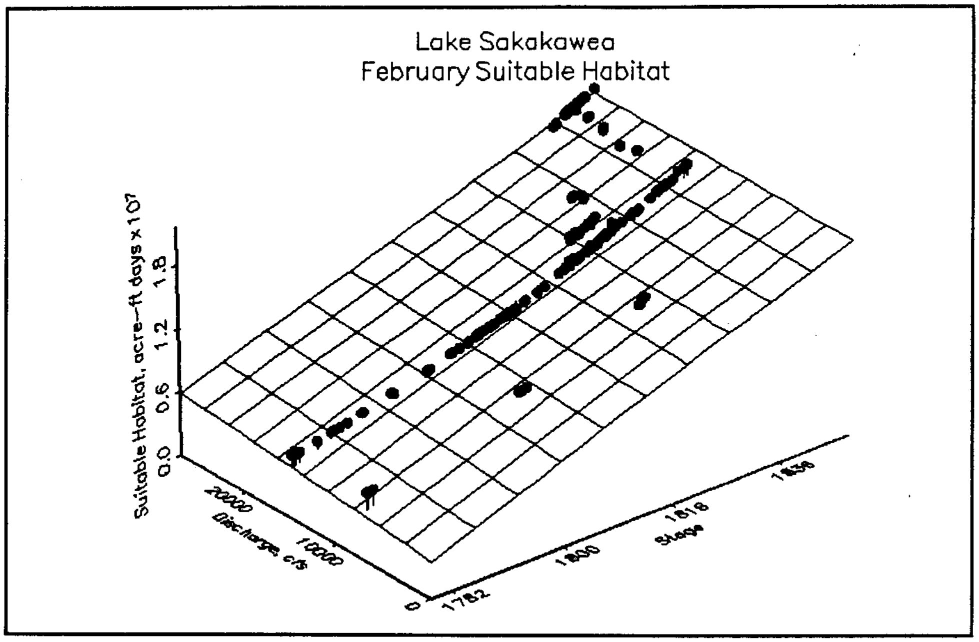

Figure 389. Lake Sakakawea plot of stage-discharge versus suitable habitat for February

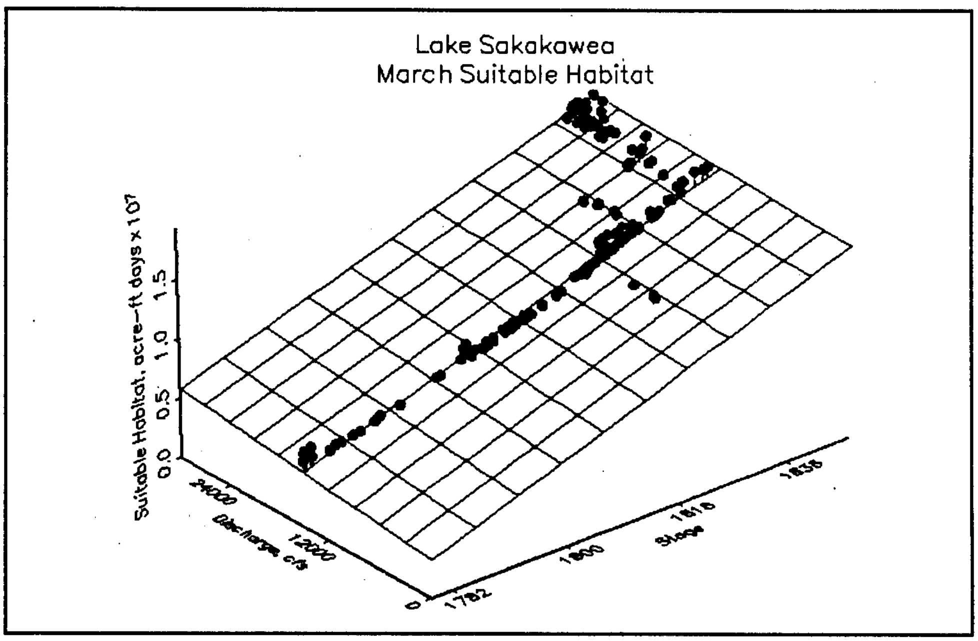

Figure 390. Lake Sakakawea plot of stage-discharge versus suitable habitat for March

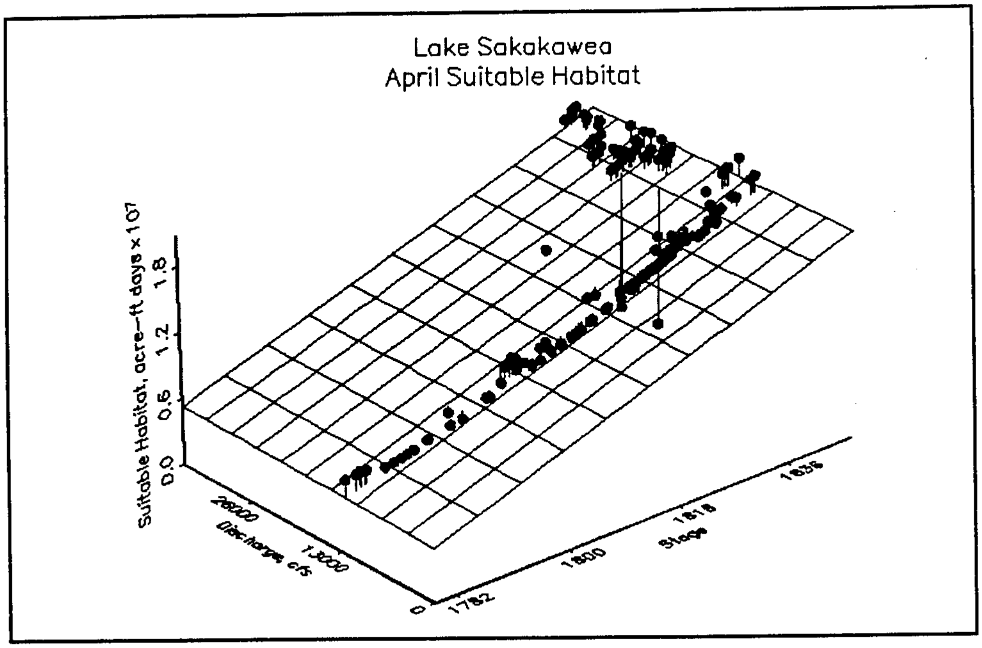

Figure 391. Lake Sakakawea plot of stage-discharge versus suitable habitat for April

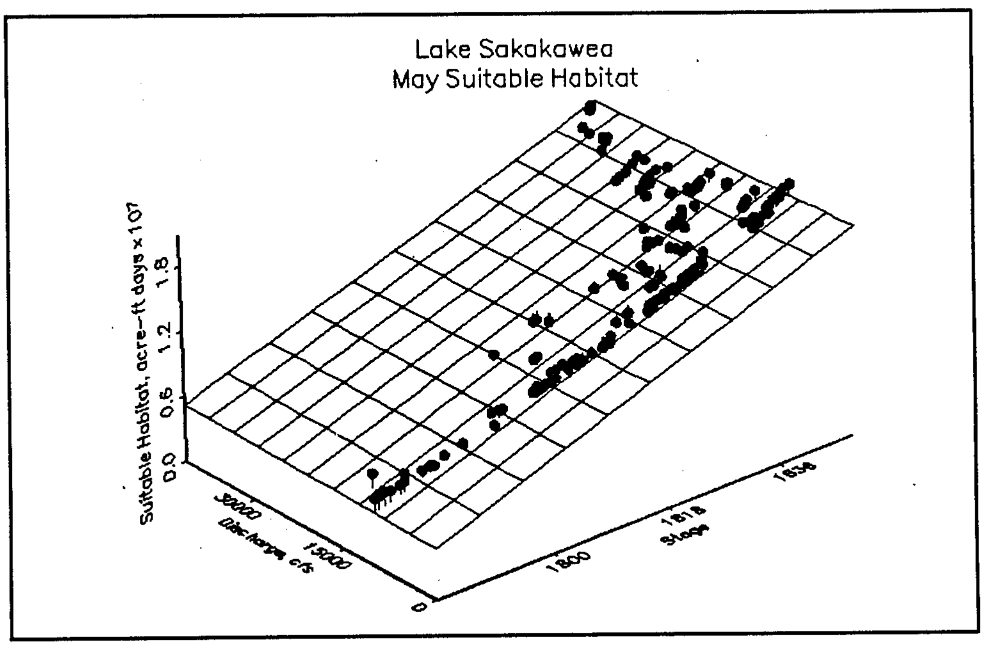

Figure 392. Lake Sakakawea plot of stage-discharge versus suitable habitat for May

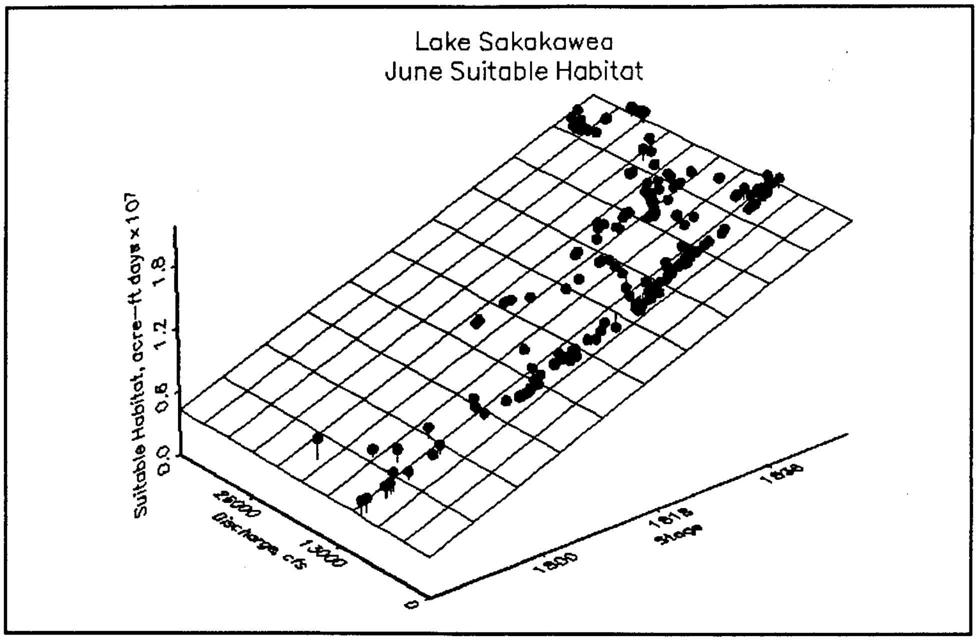

Figure 393. Lake Sakakawea plot of stage-discharge versus suitable habitat for June

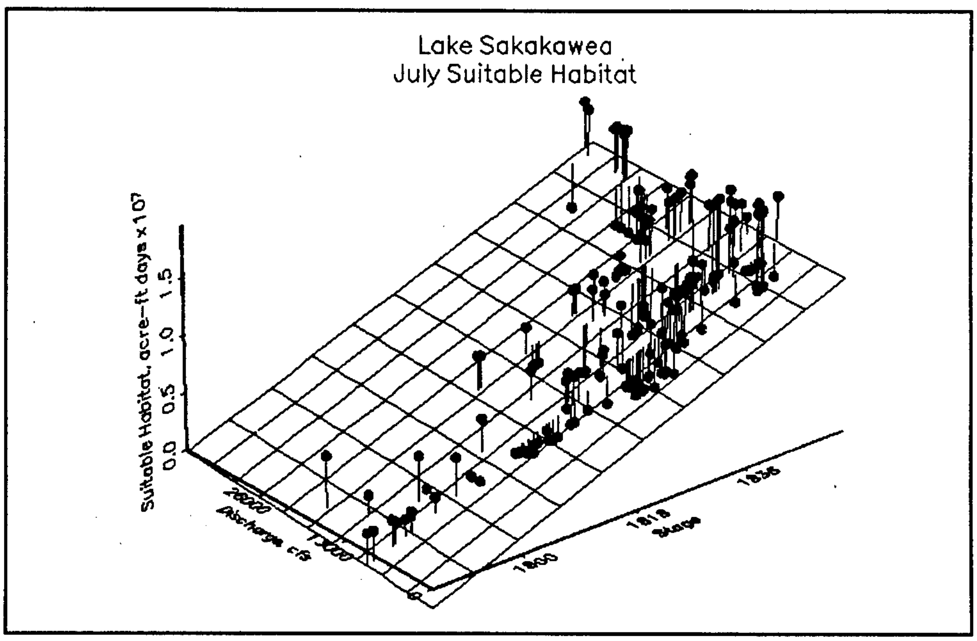

Figure 394. Lake Sakakawea plot of stage-discharge versus suitable habitat for July

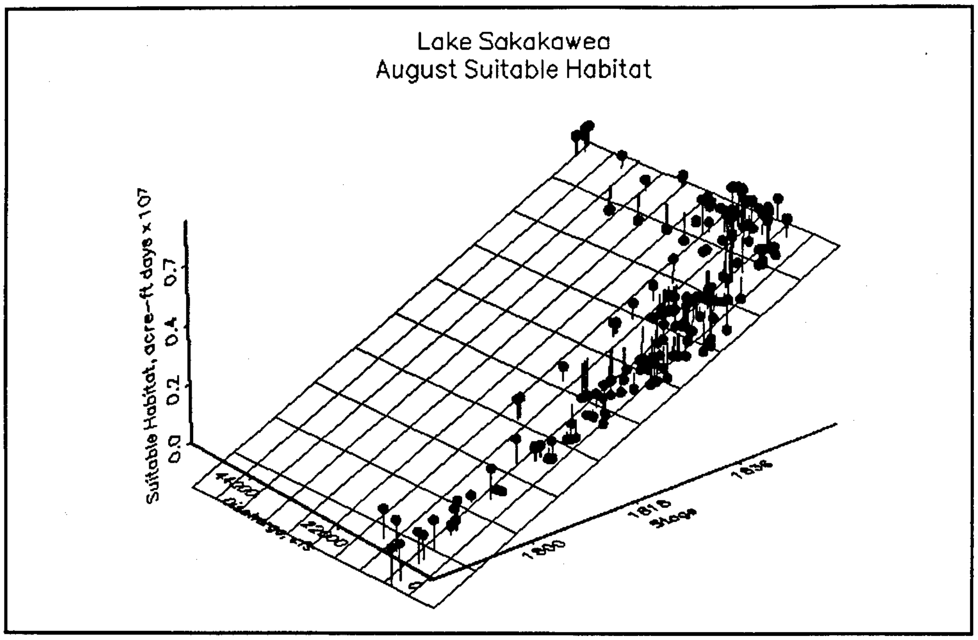

Figure 395. Lake Sakakawea plot of stage-discharge versus suitable habitat for August

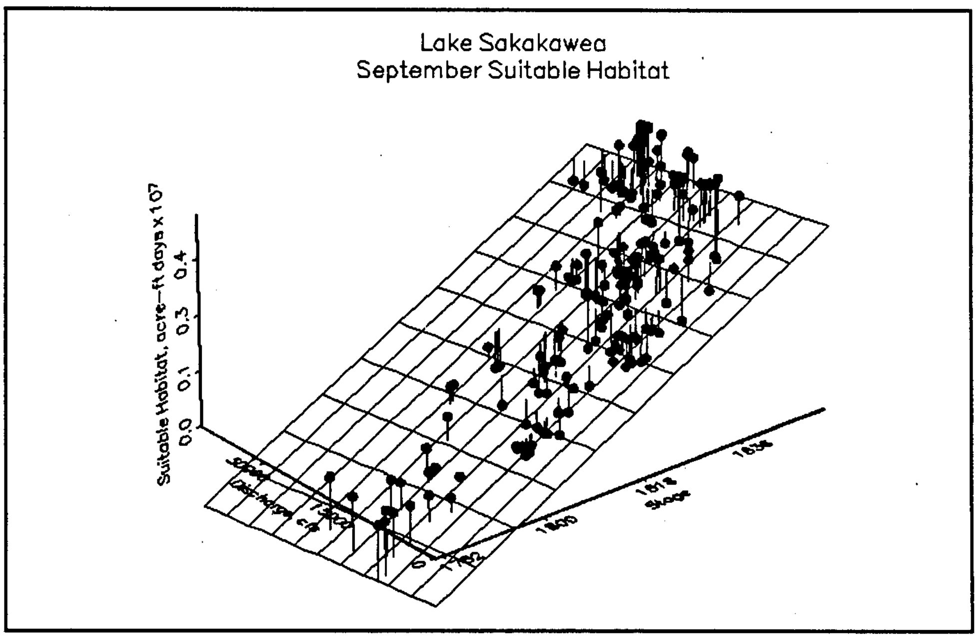

Figure 396. Lake Sakakawea plot of stage-discharge versus suitable habitat for September

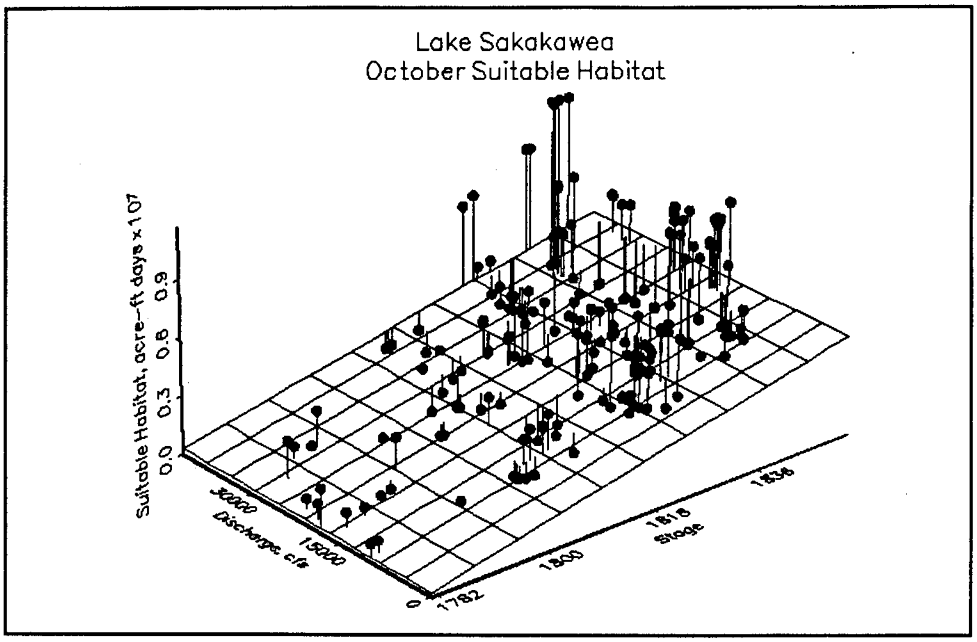

Figure 397. Lake Sakakawea plot of stage-discharge versus suitable habitat for October

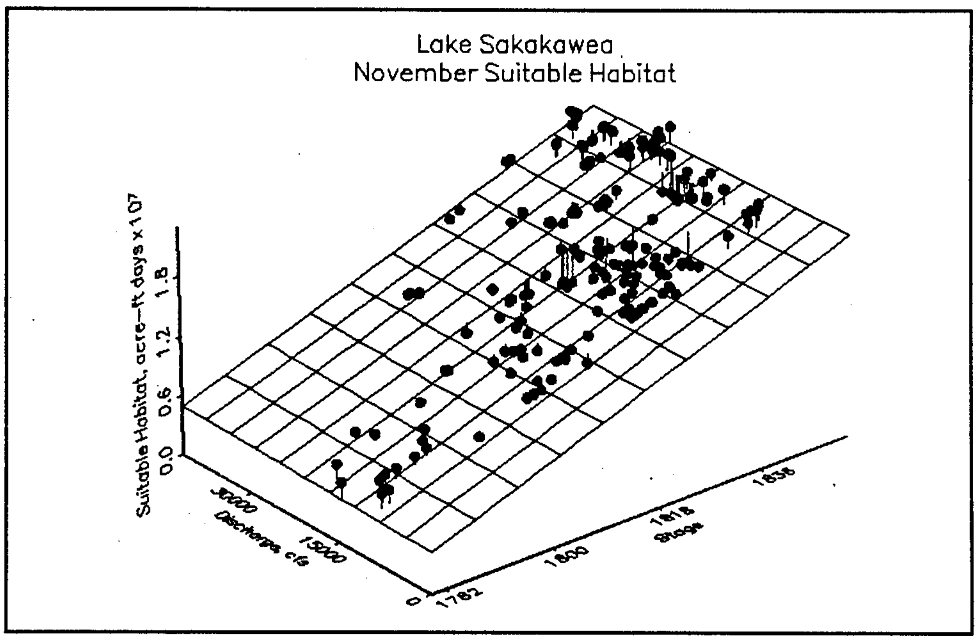

Figure 398. Lake Sakakawea plot of stage-discharge versus suitable habitat for November

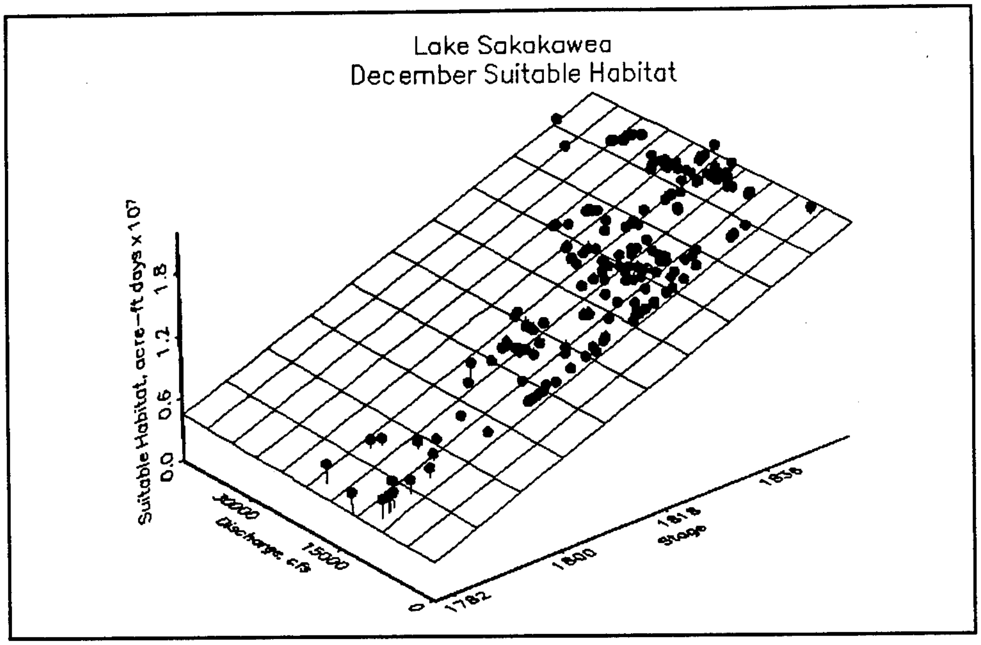

Figure 399. Lake Sakakawea plot of stage-discharge versus suitable habitat for December

Lake Oahe

Regression results are summarized in Table 14. Plots of stage and discharge versus suitable habitat are given in Figure 400-Figure 411.

Table 14. Lake Oahe suitable habitat regression coefficients and statistics

Month	Intercept	Discharge	Stage	$Stage^2$	R^2	Pr > F
January	2.36×10^{14}	3.17×10^{7}	-10.0×10^{11}	10.7×10^{8}	0.989	0.0001
February	2.33×10^{14}	1.73×10^{7}	-9.89×10^{11}	10.5×10^{8}	0.986	0.0001
March	2.14×10^{14}	1.74×10^{7}	-9.09×10^{11}	9.68×10^{8}	0.982	0.0001
April	2.07×10^{14}	-14.1×10^{7}	-8.82×10^{11}	9.41×10^{8}	0.618	0.0001
May	0.40×10^{14}	2.61×10^{7}	-1.94×10^{11}	2.32×10^{8}	0.852	0.0001
June	1.47×10^{14}	5.16×10^{7}	-6.40×10^{11}	6.96×10^{8}	0.935	0.0001
July	2.01×10^{14}	2.90×10^{7}	-8.47×10^{11}	8.95×10^{8}	0.581	0.0001
August	0.71×10^{14}	1.50×10^{7}	-3.05×10^{11}	3.28×10^{8}	0.738	0.0001
September	0.45×10^{14}	0.91×10^{7}	-1.93×10^{11}	2.08×10^{8}	0.681	0.0001
October	0.21×10^{14}	4.49×10^{7}	-0.94×10^{11}	1.05×10^{8}	0.546	0.0001
November	0.58×10^{14}	3.02×10^{7}	-2.64×10^{11}	2.99×10^{8}	0.421	0.0001
December	1.82×10^{14}	-1.02×10^{7}	-7.84×10^{11}	8.43×10^{8}	0.616	0.0001

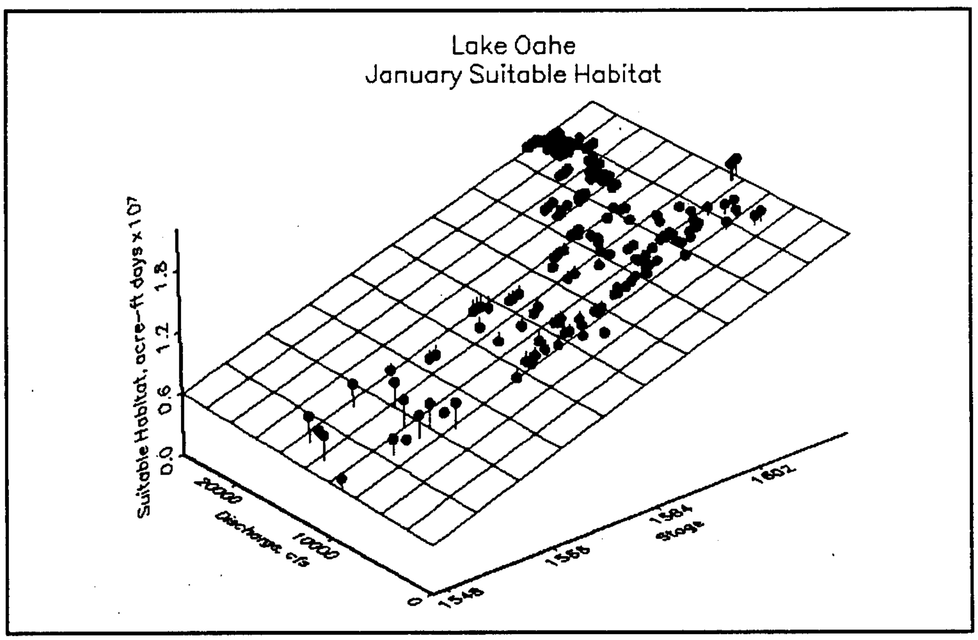

Figure 400. Lake Oahe plot of stage-discharge versus suitable habitat for January

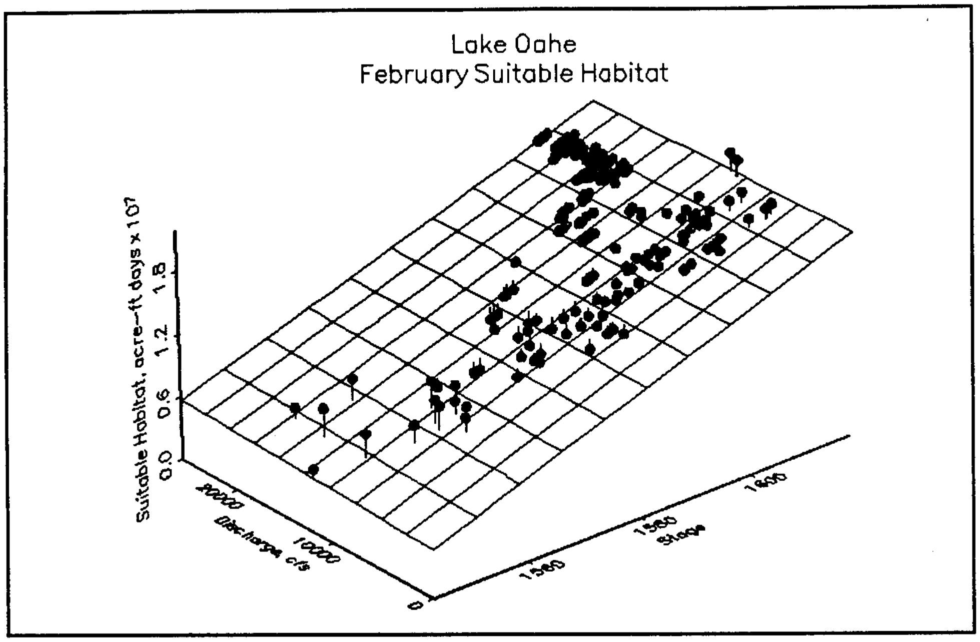

Figure 401. Lake Oahe plot of stage-discharge versus suitable habitat for February

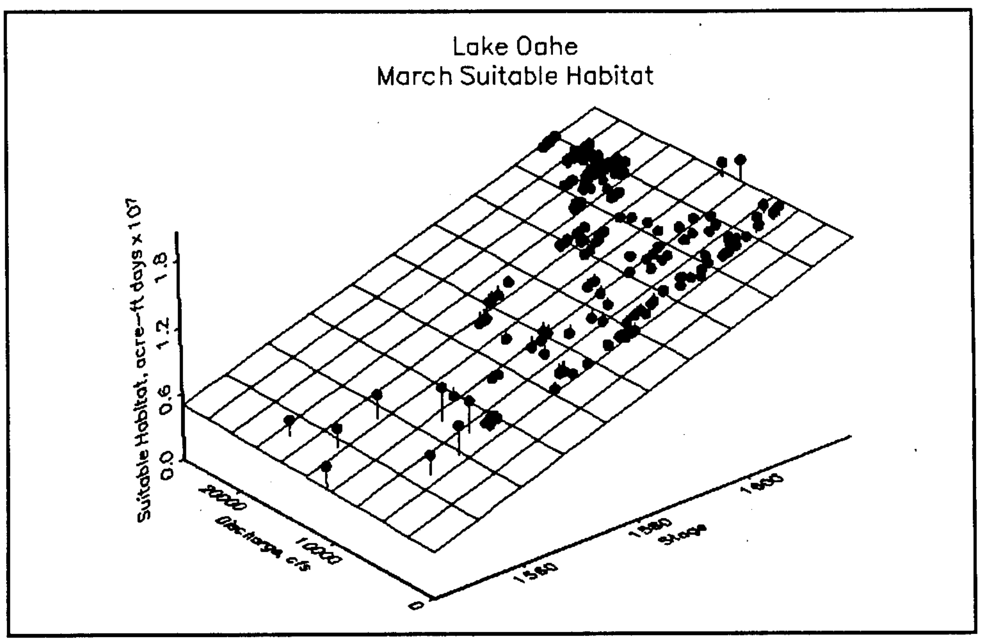

Figure 402. Lake Oahe plot of stage-discharge versus suitable habitat for March

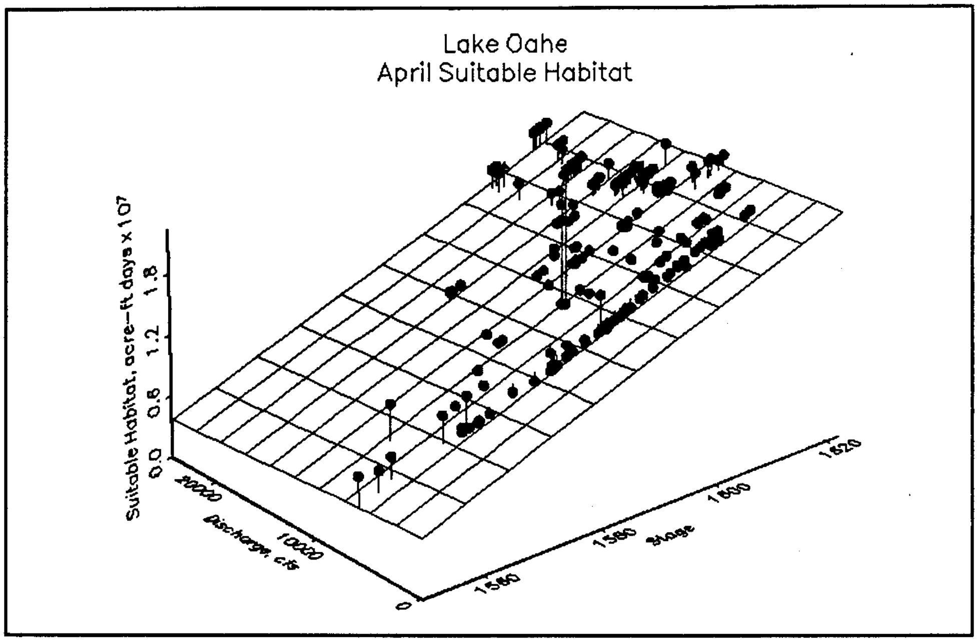

Figure 403. Lake Oahe plot of stage-discharge versus suitable habitat for April

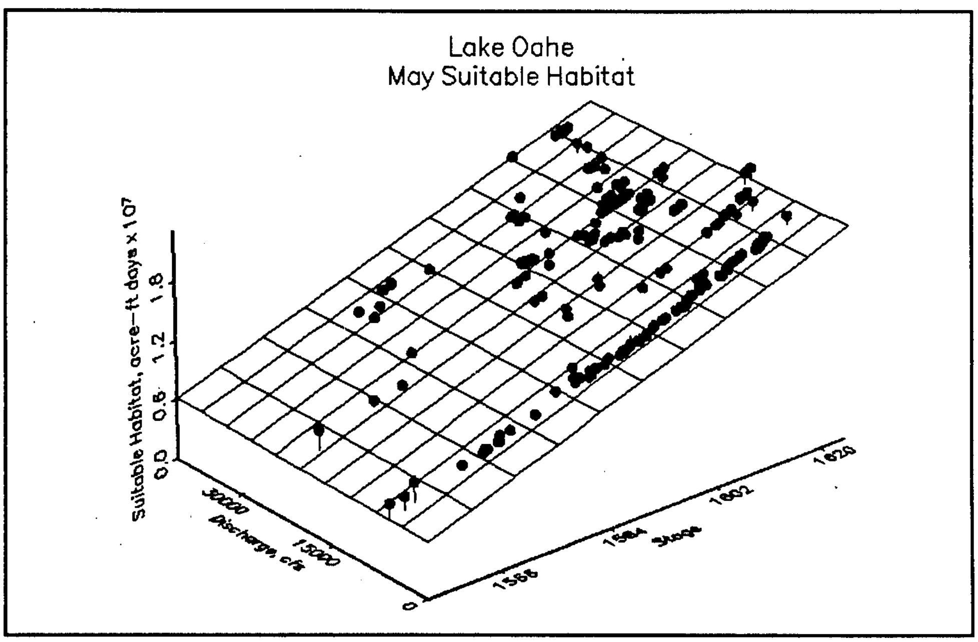

Figure 404. Lake Oahe plot of stage-discharge versus suitable habitat for May

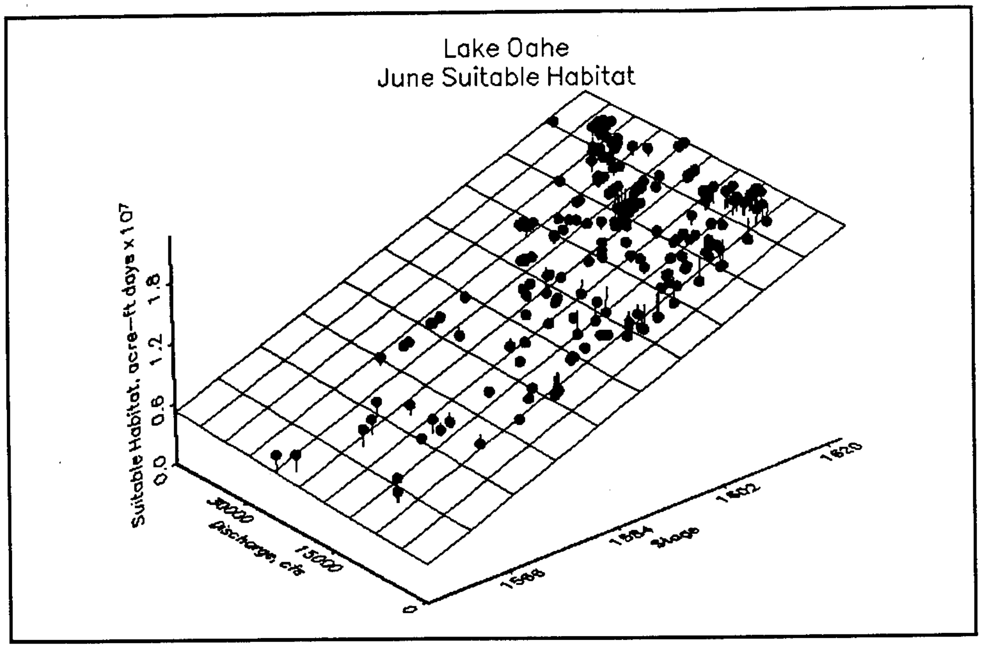

Figure 405. Lake Oahe plot of stage-discharge versus suitable habitat for June

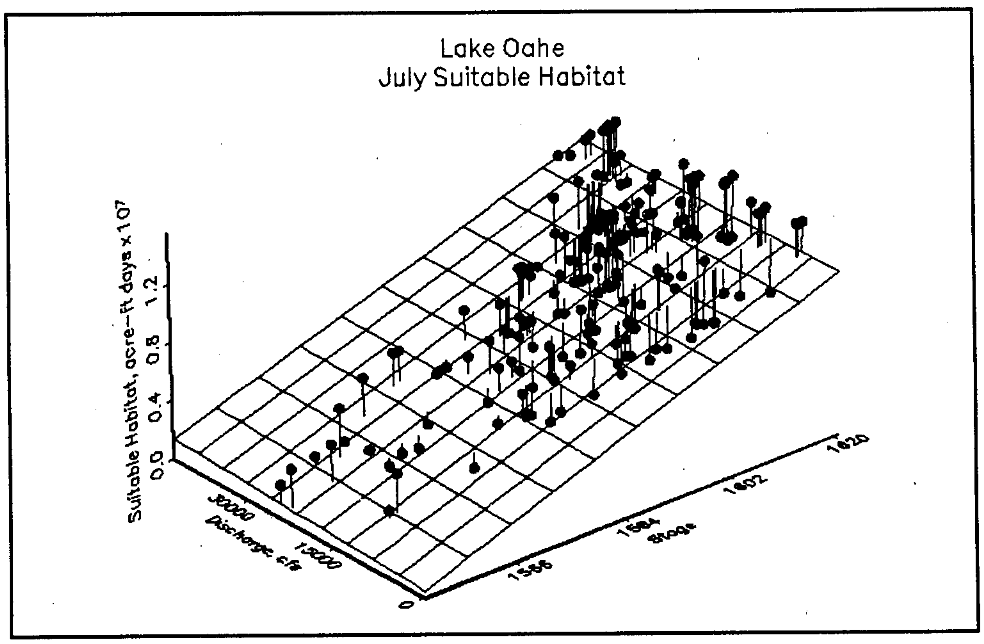

Figure 406. Lake Oahe plot of stage-discharge versus suitable habitat for July

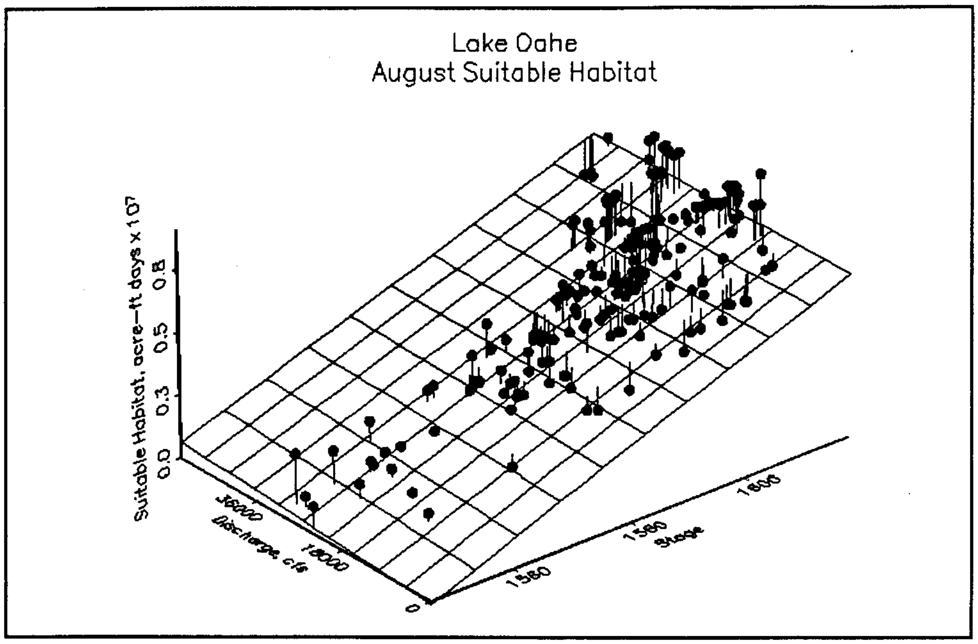

Figure 407. Lake Oahe plot of stage-discharge versus suitable habitat for August

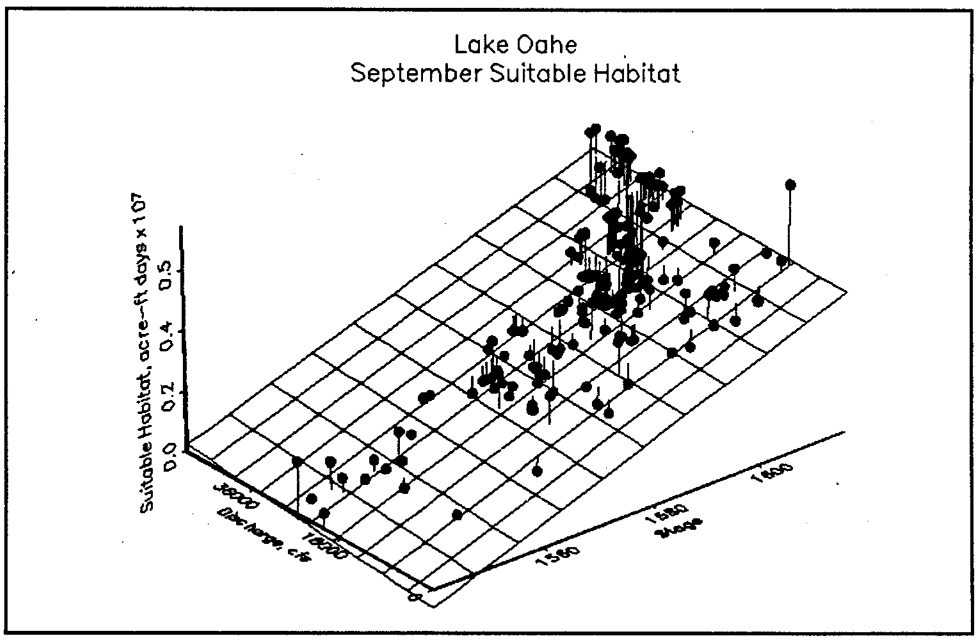

Figure 408. Lake Oahe plot of stage-discharge versus suitable habitat for September

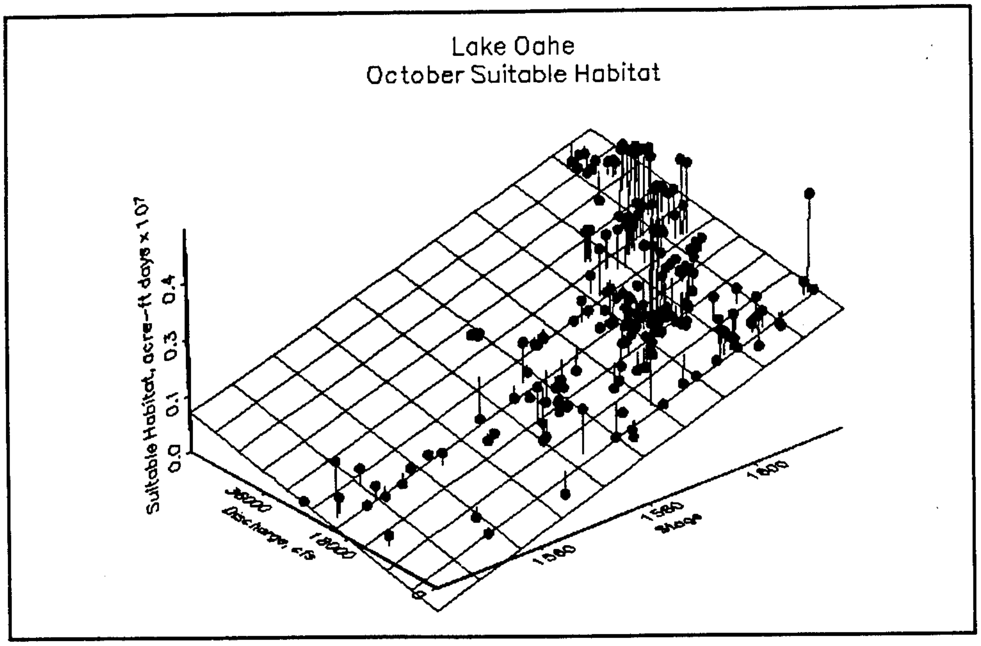

Figure 409. Lake Oahe plot of stage-discharge versus suitable habitat for October

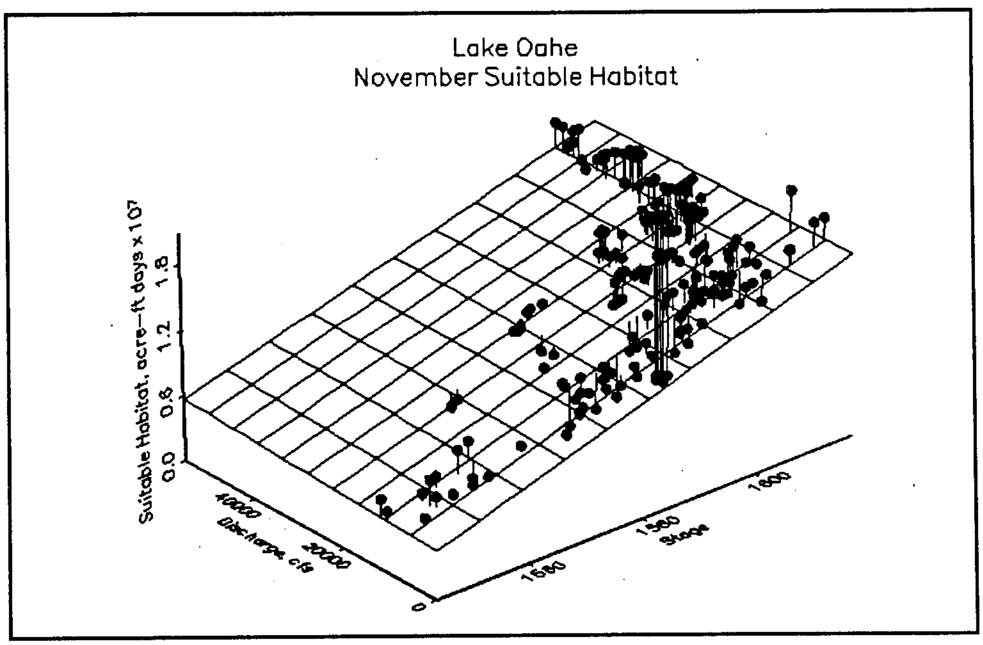

Figure 410. Lake Oahe plot of stage-discharge versus suitable habitat for November

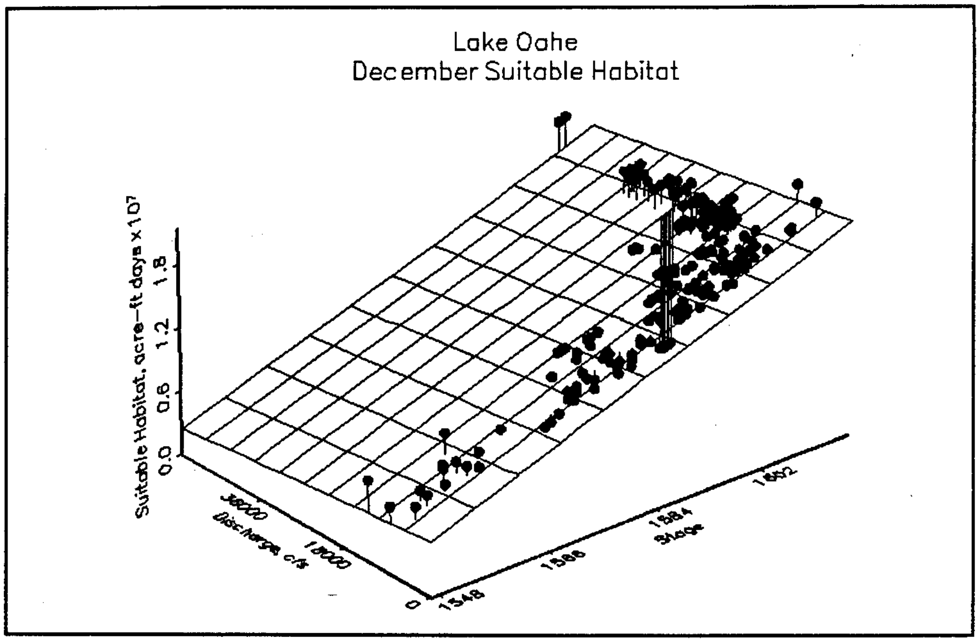

Figure 411. Lake Oahe plot of stage-discharge versus suitable habitat for December

Lake Francis Case

Regression results are summarized in Table 15. Plots of stage and discharge versus suitable habitat are shown in Figure 412-Figure 422. Regressions for Lake Francis Case were the poorest of the four reservoirs due to intermittent stratification during the summer.

Table 15. Lake Francis Case suitable habitat regression coefficients and statistics

Month	Intercept	Discharge	Stage	$Stage^2$	R^2	Pr > F
January	-0.28×10^{14}	1.12×10^{7}	1.21×10^{11}	-1.31×10^{8}	0.992	0.0001
February	-3.26×10^{14}	-0.75×10^{7}	15.66×10^{11}	-18.7×10^{8}	0.965	0.0001
March	8.45×10^{14}	-0.92×10^{7}	-41.05×10^{11}	49.85×10^{8}	0.673	0.0001
April	-4.67×10^{14}	-2.76×10^{7}	22.50×10^{11}	-27.1×10^{8}	0.124	0.0001
May	-0.93×10^{14}	-0.04×10^{7}	4.43×10^{11}	-5.23×10^{8}	0.865	0.0001
June	1.22×10^{14}	1.28×10^{7}	-6.01×10^{11}	7.39×10^{8}	0.272	0.0001
July	0.82×10^{14}	-1.22×10^{7}	-4.02×10^{11}	4.93×10^{8}	0.078	0.0002
August	1.63×10^{14}	-0.68×10^{7}	-7.94×10^{11}	9.64×10^{8}	0.170	0.0001
September	1.35×10^{11}	-3.70×10^{3}	-6.54×10^{8}	7.94×10^{5}	0.074	0.0004
October	-0.22×10^{14}	1.56×10^{7}	1.07×10^{11}	-1.30×10^{8}	0.260	0.0001
November	1.22×10^{14}	0.90×10^{7}	-6.00×10^{11}	7.37×10^{8}	0.033	0.0456
December	0.99×10^{14}	-0.72×10^{7}	-4.89×10^{11}	6.05×10^{8}	0.467	0.0001

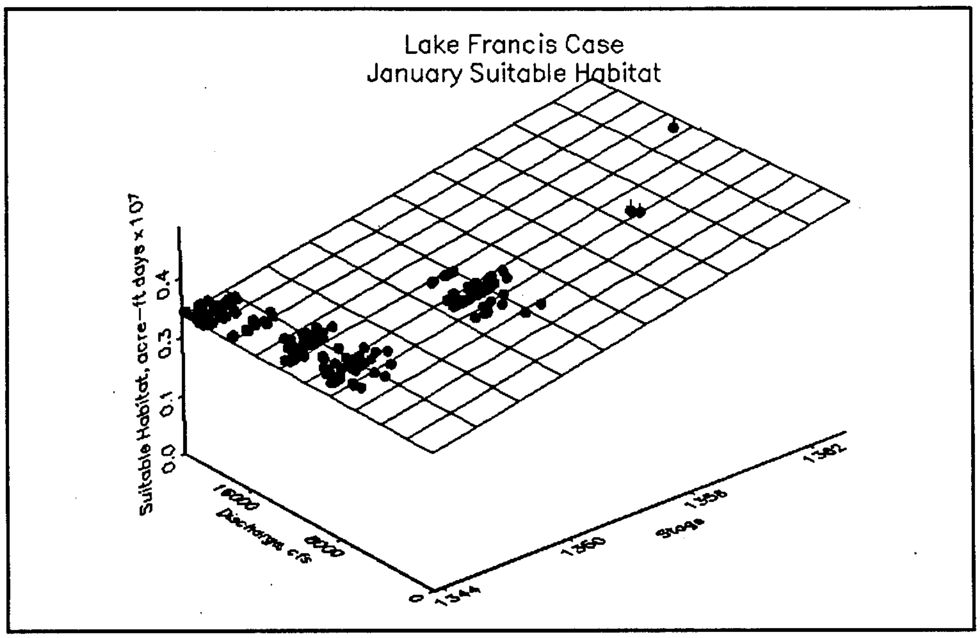

Figure 412. Lake Francis Case plot of stage-discharge versus suitable habitat for January

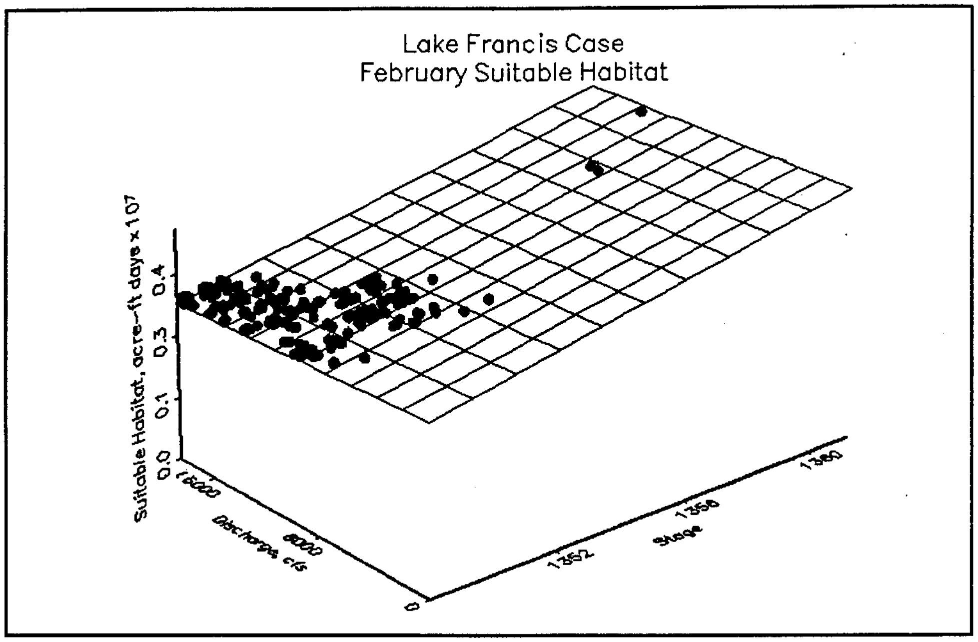

Figure 413. Lake Francis Case plot of stage-discharge versus suitable habitat for February

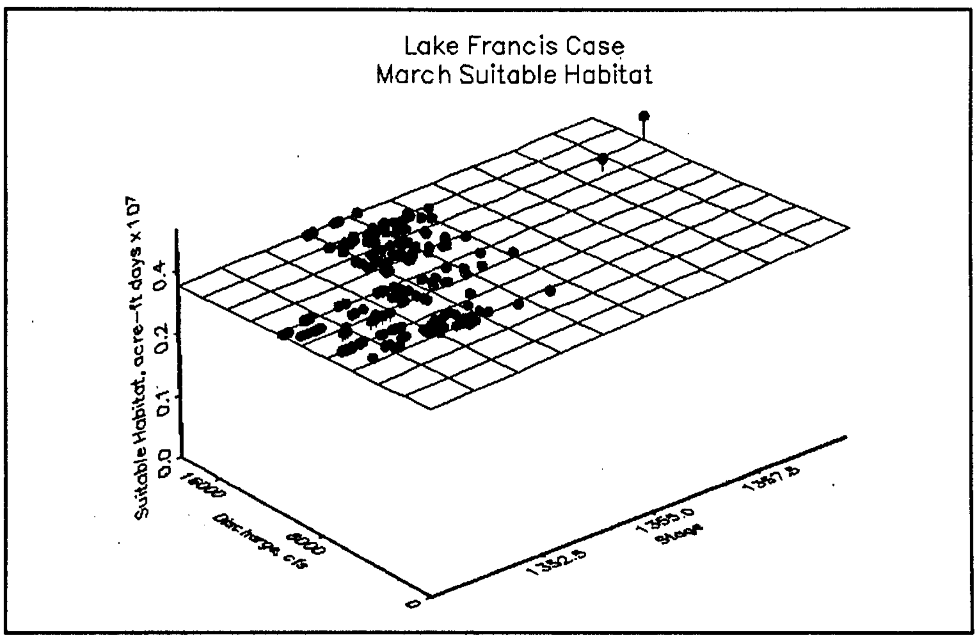

Figure 414. Lake Francis Case plot of stage-discharge versus suitable habitat for March

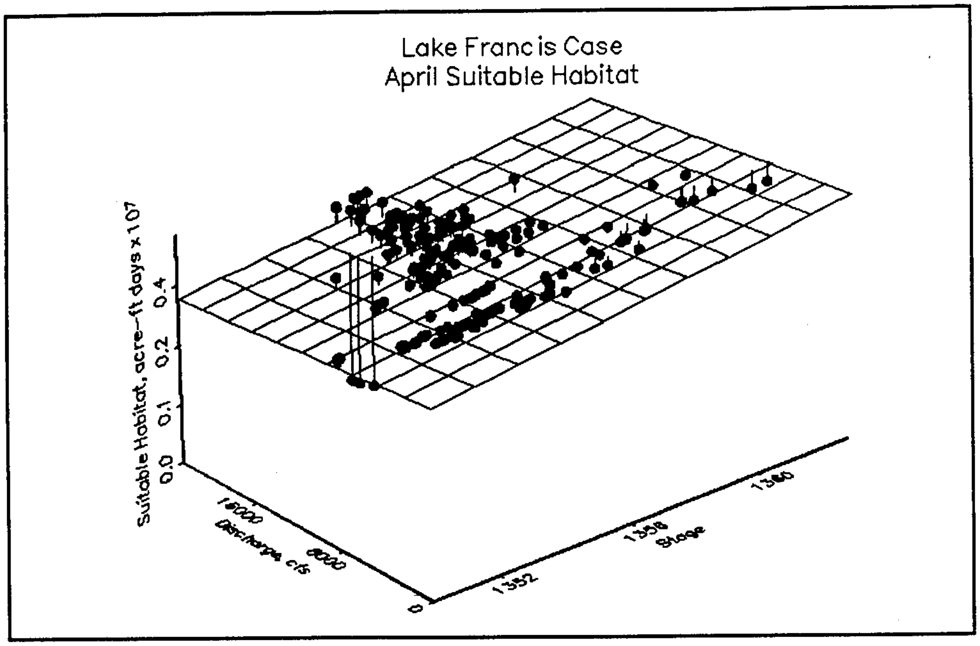

Figure 415. Lake Francis Case plot of stage-discharge versus suitable habitat for April

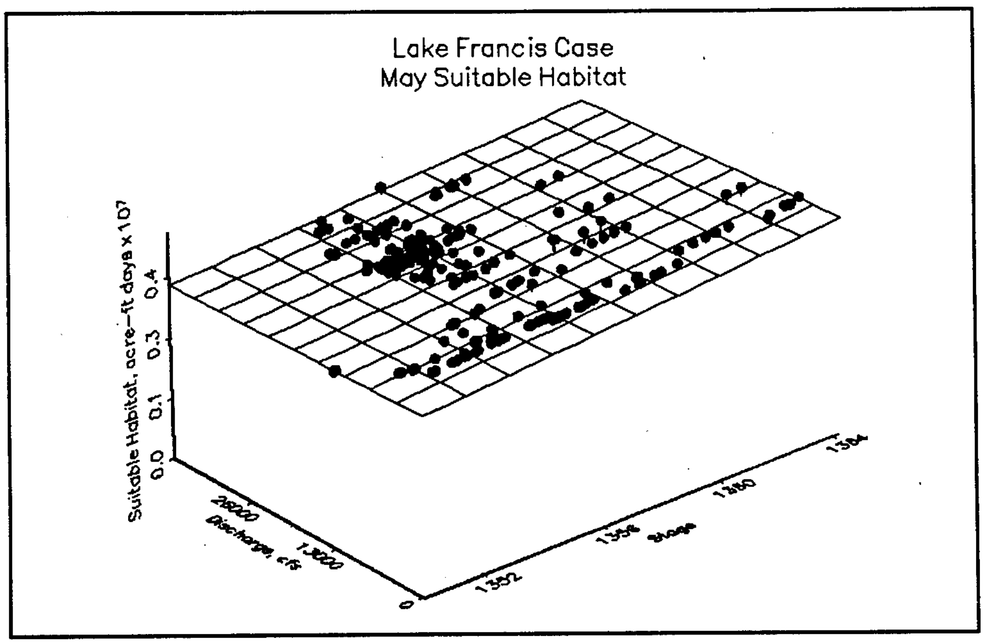

Figure 416. Lake Francis Case plot of stage-discharge versus suitable habitat for May

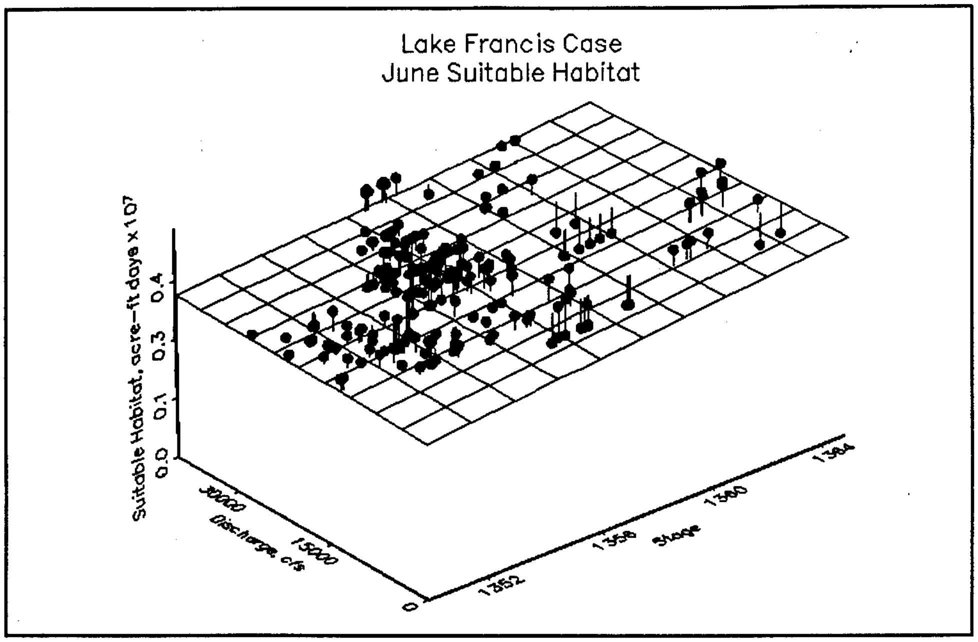

Figure 417. Lake Francis Case plot of stage-discharge versus suitable habitat for June

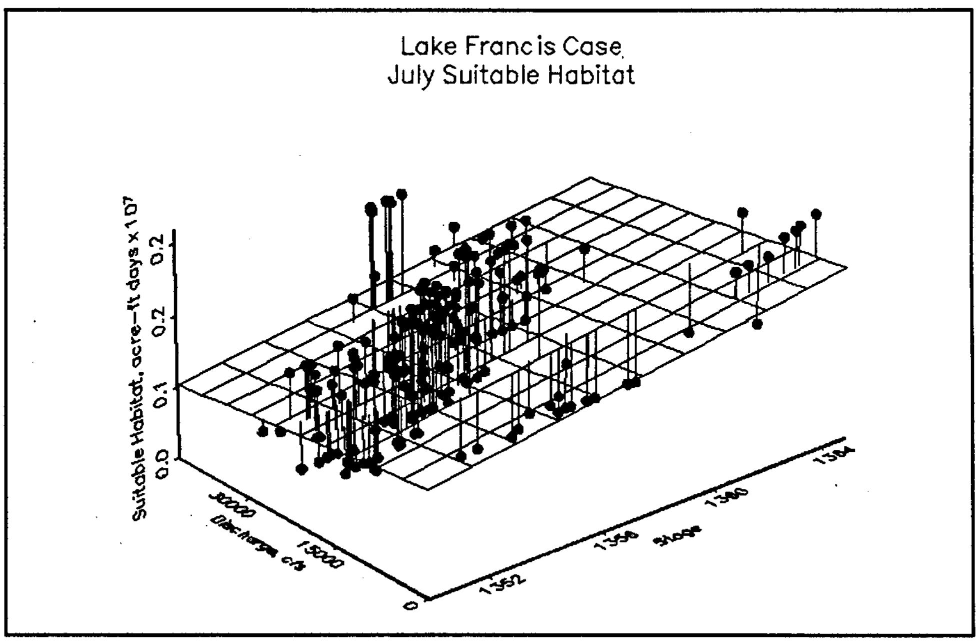

Figure 418. Lake Francis Case plot of stage-discharge versus suitable habitat for July

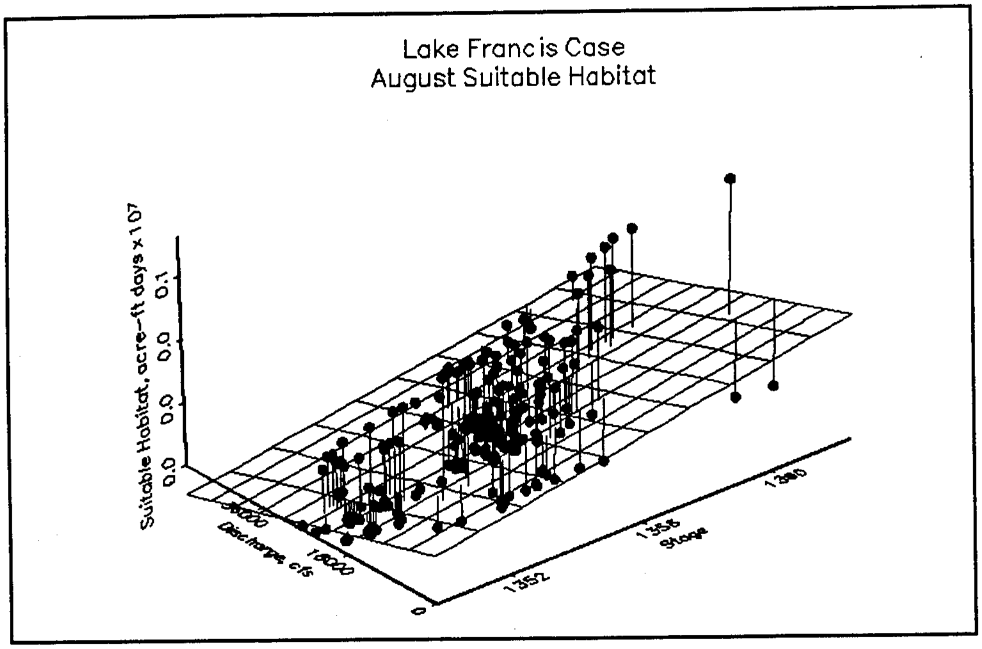

Figure 419. Lake Francis Case plot of stage-discharge versus suitable habitat for August

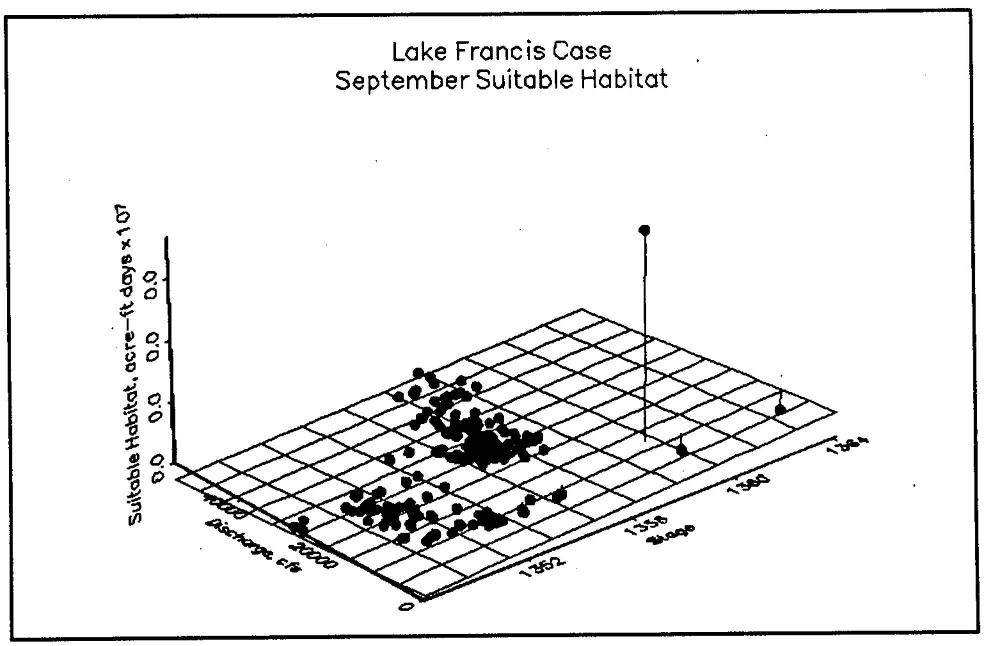

Figure 420. Lake Francis Case plot of stage-discharge versus suitable habitat for September

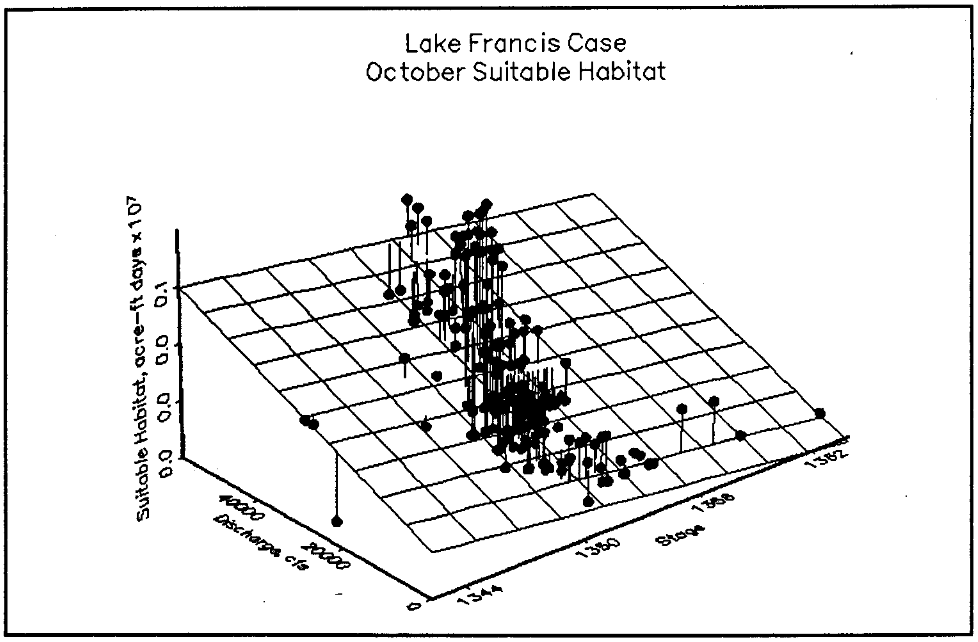

Figure 421. Lake Francis Case plot of stage-discharge versus suitable habitat for October

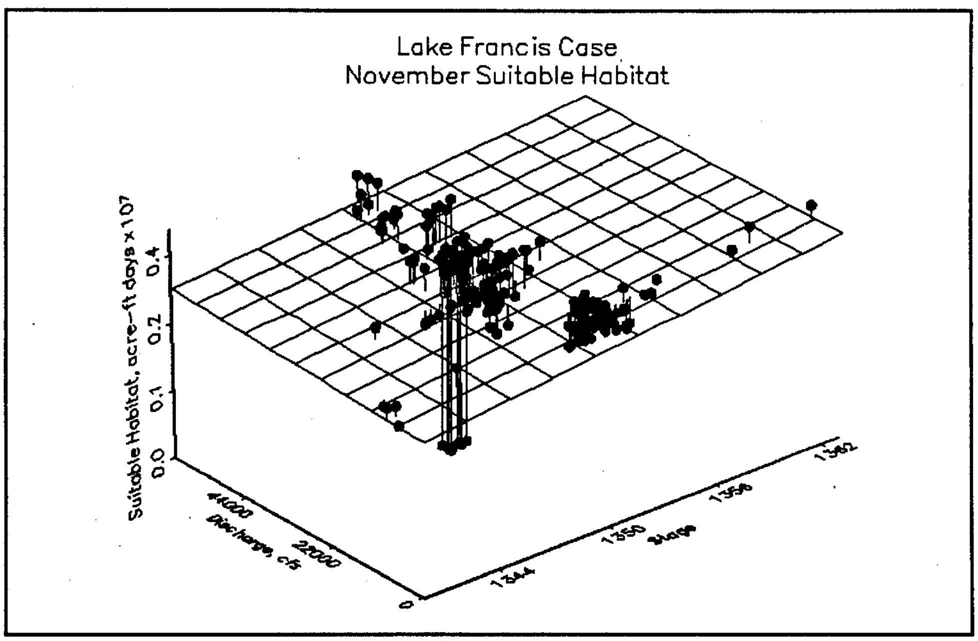

Figure 422. Lake Francis Case plot of stage-discharge versus suitable habitat for November

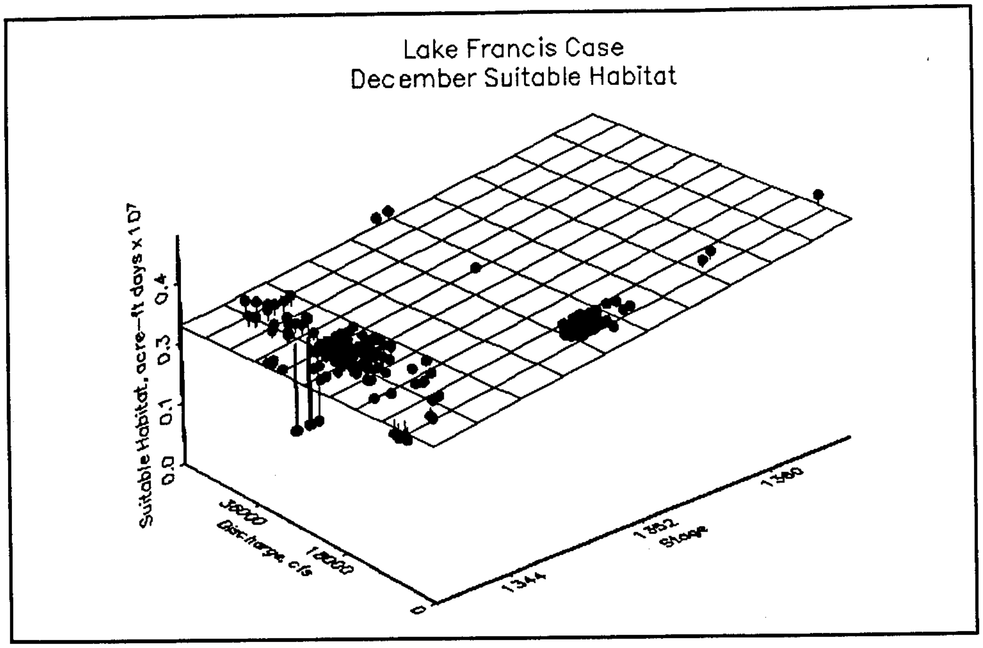

Figure 423. Lake Francis Case plot of stage-discharge versus suitable habitat for December

6 Summary and Recommendations

CE-QUAL-W2 accurately reproduced observed temperature dynamics including in-pool and release temperatures in the four reservoirs modeled. All coefficients affecting temperature were the same among the reservoirs. The model reproduced the major patterns of long-term DO dynamics through a gross sediment and water column oxygen demand without explicitly modeling algal/-nutrient/DO interactions. As a result, model predictions during scenario runs represent only how physical factors affect DO and do not include the effects of reservoir operations on algal/nutrient dynamics and their effects on DO. To include algal/nutrient effects would require at least one year's worth of detailed algal/nutrient data for each reservoir that were not and could not be made available during the time frame of this study.

Results from nine 30-year scenarios were used to determine monthly suitable coldwater fish habitat (volume of water > 5 mg l^{-1} DO and < 15 °C) for each month of the year. Results were then used to generate monthly regression relationships relating end-of-month stages and monthly discharges to suitable coldwater fish habitat. Suitable coldwater fish habitat was strongly correlated to stages which is intuitively obvious - higher stages result in larger volumes of water in the reservoir. However, the regression relationships developed during this study will allow MRD to quickly quantify the monthly habitat volumes for future scenarios of their choosing. Monthly volumes of coldwater fish habitat can now be objectively determined without the need to run the model for additional scenarios.

CE-QUAL-W2 is an extremely powerful tool to aid in addressing reservoir water quality management issues. The present implementation does not include algal/nutrient/DO interactions because of a lack of sufficient data to characterize these interactions in the model. However, a large portion of the work involved in setting up the complete model for the four reservoirs in this study has been completed. Steps should be taken to obtain a suitable database that can be used to calibrate the entire suite of water quality algorithms in the model. It is almost a certainty that water quality issues will remain important in the future. A fully calibrated water quality model for each of the reservoirs will allow management to quickly address future water quality issues based on state-of-the-art environmental engineering practices.

References

Leonard, B. P. 1979. "A Stable and Accurate Convective Modeling Procedure Based on Quadratic Upstream Interpolation", *Computer Methods in Applied Mechanics and Engineering*, Vol. 19, 59-98.

Cole, T. M. and H. H. Hannan. 1990. "Dissolved Oxygen Dynamics", in *Reservoir Limnology - Ecological Perspectives*, (Thornton, Kimmel, and Payne, eds.), John Wiley & sons, Inc., New York, NY.

Edinger, J. E. and E. M. Buchak. 1978. "Reservoir Longitudinal and Vertical Implicit Hydrodynamics". Presented at the international conference *Environmental Effects of Hydraulic Engineering Works*, ASCE, September, Knoxville, TN.

Environmental and Hydraulics Laboratories. 1986. "CE-QUAL-W2: A Numerical Two-Dimensional, Laterally Averaged Model of Hydrodynamics and Water Quality; User's Manual", *Instruction Rpt. E-86-5*. U.S. Army Engineer Waterways Experiment Station, Vicksburg, MS.

Martin, J. L. 1988. "Application of a Two-Dimensional Model of Hydrodynamics and Water Quality (CE-QUAL-W2) to DeGray Lake, Arkansas", *Technical Rpt. E-87-1*, U.S. Army Engineer Waterways Experiment Station, Vicksburg, MS.

Martin, J. L. 1988. "Application of Two-Dimensional Water Quality Model". *J. Envir. Engrg.*, 114(2), 317-336.

CE-QUAL-W2 Bibliography

Peer Reviewed Publications

Boatman, C.D. and E.M. Buchak. 1987. " Application of an Ecosystem/Water Quality Model as a Tool for Managing Estuarine Water Quality", in *Proc. Fifth Sym. on Coastal Ocean Management, ASCE, Vol. 3*, Seattle, Washington, 3932-3945.

Edinger, J. E. and E. M. Buchak. 1980. "Numerical Hydrodynamics of Estuaries" in *Estuarine and Wetland Processes with Emphasis on Modeling*, (P. Hamilton and K. B. MacDonald eds.), Plenum Press, New York, NY, 115-146.

Edinger, J. E., E. M. Buchak and D. H. Merritt. 1983. "Longitudinal-Vertical Hydrodynamics and Transport with Chemical Equilibria for Lake Powell and Lake Mead", in *Salinity in Watercourses and Reservoirs*, (R. H. French, ed.). Butterworth Publishers, Stoneham, MA, pp. 213-222.

Edinger, J. E., E. M. Buchak and S. Rives. 1987. "GLVHT Model Verification Using Field Data", in *Proc. 1987 National Conference on Hydraulic Engineering*, (R. M. Ragan, ed.), 3-7 August 1987. Hydraulics Division of the Americanv Society of Civil Engineers. Williamsburg, VA.

Gordon, J. A. 1980. "An Evaluation of the LARM Two-Dimensional Model for Water Quality Management Purposes", in *Proceedings of the Symposium on Surface-Water Impoundments*, (H. G. Stefan, ed.), Minneapolis, Minnesota, June 2-5, 1980, Vol. 1, Paper 4-34, pp. 518-527. American Society of Civil Engineers, New York, NY.

Gordon, J. A. 1981. "LARM Two-Dimensional Model: An Evaluation". *J. Envir. Engrg.*, 107(5), 77-886.

Gordon, J. A. and J. S. Lane. 1983. "Short-Term Hydrodynamics in a Stratified Reservoir", in *Proceedings of the 1983 National Conference on Environmental Engineering*, (A. Medine and M. Anderson, eds.), Boulder, Colorado, July 6-8, 1983, pp. 524-531. American Society of Civil Engineers, New York, NY.

Johnson, B. H., M. B. Boyd and R. R. Copeland. 1987. "Lower Mississippi River Salt Intrusion Modeling", in *Proceedings 1987 National Conference on Hydraulic Engineering*, (R. M. Ragan, ed.), 3-7 August 1987. Hydraulics Division of the American Society of Civil Engineers. Williamsburg, VA.

Kim, B. R., J. M. Higgins and D. J. Bruggink. 1983. "Reservoir Circulation Patterns and Water Quality". *J. Envir. Engrg.*, 109(6), 1284-1294.

Martin, J. L. 1988. "Application of Two-Dimensional Water Quality Model". *J. Envir. Engrg.*, 114(2), 317-336.

Presentations at Scientific Meetings

Buchak, E. M. and J. E. Edinger. 1989. "Comparison of Computed and Observed Velocities at Three Estuarine Sites". Presented at *Estuarine and Coastal Circulation and Pollutant Transport Modeling: Model-Data Comparison*. Waterway, Port, Coastal and Ocean Division, American Society of Civil Engineers, November 17, Newport, RI.

Buchak, E.M., J.E. Edinger, J.J. Loos and E.S. Perry. 1989. "Larval Transport and Entrainment Modeling for the Patuxent Estuary". Presented at the *Tenth Biennial International Estuarine Research Conference*, Estuarine Research Federation, October 11, Baltimore, MD.

Buchak, E. M., C. B. James and A. C. Mitchell. 1991. "Nechako Reservoir Mathematical Modelling Studies". Presented at the *1991 Annual Conference of the Canadian Society for Civil Engineering, 10th Canadian Hydrotechnical Conference and Engineering Mechanics Symposium*, May 29, Vancouver, BC.

Cole, T. M., and Hannan, H. H. 1979. "Computer Simulations of Canyon Reservoir". Presented at the *Texas Academy of Sciences Annual Meeting*. Austin, TX.

Edinger, J. E. and E. M. Buchak. 1978. "Reservoir Longitudinal and Vertical Implicit Hydrodynamics". Presented at the international conference *Environmental Effects of Hydraulic Engineering Works*, ASCE, September, Knoxville, TN.

Johnson, M. C., D. E. Ford, J. E. Edinger and E. M. Buchak. 1981. "Analyzing Storm Event Data from DeGray Lake, Arkansas Using LARM". Presented at the *American Society of Civil Engineers Convention and Exposition*, October, St. Louis, MO.

Reports and Miscellaneous Articles

Adams, R. W., Thackston, E. L., Speece, R. E., Wilson, D. J., and Cardozo, R. 1993. "Effect of Nashville's Combined Sewer Overflows on the Water Quality of the Cumberland River", *Technical Report No. 42*, Environmental and Water Resources Engineering, Vanderbilt University, Nashville, TN.

Barnese, Lisa E., Neichter, Patrick L., and Bohanon, Joseph A. 1993. "Evaluation of Water Quality in Caesar Creek Lake, Ohio using the CE-QUAL-W2 Water Quality Model", U.S. Army Corps of Engineers, Louisville, KY.

Buchak, E. M. and J. E. Edinger. 1982. "Hydrothermal Simulation of Quabbin Reservoir Using Longitudinal-Vertical Hydrodynamics", Final Report, prepared for Wallace, Floyd Associates, Inc., Cambridge, MA.

Buchak, E. M. and J. E. Edinger. 1982. "Hydrothermal Simulations of Pool 3, Monongahela River Using Longitudinal-Vertical Numerical Hydrodynamics", prepared for Energy & Environmental Management, Inc., Murrysville, PA 15668-1809. Prepared by J. E. Edinger Associates, Inc., Wayne, Pensylvania 19087-3226.

Buchak, E. M. and J. E. Edinger. 1982. "User Guide for CE-QUAL-ELV2: A Longitudinal-Vertical, Time-Varying Estuarine Water Quality Model", *Instruction Rpt. EL-82-1*, U.S. Army Engineer Waterways Experiment Station, Vicksburg, MS.

Buchak, E. M. and J. E. Edinger. 1982. "User Guide for LARM2: A longitudinal-Vertical, Time-Varying Hydrodynamic Reservoir Model", *Instruction Rpt. E-82-3*, U.S. Army Engineer Waterways Experiment Station, Vicksburg, MS.

Buchak, Edward M. and John Eric Edinger. 1985. "Simulation of Cooling Operations at Oak Knoll Reservoir, Phase II of Cooling Reservoir Modeling Program", *Document No. 85-41-R*, prepared for Environmental Department, Texas Utilities Generating Company, Dallas, Texas 75201 by J. E. Edinger Associates, Inc., Wayne, PA.

Buchak, Edward M. and John Eric Edinger. 1988. "Hydrothermal Analysis of Jersey Central Power and Light Sayreville and Werner Generating Stations", *Document No. 88-103-R/L*, prepared for EA Engineering, Science, and Technology, Inc., Hunt Valley/Loveton Center, Sparks, Maryland by J. E. Edinger Associates, Inc., Wayne, PA.

Buchak, Edward M., John Eric Edinger and Nuh-Chao Luke Huang. 1989. "Hydrothermal Analysis of Public Service Electric and Gas Linden and Sewaren Generating Stations", *Document No. 89-79-R*, prepared for EA

Engineering, Science, and Technology, Inc., Hunt Valley/Loveton Center, Sparks, Maryland by J. E. Edinger Associates, Inc., Wayne, PA.

Buchak, E. M., J. E. Edinger, and N. C. Huang. 1990. "Stationary State Dilution Studies of Lake Sinclair and Plant Harlee Branch", *Document No. 90-068-R*, prepared for Georgia Power Company Environmental Affairs, Atlanta, Georgia 30302. Prepared by J. E. Edinger Associates, Inc., Wayne, PA.

Cole, T. M. 1982. "Application of the LARM Two-Dimensional Computer Model to Canyon Reservoir", M.S. Thesis, Southwest Texas State University, San Marcos, TX.

EA Engineering, Science, and Technology, Inc. 1987. "Perryman Site Cooling Water Alternatives Study", *Report No. BSC43D*, prepared for Baltimore Gas and Electric Company, Baltimore, MD.

EA Engineering, Science, and Technology, Inc. 1993. "Comparison of the Lake Sinclair GLVHT Model Predictions with Current Meter Measurements", *EA Project No. 11987.01*, prepared for Georgia Power Company.

Edinger, J. E. and E. M. Buchak. 1978. "Hydrodynamics and Transport of Chlorine in Panther Branch Arm, Squaw Creek Reservoir for Comanche Peak S. E. S., Development Document", prepared for Texas Utilities Services, Inc., Dallas, TX.

Edinger, J. E. and Buchak, E. M. 1981. "Estuarine Laterally Averaged Numerical Dynamics: The Development and Testing of Estuarine Boundary conditions in the LARM Code", *Miscellaneous Paper EL-81-9*, U.S. Army Engineer Waterways Experiment Station, CE, Vicksburg, MS.

Edinger, J. E. and E. M. Buchak. 1982. "Analysis and Development of Carbonate-Bicarbonate Chemical Subroutine", Phase II, Development, Verification, and Use of Methods to Model Chemical and Thermal Processes for Lakes Mead and Powell. *Contract No. 2-07-DV-00131*, United States Department of the Interior, Bureau of Reclamation, Denver, CO.

Edinger, J. E. and E. M. Buchak. 1983. "Developments in LARM2: A Longitudinal-Vertical, Time-Varying Hydrodynamic Reservoir Model", *Technical Rpt. E-83-1*, U.S. Army Engineer Waterways Experiment Station, Vicksburg, MS.

Edinger, J. E., E. M. Buchak, J. Loos, and E. Krueger. 1986. "Effects of the Chalk Point Steam Electric Station on BOD and DO in the Patuxent Estuary", *Document No. 86-56-R*, Potomac Electric Power Company, Environmental Affairs Group, Water and Land Use Department, Washington, DC 20068, prepared by J. E. Edinger Associates, Inc., Wayne, PA.

Edinger, J. E. and E. M. Buchak. 1987. "Summary of Plant Hammond Coosa River - Weiss Reservoir Hydrothermal Analysis and Compliance Temperatures Reporting Procedures", *Document No. 87-119-R*, prepared for Georgia Power Company by J. E. Edinger Associates, Inc., Wayne, PA.

Edinger, J.E., E.M. Buchak, and N.C. Huang. 1988. "Chalk Point Steam Electric Station Patuxent Estuary Hydrodynamic and Transport Model Verification and Real Time Intake Entrainment Rates for 1985 Larval Sampling", *Document No. 88-77-R*, prepared for Potomac Electric Power Company, Environmental Affairs Group, Water and Land Use Department, Washington, D.C. 20068. Prepared by J. E. Edinger Associates, Inc., Wayne, PA.

Edinger, J. E. and E. M. Buchak. 1989. "Probabilistic Hydrothermal Modeling Study of Clinton Lake, Exhibit D", *Document No. 89-15-R*, prepared for Illinois Power Company, Decatur, IL 62525. Prepared by J. E. Edinger Associates, Inc., Wayne, PA.

Edinger, J. E., E. M. Buchak, and N. C. Huang. 1989. "Verification of Nechako Reservoir Hydrothermal Model", *Document No. 89-130-R*, prepared for Triton Environmental Consultants, Ltd., Burnaby, British Columbia V5M 3Z3. Prepared by J. E. Edinger Associates, Inc., Wayne, PA.

Edinger, J. E. and E. M. Buchak. 1993. "Harlee Branch Impact on Dissolved Oxygen of Lake Sinclair", *Document No. January 18*, prepared for Georgia Power Company Environmental Affairs, Atlanta, Georgia. Prepared by J. E. Edinger Associates, Inc., Wayne, PA.

Envirocon Pacific Limited and J. E. Edinger Associates, Inc. 1989. "Nechako Reservoir Mathematical Modeling Program Preliminary Results and Conclusions", prepared for Alcan Smelters & Chemicals Ltd., Vancouver, British Columbia.

Environmental and Hydraulics Laboratory. 1986. "CE-QUAL-W2: A Numerical Two-Dimensional, Laterally Averaged Model of Hydrodynamics and Water Quality; User's Manual", *Instruction Rpt. E-86-5*. U.S. Army Engineer Waterways Experiment Station, Vicksburg, MS.

FERC. 1992. "Proposed Modifications to the Lower Mokelumne River Project, California", Draft Environmental Impact Statement, Federal Energy Regulatory Commission Office of Hydropower Licensing, FERC Project No. 2916-004.

Georgia Power Company. 1992. "Hydrological and Limnological Study of Lake Sinclair in Support of Application for Renewal and Modification of a Thermal Variance for Plant Branch (NPDES Permit No. GA00026051)", prepared for Georgia Power Company, Atlanta, Georgia by EA Engineering Science and Technology, Atlanta, Georgia and J. E. Edinger Associates, Inc., Wayne, PA.

Hall, R. W. 1987. "Application of CE-QUAL-W2 to the Savannah River Estuary", *Technical Rpt. EL-87-4*, U.S. Army Engineer Waterways Experiment Station, Vicksburg, MS.

Johnson, B. H. 1981. "A Review of Numerical Reservoir Hydrodynamic Modeling", *Technical Rpt. E-81-2*, U.S. Army Engineer Waterways Experiment Station, Vicksburg, MS.

Johnson, B. H., M. J. Trawle and P. G. Kee. 1989. "A Numerical Model Study of the Effect of Channel Deepening on Shoaling and Salinity Intrusion in the Savannah Estuary", *Technical Rpt. HL-89-26*, Hydraulics Laboratory, Department of the Army, Waterways Experiment Station, Vicksburg, MS.

Kinhill Cameron McNamara Pty Ltd. 1991. Proposed Third Runway Sydney (Kingsford-Smith) Airport, Botany Bay Borrow Pit, Water Quality", Milton Queensland, Australia.

Martin, J. L. 1988. "Application of a Two-Dimensional Model of Hydrodynamics and Water Quality (CE-QUAL-W2) to DeGray Lake, Arkansas", *Technical Rpt. E-87-1*, U.S. Army Engineer Waterways Experiment Station, Vicksburg, MS.

McKee, C. P., Thackston, E. L., Speece, R. E., Wilson, D. J., Cardozo, R. J. 1992. "Modeling of Water Quality in Cheatham Lake", *Technical Rpt. No. 42*, Environmental and Water Resources Engineering, Vanderbilt University, Nashville, TN.

Tillman, D. H., and Cole, T. M. 1993. "Bluestone Phase 2 Temperature and Dissolved Oxygen Modeling Study", *Technical Rpt. EL-93-* , U.S. Army Engineer Waterways Experiment Station, Vicksburg, MS.

URS Corporation. 1986. "Southern Puget Sound Water Quality Assessment Study, Final Report, Comprehensive Circulation and Water Quality Study of Budd Inlet", prepared for Washington State Department of Ecology. By URS Corporation, Seattle, WA.

Waide, J. B., Dortch, M. S., and Cole, T. M., 1984. "Two-Dimensional Reservoir Model", *EWQOS Information Exchange Bulletin, Vol. E-84-3*, U.S. Army Engineer Waterways Experiment Station, Vicksburg, MS.

Wells, S. A. 1992. "Assessment of Management Alternatives for Water Quality Improvement in the Columbia Slough System, Volume 1: Technical Report", *Technical Rpt. EWR-001-92*, Department of Civil Engineering, Portland State University, Portland, OR.

Wells, S. A. 1992. "User Manual for the Columbia Slough Model using CE-QUAL-W2", *Technical Rpt. EWR-003-92*, Department of Civil Engineering, Portland State University, Portland, OR.

Wells, S. A., Berger, C., and Knutson, M. 1992. "Modeling the Tualatin River System Including Scoggins Creek and Hagg Lake: Model Description, Geometry, and Forcing Data", *Technical Rpt. EWR-010-92*, Department of Civil Engineering, Portland State University, Portland, OR.

REPORT DOCUMENTATION PAGE

Form Approved
OMB No. 0704-0188

1. AGENCY USE ONLY *(Leave blank)*

2. REPORT DATE
September 1995

3. REPORT TYPE AND DATES COVERED
Final report

4. TITLE AND SUBTITLE
Temperature and Dissolved Oxygen Simulations for the Upper Missouri River Reservoirs

5. FUNDING NUMBERS

6. AUTHOR(S)
Thomas M. Cole, Michael L. Schneider, John G. Skogerboe, Ronald E. Heath, Herman O. Turner

7. PERFORMING ORGANIZATION NAME(S) AND ADDRESS(ES)
U.S. Army Engineer Waterways Experiment Station
3909 Halls Ferry Road
Vicksburg, MS 39180-6199

8. PERFORMING ORGANIZATION REPORT NUMBER
Miscellaneous Paper EL-95-7

9. SPONSORING/MONITORING AGENCY NAME(S) AND ADDRESS(ES)
U.S. Army Corps of Engineers,
Washington, DC 20314-1000;
U.S. Army Engineer Division, Missouri River,
P.O. Box 103, Omaha, NE 68101-0103

10. SPONSORING/MONITORING AGENCY REPORT NUMBER

11. SUPPLEMENTARY NOTES
Available from National Technical Information Service, 5285 Port Royal Road, Springfield, VA 22161.

12a. DISTRIBUTION/AVAILABILITY STATEMENT
Approved for public release; distribution is unlimited.

12b. DISTRIBUTION CODE

13. ABSTRACT *(Maximum 200 words)*

This report describes the application of CE-QUAL-W2, a longitudinal/vertical hydrodynamic and water quality model to four reservoirs on the Upper Missouri River. Calibration results are presented for Fort Peck, Sakakawea, Oahe, and Francis Case reservoirs for water surface elevations, temperature, and dissolved oxygen. Monthly regression relationships are also presented which relate suitable fish habitat volume-days to average monthly discharge and end-of-month water surface elevations for each reservoir.

14. SUBJECT TERMS

Lake Fort Peck	Lake Sakakawea	Suitable fish habitat
Lake Francis Case	Reservoir temperature modeling	Upper Missouri River
Lake Oahe	Reservoir water quality modeling	

15. NUMBER OF PAGES
284

16. PRICE CODE

17. SECURITY CLASSIFICATION OF REPORT	18. SECURITY CLASSIFICATION OF THIS PAGE	19. SECURITY CLASSIFICATION OF ABSTRACT	20. LIMITATION OF ABSTRACT
UNCLASSIFIED	UNCLASSIFIED		

NSN 7540-01-280-5500

Standard Form 298 (Rev. 2-89)
Prescribed by ANSI Std. Z39-18
298-102